Modelling spatial variation and environmental impacts of land use change in the exploitation of land-based renewable bioenergy crops

A Thesis: By Amy Thomas

This thesis is submitted for the degree of Doctor of Philosophy
in the School of Environmental Sciences
University of East Anglia

Submission Date: June 2014

Previously published

Thomas, A.R.C., Bond, A.J., Hiscock, K.M., 2013. A GIS based assessment of bioenergy potential in England within existing energy systems. Biomass and Bioenergy. 55, 107-121

Cited in the thesis as Thomas *et al.*, 2013a
All calculations and analysis were performed by the first author. This paper forms the basis for Chapter 2, and a copy is included after the appendices.

Thomas, A.R.C., Bond, A.J., Hiscock, K.M., 2013. A multi-criteria based review of models that predict environmental impacts of land use-change for perennial energy crops on water, carbon and nitrogen cycling. GCB Bioenergy 5, 227-242.

Cited in the thesis as Thomas *et al.*, 2013b
All literature appraisal and analysis were performed by the first author. This paper forms the basis for Chapter 3, and a copy is included after the appendices.

DayCent parameterisation for SRC willow in this thesis is derived from material produced by Forest Research and The Forestry Commission by permission of Forest Research and the Forestry Commission on behalf of the Controller of Her Majesty's Stationery Office. © 2012 Crown Copyright.

Modelling spatial variation and environmental impacts of land use change in the exploitation of land-based renewable bioenergy crops

Amy Rose Carmel Thomas

Abstract

Spatial factors are of particular importance to the sustainability of land based energy crops, due both to the need to minimise feedstock transport, and to the importance of cultivation site attributes in determining key environmental impacts. This study uses geographical information system (GIS) mapping to identify sites suitable for the cultivation of *Miscanthus* or short rotation coppiced (SRC) SRC willow for co-firing with coal or generation of combined heat and power (CHP). Modelling using an adapted version of DayCent was performed for typical sites to assess variation in yield, nitrous oxide (N_2O) emissions, evapotranspiration (ET) and change in soil organic carbon (SOC) according to soil properties, hydrologic regime and previous land use.

Development of the DayCent model as part of this research gave improved simulation of the impacts of tillage on soil porosity, and resultant N_2O emissions from soil, and improved simulation of growth of SRC willow following coppicing management, leading to improved yield predictions. For land use change from arable to perennial cultivation, increased SOC was simulated, along with reduced N_2O emissions, particularly on soils prone to anoxia. However, in general, benefits of cultivation of *Miscanthus* and SRC willow for energy are maximised when the crops are grown at sites where high yields are achieved, and used to generate CHP, since this minimises the land area required per unit energy generated. Further model development work and additional field data for model verification are necessary for firmer conclusions on the change in net greenhouse gas (GHG) emissions following land use change. Additionally, indirect land use change may negate perceived benefits, and locations are difficult to predict or identify in a complex global system.

Given the magnitude of identified variations in yields and changes in N_2O emissions, spatial variation in benefits of bioenergy cultivation should be a factor in decisions to provide economic support for cultivation. However, calculations suggest that emissions offset by replacing energy generation from fossil fuels may have greater impact on GHG savings per gigajoule (GJ) than cultivation site attributes. Since total energy conversion efficiency may be in the region of 30% for electricity-only generation and up to 90% for CHP generation, planning feedstock supply chains to maximise efficiency of feedstock end use is therefore beneficial.

Contents

List of tables

Chapter 2

Chapter 3

Chapter 4

Chapter 5

Chapter 6

List of figures

Chapter 4

Chapter 5

Chapter 6

Chapter 7

List of accompanying material

One CD, containing

Data for Scenario analysis:

<site> .100 files (1 to 12)

<site>.sch files (1M to 12M, 1W to 12W)

ask.wth

bridgewater.wth

burnley.wth

newbry.wth

preston.wth

romsey.wth

staple.wth

suffolk.wth

waddington.wth

wakefield.wth

crop.100

cult.100

fert.100

fix.100

graz.100

harv.100

irri.100

omad.100

tree.100

trem.100

outfiles.in

sitepar.in

soils.in

Applications used in scenario analysis:

DailyDayCent_file100.exe

DayCent_list100.exe

model.exe

Acknowledgements

I would like to express the deepest gratitude to my supervisor, Professor Kevin Hiscock, for giving me the opportunity to work on this project, and for all his guidance and advice. I would also like to give special thanks to my secondary supervisor Dr. Alan Bond for his invaluable comments on this thesis, and finding the time to read through drafts.

I am very grateful to the research groups who provided me with data to aid in development of the DayCent model: Tony Scott and Colin Webster of the Department of Sustainable Soils and Grassland Systems at Rothamsted Research, for providing data from a tillage experiment for use in calibration work in Chapter Four; Eric Casella at The Forestry Commission for providing data on SRC willow field trials for parameterisation work in Chapter Five; and Emily Bottoms and Niall McNamara of CEH Lancaster for providing data on *Miscanthus* and SRC willow field trials for validation work in Chapter Five. In addition, I would like to thank Cindy Nevison at Colorado State University for providing me with the DayCent model code, and other files I required to complete the work. I would also like to thank Andrew Lovett and Gisela Sünnenberg for providing me with GIS data on potential *Miscanthus* yields based on their constraints mapping research. I would also like to thank Sarah Davis for providing crop parameters for Miscanthus, which were invaluable for my scenario analysis.

I would like to thank my family and friends for providing support throughout my studies. In particular: my parents, and sister Em; my cake Friday friends Emma, Alison, Adam and Mike; fellow UKERC students Rob Tina and Ellie; and my team-mates at Norwich Pikes and Ipswich White Horses Octopush clubs.

This work is dedicated to my partner Darius, for his endless support in all my endeavours, and reminding me to come home from the office to eat from time to time.

This research was supported by The UK Energy Research Centre.

Abbreviations:

Carbon (C)

Combined Heat and Power (CHP)

Department for Environment, Food and Rural Affairs (Defra)

Dissolved Organic Nitrogen (DON)

District Heating (DH)

Emission Factor (EF)

Energy Crop Scheme (ECS)

Environmental Impact Assessment (EIA)

Evapotranspiration (ET)

Feed In Tariffs (Fits)

Geographical Information System (GIS)

Global Warming Potential (GWP)

Greenhouse Gas (GHG)

Lifecycle Analysis (LCA)

Mega Oven Dry Tonnes (M Odt)

Multi Criteria Decision Analysis (MCDA)

Nitrogen (N)

No Till (NT)

Non-Fossil Fuel Obligation (NFFO)

Nutrient Use Efficiency (NUE)

Organic Matter (OM)

Relative Deviation (RD)

Renewable Heat Incentive (RHI)

Renewable Obligation Certificates (Rocs)

Senescence Month (SENM)

Short Rotation Coppice (SRC)

Soil Organic Carbon (SOC

Soil Organic Matter (SOM)

The European Commission (EC)

Tilled (T)

Towards A Sustainable Energy Economy (TSEC)

Water Filled Pore Space (WFPS)

1. Introduction

This chapter identifies key impacts of land use change for perennial energy crops, and sets out how the thesis will investigate variation in this for locations where perennial crops may be grown for energy end uses in England. The chapter begins with an overview of bioenergy in Section 1.1. Section 1.2 considers both the efficiency of conversion to energy and the fit with existing energy infrastructure; issues which are highly significant in the debate between perennials and arable crops for energy. Section 1.3 introduces *Miscanthus* and SRC willow, the two energy crops which will be the focus of this research, and Section 1.4 then discusses key issues pertaining to the sustainability of these, and other, perennial energy crops. Section 1.5 then draws out the need for this study, and is followed by the study aims in Section 1.6 and objectives in 1.7. Finally, the structure of the thesis is laid out in Section 1.8.

1.1 Overview

Biomass has long been used as a traditional energy source in the burning of wood for cooking and heating. Usage has decreased in industrialised countries, but traditional biomass remains the main energy source for an estimated 2.5 billion people in developing countries (International Energy Agency, 2008). Although this is a renewable energy source, it is not always sustainably sourced, and conversion is inefficient, often around 10 % (International Energy Agency, 2009; Kishore, 2004; McKendry, 2002b).

The European Commission (EC) prescribes an increase in renewable energy generation, in order to combat rising energy demand, reduce GHG emissions from energy, and overreliance on non-renewable energies (European Commission, 2008b). Reducing anthropogenic GHG emissions is of particular importance for climate change, for which the IPCC state that long lived GHGs, such as CO_2, N_2O, CH_4 and halocarbons, are most significant (IPCC, 2007). The UK has set a target of 60% reduction in carbon emissions by 2050; part of the pathway to achieving this is to reduce fossil fuel combustion by increasing renewable energy to 15% of total generation by 2020 (The UK Department for Business, Enterprise and Regulatory Reform, 2008).

Bioenergy currently contributes two thirds of renewable energy in Europe: 70% of this is in the form of transport fuel, which fits conveniently into existing systems of agriculture and energy infrastructure (Don *et al.*, 2012; European Commission, 2008a; Powlson *et al.*, 2005; Sims *et al.*, 2006). Energy crops can be used for electricity and heat production, as biomass for combustion, pyrolosis or gasification or as transport fuel, in the form of liquid biofuels, bio ethanol or biodiesel (McKendry, 2002b). Usage of bioenergy for electricity, heat and transport in industrialised countries was 11.3 EJ in 2008 (Chum, 2011). Since timing of generation is controlled, electricity from perennial crops has advantages over intermittent renewables such as wind and solar, however the need for changes to agriculture and energy systems are significant limiting factors (Dondini *et al.*, 2009; Powlson *et al.*, 2005).

Studies assessed by Slade *et al.* (2011) predicted future global bioenergy generation ranges from 100 to 1200 EJ, with a maximum of 200 EJ from wastes and residues and between 0.4 Gha and 2.5 Gha of land being used to cultivate bioenergy feedstock; upper estimates of land area assume yield improvements and or population and dietary changes which reduce land area requirements for food production. As part of the 2007 UK biomass strategy, there was an aim to increase the area of the UK covered by perennial energy crops, up to 0.35 Mha by 2020 (Defra, 2007) and more recent assessment has suggested that as much as 0.93–3.63 Mha could be cultivated in England and Wales without reducing food production, although socioeconomic and practical issues may prevent these figures from being realised (Aylott and McDermott, 2012; Department of Energy & Climate Change, 2012). Since currently energy crops are cultivated mostly on land suitable for food cropping, it is expected that cultivation of dedicated energy crops will increase pressure on land resources, and competition with food agriculture (Don *et al.*, 2012; Miyake *et al.*, 2012; Slade *et al.*, 2011). To avoid reduction in food production, it may be necessary to expand agricultural land reduce setaside or increase fertiliser and pesticide inputs (CBD, 2008).

In common with other renewables, bioenergy is not always a sustainable low carbon energy source; given the land area requirements, the cultivation stage may be particularly important (Clair *et al.*, 2008; Department of Energy & Climate Change, 2012; Hillier *et al.*, 2009). Conversion of agricultural land to cultivate energy crops may involve change in cropping or management scheme, and change in GHG balance may be positive or negative depending on specific cropping systems involved (Don *et al.*, 2012). Indirect land use change may then occur to accommodate food agriculture displaced by cultivation for energy. Where land use change applies to native and un-cultivated ecosystems, associated CO_2 emissions are high, and may offset the reduction in

fossil fuel emissions (Fargione *et al.*, 2008; Searchinger *et al.*, 2008). Conversion of non-agricultural land for energy crop cultivation or for food agriculture displaced by energy crops, particularly native ecosystems or land currently in set-aside schemes can be the most significant environmental cost of bioenergy (Tonini *et al.*, 2012). Indirect land-use change for displaced food agriculture, and increased fertiliser inputs with intensification of existing food production may be responsible for much of the emissions linked to bioenergy (Melillo *et al.*, 2009).

Agriculture contributes 10-12% of anthropogenic GHG emissions globally (Smith, 2007), and in particular is responsible for 84% of anthropogenic N_2O emissions (Smith *et al.*, 2008), largely from fertiliser inputs and soil disturbance (Brown *et al.*, 2002; Curley *et al.*, 2009). Soil C storage has been identified as the greatest climate change mitigation potential from agriculture (Smith, 2007), however Li *et al.* (2005a) observed increased N_2O emissions associated with soil C storage, which offset this mitigation by 75-310%. N_2O emissions in response to agricultural land management vary significantly between sites, hence the change in emissions with land use change will also be site specific (Chatskikh and Olesen, 2007). Since N_2O has a global warming potential (GWP) of 310 compared to 1 for CO_2, this may have a significant impact on the GHG balance of bioenergy (1995 IPCC).

1.2 Effectiveness of perennial crops for bioenergy; with comparison to annual alternatives

Energy crops can include annuals such as oil seed crops and sugarcane, or perennials with higher lignin content. Desired qualities include high yield, low energy, water and nutrient input requirements, and low levels of contaminants in the combusted feedstock (McKendry, 2002a).

1.2.1 Energy Ratios

Energy ratios, expressed as energy return on energy invested (with values over 1 representing net gain in energy) are useful in making absolute and comparative judgements on the efficiency of bio energy (Mulder *et al.*, 2010; Powlson *et al.*, 2005). Higher values are preferable, although since direct conversion of fossil fuels for energy has an energy ratio less than one, it could be argued that energy ratios less than one still represent an acceptably productive system if inputs are

renewable energy (Powlson *et al.*, 2005). Promising values have been reported for perennials, for example 10.34:1 for CHP produced from SRC willow via gasification, and 3.68:1 for large scale electricity generation from *Miscanthus*, (Rowe *et al.*, 2009). Annual crops tend to require greater energy input due to requirement for fertilisers and the additional fuel demands of annual tillage and planting. Calculations for corn bioethanol vary from below one Patzek (2004) to 1.5:1 (Farrell AE, 2006). Other annuals show better performance, for example 7:1 for sorghum ethanol and 8 for sugarcane ethanol and around 4:1 for palm oil biodiesel (de Vries *et al.*, 2010). Reported figures can be misleading however, for example the energy ratio of 8:1 for sugarcane ethanol excludes renewable energy inputs (Howarth, 2009). The energy ratio calculated for a given energy crop will vary with yield fluctuations, system boundaries and how much energy cost is attributed to co-products (Cherubini *et al.*, 2009; Rowe *et al.*, 2009).

Given that land is a limited resource, net energy generation per hectare is significant, so yield and energy density of the chosen crops must be compared. Annuals commonly provide less energy, such as around 2 GJ ha^{-1} a^{-1} for grain ethanols and 10 GJ ha^{-1} a^{-1} for corn and soy biofuels, compared to 110 GJ ha^{-1} a^{-1} for SRC electricity generation, and even more if heat is utilised (de Vries *et al.*, 2010; McKendry, 2002b). However some annuals such as sugarcane and palm oil can provide up to 135 GJ ha^{-1} a^{-1} (de Vries *et al.*, 2010). Use of waste residues from food crops such as rice husks and bagasse from sugar cane may show better performance than dedicated energy crops, since cultivation energy, agrochemical inputs and land use are often regarded as zero. However, quantities may be limited, and residue removal can result in soil erosion, decreased soil fertility and loss of soil carbon storage, so it has been suggested that collection should be limited to 20 – 30% of residues (Mollersten, 2003; Wilhelm, 2004). High diversity mixed grasses are suitable as a biomass feedstock, and provide a range of ecosystem benefits including increased nitrogen use efficiency, increased microbial activity and reduced nutrient leaching (Fornara, 2009; Weigelt, 2009). However net energy is less than SRC willow at 18.1 GJ ha^{-1} (Tilman *et al.*, 2006). It is also important to consider potentially restricting factors such as water availability, climate, soil type and nutrient availability which may affect relative yields of different crops (Aylott *et al.*, 2008; Lovett *et al.*, 2009; Richter *et al.*, 2008).

1.2.2 Processing and conversion

Processing of wheat and sugar beet bioethanol made up 44% , and 71% of energy inputs and 36% and 66% of GHG emissions (Mortimer, 2004). Higher lignin content means perennial crops require more processing to be used for liquid transport fuels, increasing costs, and requiring plant sizes around 1 gigawatt-thermal (GWth) for good efficiency; technology is not yet available at commercial scale, so improvements cannot yet be anticipated (Edwards, 2008; Wetterlund *et al.*, 2012). Technical improvements making processing of lignocellosic biomass for liquid transport fuel more commercially attractive may increase this usage in future (Chum, 2011), however generation of electricity and or heat is currently the preferred end use (Edwards R, 2008; Powlson *et al.*, 2005; Wetterlund *et al.*, 2012). Processing of perennials for combustion may be limited to drying, which has little impact on the GHG and energy balance (McKendry, 2002b; Powlson *et al.*, 2005), although chopping of *Miscanthus* and chipping and pulverisation of SRC willow where necessary will have some effect on the overall balance (Styles and Jones, 2007).

At the end-use stage, energy loss for conversion in ethanol transport engines is around 64-74%, whilst blending biodiesel into conventional diesel has little effect on the 58 % loss at conversion (Sims *et al.*, 2006). Perennial feedstock has wide ranging conversion efficiencies; losses for combustion to electricity varies from 80- 60% depending on plant size, or where heat and electricity are utilised, losses can be reduced to 10% (Sims *et al.*, 2006).

1.2.3 GHG emission balance

Mitigation of climate change is one of the two key stimuli for renewable energy; failure of energy crops on these issues undermines the purpose of renewable energy (Cherubini *et al.*, 2009; Clair *et al.*, 2008). Perennials generally require less agrochemical inputs such as nitrogen based fertilisers, which can halve N_2O emissions, and long periods between tillage encourage soil carbon accumulation, hence they tend to have favourable greenhouse gas balance compared to annual crops (Kavdir *et al.*, 2008; Powlson *et al.*, 2005; Rowe *et al.*, 2009). For biofuels from annual crops, N_2O emissions from soil make up from 5-80% of their GHG emissions (Don *et al.*, 2012).

Greenhouse gas emissions savings are highly variable for biofuels depending on processing methods and input energy type. For example sugarcane bioethanol in Brazil processed using biomass energy from bagasse has only 10 – 20% of the GHG emissions of gasoline, whereas corn bioethanol in the US has 70-90% of the GHG emissions of petrol based fuel (International energy agency, 2008). Variation is also seen for electricity from biomass according to land management, yield, processing and transport distances as well as system boundaries, for example inclusion of emissions from indirect land use change. *Miscanthus* has 23% of the GHG emissions of generation from coal, or 38% of the emissions from natural gas, and SRC willow generates 4-23% of the GHG emissions of coal, or 6-38% of emissions from natural gas (Rowe *et al.*, 2009).

1.2.4 UK Market penetration

In general, multiple benefits have been identified for perennial crops over annuals, in terms of energy return on energy invested, energy return per ha, and greenhouse gas emissions associated with cultivation and processing. Between 2010 and 2011, domestically cultivated energy crops offset an estimated 0.4 % of UK energy usage (Hastings *et al.*, 2014) compared to 3.1 % of total road transport fuel supplied by biofuel (Department for Transport, 2011). Powlson *et al*. (2005) suggest that, in spite of better energy ratios and greater reductions in CO_2 emissions for electricity and heat generation from perennials, biofuels from arable crops have been a preferred focus for energy cropping, since they fit easily into existing systems of agriculture and energy infrastructure. Technological research and development have the potential to make big changes in the bioenergy sector; improvements in processing enabling crops with lower pre harvest energy input to be used for biofuel, or improvements in efficiency of conversion of biomass may increase potential energy ratios (Powlson *et al.*, 2005).

Energy Crop Scheme (ECS) funding aims to assist market penetration from perennials by providing funding to cover 50% of establishment costs, however as of 2011 total uptake only amounted to 10 kha, and was seen to fall during the second phase, in spite of increases in grants (Aylott and McDermott, 2012). Issues of policy support for energy crop cultivation will be discussed further in Section 2.6. From current levels, significant increase in area planted to bioenergy crops would be necessary to meet government targets; given timescales such as the three to six year lead in period for establishment of crops (Natural England, 2009) and the long development times for bioenergy plants (Thornley, 2006) this issue should be addressed urgently (Hastings *et al.*, 2014).

1.2.5 Fit to existing energy infrastructure

It is important to assess the fit between perennial feedstock and existing energy infrastructure, since this issue is considered partly responsible for the failure of energy generation from perennials to achieve the same market penetration as biofuel from annuals (Powlson *et al.*, 2005). Although improvements in processing may ultimately enable high lignin perennials to replace annuals for liquid transport fuels, it is useful to consider more currently available end uses.

Biomass feedstock is bulky and has a low energy density compared to fossil fuels meaning it is necessary to minimise road transport distances to achieve emissions savings and ensure energy returns greater than energy invested (McKendry, 2002a; Powlson *et al.*, 2005). As a result, it is necessary to establish localised supply chains, and agreements between farmers and plant operators are of particular importance. This also limits the potential scale of generation from biomass only feedstock; since smaller plants tend to have low conversion efficiency, alternative approaches must be considered to make efficient usage of relatively small quantities of feedstock (Gross, 2003).

In order to minimise impacts per unit energy generated, it is therefore important to identify the most efficient potential end uses for relatively small quantities of biomass feedstock, and assess potential availability of feedstock close to those end uses. Issues of fit to existing energy infrastructure, and potential bioenergy generation once these issues have been taken into account will therefore be explored in Chapter 2. Fit to infrastructure is one of many issues which may potentially limit generation from bioenergy, including farm scale economics and farmer choices, public attitudes to landscape change and perceptions of impacts on food production (Alexander *et al.*, 2014; Department of Energy & Climate Change, 2012; Dockerty *et al.*, 2012; Jensen *et al.*, 2007). Socioeconomic factors are not an intended focus for this study, but will be discussed briefly where necessary to address issues of feasibility; in particular, issues regarding supply chains, competition between local and imported feedstock, profitability for farmers and generators and perceptions of food versus fuel will be discussed in Chapter 2.

1.3 *Miscanthus* and SRC willow

Perennials have been chosen as a focus for this research, due to lower agrochemical input requirements, and evidence for increased soil C storage, leading to favourable greenhouse gas balance. Popular perennials include trees suitable for short rotation coppicing, such as SRC willow or poplar, and rhizomatous grasses, such as switchgrass, reed canarygrass and *Miscanthus* (Powlson *et al.*, 2005). Of these *Miscanthus* and SRC willow are most popular in the UK (Rowe *et al.*, 2009).

Miscanthus, is a tall rhizotomous grass, becoming popular in England, due to potential high energy ratio of 32:1 (before transport, processing and conversion of feedstock have been taken into account) and high rates of photosynthesis in a range of European and Asian climates, producing high yields (Atkinson, 2009). *Miscanthus* also benefits from translocation of nutrients; reducing contaminants in the combusted feedstock, as well as providing nutrients for the next year's growth (Heaton *et al.*, 2010). Recommended *Miscanthus* lifecycle is around 15 to 20 years (Department for Environment Food and Rural Affairs, 2007); decline in productivity with age occurs due to increasing space taken up by unproductive rhizome (Christian *et al.*, 2008; Don *et al.*, 2012).The hybrid *Miscanthus x giganteus* is preferred in the UK, and for brevity will be referred to simply as Miscanthus throughout this thesis.

Willow is a fast growing shrub, with quickly establishing root systems and responds to coppicing with rapid new growth, giving a potential energy ratio of 30:1 with short rotation coppicing (SRC) (Atkinson, 2009; Smart, 2005). Multiple genotypes have shown good performance for cultivation in the UK, and can be grown together to increase resistance to disease and mitigate against low yield years (Boyd, 2000; Tallis *et al.*, 2013). Winter harvesting enables recycling of nutrients through senescence (Boyd, 2000) and nutrient and water demands may be met using treated sewage sludge at some sites (Hilton, 2002). Harvested every three years, SRC willow has a lifecycle around 21 to 30 years (Keoleian and Volk, 2005), after this stems can become too thick to harvest (Don *et al.*, 2012). In a commercial agricultural context a field of SRC willow is generally planted as a number of varieties, whilst field trials for research which provide yield data for modelling may prefer to plant a single variety on each plot.

1.4 Sustainability of perennial energy crop cultivation

For some forms of bioenergy, land use change can have a significant environmental cost, while for perennials, there is evidence of potential environmental benefits from the cultivation stage, in the form of increased soil carbon storage, and reduced N_2O emissions from agrochemical inputs (Brandão *et al.*, 2011; Clair *et al.*, 2008; Rowe *et al.*, 2009; Tonini *et al.*, 2012). As well as the environmental impacts of cultivation of the new crop, the removal of existing biomass and the interaction of a new crop and management regime with the soil conditions produced by previous land use must be considered (Brandão *et al.*, 2010; Fargione *et al.*, 2008; Searchinger *et al.*, 2008). Spatial variation in existing land use is therefore a factor; as well as the major differences between arable and grassland, variation within these broad categorisations must be considered. In terms of available data on land use, the Centre for Ecology and Hydrology 2007 land cover map (Centre for Ecology and Hydrology, 2011) lumps arable land, hence the specific crop and nutrient application regime for a location cannot be identified. Grassland is split into improved, neutral, acid and calcerous; some of the differences between these may be difficult to represent in the context of modelling, as will be discussed in Section 2.10 and Section 6.2.

Perennial crops differ from common arable crops in terms of management requirements and growth patterns; change to these affects water cycling and availability, as well as soil physical and chemical properties and resulting carbon (C) and nitrogen (N) cycling and emissions (Haughton *et al.*, 2009; Rowe *et al.*, 2009). It is necessary to have a good understanding of these changes, and how they may interact with existing site properties, in order to understand how the impacts of land use change for perennials may vary between sites. Figure 1.1 illustrates C, N and water cycling for an agroecosystem, and Sections 1.4.1 through to 1.4.3 describe how these cycles may be affected by land use change for perennial energy crops.

The discussion of nutrient cycling in relation to energy crops tends to focus on N and C (Hellebrand *et al.*, 2008; Kavdir *et al.*, 2008; Keoleian and Volk, 2005; Kramer, 2006) , because of the importance of N_2O and CO_2 in global warming, and the eutrophication and acidification impacts of N inputs to fluvial ecosystems. There are also some studies on P (e.g. Ekholm *et al.*

2005) since this is also important in Eutrophication, but less so than N since it is often bound to sediments in fluvial ecosystems. This study also focusses on C and N, because of the importance of assessing GHG balance to ensure that emissions savings promised by bioenergy are achieved.

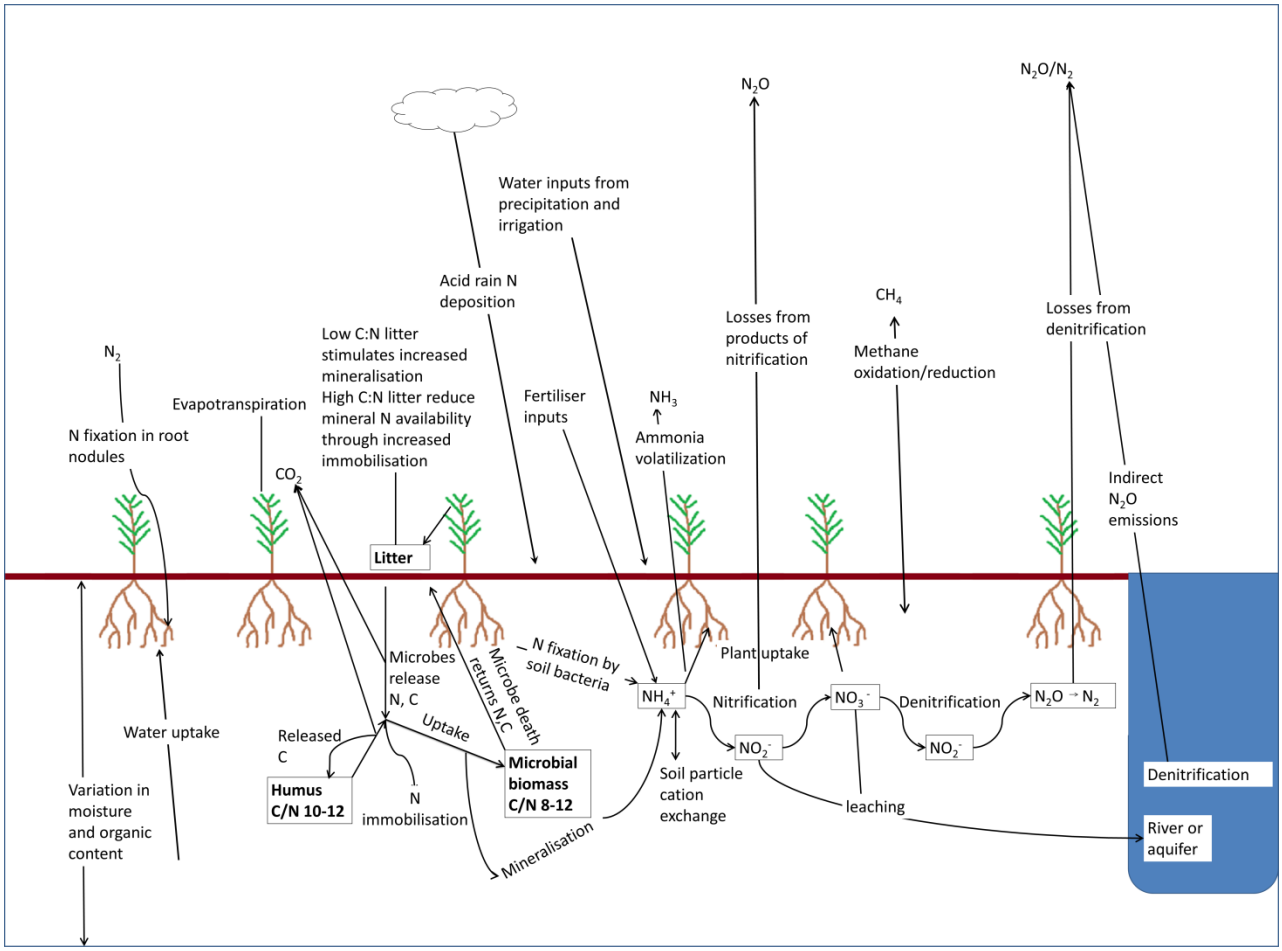

Figure 1.1 C, N and water cycling for an agroecosystem.

1.4.1 Soil Carbon cycling

Atmospheric CO_2 is used by crops in photosynthesis; in the case of energy crops, the C stored in harvested parts will be released on their combustion, however non-harvested C will move into soil storage in the form of litter, roots and exudates (Powlson *et al.*, 2005). For SRC willow and *Miscanthus*, around 85% of C uptake is re-released as CO_2 once cultivation and energy generation stages have been considered (Tonini *et al.*, 2012). Soil C storage is only temporary; CO_2 is also emitted from soil organic matter (SOM), by soil respiration which can also be accelerated by erosion (Fargione *et al.*, 2008; Keoleian and Volk, 2005) or can be adsorbed by crop roots from the

soil (Thornley, 2006). Given the unpredictability of duration of soil C storage, it has been suggested that sequestration should not be a focus for carbon mitigation efforts, however it remains important that activities are not reducing plant and soil C storage (Clifton-Brown *et al.*, 2007; Keoleian and Volk, 2005). Soil C storage has been identified as the source of greatest uncertainty in predicting GHG balance of bioenergy crop cultivation (Cannell, 1999).

The balance of C storage varies with land use e.g. oil seed rape releases 0.40 to 0.24 t C ha^{-1} a^{-1} depending on management; and forest can store around 0.32 t C ha^{-1} a^{-1} (Brandão *et al.*, 2011). For a given crop, C storage rates will vary due to variation in C inputs with yield and management, and variation in rates of C breakdown and loss according to soil type and climate factors (Hamelin *et al.*, 2012; Tonini *et al.*, 2012). Since tillage aerates soil increasing decomposition rates, and resulting CO_2 loss from soil; the no till (NT) practice for perennials should reduce gaseous losses of C inputs (Ball *et al.*, 1999; Del Grosso *et al.*, 2008; Keoleian and Volk, 2005; Li *et al.*, 2005a). Year round soil cover and reduced surface disturbance means perennial biomass crops also reduce soil erosion, increasing soil accumulation in the field and reducing sediment inputs to the river (Thornton, 1998; Jørgensen and Schelde, 2001; Powlson *et al.*, 2005). However depending on weather conditions, there is also a risk that winter harvesting can lead to soil compaction and loss of sediment to streams (McKay, 2011) and planting operations may cause erosion on slopes (Finch *et al.*, 2009). Borzêcka-Walker (2008) cite C sequestration rates from 0.15 to 0.41 t C ha^{-1} a^{-1} for SRC willow SRC and 0.13 to 0.91 t C ha^{-1} a^{-1} for *Miscanthus*. High levels of soil C sequestration observed for *Miscanthus* and SRC willow may exceed both arable land and recent setaside, but are likely to be less than more natural habitats, unimproved grasslands and former arable land in longer term setaside programs (Fargione *et al.*, 2008; Rowe *et al.*, 2009; Smith, 2004). Soil C stocks prior to land use change, which can be related to previous land use and management as well as site factors, may be the greatest determinant of GHG balance (Hillier *et al.* 2009). Alternatively, if maximum postulated increases in SOC storage were achieved by SRC, this would outweigh all other GHG flows involved (Keoleian and Volk, 2005). Since change in soil C storage is dependent on previous land use type, duration and management, as well as type and management of new crop, these issues should be factored into decisions about land use change.

Following change in land use, there is a variable period before a catchment reaches steady state due to: time taken for establishment of new vegetation (canopy, roots etc.); and rates of processes, such as soil organic matter accumulation, decay or erosion (Breemen *et al.*, 2002, Keolian and Volk, 2005, Darracq *et al.*, 2007). New C inputs occur at or near soil surface; these will

be mixed through the soil by tillage, or can result in soil C stratification for NT systems (Soane *et al.*, 2012). For example, Hellebrand *et al.* (2010) note that most of increase in SOC with SRC willow is in the top 4cm of the soil. Annual soil C changes such as those observed for Willow are often very small compared to the total soil C store (Verlinden *et al.*, 2013). Soil organic carbon (SOC) accumulation rate for a new land use will also vary over time, it is often greatest during establishment and usually curvilinear until SOC reaches equilibrium, under constant conditions (IPCC, 2006; Smith, 2004). Whilst soil C storage at equilibrium may be higher for *Miscanthus* or SRC willow than for an existing NT land use, time taken to reach equilibrium is unpredictable, and there will be a carbon debt associated with C released during land preparation, until C storage reaches previous levels.

Once at equilibrium, soil C storage levels can be maintained until there is a change in land use or management (Lal, 2004). Equilibrium may not have been achieved by the end of crop lifecycle; around 21 to 30 years for SRC willow (Keoleian and Volk, 2005) and 15 to 20 years for *Miscanthus* (Department for Environment Food and Rural Affairs, 2007). Removal of roots and ploughing of soil at the end of the energy cropping cycle will release C stored in belowground plant matter and some of the stored soil C. This loss should be offset by the next cropping cycle if land use is maintained (Keoleian and Volk, 2005).

1.4.2 Nitrogen cycling

N_2O has a global warming potential (GWP) of 310 compared to 1 for CO_2, hence it is crucial to also assess N cycling in order to fully consider GHG emissions (IPCC, 1995). Although N_2O emissions predictions are often based on type and amount of N fertiliser input (Bouwman, 1996), this relationship varies with factors such as climate and soil type, and will also be affected by interaction between new land management and crop factors, such as leaf litter inputs or timing of application relative to crop uptake (Brown *et al.*, 2002; Chatskikh *et al.*, 2005; Keoleian and Volk, 2005; Müller *et al.*, 1997). Site specific variation in nutrient cycling response to new land use must be anticipated; however prediction of these impacts is hampered by an incomplete understanding of processes.

Nitrogen naturally exists mostly as inert N_2 which can be fixed into useable nitrogen nutrients such as NH_4^+ by bacteria in soil and root nodules. This NH_4^+ can then be nitrified to NO_3^- in soil where both nutrients can be taken up by plants or leached downwards (Socolow, 1999). These N nutrients can be stored, leached, or transformed and lost as N_2O or N_2 gas, with varying proportions and timings (Cherubini *et al.*, 2009). Nitrogen retention in soils and aquifers can last for decades to centuries (Haag and Kaupenjohann, 2001, Breemen *et al.*, 2002). Agriculture has significant impacts on nitrogen cycling; the addition of fertilisers increases the N nutrient pool, tillage breaks up soil aggregates speeding decomposition, and irrigation can speed the anaerobic process of denitrification, producing increased N_2O and N_2 (Cherubini *et al.*, 2009; Del Grosso, 2008).

C and N are coupled in organic systems, and hence N cycling will also be affected by changes to soil C associated with land-use change for perennial energy crops (Ball *et al.*, 1999; Li *et al.*, 2008). The form of organic matter inputs to soil is significant since decomposition and mineralisation rates are affected by factors such as lignin content and C:N ratio (Del Grosso *et al.*, 2008; Parton *et al.*, 2010; Porporato *et al.*, 2003). High C:N inputs to soil increase microbial immobilisation of soil N, thus reducing availability for plant uptake and gaseous losses (Delgado *et al.*, 2010). Mineralisation is the reverse process, increasing soil N availability, and may be stimulated by inputs of residues with low C:N ratios, or by decomposition losses of C following tillage (Curley *et al.*, 2009). *Miscanthus* has been shown to increase the proportion of insoluble C in SOM and due to translocation of N prior to senescence, organic matter in *Miscanthus* leaf litter has a high C:N ratio reducing rates of microbial decomposition of SOM (Foereid *et al.*, 2004; Heaton *et al.*, 2010). Organic matter inputs to soil from SRC willow also have low N content, due to high C:N ratio of both leaf litter and root inputs (Jug *et al.*, 1999). Given that crop inputs with high C:N will encourage N immobilisation, and the NT system means no tillage associated decomposition and mineralisation, soil N availability may be relatively low under these perennial energy crops.

Soil N_2O emissions vary according to rates of nitrification and denitrification, and rates of diffusion out of soil, which affect whether N_2O is consumed by further reactions (Del Grosso *et al.*, 2000; Li *et al.*, 2005b). Nitrification and denitrification can occur concurrently, in aerobic and anaerobic soil pores respectively (Boyer *et al.*, 2006; Chen *et al.*, 2008). Kavdir et al (2008) explain that soil texture and drainage of soils are important controls of soil pore water and oxygen status, which affects N cycling. For example fine grained soils with many capillary pores to retain moisture are more prone to anaerobic conditions favouring denitrification, whilst well drained soils with low

bulk density favour nitrification. Between 35–60% water filled pore space (WFPS) nitrification is dominant, whereas above 70% WFPS denitrification is the only source of N_2O (Bateman and Baggs, 2005). Linn and Doran (1984) suggest that N_2O emissions are highest around 60% WFPS; at lower levels denitrification is less common, and at higher levels completion of reactions to produce N_2 is more likely. Aerobic denitrification has been theorised at 20% WFPS by some genera of bacteria capable of aerobic N respiration (Bateman and Baggs, 2005).

N_2O emissions response to changes in soil water and nutrient inputs is dependent on whether nitrification or denitrification is dominant. For example, if nitrification is dominant, emissions will decrease with increasing soil water content, due to reduction in aerobic processes and increased leaching, whereas if denitrification was dominant emissions would be likely to increase (2008). Since nitrification acts primarily on ammonium, whilst denitrification acts on nitrates; saturation of soil causes a greater increase in emissions from nitrate based than ammonium based fertiliser (Keoleian and Volk, 2005). Differences in soil texture and drainage between sites can be used to explain observed differences in rates of nitrification and denitrification, and how these processes respond to changes in management. However due to complexity of soil structural changes controlling WFPS and nonlinearity of denitrification and N_2O emissions response to changes in WFPS, N_2O emissions response to change in land use and management can be difficult to predict.

As well as water filled pore space (WFPS), nitrification and denitrification are controlled by: diffusion and temperature, which control microbial activity and diffusion of products from soil (Chatskikh *et al.*, 2005; Müller *et al.*, 1997) as well as pH (Li *et al.*, 2005a), labile C and inorganic nitrogen available to microbial biomass (Davidson *et al.*, 1998; Li *et al.*, 2005a; Müller *et al.*, 1997; Parton *et al.*, 2010; Verchot *et al.*, 2006). These variables interact, for example microbial decomposition of C and N consumes soil pore oxygen (Boyer *et al.*, 2006).

1.4.2.1 Spatiotemporal variation

Controls on N cycling vary at field scale, particularly with factors affecting water movement such as topography and soil texture and compaction. As a result, nitrification and denitrification processes and associated emissions are highly spatially variable (Boyer *et al.*, 2006; Li *et al.*, 2005a). Processes also have significant temporal variation with ambient temperature change, soil

disturbance, inputs of water and movement through soil, and nutrient input or uptake events (Beheydt *et al.*, 2007; Grant *et al.*, 2006). Jarecki *et al.* (2008) identified a pattern of significant spatial and temporal variation in N_2O throughout the literature, with emissions varying by 3 orders of magnitude over a period of days, and greater than 100% variation in coefficients of spatial variation. Heide *et al.* (2010) suggest that this may partially be explained by "hot-spots" of denitrification related to non-homogenous distribution of soil C and N and microbial biomass although at some sites, (e.g. Hellebrand, 2008) hot-spots may only occur with additions of N fertiliser.

Some existing studies on energy crops, which will be discussed in Section 1.4.2.5, measure N_2O emissions from field trials; however spatiotemporal variation in emissions must be taken into account when interpreting these data.

1.4.2.2 N_2:N_2O

N_2O is an intermediate product of the denitrification process, with N_2 as the final product, hence factors controlling the N_2:N_2O ratio of gaseous losses from soil will have a significant impact on GHG emissions (Basset-Mens *et al.*, 2006; Groffman *et al.*, 2000a; Kramer, 2006). N_2:N_2O ratio varies with soil type and changes in WFPS, temperature, pH, and C and N composition; further study is needed to improve understanding of the influence and interaction of these variables (Frolking *et al.*, 1998; K. L. Weier, 1993). Del Grosso *et al.* (2000) note that ratio is even less predictable in disturbed soils due to changes in diffusivity and disruption of pore connectivity.

Heide *et al.* (2010) state that increased residence time allows increased production of N_2O in groundwater, but also results in more N_2O being fully reduced to N_2. Soil type and structure control diffusivity of gases in and out of soil; affecting both amount of N_2O lost before completion of denitrification, and the amount of O_2 entering soil, creating conditions unsuitable for denitrification. N_2:N_2O is reduced by low pH and high O_2 which reduce completion of denitrification to N_2, since the enzymes which reduce N_2O are denatured (Groffman *et al.*, 2000a). Likewise NO_3 acts as an electrons accepter and thus can inhibit completion of denitrification at high concentration (Weier, 1993). Conversely high denitrification rates and low NO_3 create high demand for electron acceptors, increasing rates of N_2O reduction, leading to increased N_2:N_2O

(Groffman *et al.*, 2000a). Stratification of SOM under NT systems means that soil N may be concentrated near the surface, and thus more easily lost, meaning denitrification reactions are less likely to complete to N_2, increasing the relative proportion emitted as N_2O (Soane *et al.*, 2012).

N_2:N_2O ratio is difficult to predict under tilled or NT conditions, hence it is uncertain what the impacts of land use change for perennial energy crops might be. High denitrification rates under NT combined with, low NO_3 due to low inputs and tendency towards immobilisation as opposed to mineralisation could act to increase N_2:N_2O ratio. However lack of mixing will mean available N is concentrated near surface so the intermediate products of denitrification are more easily lost. Soil structural changes immediately following tillage will act to increase diffusivity of intermediate products from soil, whereas soil structure develops over time under NT, which may result in faster diffusion from soil through macropores.

1.4.2.3 Impacts of change in tillage

Impacts of change in tillage regime on N_2O emissions may be highly significant; Li, *et al.* (2005a) found that the GWP of N_2O emissions following reduction in tillage offset the benefits of increased soil C storage by 75-310%. This response of C and N cycling to land use change is complex; further studies found a decrease in N_2O emissions with no till practice (Del Grosso *et al.*, 2008; Kavdir *et al.*, 2008; Regina and Alakukku, 2010). Changes in N_2O with tillage are not well understood or quantified, however, variables identified as affecting response include; previous land use and associated C and N accumulation, amount and type of fertiliser inputs (Hellebrand *et al.*, 2008; Novoa and Tejeda, 2006), soil type (Rochette *et al.*, 2008), humidity (Regina and Alakukku, 2010), soil moisture, climate, soil physical properties and topography (Li *et al.*, 2005a).

Higher field emissions of N_2O from tilled soil have been attributed to higher levels of available N: since tillage aerates soil and redistributes surface residues to more microbially active layers, decomposition and mineralisation of N within soil are increased (Almaraz *et al.*, 2009; Del Grosso *et al.*, 2008; Metay *et al.*, 2007). Tillage also breaks down aggregates, making organic matter more physically available for decomposition (Drury *et al.*, 2004). Emissions may be reduced under NT due to the cooling effect of surface residues, since lower temperatures may mean slower rates of

microbial processes (Kaharabata *et al.*, 2003). Residues also protect soil from aggregate breakdown by precipitation, erosion, surface crusting and splash infilling of macropores (Bradford and Huang, 1994).

Observed increases in N_2O emissions under NT have been attributed to the increase in soil C over time under NT, which may stimulate microbial activity and release of N_2O. This may be offset by a reduction in soil loss, meaning a decrease in indirect emissions from eroded soils (Ball *et al.*, 1999; Li *et al.*, 2005a). Elsewhere, studies have posited an increase in rates of denitrification under NT due to structural changes to the soil increasing rates of denitrification (Heinen, 2006; Soane *et al.*, 2012).

Tillage increases porosity over the affected depth, whilst compaction from precipitation, freeze-thaw settling, or traffic may reduce porosity; severity of compaction may increase at higher organic matter content, and inter-aggregate pores are more easily lost than textural pores (Alletto and Coquet, 2009; Balland *et al.*, 2008). As a result, porosity tends to be lower for NT soil, and may decrease over time under NT (Bateman and Baggs, 2005).

Decrease in porosity, produces increase in the percentage of water filled pore space (WFPS) and reduction in drainage, leading to reduced O_2 diffusivity, and increased tendency for anoxic conditions, increasing rates of denitrification, whilst decreasing rates of nitrification (Ball *et al.*, 1999; Hellebrand *et al.*, 2008; Regina and Alakukku, 2010; Rochette *et al.*, 2008; Six *et al.*, 2004). As such, a review of published studies by Rochette (2008) identified that the increase in rate of denitrification under NT commonly occurred in poorly drained soils, whilst well drained soils experienced decreased rates of nitrification, or no change to soil pore water contents. Soil porosity changes due to tillage regime may be less important for soils with good drainage or high evaporation from surface layers (Metay *et al.*, 2007). Where change to NT increases N_2O emissions, store exhaustion may occur, causing a later drop in emissions, as observed by Six *et al.* (2004) for humid climates after 20 years of NT.

Structural changes to macroporosity and organic structure may also be significant. Macropore connectivity affects flow of water through soil, impacting both on leaching (affected by flow rate and contact with soil matrix N) and soil pore water: vertical channels are particularly important

(Logsdon, 1995). Macropore connectivity is disrupted by tillage, and builds over time with root channels, and vertical fracturing or burrowing (Jarvis, 2007; Soane *et al.*, 2012). Disruption of these pores also affects rates of gaseous losses from soil, thus impacting N_2:N_2O ratio as described above (Section 1.4.2.2) (Del Grosso *et al.*, 2000). Organic matter also contributes to structure, and correlates with porosity, SWC, soil water retention and aggregate stability (Azooz and Arshad, 1996; Gupta, 1991; Gupta and Larson, 1979; Rawls *et al.*, 2003; Six *et al.*, 2000). Increase, or stratification of soil carbon under no till will therefore affect soil water profile, and anoxic conditions may increase near the surface where SOM is concentrated (Yang *et al.*, 2008). Since gases produced in surface layers have less distance to escape, this may increase N_2O emitted. Aggregate size is also a control; when structural pores have low WFPS, aggregates may still contain anaerobic zones favourable for denitrification; in contrast under anoxic conditions, aggregate size has been found to correlate negatively with N_2O and CO_2 emissions (Drury *et al.*, 2004; Parkin and Tiedje, 1984; Uchida *et al.*, 2008).

Changes to tillage regime will affect porosity and pore connectivity of soil, however the impacts on WFPS and rates of N_2O production will be dependent on soil texture and drainage, form and availability of N and C:N ratio of inputs to soil. Understanding and prediction of these impacts is hampered by an incomplete understanding of processes and their interactions.

1.4.2.4 Nutrient requirements of willow and *Miscanthus*

Both SRC willow (Adegbidi *et al.*, 2001) and *Miscanthus* (Cadoux *et al.*, 2012) are often described as having high nutrient use efficiency (NUE) compared to arable crops, however Jørgensen and Schelde (2001) note that NUE data for energy crops is often calculated as dry yield/nutrient content. Although this is useful to calculate ash and emissions likely to be produced at combustion, it is not informative in terms of input requirements unless crop uptake efficiency is also considered along with below ground crop N storage, and any symbiotic N fixation relationships (Cadoux *et al.*, 2012; Jørgensen and Schelde, 2001). NUE assessment tends not to consider internal nutrient requirement of crops, as this is harder to assess (Adegbidi *et al.*, 2001). Broad distinctions can be made, for example C4 photosynthesis is more nitrogen efficient than C3, and so *Miscanthus*, a C4 perennial plant is likely to make very efficient use of nitrogen and thus require less artificial inputs (Curley *et al.*, 2009).

NUE is increased by delaying harvest to winter, to allow recycling of nutrients by translocation from stems and branches into the rhizome for *Miscanthus* (Beale and Long, 1997; Heaton *et al.*, 2009) and in the case of SRC willow to roots in winter (Bollmark, 1999) and back to new growth in spring (Jug *et al.*, 1999; Shibu *et al.*, 2012). Nutrients remaining in leaves are returned to the soil at senescence; in the case of SRC willow, this can provide up to two thirds of nutrient requirements for the following year (Keoleian and Volk, 2005).

Several studies have identified N fixing communities associated with *Miscanthus* roots (Davis *et al.*, 2010; Eckert, 2001; Keymer and Kent, 2013). A review by Cadoux (2012) suggested the need for proof the crop is able to use this N; this appears to have been resolved by N isotope dilution studies by (Keymer and Kent, 2013). Furthermore Davis (2010) and Gopalakrishnan (2012) required an assumption of symbiotic N fixation to explain observed nutrient balance and crop yield for *Miscanthus* modelling, suggesting fixed N is available to the crop. There is evidence of symbiotic N fixation for SRC willow also (e.g.Doty, 2009) in the form of association with diazotrophic endophytic bacteria, which they use to explain survival in N poor environments. However Knoth (2012) state that cultivated energy crops may not display the same relationships, and Moukoumi *et al.* (2012) found improved yield for intercropping of SRC willow with Caragana species in which N fixation takes place within root nodules, and is therefore less sensitive to the disruptions of commercial farming. Further nutrient support comes from mycorrhizae communities, which thrive under the NT system required for perennials and provide N and P to the roots of both SRC willow and *Miscanthus* in exchange for C (An *et al.*, 2008; Rooney *et al.*, 2009).

It has been postulated that extensive deep rooting systems, enable high efficiency of nutrient uptake, reducing the proportion of inputs lost from the crop soil system (Hellebrand, 2005; Keoleian and Volk, 2005; Rowe *et al.*, 2009). However experiments at Rothamsted have observed very low uptake of fertiliser applied to one year old *Miscanthus*; 60 kg N ha^{-1} labelled fertiliser was applied as NH_4 and NO_3, of this 22% was retained in soil, 38% was taken up and 40% was lost from the crop soil system (Christian, 1997). Losses were reduced to 16-24% with increased crop uptake in years two and three ; these values are proportional to those for arable crops, but due to lower inputs, absolute values of N loss would be reduced (Christian *et al.*, 2006). It has been postulated that lower than expected N uptake efficiency may reflect a delayed root emergence, which takes place one month after shoot emergence, meaning N uptake only occurs for around six months

(compared to around nine months for some cereals), and timing of applications should be delayed (Christian *et al.*, 2006; Christian *et al.*, 2008).

Cycling and fixation of N should reduce input requirements of SRC willow and *Miscanthus*, and numerous field studies have identified no significant yield response to fertiliser in *Miscanthus* (e.g. Beale and Long, 1997; Christian and Riche, 1998; Culman *et al.*, 2010; Heaton *et al.*, 2010). However yield dependence on N inputs is recorded at some sites e.g. (Danalatos *et al.*, 2007; Lewandowski and Schmidt, 2006). *Miscanthus* response to N inputs varies with genotype and site (Karp and Shield, 2008), hence intermittent test applications of fertiliser at commercial plots have been recommended to identify where yield may be N limited (Christian *et al.*, 2008), although some studies suggest that energy ratio and system efficiency may be maximised at little or no N input (Danalatos *et al.*, 2007; Lewandowski and Schmidt, 2006). A reduction in soil N of 150 kg N ha^{-1} was recorded over the first 150 cm soil depth, during a three year period including rhizome establishment for a *Miscanthus* field trial in France indicating risk of N depletion for some sites where plant requirements are met from soil alone (Dufossé *et al.*, 2012). In 2001, Defra recommended inputs of 88 kg N $ha^{-1}a^{-1}$ in the UK (Nixon P, 2001), but their 2007 (Department for Environment Food and Rural Affairs, 2007) handbook does not give a recommended application rate, and cites the lack of yield response observed by Christian *et al.* (2008).

For SRC willow cultivation, Jug *et al.* (1999) found SRC willow to require N inputs for good yield, and several studies have found yield improvements with fertiliser input to SRC willow. Lack of agreement on recommended inputs may indicate site variation in needs (H. G. Adegbidi *et al.*, 2001). Recommended average application rates vary between countries, for example 70 kg N $ha^{-1}a^{-1}$ is recommended in Sweden (Boyd, 2000) and 100 kg N $ha^{-1}a^{-1}$ every 3 years for the US (Keoleian and Volk, 2005). In the UK recent field trials have achieved reasonable yield over short term with no applications (e.g. Aylott *et al.*, 2008), however best practice guidelines (Hilton, 2002) recommend a cycle of 40 (post coppice), 60, 100 kg N $ha^{-1}a^{-1}$, and (Bullard *et al.*, 2002) note that commercial low input, low management approaches often produce yields below the economically viable threshold. These values can be considered low, compared to the maximum allowable rate of 250 kg N $ha^{-1}a^{-1}$ in the UK.

UK field trials tend not to apply N fertiliser for SRC willow or *Miscanthus*, however researchers at Rothamsted (personal communication) have observed store depletion in later years with no nutrient input at former arable sites, although former grass sites remain N rich. It has been

suggested that nutrient inputs may be necessary to avoid depletion, but should not exceed removal at harvest, which for *Miscanthus* is around 4.9 g kg^{-1} of N, 0.45 g kg^{-1} P and 7.0 g kg^{-1} of K, although these values will vary with yield (Cadoux *et al.*, 2012). Removal is generally below average atmospheric deposition rates for Europe (Don *et al.*, 2012) hence depletion may not be seen without N inputs, even after 14 years of growth (Christian *et al.*, 2008). For SRC willow, N removal at harvest is seen to vary with nutrient input levels, in the range of 29-47% of inputs (Jug *et al.*, 1999). Lower agrochemical requirements, combined with high efficiency of uptake and low levels of N in harvested biomass give perennial energy crops potential to reduce N_2O emissions compared to annual crops, although where N inputs are required there may be significant impacts (Cherubini *et al.*, 2009).

1.4.2.5 Observed N_2O emissions for willow and *Miscanthus*

Field studies on perennial energy crops often do not measure emissions of N_2O (e.g. Christian *et al.*, 2008; Christian and Riche, 1998; Dondini *et al.*, 2009; Heaton, 2004; Price *et al.*, 2004) perhaps in part due to issues of high spatiotemporal variation. Given the expectation of low N inputs, low N_2O emissions may be expected and a reduction in N_2O emissions compared to arable is generally postulated (Kavdir *et al.*, 2008; Powlson *et al.*, 2005; Rowe *et al.*, 2009). Since N cycling is highly complex, further consideration and field observation is warranted.

In a review of studies by Don *et al.* (2012) total N_2O emissions and emissions as a proportion of N inputs (emissions factor (EF)) were lower for SRC willow and *Miscanthus* when compared to annuals, with the exception of a one year study (Jørgensen, 1997) comparing *Miscanthus* and rye, in which emissions were similar without fertiliser, and EF for *Miscanthus* was three times that of rye. Additionally Kavdir *et al.* (2008) found higher emissions for SRC willow than for a rotation of annuals (rape/rye/triticale) where fertiliser was not applied to the perennials or the annuals . It is significant that these experimental conditions do not reflect conventional farming approaches, i.e. that annuals usually receive higher fertiliser applications than perennials. A study by Drewer *et al.* (2012) on loam over clay recorded much higher N_2O emissions for wheat and OSR compared to *Miscanthus* and SRC willow, which they attribute largely to differences in fertiliser regime, and state that *Miscanthus* only reduces N_2O if little or no fertiliser is applied. Christian *et al.* (2008) note that fertiliser inputs may be required to maintain yields on nutrient poor soils, and that warm moist soils may experience enhanced denitrification, hence a significant proportion of

observed losses of 16- 40% of N fertiliser inputs to *Miscanthus* plots in Christian *et al.* (1997) and (2006) may have been in the form of N_2O emissions.

Hellebrand *et al.* (2008; 2005) and Kavdir *et al.* (2008) suggest that their finding of an EF for perennials to be around half that for annual crops is a result of the impacts of NT, whilst Don *et al.* (2012) attribute this difference to more efficient nutrient uptake by perennials. Drewer *et al.* (2012) observed similar rates of denitrification in response to fertiliser inputs for *Miscanthus* and OSR, however gaseous losses for the *Miscanthus* field had a higher N_2:N_2O ratio, which may reflect higher pH or lower diffusivity due to the NT system. Hellebrand *et al.* (2010) record higher WFPS for SRC willow (38.4%) than annual crops (35.4%); since nitrification is dominant under these conditions, lower oxygen availability under SRC willow may reduce rates of N_2O production. Jørgensen *et al.* (1997) suggest that low emissions for their study were due to low precipitation and sandy soil; their finding of higher N_2O emissions for *Miscanthus* is therefore attributed to NT soil structure and residues increasing WFPS and associated levels of denitrification; emissions were higher from *Miscanthus* than rye, in spite of lower fertiliser inputs.

A range of modelling approaches have identified lower N_2O emissions for perennial energy crops e.g. (Davis *et al.*, 2010; Hamelin *et al.*, 2012; Tonini *et al.*, 2012). Using the IPCC methodology Tonini *et al.* (2012) calculate N_2O emissions of 5.8 kg N ha^{-1} a^{-1} for Rye, 2.3 kg N ha^{-1} a^{-1} for SRC willow and 2.0 kg N ha^{-1} a^{-1} for *Miscanthus* according to assumed levels of of fertiliser input. Calculations elsewhere identified almost twice the N_2O emissions associated with leaf litter compared to direct fertiliser inputs for Willow with 100 kg N ha^{-1} ammonium sulfate added every three years (Keoleian and Volk, 2005). Modelling by Dufossé *et al.*, (2012) of *Miscanthus* cultivation over a 20,000 km^2 region of France identified that N_2O from *Miscanthus* could contribute an average of 13-8.8 kg ha^{-1} CO_2 equivalent per ha per year, depending on estimation methods, with significant spatial variation in both yield and N_2O emissions according to soil type; the resultant variation in N_2O emissions per unit energy contributes to relative benefits of bioenergy. For land use change, existing N_2O emissions should also be considered; for arable usage of the same area, simulated emissions varied from 93 to 1744 kg ha^{-1} a^{-1} CO_2 equivalents due to site factors (Dufossé *et al.*, 2012), meaning that spatial variation in potential emissions reduction is of even greater significance.

Prior to establishment of perennial energy crops, soils are often left fallow over winter, leaving them vulnerable to erosion and leaching, then tilled for planting in Spring, causing significant mineralisation loss of N from soil in the case of former grassland or otherwise undisturbed soil (Christian and Riche, 1998; Jug *et al.*, 1999). Losses due to mineralisation from soil disturbance accounted for 24.7Gg of the 78.4Gg of UK soil N emissions in 1990 (Brown *et al.*, 2002; Curley *et al.*, 2009). A further important consideration which has not been well assessed is the risk of high emissions following an N pulse on ploughing in of the significant N storage in *Miscanthus* roots and rhizomes at the end of the crop lifecycle (Christian *et al.*, 2006).

In general, N_2O emissions losses appear to be lower for SRC willow and *Miscanthus* than for arable crops to which they have been compared. However there is variation with site factors and N fertiliser inputs, and emission during site preparation and crop removal must be included in assessments. Comparisons are rarely made for grazed lands; emissions from these relate to compaction of soil by trampling of livestock and N inputs in manure and urine, leading to emissions (Mosier, 1998).

Variation in change in N_2O emissions between sites according to current land usage, as well as site and land management factors will affect the relative benefits of bioenergy cultivation.

1.4.2.6 Leaching

Leaching losses are expected to be lower for *Miscanthus* and SRC willow compared to annuals, due to low N inputs and efficient uptake (Curley *et al.*, 2009; Powlson *et al.*, 2005). The IPCC emission factor (EF) for leached N is twice that for applied N, hence indirect emissions of N_2O must be regarded a key component of the GHG balance (Groffman *et al.*, 2000b; Nevison, 2000). Leaching also has ecological implications, polluting river systems and coastal waters, causing eutrophication (Brown *et al.*, 2002; Kramer, 2006).

Haag and Kaupenjohann (2001) state that at a watershed scale, most applied N is retained, and often stored for decades, whilst Breemen *et al*. (2002) suggest retention can last from decades to centuries. This may explain why leaching can be traced to historic land management Koh *et al*.

(2010). Land use change may encourage either release or accumulation of N in catchment stores, making them a significant area for research. Differences between inputs and outputs in N budget calculation are often attributed to retention (Alexander, 2002), however other factors should be considered first (Galloway 1995). For example N budgets often overlook dissolved organic nitrate (DON) which contributes around 20% N leaching (van Kessel *et al.*, 2009), as well as emissions from shallow aquifers (Heide *et al.*, 2009) and flow interaction between surface and subsurface water systems (Baresel and Destouni, 2006) both of which remain poorly understood

The IPCC standard methodology used for governmental calculations assumes that 30% of fertiliser input is leached; calculations by Tonini *et al.* (2012) gave values of around 74 kg N ha^{-1} a^{-1} for Rye, 10 kg N ha^{-1} a^{-1} for SRC willow and 10 kg N ha^{-1} a^{-1} for *Miscanthus*, although these are dependent on assumptions about fertiliser application rate. The ultimate fate of N from fertiliser is poorly understood in agricultural studies, and use of a default value for leaching rates may compound inaccuracies (Nevison, 2000; Van Breemen *et al.*, 2002). Variation in leaching rates is significant; an analysis of 16 US catchments by Breemen *et al.* (2002) found that 20-60% N inputs were lost as leached N, whilst Meisinger and Delgado (2002) suggested a value of 10-30% leaching for grain systems. A review by Alexander *et al.* (2002) of several catchment studies suggested that predictions of fluvial N export could be improved by mapping patterns of variation in processes controlling Nitrogen cycling. Other crucial factors include timing and amount of fertiliser application, nitrates applied faster than they can be used by plants will remain in soil and can be easily leached in the event of rain (Christian and Riche, 1998). Precipitation and soil structure and drainage are also important controls, since good drainage and increased precipitation increase leaching and decrease in-field N_2O losses (Basset-Mens *et al.*, 2006; Christian and Riche, 1998; Hutchins *et al.*, 2010).

Mineralisation due to over-winter fallow and tillage pre-planting can leave soils rich in available N, leading to higher leaching during the first year of establishment; SRC willow leaching has been recorded at levels comparable with maximum values for arable crops (Mortensen, 1998), and *Miscanthus* leaching at significantly higher levels (Christian and Riche, 1998). Reduced mineralisation under the NT system may mean lower levels of available soil N in subsequent years, and thus leaching is often much below that seen for annuals (Jørgensen and Schelde, 2001). Soil type affects pattern of nutrient loss during establishment; Mortensen (1998) found that leaching was reduced in year 2 for coarse sand and year three for loamy sand. Structural changes which develop in soil under NT systems may increase bypass flow, which avoids contact with N

stored in the soil matrix, thus reducing concentration of N in percolating water (Soane *et al.*, 2012).

Energy crops such as SRC willow with high uptake have been recommended as riparian buffers to protect water quality by uptake of nutrients in throughflow (Delgado *et al.*, 2010; Elowson, 1999; Jørgensen and Schelde, 2001). Growing season is a significant factor; Lesur *et al.* (2013) suggest that N uptake in autumn by perennial energy crops can reduce leaching in response to high rainfall inputs in autumn and winter, whereas Christian *et al.* (2008) note that *Miscanthus* root activity is delayed by a month compared to shoot activity, and suggest that period of root uptake is shorter than for arable crops. The year round cover provided by perennials also reduces soil and N losses from surface runoff (Jørgensen and Schelde, 2001).

Measurements by Behnke *et al.* (2012) show leaching of 8 kg N ha^{-1} a^{-1} for *Miscanthus* with no fertiliser input, and 28 kg N ha^{-1} a^{-1} leaching with 120 kg N ha^{-1} a^{-1} fertiliser input. Even at slurry application rates of 180 kg N ha^{-1} a^{-1} *Miscanthus* N levels remain within safe drinking water limits, and at similar levels to annuals (Curley *et al.*, 2009). A study in Denmark (Mortensen, 1998) found increased leaching with N input during the first year of SRC willow, but thereafter 75 kg N ha^{-1} a^{-1} was added without increased leaching and values around 10 kg N ha^{-1} a^{-1} were recorded, comparable with other studies. It is therefore likely that land use change to perennial energy crops could reduce N leaching compared to annual arable crops, although soil N and amount and timing of any fertiliser inputs will affect the overall outcome.

1.4.3 Water cycling

Due to high production, perennial crops such as *Miscanthus* may have high water requirements compared per hectare to annual crops which may be used for energy such as maize, although given a lower energy yield per ha for maize, this does not indicate a better energy return on water invested for annuals (Vanloocke *et al.*, 2010). *Miscanthus* also has higher water usage per MJ compared to fossil fuel generation, for which the water requirements are largely non consumptive (Mulder *et al.*, 2010). Since energy crops are not for consumption, different management standards are applied, and there is potential to use wastewater for irrigation, reducing demand

for freshwater, fertilizing crops and treating the wastewater at the same time, although this may increase contaminants on combustion (Paine *et al.*, 1996).

Without irrigation or high precipitation, high water use of perennial energy crops can reduce both soil and groundwater storage; the water resources and environmental impacts of this depend upon the previous hydrological regime (Jørgensen and Schelde, 2001). As well as land availability, water resources may be a limiting factor in many areas, so water use efficiency is an additional limiting factor on bioenergy (de Fraiture *et al.*, 2008; Mulder *et al.*, 2010). The change in water usage with cultivation of perennial energy crops is dependent on previous land use, new crop species, amount of rainfall and hydraulic properties of soil (Finch *et al.*, 2004). Key factors controlling evapotranspiration (ET) are: growing season (which dictates the timing of water usage and interception (Goodrich *et al.*, 2000; McKendry, 2002; Vanloocke *et al.*, 2010)); rooting depth (deeper roots may enable water access during shortages (Finch *et al.*, 2004)); and photosynthesis type (C4 plants have double the water use efficiency of plants using C3 photosynthesis (Smeets *et al.*, 2009)).

Although *Miscanthus* uses efficient C4 photosynthesis, other variables may lead to higher ET than a C3 annual at some sites (McKendry, 2002; Smeets *et al.*, 2009). High productivity increases transpiration and longer ground coverage increases evaporation due to interception (Berndes, 2002; Finch *et al.*, 2004; McKendry, 2002a). Finch *et al.* (2004) speculate that *Miscanthus* may require less water than annuals but suggest that more data are needed to confirm this.

If SRC willow has access to water, usage is likely to exceed that of annuals, whilst if access to water is limited, growth will be restricted (Finch *et al.*, 2004). Water use is lowest in the year following coppicing, increasing to year three of the cycle when stems are harvested (Borek R, 2010).

Miscanthus growing season varies with species and climate factors; studies in the Midwest US recorded longer growing season and greater associated ET than arables (Gerbens-Leenes *et al.*, 2009; Vanloocke *et al.*, 2010). Growing season may also be limited by water availability, which will also result in restricted yield (Richter *et al.*, 2008). Depending on depth to water table, deep roots of SRC willow and *Miscanthus* may have access to groundwater, meaning that evapotranspiration

is not limited by recent precipitation, reducing water limitation on growth, but increasing risk of groundwater depletion (Don *et al.*, 2012; Finch *et al.*, 2004). Where these crops are grown as a riparian buffer access to groundwater is good, but impacts on stream flow may be more severe (Goodrich *et al.*, 2000). ET will also vary for annual arable crops, according to species, site factors and management choices which affect growing season, yield and water use efficiency. As a result of these factors, the difference in ET between annuals and perennials may vary considerably between sites (Berndes, 2002).

Increased water use has environmental impacts including; increased depth to water table, shrinking lakes, rivers with reduced flows (also leading to reduced flushing of coastal ecosystems and reduced flooding) altered sedimentation patterns, and unspecified impacts on fisheries and biodiversity (de Fraiture and Berndes, 2008; de Fraiture and Berndes, 2009; Vanloocke *et al.*, 2010). Reduction in effective rainfall may be detrimental to water resources in some locations, or may reduce flood risk in others (Rowe *et al.*, 2009). In order to reduce transport, perennial energy crops may be planted heavily in regions around power plants, meaning the reduction in available water would be concentrated in these areas (de Fraiture *et al.*, 2008; Vanloocke *et al.*, 2010).

Increasing proportions of bioenergy with higher water usage per hectare than annuals and per MJ than fossil fuel generation will increase pressure on water resources, which may create competition for water between energy and food (Gerbens-Leenes *et al.*, 2009; Hoogeveen *et al.*, 2009; Mulder *et al.*, 2010). Concentrated planting of perennials in areas around power plants to minimise transportation may cause significant regional impacts and exacerbate local water shortages (de Fraiture *et al.*, 2008; Mulder *et al.*, 2010). These issues would likely be greatest in countries with growing populations and increasing demand for food and energy (Hoogeveen *et al.*, 2009). In China, competition for water with increases in energy crop cultivation was blamed for rising food prices, and this has led to downscaling of plans for bioenergy (de Fraiture *et al.*, 2008). Pressure on water resources may be compounded by population increases, as well as increasing demand for meat, and associated cultivation of feed (de Fraiture and Berndes, 2008; Hoogeveen *et al.*, 2009; Mulder *et al.*, 2010).

1.5 Need for this study

As discussed in Section 1.2, research suggests that energy generation from perennial crops often performs better than biofuel from annuals in terms of energy return on energy invested (Cherubini *et al.*, 2009; Rowe *et al.*, 2009), energy return per ha (de Vries *et al.*, 2010; McKendry, 2002b), and greenhouse gas emissions associated with cultivation and processing (Powlson *et al.*, 2005; Rowe *et al.*, 2009). However biofuels make up 70% of bioenergy in Europe (Don *et al.*, 2012) due in part to the greater convenience of fit with the existing energy use and distribution systems; bioethanol can be mixed into gasoline up to 10% without requirement for engine modifications or additional infrastructure for transport, storage etc. (Sims *et al.*, 2006).

By contrast perennial biomass feedstock does not fit easily into the large scale electricity generation system currently operating in England; biomass is a distributed feedstock with a low energy density, hence it is necessary to minimise transport distance and associated costs and emissions (Powlson *et al.*, 2005). As will be argued in Section 2.3, it is therefore useful to assess existing potential energy end uses for this feedstock in England within the current system of supply and demand.

Previous assessments of Biomass feedstock energy end uses have looked at potential demand for CHP for district heating in the UK (Jablonski *et al.*, 2008), Denmark (Möller and Lund, 2010) and Austria (Schmidt *et al.*, 2010). Schmidt *et al.* (2010) integrate data on potential supply from forestry according to region to make some assessment of the capacity to meet demand. Relationships between supply and demand have been assessed in detail for a UK co-firing power plant by mapping potential yield and production costs to create a supply curve for Drax (Bauen *et al.*, 2010). This study aims to extend these approaches to the national scale for England, using spatial relationships between potential supply and demand, to identify locations where perennial energy crops could usefully be grown, and the energetic magnitude and land use requirements of potential generation.

More recently, work by Wang *et al.* (2014) in a Global Change Biology special issue matched spatial data on potential supply of feedstock crops to spatial data on space-heating demands (domestic plus nondomestic as calculated in the “Disaggregated Scenarios for Demand Studies”

project (DS4DS, 2013)) and applied an optimisation model to identify locations and capacities of generation. The research presented here differs in mapping point demands for heat, including industrial process heat and space heating. This simpler approach was selected based on the preference of generating companies for a single heat off-taker due to the complexity of contractual agreements (Bailey, 2011), and availability of data at the time the mapping exercise was performed. Potential demands for domestic space heating and co-firing with coal will be considered separately, due to specific socioeconomic issues which will be discussed in Sections 2.3.2 and 2.3.1 respectively.

Spatial studies modelling potential for perennial biomass crop cultivation in the UK tend to focus on yield, e.g. Hastings *et al.* (2014) compared simulated spatial variation in yields for a range of potential feedstocks. In dictating land area required for a given level of generation, variation in yield may be a key contributing factor to the extent of other impacts. However, spatial variation in impacts on changes in SOC and N_2O emissions, which contribute to GHG balance, must be considered, to identify contribution to emissions per unit energy. Due to impacts on yield, ET associated with perennial energy crops is often considered (e.g. Lindroth, 1994; Lindroth, 1999; Zeri *et al.*, 2013) and variation in *Miscanthus* yield with precipitation and soil available water capacity has been modelled for the UK (Richter *et al.*, 2008). Changes in ET due to land use change for perennials may deplete soil and groundwater reserves (Jørgensen and Schelde, 2001), and reduce streamflow (Goodrich *et al.*, 2000), with impacts varying between sites (Rowe *et al.*, 2009) which should also be taken into account.

It has been suggested that current SOC may be the most significant variable in dictating overall GHG balance of land use change for energy crops (Hillier *et al.*, 2009). Potential change in C storage is well studied; average values are available for a range of land use changes (e.g. Smith *et al.*, 2008) and IPCC guidelines are available for estimations (IPCC, 2003). Field values for change in soil carbon will vary with yield and associated C inputs to soil, and with temperature and other variables affecting the rate of C accumulation or loss (Lal, 2004). Studies often apply standardised values from databases, hence there is scope to consider spatial variation in changes in SOC, since where maximum values are achieved, this may control overall GHG balance (Keoleian and Volk, 2005).

There is less research on N_2O emissions for perennial energy crops due to low N input requirements, meaning emissions savings can be expected compared to annual crops. Field data generally uphold this expectation, although there are exceptions (e.g. Jørgensen, 1997), and there is concern about ploughing in of high N below ground crop biomass at end of lifecycle (Christian *et al.*, 2006). Change to NT system for conversion from arable to energy crops causes structural changes leading to increased N_2O emissions in poorly aerated soils where denitrification is dominant (Rochette, 2008); although this is likely to be offset by reduction in emissions associated with N fertiliser inputs (Don *et al.*, 2012), these structural changes may reduce the N_2O emissions savings at relevant sites.

Dufossé, *et al.* (2012) simulated direct N_2O emissions around 13 kg ha^{-1} a^{-1} CO_2 equivalent, with significant variation observed between sites, from around 0 to 272 kg ha^{-1} a^{-1} CO_2 equivalent according to soil type. Given that simulated emissions for an annual crop varied from around 93 to around 1744 kg ha^{-1} a^{-1} CO_2 equivalent for the same area, the potential reduction in direct N_2O emissions may make a significant contribution to overall GHG balance (Dufossé *et al.*, 2012). Assuming similar or greater spatial variation in current N_2O emissions from UK arable land, it is likely that current emissions level could be more significant than other factors in determining the change in N_2O emissions at a site following land use change; hence this is of particular importance.

Assessments of the impacts of perennial crop cultivation generally do not consider the impacts of site variation on change in N_2O emissions; field comparison of perennials and annuals is usually for an individual site (e.g. Hellebrand *et al.*, 2010; Jørgensen, 1997) whilst calculations often use generalised approaches such as IPCC EFs (e.g. Clair *et al.*, 2008), which do not account for site differences (Stehfest and Bouwman, 2006). As a result, understanding of spatial variation in N_2O emissions associated with land use change for perennial energy crops is incomplete, and there is scope for a study to simulate potential variation for sites in England where the crops could be cultivated. Due to the data requirements of process based models advocated by the IPCC Tier 3, it would be impractical to perform modelling for all potential sites, however, the application of such a model at a range of sites, combined with appropriate assessment of the findings, may improve current understanding of site specific factors controlling GHG impacts of land use change.

Policy should seek to maximise both efficiency of energy generation and GHG benefits of renewable energy. If the cultivation of these crops is to be encouraged, it is therefore important to fully assess GHG balance, and to consider spatial variation in change in emissions, as well as spatial and crop variation in energy yield per ha, which affects the land use requirements. Understanding of variation in benefits such as efficiency and emissions is crucial to inform policies which can affect the economics of choices about energy generation (Thomas *et al.*, 2013; Waller *et al.*, 2011).

The intention is to evaluate variation in the sustainability of land based renewable energy by looking at the impact of energy crops on both the host catchment and the wider environment. This will include study of water flows, nutrient cycling and leaching and GHG emissions. Nitrate leaching and N_2O loss both have serious environmental impacts, and both increase for managed land, so it will be worthwhile to study how these factors vary under different energy crops (Brown *et al.*, 2002; Kramer, 2006). Change in SOC storage is a major factor in controlling GHG balance, so this should also be assessed (Fargione *et al.*, 2008; Keoleian and Volk, 2005).

1.6 Aims

This research aims to assess the potential for land-based renewable energy in England, and simulate likely impacts at potential cultivation sites. Assessment of sustainability of perennial energy crop cultivation in Section 1.4 identified potentially significant impacts on soil carbon storage (Section 1.4.1), N_2O emissions (Section 1.4.2), leaching of nitrates and associated indirect N_2O emissions (Section 1.4.3) and hydrology (Section 1.4.4). Therefore this research seeks to take an approach which can simulate all of these impacts. It is also useful to simulate yield variation between sites, as it dictates economic viability and the land area required for a given amount of energy, as well as extent of competition with other land use.

To do this it is necessary to take a whole system approach, first looking at supply and demand of energy (heat and electricity), given the importance of minimising feedstock transport as introduced in Section 1.3, and then identifying impacts of land use change where cultivation could usefully take place. Lifecycle analysis of bioenergy often applies an assessment approach for the cultivation stage which does not take into account site specific factors affecting GHG emissions, water use and yield. This study does not aim to undertake complete lifecycle assessment of the

bioenergy systems considered, but the intention is that findings should be informative in terms of spatial variation in costs and benefits of bioenergy.

1.7 Objectives

In order to explore the potential for land-based renewable energy in England, and identify how the impacts of land use change might vary in terms of impact on N_2O emissions, soil C and ET, the following objectives will be set;

1. **Assess potential for willow and *Miscanthus* feedstock to be used for bioenergy at high efficiency within the existing energy system in England**
2. **Assess spatial relationships between potential supply and demand for the identified forms of biomass energy using GIS mapping techniques.**
   Based on data from Objective 2, locations where the crops could usefully be cultivated will be identified, and analysed to extract common combinations of site properties.
3. **Assess approaches for simulating perennial energy crop yield along with change in N_2O emissions, soil C and ET for land use change at these sites.**
   A model will be selected to apply to a range of "typical" sites based on common combinations of site variables identified following Objective 2.
4. **For simulated cultivation of *Miscanthus* and SRC willow, assess spatial variation in: yield; N_2O emissions; soil C storage; evapotranspiration.**
   This will be done for sites typical of those identified as suitable for energy crop cultivation following Objective 2, using the model selected following Objective 3. Findings will be analysed in terms of how spatial variation may affect the benefits of bioenergy.

1.8 Thesis structure

Chapters 2 to 5 outline the stages of the methodology;

Chapter 2 details the site identification approach, in which factors affecting potential for supply and demand of perennial biomass feedstock are used to identify possible cultivation sites. This chapter addresses Objective 1 through discussion of factors affecting potential biomass energy generation and identification of high efficiency potential feedstock end uses. To meet Objective 2,

a GIS mapping approach is applied to predict potential energy generation and locations of land use change under two policy scenarios for two identified end uses. Output from the mapping were used to identify “typical” sites of potential land use change, in terms of soil and climate properties which may affect response to land use change; tables of variables are included.

Chapter 3 discusses potential approaches to predicting how change in N_2O emissions and soil C, as well as crop yield and ET may vary between sites, outlining the potential for an agroecosystem modelling approach, and what the requirements of such a model might be, in order to meet Objective 3.

Chapters 4 and 5 outline the development and verification of the chosen model including description of improvements to process representation and remaining limitations of the model to enable Objective 4 to be met in Chapter 6. Chapter 6 details the process of running the model for the identified land use change scenarios.

Objective 4 is then addressed in Chapter 6 by a process of scenario development and analysis of model output. This chapter identifies some of the factors which may influence simulated spatial variation in the benefits of land use change for bioenergy, and looks at the extent of that variation. Finally Chapter 6 identifies limitations in the model which could be addressed in future research.

Chapter 7 highlights the main conclusions from the study, and how they address the objectives listed in Section 1.7. The key impacts of all cultivation to meet demand in an example location are calculated and contextualised, followed by a critical appraisal of the research project as a whole.

2. Site identification approach

This chapter describes the approach taken to identify sites where SRC willow or *Miscanthus* could usefully be grown for bioenergy generation. This chapter fulfils Objectives 1 and 2 as outlined in the introduction.

Biomass feedstock is bulky, and has low energy density compared to fossil fuels, meaning that it is necessary to minimise feedstock transport, making the spatial relationship between supply and demand important, as detailed in Section 2.1. This creates a need for localised supply chains, which are discussed in Section 2.2, and limits the scale of bioenergy generation, according to the amount of feedstock which can be cultivated within that localised area. Section 2.2 also introduces specific issues affecting the establishment of these supply chains.

As a distributed low energy density feedstock, biomass does not fit easily into the existing energy infrastructure in England of large scale, centralised generation of electricity with a national grid distribution system. It is therefore necessary to assess potential for SRC willow and *Miscanthus* feedstock to be used for bioenergy at high efficiency within the existing energy system in England, as was stated in Objective 1. Chapter 2 addresses this issue in Section 2.3 by identifying end uses for biomass feedstock which can be efficient at relatively small scales, requiring relatively little feedstock, compared to more typical large scale fossil fuel plants. Government incentives can significantly affect economics of different energy forms, so existing policy relating to these forms of generation is examined in Section 2.4 to consider issues of economic feasibility or risk.

Sections 2.5 through to 2.8 address Objective 2; to assess spatial relationships between potential supply and demand for the identified forms of biomass energy using Geographical Information System (GIS) mapping techniques by integrating data on these demand types with data on potential for supply and calculating local potential feedstock availability. Section 2.5 describes the approach used by Lovett *et al.* (2009) to rule out sites unsuitable for *Miscanthus* feedstock cultivation, and the calculation of predicted yields at remaining sites using the Richter *et al.* (2008) model. These spatially referenced values of potential yield for the locations where crops could be grown enable calculation of available feedstock to meet demand in later stages of the

methodology. Section 2.6 then discusses issues of policy relating to feedstock cultivation, in terms of how they may affect feedstock availability. Section 2.7 outlines the mapping approach by which data on supply and demand are integrated, and Section 2.8 details the mapping of locations with energy demands which could efficiently be met using bioenergy feedstocks, along with the hindcasting calculations to establish how much feedstock would be required to meet these energy demands. Section 2.9 then uses the data introduced in Section 2.5 to calculate the extent to which feedstock could be cultivated locally to meet the demands calculated in Section 2.8.

In addressing Objective 2, this chapter also makes broad calculations of theoretical potential for biomass energy generation in England, which are discussed in Section 2.9, and can be compared to government targets for bioenergy to assess how achievable they may be. Current land use for the locations where energy crops may be grown is significant, in terms of environmental impacts and impacts on food production, which are also considered in Section 2.9. This research considers England as opposed to the whole UK due to availability of appropriate data.

Output from the mapping was also used in Section 2.10 to collate site data for areas where perennial energy crops might be grown. These data were then analysed using cluster analysis, to extract common combinations of site properties, to provide input data for predictive modelling to meet Objective 4 in Chapter 6.

2.1 Importance of spatial relationships between supply of biomass and demand for energy feedstock

Biomass feedstock is a distributed resource with a low energy density, meaning that transport can account for up to 70% of delivered feedstock costs, as well as requiring fossil fuel use and associated emissions (McKendry, 2002a; Powlson *et al.*, 2005). As a result, bioenergy is only economically feasible in Europe with localised supply chains (Upham and Speakman, 2007) or using feedstock grown more cheaply elsewhere, for example Latin America, and then imported by ship (Hamelinck *et al.*, 2005). Energy consumption and associated GHG emissions from biomass transport vary with bulk density of feedstock, load per truck and distance transported. For example for 100km road transport, *Miscanthus* uses 1738 MJ $ha^{-1}a^{1}$ baled; chopping reduces usage to 1436 MJ $ha^{-1}a^{-1}$ but requires an additional 2280 MJ $ha^{-1}a^{-1}$ for drying (Venturi, 1999). Additionally, around 15 % dry matter may be lost during transport (Hamelinck *et al.*, 2005).

The requirement to source feedstock locally reduces the potential scale of generation from biomass only feedstock, which does not fit conveniently into the conventional energy supply system in England, of centralised generation at large scale for efficiency (Gross, 2003). Spatial relationships between supply and appropriate demand types for smaller scale or co-firing generation are therefore significant. As a result, biomass supply and demand issues have been the subject of much research, for example by the Towards a Sustainable Energy Economy (TSEC) group (Akgul *et al.*, 2012; Aylott *et al.*, 2008; Hosseini and Shah, 2011; Sims *et al.*, 2006). Previous studies have identified potential for biomass generation at individual sites, according to local factors dictating viable transport distances and costs. When allocating feedstock to an individual plant, it is necessary to assess both supply and demand side economics, as well as spatial distribution of feedstock, to identify whether demand can be met at an acceptable cost.

Supply curves have been created for a range of crops (*Miscanthus* (Bauen *et al.*, 2010), corn stover and switchgrass (Brechbill *et al.*, 2011)). These curves indicate how cost per tonne increases with the total amount of feedstock required, due to the need to source feedstock from a greater distance, and transport costs per km. Feedstock price for these curves is generally based on cultivation cost, however, opportunity cost may also be relevant (Brechbill *et al.*, 2011), hence it may be more appropriate to use market prices, since competition with other end uses can push up feedstock cost, e.g. animal bedding or conversion to second generation biofuel. Cost of delivered feedstock is therefore dependant on: required quantity, fuel costs and road network tortuosity, cost of cultivation, availability of cheaper alternatives such as wastes or residues, market price of feedstock and spatial patterns of yields (Bauen *et al.*, 2010; Brechbill *et al.*, 2011). Supply curves can be used in conjunction with data on feedstock availability to establish total cost of delivered feedstock up to the required demand for an individual plant (Bauen *et al.*, 2010; Brechbill *et al.*, 2011). The affordable total feedstock cost will be dependent on plant size and efficiency, sale price of energy, and any additional policy factors such as renewable obligation certificates (ROCs), renewable heat incentive (RHI) and feed in tariffs (FITs) which will be discussed in section 2.4. Therefore economics will dictate a different supply radius for any given biomass plant, and this will vary with fluctuations in transport costs, feedstock costs, spatial patterns of yields, energy sale price and changes to incentive schemes yields (Bauen *et al.*, 2010; Brechbill *et al.*, 2011). To analyse the relationship between feedstock supply and demand at a national scale the analysis must be simplified, compared to assessment of individual plants. The research presented here necessarily takes a more generalised approach, to allow national scale

assessment of capability to meet fixed location demands, and quantify theoretical potential generation under relevant scenarios.

Several studies have applied a sourcing radius of 25 km to limit emissions and costs from transport (Aylott *et al.*, 2008; Gasol *et al.*, 2011; Sims and Venturi, 2003). For England the 25 km sourcing radius was previously justified e.g. Aylott *et al.* (2008)) by the stipulation from the Department for Environment, Food and Rural Affairs (DEFRA) that Energy Crop Scheme (ECS) funding was only available where an end use within 25 km could be demonstrated. Updated regulations require end use to be within a "reasonable distance" meaning other economic factors will now dictate distance. Drax, the largest coal plant in England, currently sources from a supply radius of 96 km, but these distances would not be necessary or economic for smaller plants (Farmer's Weekly Interactive, 2012). Biomass demand for 10% co-firing at Drax is over double almost all other potential feedstock demands identified by this study. To make a more conservative assessment of potential, the 40 km radius applied by International Energy Crops is used here (Farmer's Weekly Interactive, 2011). Another radius might be more appropriate for assessment in another country, depending on local regulations, stipulations in incentives, or industry specifications. Based on market prices paid by Drax for 2012, of £63/t and road network tortuosity factor of 1.6 (to account for the fact that roads to not take a direct route) and transport costs of £2.72 + £0.27/km (Bauen *et al.*, 2010) delivered feedstock from a 40 km radius would cost £83/t, and from 25 km would cost £76.52/t. However this is variable with fuel costs and market prices so may differ for subsequent years. It is useful to compare potential generation applying a 40 km radius to the likely potential if the 25 km stipulation of the previous regulation had been maintained, so that the implications of such policies can be considered.

Relationship between supply and district heating (DH) demand has been assessed previously using modelling (Schmidt *et al.*, 2010) and GIS (Möller and Lund, 2010) analyses. For the UK, GIS has also been used with supply curves for co-firing at a single plant (Bauen *et al.*, 2010), supply based analysis has been used to identify 40 km radius supply areas with most feedstock potential (Aylott *et al.*, 2008) and a thorough assessment has been made of demand side factors for residential heat from bioenergy (Jablonski *et al.*, 2008). The study presented in this thesis extends these ideas to use a Geographical Information System (GIS) mapping approach to assess the relationship between the potential supply of local feedstock and the identified likely demand forms, and thus identify theoretical potential generation. The approach is illustrated using ArcMap software to

assess the relationship between yield data for *Miscanthus* feedstock, and combined heat and power (CHP) and co-firing demands in England.

2.2 Biomass feedstock supply chains

As well as the need for spatial proximity of supply and demand, there is also a temporal component to the relationship; bespoke feedstocks such as SRC willow and *Miscanthus* have relatively long preparation and establishment periods before useful harvests are achieved, creating a three to six year lead in period (Natural England, 2009a). Supply chain establishment is complicated by the conflict between a need for long term contracts (both for farmers to commit land (Styles and Jones, 2007), and for construction of new plants) and the economic and technical uncertainties surrounding new technology, preventing set long term pricing. Land use change to *Miscanthus* or Willow requires high initial investment and long term commitment of land compared to traditional annual crops (Clifton-Brown *et al.*, 2007; Jensen *et al.*, 2007; Styles and Jones, 2007). Farm scale economics may be used to calculate where energy crop cultivation would be more profitable than alternative land uses, however several sources of uncertainty (such as variations in feedstock price and yield) must be considered, and market uncertainty or reluctance to try novel crops is likely to prevent cultivation potential from being attained (Alexander *et al.*, 2014a; Alexander *et al.*, 2014b).

For a dedicated energy generation feedstock, with limited alternative market, farmers want security of demand before they will invest in cultivation and commit land (Styles and Jones, 2007). Bioenergy plants have long development times relative to other forms of energy generation, and unwillingness of farmers to cultivate feedstock until the end use is guaranteed and construction is near completion may add an additional time lag (Thornley, 2006). The change to the farming system involved in uptake of perennial energy crops makes farmer choice an important and perhaps less predictable variable when considering where energy crops may be grown (Jensen *et al.*, 2007).

Although the requirement for long-term feedstock supply to a plant should theoretically provide farmers with a secure on-going demand, operators may be unwilling to commit to a long-term supply contract. Whilst plant operators require guaranteed availability to construct a plant, they may prefer to maintain choice of suppliers in an uncertain market. Since imported or alternative

feedstocks may be preferred, potential demands identified by this study may not represent a secure market for local feedstock suppliers, making cultivation economically risky. Planned biomass plants 100 MWe or greater are mostly on the coast (Table 2.1), which enables plant operators to maintain choice of feedstock suppliers, avoiding the need for long term contracts. Ocean transport is less costly than road transport, which combined with cheaper cultivation overseas, means that European bioenergy using feedstock shipped from Latin America can be economically competitive with fossil fuel generation (Hamelinck *et al.*, 2005).

As well as economics, environmental considerations should be applied to restrict transport distances, to ensure that GHG savings compared to fossil fuel generation are preserved. Sourcing feedstock from Latin America may entail deforestation and land use change, damaging habitats and causing significant losses of above and below ground carbon stores (Fargione *et al.*, 2008; Hamelinck *et al.*, 2005). Planned UK regulations from 2015 will require bioenergy plants to prove that fuel is sustainable to receive financial support; sustainability criteria will be set until 2027 to reduce uncertainty for investors (Department of Energy and Climate Change, 2013b).

Due to difficulties establishing supply chains and contracts for dedicated feedstocks, many existing plants use residues from agriculture and waste from industry (Thornley, 2006). Limited availability of these feedstocks reduces potential scale of generation, and removal of agricultural residues may reduce soil fertility (Lal, 2004). Renewable energy policies have facilitated contracts for existing bioenergy plants using bespoke feedstocks (Thornley, 2006). Investing up the supply chain by plant operators has been suggested as a potential solution to the issue of market and supply chain security.

Biomass can be processed to increase energy density and enable increased transport, and hence increased scale of generation. The large planned inland plants in Table 2.1 (Drax and Ironbridge), plan to use pellets, which reduces storage and transport space and costs, and improve fit with the coal plant systems of fuel injection and combustion (Spackman, 2011). Integrated modelling of logistics and processing has been advocated (Hosseini and Shah, 2011) and will become more relevant if processing by torrefaction moves past the demonstration stage (International Energy Agency, 2009; Jaap Koppejan *et al.*, 2012). Processing is likely to entail some energy use and GHG emissions, as well as material losses, which may or may not be compensated for by efficiencies of scale and improved fit with the existing centralised generation system (Hamelinck *et al.*, 2005).

Table 2.1 Planned and proposed new bioenergy generation facilities in England (Forestry Commission, 2013)

Project - in planning	**Location**	**Company**	**Fuel**	**Output (MWe)**	**Output**
Avonmouth	Avonmouth	Helius	Pellets	100.0	Electricity
Billingham	Teesside	Gaia Power	Recycled wood	45.0	Electricity
Blackburn Meadows	Sheffield	E.ON	Wood	25.0	Electricity
Brigg	North Lincolnshire	Eco2	Straw	40.0	Electricity
Castle Cary	Castle Cary	Bronzeoak	Wood	12.7	Electricity
Drax	Yorkshire	Drax	Pellets	2000.0	Electricity
Enfield Biomass	London	Kedco	Wood	12.0	CHP
Ferrybridge	Nr Castleford	SSE	Multifuel, RDF	68.0	Electricity
Ironbridge	Ironbridge	E.ON	Pellets	1000.0	Electricity
Mendlesham	Mendlesham, Suffolk	Eco2	Straw	40.0	Electricity
Pollington	Pollington	Dalkia Bioenergy		52.0	Electricity
Portbury Docks	Bristol	E.ON	Wood	150.0	Electricity
Sleaford	Lincolnshire	Eco2	Straw	40.0	Electricity
Stallingborough	Stallingborough, Lincs.	Helius/RWE npower	Wood	65.0	Electricity
Tansterne	Hull	GB Bio	Straw	12.5	Electricity
Tees REP	Middlesborough	MGT Power	Wood	300.0	Electricity
Tilbury Biomass	Tilbury	RWE npower	Pellets	870.0	Electricity
Tilbury Green Power	Tilbury	Express Energy	Biomass & SRF	60.0	Electricity
Tyne REP	Tyneside	MGT Power	Imported wood	295.0	Electricity
Wetwang	Yorkshire	E Yorks Power	Wood & straw	15.0	Electricity
			total	5202.2	Electricity
Project - proposed	Location	Company	Fuel	Output (MWe)	Output
Blyth	Blyth	RE Systems	Wood	100	Electricity
Claycross	Derbyshire	Kedco	Wood	12	CHP
Drakelow	Drakelow	E.ON	Wood		Electricity
Greenpower.54	Wolverhampton	Express Energy	Biomass & SRF	30	Electricity
Hull	Hull	Dong		300	Electricity
Peterborough	Peterborough	Peterborough RE	Agricultural waste	66	Electricity
Southampton	Southampton	Helius	Pellets	100	Electricity
Thetford Wood	Thetford	EPRL	Wood	40	Electricity
			total	648	Electricity

Processing techniques currently under development aim to make biomass feedstock more comparable to fossil fuels, for improved fit with existing energy technologies and perspectives; however it may be more beneficial to apply energy conversion technologies appropriate to bioenergy feedstocks (Robbins *et al.*, 2012).

2.3 Integrating biomass feedstock with existing energy infrastructure

Minimising feedstock transport improves supply side economics, but reduces effectiveness of electricity-only generation, since plant capacity is limited by local feedstock growing area, and smaller plants tend to achieve lower energy conversion efficiency (Gross, 2003; Powlson *et al.*, 2005; Schmidt *et al.*, 2010). This means that bioenergy generation must be in a form able to achieve high efficiency with relatively small feedstock availability, compared to fossil fuel plants, in order to make effective use of feedstock, and improve economics for the generator. Hence there is a problem with the tendency to base calculations of potential bioenergy generation on supply side data only, as noted in (Jablonski *et al.*, 2008), since locations and magnitudes of appropriate demand must also be considered. Assessments of the future potential of bioenergy must therefore take into account spatial factors for both supply and demand in order to minimise transport of feedstock whilst maximising efficiency of generation (Aylott *et al.*, 2008; Berndes *et al.*, 2010; Schmidt *et al.*, 2010).

Without significant energy densification processing, there are two main approaches through which penetration of generation from biomass may be increased in countries like England with developed energy systems. First, integrating with the existing large scale centralised generation systems by co-firing with coal (e.g. Berndes *et al.*, 2010; Perry and Rosillocalle, 2008); or second through decentralised co-generation of heat and power, which can achieve higher efficiency at small scales by avoiding waste of generated heat (e.g. Schmidt *et al.*, 2010; Speirs *et al.*, 2010). For countries with less developed infrastructure, or significant off-grid rural areas, assessment based on supply and population density would be a more appropriate methodology.

2.3.1 Potential for co-firing biomass with coal

In 2010, co-firing with coal was operational using a range of feedstocks at 228 plants worldwide (Al-Mansour and Zuwala, 2010). By using feedstock in large plants, efficiency benefits of large scale generation are maintained (Berndes *et al.*, 2010; Cherubini, 2010). Co-firing up to 10% requires little investment in plant conversion, and can be implemented more rapidly compared to the establishment of new biomass only generating facilities, 20% is also possible with relatively little modification (Berndes *et al.*, 2010; Perry, 2006). Since the proportion of co-fired biomass can be varied, flexibility is maintained; the plant does not commit to a certain feedstock, which removes the uncertainty issue of feedstock availability for the plant operator, but not the issue of demand security for the farmer (Berndes *et al.*, 2010). There is also the added certainty of using established technology (Wood and Dow, 2011). If a shortfall in meeting required renewables targets is anticipated, the flexibility and speed with which the proportion of co-firing can be increased may enable the gap to be bridged at relatively short notice, if feedstock is available. For 2012, bioenergy co-firing generated 1,783 GWh, well below the theoretical capacity of around 14,318 GWh (Department of Energy and Climate Change, 2013b). To assess the potential for co-firing local biomass feedstock with coal, it is necessary to identify plant locations, calculate the feedstock requirement for 10% (or 20%) co-firing, as described in Section 2.8.1, and then calculate if the required feedstock could be cultivated within the local area, taking into account constraints on land where the feedstock may be grown and appropriate transport distances as described in Section 2.9.1.

2.3.2 Potential for co-generation of heat and power

Since generation using biomass feedstock must be small scale to minimise transport, it is likely that biomass only generation of electricity would achieve comparatively low efficiency (Gross, 2003; Powlson *et al.*, 2005). However, on combustion, a significant proportion of the energy stored in the biomass will be released as heat; using this otherwise wasted heat could dramatically increase total efficiency of energy production (Babus'Haq and Probert, 1996; Hawkes and Leach, 2008; Powlson *et al.*, 2005). Transmission losses and costs of distribution infrastructure are significant; therefore, heat must be generated close to demand, meaning that distributed generation of heat is more efficient than centralised generation, making combined heat and power (CHP) an appropriate end use for distributed feedstock (McKendry, 2002b; Rowe *et al.*, 2009). Whilst geothermal and solar energy may be suitable for supplying low temperature

heat for space and water heating, biomass generation is unique among renewables in being able to efficiently supply high temperature heat for industrial processes (Thornley, 2006). Improvements in efficiency and carbon savings through CHP generation, compared to separate generation of heat and electricity, are dependent upon the appropriate reference systems (Martens, 1998).

Total efficiency of CHP drops with electric power increase, so in order to maximise efficiency gains compared to electricity alone, heat generation should be maximised, but should not exceed heat demand (International Energy Agency, 2009; Martens, 1998). Policy can also be a factor in the decision to shift generation towards heat or electricity, so it is important that financial incentives do not encourage less efficient use of plants.

CHP is most efficient where the heat off-taker has a large, consistent demand; industry tends to require higher temperatures than domestic users, with less seasonal variation, enabling more efficient supply (Hawkes and Leach, 2008). However, a generation plant may produce heat energy at a range of temperatures; reducing the demand temperature increases the proportion of this heat that can be used, and therefore may be a more efficient application (Mortensen and Overgaard, 1992). In the UK in 2008, 58% of domestic energy consumption was for space heating and 24% for hot water (Department of Energy and Climate Change, 2010) suggesting that biomass district heating (DH) in England could significantly reduce carbon emissions. Although existing domestic heat demand is significant, it is important to take into account that new housing will be built to higher thermal efficiency specifications, which can reduce peak heat demand by 50-90% (Roberts, 2008; Wood and Dow, 2011). Although this would reduce the heat generation displaced by DH, the electricity proportion of generation can increase (Martens, 1998; United Nations Environment Programme, 2007). The infrastructure costs of DH installation may be prohibitive in many cases, however payback periods can be as low as 4 years, assuming sufficiently cheap biomass supply, compared to an average system lifetime of 25 years (Vallios *et al.*, 2009). Although DH is considered likely to be profitable at demand densities over 180 MJ m^{-2} a^{-1} (Bøhm *et al.*, 2008), cultural factors such as lack of familiarity may prevent investment in new projects, whereas areas with existing DH systems can convert to biomass, and are more likely to build new DH (Vallios *et al.*, 2009).

To assess the potential for CHP using local biomass feedstock, it is necessary first to identify the location and magnitude of appropriate heat demands and calculate the feedstock requirement to generate the required heat according to methodology laid out in Section 2.8.2 for large demands and Section 2.8.3 for DH. Having calculated the feedstock demands, it is then necessary to calculate if the required feedstock could be cultivated within the local area, taking into account constraints on land where the feedstock may be grown and appropriate transport distances; methodology for this is detailed in Section 2.9.2 for large demands and Section 2.9.3 for DH.

Since both DH and large demand applications of bioenergy CHP have the potential for improved efficiency and economics compared to separate heat and electricity generation, the potential for both should be assessed to some extent.

2.4 Policy for energy generation factors

Fossil fuels are advantaged over bioenergy feedstocks by higher energy density, existing infrastructure, and commodities markets (Thornley, 2006). Jablonski *et al.* (2008) note a lack of focus on demand side policy to increase generation from bioenergy. Bioenergy may be an important contributor to the renewable energy mix with advantages over intermittent renewables such as wind and solar, in that timing of generation can be controlled, however it may require greater economic incentives and support for supply chain establishment (Finney *et al.*, 2012; Schmidt *et al.*, 2010; Thornley, 2006). To effectively encourage investment in renewable energy, policy must provide long term stability and risk reduction (Mitchell *et al.*, 2006). Recent policy initiatives may have contributed to the increase in UK biomass energy capacity from 159.7 MWe in 2004 to 1090.2 MWe in 2013, however there remains much unfulfilled potential (Department of Energy and Climate Change, 2013b; Finney *et al.*, 2012; Forestry Commission, 2013; Thornley, 2006). Although incentives are targeted at both ends of the supply chain, failure to address the issue of agreements between farmers and plants may contribute to low levels of expansion.

Renewable obligation certificates (ROCs) were brought in in 2002 to replace the non-fossil fuel obligation (NFFO) as a stimulus for renewable energy. Suppliers are obligated to supply a proportion of energy from renewables in return for ROCs, or to pay a buyout price for any shortfall; the buyout money will then be redistributed among suppliers according to the number of ROCs they received to maintain a market value above the buyout price (Ofgem, 2013c;

Thornley, 2006). Lack of banding meant that the initial ROC scheme favoured more profitable schemes without taking into account environmental or community benefits, or the energy mix, and as a result no new bioenergy plants were proposed in the first few years (Thornley, 2006).

Energy policies from 2006 have aimed to stimulate distributed generation (Upham and Speakman, 2007), however uptake of policy incentives was initially curtailed by problems such as the lack of long term security and insufficiencies of grants to cover start-up costs for smaller generators (Finney *et al.*, 2012).

Since April 2009, banding of ROCs provided differing levels of support for different technologies to increase support for less economically favoured generation which has additional socioeconomic or energy security benefits; for example doubled ROCs for small scale generation attempted to compensate for greater investment risks (Finney *et al.*, 2012). Previous policy stated that co-firing would only receive ROCs until March 2016, and could not make up more than a set proportion of a supplier's total ROCs (Thornley, 2006), however the cap has been replaced by different banding for co-firing (Ofgem, 2013c). In 2010 the ROC legislation end date was increased from 2027 to 2037, with the aim of providing stability and reducing risk, however bandings will be reassessed every four years (Finney *et al.*, 2012; Ofgem, 2013c). Required percentage renewable generation and buyout price are both increased every year; the 2010-2011 price was £36.99 for every MWh which increased to £42.02 for 2013-2014 (Ofgem 2013b).

Feed in tariffs (FITs) introduced in the UK in 2010 require energy companies to pay small scale generators, however lack of contracts reduces long-term security, limiting the appeal for investors (Finney *et al.*, 2012). FITs are the only incentive scheme for renewables in most other European countries; differences in the policy overseas have provided greater long-term security and often improved success, but recent economic decline has reduced support for new contracts (Finney *et al.*, 2012; Mitchell *et al.*, 2006).

Renewable heat incentive (RHI) was brought in in 2011 in the UK to provide an additional incentive for growth in CHP, since heat generation produces 50% of carbon emissions (Finney *et al.*, 2012). The incentive includes DH schemes, with plans to extend to individual households (Department of Energy and Climate Change, 2011; Ofgem 2013a). However, plans to exclude

bespoke feedstock from RHI if there is significant expansion remove long-term guaranteed returns and may discourage cultivation (Department of Energy and Climate Change, 2011; Jensen *et al.*, 2007; Sherrington and Moran, 2010; Styles and Jones, 2007). Initial uptake has also been reduced by lower than proposed tariffs (Finney *et al.*, 2012). Extra ROCs are also available for generation of electricity in CHP schemes (Ofgem, 2013c). Since overall efficiency of CHP is greater for lower electricity to heat ratios (provided a suitable heat off-taker is available) policy should not incentivise electricity over heat, as this would encourage plant inefficiency.

2.5 Mapping of biomass feedstock supply

Lovett *et al.* (2009) performed constraints mapping to rule out locations unsuitable for the cultivation of perennial energy crops in England, and mapped predicted *Miscanthus* yield for suitable sites, using spatial data on site properties and regression equations from Richter *et al.* (2008). Yield predictions are crucial, due to significant spatial variability, the threshold of economically viable yields, and the use of predicted yields in forecasting generation potential. Equally it is vital to rule out locations where perennial crops cannot or should not be grown to make meaningful assessments of technical potential feedstock availability (Lovett *et al.*, 2009).

Briefly, the constraints ruled out: specific areas where high C losses might be expected (organic soils, forest, improved grassland); areas where the crops physically could not be grown (urban areas, major rivers, lakes); as well as natural and semi-natural habitats, sensitive landscape areas and designated areas such as nature reserves to protect ecosystems; and cultural heritage sites, to minimise socioeconomic detriment. Slope steepness places a practical constraint on agricultural uses; slopes over 15% were constrained out based on locations of existing *Miscanthus* cultivation; agricultural SRC willow cultivation is also predominantly on gentler slopes, so this constraint is also appropriate for this study. Improved grassland and landscape sensitivity are considered secondary constraints but these areas are excluded for the purpose of this study to produce more conservative findings. Research elsewhere e.g. Wang *et al.* (2014) following Lovett *et al.* (2014) does not exclude higher grade farmland on economic grounds, since this is potentially available if energy crop cultivation were economically advantageous, however excluding high grade farmland reduces the need to include farm scale economic analysis as per Alexander *et al.* (2014b). Land which has thus far been converted under ECS schemes is predominantly agricultural land classification grades three and four, so higher and lower grades were also constrained out.

Applying 11 constraints and assuming crops would only be grown on grade 3 or 4 land for socioeconomic reasons left 3.12 M ha of suitable land, with predicted annual yield of 38.9 oven dry mega tonnes (odMt) (Lovett *et al.*, 2009). For the purposes of this thesis, land where simulated *Miscanthus* yields fell below the economically viable threshold was also excluded from analysis.

Although the study detailed in this thesis considers the impacts of cultivation of SRC willow as well as *Miscanthus*, it is convenient to use yield data for a single feedstock type for the purposes of national scale analysis. SRC willow yields are likely to differ from those predicted for *Miscanthus*, however the differrence may not be consistent, or significant in comparisson to interannual yield variation or model error. Predicted *Miscanthus* yield data from the constraints mapping study was therefore used in this thesis to estimate potential feedstock availability.

2.6 Existing policy for biomass feedstock cultivation

Energy Crop Scheme (ECS) grants are available from Natural England to incentivise the cultivation of SRC willow and *Miscanthus* for energy end uses. In phase one these were too low to stimulate much uptake and many of the farmers who did plant were left without an energy end use when a 40 MWe biomass only project was decommissioned without coming into operation due to financing and technical issues (Aylott and McDermott, 2012; Piterou *et al.*, 2008). This combined with a two year hiatus in the funding may have reduced farmer confidence, and there has been even less uptake in the 2008-2012 period of the second phase of the grant, in spite of payments being increased from a flat rate per ha (£900-£1000 depending on region (Natural England, 2006)) to cover 50% start-up costs of SRC willow and *Miscanthus* cultivation for energy. It has been suggested that current assessments may be too complex, and that a return to a flat rate, with clear maps outlining payment level for each region may be more appealing to farmers (Lindegaard, 2013). Nonetheless, market analysis by Alexander *et al.* (2014a) suggests that ECS is an economically efficient scheme, and Lindegaard (2013) advocate a third phase. Supply chain issues as discussed in Section 2.2 may thus be considered a greater barrier to energy crop cultivation than a lack of policy support for cultivation.

2.7 Mapping approach

The GIS approach developed in this study is based on application of mapping and spatial analysis actions as detailed in Figure 2.1. The approach is designed to be applied at national scale to provide an initial forecast of biomass generation potential, to identify regions or plants with limitations, and to calculate potential land area taken out of food production. The underlying logic is similar to the WISDOM methodology (Drigo *et al.*, 2002); data on supply must be assessed in relation to demand due to the need to view biomass as a local feedstock in order to minimise costs and emissions from transport. It differs in scale from research for individual plants or regions (e.g. Aylott *et al.*, 2008; Brechbill *et al.*, 2011), and from other national scale assessments (e.g. Akgul *et al.*, 2012; Drigo *et al.*, 2002) in the incorporation of multiple fixed site potential end uses and analysis of interaction of demand zones.

Elsewhere, Wang *et al.* (2014) have performed more detailed analysis integrating spatial data on predicted yields with spatially disaggregated energy demand, including combined domestic and non-domestic space heating and as well as electricity, using an optimisation model to determine size and location of plants for maximum profit whilst meeting all demands. This output formed part of a large research project, incorporating data from Taylor *et al.* (2014) and modelling approaches developed in Wang *et al.* (2012). This level of assessment is outside the scope of this thesis, instead, the approach taken considers preferences in the energy industry for single offtaker heat agreements (Bailey, 2011) and for convenient, low investment, low commitment incorporation of renewables as co-firing in existing coal plants. This approach seems reasonable given the assertion by Lovett *et al.* (2014) that the current energy crop cultivation in England is located to meet feedstock demand for co-firing and small CHP or local biomass heating systems.

Locations and magnitudes of these existing demands were mapped, and data on potential yields for the surrounding area was used to identify where demand can be met. The analysis in this thesis is intended to broadly indicate generation potential; subsequent, more detailed individualised analysis would be necessary to calculate economic merits and relative GHG savings of individual plants.

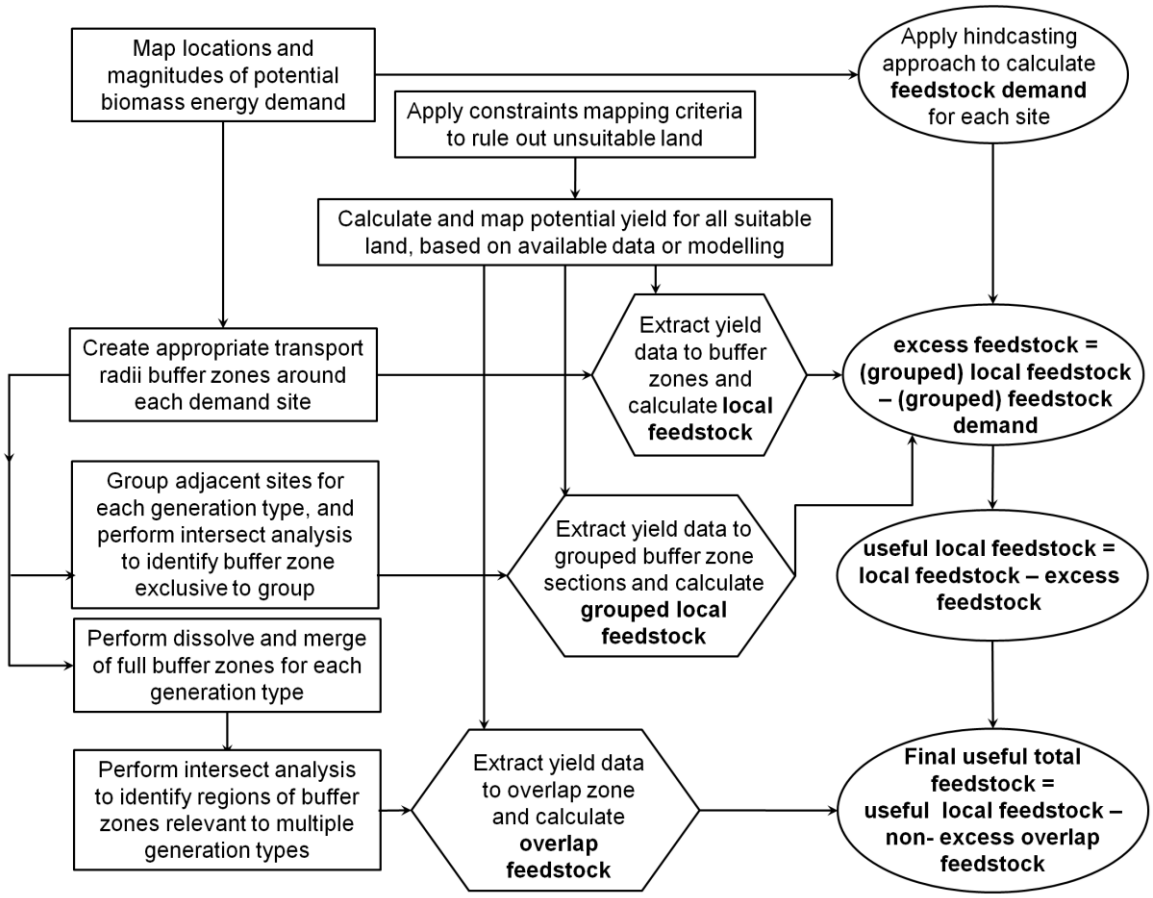

Figure 2.1 Methodology relating potential yield data spatially to identified potential energy end uses. Data were extracted using the "extract by mask" tool in ARCGIS; this creates a new raster of values from the selected raster dataset which spatially coincide with a selected "mask" raster or polygon.

Locations of potential end users of feedstock in the three categories identified in Section 2.3 were identified, and hindcasting calculations using methodology from Table 2.2 and Table 2.3 were performed to identify the potential demand for feedstock in odMt of *Miscanthus*.

2.8 Mapping of demand

2.8.1 Mapping potential bioenergy generation as co-firing

To assess the potential for co-firing local biomass feedstock with coal, it is necessary to identify plant locations, calculate the feedstock requirement for 10% (or 20%) co-firing. Location data for existing coal generation were used to map existing plants for England with data available from energy providers (Perry, 2006). Potential demand for biomass feedstock for co-firing in existing coal powered stations is likely to be up to 10% of total fuel. A greater proportion, up to 20% is

feasible, but would require willingness of owners to invest in modifications to deal with by-products and potential sources of corrosion (Perry and Rosillocalle, 2008). The tonnage of feedstock required is calculated based on plant output, using a measure of efficiency to calculate the energy input required, and dividing by the energy density of *Miscanthus* to calculate the mass required. Detailed steps for co-firing up to 10% or 20% are outlined in Table 2.2.

Table 2.2 Calculations used to establish tonnage of biomass required for 10% co-firing at a coal fired plant

Power	**Energy output = Power × utilization factor × hours in a year** **1 kWh =3.6 MJ**	**Energy input required; based on average efficiency (Berndes *et al.*, 2010)**	**Biomass energy assuming 10% co-firing**	**Oven-dry *Miscanthus* demand at 17 GJ t^{-1} (Department for Environment Food and Rural Affairs, 2007)**
kW	Capacity×0.6 ×8760×3.6 MJ	Energy×(100/30)	Input× (10/100)	Biomass energy/17 000

Utilization factor is taken from the UK biomass strategy (Department of Energy and Climate Change, 2011). These calculations can be performed in reverse to calculate energy generation from figures for available feedstock.

Since co-firing is flexible, for coal-fired plants, the proportion of biomass fired was assumed to be variable up to the 10% or 20% demand figure (calculated as per Table 2.2). Therefore any feedstock up to this amount could be used, so the total feedstock available for co-firing was calculated, applying the specified radius, and subtracting excesses up to both 10% and 20% demand for individual English coal plants. To assess whether this demand could be met, the potential local feedstock cultivation is calculated in Section 2.9.1 according to constraints on land use detailed in Section 2.5, and the two theoretical transport distance limits considered by this study.

2.8.2 Mapping potential bioenergy generation as CHP for industrial and other large demand sites

To assess the potential for CHP using local biomass feedstock, it is necessary first to identify the location and magnitude of appropriate heat demands and calculate the feedstock requirement to generate the required heat. Potential locations for industrial scale CHP were established from the UK Government's Department for Energy and Climate Change (DECC) heat map; data were compiled for all large heat demands not already utilising CHP. The tonnage of feedstock required to supply a CHP plant meeting heat demand is calculated from the heat energy requirement,

maximum thermal energy generation efficiency and energy density of *Miscanthus*, according to the steps outlined in Table 2.3.

Table 2.3 Calculations used to establish tonnage of biomass required to provide industrial CHP

Heat demand	**Heat energy demand = Power × utilization factor × hours in a year, 1 kWh = 3.6 MJ**	**Energy input required; based on maximum thermal efficiency (Hans Falster *et al.*, 2002)**	**Oven-dry *Miscanthus* demand at 17 GJ t^{-1} (Department for Environment Food and Rural Affairs, 2007)**
kW	Demand × 0.569 × 8760 × 3.6 MJ	Output × (100/70)	Energy input/17 000

Utilization factor is based on UK statistics (Department of Energy and Climate Change, 2012). These calculations can be performed in reverse to calculate energy generation from figures for available feedstock. Hindcasting calculations are based on meeting heat demand. Therefore, efficiency values for generation to maximise heat production are applied to calculate energy input; 70% efficiency of conversion to heat can be expected and 20% efficiency for conversion to electricity are applied when reversing calculations to calculate total energy generation (Falster et al., 2002).

Calculations assume that generation would target meeting heat demand, although excess feedstock may be used to increase the electricity component of generation. A utilisation factor must be applied to account for downtime of the heat demand; existing CHP in the UK has 57 % utilisation, although variation with end use is likely (Department of Energy and Climate Change, 2012). To assess whether this demand could be met, the potential local feedstock cultivation is calculated in Section 2.9.2 according to constraints on land use detailed in Section 2.5, and the two theoretical transport distance limits considered by this study.

For industrial and other large heat demands, feedstock requirement may not be flexible unless alternative feedstock can be used, hence ability to meet total demand for sites individually is more important. The feedstock demand for each potential unit (calculated as per Table 2.3) was compared to potentially available feedstock within the applied radius to assess viability. Where there is excess feedstock available for CHP relative to heat demand, it is possible to increase the electricity component of generation to utilise this, although total efficiency may decrease as a result.

2.8.3 Mapping potential bioenergy generation as CHP for district heating

Due to expected profit margins, DH is likely to be installed only in regions with heat demand densities over 180 MJ m^{-2} a^{-1} (Bøhm *et al.*, 2008). Areas of profitable demand were identified for England based on annual total gas consumption statistics, obtained from government databases, provided per district (divided by district area to obtain demand density) assuming 98% of gas usage to be for space and water heating (Department of Energy and Climate Change, 2010) and an 80% efficiency for conversion to heat in domestic boilers (Martens, 1998).

In rural areas, such as the south-west of England where 16% of homes are not connected to the gas grid (Lindegaard, 2013), biomass DH systems would be likely to have high uptake due to economic benefits for residents. Although high uptake increases potential for DH, low population density may mean that heat demand is not over the threshold quoted here; since these areas are not on the gas grid, demand density must be calculated using a different approach, and these regions are excluded from this assessment.

Demand will vary over time with outside temperatures, changes to housing standards and the age and income of occupants, as well as how much time they spend at home (Taylor *et al.*, 2014). Increasing temperatures with climate change and improved household insulation funded by initiatives such as the green deal may therefore reduce demand over time (Taylor *et al.*, 2014). Conversely if DH was supplied at a low price, demand for some houses may increase.

Modelling approaches to identify optimum potential DH plant locations in terms of energy supply and demand are illustrated elsewhere (Schmidt *et al.*, 2010) and ideally incorporate detailed information on individual buildings (Möller and Lund, 2010). As well as modelling, additional consideration of site factors may be required to identify feasible locations for generation to supply an individual district. Furthermore, distribution losses for potential DH are dependent on the system specification, lengths of pipes and distribution temperatures (Bøhm *et al.*, 2008), and many variables such as household level choice and local demand density variations must also be taken into account (Möller and Lund, 2010; Schmidt *et al.*, 2010). Estimates can be made to cover

some of these parameters, for example based on existing systems DH network radius can be up to 30 km, however without known system specification it is not possible to analyse this issue fully.

Because national scale analysis cannot take into account factors such as availability of sites for DH CHP plant, distribution system specification, and level of uptake, it was decided to perform a basic level of assessment for DH. Therefore, calculations have been limited to approximations based on locations and magnitude of end user demand. Calculations are based on total gas usage, so it is not relevant to apply a utilisation factor to allow for down time, however seasonal and daily variability in heat demand is likely to be significant. This analysis is best used for initial visual assessment of potential for DH, and for identifying competition with other potential feedstock end uses. A map has been produced (Figure 2.5) to visualise the general potential of feedstock availability for this purpose, with potential yield extracted to 40 km and 25 km buffers of districts with potential for DH installation. Modelling approaches could be applied following on from this to identify optimum sites and capacity (Schmidt *et al.*, 2010).

2.8.4 Calculating potential generation of bioenergy at identified end uses

Table 2.4 compares total potential for *Miscanthus* cultivation in England (based on predicted potential yield data (Lovett *et al.*, 2009)) to demands from hindcasting calculations. Without taking into account spatial factors, there is sufficient potential supply for both 10% co-firing with coal, and for all industrial and large-scale heat demand to be supplied by biomass CHP.

The potential generation identified in Table 2.4 does not take into account spatial relationship between supply and demand. To assess how the need to localise biomass road transport-based supply chains will affect generation potential, data on locations of demands was then integrated into the assessment.

Table 2.4 Potential Miscanthus yield calculations for the whole of England, compared to demand of identified potential end uses of feedstock

Predicted oven-dry yield range (t ha^{-1}a^{-1})	**Available land (ha)**	**Oven-dry *Miscanthus* production (Mt)**
9 or less	591,900	N/A
9 – 12	520,600	5.47
12 – 15	1,211,900	16.36
15 or more	789,500	11.84
	Total	33.67
Potential usage		**Required oven-dry feedstock (Mt)**
Co-firing at 10% of capacity		8.6
Industrial CHP for identified heat demand		2.2
Total		10.8

Yield data are from a previous study (Lovett et al., 2009)modelling potential yield of Miscanthus for sites identified as suitable for cultivation based on 11 constraints (Lovett et al., 2009). Since 9 oven- dry t ha-1a-1 is the minimum economically viable yield, areas with lower yield are considered unattractive for cultivation and are not included in calculations (Lovett et al., 2009; Richter et al., 2008).Total yields for viable areas are calculated conservatively, as the average for each yield range, or as the minimum for the 15 or more range.

For the coal fired stations identified in 2.8.1, the potential large demand CHP sites identified in 2.8.2, and the DH zones identified in 2.8.3 a transport radius buffer was produced in ArcMap, and spatial data on potential *Miscanthus* yield were extracted for each feedstock catchment area to give potential local feedstock. Comparison of potential supply and demand was made individually for large scale CHP and co-firing, whilst for DH the assessment was made for the whole regions, since locations of potential generation cannot be pinpointed, and adjacent demand regions may be supplied together or separately. Adjacent CHP or co-firing demand sites with mutually overlapping feedstock demand zones were grouped as illustrated in Figure 2.2, and feedstock extracted to the group buffer zone.

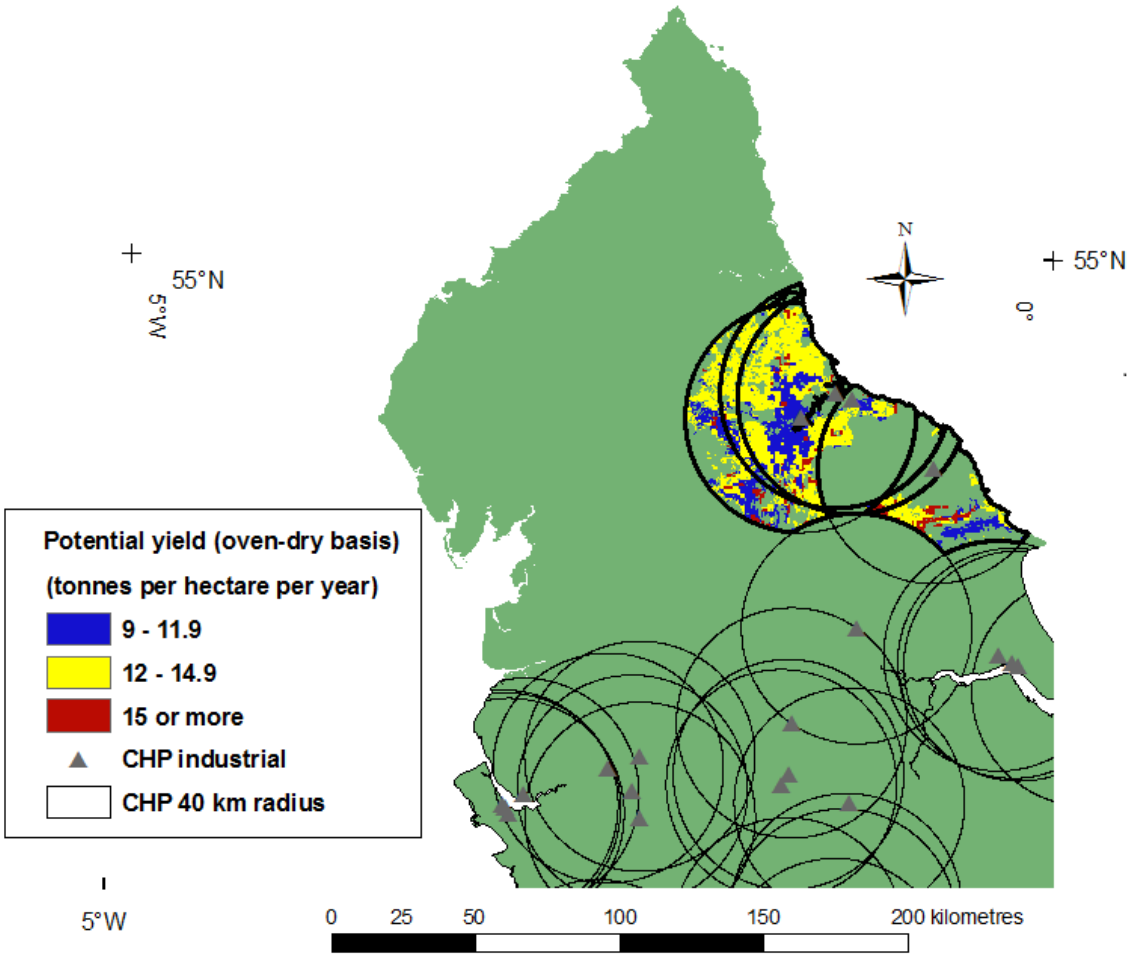

Figure 2.2 Map to illustrate calculation of available feedstock for a group of individually viable demands. Demand sites (in this case for CHP) are grouped for convenience of calculations, with groups selected to have intersections between all included buffers. Thick black lines indicate buffer zones for the group of CHP sites being assessed, and the predicted yield data extracted to this group is displayed.

Using feedstock demands calculated as per Table 2.2 and Table 2.3, any excess feedstock was calculated as:

Excess feedstock = (group) Local feedstock – (group) Feedstock demand.

Finally, total potential local feedstock was calculated by applying the "dissolve and merge" GIS tool to the original buffer zones, and again extracting potential yield data to this mask. An intersect analysis was then performed on these buffers to identify where feedstock catchment areas overlap, and predicted yield data were extracted for these zones to give overlap feedstock. The usable total feedstock for all England, for the identified demand type, can then be calculated according to:

Total useful feedstock = Useful local feedstock – non excess overlap feedstock.

Where:

Non excess overlap feedstock = Overlap feedstock – excess feedstock.

When applying this method to project maximum potential generation, overlap feedstock should be included in calculations for the most efficient generation type to which it is applicable. Therefore, since large scale CHP has higher conversion efficiency than co-firing, feedstock which was also suitably located for CHP was subtracted from co-firing figures before calculation of excess. DH was prioritised last due to significant cultural barriers in England; non-excess feedstock overlapping between DH and large-scale CHP or co-firing was subtracted from the total within the DHP catchment zone to give an estimate of potential generation.

2.9 Results

2.9.1 Co-firing

Having calculated the feedstock demand in Section 2.8.1, it is then necessary to calculate if the required feedstock could be cultivated within the local area, taking into account constraints on land where the feedstock may be grown and appropriate transport distances. Predicted *Miscanthus* yield data from Lovett *et al.* (2009) for the locations suitable for energy crop cultivation were clipped to the 40km and 25km feedstock transport zones using the methodology described in Section 2.7 to calculate potential feedstock available to each demand. Where demand zones overlapped, values were calculated for the group as indicated in Figure 2.2. Tables A1.1 and A1.2 in Appendix Section 1 contain data on feedstock demands and potential local cultivation, and the associated Figures A1.1 and A1.2 indicate the demand groups as referred to in the tables. Figure 2.3 displays the data visually; there is most coal fired capacity and potential local biomass cultivation in Yorkshire and the Midlands, giving these locations the best potential for co-firing of locally grown *Miscanthus*.

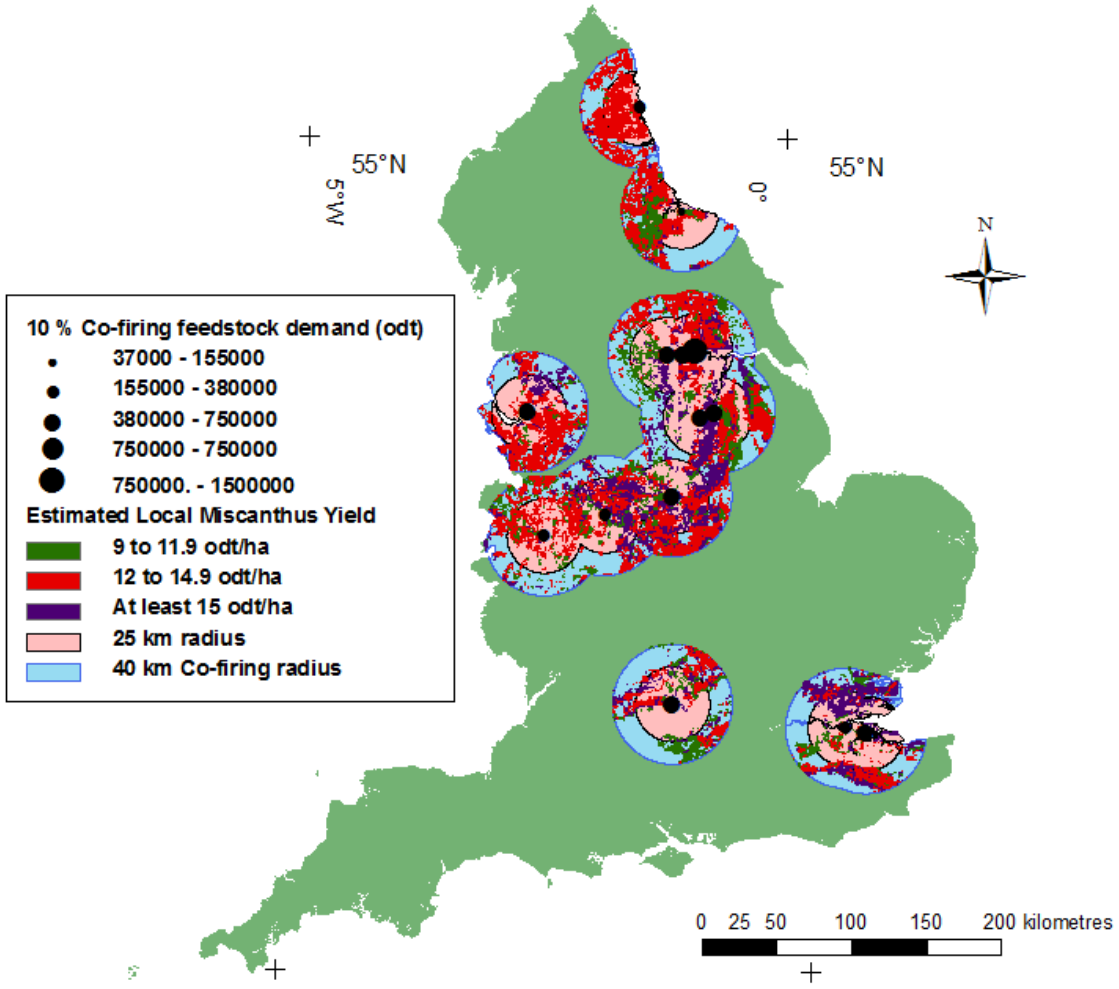

Figure 2.3 Map to show potential Miscanthus feedstock supply and demand for co-firing.

Table 2.5 Potential biomass availability for co-firing (assuming conservative potential cultivation within 40km of all existing coal plants)

Percentage biomass to be co-fired	Total PJ that could be from biomass	*Miscanthus* demand (odMt)	Transport radius	Potentially available *Miscanthus* (up to specified local demand) within supply radius (odMt)	Generation for potentially available *Miscanthus* (PJ)
10%	43	8.6	40 km	8.2	42
			25 km	7.9	41
20%	86	17.2	40 km	10.7	55
			25 km	8.6	44

As indicated in Table 2.5; based on useful feedstock figures from Table A1.1 and Table A1.2, 42 PJ could be generated from locally-sourced *Miscanthus* with co-firing at 10%, or 55 PJ at 20%. Of 13 odMt, 11 are also suitably located for industrial CHP. Were a 25 km transport restriction imposed, 41 PJ could be generated with co-firing at 10%, or 44 PJ at 20%.

2.9.2 CHP for Industrial and large demand sites heat

Having calculated the feedstock demand in Section 2.8.2, it is then necessary to calculate if the required feedstock could be cultivated within the local area, taking into account constraints on land where the feedstock may be grown and appropriate transport distances. Predicted *Miscanthus* yield data from Lovett *et al.* (2009) for the locations suitable for energy crop cultivation were clipped to the 40km and 25km feedstock transport zones using the methodology described in Section 2.7 to calculate potential feedstock available to each demand or demand group. Proximity of sites with potential for industrial CHP means that there is significant overlap of catchment regions for adjacent sites, meaning that competition for feedstock must be considered as well as potential local yields. To assess whether this overlap reduces total potential, adjacent sites whose individual demands can be met within the defined radius were grouped, extracting feedstock availability data to this zone as indicated in Figure 2.2, and viability assessed as for an individual plant. Tables A1.3 and A1.4 in Appendix Section 1 contain data on feedstock demands and potential local cultivation, and the associated Figures A1.3 and A1.4 indicate the demand groups as referred to in the tables; data are displayed here visually in Figure 2.4. Significant feedstock potential in these regions combined with mostly low demands mean CHP groups remain viable, and have excess feedstock when assessed as per Figure 2.2. Viability of adjacent demands is dependent on appropriate feedstock allocation; in a free market, feedstock purchasing is likely to be based on proximity not optimising national generation, and competition may also have economic impacts. The issue of overlapping demand zones is likely to be common, since industry, and therefore industrial heat demand, is likely to be clustered in most countries, due to spatial patterns of transport links and raw material availability (Henderson, 1988).

Total potential large demand CHP generation from local *Miscanthus* in England identified by this analysis is 25 PJ of heat and 7 PJ of electricity (see Table A1. 3). Calculated potential generation is reduced to 18 PJ of heat and 5 PJ of electricity by restricting feedstock transport, since two of the sites cannot be supplied from 25 km (see Table A1. 4). Since calculations are based on cultivation at 100% of suitable sites, it is likely that restrictions on feedstock transport distance would further impact generation potential. Whilst identified locations are indicative of heat demand, social and economic factors are critical to the potential for bioenergy CHP being used to meet this demand; non-renewable CHP, or generation of heat only, may be preferred. The use of an average utilisation factor of 57 % based on data for 2009 CHP may underestimate total potential, due to

exclusion of incomplete months from dataset, or failure to account for variation in proportions of heat and electricity, or on site usage. Furthermore current rates of downtime due to technical factors may be significantly reduced as the technology develops; utilisation factors of up to 80% are theoretically achievable (Thornley, 2006). This would increase competition for feedstock, and may make several sites no longer viable.

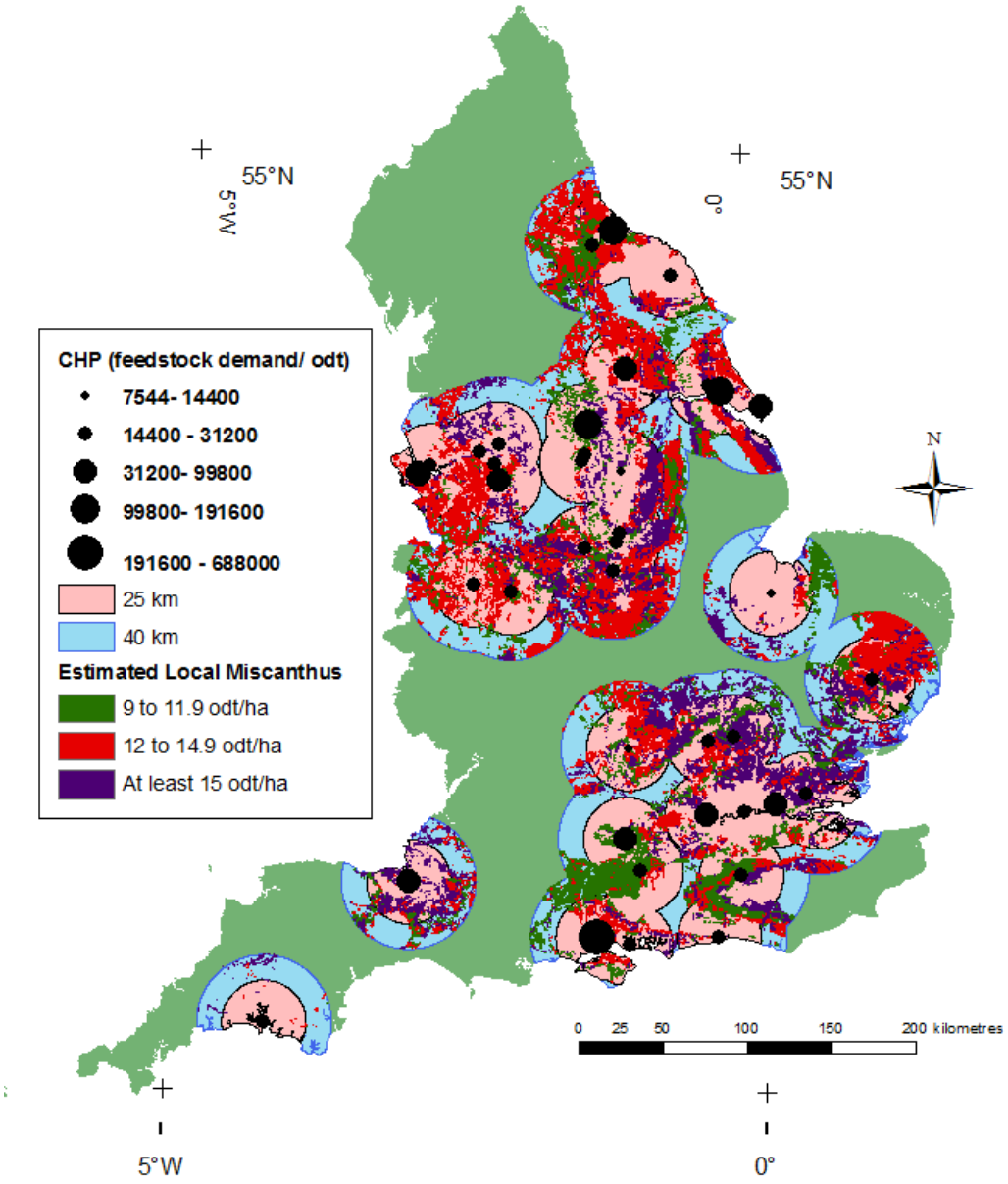

Figure 2.4 Map to show potential Miscanthus feedstock availability in relation to locations of potential demand for industrial and large scale Combined Heat and Power

2.9.3 CHP for district heating (DH)

As before, predicted *Miscanthus* yield data from Lovett *et al.* (2009) for the locations suitable for energy crop cultivation were clipped to the 40km and 25km feedstock transport zones using the methodology described in Section 2.7, and total local feedstock was calculated. Calculations were not performed for individual DH systems due to the complications described in Section 2.8.3. Figure 2.5 shows that potential DH installations are distributed in clusters throughout England. The map shows significant feedstock potentially available within 40 km of many of these sites. In regions with potential for DH, there is a total end user demand of 461 PJ of delivered heat, which would require 39 odMt of biomass feedstock, assuming 70% conversion efficiency, and without taking into account additional generation to cover distribution losses. Calculations indicated that in England 31 odMt could be cultivated for this purpose, producing 366 PJ of DH as well as 104 PJ of electricity; hence not all of England's potential for DH could be realised through local *Miscanthus* feedstock.

These values do not exclude feedstock which is also suitably located for other end uses; once this feedstock has been subtracted, the total combined energy generation potential from DH is 334 PJ, although distribution losses will apply to the generated heat. Were a 25km transport restriction imposed, feedstock availability drops to 25 OdMt, producing 295 PJ of heat and 84 PJ of electricity.

In practice, feasibility of meeting DH demand is dependent on heating requirements which vary with temperature, housing standards and population density, and the potential for cultivation close to higher population densities (Möller and Lund, 2010; Schmidt *et al.*, 2010). Total efficiency is increased by linking demands with different timings of demand i.e. accommodation and schools or offices, to facilitate a more consistent plant running capacity (Roberts, 2008). Previous work suggests optimum locations for DH generation are at the edge of urban areas (Schmidt *et al.*, 2010), with highest demand likely to coincide with urban centres such as capital cities. In England, greatest demand density is in London, which is entirely urbanised with no cultivation potential; however, data displayed in Figure 2.5 indicate significant local feedstock potential to the north of the city.

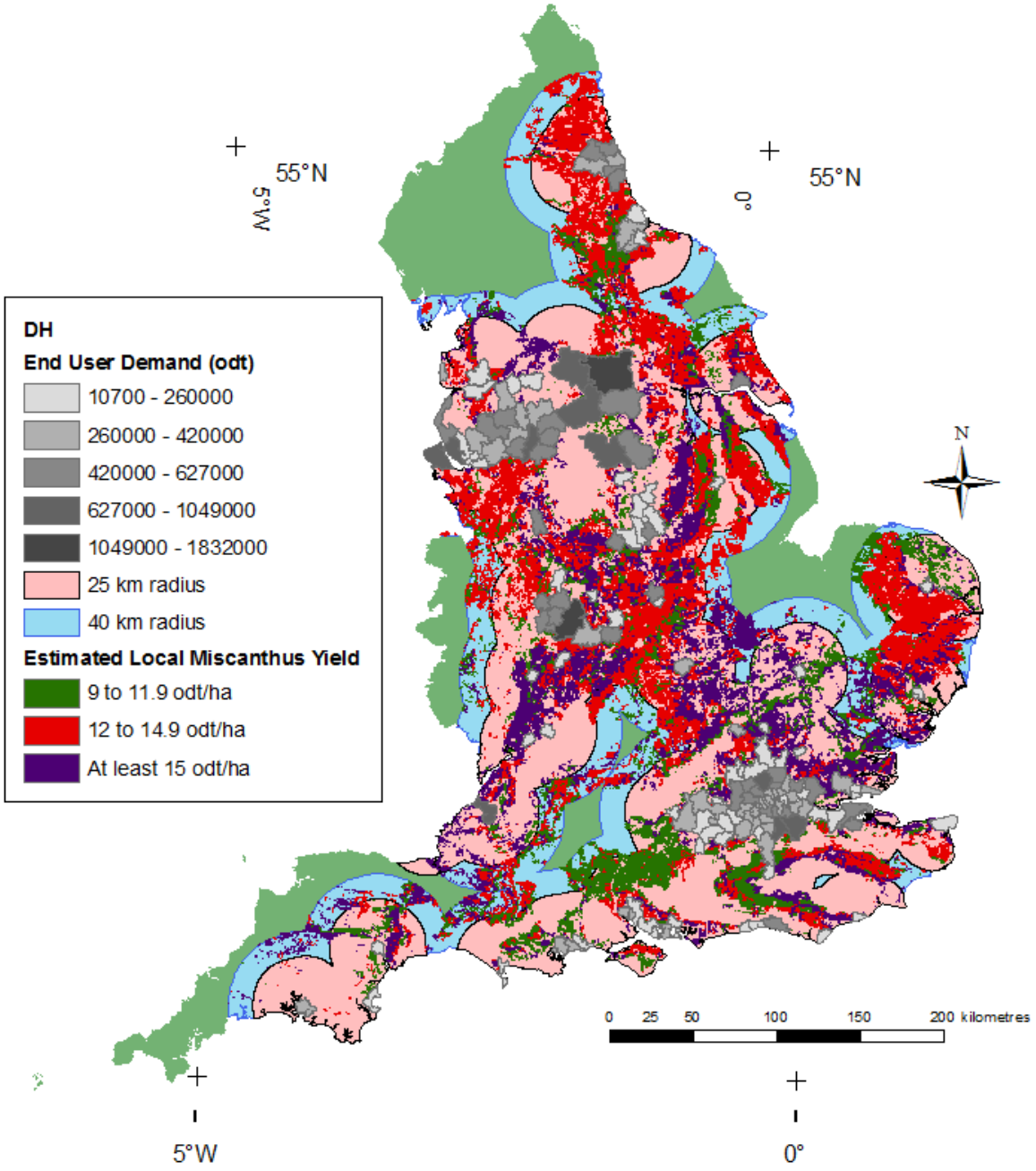

Figure 2.5 Map to show potential Miscanthus feedstock availability in relation to locations of potential District Heating installations. Grey and white zones indicate regions with potential for profitable DH systems, and feedstock located within 40 km of these zones is displayed

2.9.4 Competition for feedstock between identified end uses

Overlap of feedstock catchment zones for different forms of demand must also be taken into account since demand sites of each type tend to cluster in similar locations (Henderson, 1988). Figures 2.6 and 2.7 show the overlap between catchment zones of different potential end uses of biomass for energy. Overlap between feedstock catchment zones for different forms of demand can be significant; calculations for England applying 40 km radius showed that 11 odMt of feedstock have potential end-use competition between co-firing and large scale CHP. Generalised 40 km catchment zones for regions of DH potential cover much of England, with 10 odMt *Miscanthus* on areas coinciding with co-firing, and 21 odMt coinciding with industrial CHP.

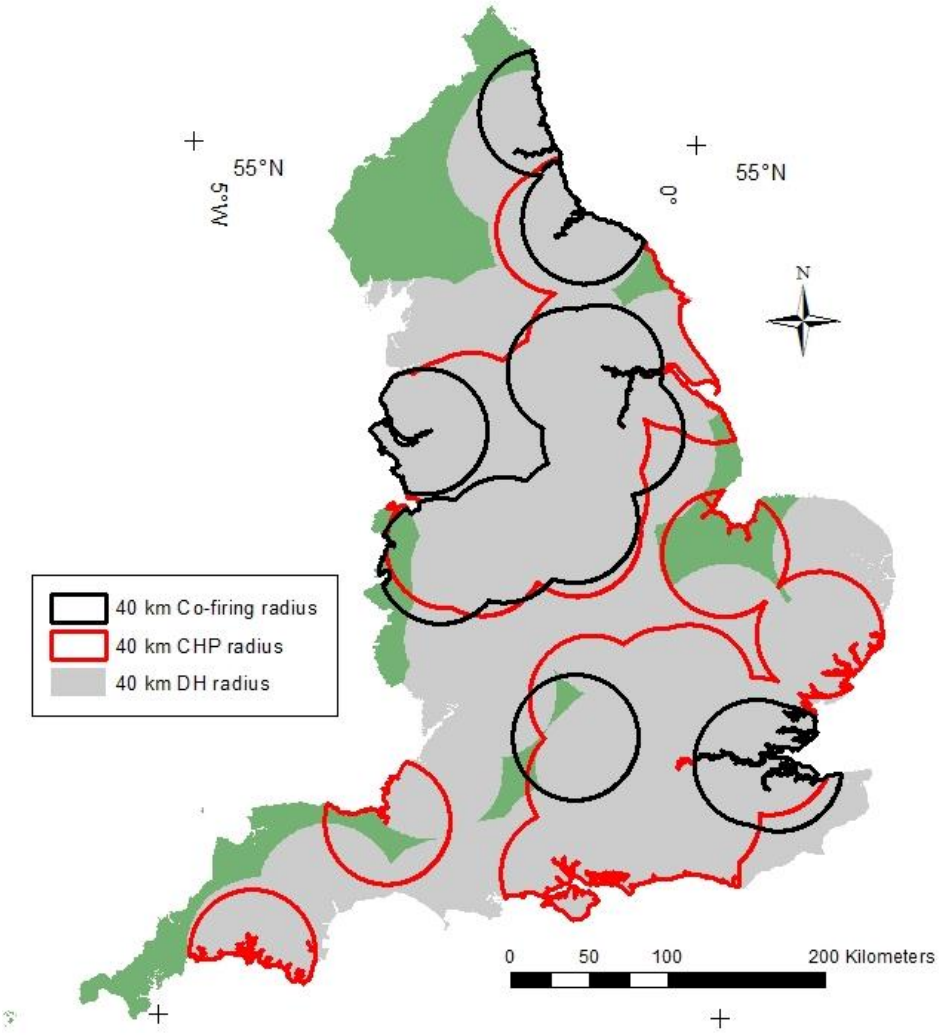

Figure 2.6 Map to illustrate overlapping of 40 km demand zones for identified Miscanthus energy end uses

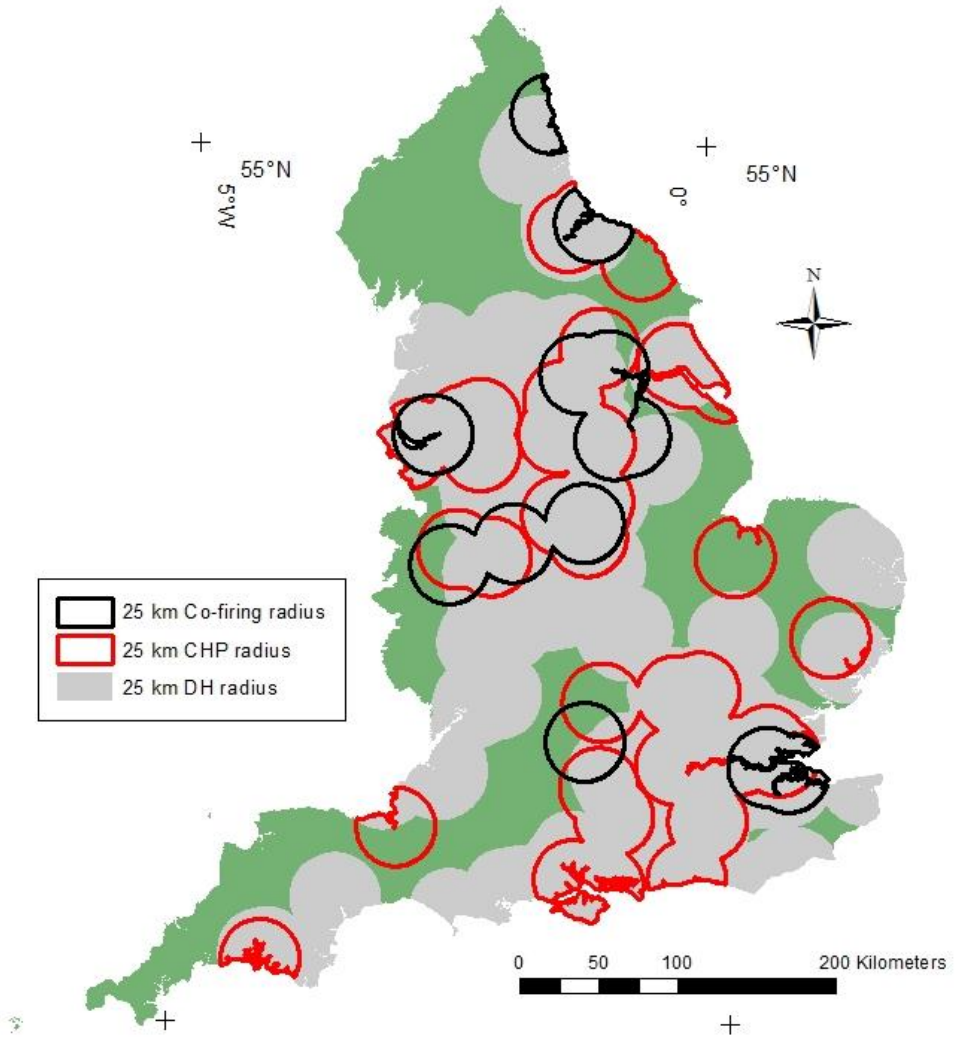

Figure 2.7 Map to illustrate overlapping of 25 km demand zones for identified Miscanthus energy end uses

Feedstock from areas identified in England as within 40 km of both industrial CHP and coal plants has a generation value of 38 PJ of electricity and 134 PJ of heat as CHP (at 20 % and 70 % conversion efficiency), or 57 PJ of electricity from co-firing with coal (at 30% conversion efficiency). This would appear to suggest that CHP may be a better choice if the objective is to increase the proportion of generation from renewables. Although in the scenario analysed here there is sufficient feedstock not to make allocation decisions between industrial CHP and co-firing, in practice cultivation is unlikely to take place on all available land, and competition for feedstock will be dependent on economics and spatial pattern of availability. Additionally, the associated CO_2 mitigation achieved through deployment of bioenergy generation is dependent on the reference system (i.e. the emissions from the generation replaced) as well as the life cycle analysis (LCA) of the bioenergy process (including cultivation and transport of feedstock as well as the power generation step).

Bioenergy LCA requires consistent, well defined, ideally inclusive system boundaries, as well as incorporation of site specific factors, particularly in terms of GHG balance of cultivation (Cherubini *et al.*, 2009). Therefore, if GHG emissions reduction is taken into account as a secondary aim, many other factors must be considered when comparing potential bioenergy generation. There is a need for system-specific LCA to gain a true picture of any benefits in terms of energy and GHG savings of CHP in practice (Martens, 1998).

Before transmission losses have been considered, DH efficiency is more than double co-firing efficiency, with potential generation from overlap feedstock of 168 PJ compared to 56 PJ. However, DH was prioritised last for overlap feedstock in these calculations due to significant socioeconomic obstacles in England.

When comparing DH and industry as end users of CHP there are further variables affecting efficiency, and therefore generation proportion; the large, consistent demand of industrial type users enables more efficient generation patterns (Hawkes and Leach, 2008), however the lower temperatures required by domestic end users enable a more efficient use of the full temperature spectrum of generated heat (Martens, 1998). Combination of industry and DH may, therefore, be the most efficient approach in terms of heat utilisation, although generation companies tend to prefer a single heat off-taker due to the complexity of contractual agreements (Bailey, 2011). Large demand sites such as hospitals, airports and public buildings may combine the benefits of domestic lower temperature requirements, with the large demand advantage of reduced infrastructure requirements, making an optimum location for CHP (Chicco and Mancarella, 2009).

2.9.5 Total potential bioenergy generation from identified end uses

Observations in section 2.9.4 suggest an order of preference for allocating feedstock of: large demand CHP, then co-firing, then DH, in order to achieve efficient usage of feedstock, whilst allowing for socioeconomic influences. Therefore, in Table 2.6, feedstock is allocated to CHP and co-firing up to the useful value, then non-excess overlap between DH and other uses is subtracted before total potential DH is calculated. A total of 406 PJ of energy could be generated annually

from local *Miscanthus* in England. This exceeds the DECC (2009) UK biomass generation target of 259 PJ or 30 % of the UK renewables target.

Table 2.6 Calculations of total potential generation applying a transport radius of 40 km

40 km	Useful local feedstock (odMt)	Electricity (PJ)	Heat (PJ)	Total (PJ)	Overlap (odMt)	Local excess (odMt)	Excesses - overlap (odMt)
Useful CHP	2.01	7	24	31	11.24	20.16	13.85
Useful co-firing	8.16	42		42		4.93	
						Non-excess overlap (odMt)	
DH	30.76				22.79	8.94	
DH-overlap	21.82	74	260	334			

Table 2.7 indicates that the target could, in fact, theoretically be met taking feedstock only from within the 25 km radius originally stipulated. However, since *Miscanthus* is unlikely to be grown at all potential sites, increasing the allowable transport distance improves prospects for bioenergy.

Table 2.7 Calculations of total potential generation applying a transport radius of 25 km

25 km	Useful local feedstock (odMt)	Electricity (PJ)	Heat (PJ)	Total (PJ)	Overlap (odMt)	Local excess (odMt)	Excesses - overlap (odMt)
Useful CHP	1.49	5	18	23	4.71	11.75	8.38
Useful co-firing	4.22	22		22		1.34	
						Non-excess overlap (odMt)	
DH	24.84				13.09	4.72	
DH-overlap	20.12	68	239	308			

Of the 407 PJ of energy identified in Table 2.6, 123 PJ would be electricity, around 1.4 % of the UK 2013 demand of 8972 PJ (Department of Energy and Climate Change, 2013a). Policy, regulation, economics and local choices would affect the generation balance and capacity achieved. The end use may affect the carbon and energy savings, and policy reflecting this may encourage optimum utilisation of potentially available biomass feedstock.

2.9.6 Land area requirements for identified potential biomass feedstock cultivation

The UK Biomass Strategy aims for 350,000 ha of land to be converted for perennial energy crops. This figure has been identified elsewhere as the maximum UK land availability for biomass (2008).

Therefore the 2.4 Mha identified here for England as viable for cultivation of *Miscanthus* within 40 km of the identified potential end uses of feedstock, may require further consideration of competition with other land uses, which could significantly reduce bioenergy generation potential.

Total potential cultivation area for Co-firing, large scale CHP and DH areas is shown in Figure 2.8, and has been mapped according to CEH data on 2007 land use using the extract tool, with CEH land use data as the input raster and identified cultivation locations as the mask. Potentially displaced land-uses include 1.5 Mha arable and horticulture, 0.69 Mha grassland as well as 0.05 Mha broadleaved woodland. To achieve the maximum potential generation of 406 PJ identified by this study, roughly 94 % of this land would need to be used. It has been suggested that 0.9- 3.6 Mha in the UK may be available for bioenergy (Hastings *et al.*, 2014). Upper estimates for the UK may indicate that the area of land indicated by this study could be made available in England, however land may still not be available in the identified areas or from the identified current land uses.

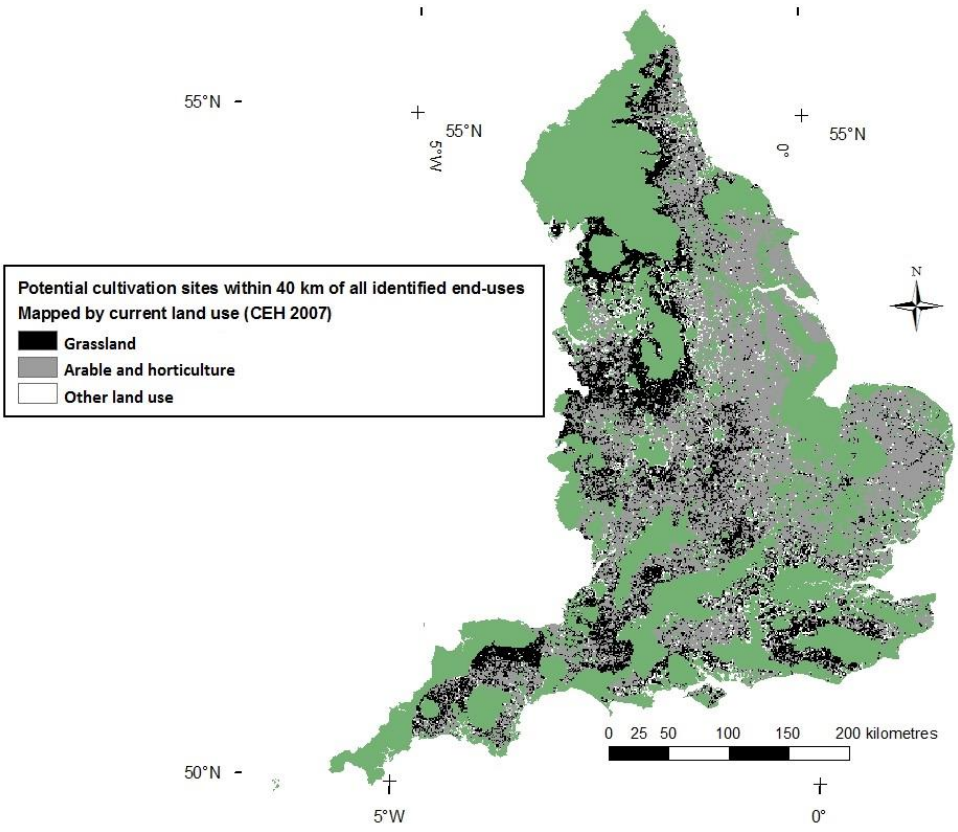

Figure 2.8 Map to illustrate current land use for potential cultivation sites identified by this study

To meet the 2011 UK biofuel target of 27 PJ using wheat bioethanol, 3 Mt of cereal would be required (Akgul *et al.*, 2012), threatening food availability. Generating the same amount of energy from industrial CHP would require 1.7 odMt feedstock; assuming a distribution of yields and land use representative of the whole area, this would require 0.13 Mha, which would displace approximately 0.08 Mha arable as well as loss of 0.04 Mha grassland. Assuming average cereal yields for converted land (based on 2012 data (Department for Environment Food and Rural Affairs, 2012)), this would result in a loss equivalent to roughly 0.51 Mt cereal. Highly productive agricultural land was excluded from consideration (as described in Lovett *et al.*, 2009) so use of average yields should not underestimate the impacts. Due to lower than expected yields in the UK in 2012, there was net import of 0.97 Mt cereal, compared to 1.2 Mt net export from the UK for 2011. Whether the impacts of land use change could be offset by reducing exports to maintain food security is therefore uncertain, and dependant on yields; in either case there will be economic trade-offs and changes to balance of trade. As well as considering economics and impacts on food security, GHG emission associated with land use change must be considered (Del Grosso *et al.*, 2005; Li *et al.*, 2005); Chapters 3, 5 and 6 look to address this. Indirect land use change to replace cereal losses may take place in the UK or overseas in countries previously receiving the imports. Accounting for and attributing land use change is complicated when considering a global system with a range of drivers in addition to bioenergy cultivation (Kim *et al.*, 2012). Although it has been suggested that improvements in farming techniques and cereal genotypes may offset some losses, data for the UK indicate reduction in average yield since 2008 (Department for Environment Food and Rural Affairs, 2012). Previous work has suggested that much of the emissions linked to bioenergy may be caused by land-use change and increased fertiliser inputs to compensate for land coming out of food agriculture (Melillo *et al.*, 2009).

2.9.7 Other factors affecting total potential bioenergy generation as identified in this chapter

The complexity of agricultural systems dictates that yield predictions based on model output should be regarded only as a guide (Price, 2004; Schoumans *et al.*, 2009). Model *Miscanthus* yield predictions were supplied as three ranges, and although average estimates were used in calculations, this is not a guarantee of feedstock availability. Based on these ranges, total potential cultivation on land identified by this study would range from 30 odMt to 35 odMt, as indicated in Table 2.8.

Table 2.8 Data for calculation of range in simulated yield

Simulated yield range	Relevant area (ha)	Minimum yield prediction (odt)	Maximum yield prediction (odt)
9-12.9	490783	4417047	5840318
13-14.9	1154703	13856436	17205075
15 or greater (16 used)	764055	11460825	12224880
Total	2409541	29734308	35270272

Inter-annual yield variability with temperature, radiation and precipitation may exceed model predicted ranges, and yield variation between genotypes and between species interacts with spatial and climate factors (Lovett *et al.*, 2009; Richter *et al.*, 2008). Feedstock type is also significant; predicted yields are for a the hybrid *Miscanthus* x giganteus, chosen due to its high yield in field trials in England (Lovett *et al.*, 2009), however other *Miscanthus* variants, or alternative energy crops such as SRC willow or SRC poplar may produce higher yield at some sites, hence a mosaic of different feedstocks may give higher total yield (Clifton-Brown *et al.*, 2001). Contracts between biomass power plants and farmers tend to be agreed based on minimum expected yield for a specific site, to ensure that the plant has reliable supply (Spackman, 2011). Annually varying spatial patterns of availability will affect feedstock costs as well as required transport distances and costs. An increase in allowable transport distance may be helpful in enabling demand to be met in years when more local sites experience low yield, hence capping transport distances to minimise emissions may diminish feasibility.

Feedstock demand calculations were based on average efficiency values for existing power plants. As well as existing variation in efficiency, future technological improvements in efficiency may affect demand. Coal is a mature technology and CHP already has high efficiency in terms of total output, making efficiency improvements unlikely, although future developments in CHP could improve efficiency at higher proportional electricity generation, which would allow efficient generation flexibility (Gross, 2003). This would be particularly beneficial for DH systems, since heat demand is likely to drop with increasing insulation standards, whilst electricity demand tends to rise with proliferation of technologies (Roberts, 2008).

A radius of 40 km was used to approximate 40 km road transport regions, since it is impractical to incorporate site specific data on potential transport routes. Hence, this approach may generate optimistic estimations of local cultivation potential, particularly in regions with limited road networks. Lower emissions for boat transport may mean that GHG emissions savings can be

maintained over longer distances for non-road transport, however costs may be prohibitive, depending on feedstock costs.

Due to differences in parameters and considerations, total generation values calculated here were much lower than the 809 PJ heat and 405 PJ electricity calculated by Wang *et al.* (2014) and higher than the 0.21-0.83 PJ primary energy mentioned in Hastings *et al.* (2014). Wang *et al.* (2014) performed calculations for the whole UK, and incorporated greater heat demand by combining domestic and non-domestic space heating demands, and applying a model to meet all demands as opposed those over a set threshold. Additionally, for this thesis, analysis in Section 2.9.5 allocated feedstock to co-firing (lower energy output) before DH (higher energy output) due to lower investment requirements, and less socioeconomic considerations. Hastings *et al.* (2014) also consider the whole UK, however total values quoted are based on an average energy ratio (or "energy intensity" from Hastings *et al.*, 2009), and thus energy inputs to the system have already been subtracted from the values quoted.

Land availability for biomass is based on holistic GIS assessment of land use impacts (Lovett *et al.*, 2009), although in practice an in-depth site specific assessment may identify reasons why land use change should not or would not take place. Potential reasons include: habitat mosaic impacts on food webs (Firbank, 2008); excessive GHG emissions from disruption of soil (Brandão *et al.*, 2011; Fargione *et al.*, 2008; Natural England, 2009a); and water use of *Miscanthus* compared to existing land cover (Richter *et al.*, 2008; Vanloocke *et al.*, 2010). Conversely, constraints mapping rules out environmentally sensitive landscapes and grasslands which, if economically attractive, may be converted for biomass. This may increase local potential capacity of biomass generated energy, but the potential environmental impacts should also be taken into account (Lovett *et al.*, 2009).

CHP has a conversion efficiency over double that of co-firing, reducing environmental impact per unit of useful energy. However economic not environmental issues are likely to control the rate of expansion in generation from biomass; co-firing may be initially cheaper since little investment is required, whereas new district heating would require significant investment in infrastructure, which may deter energy generators. The costs and commitment of land required for perennial feedstock cultivation mean that guaranteed income may be a pre-requisite for cultivation. Where policy has economic implications, it can become a deciding factor, making it crucial that low-carbon future objectives are supported without unsustainable detriment to the environment or

food production. Encouraging cultivation of biomass feedstock for CHP whilst minimising food security detriment, as well as safeguarding the environment, is highly complex. Ideally policy incentives and sustainability assessment should reflect this, without adding uncertainty to an already imperfect market.

Socioeconomic factors which complicate supply chain establishment (as discussed in Section 2.2 above) may present the greatest obstacle to the expansion of bioenergy generation, along with policy factors affecting confidence in profitability of generation and cultivation (as discussed in Sections 2.4 and 2.6). Incomplete usage of installed bioenergy generation was observed in in part due to co-firing with cheaper non-renewable feedstock and, unplanned plant downtime due to technical problems (Thornley, 2006).

Existing housing stock represents a significant heat demand, however retrofitting of district heating systems is costly and disruptive, and homeowners may choose not to be connected, reducing demand density, potentially below profitable levels (Rüdig, 1986; Vallios *et al.*, 2009). On the other hand it is easier and cheaper to fit DH systems when building new housing, and planning permission can be used as leverage to encourage this; however greater thermal efficiency of new build may reduce peak heat demand by 50-90%, thus reducing viability in terms of demand density threshold, as well as emissions and energy savings (Hawkes and Leach, 2008; Roberts, 2008; Wood and Dow, 2011). In addition to this, lack of familiarity may mean lower investor interest and homeowner confidence in DH systems, and is likely to be a significant obstacle to new projects in the UK (Vallios *et al.*, 2009). These socioeconomic barriers to uptake of DH could significantly affect total bioenergy generation potential; without DH, total potential generation for England drops from 406 PJ to 72 PJ. Current land use for the area suitable for cultivation of perennial energy crops for large scale CHP or co-firing is indicated in Figure 2.9, and consists of around 0.7 Mha arable and 0.3 Mha grassland.

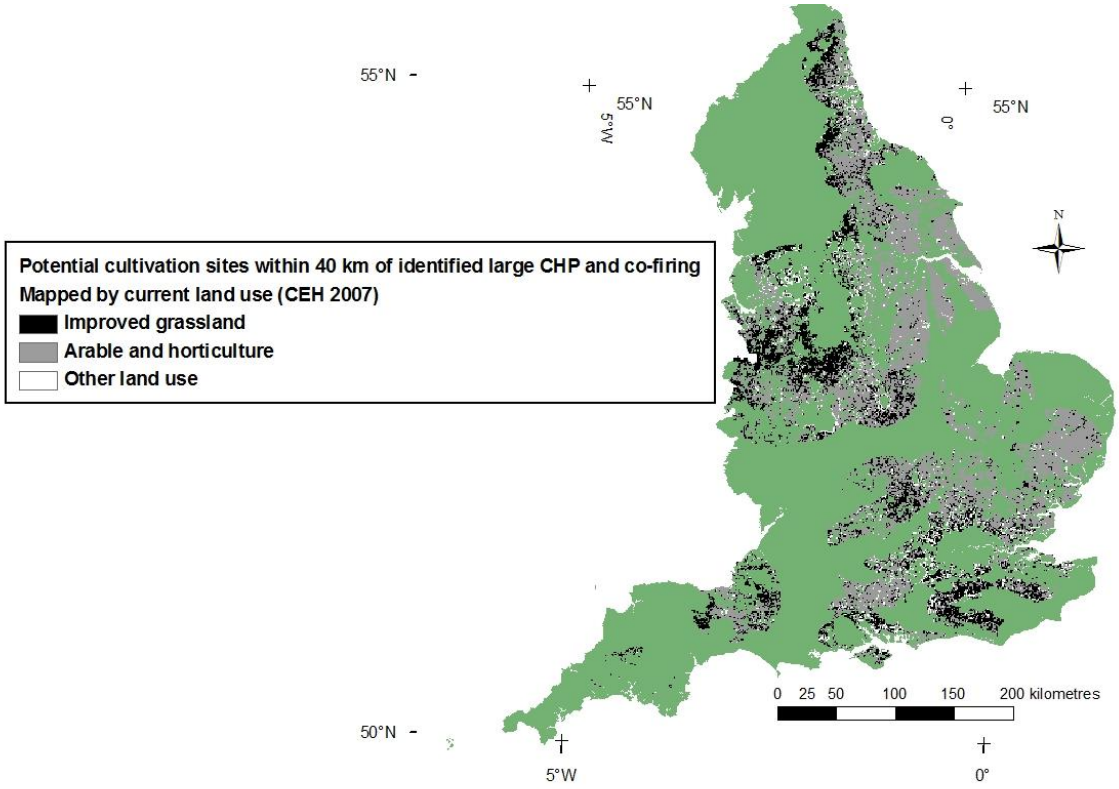

Figure 2.9 Current land use for suitable cultivation sites within 40 km of potential CHP and co-firing end uses

Social opposition to land use change must also be considered; there is a perception of a conflict between cultivation of food and fuel, since it is assumed that food could have been cultivated on land which may be taken up for cultivation of energy crops, and there is evidence of rising prices and declining production (Mitchell, 2008; Nonhebel, 2005). However the significance of pressure on land varies between countries. For England, food production is not limited by land or water availability, and food export was increasing prior to reductions in yield associated with poor weather conditions in 2012 (Department for Environment Food and Rural Affairs, 2012; Paice, 2011). Kim *et al.* (2012) suggest that the "food versus fuel" problem should in fact be reframed as "nutrition versus fuel" with consideration of the land use efficiency of human dietary choices, and resultant impacts of cultural preferences and trends.

Unlike other energy types, bioenergy may have focussed regional impacts, particularly in rural areas, due to spatial constraints on supply chains. Objections to associated infrastructure, traffic and landscape change may create a barrier to planning permission for plants. Alternatively, there may be many benefits to the rural economy, and for rural areas not connected to the gas grid, bioenergy heating schemes can offer significant savings over alternatives (Thornley, 2006).

2.10 Soil data analysis for potential sites

Given the significant socioeconomic barriers to district heating systems in England and the incomplete nature of the assessment of DH in this thesis, locations suitable for cultivating feedstock for co-firing and larger scale CHP were chosen for the final analysis. These were overlaid in GIS with the Centre for Ecology and Hydrology 2007 land cover map at 1km resolution (Centre for Ecology and Hydrology, 2011), and harmonised soil data layers from JRC (European Commission - Joint Research Centre and Institute for Environment and Sustainability) including bulk density and texture of topsoil and subsoil, the depth to textural change and organic carbon and pH of topsoil at 1km resolution. The ARC GIS sample tool was then used to produce a table of values from these soil and land use data layers, at points spatially coinciding with yields over 9 odt ha^{-1} from the raster file of the identified potential cultivation sites. Sample points were taken from these data on a 10 ha by 10 ha grid, creating a database of over 30,000 cases.

It has been noted by Aylott *et al.* (2008) that energy crop yield is controlled by interaction between site properties. Given the likelihood that change in ET and soil C storage will be affected by yield, the occurrence of site factors in combination as opposed to individually may be more significant in controlling these outputs, than individual site properties. The same is true of N_2O emissions, given that different processes are responsible for N_2O production in different soil types, and taking into account the complexity of controlling processes, which will be introduced in Section 3.4. Therefore to extrapolate from model output to multiple sites it is necessary to look at combinations of site properties.

A two-step cluster analysis was run to identify the most common combinations of site properties in this sample, in order to produce input files for modelling representative sites. Two-step clustering was chosen because this test is the most appropriate for datasets with over 1000 cases, and can be performed for data which are not normally distributed, and include categorical variables (Kaufman and Rousseeuw, 2009). It was necessary to use log-likelihood as the measure of distance between cluster centres, since Euclidean is only appropriate for continuous variables. The data are categorical, with each category covering a range of numerical values, as can be seen in Table 2.9 and 2.10. To account for the maximum and minimum numerical values in each category, two model runs must be performed for each site. Given the time demands for compiling input data, running the model and analysing output, and limited time availability at the modelling

stage, it was decided to limit the number of sites analysed to 12 (i.e. 24 model runs). Since each soil type and land use combination will be modelled for one location with low precipitation and one with high, this means that six clusters are required as output from this analysis. In order to have three clusters at arable sites and three at grassland sites, the number of clusters was set to three.

Because the model sets soil organic matter pools by simulating historic land use using a "spin up" period approach (described in Section 4.2), numeric SOC values are not required for model input, hence category values from high to very low (according to JRC classifications) are used for this variable also.

The three clusters indicated in Table 2.9 all have land use as arable and horticulture, which can be seen in Figure 2.9 to apply to the majority of identified sites. However, grassland has less economic value, so may be more likely to be used for cultivation of energy crops, assuming high yields can be expected. Tillage of grassland may cause significant carbon loss, so it is particularly useful to perform modelling for these sites. Therefore a second cluster analysis was performed on the grassland subset of the data, which is shown in Table 2.10. The 25km CEH land cover map differentiates between improved, neutral, acid and calcerous grassland, however the 1km resolution version used for data extraction has aggregated classifications, so grassland is either improved or unimproved. Improved grassland was ruled out for economic reasons as part of the original constraints mapping, so grassland considered in Table 2.10 is in the broad category "unimproved grassland". The pH differences between acid, neutral and calcerous grassland may be accounted for by the soil pH layer from the JRC harmonised soil layers, however resulting differences in other site properties may not be completely represented in the model, as will be discussed in Section 6.2.

Other parameters which will interact with the soil parameters tabulated in determining yield and other outputs include latitude and climate variables; these will be discussed when scenario analyses are developed in Sections 6.1 and 6.2.

Table 2.9 Combinations of site properties typical of identified locations, as extracted by cluster analysis

Cluster1	**Cluster 2**	**Cluster 3**
39%	32%	26%
15140 cases	12564 cases	11556 cases
Depth to textural change	**Depth to textural change**	**Depth to textural change**
>120 cm	20-40 cm	20-40 cm
82 %	57 %	26 %
Depth to gleyed horizon	**Depth to gleyed horizon**	**Depth to gleyed horizon**
<40 cm	<40 cm	>120 cm
59 %	100 %	75 %
Subsoil Packing Density	**Subsoil Packing Density**	**Subsoil Packing Density**
high	high	medium
90 %	100 %	93 %
Topsoil Packing Density	**Topsoil Packing Density**	**Topsoil Packing Density**
medium	low	medium
99 %	100 %	75 %
Soil organic carbon	**Soil organic carbon**	**Soil organic carbon**
very low	medium	very low
29 %	81 %	37 %
pH	**pH**	**pH**
5-6	5-6	6-7
62 %	84 %	51 %
Subsoil texture	**Subsoil texture**	**Subsoil texture**
fine (35%< clay<60%)	fine (35%< clay<60%)	medium (18%<clay < 35% and sand>=15% or18%<clay and 15%<sand<65%)
91 %	82 %	52 %
Topsoil texture	**Topsoil texture**	**Topsoil texture**
fine (35%< clay<60%)	medium (18%<clay < 35% and sand>=15% or18%<clay and 15%<sand<65%)	coarse (18% < clay and > 65% sand)
57 %	100 %	50 %
Water regime	**Water regime**	**Water regime**
Wet within 80 cm for over 6 months, but not wet within 40 cm for over 11 months	Wet within 40 cm depth for over 11 months	Not wet within 80 cm for over 3 months, nor wet within 40 cm for over 1 month
69 %	100 %	87 %
Land use	**Land use**	**Land use**
arable and horticulture	arable and horticulture	arable and horticulture
70 %	50 %	67 %

Table 2.10 Combinations of site properties typical of identified locations, as extracted by cluster analysis of grassland sites only

Cluster1	**Cluster 2**	**Cluster 3**
48 %	31 %	19 %
5424 cases	3581 cases	2216 cases
Depth to textural change	**Depth to textural change**	**Depth to textural change**
>120	>120	>120
53 %	60 %	100 %
Depth to gleyed horizon	**Depth to gleyed horizon**	**Depth to gleyed horizon**
<40 cm	>120 cm	<40 cm
100 %	87 %	90 %
Subsoil Packing Density	**Subsoil Packing Density**	**Subsoil Packing Density**
high	medium	high
98 %	75 %	100 %
Topsoil Packing Density	**Topsoil Packing Density**	**Topsoil Packing Density**
low	medium	medium
100 %	76 %	100 %
Soil organic carbon	**Soil organic carbon**	**Soil organic carbon**
medium	very low	medium
76 %	49 %	58 %
pH	**pH**	**pH**
5-6	6-7	5-6
82 %	47 %	82 %
Subsoil texture	**Subsoil texture**	**Subsoil texture**
fine (35%< clay<60%)	medium (18%<clay < 35% and sand>=15% or 18%<clay and 15%<sand<65%)	fine (35%< clay<60%)
76 %	34 %	100 %
Topsoil texture	**Topsoil texture**	**Topsoil texture**
medium (18%<clay < 35% and sand>=15% or 18%<clay and 15%<sand<65%)	medium (18%<clay < 35% and sand>=15% or 18%<clay and 15%<sand<65%)	fine (35%< clay<60%)
94 %	45 %	100 %
Water regime	**Water regime**	**Water regime**
Wet within 40 cm depth for over 11 months	Not wet within 80 cm for over 3 months, nor wet within 40 cm for over 1 month	Wet within 80 cm for over 6 months, but not wet within 40 cm for over 11 months
93 %	62 %	70 %
Land use	**Land use**	**Land use**
grassland	grassland	grassland
100%	100%	100%

2.11 Summary

This chapter has outlined the approach taken to identify sites where perennial bioenergy crops such as SRC willow or *Miscanthus* could be grown in England. The approach was based on integrating data on where the crops could be grown with data on locations of high efficiency potential end uses. The approach aims to avoid excessive transport of feedstock and low efficiency energy conversion, both of which reduce the overall ratio of energy out to energy in, as well as increasing relative and absolute GHG emissions. Potential generation of 406 PJ of energy was identified; reducing to 72 PJ if DH schemes are excluded. The approach taken is based on logical decisions about feedstock cultivation and allocation in order to maximise energy generation, whilst in reality socioeconomic factors will control such decisions. Additionally, socioeconomic barriers to expansion of bioenergy such as establishment of supply chains for bioenergy feedstock, uncertainty about government incentive schemes and lack of familiarity with DH have been identified.

The land area identified here as potentially suitable for cultivation of bioenergy crops is largely arable, and could have significant impacts on food production, although per PJ of energy, these would be much lower than for cultivation of cereal crops for liquid biofuels. Data on the locations identified as suitable for cultivation was used to identify common combinations of soil properties which affect site specific impacts of land use change, in terms of soil and climate properties which may affect change in N_2O emissions and soil C, as well as crop yield and ET. Cluster analysis has been used to identify three common arable site types, and three common grassland site types. The following chapter (Chapter 3) assesses approaches for predicting change in N_2O emissions, soil C and ET for land use change at these sites. These data were used as input to modelling in Chapter 5, wherein the selection of geographic locations at which each typical soil type occurs, and creation of site and weather input data files is also described.

3. Selecting a model to predict environmental impacts of land use change for perennial energy crops

This chapter addresses Objective 3; to assess approaches for predicting perennial energy crop yield along with change in N_2O emissions, soil C and ET for land use change.

Section 3.1 identifies gaps in existing assessment of the impacts of land use change for SRC willow and *Miscanthus* on water use, direct GHG emissions from soil, and indirect GHG emissions from downstream transformation of leached nitrates. The need for assessment approaches which can adequately represent how site factors interact to control these impacts is articulated. Section 3.2 gives the rationale for taking a whole agroecosystem approach in order to simulate interaction between crop, soil and atmospheric systems, which is supported by the illustration of C, N and water cycling for an agroecosystem in Figure 1.1 of Chapter 1. Section 3.3 explains multi criteria decision analysis (MCDA), and how the stages of identifying and addressing multiple criteria are appropriate for selecting a whole-agroecosystem model. Section 3.4 takes a literature based approach to identify required representation of potential agroecosystem impacts of land use change for perennial energy crops and variation between sites. Section 3.5 states the approach taken to compile a database of potential models. A two-step MCDA is then applied; Section 3.6.1 takes a conjunctive approach to rule out models which do not meet crucial criteria, and Section 3.6.2 applies factors specific to this study to select which of the suitable models will be used. The chosen model is described in Section 3.7 and will be refined in Chapters 4 and 5, and then in Chapter 6, will be applied to the locations identified by Chapter 2.

3.1 Limitations of existing assessment of site variation in identified impacts of land use change for perennial energy crop cultivation

Chapter 1 discussed several factors which could lead to site variation in the identified impacts of land use change for perennial energy crops. Specifically;

- Section 1.4.1 outlined how anticipated increase in soil C storage will be dependent on current crop type, management and C storage
- Section 1.4.2 described how change in N_2O emissions will be dependent on current nutrient inputs, rates of nitrification and denitrification and soil texture and drainage
- Section 1.4.3 identifies that change in ET and impacts on water availability or flood risk will be dependent on climate, root access to water table and how perennial crop growing season varies from that of current land cover

Section 2.6 of Chapter 2 introduces ECS funding, which covers 50% of establishment costs, reducing the economic barrier for farmers considering cultivating perennial energy crops. Currently, the extent of environmental appraisal required for ECS is dependent on recent land use history. Environmental Impact Assessment (EIA) is required for crop cultivation on natural or semi natural land (as defined by flora and fauna), or land that has not been managed for 15 years. In the EU, there is variation in the level of permits required for a bioenergy project, and no universal requirement for prediction of environmental impacts of associated land use change (IPCC, 2006a). Policy for indirect land use change is limited and there is added complexity with the difficulty of attributing land use change for agriculture to displacement by energy crops, as opposed to population increase and dietary change (Gawel and Ludwig, 2011; Kim *et al.*, 2012; Smith *et al.*, 2010b). Alternatively it has been suggested that increases in yield due to agronomic improvements and new varieties may reduce land use requirements for food provision, for example, assuming 50 % increases in arable yields, Perlack *et al.* (2005) suggest that by 2030 24 Mha of agricultural land in the U.S. could be converted to biomass without reducing food production. In a global system, with other changes to agricultural systems and efficiencies to account for, attributing land use change to energy crop cultivation, and identifying particular schemes as responsible is even more complex (Kim *et al.*, 2012).

Where EIA is required for ECS some of these issues are likely to be assessed if they are identified as important for that site. For example where water shortages are a concern, the risk of exacerbating these would be considered by EIA. ECS appraisal suggests that sandy soils and low rainfall may cause water availability to limit yields, but does not discuss potential impacts on local hydrology if roots have access to groundwater. Economically it would be unwise for perennial energy crops to be cultivated where irrigation might be required, or where yields might be limited by water availability, and therefore some level of consideration by a farmer is likely before land use conversion

The issue of GHG emissions associated with bioenergy cultivation was not well considered until assessments by Fargione *et al.* (2008) and Searchinger *et al.* (2008) in 2008. However, there are a standard set of IPCC guidelines set out for calculating the GHG impacts of land use change (IPCC, 2006b). Underestimating impacts of direct and indirect land use change risks failing to identify net increase in GHG emissions, as well as ecological impacts such as biodiversity loss, whereas overestimation stifles bioenergy development unnecessarily (Gawel and Ludwig, 2011). In theory ECS provides leverage to put a more thorough sustainability assessment in place, however such assessment should not be too costly or off-putting to farmers.

Woody perennial energy crops fall under the forestry commission 1999 regulations requiring EIA for afforestation on designated sites, or for plots over 2 hectares on all other land (Natural England, 2009). Although EIA is intended to ensure sustainable development, there is often a focus on socioeconomic sustainability and local ecological impacts, as opposed to broader environmental impacts, and there is not always a requirement to predict GHG balance or change in water use (Bond *et al.*, 2010). There is an intention to build in consideration of sustainability in terms of GHG emission savings and variation with feedstock and site, however this is not included in the latest appraisal guidelines (Natural England, 2013).

The IPCC methodology for calculating GHG from land use change is a three tiered approach. Tier 1 requires least data, applying previous C storage assumptions based on ecosystem type, and biomass accumulation rates according to agroecosystem and climate region. Tier 2 improves on Tier 1 by application of country specific rates for new biomass accumulation, and accounting for incomplete removal of previous biomass. Tier 3 is most data intensive, and applies measured data on existing biomass and calculates accumulation rates based on species and management specific factors, local climate and soil, and process based models (IPCC, 2006a). Similarly the IPCC methodology for emissions from N inputs has three tiers building from generalised emissions factors (EF) to more process based modelling for Tier 3, for which data may be difficult to acquire. Site specific variation in response to land use, and land use change outlined in Section 1.3 is not incorporated into Tiers 1 and 2 of the IPCC approach.

To minimise data requirements and costs, in most cases either Tier 1 or 2 is applied, with Tier 3 only applied where the land classification has been identified as significant for changes in C stocks (IPCC, 2006a). However, current understanding of crop soil processes is incomplete making such change difficult to anticipate, and furthermore change in N may be more relevant in terms of GHGs. Due to the data requirements of process based models advocated by the IPCC Tier 3, it would be impractical to perform modelling for all potential sites, however, the application of such a model at a range of sites, combined with appropriate assessment of the findings, may improve current understanding of site specific factors controlling GHG impacts of land use change.

The IPCC land use change assessment focuses on GHG emissions, meaning that change in ET for a new crop is not considered, although it could be an output for a Tier 3 process based model, and would be incorporated by a full EIA. This consideration may be restricted to economics, and may not give in depth consideration to ecosystem impacts where it is not obligatory. To avoid increasing flood risk by physical obstruction of water flow, ECS applies restrictions to locations on the one in 200 year flood plain; planting is not permitted 500m upstream or downstream of urban areas, or within 10m of the river channel (or five times the river width if larger)(Natural England, 2013).

Since both Willow and *Miscanthus* have low nutrient input requirements, potential N_2O emissions are unlikely to be thoroughly assessed. It is likely that tier 1 and 2 of the IPCC methodology would be applied, as described in section 2.6. These approaches do not take into account variables such as tillage, crop species, fertiliser type and timing of application or site specific factors such as soil type and drainage, all of which influence field N_2O emissions response to fertiliser (Brown *et al.*, 2002; Keoleian and Volk, 2005). There is some broad allowance for variation in soil and climate, such as country specific values, and an additional EF for organic soils, but this is not adequate to capture likely variation between sites as identified in Section 1.4, and is more useful for national scale assessment than choosing between sites (IPCC, 2000; Smeets *et al.*, 2009). The IPCC tier 1 and 2 approach also fails to account for the varying rate of residue decomposition with species and part of plant (Novoa and Tejeda, 2006) which is of particular importance for representing inputs with high C:N ratios such as those from SRC willow (Jug, 1999) and *Miscanthus* (Foereid *et al.*, 2004a; Heaton *et al.*, 2010), as these increase N immobilisation (Delgado *et al.*, 2010).

For changes in soil C tiers 1 and 2 of the IPCC methodology are usually applied, requiring application of emission factors, or use of inventory values, which may be specific to country and land use type, but again these will not identify differences for soil properties and precipitation regime identified for the sites to be assessed in this thesis. Where land classification has been identified as significant for changes in C stocks tier 3 assessment will be applied, although for many sites the data required may be difficult to acquire (IPCC, 2006a).

For both C and N, IPCC tier 3 involves site specific modelling studies; this can provide site specific output on changes in soil C stocks, N_2O emissions and water availability, enabling comparison of relative benefits of cultivation at different sites. This would also identify potentially significant impacts of soil disturbance in terms of N_2O and CO_2 emissions for sites not currently tilled.

Since the IPCC tier 1 and 2 approaches cannot identify where interactions of site factors will create variation between sites in terms of the identified impacts of land use change for bioenergy, there is arguably a need for tier 3 assessment, using process based models. This study aims to identify an existing model suitable for predicting water usage, soil carbon storage as well as GHG emissions from land use change for SRC willow and *Miscanthus* in the UK, in line with the IPCC tier 3 approach. Associated time and data requirements make it prohibitive to do such assessment for all sites at which land use change may occur, however by applying the model at each of the typical sites identified by cluster analysis in 2.10, inferences can be made about other sites with similar properties, and could be used to inform policy decisions.

3.2 Potential for a whole agroecosystem predictive modelling approach

Ideally, field data would be available on the relevant impacts for land use change for, and cultivation of, perennial energy crops at a range of sites reflecting typical soil properties and climate conditions. Although field experiments are costly, and considerable time is required for assessment of a full lifecycle, there are multiple studies underway, for example the Forestry Commission are cultivating experimental plots of SRC willow at multiple sites throughout the UK, and researchers at Rothamsted, led by Angela Karp, have plots of *Miscanthus* which have been studied for 20 years. Given that N_2O emissions may vary by 3 orders of magnitude over a period of days, and exhibit greater than 100% variation in coefficients of spatial variation, point

measurements from field studies may not be informative (Jarecki *et al.*, 2008). Since field studies tend to apply little or no N fertiliser, N_2O is often not measured at test plots, and furthermore, to assess change in N_2O emissions would also require field data for previous land use, which is unlikely to be available.

Comparatively, models are a cheap, quick and convenient way of predicting impacts of possible land use and management changes (Chirinda *et al.*, 2010). Models can apply equations to represent relevant processes, and how these interact to produce changes to the system. Models tend to apply temporal discretisation to solve these equations for a given point in time - i.e. using a daily or hourly time step, and calculating the change in the system over this time. Spatial discretisation is also applied, for example in a one dimensional model; a finite difference approach can be used to simulate vertical water movements through a continuum of soil, by splitting it into layers, and solving the relevant equations for each layer separately (Li *et al.*, 2007).

N cycling is complex and there is incomplete understanding of many of the factors required for representation, for example: factors affecting N_2:N_2O ratio (Section 1.4.2.3); changes in N_2O production and emission with tillage (Section 1.4.2.4). Prediction and model representation is also complicated by spatial variation in processes. Wagener and Gupta (2005) state that statistical models can perform better when representing poorly understood processes, however statistical models are based on input output data relationships, meaning that performance decreases when applied to new situations.

The impacts of land use change for cultivation of perennial energy crops on carbon, nitrogen and water cycling are site specific, and variation in these affects overall benefits of bioenergy. Statistical models are therefore inappropriate for scenario analysis where differences between sites are significant, and site calibration data are unavailable (Frolking *et al.*, 1998; Groffman *et al.*, 2000a). Process based models show better performance for scenario analysis (e.g. in the EUROHARP studies Perrin *et al.*, 2001; Schoumans *et al.*, 2009b), provided that processes, and process interactions, are represented appropriately. This explicit process representation increases input data demand for running the models (Chen *et al.*, 2008; Clifton-Brown *et al.*, 2007; Keoleian and Volk, 2005).

For the purposes of this study, it is unlikely that sufficient calibration data will be available, due to the difficulty of measuring N_2O emissions, the relatively limited area of existing *Miscanthus* and SRC willow in the UK, and the need to take into account variations throughout the 20 year cropping cycle (Clifton-Brown *et al.*, 2007; Keoleian and Volk, 2005), therefore process based models may perform better (Chen *et al.*, 2008) and this will be one of the initial selection criteria.

Objective 3 seeks to assess approaches for predicting perennial energy crop yield along with change in N_2O emissions, soil C and ET for land use change. Figure 1.1. in Chapter 1, showing C, N and water cycling for an agroecosystem, illustrates how these systems are linked; C and N are coupled in soil organic matter (SOM) pool cycling and C fixation, water and N uptake of a plant are all part of the same photosynthesis and crop growth processes resulting ultimately in yield. Simulation of small scale short term fluxes of organic matter is important to facilitate simulation of nutrient dependant crop processes (Stockle *et al.*, 2012). Similarly, crop growth representation is dependent on accurate simulation of water availability, which may limit yield, or may be over extracted where crops have access to the water table (Fraiture *et al.*, 2008; Vanloocke *et al.*, 2010). Resulting changes in soil water will themselves impact SOM cycling processes by altering soil pore oxygen status. It therefore makes sense to model yield and water use together, and to bring C and N cycles into the crop growth and water use model, enabling prediction of direct and indirect GHG emissions, yield and water usage together, taking a whole agroecosystem approach.

The whole agroecosystem approach taken here is not common in research on land use impacts, which tends to focus on a single output (e.g. Grant and Pattey, 2003; Hendriks *et al.*, 2008; Richter *et al.*, 2008; Toma *et al.*, 2010; Vanloocke *et al.*, 2010). This may be because agricultural GHG emissions and evapotranspiration are separate issues in terms of impact scale; evapotranspiration is likely to impact local water resources and ecosystems (de Fraiture and Berndes, 2008; Vanloocke *et al.*, 2010); whereas GHG emissions are a global issue in terms of climate change, which will have feedback on the agroecosystem via changes in CO_2, temperature and precipitation, which directly affect rates of crop growth (Dondini *et al.*, 2009). However, the whole agroecosystem approach is well recognised in agriculture, and is often utilised for improving efficiency of amounts and timings of fertiliser inputs and irrigation, and has also been recommended in the literature for approaching land use problems (e.g. by Li *et al.*, 2007; Stockmann *et al.*, 2013).

Land use change and energy crop cultivation impacts falling outside the scope of the physiological crop growth process such as; ecology and biodiversity, landscape structure, socioeconomic systems and emissions from fuel use, will not be represented by a crop-soil system based model (Cherubini, 2010; Hanegraaf *et al.*, 1998; Paine *et al.*, 1996). It is not practical to model these issues together with nutrient and water cycling, as they are not directly involved in crop growth in the same way. Fuel use associated with cultivation and harvesting of the crop is crucial in terms of the greenhouse gas balance of the crop, and should be included in a full lifecycle analysis (LCA), however this will not be included here since it also falls outside of the scope of the physiological crop growth process. Full LCA should take into account emissions and energy used for construction and operation of plant, as well as emissions and energy use from transport of feedstock in addition to the emissions from land use change and cultivation of feedstock (Thornley, 2006). A fully inclusive LCA should also consider emissions from indirect land use change, however allocation is complex.

LCA including GHG costs of all stages of energy crop cultivation should be compared to a fossil fuel reference system in order to ensure that the GHG reduction aims of bioenergy are met. The predictive models considered are not intended to give a complete assessment, but could contribute a useful input to a broader LCA.

3.3 Multi criteria decision analysis (MCDA)

This research sets out an objective approach to identify the most appropriate model(s) to assess the environmental impacts of land use change for perennial energy crops, in terms of carbon, nitrogen and water cycling. The approach takes the form of multi-criteria based decision analysis (MCDA) which is a robust, logical approach to meeting multiple demands. The term MCDA covers a wide range of approaches to structured decision making, using ranking and multiple stakeholders, or individual decision makers as appropriate. MCDA comprise four stages:

1. Structuring and framing the decision problem;
2. Articulating preferences;
3. Aggregating alternative preferences;
4. Making recommendations.

In this case, the decision problem is structured as a need to predict site-specific changes in crop and soil processes and resulting GHG balance and ET, for land use change to perennials.

For stage two, the relative importance of criteria must be considered, and this may incorporate weighting and ranking, or a compensatory approach where poor performance on one criterion can be balanced by good performance on another criterion (Guitouni and Martel, 1998). Alternatively, where several criteria are essential, a conjunctive method, as used by Hwang and Youn (1981) and Chen and Hwang (1992), may be necessary, where all approaches not meeting these key criteria are ruled out. A wide range of other approaches to MCDA have been developed for different situations. A comprehensive review of MCDA is provided by Guitouni and Martel (1998).

The objectivity of the MCDA approach is dependent on the objectivity of the criteria identification in the first two stages, so it is crucial that a transparent approach is used, based on appropriate stakeholder input, or data and literature. MCDA often incorporates stakeholder input for criteria identification, however a literature review may be used in proxy. Therefore, the purpose of stage two is to identify what potential impacts have been discussed in the literature, and use these to map out criteria to be represented by the chosen approach. The decision problem structure is then used to outline the relative benefits of different assessment approaches, and the relative importance of different factors to be included in the assessment according to the second stage of MCDA. These considerations are then aggregated to select an appropriate MCDA approach, and an appropriate set of criteria on which to base recommendations.

3.4 Required representation of potential agroecosystem impacts of land use change for perennial energy crops

Land use change for perennial energy crops often represents major change to tillage regime, evapotranspiration, crop rooting depth and seasonality of land cover. This will have knock on effects on soil chemical and physical properties such as texture, water filled pore space (WFPS) and available C and N, and resulting GHG emissions of CO_2 and N_2O. In the case of conversion from grassland to perennial energy crops, there is also the issue of soil disturbance, resulting in loss of stored C and N through mineralisation and decomposition. Also, water usage may differ from previous vegetation, affecting the catchment regime, and potentially limiting crop yield.

Hence, understanding these variables and how they interact may help to minimize negative impacts and to fulfill the emissions savings potential of bioenergy crops.

An important review by Chen *et al.* (2008) makes a general assessment of existing N_2O emission model characteristics, intended to inform researchers to select a model suitable for their purposes. This chapter builds on this, and similar reviews, by making specific assessment of model capability to represent an agroecosystem, in terms of soil C and N cycling and effects on of soil formation, and GHG emissions, as well as changes to ET, and how these might affect water resources or flood risk locally. Overall there is no existing comparative assessment of model (or sub model combination) suitability to predict these outputs and assess impact of land use change for perennial energy crops on a catchment. Figure 3.1 is a schematic representation of the conceptual model in Chapter 1 (Figure 1.1); it shows how the processes described below are linked, and how they interact to produce the desired outputs. It is difficult to include all processes in a model and the importance of some processes is uncertain; therefore it is necessary to assess literature and existing data to establish which processes are important and need to be included within the model.

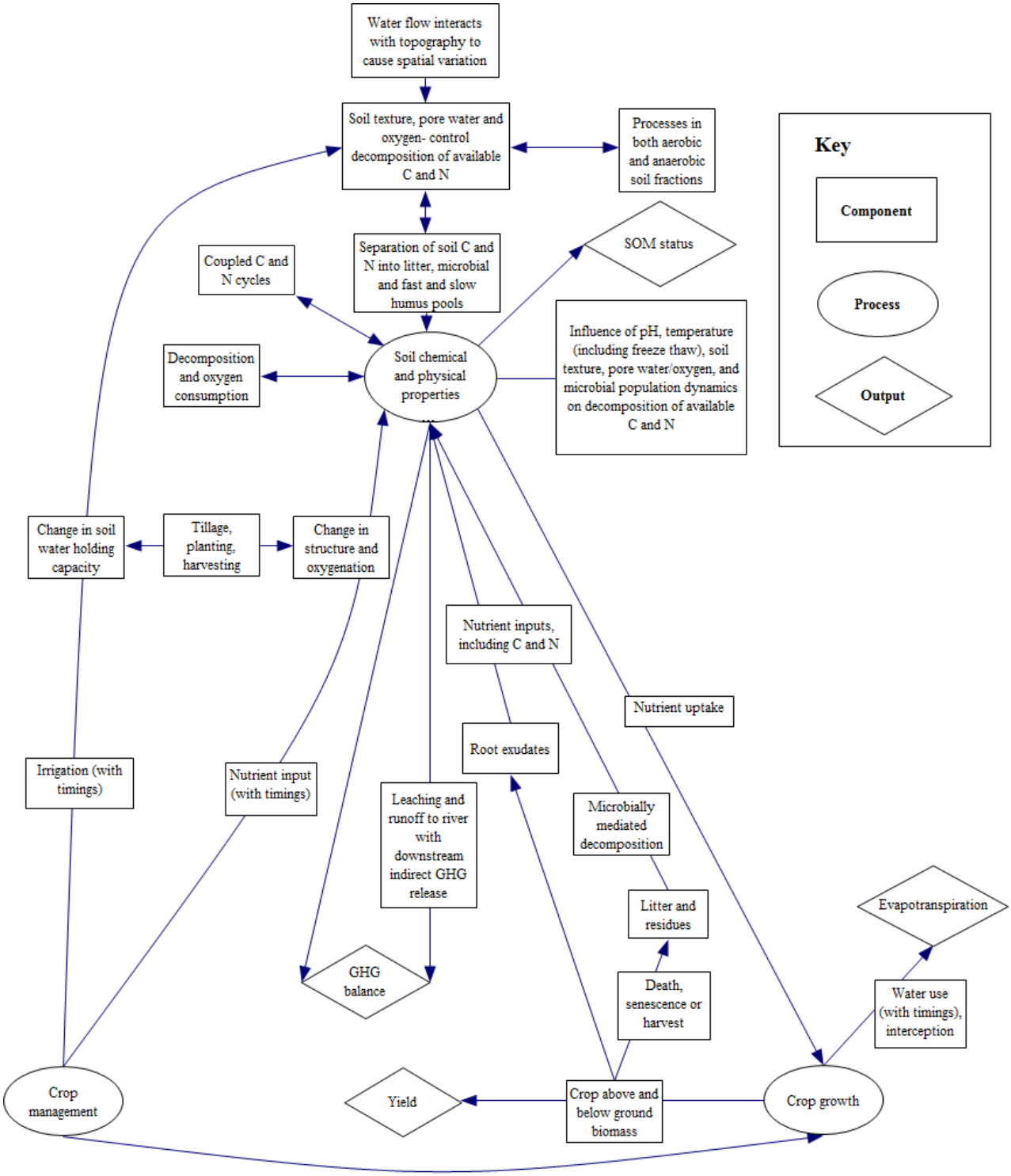

Figure 3.1 Conceptual model of whole agroecosystem; includes the components and processes required to produce the desired outputs. This is a schematic version of Figure 1.1 in Chapter 1, produced to enable additional processes to be included.

Previous land use is highly significant, and in some cases, removal of existing biomass and disruption of soil to allow cultivation of energy crops causes CO_2 emissions which exceed any savings from avoided fossil fuel use (Fargione *et al.*, 2008). These may be significant for conversion of mature grassland, whilst in the case of arable land, there is annual soil disruption

and plant biomass removal, meaning these losses need not be considered. In either case, soil C and N levels resulting from the previous ecosystem will contribute to nutrient cycling and crop growth in the new ecosystem (Brandão *et al.*, 2011; Fargione *et al.*, 2008; Searchinger *et al.*, 2008). For useful prediction, the model must therefore be able to simulate any biomass removal and soil disruption, soil conditions produced by previous land use in the form of N and C storage and availability, as well as the new crop and management regime, and how all of these interact to produce the new crop-soil-atmosphere system.

After change in land use, there is a variable period before a catchment reaches steady state due to: nitrogen retention in soils and aquifers; time taken for establishment of new vegetation (canopy, roots etc.); and rates of processes, such as soil organic matter accumulation, decay or erosion (Breemen *et al.*, 2002, Keolian and Volk, 2005, Darracq *et al.*, 2007). Models often predict equilibrium at steady state for a given system, whereas to simulate land use change, it is necessary to also represent the transition period (Hutchins *et al.*, 2010). This is particularly important due to the impacts of small scale short term organic matter fluxes on crop growth (Stockle *et al.*, 2012) and variation in the proportion of N lost from soil as N_2O emissions according to ephemeral soil properties.

The first year's model results will not be representative of a full cycle average for C or N, since C accumulation is greatest during establishment, as identified in Section 1.2.3, whilst N uptake is initially high, then lower in later years due to internal N recycling by both SRC willow and *Miscanthus*. The model must therefore be run over at least a full growing cycle for both SRC willow and *Miscanthus* (25 and 20 years respectively) to predict total changes. It would be preferable to run the model until equilibrium is reached, if applicable, so the impacts at steady state can also be assessed. Disturbance of soil at the end of each growing cycle is likely to prevent a constant equilibrium from being reached; accumulation from a second growing cycle can be expected to offset emissions from decomposition of old roots, which may mean a dynamic equilibrium is reached as opposed to a constant level of storage (Keoleian and Volk, 2005). Therefore the model could be run for multiple growing cycles to gain a more complete picture of long term impacts. Basset-Mens *et al.* (2006) highlight the difficulty of creating and validating models to predict steady state for a system which is unlikely to reach equilibrium in reality due to the constant changes in farming practices and potentially long timescales of slow transport and storage of N.

As discussed in Section 1.4.1, soil C storage under perennial energy crops is likely to exceed that of the previous ecosystem, particularly at arable sites. This is due to higher inputs, in the form of leaf litter and root exudates, compared to arable crops where less aboveground material remains after harvest. Soil organic matter (SOM) exists as a range of compounds with different availability and reactivity; C and N flows generally make up a small proportion of the store, annual turnover may be around 2%, whilst short term changes can have significant impact on crop growth processes. To give useful simulation of this multiscale system, pools can be separated according to turnover rate and composition, for example; microbial, litter, and labile and passive humus (Parton *et al.*, 2010; Porporato *et al.*, 2003). Since data are not available on SOC distribution over the relevant soil pools, the model must be able to assign these partitions according to land use and management history.

As well as storage pool, the model should represent variation in decomposition according to soil pH (relationship varies with soil type), soil moisture (decomposition rate increases with moisture until oxygen availability becomes limiting), and temperature (tends to increase decomposition rate e.g. Dao (1998)). It would also be useful to represent variation according to proportions of: clay (provides physical protection Parton *et al.* (1994)); organic matter (increases soil water holding capacity Gupta and Larson (1979)); and sand (increases decomposition rate and CO_2 loss Parton *et al.* (1987)). Decomposition should be represented both as transfer of C to a more active pool and loss as CO_2 from microbial respiration (Stockle *et al.*, 2012). Since C and N are coupled in soil, transfers of N out of pools should occur according to the C:N ratio, and N immobilisation or mineralisation should be simulated to ensure that the C:N ratio of the receiving pool is also maintained (Del Grosso *et al.*, 2008; Parton *et al.*, 2010; Porporato *et al.*, 2003). As mentioned in Section 1.4.2, organic matter inputs associated with SRC willow and *Miscanthus* tend to have high C:N; in this case transfers of N from more available to less available pools will simulate impacts on N availability via increased N immobilisation.

To represent the previous arable system, the model must be able to represent tillage in terms of the oxygenation and physical breakdown of organic matter which will cause transfers to more available pools and increased gaseous losses of C. If there is no explicit representation of soil particle aggregation, a proxy factor will suffice.

Since tillage increases erosion and aerates soil increasing decomposition rates, and resulting CO_2 loss from soil, the no till practice for perennials should encourage SOC accumulation producing a CO_2 sink (Ball *et al.*, 1999; Keoleian and Volk, 2005; Li *et al.*, 2005a). However, as discussed in Section 1.4.2.3, there are also potential negative environmental impacts; since C and N cycles are coupled, it has been suggested that increase in soil C with NT practice may stimulate microbial activity and release of N_2O (Ball *et al.*, 1999; Li *et al.*, 2005a) or that reduction in soil porosity under NT may create anoxic conditions increasing denitrification (Heinen, 2006; Soane *et al.*, 2012), whilst elsewhere reduction in N_2O emissions under NT is attributed to reduction in decomposition and associated N availability (Metay *et al.*, 2007), or reduction in porosity reducing oxic conditions for nitrification (Hellebrand *et al.*, 2008). As described in Section 1.4.2.3, interaction between soil drainage, the dominant N_2O producing process, N availability for that process, and change in soil pore oxygen status will dictate whether N_2O emissions increase or decrease under NT. To represent this interaction it would be useful if the model could simulate soil porosity changes induced by tillage, and their impacts on WFPS.

New land management will interact with precipitation regime, leaf litter inputs, and fertiliser application schedule and relative timings of uptake. Lower agrochemical requirements give perennial energy crops potential to reduce N_2O emissions compared to annual arable crops (Cherubini *et al.*, 2009) and field observations for SRC willow and *Miscanthus* as discussed in Section 1.2.4.6 have recorded reduction in N_2O where fertiliser was not applied. The extent of N_2O emissions reduction will vary by site, according to the interaction of N inputs, N storage, and factors controlling rates of N_2O emission both before and after land use change. It is therefore necessary to represent these processes, rather than apply default emission factors (EFs) to predict emissions based directly on fertiliser values (Chamberlain *et al.*, 2011; IPCC, 2006).

Because of the complexity of nitrogen cycling it is useful to identify key processes controlling N flows to ensure that these are also properly represented in the chosen model (Delon *et al.*, 2007). In Chapter 1, Section 1.4.2.1 nitrification and denitrification controls were identified as; soil texture and lateral water movement, which control WFPS and diffusion; temperature, which controls microbial activity and nitrogen availability for reaction. Although microbial population dynamics are a crucial control, changes may be represented implicitly through the relationship to other variables (Del Grosso *et al.*, 2000; Müller *et al.*, 1997). For the UK, it is also necessary to model impacts of freezing temperatures, which reduce oxygen diffusion into soil, can kill microbes and reduce available soil water (Frolking *et al.*, 1998).

Chatskikih *et al.* (2005) note that assessments of N_2O emission models often focus on capability to replicate timings of emission peaks and troughs (e.g. Beheydt *et al.*, 2007; Chen *et al.*, 2008; Grant and Pattey, 2003; Li *et al.*, 2005b). Given that N_2O emissions are a result of highly nonlinear reactions affected by changes in soil pore oxygen status, time series predictions are unlikely to be accurate without incorporation of complex data on water movement and spatial heterogeneity of soil (Del Grosso *et al.*, 2005; Li *et al.*, 2005b). However, since N_2O emissions peaks make a significant contribution to annual totals, failure to simulate these can create inaccuracies in longer term predictions (Beheydt *et al.*, 2007; Bessou *et al.*, 2010). The temporal resolution of a model is also important in terms of process representation, for example, the DNDC model uses a finer temporal scale to model denitrification because of the rates and variability of the process; a finer (daily) timescale version of the CENTURY model has shown improved performance (Chen *et al.*, 2008).

Soil saturation, which varies with water movements and diffusion is crucial in controlling oxygen availability and therefore decomposition, nitrification and denitrification; as well as diffusion and release of produced gases (Metivier *et al.*, 2009). Given spatiotemporal variation in controlling processes, model representation can be expected to perform better at an appropriate resolution, incorporating data on this variation. Different processes may become important at different spatial scales; to produce accurate representation of spatiotemporal variation in gas emission, small scale processes must be considered (Giltrap *et al.*, 2010). By taking a distributed approach to simulating processes closer to the scale at which they are occurring, incorporating spatial variation in controlling variables has the potential to also produce a more accurate average value; assuming that data on the controlling variables is accurate. There is a trade-off; although aggregating processes enables reduction in input data making the model easier to apply to data poor sites, this comes at the cost of reduced quality of output data.

Models such as Ecosys, which include topographic data, simulate water movement through the landscape, and associated changes in soil saturation and oxygen availability (Grant and Pattey, 2003). Soils are often highly heterogeneous, hence variability texture is also a key control on spatial variation in WFPS (Boyer *et al.*, 2006; Li *et al.*, 2005a). N_2O flux is also affected by spatial variation in soil N concentration (Hellebrand, 2006). A lack of distributed data on soil texture and N content may necessitate use of interpolated or average values, which may negate the

improvement on a lumped approach (Chen *et al.*, 2008; Potter *et al.*, 1996; Schoumans *et al.*, 2009a). Without representation of spatial variation in controlling factors, it has been suggested that explicit representation of microbial processes will not improve model performance (Chen *et al.*, 2008; Potter *et al.*, 1996).

Elsewhere it has been suggested that a lumped approach is sufficient to simulate N_2O emissions at annual field scale, as required for identifying the impacts of change in land use (Del Grosso *et al.*, 2005; Del Grosso *et al.*, 2008; Grant and Pattey, 2003). Therefore in spite of high spatiotemporal variability, assessment will focus on model ability to predict field scale average impacts of change in conditions (Chatskikh *et al.*, 2005).

Vertical spatial resolution must be considered as well as horizontal; discretisation into layers enables the model to represent vertical water movement. C and N cycling controls such as texture, porosity and soil water content vary with depth, and deeper soil layers may make an important contribution to N_2O emissions (Bessou *et al.*, 2010; Rochette *et al.*, 2008). Accurate representation of changes in soil texture with depth would significantly increase data demand; the site data compiled in Section 2.10 only includes textural properties for two layers. However by splitting the soil into more layers, representation of soil water movement and resultant soil water content will be greatly improved, so multi-layered models should still be preferred.

Based on an opinion study for switchgrass by Jensen *et al.* (2007) not all farmers with suitable land would be keen to grow perennial energy crops; thus it is likely that land use change would occur at plot or farm scale as opposed to over an entire region, and plot scale representation is most appropriate. Plot scale is a convenient level of discretisation due to spatial variability in current land use and its vintage. However; as well as affecting the soil and ecology within the altered plot, there will be interaction with atmosphere and impacts from and to areas upslope and downslope respectively, meaning adjacent land use and landscape composition are also relevant (Lane *et al.*, 2009). Therefore there is a choice between; modelling the full catchment; or modelling at plot scale (including atmosphere) and making separate consideration of the impact of altered ET and leaching on the wider area. Simulating land use and site properties for an entire catchment, as well as the hydrological linkages between plots as discretised would significantly add to computational demands. Additionally plot location within the catchment would be different for other sites of the same “typical” profile as identified in Section 2.10, hence a whole-

catchment approach would make it more difficult to make inferences for other sites based on output. Therefore modelling will be performed at plot scale, and consideration of wider catchment impacts will be made separately.

As well as direct N gas emissions from soils, the model must be able to represent indirect emissions from leached or stored nitrates, in particular due to proportionally high emissions from leached N (Groffman *et al.*, 2000b; Nevison, 2000; Reay *et al.*, 2009). Soil profile representation is therefore also important to simulate leaching and associated indirect downstream emissions which may offset changes in field emissions (Chen *et al.*, 2008). Additionally, the model must not assume annual turnover rates, since N released from storage can have greater impact on fluvial N concentration than current application rates (Baresel and Destouni, 2006; Nevison, 2000).

As indicated in Section 1.4.4; due to variation in relative productivity and timing of growing season, change in rates of ET will vary between sites, and may affect water availability and flood risk, as well as whether water availability limits yields (McKendry, 2002; Rowe *et al.*, 2009; Vanloocke *et al.*, 2010). It is therefore useful to represent water usage and availability in terms of both catchment and productivity impacts, using explicit representation of crop growth and water uptake, according to local climate and soil data (Aylott *et al.*, 2008; Lovett *et al.*, 2009; Richter *et al.*, 2008). To do this, the model must have capability for representing differences between the crops considered, in terms of timing of growth processes, and water uptake.

Representing nutrient cycling for the specific crops is also important, since inputs from crop to soil feed back into representation of soil C and N cycling; forms of nutrient input from crops include root exudates and dead root matter, senesced leaves and residue left after harvest (Heaton *et al.*, 2009; Jørgensen and Schelde, 2001; Jug *et al.*, 1999). Models which have already been successfully validated for specific perennials will be preferred, since relevant process representation can be ascertained.

Models tend to perform better in a similar environment to where they were developed, and may sometimes fail to include processes occurring at new sites such as snow melt and fluvial retention (Frolking *et al.*, 1998; Groffman *et al.*, 2000a; Schoumans *et al.*, 2009a). Therefore a geographical scope must be outlined for each model, in terms of development location, and validation regions.

Due to the required range of outputs, it may be necessary to couple models; in particular, indirect GHG emissions tend not to be a standard output for agroecosystem models. Potential impacts of coupling must be considered; accuracy can be reduced depending on quality and suitability of data feeding into the coupled model (Smith *et al.*, 1997). Model complexity may increase scope, however simple models may perform better when coupled, and structure may be more important than complexity in determining model accuracy (Perrin *et al.*, 2001; Smith *et al.*, 1997). While structure and complexity may be considered, validation performance is likely to be most indicative of suitability.

3.5 Compiling a database of suitable models

The next step is to identify a process based model which can fulfil the requirements outlined in Section 3.4, and be applied at individual sites where land use change is planned, perhaps as part of a Tier 3 IPCC approach. There are a great number of models available which could be used to predict part(s) of the required outputs; therefore it is not possible to consider every existing model. Given the availability of models meeting the review criteria, it is not necessary to build a new model for application to perennial energy crops, although it may be useful to adjust existing models to refine relevant processes and eliminate any unnecessary input data requirements.

A database of several models widely utilised by existing studies (for which it is therefore possible to establish reliability, scope etc.) was compiled from the literature. A Scopus search was run to find models using "TITLE-ABS-KEY-AUTH (soil greenhouse gas emission model)"; this gave 765 results. Of these 765 results several models were featured strongly; 325 discussed the IPCC methodology, 124 DNDC, 83 DayCent (182 CENTURY), 11 Expert-N, 19 ecosys, 1 hole in the pipe, 8 artificial neural networks, 4 NLOSS, 3 WNMM, 3 CASA, 10 STICS, 8 FASSET, 10 InfoCrop, 2 NL-CAT, 7 FullCAM (12 Roth C), 2 MCROPS and MGRASS, 1 INCA, 29 EPIC, 5 CropSyst, 13 APSIM, 4 3PG simulation model and 23 CERES.

Detailed model descriptions can be found in the IPCC Guidelines For National Greenhouse Gas Inventories (IPCC, 2006a) for the IPCC methodology; Davidson *et al.* (1998) for HIP; Ryan *et al.* (2004) for ANN; Brisson *et al.*(1998) for TNT-STICS-NEMIS; Aggarwal *et al.* (2006) for InfoCrop;

Potter *et al.* (1996) for CASA; Renaud *et al.* (2006) for NL-CAT; Lokupitiya and Paustian (2006) for FullCAM; Roelandt *et al.* (2005) for MCROPS and MGRASS; Whitehead *et al.* (1998) for INCA; Chen *et al.* (2008) for DNDC, DayCent, FASSET, Expert-N, Ecosys, NLOSS, WNMM and CERES; Williams (1990) for EPIC; Stockle *et al.* (2003) for CropSyst; McCown *et al.* (1996) for APSIM; Landsberg *et al.* (1997) for the 3PG simulation model.

3.6 Comparison

As indicated in Section 3.4, multiple criteria must be taken into account in choosing a model appropriate to the purposes of this thesis, and selection requires a transparent, well-structured decision making process, for clarity. Model criteria were therefore established based on the processes which would be affected by land use change for perennials and appropriate resolution, and models unable to meet these requirements were ruled out.

From Sections 3.2 and 3.4, primary criteria to compare process based models were identified as;

- Representation of complete agroecosystem
- Potential to produce required output (diamond boxes in Figure 3.1)
- Explicit representation of required soil, crop and land management processes (square boxes in Figure 3.1)

Traditionally MCDA incorporates weighting of criteria at this stage (stage two); however as illustrated in Figure 3.1; crop soil and site properties interact to control output. Process based models are unlikely to perform well unless the whole system and all relevant processes are represented, making it difficult to separate the importance of these primary criteria. As a result an analytic hierarchy process ranked many criteria (soil chemical and physical properties, soil nutrient cycling, crop growth and management, site specific interactions between variables, whole agroecosystem representation) equally (Del Grosso *et al.*, 2005; Frolking *et al.*, 1998; Groffman *et al.*, 2000a; Schoumans *et al.*, 2009a; Smith *et al.*, 1997). Therefore a partially-compensatory MCDA framework was adopted as per Guitouni and Martel (1998), and models not meeting all primary criteria were excluded at the initial assessment stage, with lesser or study-specific criteria grouped in a second table. Indirect emissions do not affect representation of other processes, and could be represented by a separate sub-model. However, the high IPCC

indirect GHG EF suggests that failing to represent indirect emissions would give poor representation of the system impacts, so potential to meet this output was included as a primary criterion (Groffman *et al.*, 2000b; Nevison, 2000). Table 3.1 shows application of these primary criteria to identified models. Although the analytic hierarchy process was performed by an individual decision maker, the extensive use of literature to support rankings should ensure robust objectivity.

Microbial population dynamics correlate with other parameters and may be represented implicitly, and hence were identified as of lesser importance by the analytic hierarchy process (Del Grosso *et al.*, 2000; Müller *et al.*, 1997). Therefore models unable to represent these processes will not be ruled out, but this ability will be considered as a limiting factor.

Since resolution appears to be of secondary importance, this was included in a second criteria matrix in Table 3.2, along with locations and crops to which the model has been applied (Del Grosso *et al.*, 2005; Del Grosso *et al.*, 2008; Grant and Pattey, 2003). These secondary criteria are of varying importance depending on the location, crops and data availability of the study in which a land use change model is required; in the case of this study, it is preferable that the model has been applied to SRC willow and or *Miscanthus* in the UK or Europe.

3.6.1 Aggregating alternative preferences: application of primary criteria

Given the need to apply the model at sites where calibration data are unavailable, non-process-based models were ruled out first.

Tiers 1 and 2 of the IPCC methodology apply a statistical approach to calculate N_2O emissions from fertiliser input multiplied by an EF (which may be specific to country and land use type) and soil C loss from use of inventory values (IPCC, 2006a). These approaches may be applied to assess average GHG emissions associated with land use change for perennial energy crops; however they cannot identify how these vary with site specific factors.

MCROPS and MGRASS are empirical models, which use statistical relationships to calculate N_2O emissions according to fertiliser input and seasonal climate variability, to improve on the generalised factors used by the IPCC tier 1 approach (Roelandt *et al.*, 2005). Artificial neural networks (ANN) use recursive pattern recognition techniques and can be applied to optimise calculation of statistical relationships between input and output data; excellent validation performance has been observed for prediction of daily N_2O from climate and N availability properties (Ryan *et al.*, 2004). Due to the lack of appropriate calibration data for the sites to be modelled in Chapter 5, ANN and MCROPS and MGRASS may not give good representation, and are therefore ruled out.

Where the data demands of a process based model cannot be met, one of these models could be applied if it had been calibrated at a similar site. However predictions will be less reliable than for calibrated sites, or than from an appropriate process based model. Having ruled these statistical models out, the remaining models identified from the Scopus search were then compared on primary criteria (see Table 3.1).

***Table 3.1** Primary criteria to select a model capable of representing impacts of land use change for perennial energy crops. Where models can be ruled out due to a failure to meet key criteria this is stated. References are given as subscript numbers, and cited at the end of the table.*

	Full agroecosystem	**Processes modelled explicitly**	**Outputs met/ Potential to produce all output**
TNT2 (TNT-STICS-NEMIS)	Full [20].	Separate root and shoot growth, tillage, water balance, leaching, soil aquifer exchange and riparian zone circulation soil N, C and temperature. [20.22.35]. **Ruled out:** No separation of slow and fast soil pools.	Direct GHG emissions, leaching, ET, yield, SOM. [20. 22. 35]. Downstream N transformation can be separate or coupled.
INCA	Ruled out: Partial 26.	Nitrification and denitrification, seasonal average plant uptake. Surface and subsurface flow pathways, river flow and N concentration and transformation [26].	Direct and indirect N GHG emissions, ET, SOM. [26]. Requires additional crop model
FullCAM (CAMFor, CAMAg, GENDEC, Roth-C)	Ruled out: Partial 32.	Soil C turnover, separated slow and fast C pools, residue decomposition, tillage, afforestation/deforestation [24].	Direct C GHG emissions, SOM. [32. 24]. Requires additional sub models for N, yield and leaching.
Hole In the Pipe	**Ruled out:** Soil system only. [16].	Nitrification, denitrification, biological assimilation and lumped non biological retention reactions [16].	Direct GHG emissions, SOM. [16]. Requires additional sub models for ET, yield and leaching.
CASA (19. Describe soil component as a "HIP" method)	Coupled crop and soil system submodels. [18. 19].	Plant carbon fixation, nutrient allocation, litterfall, separated slow and fast coupled C and N pools, N mineralisation and immobilisation are represented implicitly according to C cycling [19]. No ecological succession, compaction, or irrigation, implicit representation of tillage [18].	Direct GHG emissions, SOM, NPP [18. 19] **Ruled out:** N leaching not modelled, actual ET not modelled [6].
CERES-NOE	Full [2].	Nitrification, denitrification, separated slow and fast coupled C and N pools, water movement and nutrient leaching. No methane balance or gas diffusion [2]. NOE2 represents compaction and tillage. [36].	Direct GHG emissions, SOM, ET and yield. [2].

EPIC	Full [38.]	Erosion, nitrification, denitrification (only at > 90% WFPS), separate root and shoot growth, nutrient uptake, water flows, tillage, N mineralisation and immobilisation [38.] C cycling routines from DayCent added [39.] **Ruled out:** Trace gas emission from soil not modelled [40.] Crop representation simplistic and generic [41.]	C and N loss from soil, yield, SOM. leaching, ET [38.]
CropSyst	Full [41.]	Net mineralization, nitrification, denitrification, tillage, irrigation [41.] crop growth, residue decomposition, slope runoff, erosion, freeze thaw [43.] Separated slow and fast C pools, N_2O emissions [42.]	ET, yield, changes in soil N and C leaching [41.], direct GHG emissions [42.]
APSIM	Full [44.]	N mineralisation, N immobilisation and nitrification, denitrification [45.] Erosion, crop growth, soil C [44.]	Yield, leaching, ET, soil C [44.] Adapted to give N_2O emissions [46.]
3PG	**Ruled out:** Crop system only. [47.]	Root growth, multiple shoot growth, soil water balance [47.]	Yield, ET [47.]
Ecosys	Full [2.]	Freeze thaw, multiple crop layers, leaf and root vertical distribution, tillage, simultaneous denitrification and nitrification lateral flows simulated from topography, microbial dynamics, separated slow and fast coupled C and N pools [8. 11. 33.]	Direct GHG emissions, leaching, yield, ET, SOM. [2. 10.] Downstream N transformation can be separate or coupled.
NLOSS	Full [2. 28. 29.]	Microbial dynamics, separated slow and fast coupled C and N pools, simultaneous denitrification and nitrification, water/gas/heat translocation, not tillage or freeze-thaw [1. 21.13.] **Ruled out:** no representation of freeze thaw or variation in tillage	Direct GHG emissions, ET, leaching, yield, SOM. [2. 28. 29.] Downstream N transformation can be separate or coupled.
WNMM	Full [11.]	Freeze –thaw, tillage, separated slow and fast coupled C and N pools, simultaneous denitrification and nitrification, microbial dynamics. [22. 7.]	Direct GHG emissions, ET, Yield, Leaching, SOM. [11. 2.] Downstream N transformation can be separate or coupled.

InfoCrop	Full [23.]	Microbial dynamics, separated slow and fast coupled C and N pools, simultaneous denitrification and nitrification. No soil tillage or cold temps. [9.] **Ruled out:** no representation of variation in tillage	Direct GHG emissions, leaching, ET, yield, SOM. [23.] Downstream N transformation can be separate or coupled.
ExpertN	Full [6. 9.]	Freeze thaw, snow, tillage, separated slow and fast coupled C and N pools, simultaneous denitrification and nitrification, microbial dynamics. [1. 20. 31.]	Direct GHG emissions, ET, Yield, SOM, Leaching. [6. 9.] Downstream N transformation can be separate or coupled.
FASSET (agroecosystem submodel) (11. Describe N_2O calculation as a "HIP" method)	Full [2. 11.]	Grazing/cutting, separate root and shoot growth, tillage levels, separated slow and fast coupled C and N pools, freeze-thaw, simultaneous denitrification and nitrification, microbial dynamics. [2.]	Direct GHG emissions, leaching, ET, SOM, yield. [2. 11.] Downstream N transformation can be separate or coupled. Code available for coupling. [2.]
NL-CAT (ANIMO coupled with SWAP, SWQN, SWQL)	Requires additional coupled external crop model [12. 13.]	Freeze –thaw, snowmelt, tillage, retention in surface waters, simultaneous denitrification and nitrification, microbial dynamics, can have external crop model. [2. 14. 16.]	Leaching, yield, ET, SOM, extended for direct GHG emissions. [13. 31.12.]
DayCent	Full [27. 7.]	Freeze –thaw, snow, tillage, root turnover rates (FORCENT), simultaneous denitrification and nitrification, separated slow and fast coupled C and N pools. No microbial dynamics. [17. 18. 19. 19. 23.]	Direct GHG emissions, ET, Yield, Leaching, SOM. [27. 7. 8.] Downstream N transformation can be separate or coupled.
DNDC	Full [4.]	Freeze –thaw, cold temp (-5 activation), snow coverage, weeding, tillage, water/gas/heat translocation, simultaneous denitrification and nitrification, microbial dynamics, separated slow and fast coupled C and N pools. [1. 5.]	Direct gas emissions, ET, Yield, Leaching, SOM. [4.5.] Potential to couple to SWAT for downstream transformation, code available for coupling. [2. 34.]
ECOSSE	Full [37.]	Tillage, separated slow and fast coupled C and N pools, simultaneous denitrification and nitrification. [37.]	Direct GHG emissions, ET, Yield, Leaching, SOM. [37.] Downstream N transformation can be separate or coupled.

References	**1.**(Nevison, 2000) **2.**(Chen *et al.*, 2008) **3.**(Brown *et al.*, 2002) **4.**(DNDC User Guide, 2009) **5.**(Li *et al.*, 1992) **6.**(Frolking *et al.*, 1998) **7.**(Davis *et al.*, 2010) **8.**(Parton *et al.*, 1998) **9.**(Stenger *et al.*, 1999) **10.**(Grant, 1995) **11.**(Chatskikh *et al.*, 2005) **12.**(Silgram *et al.*, 2009) **13.**(Renaud *et al.*, 2006) **14.**(Wolf *et al.*, 2005) **15.**(Ryan *et al.*, 2004) **16**.(Verchot *et al.*, 1999) **17.**(Groffman *et al.*, 2000a) **18.**(Potter *et al.*, 1996) **19.**(Davidson *et al.*, 1998) **20.**(Brisson *et al.*, 1998) **21.**(Beaujouan *et al.*, 2002) **22.**(Gascuel-Odoux *et al.*, 2010) **23.**(Aggarwal *et al.*, 2006) **24.**(Lokupitiya and Paustian, 2006) **25.**(Roelandt *et al.*, 2005) **26.**(Whitehead *et al.*, 1998) **27.**(Del Grosso *et al.*, 2005) **28.**(Riley and Matson, 2000) **29.**(Christensen *et al.*, 2006) **30.**(Li *et al.*, 2005b) **31.**(Hendriks *et al.*, 2008) **32.**(Richards, 2001) **33.**(IPCC, 2006a) **34.**(Gassman *et al.*, 2007) **35.**(Brisson *et al.*, 2003) **36.**(Bessou *et al.*, 2010) **37.** (Smith *et al.*, 2010a) **38.** (Williams, 1990) **39.** (Farina *et al.*, 2011) **40.** (David *et al.*, 2009) **41.** (Claudio O. Stockle, 2003) **42.** (Stockle *et al*., 2012) **43.** (Stöckle *et al*.1994) **44.** (McCown *et al.*, 1996) **45.** (Vogeler *et al.*, 2013) **46.** (Thorburn *et al.*, 2010) **47.** (Landsberg and Waring, 1997)

3PG, HIP, INCA, and FullCAM were ruled out as not representing linked crop-soil systems. In terms of required process representation, STICS does not separate SOM pools according to availability and rates of decay, and so was ruled out. NLOSS and InfoCrop are ruled out due to poor representation of tillage, which is crucial to modelling difference in management (Del Grosso *et al.*, 2008; Li *et al.*, 2005a; Rochette *et al.*, 2008). NLOSS also cannot represent freeze thaw, which is crucial to representation of winter denitrification in temperate climates such as the UK (Frolking *et al.*, 1998). EPIC does not represent trace gas emissions from soil, making it unsuitable for GHG predictions in its current form (David *et al.*, 2009).

Table 3.1 then lists which of the desired outputs of Direct and indirect GHG emissions, yield and ET are produced. Leaching is included where the model does not simulate indirect GHG, since leaching can be used to give a value for indirect fairly easily (Gassman *et al.*, 2007). CASA was ruled out due to not simulating leaching or actual ET.

All of the remaining models can represent rain, flooding and irrigation, gaseous losses from soil, crop uptake and growth, fertiliser and residue application, tillage and simultaneous denitrification and nitrification; using partitioning based on WFPS or aerated fraction of soil (Chen *et al.*, 2008; Chirinda *et al.*, 2010; Frolking *et al.*, 1998; Li *et al.*, 2000; Renaud *et al.*, 2006). The remaining models are; NL-CAT, DNDC, DayCent, Expert-N, Ecosys, WNMM, CERES-NOE, ECOSSE, CropSyst, FASSET, APSIM.

Of these, some have limitations in representation of certain processes which must be taken into account. DayCent, WNMM and CERES-NOE don't represent SOM below 20 cm, so conclusions cannot be drawn for changes at greater depth (Chen *et al.*, 2008; Del Grosso *et al.*, 2008; Del Grosso *et al.*, 2000; Müller *et al.*, 1997). However since deeper soil tends to consist of older, less available C, and since NT means no OM inputs to deeper layers from mechanical mixing, this may be of limited importance (Jenkinson, 1992). DayCent also does not explicitly model microbial dynamics (Del Grosso *et al.*, 2008). FASSET applies a constant value for N_2:N_2O ratio of emissions, and function parameters for denitrification and nitrification controls are derived from site specific data, which may impede performance at new sites (Chen *et al.*, 2008).

In representing the same processes, these models tend to draw from the same theories, often applying the same approaches or equations, for example, the empirical equations to represent solute movement, and the crop model in WNMM are both based on EPIC (Li *et al.*, 2007), whilst EPIC takes on soil C partitioning equations from DayCent (Farina *et al.*, 2011) and EXPERT-N can incorporate the CERES crop model (Chen *et al.*, 2008). Given the history of model development, whereby a model is designed to solve a specific problem in the context of specific (usually localised) sites, the duplication identified in the literature search is, to some extent, inevitable.

3.6.2 Application of secondary criteria and resulting recommendations

The remaining models were then assessed and compared in Table 3.2 on the basis of the following secondary criteria;

- Existing studies applying the model in the UK and to *Miscanthus* and SRC willow; it would be advantageous if the model selected had already been tested and parameterised for UK conditions and perennial crop physiology and management. However this is not crucial provided that the required processes can be represented.

- Resolution; although this study does not require fine resolution output (lumped annual output is sufficient), the spatial and temporal scale of processes means that finer resolution models may be expected to perform better.

Preference should be given to models tested and developed for appropriate locations and crops, and of a resolution appropriate to study data availability. Discussion will also consider processes which are not represented explicitly by all models; variation in tillage (which is crucial to modelling difference in management (Del Grosso *et al.*, 2008; Li *et al.*, 2005a; Rochette *et al.*, 2008)) and microbial dynamics (which may influence spatiotemporal variation in activity (Del Grosso *et al.*, 2000; Müller *et al.*, 1997)).

Table 3.2 Secondary criteria to select an appropriate model from those capable of representing impacts of land use change for perennial energy crops. References are given as subscript numbers, and cited at the end of the table.

	Regions applied	**Crops parameterised for**	**Spatial resolution**	**Temporal resolution**
NL-CAT (ANIMO coupled with SWAP, SWQN, SWQL)	Europe [3. 1.]	Grassland, woodland, annual crops [1.] (option to use external crop model)	1m vertical / horizontal 0.01 km^2 (1 ha) up to 100 km^2 [3.]	Daily [3.]
DNDC	USA, Canada, Australia, New Zealand, Europe, China and India [4. 5.]	Grassland, forest, annual crops, perennials [4. 6. 16.]	Region mode; heterogeneous polygons – use coarsest resolution dataset Site mode; lumped [6.]	Daily input data and decomposition. Hourly denitrification handling [4. 6.]
DayCent	USA, Canada, Australia, New Zealand and Europe [4.7.]	Grassland, forest, annual crops [4. 8.]	Lumped at plot scale [9.]	Daily [4.]
Expert-N	Germany, UK, USA and Canada [4. 10.]	Annual crops [4.]	Lumped at plot scale [12.]	Daily [11.]
Ecosys	USA and Canada [4.]	Grassland, forest, annual crops [4.]	Spatially referenced (coupled with GIS)	Hourly [13.]

			e.g. 50m by 50m 28. [13.]	
WNMM	China, Australia, Korea and Mexico [4.]	Grassland, annual crops [4.]	Spatially referenced (coupled with GIS) 100-1000 m2 common for regional [11. 15.]	Daily/ hourly [4. 14.]
CERES-NOE	France, Puerto Rico [2.]	Annual crops [2.]	Spatially lumped at plot scale, or may be applied at regional scale with compromises on input data [4.]	Daily [2.]
ECOSSE	Scotland, France, Germany [17. 18.]	Grassland and forest [17. 18.]	Spatially lumped, input parameters as available for regional scale [18.]	Daily. [18.]
CropSyst	Mediteranean Argentina, Australia [21. 22.]	Arable [21.] fallow [22.]	Spatially lumped at plot scale, or may be applied at regional scale with compromises on input data [4.]	Daily [20.]
FASSET	Europe [24.]	Grassland, legumes, ryegrass and catch crops [24. 25. 26.]	Lumped at plot scale [27.]	Daily [4. 24.]
APSIM	Australia [29.]	Sugarcane cereal and grain legumes [28. 29.]	Lumped at plot scale [28.]	Daily [28.]
Refs.	**1.** (Wolf *et al.*, 2005) **2.** (Gabrielle *et al.*, 2006) **3.**(Schoumans *et al.*, 2003) **4.**(Chen *et al.*, 2008) **5.**(Brown *et al.*, 2002) **6.**(DNDC User Guide, 2009) **7.**(Abdalla *et al.*, 2010) **8.**(Davis *et al.*, 2010) **9.**(Del Grosso *et al.*, 2005) **10.**(Frolking *et al.*, 1998) **11.**(Li *et al.*, 2007) **12.**(Stenger *et al.*, 1999) **13.**(Metivier *et al.*, 2009) **14.**(Li *et al.*, 2005a) **15.**(Li and Chen, 2010) **16.**(Gopalakrishnan *et al.*, 2011) **17.**(Smith *et al.*, 2010a) **18.**(Bell *et al.*, 2011) **19.** (Nelson, 1993) **20.** (Stockle *et al.*, 2012) **21.** (Pala, 1996) **22.** (Monzon, 2006) **23.** (Silgram *et al.*, 2009) **24.** (Chatskikh *et al.*, 2005) **25.** (Doltra *et al.*, 2010) **26.** (Berntsen *et al.*, 2006) **27.** (Hutchings *et al.*, 2007) **28.** (Huth *et al.*, 2010) **29.** (Thorburn *et al.*, 2010)			

WNMM, DayCent and DNDC have been applied over the widest geographical scope. However, the models identified are only as good as their performance at validation, and this must be considered both in model selection, and also in inferences based on model output. Good performance over a wide range of geographic regions suggests good representation of processes, although further work on validation in England or similar climate is necessary where not already performed. NL-CAT, DNDC, DayCent and FASSET have been applied in Europe, and ECOSSE and Expert-N have been tested in the UK; all of these could be expected to be suitable for scenario analysis in England, in terms of being able to represent the relevant climate conditions, although

more detailed assessment of validation performance under relevant conditions should be made for the chosen model. Further validation studies could increase the geographical scope of the other models, or highlight regions where they should not be applied. Models cannot be tested for future climates, which may affect longer term predictions.

In terms of crops, NL-CAT, Ecosys, DNDC and DayCent are well tested over a useful range of crop types (annual arable crops, and perennial grassland and forest) and should therefore perform well for land use change to perennial energy crops, although calibration and validation may be necessary to add specific new crop types. To see which models have been specifically applied to SRC willow or *Miscanthus*, a Scopus search of the literature was performed using "((TITLE-ABS-KEY(*Miscanthus*) OR TITLE-ABS-KEY(SRC willow)))". None of the papers found applied Ecosys, Expert-N, CERES-NOE, WNMM, ECOSSE, CropSyst, FASSET or APSIM. NL-CAT requires an external crop model, so it is possible that a SRC willow or *Miscanthus* model could be coupled, however, no articles using NL-CAT for these crops were identified. MISCANMOD or the FORTRAN modified version MISCANFOR are often used to predict *Miscanthus* yield. However, predictions are only of non-nutrient limited growth, and additional modelling is necessary to assess change in soil C (e.g. using DNDC (Hastings *et al.*, 2009), or the Matthews and Grogan model (Mishra *et al.*, 2013)).

DayCent has been calibrated for *Miscanthus*, using evidence for N fixation to balance N cycling and match observed yields (Davis *et al.*, 2010). The model was subsequently applied regionally to look at GHG impacts of replacing corn with *Miscanthus* for ethanol production in the U.S.; simulated yield and N_2O emissions closely matched available field data (Davis *et al.*, 2012). DayCent also has a separate option for modelling forest systems, which could be adapted to represent SRC willow.

Gopalakrishnan *et al.* (2012) applied DNDC to model *Miscanthus*, with parameterisation values taken from the literature. Yield predictions for *Miscanthus* grown as a buffer strip in the U.S. Midwest were improved by incorporating evidence for N fixation from Davis *et al.* (2010). Yield predictions were reasonable, but overestimated for some years, and they suggest greater understanding of N fixation would improve model performance. The model is intended to simulate potential yield according to climate and nutrient factors, but does not take into account possible pests or other damage, which may prevent potential yield from being achieved. The crop model for DNDC is relatively simple, with 12 parameters, compared to 108 in DayCent.

In terms of temporal resolution, all models implement at least a daily time-step, and are therefore capable of providing output more detailed than the annual values required. Of the models assessed; Ecosys, WNMM and DNDC implement hourly processing, at least for N cycling, which may be expected to give improved simulation of certain processes, although validation performance would be a better indicator of whether this results in improved prediction of annual average values.

Of the models in Table 3.2, NL-CAT, Ecosys and WNMM can be coupled to GIS. Of these, only Ecosys can apply a distributed approach incorporating data on topography, however, since soil data compiled in Section 2.10 is at a 1km^2 scale, there are no data on small scale variations in soil properties to represent how they interact with topography to produce WFPS as occurring in the field (Chen *et al.*, 2008; Potter *et al.*, 1996; Schoumans *et al.*, 2009a). WNMM and DNDC apply a one dimensional representation of soil water, so there is no capability for factoring in impacts of topography or lateral subsurface water movement (Li *et al.*, 2007). NL-CAT splits the modelled area into hydrologic response zones, and may therefore be appropriate for a more detailed site specific study incorporating impacts of landscape composition (Schoumans *et al.*, 2003).

Vertical spatial resolution varies significantly between the identified models; N-Loss uses 10 10 cm layers (Christensen *et al.*, 2006) CropSyst employs a system of layers and sub-layers (Stöckle *et al.*), and FASSET (Chatskikh *et al.*, 2005), APSIM (Vogeler *et al.*, 2013), Expert-N (Stenger *et al.*, 1999) and ECOSSE (Smith *et al.*, 2010a) can also have at least 10 layers. Number of layers is often user defined, for example; NL-CAT can have up to 50 (Renaud *et al.*, 2006), the soil-water component of DAYCENT has up to 10 (Lewis and McGechan, 2002), Ecosys can have up to 15 (Amthor *et al.*, 2001), WNMM has a user defined number (Li *et al.*, 2007), DNDC varies between versions, soil layers may be fixed or user defined (Chirinda *et al.*, 2010). The updated version of NOE has soil split into fine 1 cm layers, giving improved simulation of nitrification (Bessou *et al.*, 2010).

DNDC uses layer discretisation to simulate C and N profiles over the top 50cm (DNDC User Guide, 2009) and ECOSSE can simulate soil C cycling over at least the top 100 cm (Smith *et al.*, 2010a). DayCent simulates lumped SOM cycling using water and oxygen availability for upper layers to

predict process rates, on the assumption that most soil respiration and nutrient cycling occurs in the top 15 cm (Parton at al., 1998). Following decomposition DayCent distributes mineralised NO_3 through all soil water layers for N_2O calculations, whilst FASSET, WNMM and CERES-NOE only simulate N_2O production in the top 20 cm of soil (Chen *et al.*, 2008). Given that denitrification in deeper layers may make an important contribution to N_2O emissions (Bessou *et al.*, 2010), the approach applied by DayCent may be preferable.

Depth is also important when representing deep rooting crops; *Miscanthus* roots may go 250 cm into the soil, so greater representation of depth would be advantageous in simulating root access to water (Christian 2006). There is significant variation between models in the depth of water movement simulated, for example N-Loss simulates only the top 100 cm (Christensen *et al.*, 2006) whilst APSIM can simulate down to at least 200 cm (Huth *et al.*, 2010). DayCent simulates evapotranspiration uptake from the top 210 cm of soil; although where a water table is simulated evaporation can draw up deeper stores of water, although direct root access to water at these depths cannot be simulated.

Identified models are only as good as their process representation. The representation of tillage is particularly significant and often incomplete, for example DayCent represents an increase in decomposition immediately after tillage, but does not represent changes in bulk density for tilled versus no tilled systems. Similarly, WNMM only represents organic matter mixing, NL-CAT applies user-defined, as opposed to calculated values for bulk density, and Ecosys, CERES-NOE, ECOSSE and DNDC do not represent change in soil structure with tillage (Groenendijk *et al.*, 2005; Li *et al.*, 1992; Li *et al.*, 2007). Expert-N gives better representation of tillage, as some versions are able to simulate impacts on bulk density as well as mixing (Stenger *et al.*, 1999). Expert-N is a flexible modular system for combining models, often recommended for testing which combinations work, however no studies are available showing calibration for perennial crops. Furthermore documentation in English is limited (Stenger *et al.*, 1999), and the model is not currently available according to the research group website (Priesack, 2012).

DayCent does not explicitly represent microbial dynamics; accuracy of output may be reduced by assuming that rates of microbial output can be inferred implicitly from the parameters controlling microbial processes (Del Grosso *et al.*, 2000; Müller *et al.*, 1997). However Potter *et al.* (1996) and Chen *et al.* (2008) suggest that improvement in accuracy is minimal where microbial processes are

not represented at sufficiently fine scale, and Grant and Pattey (2003) and Boyer *et al.* (2006) suggest that information on topographically controlled saturation of soil is crucial to accurate representation of microbial activity. Of the models selected only Ecosys uses distributed microbial process representation and includes the impact of topography on lateral variation in soil water content. SWAT (coupled to ANIMO in NL CAT) includes lateral water flows for groundwater, but applies a vertical one dimensional approach for topsoil. Therefore explicit representation of microbial dynamics in most of the models considered here may not represent a significant improvement in performance.

Whilst several of the identified models were suitable for this study, the DayCent model has been selected, due to good validation performance for prediction of yield and N_2O emissions for *Miscanthus* (Davis *et al.*, 2012) and because good performance outside of development region suggest that the model should be appropriate for England (Foereid *et al.*, 2004b).

Model verification is crucial due to limited understanding of many of the processes discussed, and the tendency of model equations to be based at specific location. It is important to base confidence in the model on performance at validation as opposed to calibration (Perrin *et al.*, 2001). Although validation is often based on GHG emissions, the temporal variability of emissions at field scale complicates the process; validation based on change in soil C and N and proxy values for gaseous emissions may be more reliable (Bessou *et al.*, 2010; Del Grosso *et al.*, 2005; Li *et al.*, 2005b). Lastly, a model which has been calibrated for both perennial and annual crops may still not perform well for the transition between the two, where representation of relevant processes is incomplete. Ultimately the development of models identified by this review to give more complete representation of key processes should yield improved performance at validation.

3.7 Brief description of the DayCent model

The Century (Parton, 1994) agroecosystem model is designed to represent exchange of C, N and water, through biogeochemical processes including decomposition, infiltration and crop growth (Parton *et al.*, 1998). The model was originally produced by biogeochemists to improve understanding of soil C and N cycling (David *et al.*, 2009). DayCent is an adapted version of Century, which can represent soil processes at a daily time step, to enable improved representation of trace gas fluctuation with soil water and nitrogen levels through finer spatial

and temporal scale of simulation. Input data requirements include; daily weather, soil textural composition, pH and bulk density, a schedule file of types and timings of land uses and a set of parameters for the crop model. The model runs on a daily time step to solve a series of equations describing transfers and transformations of C, N and water within and between interconnected crop, soil and atmosphere systems. Parameter values for the specific site, date, crop, and any management events are read from input files of formatted text.

The main files required to run the model are; a schedule file of events to be modelled; a site file of data specific to the modelled location; a weather file of daily weather parameters; two separate files of set default values; a soil file to indicate how physical properties vary over the soil profile. These are listed in Table 3.3, along with additional "event" files which may be required depending on the scheduled events.

Table 3.3 Files to run the DayCent model

File name	Description
*.sch (where * is a name set by the user)	Dates of all events to be simulated: land use start and end dates, management activity dates
*.100 (where * is a name set by the user)	Site specific parameters: Latitude and Longitude, soil textural composition, bulk density, pH and monthly weather data.
*.wth (where * is a name set by the user)	Daily weather data: precipitation, maximum temperature, minimum temperature
Fix.100	Fixed parameters
Soil.in	Properties of texture, field capacity, wilting point, bulk density, hydraulic conductivity and pH for each soil layer
Outfiles.in	Indicates desired outputs
SItepar.in	Fixed parameters
Event files	Event type
Crop.100	Planting of a crop
Tree.100	Planting of a tree
Cult.100	Cultivation event
Harv.100	Harvest event
Omad.100	Organic matter input event
Fert.100	Fertiliser input event
Trem.100	Tree removal event
Irri.100	Irrigation event
Graz.100	Grazing event
Fire.100	Fire event

The model is run from command prompt, so before a run can be initiated, it is necessary to navigate to the folder containing the model file and all ancillary files. Commands are then input to run the model, reading from a named schedule file, and outputting data to a named bin file, as well as producing output files, with the ending ".out".

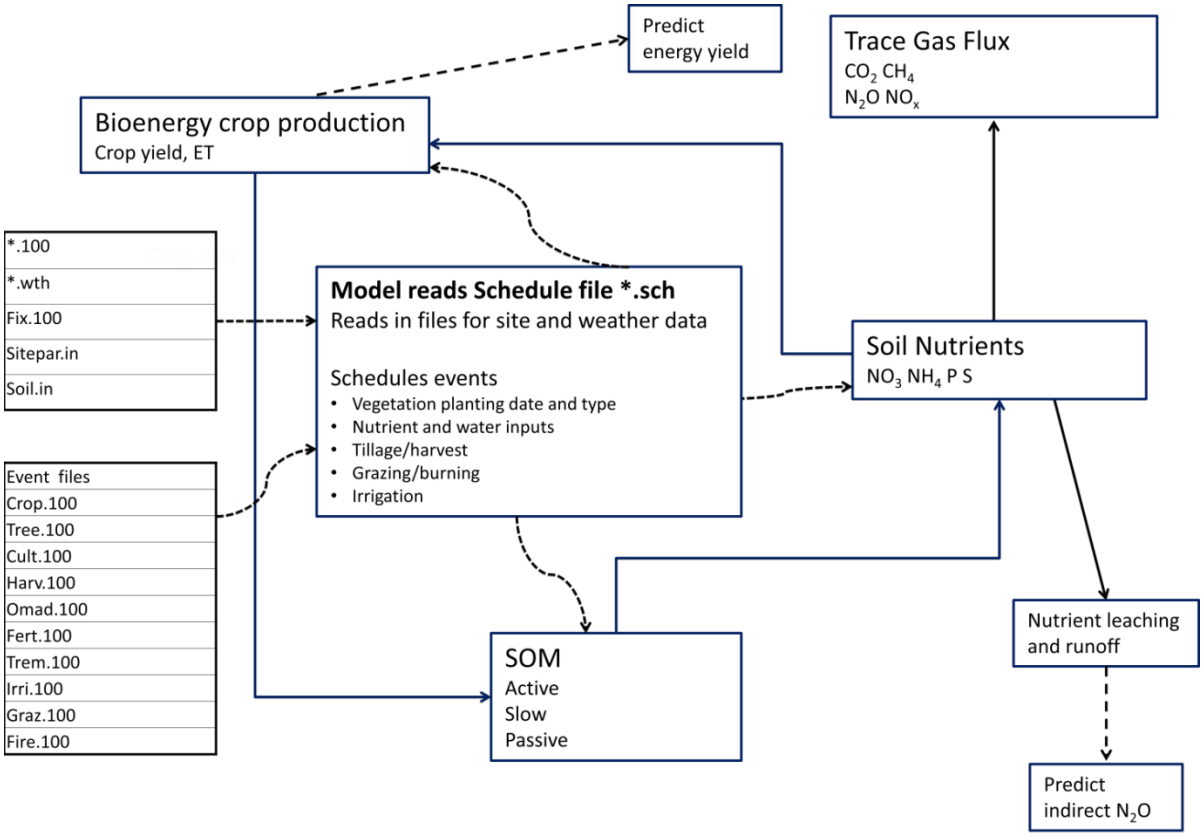

Figure 3.2 Schematic of DayCent

When running, the model reads values from input files of formatted text, beginning from the first line of the schedule file. The schedule file begins with start and end dates, and a pointer, in the form of *.100 (where * is a name set by the user) to read in the relevant site file. The modelled time period is split into blocks of land use, with a start and end time, and a pointer to read in the appropriate weather file, and the dates of events scheduled according to year and Julian day. To schedule an event, the model requires a pointer to the relevant ancillary file as per Table 3.3, and a label to indicate the event subtype within that input file. Each ancillary file is formatted into subsets of variables, each of which represents a subtype of event, and is formatted as a set number of parameters in a set order. For example an event type might be cult, and the subtype, e.g. rotovator plough, would have a label to call it from the schedule file, which would correspond to a subheading in the cult.100 file, followed by the list of cultivation parameters, each listed with a value appropriate to describe the impact of a rotovator plough. Values are thus read in

according to ancillary file name, event subtype label, and a line number and parameter label within that subtype.

Detailed model description is available in the literature, and a manual is distributed with the model, although as the model code is available to users for development, documentation does not always keep pace with changes to the model (Parton *et al.*, 1998; Parton, 1996).

3.8 Summary

Based on a literature review and conceptual model, the potential impacts of land use change for perennial energy crops were identified, as well as likely controlling variables. Based on these findings, criteria for model selection were derived. Due to interaction between crop, soil and atmosphere, a process based model representing the complete agroecosystem was identified as the best predictive tool. Crucial outputs for this study are; crop yield, direct and indirect GHG emissions, N leaching and ET. Indirect emissions may not be included in outputs, but can be easily calculated from predicted leaching rates. Crucial process representation includes rain, flooding and irrigation, crop uptake and growth, fertiliser and residue application, tillage, simultaneous denitrification and nitrification and gaseous losses from soil. Given the need to simulate all relevant aspects of the system, a conjunctive MCDA approach was applied, and models unable to represent all of these processes were ruled out.

DNDC, DayCent, Expert-N, Ecosys, CERES-NOE, ECOSSE, CropSyst, APSIM, WNMM, FASSET and NL-CAT were all identified as suitable, and cover a range of regions and crop types. For this thesis, DayCent was chosen due to calibration work for *Miscanthus* to match observed yields (Davis *et al.*, 2010), and subsequent good performance simulating yield and N_2O emissions at validation (Davis *et al.*, 2012), as well as evidence that the model performs well outside of development region and hence should be appropriate for England (Foereid *et al.*, 2004b).

4. Model development: tillage representation

This chapter follows on from Chapter 3 by developing the model which will be applied to sites typical of those which may undergo land use change for cultivation of perennial energy crops. In order to usefully predict the desired outputs of perennial energy crop yield and change in N_2O emissions, soil C and ET for land use change at these sites, some changes to the chosen model are necessary.

The key changes to the agroecosystem associated with land use change for perennial bioenergy crops are as identified in Section 3.4: change in tillage system; change in fertiliser regime; change in crop growth pattern. DayCent has only incomplete representation of tillage, as discussed in Section 3.6.2, so development to improve performance in simulation of impacts of tillage regime on N_2O is necessary to adequately simulate emissions under arable conditions prior to land use change, and how these vary between sites. Model adaptation for this purpose will be detailed in this chapter. The model is able to represent change to fertiliser regime, since nutrient inputs can be simulated in terms of quantity, timing, and C:N ratio. However, improvements to simulation of change in tillage regime should enable the model to represent interaction between changes to these two land management factors. In terms of representing new crop growth pattern, DayCent has shown good validation performance for simulation of *Miscanthus*, as mentioned in Section 3.6.2, however model capability to simulate SRC willow cultivation has not been assessed, so this issue will be addressed in Chapter 5.

Intensity of tillage is variable; different equipment will disturb the soil to differing extents and different depths. For example a moldboard plough (often described in the literature as "conventional tillage") causes inversion of the top layer of soil (around 20cm) increasing aeration significantly and redistributing residues and other surface organic matter, whilst a rotovator is designed to break up clods, and only affect around the top 10cm of soil. Secondary tillage such as tillering may also be applied for seed bed preparation, with relatively minimal disturbance, but some increase in aeration. In some cases rollering may also be applied to compact the soil increasing contact with seeds or rhizomes following planting. Images of relevant tillage equipment are included the visual glossary. As well as variations in tillage equipment, timing, particularly in

relation to precipitation events can significantly alter the impacts. Arable land in England is generally under annual tillage, whereas permanent grasslands may be tilled and re-seeded at intervals of five years, and tillage may be more frequent for improved grasslands (UK Agriculture, 2010c). A no till system is necessary for the full lifecycle of perennial energy crops, hence this will represent a reduction in tillage frequency. Disturbance at the end of the lifecycle will be necessarily intensive to remove or breakdown remnants of the crops; in the absence of calibrated values for the relevant equipment, this may be simulated as multiple passes of more conventional tillage equipment, as will be discussed in section 6.2.

Given that Section 1.4.2.3 identified structural changes to soil as the key impact of tillage on N_2O emissions, Section 4.1 identifies equations which can calculate the impacts of these changes on key soil properties, and outlines the extent to which these approaches can be incorporated into the DayCent model. The required algorithms were identified at this point, and added to the model code to recalculate variables used to calculate the rates of nitrogen cycling and decomposition processes. Section 4.2 details changes to the model code and input files to incorporate these new algorithms, although in order to be concise, some of this information is necessarily relegated to the appendix.

Model verification is then detailed in Section 4.3 to show that improvement in model performance is not merely theoretical. Section 4.3 gives descriptions of field sites and the calibration approach, followed by an assessment of model performance at simulating time series of water filled pore space (WFPS) and N_2O emissions, to identify whether the model can replicate the observed field changes occurring in response to land management. Relative deviation of model predictions from measured data over the study period is then calculated to create an objective measure of model performance which can be compared to other models and studies.

The change in porosity associated with tillage will interact with site properties, to produce different levels of SOC storage, CO_2 and N_2O emissions, depending on factors such as soil textural properties and precipitation regime. Following land use change, the NT system no longer experiences oxygenation, aggregate breakdown and increased porosity; again this change will interact with site properties such as soil textural properties and precipitation regime to produce the new levels of SOC storage, CO_2 and N_2O emissions. Given the relatively high fertiliser inputs for arable land, and the high GWP of N_2O emissions, it is particularly important to represent

impacts of tillage on N cycling, to identify current variation in emissions. Whilst perennial energy crops are likely to receive little or no fertiliser inputs, it would be useful for the model to represent impacts of changes in soil porosity and structure under NT, and how these affect emissions and cycling of retained N and the high C:N OM inputs from the new crop as discussed in Section 1.4.2.4, as well as any N inputs which become necessary in the event of soil store exhaustion. Representation of impacts of tillage is limited by incomplete understanding of processes, and the need to minimise complexity, as will be outlined in Section 4.1.

4.1 Existing and potential tillage representation

Existing complex agroecosystem models such as DayCent and DNDC tend to apply proxy factors to simulate impacts of tillage on processes such as decomposition, which limits the ability to account for variation in response with site factors such as soil texture or climate. The EPIC model uses change in bulk density with tillage to simulate change in porosity, and impacts on other parameters. However N_2O:N_2 ratio is not simulated; hence this model is less useful for consideration of GHG emissions. A similar approach could be built into the DayCent model to account for impact of tillage on bulk density, and simulate impacts of this change on other processes. DayCent is a crop-soil-atmosphere model which has been applied to a range of crops and climate zones, and was identified by MCDA in Chapter 3 as potentially suitable for simulating land use change to NT conditions (Chen *et al.*, 2008; Parton *et al.*, 1998; Parton *et al.*, 1996; Thomas *et al.*, 2013b).

Modelling of the impacts of tillage on N_2O emissions is hampered by incomplete understanding of processes, and limited research aimed at predicting soil hydraulic properties from management (Green *et al.*, 2003). There is a need for further development and testing of whole agro ecosystem model approaches to representation of tillage, to give improved potential to provide site specific guidance on appropriate tillage regimes (Gupta, 1991; Strudley *et al.*, 2008). To achieve reasonable yields, NT farming must necessarily differ from tilled farming in other aspects of land management, hence field studies do not only change tillage system in the manner of a controlled experiment (Derpsch, 2010). However, to address the topic fully, calibration in Section 4.2.4.1 focusses only on the models ability to represent tillage.

Model development is constrained both by current knowledge and available equations, and the level of representation in the existing model. It is therefore necessary to first outline how DayCent represents aspects of the soil system which are affected by tillage, before considering how the impacts of tillage might be represented. The DayCent agroecosystem model is designed to represent exchange of C, N and water, through biogeochemical processes including decomposition, infiltration and crop growth (Parton *et al.*, 1998; Parton *et al.*, 1994). The model consists of a soil water sub-model, which simulates storage and movement of water, and a SOM sub-model which simulates transfer of SOM between pools defined by availability and decomposition rates (Chen *et al.*, 2008; Parton *et al.*, 1998; Parton *et al.*, 1996). Recommendations suggest that the model is run for an 1800 year "spin-up" period with pre agricultural land-use parameters, followed by a "clear cut" (100 %) tree removal event, tillage, and 200 years of roughly modern arable land management and crops to set SOM pools.

Existing representation of tillage by DayCent is limited to a temporary increase in SOM decomposition (Parton *et al.*, 1994; Ogle *et al.*, 2012; Parton *et al.*, 1998). Thus, the model is only able to represent the aspects of tillage which cause increased N_2O emissions, and there is no representation of porosity changes controlling WFPS which may decrease emissions with tillage. The model is described in Section 3.8, and more in-depth model description is available in the literature (Chen *et al.*, 2008; Parton *et al.*, 1998; Parton *et al.*, 1996), therefore discussion of process representation in this chapter is limited to the context of tillage, in order to identify potential for improvement. The key processes affected by tillage, as identified in Section 1.4.2.4., are decomposition of organic matter, soil water retention and drainage, nitrogen cycling and gas diffusivity. These processes are affected primarily by changes in soil porosity and pore connectivity.

4.1.1 Increase in inter-aggregate porosity

Tillage produces an immediate but temporary increase in inter-aggregate porosity, whilst the breakdown of aggregates reduces intra-aggregate porosity (Ahuja *et al.*, 1998; Leij *et al.*, 2002a). This will affect water and gas flow and storage in soil according to the differing properties of intra-aggregate and inter-aggregate pores. Porosity is represented in DayCent as a constant value of inter-aggregate pore space based on ρb, and as a constant value of intra-aggregate porosity calculated from texture and organic matter content.

A range of equations could be integrated to update ρb and thus inter-aggregate pore space for tilled soil (Chen *et al.*, 1998b; Williams, 1984; Williams, 2008). Prior to development of these equations, models required experimental data input to represent such change (Gupta, 1991). Impacts of tillage on soil processes can then be represented, provided these correlate with bulk density, and are not more strongly affected by other changes occurring at tillage.

Change in bulk density (ρb) could be calculated according to the following empirical equation, based on initial ρb, and final consolidation ρb (Williams, 1984; Williams, 2008);

$$\rho b(i) = \rho b_o - \left[\rho b_{o-\frac{2}{3}} \rho b_c\right] I$$

where $\rho b(i)$ = bulk density after tillage (g cm^{-3})

ρb_o = bulk density before tillage (g cm^{-3})

ρb_c = consolidation bulk density at 33-kPa pressure (g cm^{-3})

I = tillage intensity (0-1)

This equation is applied in some existing models (APEX and EPIC), however, it relies on known consolidation bulk density, as opposed to the more readily available parameters of soil textural composition. Consolidation occurs with compaction from precipitation, freeze-thaw settling, and traffic, reducing porosity over time, potentially to below pre-tillage levels, since smaller aggregates can have closer packing (Bronick and Lal, 2005; Green *et al.*, 2003).

More recently (Chen *et al.*, 1998b) derived equations to calculate change in ρb at tillage, according to soil texture, using constants based on data from a range of published studies;

$\Delta\rho b_{ij} = a + bm_{cl} + cm_{si} + dm_{sa} + eOM$

where $\Delta\rho b_{ij}$ = change in ρb for soil layer and tillage implement

m_{cl} = mass of clay

m_{si} = mass of silt

m_{sa} = mass of sand

OM = mass of organic matter

and a,b,c,d and e are constants varying with tillage implement and soil layer

Since soil data in Section 2.10 does not include consolidation ρb value (Chen *et al.*, 1998b), equations were considered more appropriate to build into the DayCent model, although these are based on a limited number of field studies, and there is difficulty accounting for factors such as soil moisture content at the time of tillage, which may introduce error (Chen *et al.*, 1998b). Although soil data in Section 2.10 does not include potential range of ρb, it remains necessary to apply constraints to avoid simulation of ρb values outside of the likely range for a given soil texture. DayCent will not run with ρb values which are not representative of soil texture, but does not supply a ρb range for given texture, so this must be established iteratively during model development, and then built into model algorithms.

Changes in processes such as decomposition and denitrification can then be calculated using the new ρb value, to reflect impacts of change to porosity. Rates of both nitrification and denitrification are affected by soil pore oxygen status, affected by the change in porosity at tillage. DayCent represents nitrification and denitrification simultaneously, occurring in aerobic and anaerobic pores respectively. Simulated rates are controlled by WFPS, CO_2 and nitrate or ammonium per layer, as well as pH and temperature (Boyer *et al.*, 2006; Chen *et al.*, 2008; Del Grosso *et al.*, 2000; Li *et al.*, 2005b). To account for impacts of tillage on these processes, it is thus required that updated ρb be applied to calculation of WFPS.

These changes to representation of tillage will also affect SOM representation, since updated WFPS is applied to calculations for decomposition rates. Therefore tillage factor should be adjusted to account only for aggregate breakdown and change to OM availability and microbial community.

Simulation of change in ρb with tillage enables representation of some of the impacts of porosity changes on soil C, N and water cycling. System complexity and gaps in knowledge and

understanding mean that model representation is inevitably imperfect. It is important to consider possible sources of error where factors cannot be accounted for, particularly the soil moisture content at time of tillage, which will affect the change in ρb. Propagation of errors in ρb recalculation may be amplified by nonlinearity of equations representing rates of processes according to WFPS. However in the absence of field data, the changes in rates of these processes cannot be predicted for a specific site.

Impacts of tillage on soil porosity are temporary, so changes should either be applied for a set period, or gradually removed with successive rainfall events (Green *et al.*, 2003; Li, 1994). Given that calculations of settling following tillage should be independent of initial ρb, Onstad *et al.* (1984) formulated the following equation to calculate the change, based on experiments with soils ranging from sandy loam to clay loam;

$$\rho b = \rho b(i) + a\,\frac{P(t)}{1 + P(t)}$$

where ρb(i) = bulk density after tillage (g cm^{-3})

ρb = new bulk density (g cm^{-3})

P(t) = cumulative precipitation

a = empirical constant, generally around 0.1

Changes in processes such as decomposition and denitrification can then be calculated to reflect impacts of change to porosity.

Separation of porosity into inter-aggregate and intra-aggregate pores is a simplification; in particular inter-aggregate pore size is highly variable according to aggregate size and packing. Following tillage larger pores are likely to experience more change in size, and over time with natural settling a reduction in size and frequency of modal pore size is observed (Leij *et al.*, 2002b). Models with detailed structural representation can incorporate approaches such as the Fokker-Planck equation, using a stochastic approach to quantify impacts of tillage on different pore size distribution controls (Or, 2000);

$$\frac{\partial f}{\partial t} = \frac{\partial}{\partial r}\left(D(r,t)\frac{\partial f}{\partial r}\right) - \frac{\partial}{\partial r}(V(r,t)f) - M(t)f$$

Where f = frequency (μm^{-1})

t = time (s)

r = pore radius (µm)

V = drift coefficient ($\mu m\ s^{-1}$)

D = dispersion coefficient ($\mu m^2\ s^{-1}$)

M = degradation coefficient (s^{-1})

Pore size distribution and changes over time following tillage cannot be represented within the limited dual porosity approach adopted by DayCent, and therefore these equations cannot be built into the model without significant additional complexity.

Field studies have noted more impact on soil water retention under wet conditions, when inter-aggregate pores hold more water, i.e. at high matric potentials (Gupta, 1991). This indicates greater impact from the temporary increase in inter-aggregate porosity at tillage than from the breakdown of aggregates and loss of internal pores (Green *et al.*, 2003). Since intra-aggregate porosity is not strongly affected by tillage, this variable need not be recalculated.

The key range in which change to the soilwater retention curve occurs is between air entry pressure (h_b) and $10h_b$. A new gradient for this portion of the curve can be calculated according to Ahuja *et al.* (1998);

$$\lambda\text{till} = \frac{\log(\theta s, till - \theta r) - log[\theta(10h_b) - \theta r]}{log|h_b| - log|10h_b|}$$

Where λtill = new gradient

h_b= air entry pressure (cm)

Θr = residual water content (m^3m^{-3})

Θs,till = tilled soil saturated water content (which can be calculated from ρb) (m^3m^{-3})

DayCent applies the assumption that the soil water retention curve has similar slope to particle size distribution, and therefore it is not directly related to porosity in the model (Gupta, 1991). The equation above would enable updated values of effective porosity to be applied for recalculation of soil water retention curve, however, known values of h_b and $10h_b$ would also be required, and these are not included in the soil data in Section 2.10. Furthermore, the process would be complicated by the need to update only the relevant portion of the curve, hence this part of the model has not been adapted (Ahuja *et al.*, 1998; Gupta, 1991).

4.1.2 Disruption of pore connectivity

Hydraulic conductivity and diffusivity also correlate with ρb, however the impacts of tillage on this relationship are complicated by changes to pore connectivity.

As well as soil water retention curve, saturated hydraulic conductivity (Ksat) is a key variable in the calculation of drainage rates. In DayCent, K, calculated from Ksat and relative saturation, controls the rate of water entry and downward flow through soil. In the event of water input, a 4 hour saturated flow cycle is computed with initial water entry at the Ksat of the top layer, and downward flow at the rate of the slowest layer Ksat. For unsaturated periods, 2 hour time steps use Darcy's law to simulate flux of water between soil layers based on hydraulic potential and hydraulic conductivity (Parton *et al.*, 1998). Assuming a consistent relationship, it is possible to calculate a new value of Ksat for the updated ρb following tillage via effective porosity, according to (Green *et al.*, 2003);

$$K_{sat} = B\ \emptyset_e^n$$

Where K_{sat} = Saturated hydraulic conductivity ($cm\ h^{-1}$)

$\emptyset_e$ = effective porosity (cm^3cm^{-3})

B,n = empirical constants

B and n can be calculated prior to tillage from effective porosity based on Kozak and Ahuja (2005).

$$B = \frac{K_{sat}}{\emptyset_e^n}$$

$$n = 3 - \lambda$$

Where λ is a pore size distribution function which can be calculated as:

$$\lambda = e^{\frac{\log K_{sat} - 4.83}{3.62}}$$

However Ksat, is also affected by soil structure, due to faster flow through macropores, and as a result, the relationship between Ksat and effective porosity is altered by tillage. Therefore, although Ksat can be scaled with effective porosity changes at tillage, without simulation of connectivity and tortuosity this is unlikely to give good representation, and should not be recalculated using pre tillage values as constants (Moldrup, 2001; Schwen, 2011).

Changes to Ksat with tillage cannot therefore be represented in the developed model, which limits representation of affected processes (Green *et al.*, 2003; Kozak and Ahuja, 2005; Moldrup, 2001). Drainage affects two key N cycling controls; soil oxygen status (via water filled pore space (WFPS) and impacts on diffusion) and soil N (via leaching). Flux and storage of water affect N_2O emissions since leaching affects nitrate per layer, and WFPS affects soil pore oxygen status and connectivity for gas diffusion. Limitations in predicting N_2O emissions as a result of not being able to simulate these impacts must be taken into account when assessing model output. Field studies on changes in land management or crops have produced varying findings on impacts on N leaching, leading to a lack of consensus on this issue; this incomplete understanding further reduces potential for good representation (Soane *et al.*, 2012). Representation is further complicated by spatial variation in soil structure in terms of macropore numbers and connectivity, which can lead to orders of magnitude differences in Ksat, exceeding the impacts of management (Strudley *et al.*, 2008). Soil structure, pore continuity, drainage and gas diffusivity may be enhanced over time under no tillage by aggregate formation, and greater abundance and activity of soil biota (Capowiez *et al.*, 2009; Derpsch, 2010; Schwen, 2011; Six *et al.*, 2004). Although many of these changes may be measurable within months of the last tillage event, others may take

several successive seasons of NT to develop, for example macropore and SOM changes usually don't reach equilibrium within 3 years (Soane *et al.*, 2012).

Since N_2O is an intermediate product of denitrification, the rate of diffusion from soil affects the ratio of N_2O to the completed reaction product N_2 (David *et al.*, 2009; Davidson *et al.*, 1998; Green *et al.*, 2003; Moldrup, 2001; Petersen *et al.*, 2008). As well as gaseous losses, diffusivity also controls O_2 availability, so accuracy of simulation of rates of N cycling processes will also be affected (Skiba, 2002). As with hydraulic conductivity, the molecular diffusion coefficient is controlled by the continuity and tortuosity of the pore network (Gupta, 1991). The diffusion coefficient can be calculated from air filled porosity based on a range of approaches with varying complexity; better performance is seen for models which require empirical data to calculate multiple constants, and models which divide pores by size or accessibility (Moldrup, 2004). Scaling diffusivity with ρb would give increased diffusion of N_2O from soil at tillage, which may not be representative of field conditions, since connectivity of pores will be disrupted by tillage, and acts as a more significant control on fluid flow through soil. Macrostructure controls relationship between tillage and diffusivity, making it difficult to analyse what is really happening for a given site. Tillage does not always increase diffusivity e.g. (Elmi, 2003), and impacts on product ratio are low where N_2O producing processes occur close to the surface of the soil (Ball *et al.*, 1999). Again, without equations to account for the impacts of disturbance on connectivity, the potential to represent impacts of tillage on diffusivity is limited, and additional complexity may not be warranted (Leij *et al.*, 2002a; Moldrup, 2004). Connectivity can be simulated based on soil surface area for undisturbed soils, however there is no existing approach to represent variation with time and tillage (Moldrup, 2001; Strudley *et al.*, 2008). This lack of suitable equations to simulate change in connectivity limits potential for modelling, although simulation of change in such hydraulic properties may be possible where pore connectivity can be measured (Gupta, 1991). In the context of this study, such data are not available, so changes cannot be made to the DayCent model, and the original ρb must be applied for these calculations.

4.1.3 Soil aggregate breakdown and SOM mixing

SOM is linked to land management; loss may be accelerated by tillage, due to the breakdown of protective aggregates, and aeration of soil which combine to accelerate organic matter decomposition (Paustian, 2000). In models with representation of aggregate size distribution, it

may be possible to account for impacts of tillage, for example using fractal theory (Pirmoradian *et al.*, 2005). However, for simplicity, existing models usually combine the impacts of aggregate breakdown and increased pore oxygen, by applying a factor to increase decomposition rates (Li, 1994). Provided resulting decomposition rates are simulated reasonably, this approach is adequate in terms of representing change in SOM, but may not enable accurate simulation of fate of decomposition products and associated GHG emissions from soil. Therefore, to avoid the model complexity required for explicit aggregate simulation, a proxy factor for increased decomposition rates from reduced physical protection may be adequate

DayCent represents impacts of tillage on SOM by transfer of OM from surface to soil pools, and the application of tillage factors as a proxy for aeration and aggregate breakdown, to increase decomposition and microbial yield efficiency for the rest of the month (Parton *et al.*, 1994; Ogle *et al.*, 2012; Parton *et al.*, 1998). The tillage factor is applied for one month, to simulate loss of inter-aggregate porosity over time with precipitation and other natural compacting forces.

Tillage also reduces stratification of SOM by incorporating surface inputs such as residue or fertiliser over the tilled depth. Mixing of nutrients over the ploughed layer can be simulated in models with vertical disaggregation of SOM representation by transferring SOM between pools (Li, 1994; Williams, 1990, 2008).

In terms of vertical stratification, the DayCent SOM sub model is only split into surface and soil pools, hence redistribution with tillage can only be represented as a transfer from surface to soil. There is also no representation of aggregate size and stability and associated impacts on availability of SOM for decomposition or other reactions. It has been suggested (Ogle *et al.*, 2007) that this may cause bias in representation of soil C stocks, particularly under NT conditions, however it would significantly increase model complexity to resolve this issue.

4.2 Improvement – changes to code

The model code is made up of over 200 subcomponents- some are in C, some are in FORTRAN, hence both a FORTRAN and a C compiler must be used. Changes were made to both sets of code,

and the relevant ancillary files. Code changes are given in full in Appendix Section 2 and the technical details are outlined in Figure 4.1.

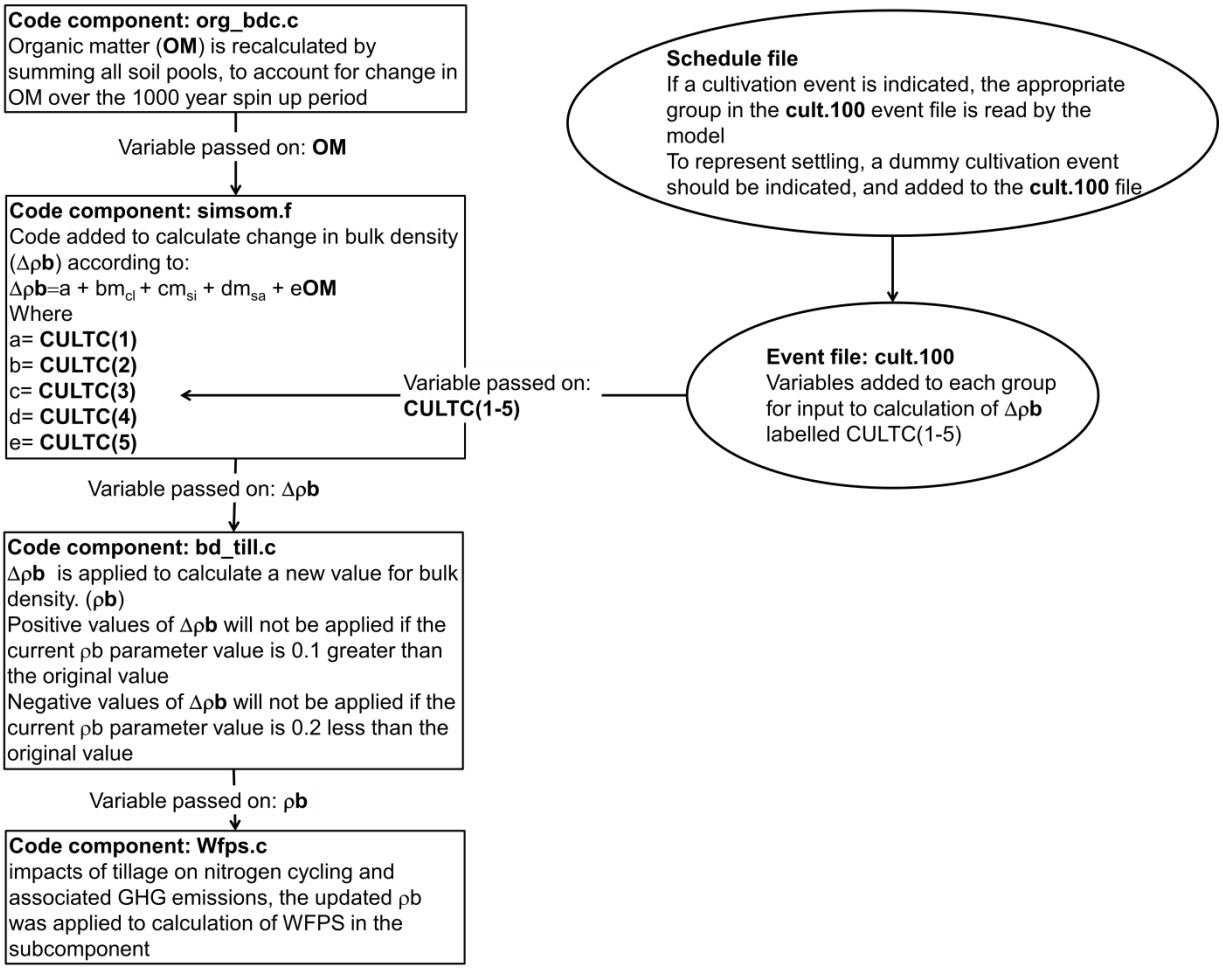

Figure 4.1 Main changes made to the model: code components and event files. Changes were made to the code components (square boxes), and these were compiled to produce the new executable. The event and schedule files (oval boxes) must be present in the same folder as the executable for the model to run. The schedule file is specific to the model run, as detailed in Section 3.7. Five parameters CULTC(1-5)were added to each event type in the cult.100 file to account for values of a – e in the algorithm added to the simsom.f model component. The values of CULTC(1-5) will vary according to tillage implement and are read in along with other variables pertaining to cultivation.

In brief, change in bulk density following a tillage event is calculated using Chen *et al.* (1998b) equation; inputs are soil textural components (set at the start of the model run) and OM (recalculated to account for change over time) and variables a-e (represented by CULTC (1-5)). The values of CULTC(1-5) will vary according to tillage implement; a number were listed by Chen *et al.* (1998b), although the terminology used does not match with that used for the existing **cult.100** types, due to variation in both implements and terminology between agriculture in

different areas. Values used and reasoning behind selection of the closest match for tillage type are listed in Appendix Section 2.2. Proportions of the textural components are set by the original input files, whilst the value for OM is recalculated in **org_bdc.c**, by summing all soil pools, as SOM may have changed significantly from the initial values, due to the 1000 year spin up period. $\Delta\rho$**b** is then calculated.

The value for change in bulk density is then added to each soil layer in the **bd_till.c** model subcomponent. It is necessary to apply constraints to avoid simulation of bulk density values outside of the likely range for a given soil texture. To do this, positive $\Delta\rho$b is not applied if ρb is too much greater than the preset value, and negative $\Delta\rho$b is not applied if bulk density is too much less than the preset value. In the absence of equations to indicate bulk density range for given texture, boundaries were established iteratively during model development, and then built into model algorithms. Based on testing, boundaries were set as indicated in the box for code component **bd_till.c** in Figure 4.1; application outside of this range caused the model run to terminate.

To account for impacts of tillage on nitrogen cycling and associated GHG emissions, the updated bulk density was applied to calculation of WFPS. The new value of bulk density is only used to recalculate water capacity for simulation of soil drainage and soil pore oxygen status, and was not applied to recalculate the diffusivity coefficient. Although bulk density is also used in the initial calculation of field capacity and wilting point, it is important that these are not recalculated for the change in bulk density, since intra-aggregate porosity is not affected in the same way.

The existing actions of a cultivation event; OM transfer and a proxy factor for increased decomposition were left in the source code and input files. Values of the proxy factor were reduced so that SOC change following till is similar to if no porosity factor was applied- i.e. the factor now no longer needs to account for the increased soil pore oxygen status, but should still be applied to account for the other impacts of tillage on decomposition rate. Graphs to indicate the calibrated values are also included in Appendix Section2.3.

To remove the impact of tillage on ρb after one month, a virtual cultivation event is applied, read from **cult.100** as before. Ideally the settling event would be applied at the first rainfall event, however due to model structure, it is more convenient to apply this at a defined interval, and this approach was also used for cultivation effects in the model as distributed, so was deemed

adequate. For the settling event CULTC(2-5) are set to 0, and CULTC(1)is set as the total value for $\Delta\rho b$, which is calculated using the settling equation from (Onstad *et al.*, 1984), and a value of average precipitation for the relevant month and site. For sites under NT, additional settling events were added for the months with highest precipitation in the first year, in order to match with field observations of higher bulk density. No OM transfers or proxy factors for aggregate breakdown are required for the settling events.

4.3 Improvement-model performance testing

After model code changes had been implemented, parameterisation and calibration of this adapted model were then carried out for appropriate datasets identified in the literature. Given the need to test model behaviour for different conditions of soil pore oxygen, study sites were selected to cover a spectrum of values for drainage and aeration status (Rochette, 2008). Land use change is accompanied by a period of soil structural changes before a new equilibrium is reached, hence preference was given to sites with data collected close to the timing of transition from T to NT conditions, in order to test model capability fully. Study location is also relevant; although the daily version of the model was originally developed and tested for Colorado and Europe (Parton *et al.*, 1998), it has shown reasonable performance in other regions (Thomas *et al.*, 2013b). It would be preferable to assess performance for a range of climates, however, the need for relatively complete datasets collected close to change in management scheme limited choice of sites.

4.3.1 Calibration datasets

Six datasets were compiled from studies in Denmark, Canada and England with available, useable data on land management, soil type and N_2O emissions, covering a spectrum of drainage and aeration states from good to poor. Three datasets begin two years after change to tillage regime (Chatskikh *et al.*, 2008; Rochette *et al*., 2008a); two begin at the time of regime change (Baggs, 2003; Webster, 2003); the remaining dataset does not record land management history prior to the start of data collection (Lemke, 1999). Daily weather data inputs as required by DayCent were either provided by the authors, or compiled from online repositories and checked against statistics provided in the study. All studies used soil chambers to collect gas measurements, and provided N_2O data in the form of both graphs and totals for stated time periods. Time series data

were not available for the published studies, except for site 5, for which Webster (2004) provided time series data, which is included in the graphs. Therefore, assessment of model simulation of the measured WFPS and N_2O emission response to land management was based on qualitative comparison to graphs included in the publications, which are reproduced in Appendix Section2.4. Excepting site 5, quantitative assessment was limited to measured versus modelled totals over the experiment time period, for both management conditions, and the difference between the two. Information missing from the published studies, such as a failure to describe tillage implements, or detail land use history is limiting both to application of published data to model testing, and to comparison of findings between studies.

Table 4.1 compares key characteristics of the datasets used; more detailed descriptions of sites and study methodology can be found in the relevant publications identified therein. In terms of land management, tillage types included moldbord plough and rotovator, with varying degrees of intensity and N application rate varied from 12 to 200 kg ha^{-1} a^{-1}. In terms of site properties, bulk density varied from 1 to 1.5, and clay percentage varied from 8 to 77. Details on the moldbord plough, rotovator and other tillage implements can be found in the Visual Glossary on page 311. The sites also encompass a reasonable range of climate types, with precipitation from 61 to 300 cm a^{-1}, minimum air temperatures ranging from -19 to 1.3°C and maximum temperatures ranging from 12.5 to 25°C.

Table 4.1 Key characteristics of calibration datasets (Images of relevant tillage equipment are included the visual glossary)

Site	**1 (Lemke *et al.*, 1999)**	**4 (Baggs *et al.*, 2003)**	**2 (Chatskikh *et al.*, 2008)**	**5 (Webster, 2004)**	**6 (Rochette *et al.*, 2008a) Kamourska soil**	**3 (Rochette *et al.*, 2008a) St Andre soil**
Drainage	intermediate	intermediate	good	intermediate to poor	poor	good
Aeration status	good	intermediate	Intermediate	poor	poor	Intermediate
Time since change to NT	Not stated	0 years	2 years	0 years	2 years	2 years
lat long	53°25N, 113°22W	51°10'18 N, 0°51'46E	56°29N, 09°34E	51°46.51'N 0°28.26'W	46°48' N, 71°23'W	46°48' N, 71°23'W
tillage type	rotovator *2 (for till only) hoe drill planting (both)	conventional zero	rotovator (for till only)	plough, press (for till only) and top tilth (both)	moldboard plough (for till only) and tillering (both)	moldboard plough (for till only) and tillering (both)
vegetation	Spring wheat	Maize/Rye	Barley/Rye	winter wheat	barley	barley
OM and nutrient inputs	Urea was applied at an N rate of 56 kg $ha^{-1}a^{-1}$	N rate of 200 kg $ha^{-1}a^{-1}$ as well as straw/residue	N rate of 12 kg $ha^{-1}a^{-1}$	N rate of 180 to 200 kg $ha^{-1}a^{-1}$	N rate of 70 kg $ha^{-1}a^{-1}$	N rate of 70 kg $ha^{-1}a^{-1}$
annual average air temp range °C	-14 to 23	-0.7 to 12.5	-2 to 23	1.3 to 23	-19 to 25	-19 to 25
annual average precipitation cm	300	79	61	68	119	119
Precipitation SD	19.14	2.20	2.04	1.51	2.45	2.45
Clay %	39	15	8	31	77	22
pH	6	5.8	6.1	7	6.2	5.9
bulk density	1.01	1.5	1.3	1.04 to 1.23	1	1.4
measurement approach	3 or 4 vented soil covers per sample date. At least twice monthly. No WFPS data	2 chambers daily or less often. No WFPS data	chambers, 3 measurements per sample date	weekly 8 chambers per field/Daily autosamples at key times	weekly chambers	weekly chambers

4.3.2 Calibration approach

Although the adapted model gives improved theoretical representation of processes relating to tillage, it is crucial to assess whether model performance is also improved. Ideally, this would

include calibration to improve model representation for an initial time period, and a validation stage where measures of model performance for a subsequent time period are used to evaluate the new model (Thomas *et al.*, 2013b). In the case of this study, the limited duration of available datasets prohibits application of both calibration and validation methodology in this manner. Taking an alternative approach, minor changes to model inputs were made to calibrate ρb, WFPS and N_2O for four of the sites, followed by validation only assessment for N_2O emissions only for the other two sites (where data on WFPS and ρb was not available).Values used and impacts on model output are detailed in Table 4.3. Conclusions about likely model performance for scenario analysis where calibration data are unavailable should be based on the latter studies.

WFPS and ρb were chosen as calibration variables because both control diffusivity and oxygen availability, and hence N_2O emissions. Given the nonlinear relationships between WFPS, and the differing rate profiles of denitrification and nitrification processes, misrepresenting the initial saturation will result in poor simulation of N_2O emissions response to change in soilwater (Frolking *et al.*, 1998). Comparison of WFPS to field data is therefore a useful start point to improving and evaluating model performance. Parton *et al.* (1996) note the importance of WFPS in simulating N_2O emissions, and that performance for DayCent may be variable over different sites and seasons.

A degree of calibration was required for some sites to achieve reasonable WFPS representation. To increase WFPS in line with field data, presence of a water table was applied for poorly drained sites, whereas an increased value for sand content and reduced value for clay was applied to match lower WFPS field data for better drained sites. Settling events were scheduled to follow tillage events, in line with common field observations (Franzluebbers, 1995; Moret and Arrue, 2007) applying equations by Onstad *et al.* (1984) set out on page 144. Since bulk density is commonly regarded as having a consolidation value i.e. a point at which further porosity is unlikely to be lost without additional compacting forces such as vehicle traffic, models such as EPIC utilise a consolidation factor. Often subsequent settling will negate impacts of tillage on ρb, however this may take more than a year (Franzluebbers *et al.*, 1999), and consolidation does not always create a stable value for ρb (Green *et al.*, 2003). Reduction from year to year may occur even where fields had previously been under long term tillage; changes of -0.14 over one year for site 5 indicate that this change can be significant, as opposed to a transitional phase leading into a plateau.

Whilst the model is required to replicate this site behaviour, it is necessary to set boundaries in the model code for change in ρb to avoid unrealistic values and prevent calculation errors. Model parameterisation therefore focussed on restricting the range for application of the factor to change ρb, to avoid simulation of unrealistic values outside the range accepted by the model for a given soil texture.

Settling factors were included in the schedule file, coded as cultivation events, scheduled to coincide with the month following tillage, and the peak rainfall months, to produce ρb values matching those in field data for sites 5 and 2. Changes to these enabled the model to give reasonable simulation of ρb, following which additional changes were made to textural composition and water table simulation as necessary to simulate field data for WFPS.

4.3.3 Time series WFPS

Field data plotted in Chatskikh *et al.* (2008) (see appendix Figure A2.4) indicated a drop in WFPS immediately following tillage; for site 2 (Figure 4.2), this was not simulated by the old model version, but the developed version of the model simulated timing and magnitude well. Simulated values of WFPS prior to tillage from both models are slightly higher than those measured by Chatskikh *et al.* (2008), whereas from May to July, simulated values from both models are lower than the field data, and at the end of the measurement period, the WFPS simulated by the developed version of the model for the tilled site is lower than measured values, whereas the other three sets of model output are slightly higher than measured values.

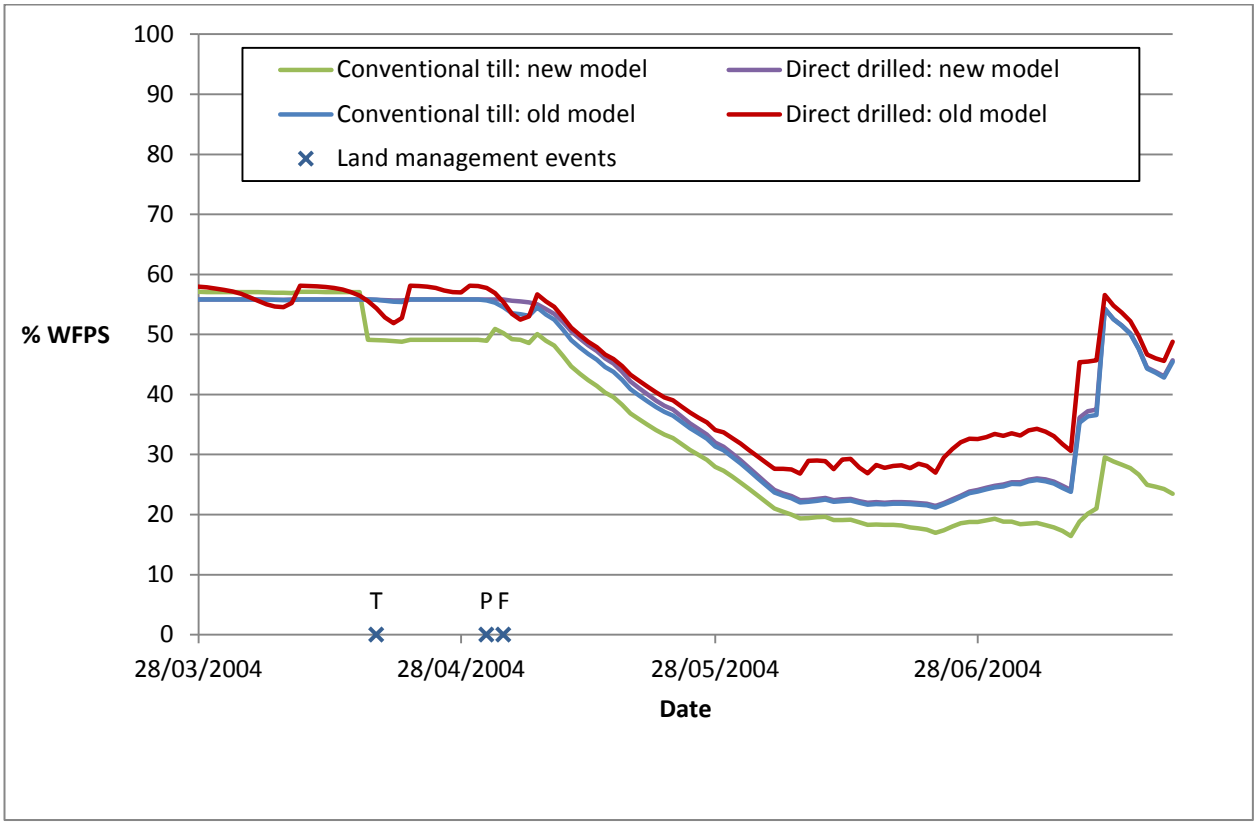

Figure 4.2 Time series WFPS at site 2, model data from Chatskikh et al. (2008). Where land management events are; T = Tillage, P = Planting, F = Fertiliser input

The pattern of WFPS measured by Rochette *et al.* (2008a) for the loamy soil (see appendix Figure A2.2) corresponding to modelled site 3 was characterised by 10-20% lower saturation for the conventional till site from September 2001 to May 2002, and May to June, as well as much of August through September in 2003 and there is no data for December through to April in any of these years. This pattern was well simulated by the updated version of the DayCent model, as can be seen in Figure 4.3, although the magnitude of the difference between conditions was underestimated in 2001-2002, and the magnitude of WFPS was sometimes overestimated by around 10%. Comparatively, there were a number of issues with output from the old model; simulated WFPS was consistently around 20% higher than measured values, and NT WFPS was often simulated as higher than T, whereas measured values indicated the reverse. Both model versions simulated peaks higher than indicated by field data. Calibration efforts tested the impact of reducing clay content to reduce simulated WFPS at peaks using the developed model, however this was not effective, and had a detrimental effect on simulation of N_2O emissions over the full measurement period.

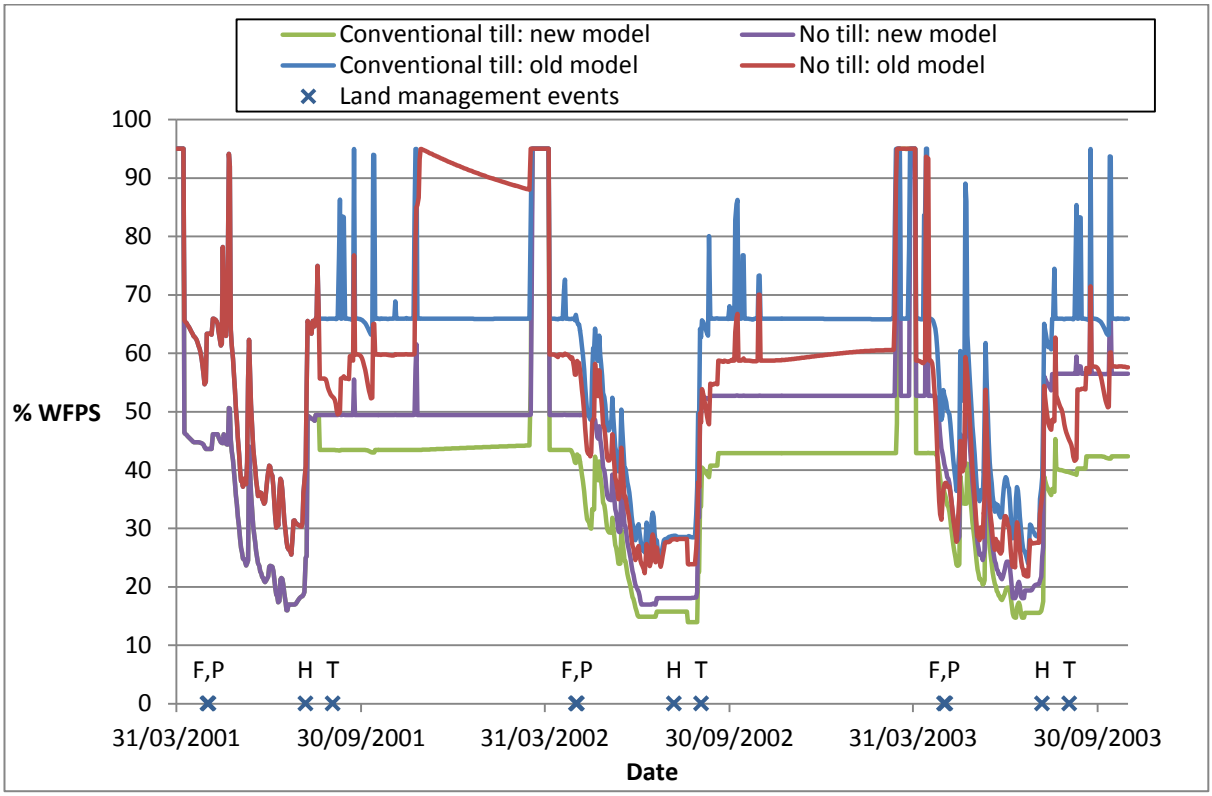

Figure 4.3 Time series WFPS at site 3, model data from Rochette et al. (2008a). Where land management events are; T = Tillage, P = Planting, F = Fertiliser input, H = Harvest

Webster *et al.* (2004; 2008) measured values of WFPS under minimum till around 20% higher than for NT for the period November to March in 2002-2003 and November to May in 2003-2004; output from the updated model for site 5 (Figure 4.4), followed a very similar pattern, although the magnitude for both conditions was simulated 5-15% too low between November and May. Output from the old model version was also 5-15% below measured values between November and May, and the old model version failed to simulate the observed difference between T and NT. The model was tested for increased clay content and presence of a water table to increase simulated WFPS at the start of the measurement period, however the general trend of simulated WFPS was still not in line with measured values, and although simulation of N_2O emissions for the T condition with the new model was improved, simulation of the NT condition was worsened.

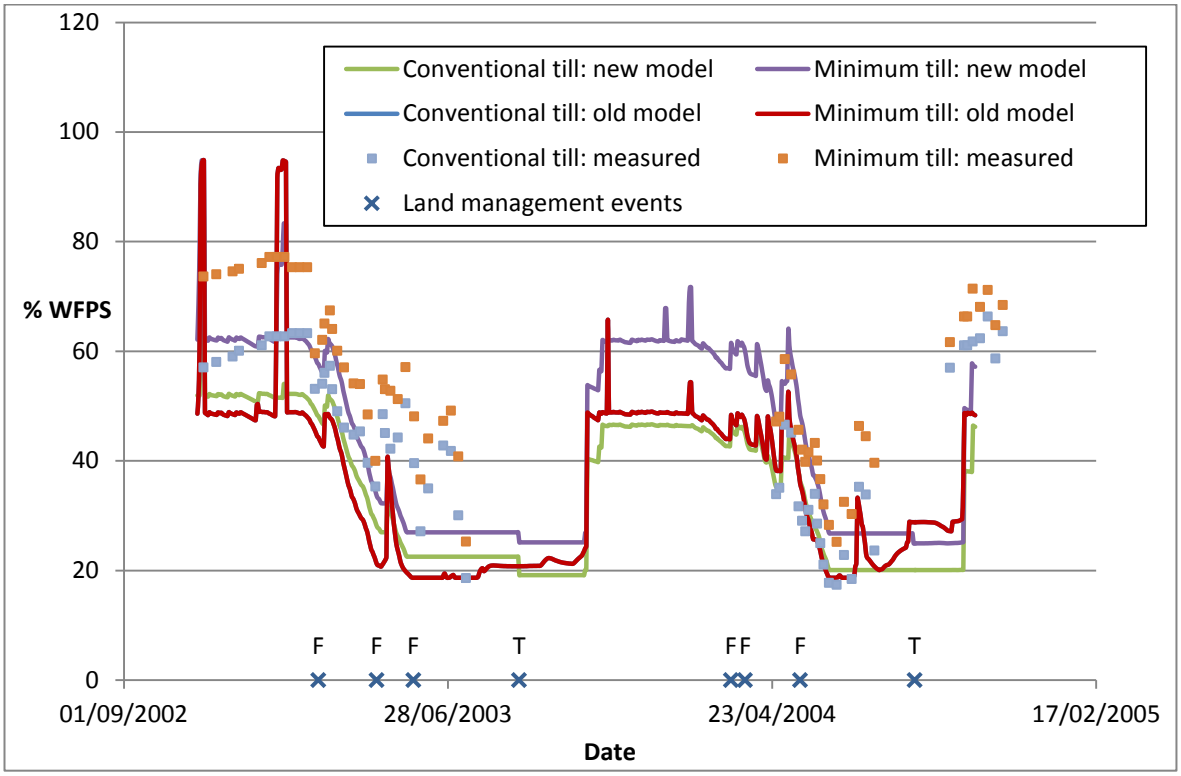

Figure 4.4 Time series WFPS at site 5, model data from Webster et al. (2008; 2004). Where land management events are; T = Tillage, F = Fertiliser input. The "conventional till: old model" line exactly matches the line for "minimum till: old model", and hence is not visible.

The pattern of WFPS measured by Rochette *et al.* (2008a) for the clay soil (see appendix Figure A2.1) corresponding to modelled site 6 was characterised by 10-20% lower saturation for the conventional till site from September to May, although they state that this was not statistically significant in 2002, and again there are no data for December through to April in any of these years. This pattern was well simulated by the updated version of the DayCent model, as can be seen in (Figure 4.5); predicted WFPS was 20-30 % too high, but the difference between management conditions was well represented. The old model version also predicted WFPS 20-30 % higher than measured values and failed to represent observed difference between T and NT conditions. Both model versions simulated very high WFPS for both sites during the period not measured by Rochette *et al.* (2008a), which cannot be validated. Overprediction of saturation level may reflect limitations for extremes of texture, since clay content for this site is particularly high (77%) which is a key control for simulation of drainage. The model was tested for 10% reduced clay content (in line with Post *et al.* (2008) spatial variation) and for presence of water table, but WFPS remained much higher than measured. The input data version chosen was therefore once again based on optimising prediction of N_2O emissions.

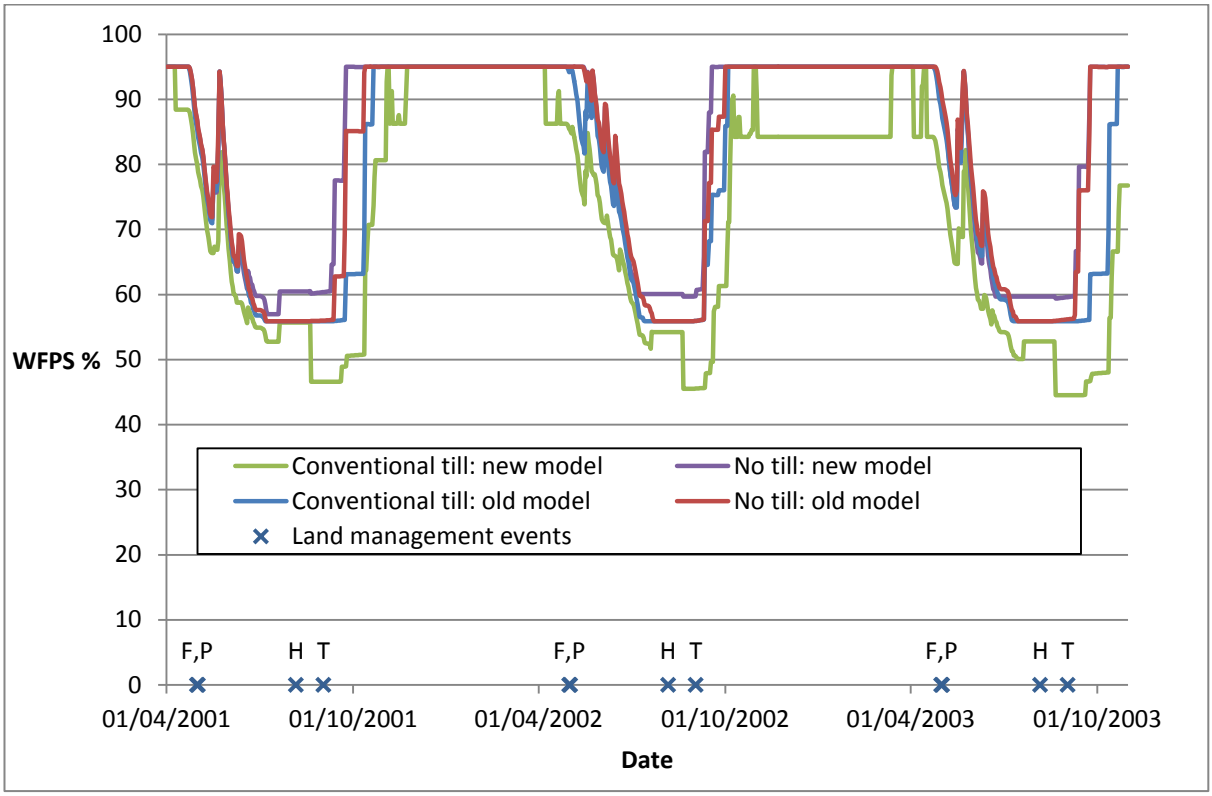

Figure 4.5 Time series WFPS at site 6, model data from Rochette et al. (2008a). Where land management events are; T = Tillage, P = Planting, F = Fertiliser input, H = Harvest

In general, the updated model seems to give good representation of trends in WFPS and, in particular, gives improved simulation of response to tillage and the difference between T and NT sites, which was not represented by the old version of the model, and is crucial to simulating the impacts of tillage on N_2O emissions. However, for both model versions, absolute values are not always well represented, which due to the nonlinear relationships between WFPS and rates of both nitrification and denitrification is likely to lead to errors in predicting both relative and absolute values for N_2O.

Having checked simulated WFPS against measured data where available, comparison of observed and predicted N_2O emissions was then performed. The remaining field sites (sites 1 and 4) do not have available data on ρb, WFPS or soil water content; validation of data was performed for these sites, to draw conclusions about potential model performance in scenario analysis.

4.3.4 Time series N_2O emissions

Field observations from Chatskikh *et al.* (2008) indicate an increase in N_2O emissions for the tilled site following tillage (see appendix Figure A2.4); this was not well simulated by either version of the DayCent model, as can be seen in Figure 4.6 for modelled site 2. The authors attribute the observed peak to an increase in diffusivity; it is a limitation of both versions of the model that there is no simulation of change in diffusivity following tillage. N_2O emissions at the start of the measured period are well simulated by both model versions, and the magnitude of the post fertiliser peak is also well represented for the T site. Measured data in Chatskikh *et al.* (2008) showed a higher, later peak for the NT condition; both model versions simulated this peak lower and beginning earlier.

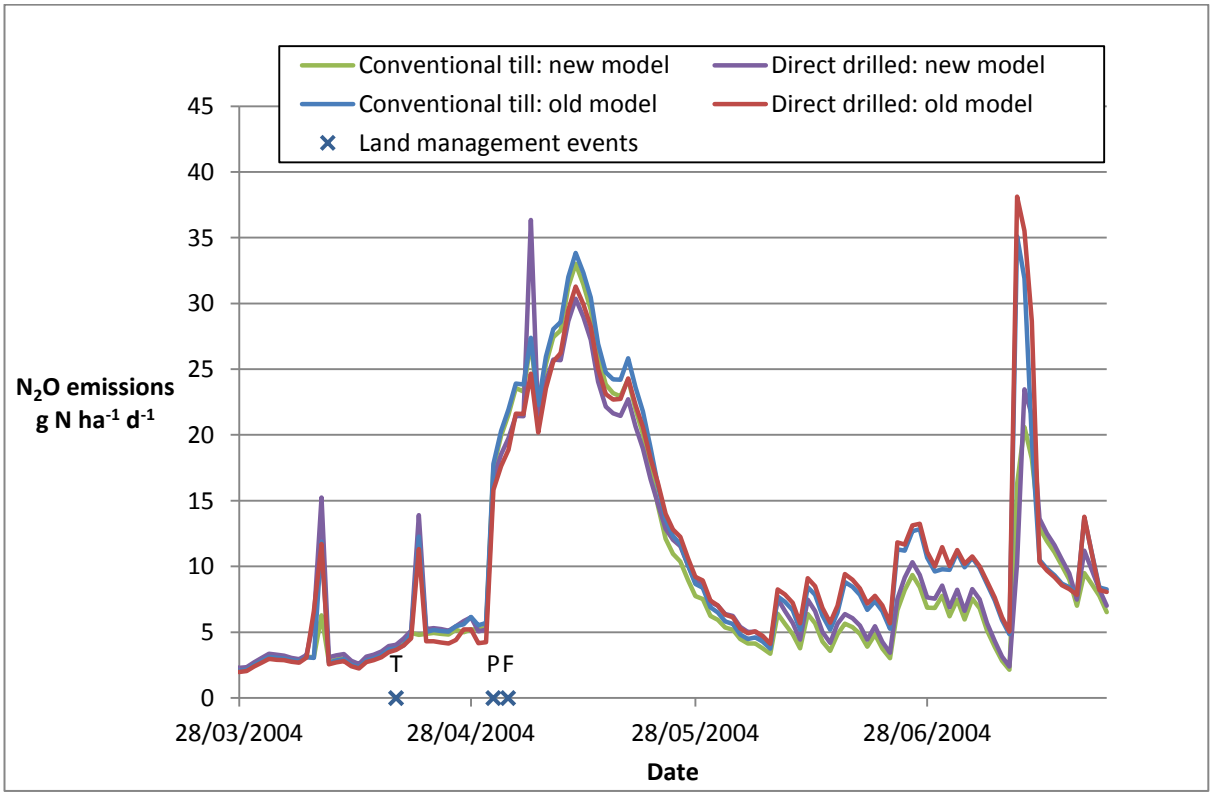

Figure 4.6 Time series N_2O emissions at site 2, model data from Chatskikh et al. (2008). Where land management events are; T = Tillage, P = Planting, F = Fertiliser input

Field data in Rochette *et al.* (2008a) for the loamy site corresponding with modelled site 3 (Figure 4.7; for measured data see appendix Figure A2.2), suggest that T generally exhibits similar N_2O to NT, except for peaks at the tilled site immediately following tillage. The developed version of the DayCent model simulated a period of higher emissions following tillage, but several peaks were simulated at the NT site during this period, which reflect observed and simulated increase in

WFPS at this time, but were not observed in the field. The old model simulated a similar pattern for both T and NT conditions to that modelled for the NT site using the developed model. Field data for site 3 is not a complete record; the excluded Spring thaw period often displays high emissions, with spatial variability due to patchy snow cover which cannot be represented in a spatially lumped model like DayCent, hence low values simulated for this period may not be representative of the site (Parton *et al.*, 1998; Smith, 2008).

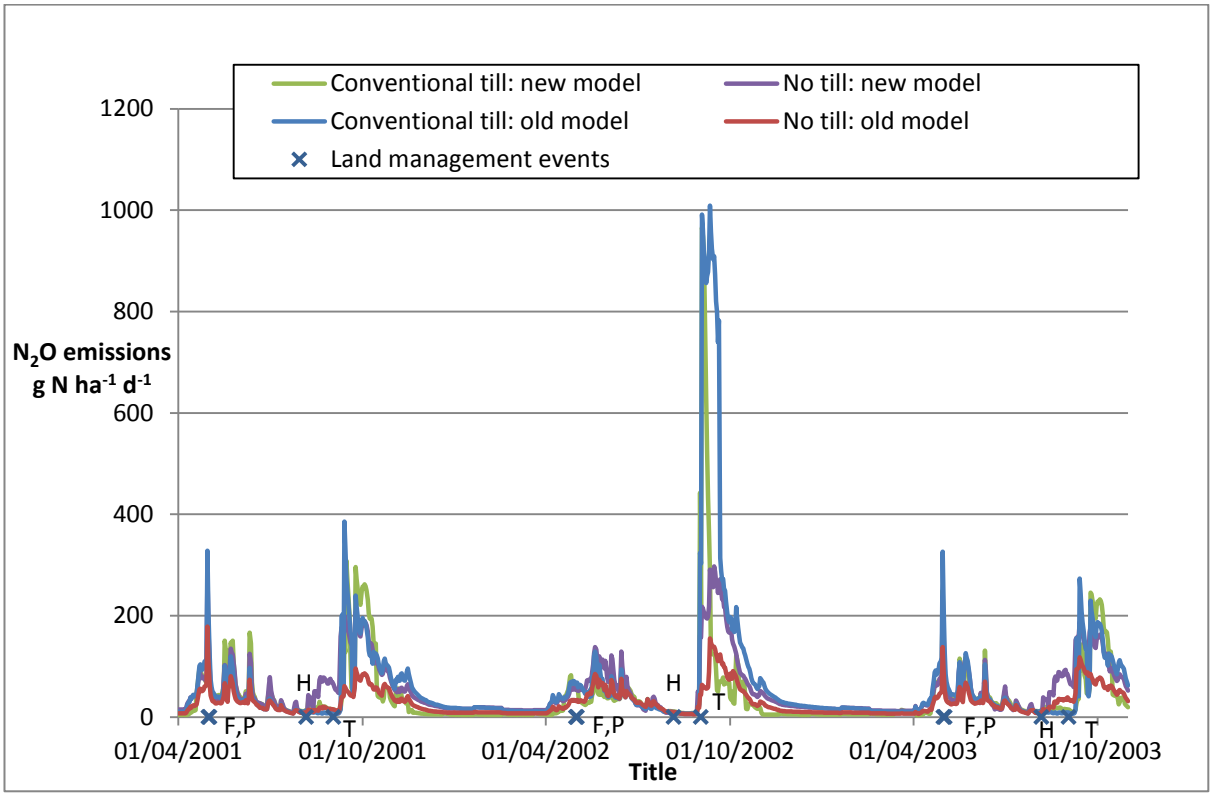

Figure 4.7 Time series N_2O emissions at site 3, model data from Rochette et al. (2008a). Where land management events are; T = Tillage, P = Planting, F = Fertiliser input, H = Harvest

Webster *et al.* (2008; 2004) recorded periods of higher emissions for their minimum tilled site in December 2002 and April through to June 2004, along with an overall trend of increase in emissions over the measured period. Simulations for site 5, shown in Figure 4.8, indicate that the updated model represented periods of greater emissions from the minimum tilled site at appropriate dates, whereas the original version of the DayCent model simulated virtually no difference in N_2O emissions between the two sites. Both the original model and the developed version generally simulated much higher emissions than were measured by Webster *et al.* (2008; 2004). This may be attributed to the simulated WFPS which was generally in the optimum zone for either nitrification or denitrification, due to being around 5-15% below measured values. Both model versions show little immediate response of N_2O emissions to tillage events; gaps in the data prevent verification with field data.

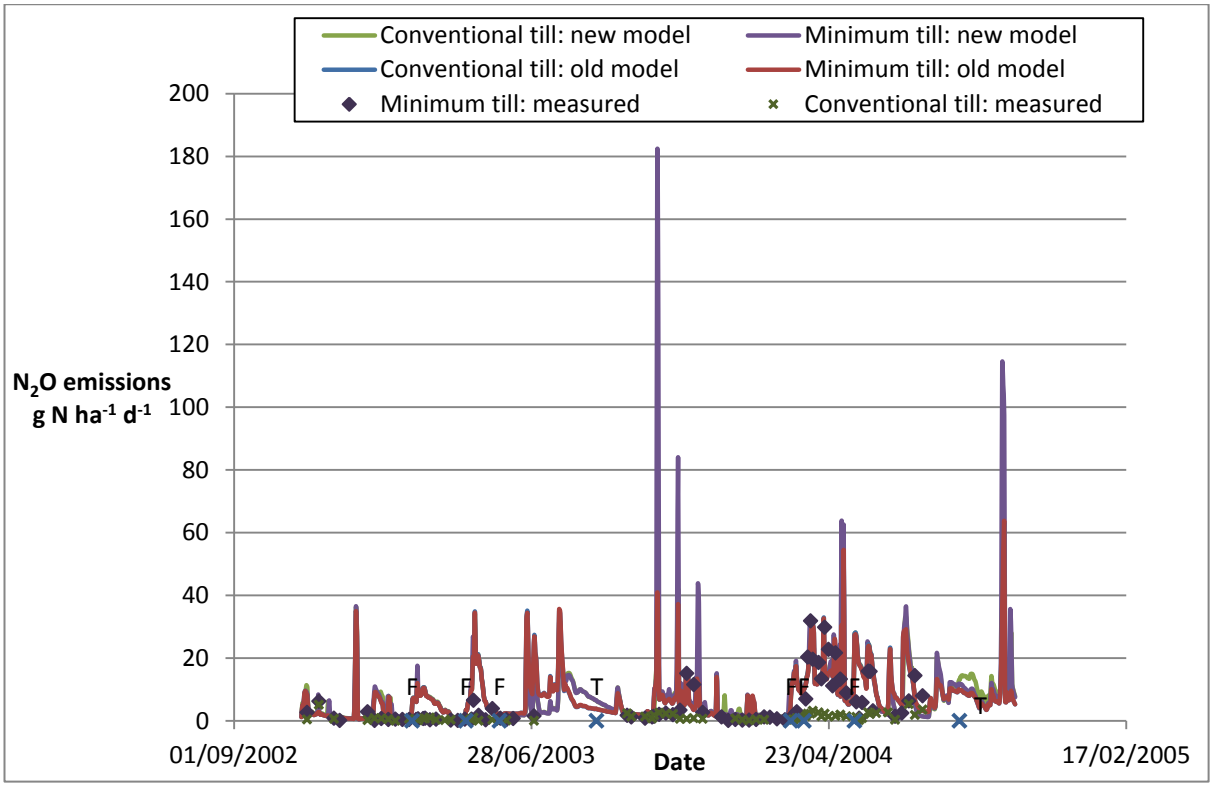

Figure 4.8 Time series N_2O emissions at site 5, model data from Webster et al. (2008; 2004). Where land management events are; T = Tillage, F = Fertiliser input

Researchers at Rothamsted made time series data (Webster, 2004) available for this study, so it was possible to complete further statistical analysis for site 5, using equations outlined in Smith *et al.* (1997); results are displayed in Table 4.2.

Table 4.2 Statistics for evaluating model performance at site 5

Updated model	Modelling efficiency (EF)	Root mean square error (RMSE)	Normalised root mean square error (NRMSE)	Coefficient of determination (CD)	Relative error (E)
N_2O NT	-0.15	10.83	237.21	0.78	-247.98
N_2O T	-59.33	13.80	1574.57	0.02	5649.06
WFPS NT	0.25	12.86	23.52	0.64	11.60
WFPS T	0.28	12.45	27.94	0.88	10.97
Old model					
N_2O NT	-0.33	11.62	254.57	0.68	-212.45
N_2O T	-72.55	15.33	1748.70	0.01	2191.59
WFPS NT	-0.94	20.73	37.91	0.36	24.55
WFPS T	0.01	14.61	32.77	0.59	11.69

The updated model has higher values for EF and lower values for NRMSE than the old model, suggesting improved representation. Using the new model, a higher proportion of N_2O emissions variance is explained by simulated values for NT, with a coefficient of determination of 0.78 than for T (0.02); again these values indicate improved performance compared to the old model version.

Field data from Rochette *et al.* (2008a) for the clay soil corresponding to modelled site 6 (see appendix Figure A2.1) indicate generally similar emissions for T and NT sites, with higher emissions from the NT site in the period following tillage. Figure 4.9 shows that both model versions simulated increased emissions from both conditions around the timing of tillage or tillering in the case of the NT site; this likely results from decomposition increasing N availability, given the high SOM at this site. Simulated reduction in WFPS to around 45% following tillage does not supress emissions, since this is in the region favouring nitrification (35-60%), whereas measured values at the tilled site for this time were around 20% WFPS, and low water availability may have limited microbial activity. Measured emissions peaks for the NT condition were very large, which may indicate that location and timing captured hotspots; simulated values were lower with both model versions.

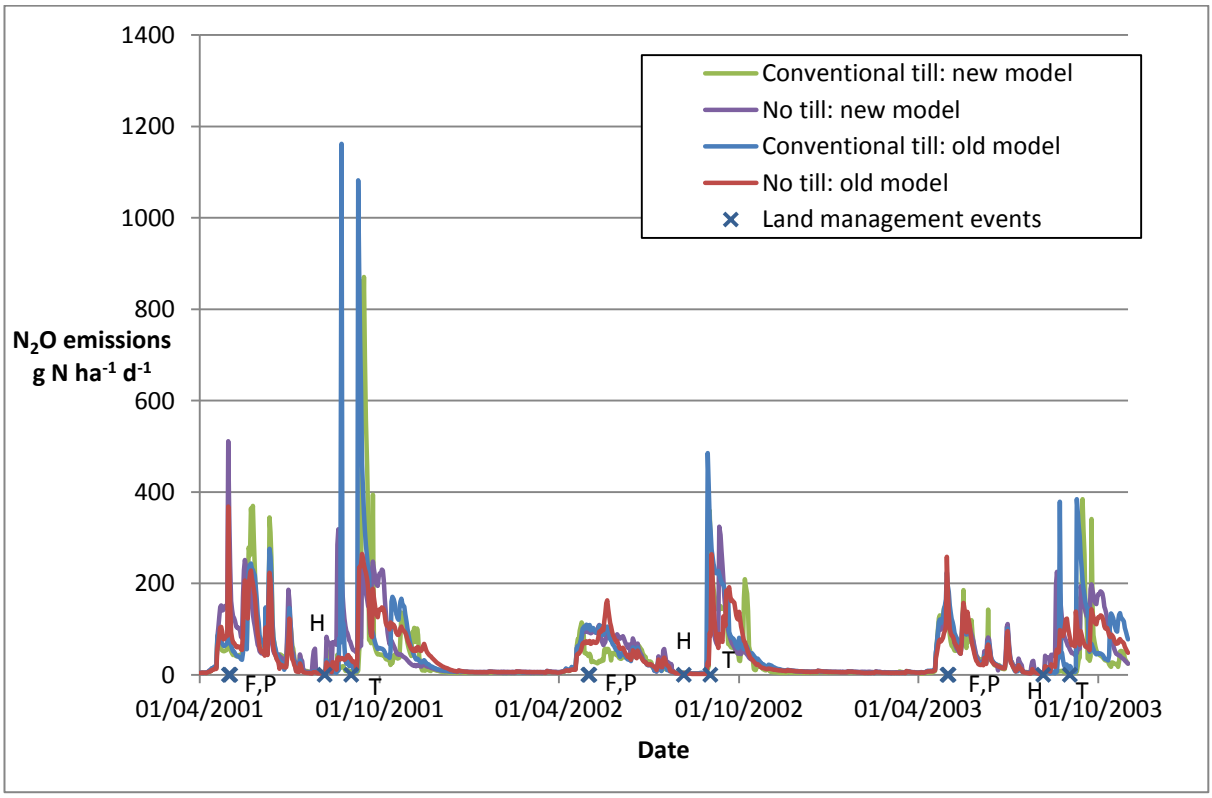

Figure 4.9 Time series N_2O emissions at site 6, model data from Rochette et al. (2008a). Where land management events are; T = Tillage, P = Planting, F = Fertiliser input, H = Harvest

N_2O emissions for sites 1 and 4 were validated against site data with no calibration stage.

Measured values in Lemke *et al.* (1999) corresponding to modelled site 1 show much higher N_2O emissions in response to fertiliser input at their intensively tilled site compared to the NT site. For site 1, both old and new versions of the model (Figure 4.10) give an appropriately timed response

to fertiliser input, with similar magnitude to the field data for NT, whilst for the CT condition, both model versions predict emissions marginally greater than for the NT site, but significantly lower than measured values (see appendix Figure A2.3 for measured values).

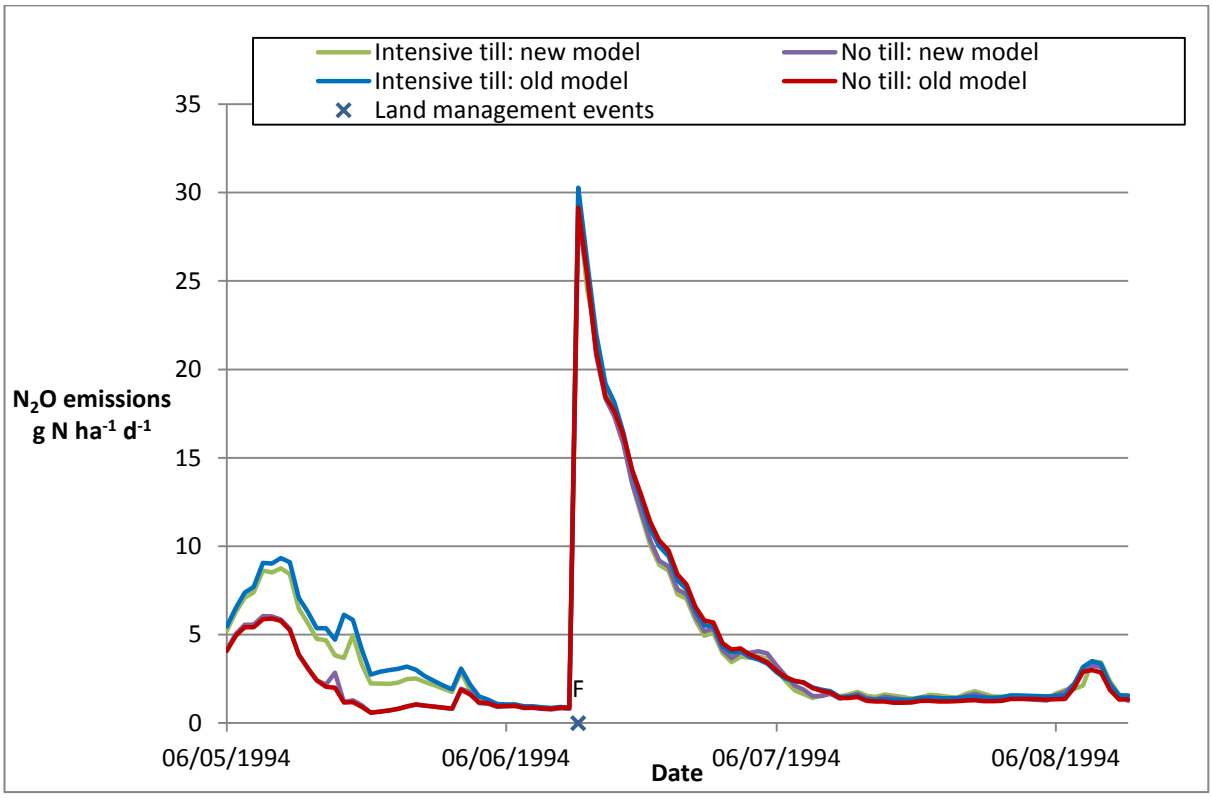

Figure 4.10 Time series N_2O emissions at site 1, model data from Lemke et al. (1999). Where land management events are; F = Fertiliser input

Field data in Baggs *et al.* (2003) (see appendix Figure A2.5) corresponding to modelled site 4 indicate a significantly higher peak with response to fertiliser for the NT condition. Both model versions simulated higher N_2O emissions from the T condition than the NT condition, although this was less extreme for the updated version of the model (Figure 4.11). This may reflect a difference in field versus simulated WFPS; predicted values for the tilled site are in the region favouring nitrification (35-60%) whereas values for the NT site are at the bottom of the range favouring denitrification (above 70%). Assuming field values of WFPS for this site were 5 or 10 % higher than modelled may explain why field values of N_2O following fertiliser input were higher for the NT condition and slightly lower for the T condition.

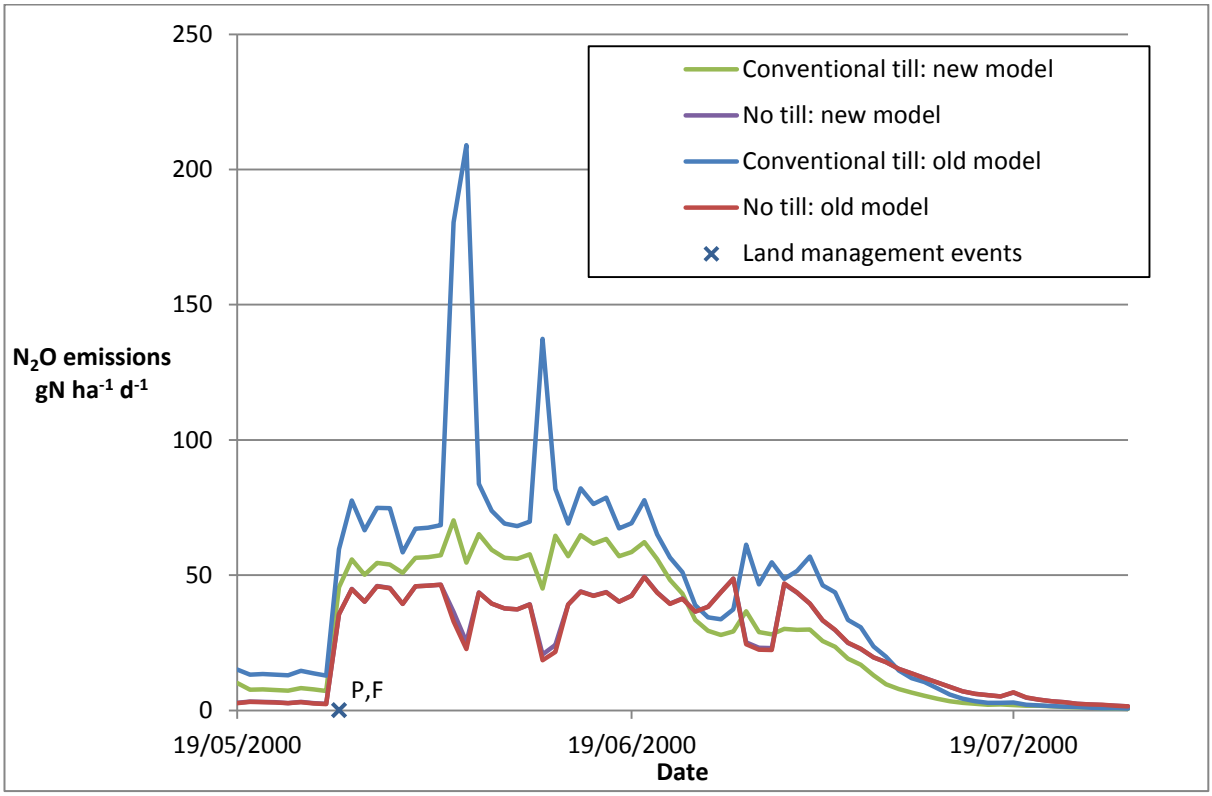

Figure 4.11 Time series N_2O emissions at site 4, model data from Baggs et al. (2003) . Where land management events are; P = Planting, F = Fertiliser input

In general, the updated model version gives greatly improved simulation of the difference in N_2O emissions response to land management between T and NT conditions. Where performance is poor, this can often be attributed to poor simulation of WFPS.

4.3.5 Relative deviation total N_2O emissions

In order to assess model performance objectively using total measured and modelled values of N_2O for the same time period, relative deviation was calculated according to:

$$RD = \frac{modelled - measured}{measured} \times 100$$

(Abdalla *et al.*, 2011)

Relative deviation of simulated versus measured N_2O emissions is shown in Table 4.3 for simulations with both the original and the adapted DayCent model. Large values of RD are common, particularly for sites with low emissions, where slight miscalculations will produce large percentage error. Figure 4.12 indicates RD compared to model testing for DNDC compiled by De Vries, *et al.* (2005) and shows best performance was found for the adapted version of DayCent. Crucially, Table 4.3 indicates that performance for validation is as good as for calibration, and that for 5 out of the 6 sites, the updated DayCent model showed improved performance for representing NT-T. In spite of identified issues in representation of Spring melt emissions, RD values for site 1 which incorporates measured and simulated data for the thaw period are good.

Figure 4.13 and Table 4.4 compare the performance of the original and the adapted DayCent model versions, in terms of the relationship between modelled and measured emissions; the adapted version showed higher r2 and correlation coefficient, although the difference was quite small.

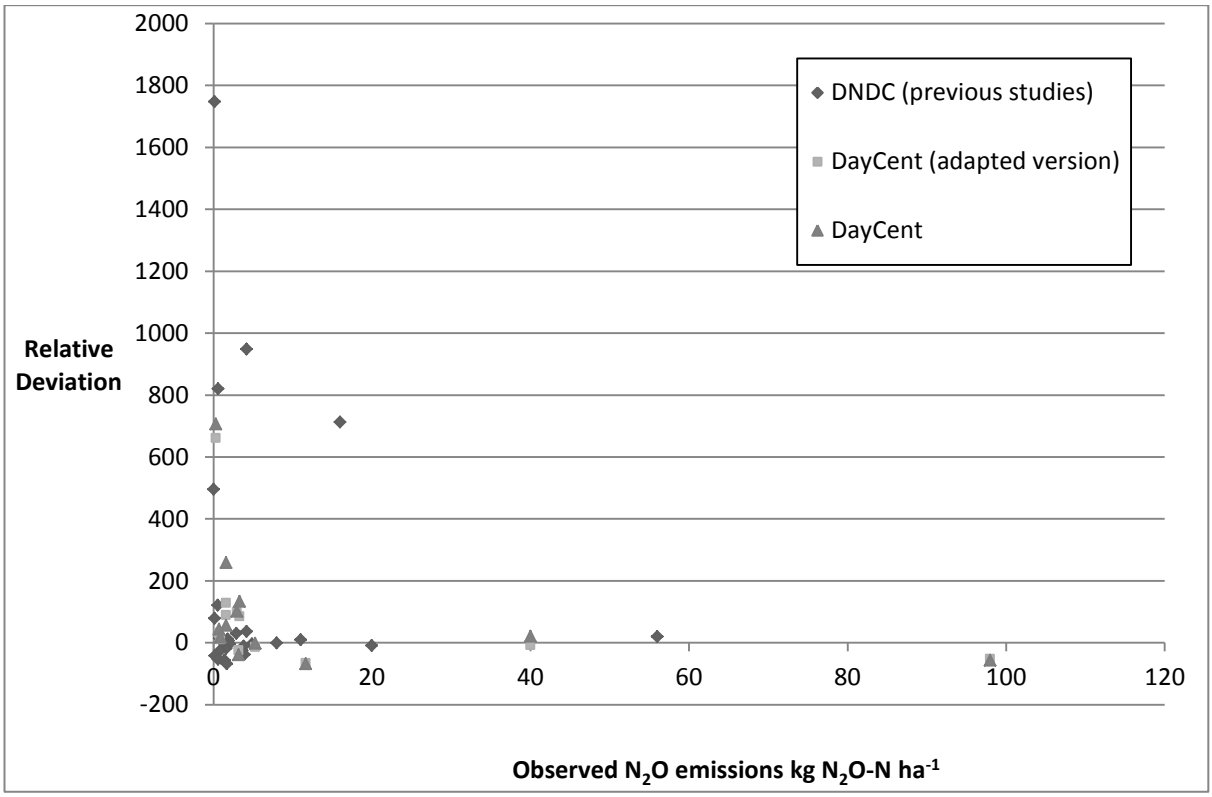

Figure 4.12 Relative deviation of simulated from observed N_2O emissions with adapted DayCent, compared to the distributed version, and the performance of the DNDC model in other studies: taken from a database compiled by de Vries et al. (2005)

Table 4.3 Relative deviation for final model runs and other values tested during calibration, using N_2O emissions over the full measured time period

Site number	Till or no till	Clay fraction	Initial ρb	Water table (months out of 12)	Measured N_2O emissions (Kg)	Updated model simulated N_2O emissions (Kg)	Original model simulated N_2O emissions (Kg)	Relative deviation updated model	Relative deviation original model	NT-T relative deviation updated model	NT-T relative deviation original model
1	NT	0.39	1.01	0	3.18	2.39	1.90	-24.77	-40.10	-0.09	54.55
1	T	0.39	1.01	0	5.28	4.49	5.15	-14.95	-2.45		
2	NT	0.081	1.3	0	0.72	0.95	0.99	31.74	36.82	-120.50	-79.97
2	T	0.081	1.3	0	0.89	0.91	1.02	2.66	14.51		
3	NT	0.22	1.2	0	3.30	6.08	7.69	84.14	132.91	-64.53	446.48
3	T	0.22	1.2	0	3.00	5.97	6.05	99.01	101.55		
4	NT	0.15	1.5	0	11.66	3.55	3.76	-69.57	-67.76	-102.36	-125.95
4	T	0.15	1.5	0	1.61	3.79	6.37	135.63	296.43		
5	NT	0.21	1.2	0	1.60	3.01	2.49	88.32	55.70	-49.13	-100.50
5	T	0.21	1.2	0	0.31	2.36	2.50	660.28	705.70		
6	NT	0.77	1	6	98.00	46.22	41.59	-52.84	-57.56	-83.14	-111.66
6	T	0.77	1	6	40.00	36.44	48.35	-8.90	20.89		
Alternative values tested during calibration											
5	NT	0.31	1.2	6	1.60	3.19	3.07	99.44	92.16	-24.30	-65.64
5	T	0.31	1.2	6	0.31	2.21	2.63	614.32	748.79		
6	NT	0.67	1.00	0	98.00	47.49	18.75	-51.54	-80.86	-55.42	-107.91
6	T	0.67	1.00	0	40.00	21.64	23.34	-45.90	-41.64		
6	NT	0.77	1.00	0	98.00	44.79	41.59	-54.30	-57.56	-83.34	-111.66
6	T	0.77	1.00	0	40.00	35.12	48.35	-12.19	20.89		
3	NT	0.12	1.2	0	3.30	5.85	9.39	77.31	184.58	-348.38	786.44
3	T	0.12	1.2	0	3.00	6.60	6.73	119.88	124.40		

Table 4.4 Correlation coefficients for relationship between modelled and measured N_2O emissions using the updated DayCent model and the original version

		Predicted values; Developed DayCent model	Predicted values; Distributed DayCent model
Field data	Spearman Rank Correlation Coefficient	0.853	0.727
	Sig. (2-tailed)	<0.001	0.007
	N	12	12

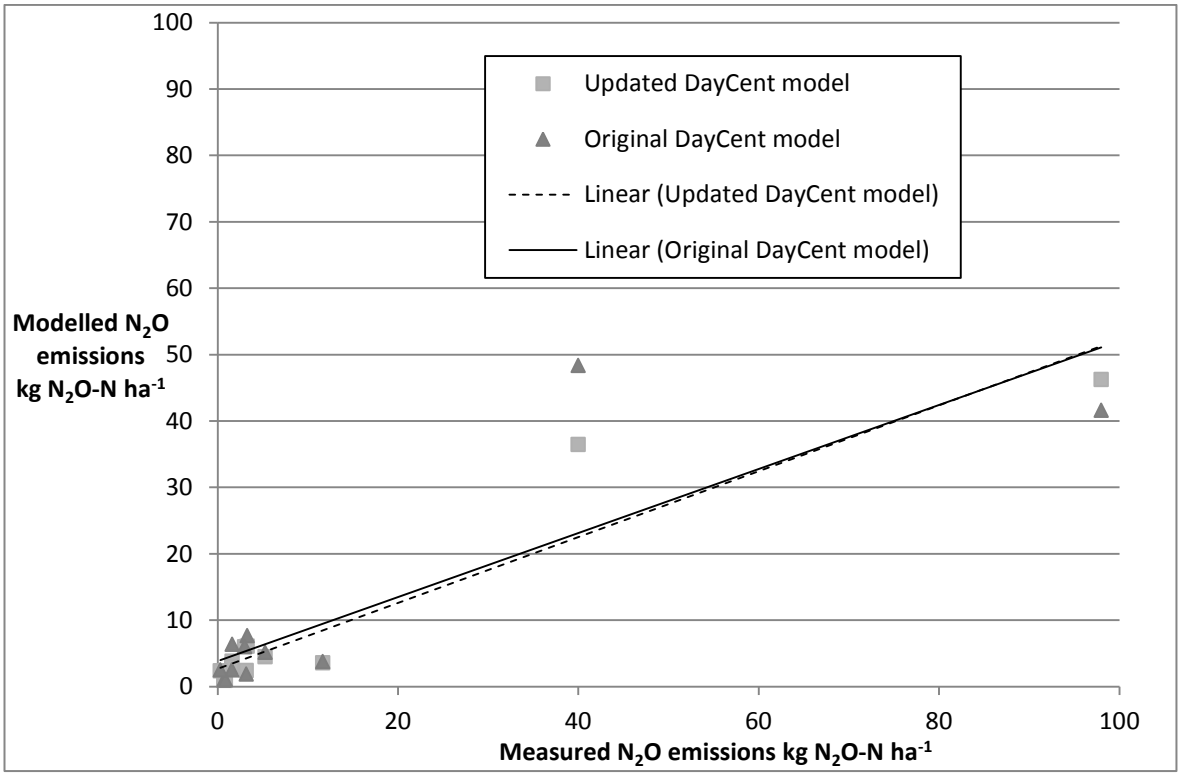

Figure 4.13 Modelled N_2O emissions with updated DayCent and the original version, plotted against measured values.
The updated model version showed a relationship of: $y = 0.4961x + 2.6935$ with $R^2 = 0.895$. Whereas for the original model: $y = 0.4826x + 3.7844$ with $R^2 = 0.7221$

Previous studies have found that DayCent tends to underestimate soil nitrate, and underestimate soil ammonium in the absence of fertiliser inputs, or overestimate shortly after fertiliser inputs (Del Grosso *et al.*, 2008; Jarecki *et al.*, 2008).

As can be seen from Table 4.3 and Figure 4.12; simulated emissions are sometimes higher than measured, and sometimes lower. Although this rules out systematic under or over prediction of soil N, it remains useful to compare model output to field data where available. Field data on

ammonium or nitrate in soil are not available for sites 1, 2 and 5, but comparisons are made for the other three. For Sites 3 and 6 shown in Figures 4.14 and 4.15 respectively, simulated ammonium is higher than field data, whilst nitrate is simulated reasonably well. Over prediction of ammonium at site 3 could contribute to over prediction of N_2O emissions, since aerobic processes are likely to be dominant at this site. For Site 4 (Figure 4.16) poor simulation of soil N may contribute directly to error in prediction of N_2O emissions since simulated ammonium is higher than field data, which may contribute to over prediction of aerobic gaseous losses, more significant at the conventional till site, where simulated N_2O emissions are higher than measured values, whereas simulated nitrate is lower than field data, which could contribute to under prediction of N_2O emissions in anaerobic conditions more common at the NT field site, where field emissions were higher than simulated.

Del Grosso *et al.* (2008) suggest that tweaking the proportion of nitrification to reduce the amount which goes to N_2O and increase the amount which goes to NO can improve simulation of both, but that the appropriate proportion is likely to be soil specific. Elsewhere Jarecki *et al.* (2008) found that both soil N and gaseous N losses of N were under predicted, hence in this case the solution must lie elsewhere; for example leaching losses may be lower than simulated, although these were not measured or discussed. As such, there is not a convenient, universal solution to the identified issues with simulating soil nitrate and ammonium; site specific calibration of nitrification products or leaching rates is likely to lead to improvements, but this is not applicable for scenario analysis.

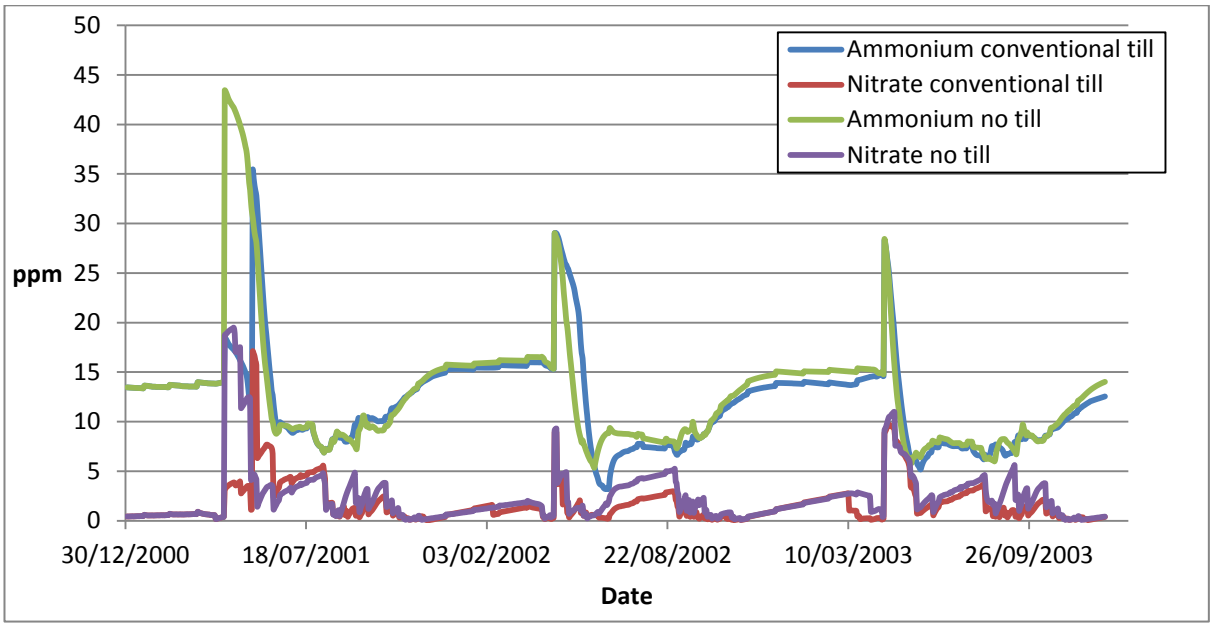

Figure 4.14 Simulated soil ammonium and nitrate for Site 3 (Rochette et al., 2008a)

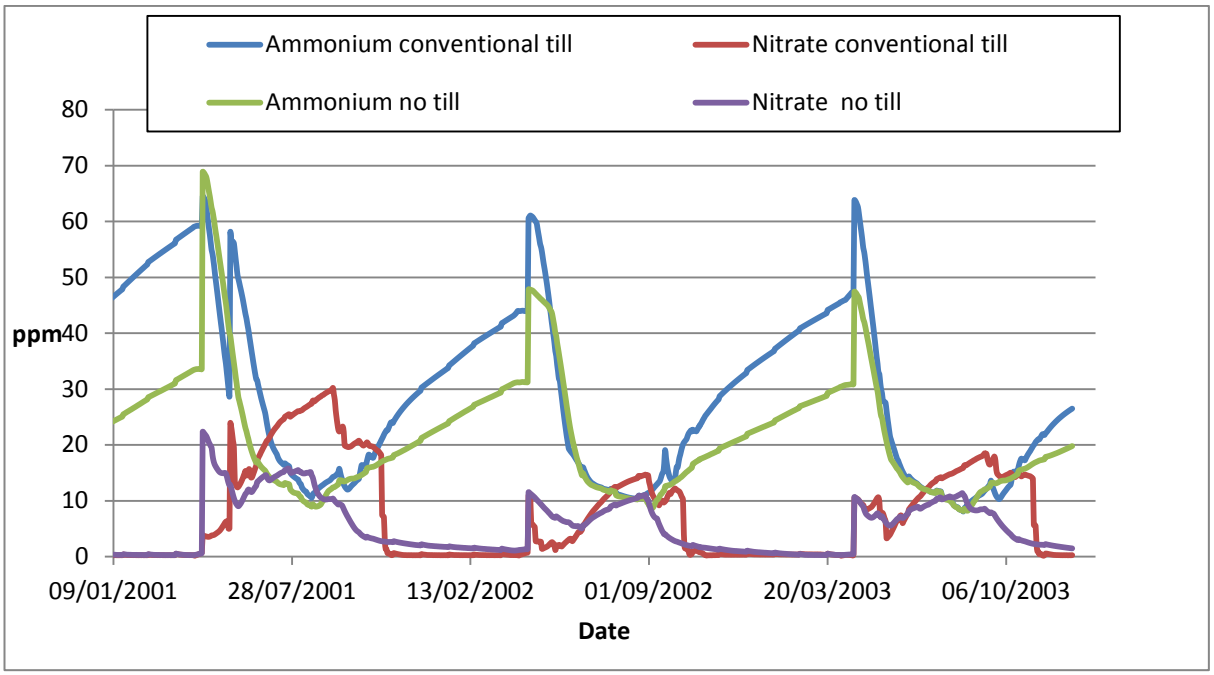

Figure 4.15 Simulated soil ammonium and nitrate for Site 6 (Rochette et al., 2008a)

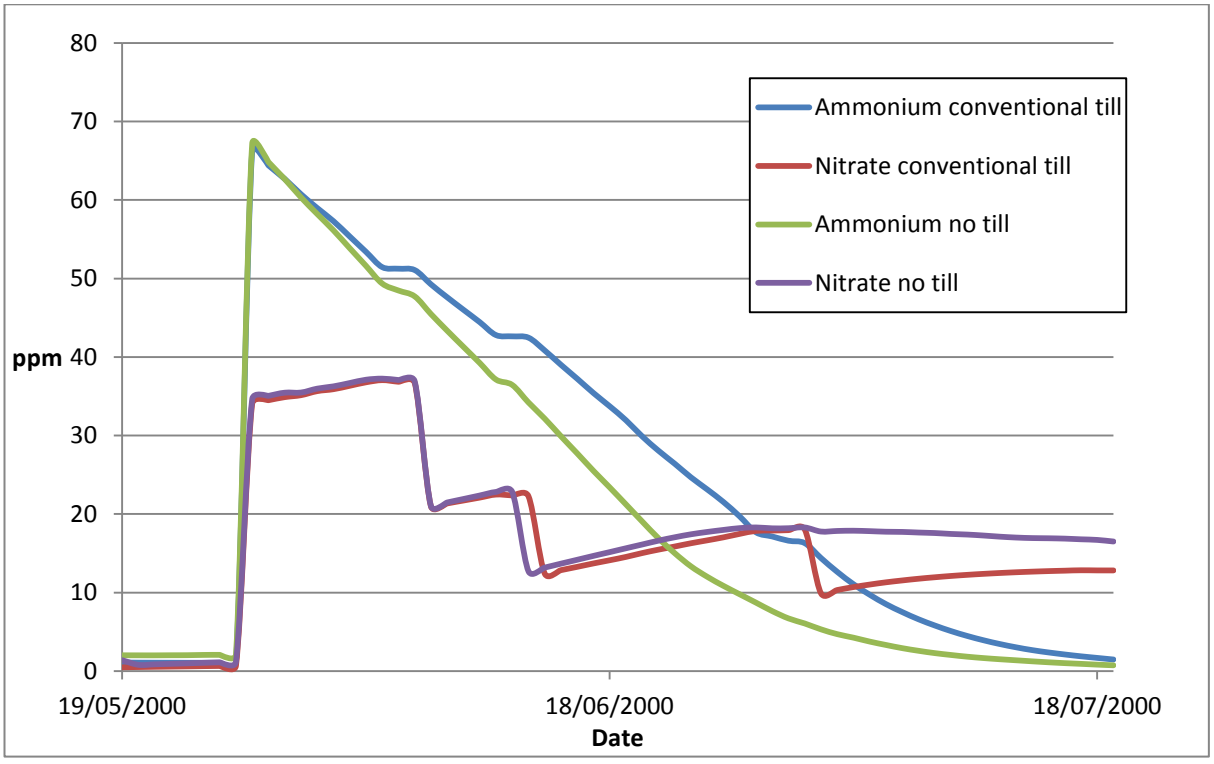

Figure 4.16 Simulated soil ammonium and nitrate for Site 4 (Baggs, 2003)

4.4 Discussion

Although models are necessarily assessed by comparison to field data, it is important to note that movement and retention of water varies over a field with small scale topographic features, textural composition, aggregate packing density and pore connectivity (Boyer *et al.*, 2006; Gupta, 1991; Li *et al.*, 2005a). This spatial variation in soil water controls oxygen availability for nitrogen cycling processes, creates variation in N_2O emissions within a field which may exceed variation for land management approach (Green *et al.*, 2003; Strudley *et al.*, 2008). As a result, there will be significant variation in chamber measurements at different locations over a field, and there are issues with scaling up point data for comparison to hectare scale simulation. Regression models used for upscaling may create significant misrepresentation of N_2O emissions (Beheydt *et al.*, 2007). Temporal variation is also a problem for scaling up; ambient temperature and soil moisture vary diurnally and with local weather patterns, and nutrient cycling or plant uptake affect availability (Beheydt *et al.*, 2007; Grant *et al.*, 2006). Although sampling strategies may be designed to capture some of the spatiotemporal variation, there remain problems for scaling up point measurements, which must be taken into account in addition to measurement error when evaluating model performance. There are similar complications with spatially lumped models, in the need to simulate at large scale using averages, given those relationships between N_2O and for example WFPS are nonlinear and affected by other factors such as tortuosity. As well as spatiotemporal scaling errors, field data will include measurement error, for example (Webster, 2003) suggest that their methodology may underestimate flux by 20%. Rochette *et al*. (2008b) cite low confidence for most studies during the time period relevant to datasets used here, and suggest that estimates of emissions are often biased, but can be useful for comparison between conditions. As a result, it may be better to draw conclusions from statistics comparing modelled and measured NT-T than from statistics on absolute values. As a result of these issues, many studies report difficulty in modelling N_2O emissions (e.g. Beheydt *et al.*, 2007; Brown *et al.*, 2002). System complexity and gaps in knowledge and understanding mean that model representation is inevitably imperfect.

As well as spatial variability and errors from scaling nonlinear relationships, potential sources of modelling error to be considered include input data uncertainty and calculation errors due to poorly understood or difficult to represent processes (Laville *et al.*, 2005; Post *et al.*, 2008).

In terms of input data for this calibration study, potential sources of error include use of data from major local weather stations as opposed to field specific climate input data for many of the sites, spatial variability in soil textural properties, and use of values for textural composition or bulk density based on published values for the soil type in the absence of measured values for the specific study site.

RD values of simulations using the modified model code suggest sub-optimal performance, but better performance than the original model code for most of the tested sites, particularly in terms of predicting the difference between T and NT conditions. General time series performance may not be reflected in RD, due to the disproportionate impact of large pulses, and variation in the total emissions value, since a small margin between measured and modelled values is more significant as a proportion of low emissions.

Table 4.3 indicates that the new model gives improved representation of N_2O emissions for the tilled land management for all but sites 1 and 6, suggesting there may be problems representing impacts of tillage at sites with high clay content. Figures in Table 4.3 also indicate that the updated model better simulates the difference in N_2O emissions between conditions for all but site 2. This may be due to the fact that the updated model has been developed to represent the greater likelihood of anoxia in the NT condition, but not any increase in diffusivity with tillage. Therefore the updated model could be expected to perform worse than the original version where increase in diffusivity with tillage has a greater impact on N_2O emissions than the increase in anoxia under NT conditions.

It is likely that impacts of tillage on soil pore oxygen are more significant than impacts on denitrification product ratio, particularly where N_2O producing processes occur close to the surface of the soil (Ball *et al.*, 1999). Additionally, tillage does not always increase diffusivity (e.g. Elmi, 2003) and increased diffusivity may increase O_2 availability (Skiba, 2002), thus reducing denitrification rates, and making any impacts on product ratio less significant. Therefore improved simulation of porosity following tillage can be expected to give improved simulation of N_2O emissions in most cases, even though change to pore connectivity cannot be simulated.

Model validation at sites 1 and 4 showed equally good performance for RD, when compared to the calibrated sites. Time series data were well simulated at site 1, whereas at site 4 both model versions gave poor representation of the impacts of tillage on response to fertiliser. This could be attributed to poor representation of WFPS, leading to misrepresentation of impacts on N_2O emissions from reduced WFPS with tillage. Simulation of absolute WFPS was often poor, however the developed model gave good simulation of changes in WFPS with land management. Although average WFPS does not theoretically enable simulation of average N_2O, due to nonlinearity of relationships, it remains one of the best available predictors for a spatially lumped model. Therefore where initial WFPS is well represented, model output can be considered a reasonable predictor of impacts of land use change on N_2O emissions. Ideally, the model should be calibrated to match field data on current WFPS (and if possible N_2O emissions) in order for more reliable conclusions to be drawn. Since these data are not available for the sites modelled in Chapter 6, it is appropriate to test the model for a range of input values at each typical site, and to consider model output with the caveat that conclusions about the impacts of tillage regime change on N_2O emissions will only hold for soils where WFPS is similar to simulated values. Thus when extrapolating from findings at the theoretical sites to consider potential impacts at actual sites where such land use change may take place, some verification of WFPS conditions under current management regime would greatly enhance the certainty of predicted change in N_2O emissions. Simulated values for N leaching should be considered carefully in comparison to field data, and model verification performance in previous studies, since this study has not performed model verification for N leaching.

4.5 Summary

Alterations were made to the model code to recalculate ρb for tillage and subsequent settling, and to apply the updated value to calculation of inter-aggregate porosity for WFPS. These changes theoretically give improved representation of N_2O producing and emitting processes by enabling the updated model to simulate the greater tendency for anoxia in poorly drained soils under NT. Since soil pore oxygen status is a key contributor to differences in N_2O emissions associated with different tillage regimes, the updated model was better able to simulate variation in field measurements between conditions. The adapted model is not able to simulate changes in diffusion and hydraulic conductivity associated with tillage, due to a lack of appropriate equations, hence where these factors have greater impact on N_2O emissions than changes in total inter-aggregate porosity, impacts of tillage regime on N_2O emissions may be poorly simulated.

The datasets used (Table 4.1) span a range of drainage and aeration statuses, and were selected as such in order to test model capability to differentiate the opposing impacts on N_2O identified in the field data with change to NT for well versus poorly aerated soils. Based on model performance over the range of sites, there may be some limitations in simulating impacts of tillage on sites with a high proportion of clay. Since model performance was better for simulating changes in WFPS with tillage than absolute values of WFPS, stronger conclusions can be drawn where the model can be calibrated to current site behaviour in terms of WFPS. Calibration involved manipulating drainage rates, by altering the textural composition values within likely site variation (10 %), and ensuring ρb matched site data by altering initial values and scheduled events to enable good representation of WFPS. For scenario analysis, such as application of the model to the "typical sites" identified in Chapter 3, data are not available to calibrate the model to give good simulation of WFPS, thus conclusions drawn about potential impacts will only hold for sites where WFPS is in the range simulated by the model, as opposed to for sites where soil texture and precipitation regime match input values. Since the developed version of the model gave improved performance for simulation of impacts of tillage regime on N_2O emissions, this version will be applied in scenario analysis.

5. Model development: SRC willow

This chapter follows on from Chapter 3 by developing the model which will be applied to sites typical of those which may undergo land use change for cultivation of perennial energy crops. In order to usefully predict the desired outputs of perennial energy crop yield and change in N_2O emissions, soil C and ET for land use change at these sites, some changes to the chosen model are necessary. The model was developed to improve simulation of WFPS and thus N_2O emissions in Chapter 4, and the changes made to the model code in Section 4.3 are retained in the version of the code edited here.

This chapter aims to improve the DayCent model to ensure good representation of crop growth processes, and their interaction with the soil and atmosphere systems. DayCent has already been successfully calibrated and validated for *Miscanthus*, and parameters used are available. Willow can be represented using the **tree.100** input file (as introduced in Table 3.3 of Chapter 3) to simulate crop parameters; parameterisation will be necessary to identify appropriate values from published ranges. Additionally, some development of model code may be necessary to simulate response of the crop to coppicing agroecosystem management.

Unlike in Chapter 4, it is not necessary to build complex new algorithms into the model; instead, change to tree growth following coppicing may be simulated by incorporating different parameter values into existing algorithms. Model performance for simulation of yield can be expected to be much better than for simulation of N_2O emissions where both prediction and measurement is complicated by high spatiotemporal variation in controlling properties, and nonlinear reaction responses (Jarecki *et al.*, 2008).

This chapter first outlines the importance of good crop representation. In Section 5.1, key processes which must be simulated to predict both overall yield and the timings of nutrient and water uptake, taking into account the impacts of coppicing management, are identified. Section 5.2 then outlines the extent of tree growth representation in the existing DayCent model, and looks at existing approaches to simulating coppicing which could be implemented in DayCent in

order to simulate variation in growth over the coppice cycle. Section 5.3 details changes to the model code to enable simulation of changes to tree growth processes immediately following coppicing, and Section 5.4 then describes parameterisation and calibration, and assesses the performance of the updated model. As part of the validation process, the model is also run for *Miscanthus*, using crop parameters from Davis (2009) to assess whether their crop parameters also gave reasonable performance under UK field conditions.

DayCent parameterisation for SRC willow in this chapter is derived from material produced by Forest Research and The Forestry Commission by permission of Forest Research and the Forestry Commission on behalf of the Controller of Her Majesty's Stationery Office.

5.1 Required crop process simulation

Perennial crops such as *Miscanthus* and SRC willow differ from annuals in terms of growing season, ET, nutrient uptake and land management requirements. The DayCent model has already shown good performance at calibration (Davis *et al.*, 2010) and validation (Davis *et al.*, 2012) for prediction of yield and N_2O emissions associated with *Miscanthus* cultivation. However, as noted in Section 3.6.2, the model has not previously been used to simulate yield or GHG emissions associated with cultivation of SRC willow or other SRC managed forest. A review of potential coppice models by Philippot (1996) identified senescence and biomass partitioning between plant organs as the most important crop processes to be simulated, so capacity to model these processes must be assessed.

As a whole agroecosystem model, DayCent simulates interaction between tree growth and soil properties: as stated in Section 3.4, it is crucial to simulate timing of water uptake and nutrient exchange associated with tree growth, due to impacts on oxygen and nutrient status of the soil, which controls carbon and nitrogen cycling processes. Similarly, availability of water and nutrients at the times they are required by the crops for growth will control whether potential yield is attained (Fraiture *et al.*, 2008; Vanloocke *et al.*, 2010). Therefore the model must simulate seasonal variation in growth (and associated water and nutrient requirements) as well as variation over coppice cycle and lifecycle.

Simulation of root growth and uptake is important to simulating supply to the tree, as well as changes to soil water, oxygen and N availability, although data to inform modelling is limited (Philippot, 1996; Tallis *et al.*, 2013). Pacaldo et al (2012) have published a 19 year dataset for SRC willow which includes root biomass measurements, and can be used to calibrate changes in the relative proportions of above and below ground biomass, but further datasets from different sites would be helpful to identify how root biomass growth varies with soil texture, water and nutrient availability. Simulation of crop root access to groundwater would also be necessary to fully simulate impact of water availability on yield and enable consideration of potential environmental impacts of any groundwater depletion. Simulation of root growth and controlling factors is described in Section 5.2, whilst limitations of lack of field data on model calibration will be discussed in Section 5.4.

Increased above ground biomass growth relative to incident sunlight immediately following coppicing can be anticipated due to translocation of nutrients stored in the below ground plant organs and above ground stool (Jug *et al.*, 1999; Shibu *et al.*, 2012). Additionally, the growing crop has a proportionally large amount of biomass in the form of leaves, but initially little selfshading, meaning a high LAI relative to total biomass (Ceulemans, 1996).

Since DayCent has not previously been used to simulate coppicing management, it will be necessary to adapt the code to enable representation of changes to above ground biomass growth following coppicing. Section 5.2 will describe existing simulation of tree growth in the DayCent model, and investigate the extent to which simulation of coppicing can be incorporated at the existing level of resolution.

5.2 Existing and potential representation

Recently developed mechanistic approaches to coppice growth simulation provide an improvement on previous statistical approaches such as Aylott *et al.* (2008) for the UK or Mola-Yudego *et al.* (2008) for Sweden, in that these models can be applied to new climate and soil conditions, provided that plant growth and interaction with soil properties are adequately simulated (Tallis *et al.*, 2013). Simulation must include: drivers and limitations to growth; partitioning of new plant C between organs, and how this may vary over the lifecycle and in response to coppicing; senescence and breakdown of dead plant components. Figure 5.1

summarises DayCent simulation of tree carbon fixation, partitioning and loss, and Sections 5.2.1 through to 5.2.4 outline the details of DayCent representation, assess appropriateness for simulating SRC willow, and discuss alternative approaches and potential model development.

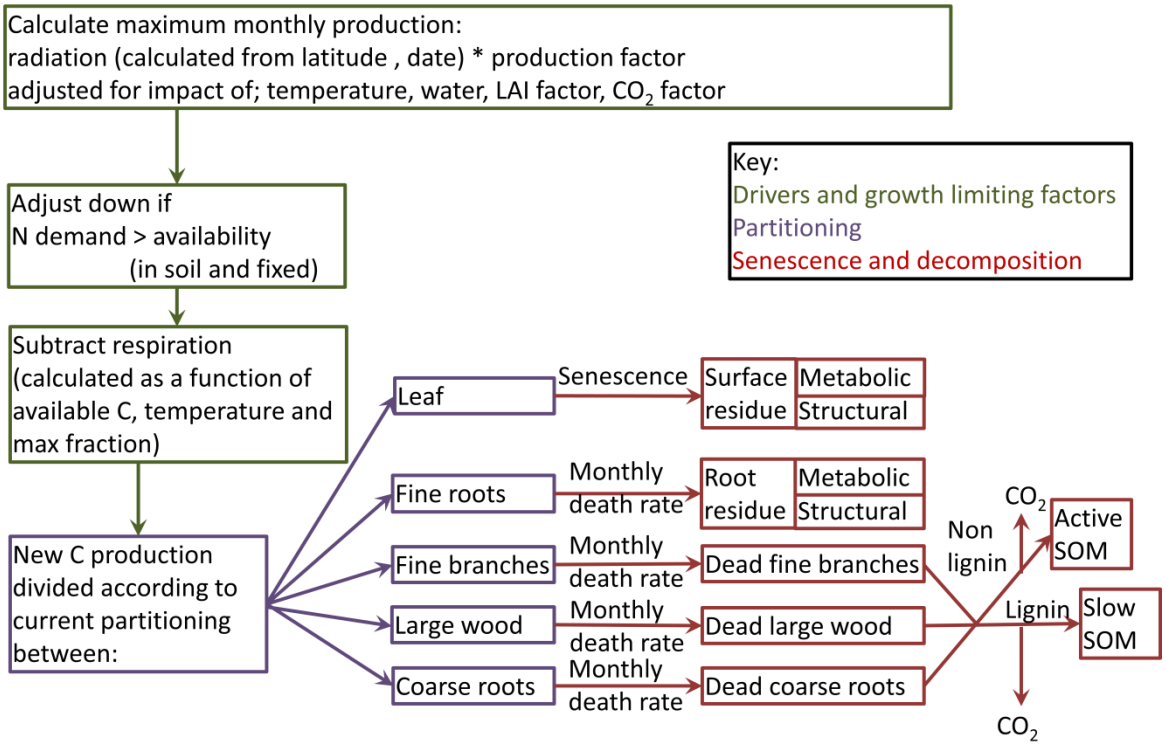

Figure 5.1 DayCent simulation of tree carbon fixation, partitioning and loss

5.2.1 Drivers and growth-limiting factors

Solar radiation, calculated from latitude and date, is the driver of crop and tree production in DayCent. Tree specific maximum monthly production is then calculated from solar radiation according to a conversion factor (**PRDX(2)** in the **tree.100** file; see Table 5.3). A factor is applied to limit growth according to leaf area index (LAI) where it is below the plant maximum (**MAXLAI** in the **tree.100** file; see Table 5.3), and therefore less light can be intercepted. Additional limitations on growth rate are factored into this calculation according to soil temperature and moisture. Soil temperature impact is calculated according to a tree specific Poisson Density Function relating temperature and growth. Soil water restriction is calculated according to the relationship between potential ET and available soil water plus precipitation and irrigation for the day, adjusted for soil texture.

Tree rooting depth can be simulated by setting the parameter to allocate the number of soil layers used for water uptake (**TLAYPG** in the **tree.100** file; see Table 5.3); for SRC willow, this should equal 7, since rooting depth can be up to 130cm (Crow and Houston, 2004) and soil water simulation layer 7 represents the 120-150 cm depth. This value is in fact only used to calculate nutrient and water access for tree survival; growth is calculated according to availability in the top 30cm of soil, since the majority of roots are found at this depth; this is true of SRC willow (Crow and Houston, 2004) as well as crops more commonly simulated with DayCent.

Following this initial calculation of maximum production, production is then reduced if N demand cannot be met. Demand is calculated according to the C:N ratio, and availability is based on soil N availability plus any N fixation: uptake of both fixed and soil available N is adjusted for total root biomass (adjustment is set according to a factor calculated in the **RTIMP.F** module). Respiration is calculated as a fraction of the maximum rate according to temperature, size of C pool and plant component C as a fraction of that plant component C at optimum LAI.

Dates of first and last growth and senescence can be set in the schedule file, according to available information on growing cycle, and coppicing dates should be set according to management practices for the site modelled, if known, or a date selected during the recommended harvest time period if not.

5.2.2 Partitioning

The **tree.100** input file (as introduced in Table 3.3 of Chapter 3) allows the user to set Juvenile and mature values for C partitioning (using **FCFRAC(1-5,1-2)**; see Table 5.3), enabling the model to simulate the difference between establishing and mature trees. Organs simulated are: leaves; fine branches; coarse wood; fine roots; coarse roots**.** Maximum, minimum and initial C:N ratios of the partitions are also pre-set (according to **CERFOR(1-3,1-5,1)**; see Table 5.3), C:N will lie somewhere between maximum and minimum depending on availability relative to demand. Maximum and minimum values for juvenile roots are set separately to allow for variation with availability of water (according to **TFRTCW(1-2)** or N **TFRTCN(1-2)** see Table 5.3); maximum values will be applied in the event of nutrient or water shortages, resulting in an increase in the proportion of below ground biomass.

Coppicing reintroduces the juvenile tendency towards rapid growth in woody plants, whilst the presence of established roots enables even faster growth by supplying water and nutrients to leaves, and energy stores in below ground and remaining above ground plant parts provide additional reserves for growth (Philippot, 1996). Spatial distribution and numbers of new stems are important in determining "free growth" through internode elongation, and the resultant leaf numbers. Therefore it has been suggested that explicit simulation of individual stem sprouting and as well as resultant leaf numbers and canopy architecture, using an individual plant level demographic approach, could give improved representation of the rate of post coppice growth (Ceulemans, 1996; Philippot, 1996). However explicit, individual tree-level simulation would require significantly greater complexity than the stand-level of simulation currently applied in DayCent, and is not synonymous with a useful simulation of coppice growth. For example the ECOPHYS model applies an individual plant level demographic approach to coppice modelling, and incorporates complex 3D simulation of individual leaf positions to calculate LAI, but cannot simulate multiple stems or self-thinning (Philippot, 1996).

Conversely, complex demographic approaches can be incorporated into stand-level simulations; for example ForestGrowth explicitly simulates average stem numbers according to user input, and can simulate stem death to represent self-thinning over the course of the coppice cycle. ForestGrowth applies a simplified approach to leaf architecture simulation, by assuming horizontal uniformity over the stand, but is still able to simulate variation in photosynthetic capacity without individual tree-level simulation, by discretising the canopy by height to simulate changes in average leaf angles and LAI with height in canopy (Tallis *et al.*, 2013).

Amichev *et al.* (2011) adapted the multi-stem approach to represent a single stem (with total mass of all separate stems) using the 3PG model to remove the need for highly specific input data on bud numbers. To simulate post coppice growth without multi-stem simulation, the 3PG model resets the age of the trees at the start of each coppice cycle, to reinstate juvenile growth patterns, but retains the root biomass from the end of the last coppice cycle (Amichev *et al.*, 2011). This enables the model to simulate fast canopy closure following coppicing, and the increase in above ground biomass growth with the first three successive coppice cycles, since the established root system creates a high root:leaf ratio enabling good supply of water to leaves (Amichev *et al.*, 2011; Philippot, 1996).

Alternatively, the PALM model, which is similar to DayCent in terms of drivers and partitioning, simulates post coppicing translocation of nutrients from root to shoot explicitly as an immediate C transfer of 20% (Shibu *et al.*, 2012). DayCent has the option to simulate root death to coincide with a tree removal event; hence a similar transfer could be built in relatively easily, with some minor changes to the model code, to transfer the root C and N to the forest C and N stores respectively.

Whilst *Miscanthus* translocates nutrients from above ground to below ground organs at the start of the dormant winter period, this would be disadvantageous for woody tree species where the perennial organs are also above ground (Brereton *et al.*, 2013). Numerous studies suggest that translocation of nutrients into roots prior to coppicing does not occur for SRC willow, hence there is no need to build such transfers into the model (Bollmark, 1999; Deckmyn *et al.*, 2004; Shibu *et al.*, 2012).

Simulation of post coppicing growth with the PALM model is initially partitioned to above ground biomass, due to application of a parameter to prevent root biomass exceeding a set proportion of above ground biomass (Shibu *et al.*, 2012). Given the evidence for variation in root: shoot over lifecycle (Amichev *et al.*, 2011; Pacaldo *et al.*, 2012), setting a fixed ratio to limit below ground growth is not ideal. An alternative approach to ensure that the transferred C and N is applied to above ground biomass growth, and thereby account for the impact of coppicing on carbon metabolism and N translocation, would be to set different C partitioning to be applied during this period. Since DayCent already applies two sets of C partitioning for juvenile and established trees, it is relatively easy to add a third set, favouring above ground growth, to be applied during a user defined post coppicing period.

Due to increased photosynthesis post coppicing, resulting from multiple shoots and limited self-shading (Ceulemans, 1996; Philippot, 1996), simulation may be further improved by applying an increased photosynthetic conversion factor to account for increased activity and to allow the model to be parameterised to fit observed levels of post coppice growth. Again, the model code can be altered to apply a different photosynthetic conversion factor for the same user-defined post-coppicing period.

5.2.3 Senescence and decomposition

Unlike some of the more complex tree growth simulation models, e.g. ECOPHYS (Philippot, 1996) DayCent incorporates full simulation of senescence, organ death and decomposition. The **tree.100** input file includes user defined values for monthly death rate for all partitions, and the proportion of leaves to senesce in the scheduled month. Following simulation of (partial) organ death, decomposition is simulated at a proportion of the maximum rate (which can be set in the **tree.100** file) adjusted for substrate lignin content, C:N ratio and the impact of temperature and relative moisture content of soil.

5.3 Improvement – changes to model code

The model code is made up of over 200 subcomponents- some are in C, some are in FORTRAN, hence both a FORTRAN and a C compiler must be used. It was only necessary to alter the FORTRAN code (and ancillary files) in this instance, since this includes most of the crop and tree growth components.

Unlike the code changes implemented in Chapter 4, there are no complex algorithms to be built in, instead alterations simply allow for transfer of C and N on coppicing, and enable a choice of parameters to be used in the existing model algorithms, depending on whether a coppice event has recently taken place. Code changes are given in full in Appendix Section 3 but are described in brief here; Figure 5.2 outlines the key code changes and introduction of new parameters to event files, whilst Figure 5.3 can be compared directly to Figure 5.1 to illustrate how this model development alters DayCent simulation of tree carbon fixation, partitioning and loss.

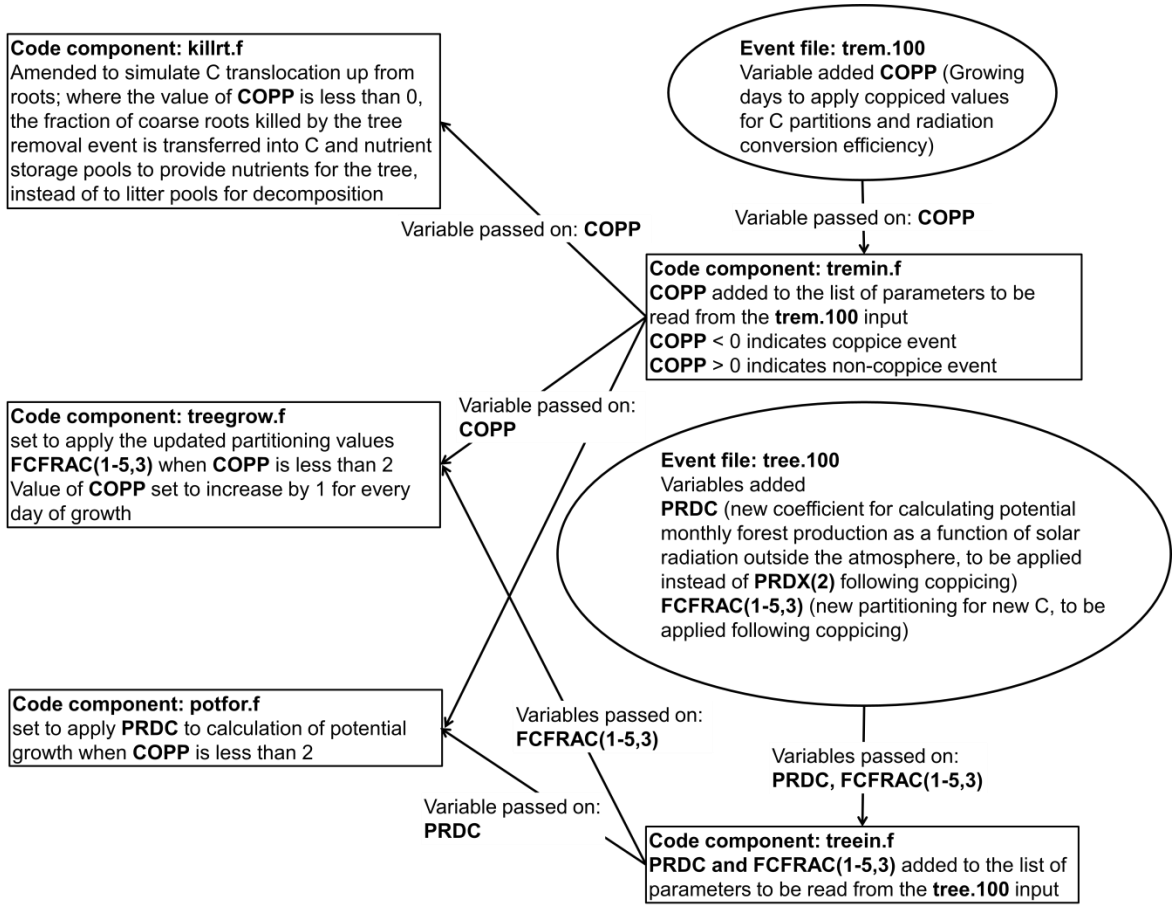

Figure 5.2 Main changes made to the model: code components and event files. Changes were made to the code components (square boxes), and these were compiled to produce the new executable. The event files (oval boxes) must be present in the same folder as the executable for the model to run.

An additional parameter **COPP** was added to each subtype of event in the **trem.100** event file, to indicate whether the tree removal event is coppicing. Negative values for **COPP** indicate coppicing; the value increases by one for every day of tree growth, to allow growth parameters to return to pre-coppicing values after a user defined period of growing days. The value for **COPP** is read in by the **tremin.f** component, and passed to the **killrt.f**, **treegrow.f** and **potfor.f** components.

The **killrt.f** component was then amended to simulate C translocation up from roots; where the value of **COPP** is less than 0, the fraction of coarse roots killed at the tree removal event is transferred into C and nutrient storage pools to provide nutrients for the tree, instead of to litter pools for decomposition.

To apply an increased value of conversion of light energy to drive a growth pulse, and altered C partitioning, to reflect more juvenile growth behaviour and preferential allocation to above ground growth, an alternative coefficient for calculating potential monthly forest production as a function of solar radiation outside the atmosphere (labelled **PRDC**) and an extra set of C partitioning parameters (labelled **FCFRAC(1-5)**) were then added to the **tree.100** input file. The **potfor.f** component was set to apply the new potential growth coefficient (**PRDC**) when **COPP** is less than 2, and the **treegrow.f** component was also set to apply the updated partitioning values (**FCFRAC(1-5,3)**) when **COPP** is less than 2.

Altering the value of **COPP** in the **trem.100** input file enables post-coppice growth parameters to be applied for a used-defined number of days as required for calibration.

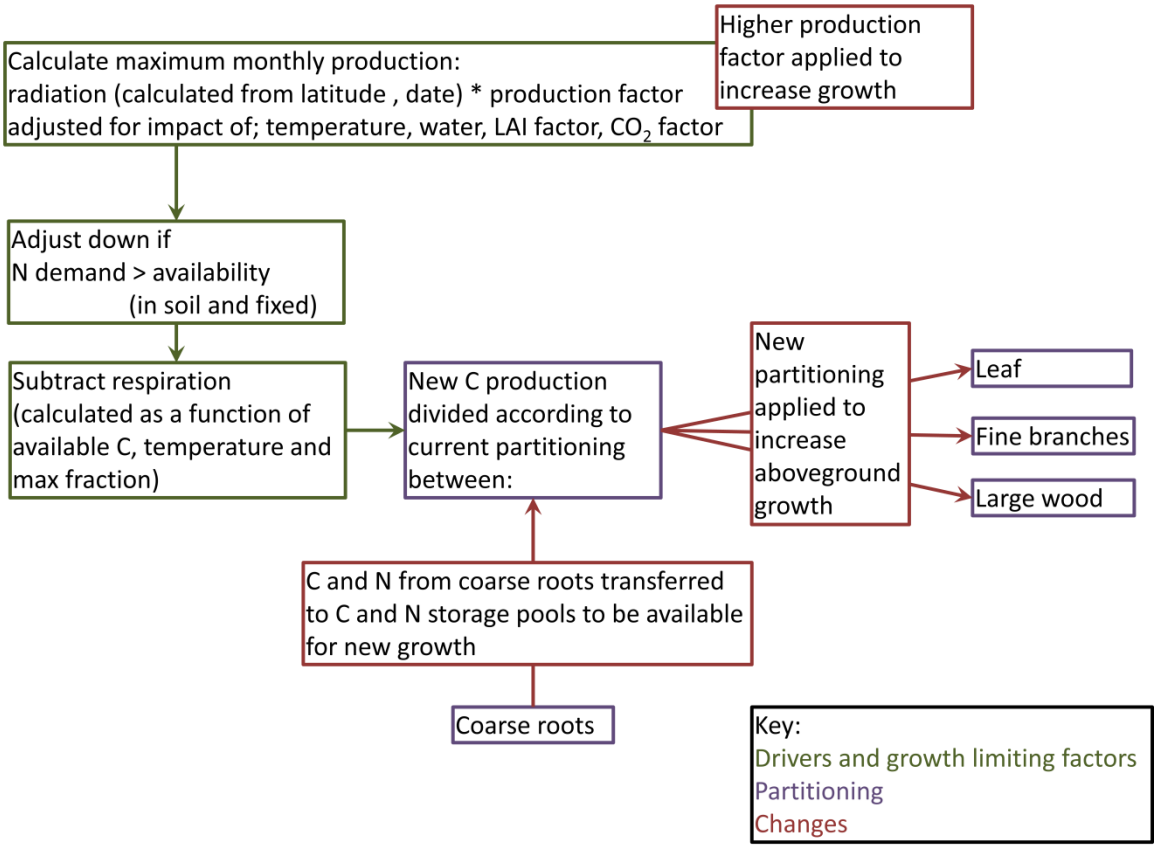

Figure 5.3 Alterations to DayCent simulation of tree carbon fixation, partitioning and loss

5.4 Improvement-model performance testing

After model code changes had been implemented, parameterisation and calibration of this adapted model were then carried out for datasets provided by Eric Cassella, from Forestry Commission field trials. The model was then validated against yield data for a Centre for Ecology and Hydrology field site in Lincolnshire, provided by Emily Bottoms and Niall McNamara for a site in Lincolnshire.

5.4.1 Calibration datasets

The Forestry Commission field trials included several different genotypes of SRC willow at 53 different UK field sites. Four of these sites were selected for calibration; the sites were chosen to cover a range of values for the drivers (latitude, temperature, water and N availability) as well as variation in parameters which affect soil water availability modelling (precipitation, soil textural composition and bulk density). Completeness of the weather datasets was also taken into account when choosing which sites to model, since many sites had gaps in the record. Site properties are listed in Table 5.1. At the field scale, spatial variation in yield is significantly less than that observed for N_2O emissions; hence biomass field data can be expected to be much more reliable.

Field studies have observed variation between genotypes in terms of response to fertilizer inputs, N utilisation efficiency and growth response, root, shoot and leaf biomass accumulation and proportional N allocation to different organs (Brereton *et al.*, 2013). As a result of observed variations, modelling studies often calibrate for one genotype (Amichev *et al.*, 2011), or identify which genotypes may perform better at different sites (Bauen *et al.*, 2010). There is generally a preference for single clone cultivation in field trials; however mixed clones may produce more consistent yields, due to varying yield responses to interannual weather variations. For the Forestry Commission field trials there is significant variation in yield; of the three genotypes trialled most frequently, average yields were: 20; 12; 15 odt ha^{-1}. The highest yielding clone varied between sites, with clone 1 (Jorunn) highest yielding at 33 sites, 2 (Germany) highest yielding at 3 sites, and 3 (Q83) highest yielding at 14 sites.

Table 5.1 Site properties for calibration sites

Site identifier Site variable	TALY	CARR	DEMO	BORE
Latitude	51.457	55.0421	53.2699	51.2101
Longitude	-3.392	-3.6356	-0.5274	0.1491
Available water capacity (mm)	No data	74.3	123	152.3
Slope	Flat	Convex	Flat	Convex
Maximum temperature (°C)	33.4	35	34.2	35
Minimum temperature (°C)	-13.4	-7.7	-11	-7.7
Average annual precipitation (cm)	150	116	74	86
pH	5.54	5.53	7.64	6.50
% sand	39.73	67.20	28.63	8.43
% silt	45.80	25.30	41.73	47.47
% clay	14.27	7.40	29.67	44.17
Bulk density	1.45	1.61	1.33	1.23
% organic matter	4.33	7.51	3.33	2.33
Extractable ammonium (mg kg^{-1})	6.7	16.4	8.2	6.8
Extractable nitrate (mg kg^{-1})	1.40	7.47	4.86	5.01
Mineral nitrate (mg kg^{-1})	19.50	26.63	10.95	6.33

However, for the four chosen calibration sites, there is limited variation between average yields for the three genotypes, as can be seen from Table 5.2.

Table 5.2 Genotype variation in average yields for calibration sites

	Genotype 1 yield (odt ha^{-1})	Genotype 2 yield (odt ha^{-1})	Genotype 3 yield (odt ha^{-1})
BORE	15.0	15.2	17.1
CARR	14.5	15.8	15.4
DEMO	12.4	11.9	12.3
TALY	19.6	18.6	17.1

To avoid the complexity of calibrating for multiple genotypes, this study will take average yield for each site, as per (Shibu *et al.*, 2012). This will have the limitation of meaning that variation in genotype performance cannot be simulated for the study sites to be assessed in Chapter 6. The model can be considered to be simulating a genotype mixture, although interspecies interactions may increase yield for mixed clones (Hofmann-Schielle, 1999), and the model is unable to account for this.

Field data on above ground biomass used for calibration from the Forestry Commission are based on allometric relationships between shoot diameter 100cm above ground level (D100) and shoot

dry mass, which were calculated as part of the study for each site and genotype. These relationships should not be affected by interannual variations in growth resulting from water or nutrient deficiencies etc, but will be altered by crop damage (Amichev *et al.*, 2011). Damage observed at field sites included aphid activity, caterpillar activity, rust, skeletonising, hail and frost; since these cannot be simulated by the DayCent model, the fact that their impact on yield is also not accounted for in field data could be expected to increase apparent agreement between model and field data. Due to the iterative nature of model calibration and parameterisation, and the need to match field data from multiple sites, a qualitative approach is taken here as opposed to use of statistical measures.

The files required for running DayCent were introduced in Table 3.3. of Chapter 3; only the files which are specific to an individual model run are discussed here. For each site, five specific input files were required including: daily weather in terms of precipitation, maximum and minimum temperature; a site file with data on latitude and longitude, soil textural composition and bulk density; and a schedule file with previous land use and management, dates of planting and coppicing of SRC willow, as well as first and last growth days for each year of SRC willow. Additionally, a **soil.in** file is required to represent the soil profile, and a **site.in** file, which in this case will be edited to simulate presence or absence of water table.

The schedule file must include a spin up period to account for the impact of previous land use on site properties such as soil C and N stores. Around 2000 years is recommended, in the form of 1800 years of native vegetation and 200 years of current cropping management (Adler, 2007) in this case arable. Therefore the schedule files began at year 0014, with land forested until 1813, followed by 200 years of arable use. This does not match with the land use history of arable land in the UK which was for the most part cleared of forestation much earlier, however the schedule file was written in this way to match the instructions distributed with the model, and applied in numerous previous studies in which the model has shown good performance. The intention of the recommended spin up approach is to set reasonable soil pools for arable land not yet at equilibrium, i.e. still losing carbon; in the absence of known soil carbon values or long term land use history, this approach is probably the most sensible. Since soil carbon will not be known for the scenario analysis sites, the spin up approach will be applied to sites in chapter 6, and is applied here also for consistency. Data on site properties and weather were provided by the Forestry Commission, with missing weather data populated based on the same dates in previous years. The weather dataset was looped for the entire spin up period. Planting dates were included

in Forestry Commission site data, and dates for first and last growth were obtained from the literature (Martin and Stephens, 2006).

There are no data on planting density, nor is there a facility to input this to DayCent, however planting density may be unimportant, since due to impacts on shading (Shibu *et al.*, 2012) and self-thinning, higher planting density may only increase yields if coppicing frequency is increased (Bullard *et al.*, 2002).

5.4.2 Calibration and parameterisation

Since DayCent had not previously been applied to SRC willow, it was first necessary to set appropriate parameters in the **tree.100** input file. The **tree.100** file has 153 parameters, many of which cannot be measured directly, therefore the parameterisation approach involved use of default values, and values from other studies where available (as per. Amichev *et al.*, 2011; Shibu *et al.*, 2012). The **trem.100** file has only 21 parameters, most of which can be set based on previous studies. The calibration approach involved fitting model output to field data on above ground biomass for the four sites, by altering carbon partitioning, the coefficients for calculating potential monthly forest production, and tree age at which to apply mature partitioning in the **tree.100** file, and duration for which to apply post-coppicing growth behaviour in the **trem.100** file. Model output for biomass is in the form of g C m^{-2}; C does not make up a consistent proportion of biomass, total biomass was calculated based on proportions as indicated by Pacaldo *et al.* (2012) since this study was also used to set composition values in the **tree.100** input file. The accepted values for **tree.100** and **trem.100** following calibration are included in full in Appendix Sections 3.2 and 3.3 respectively, with key parameters shown here in Tables 5.3 and 5.4.

The approach taken for calibration is very similar to that applied by Chamberlain *et al.* (2011) in terms of modelling for a spin-up period of 1800 years natural vegetation and 200 years of previous land management to set SOC, and parameterisation by manipulation of sensitive parameters, with calibration based on yield data only. They state that good calibration performance for yield simulation gave modest confidence in predictions of N_2O emissions and changes in system C associated with land use change

Fitted values for **tree.100** were generally within the range of model defaults, except for **PRDC** and **SNFXMX(2)**. Since the **PRDC** (or **PRDX(2)** if a coppice event has not occurred) parameter is used to calculate maximum monthly production, the use of a higher parameter value following coppicing is justified by the observed increase in photosynthetic activity, plus the supply of energy from below ground biomass. The high value of **SNFXMX(2)** , shown in Table 5.3, was necessary to match field data: regardless of values applied elsewhere, yields were significantly under predicted for values of symbiotic N fixation below the maximum of 0.0001 recommended, as can be seen from Figure 5.7. The need for a higher value for N fixation may indicate that SRC willow benefits from higher levels of symbiotic N fixation than previously modelled tree species, or may suggest that N cycling is not adequately simulated by the model, making it necessary to increase the value of **SNFXMX(2)** to prevent yield from being underestimated due to simulated N deficiencies.

Table 5.3 Key parameters in the tree.100 input file. It is necessary for NLAYER in the site.100 file to be greater than or equal to TLAYPG in order for soil water to be simulated to the required depth.

Parameter code	Parameter description		Value	Method of estimation
PRDX(2)	coefficient for calculating potential monthly forest production as a function of solar radiation outside the atmosphere	Standard	0.6	Fitted
PRDC		Following coppicing	0.8	
PPDF(1)	values for production for parameterization of a Poisson Density Function curve to simulate temperature effect on growth	Optimum temperature (°C)	20	(Amichev *et al.*, 2011)
PPDF(2)		Maximum temperature (°C)	40	
PPDF(3)		Left curve	1.7	Fitted
PPDF(4)		Right curve	3.7	
FCFRAC(1,1)	Leaves for juvenile forest		0.37	Fitted
FCFRAC(2,1)	Fine roots for juvenile forest		0.15	
FCFRAC(3,1)	Fine branches for juvenile forest		0.12	
FCFRAC(4,1)	Large wood for juvenile forest		0.21	
FCFRAC(5,1)	Coarse roots for juvenile forest		0.15	
FCFRAC(1,2)	Leaves for mature forest		0.34	
FCFRAC(2,2)	Fine roots for mature forest		0.04	
FCFRAC(3,2)	Fine branches for mature forest		0.35	
FCFRAC(4,2)	Large wood for mature forest		0.25	
FCFRAC(5,2)	Coarse roots for mature forest		0.03	
FCFRAC(1,3)	Leaves for coppiced forest		0.20	
FCFRAC(2,3)	Fine roots for coppiced forest		0.01	
FCFRAC(3,3)	Fine branches for coppiced forest		0.44	
FCFRAC(4,3)	Large wood for coppiced forest		0.34	
FCFRAC(5,3)	Coarse roots for coppiced forest		0.01	

TFRTCN(1)	Maximum C fraction to fine root, water stress		0.15	Fitted
TFRTCN(2)	Minimum C fraction to fine root, no water stress		0.01	
TFRTCW(1)	Maximum C fraction to fine root, nutrient stress		0.15	
TFRTCW(2)	Minimum C fraction to fine root, no nutrient stress		0.01	
BTOLAI	Biomass to leaf area index (LAI) conversion factor		0.013	(Lindroth, 1994)
MAXLAI	Theoretical maximum leaf area index achieved in mature forest		8	
SWOLD	Growing days after which to switch to mature C allocations		800	Fitted
WOODDR(1)	Fraction of forest deciduous		1	Fitted
WOODDR(2)	Monthly death rate fraction	Fine root (juvenile)	0.04	
WOODDR(3)		Fine root (mature)	0.04	
WOODDR(4)		Fine branch	0.01	Used default maximum to account for self-thinning
WOODDR(5)		Large wood	0.002	Fitted
WOODDR(6)		Coarse root	0.12	
SNFXMX(2)	Symbiotic N fixation maximum for forest		0.004	Fitted
TLAYPG	Number of soil layers used		7	To account for roots down to 130 cm
TMPLFF	Temperature at which leaf drop will occur (°C)		5	(Kopp, 2001)
TMPLFS	Temperature at which leaf out will occur (°C)		8	(Kopp, 2001)
CERFOR(1,1,1)	Minimum C/N ratio for leaves		22.99	Fitted based on (Pacaldo *et al.*, 2012)
CERFOR(1,2,1)	Minimum C/N ratio for fine roots		64.99	
CERFOR(1,3,1)	Minimum C/N ratio for fine branches		100.99	
CERFOR(1,4,1)	Minimum C/N ratio for large wood		120.99	
CERFOR(1,5,1)	Minimum C/N ratio for coarse roots		112.98	
CERFOR(2,1,1)	Maximum C/N ratio for leaves		40.01	
CERFOR(2,2,1)	Maximum C/N ratio for fine roots		70.01	
CERFOR(2,3,1)	Maximum C/N ratio for fine branches		200	
CERFOR(2,4,1)	Maximum C/N ratio for large wood		220	
CERFOR(2,5,1)	Maximum C/N ratio for coarse roots		200	
CERFOR(3,1,1)	Initial C/N ratio for leaves		38	
CERFOR(3,2,1)	Initial C/N ratio for fine roots		50	
CERFOR(3,3,1)	Initial C/N ratio for fine branches		98	
CERFOR(3,4,1)	Initial C/N ratio for large wood		98	
CERFOR(3,5,1)	Initial C/N ratio for coarse roots		113	
'FURGDYS'	Number of days after leaf out of unrestricted growth of woody components		100	Fitted

The value of **FD(2)**, shown in Table 5.4, is set at 0.2 to account for 20 % coarse root transfer to above ground biomass following **COPP**. This proportion was applied by Tallis *et al.* (2013) after

Deckmyn *et al.* (2004) on the assumption that carbon metabolism response to coppicing is similar to that of poplar, although there is no record of how the value was originally calculated, or whether response may vary with site factors such as soil water and nutrient availability.

Table 5.4 Key parameters in the trem.100 input file

Parameter	Definition	Value for coppice event	Method of estimation
'EVNTYP'	Event type flag 0= cut, 1= fire	0	
'REMF(1)'	Fraction of leaf live component removed	1	
'REMF(2)'	Fraction of fine branch live component removed	1	(Shibu *et al.*, 2012)
'REMF(3)'	Fraction of large wood live component removed	0.95	
'REMF(4)'	Fraction of fine branch dead component removed	1	
'REMF(5)'	Fraction of large wood dead component removed	0.95	
'FD(1)'	Fraction of fine root component that dies	0.0	
'FD(2)'	Fraction of coarse root component that dies	0.2	(Deckmyn *et al.*, 2004; Tallis *et al.*, 2013)
'RETF(1,1)'	Fraction of C in killed live leaves that is returned to the system (ash or litter)	1	
'RETF(1,2)'	Fraction of N in killed live leaves that is returned to the system (ash or litter)	1	
'RETF(1,3)'	Fraction of P in killed live leaves that is returned to the system (ash or litter)	0	
'RETF(1,4)'	Fraction of S in killed live leaves that is returned to the system (ash or litter)	0	
'RETF(2,1)'	Fraction of C in killed fine branches that is returned to the system (ash or dead fine branches)	0	
'RETF(2,2)'	Fraction of N in killed fine branches that is returned to the system (ash or dead fine branches)	0	
'RETF(2,3)'	Fraction of P in killed fine branches that is returned to the system (ash or dead fine branches)	0	
'RETF(2,4)'	Fraction of S in killed fine branches that is returned to the system (ash or dead fine branches)	0	
'RETF(3,1)'	Fraction of C in killed large wood that is returned to the system (ash or dead large wood)	0	
'RETF(3,2)'	Fraction of N in killed large wood that is returned to the system (ash or dead large wood)	0	
'RETF(3,3)'	Fraction of P in killed large wood that is returned to the system (ash or dead large wood)	0	
'RETF(3,4)'	Fraction of S in killed large wood that is returned to the system (ash or dead large wood)	0	
'COPP'	Growing days to apply coppiced values for C partitions and radiation conversion efficiency	-150	Fitted

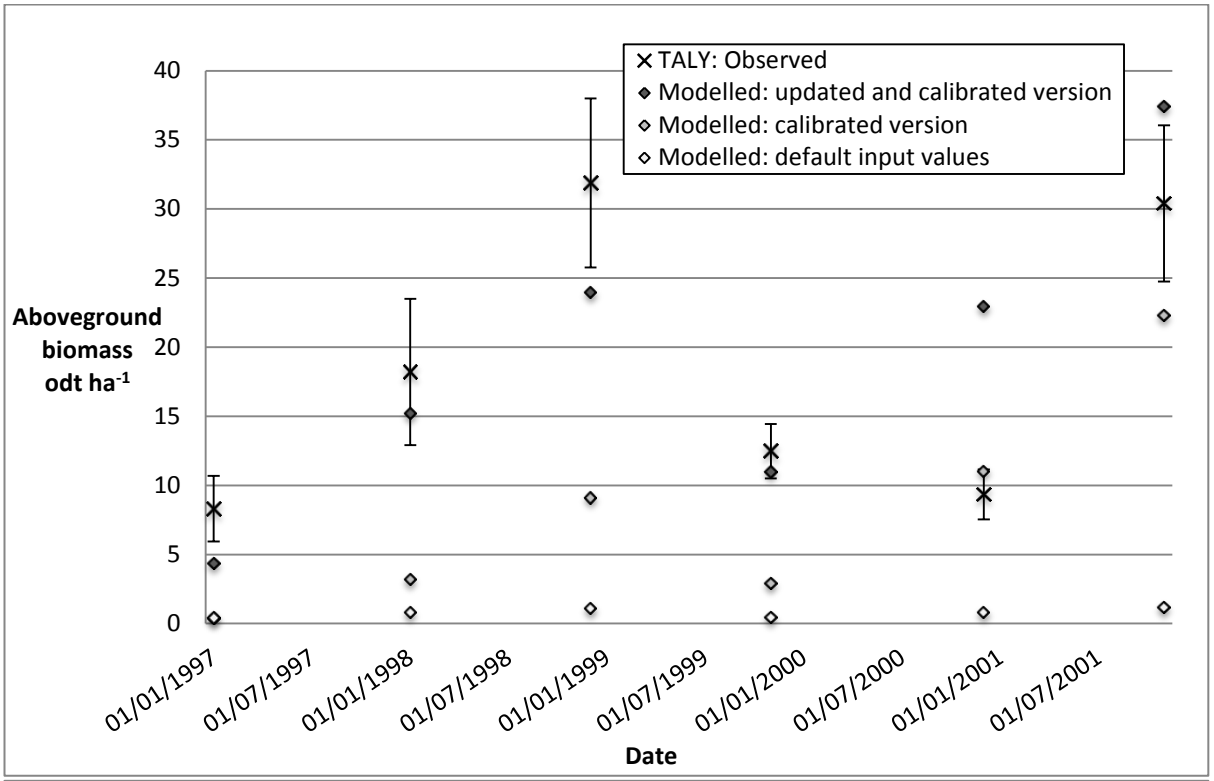

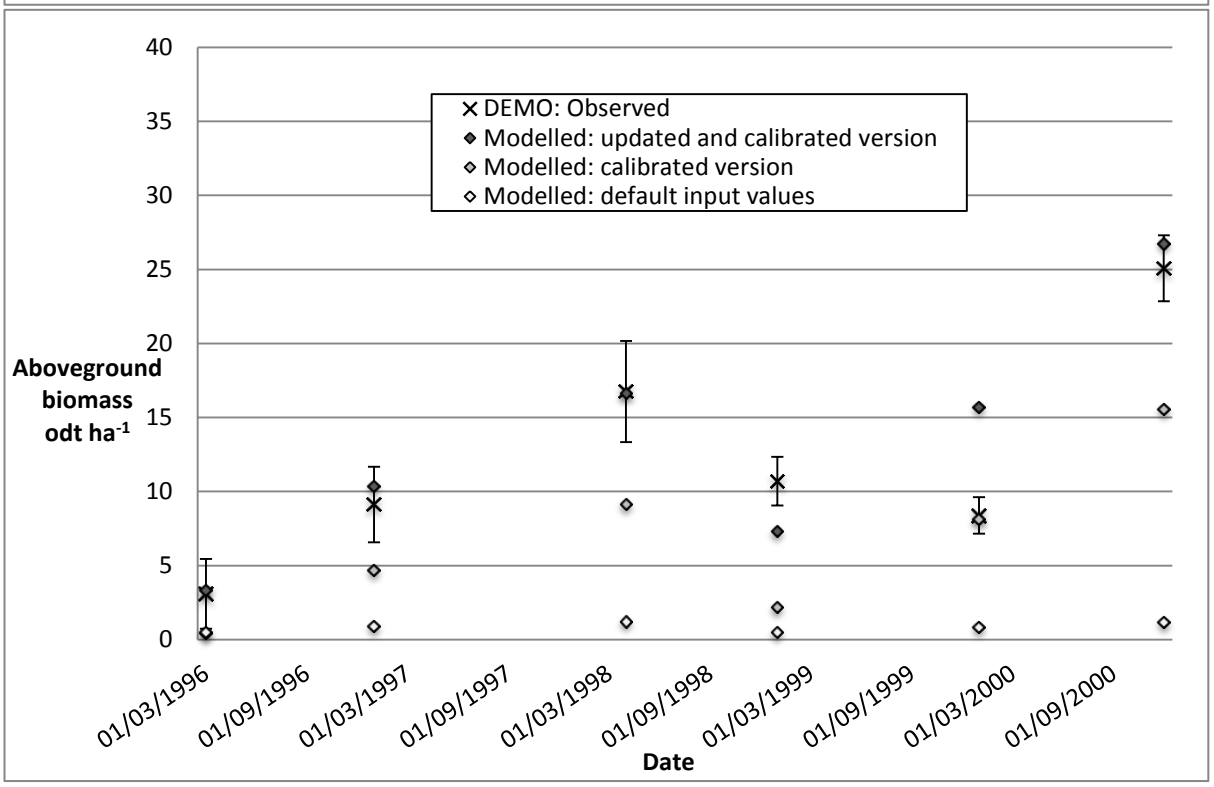

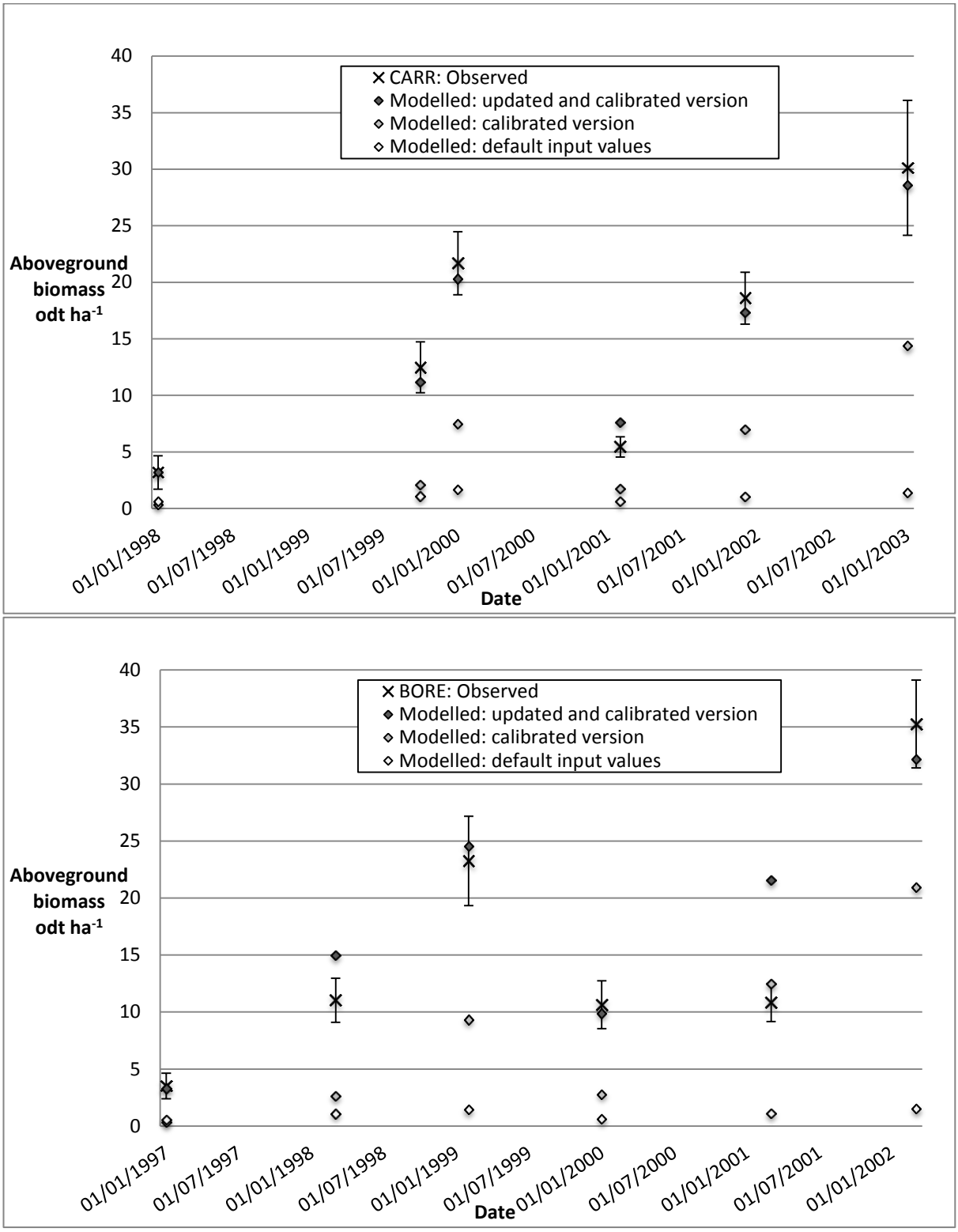

Figure 5.4 Measured and modelled time series above ground biomass for the four calibration sites with error bars showing ± one standard deviation of measured data. Owing to the relationship between precipitation and site moisture in the dataset provided by the Forestry Commission, presence of water table was simulated for six months of the year at sites BORE and DEMO, and none of the year at sites TALY and CARR. The three sets of model output are: updated and calibrated version= Impacts of coppicing simulated, parameters as set in Tables 5.3 and 5.4; calibrated version= Impacts of coppicing not simulated, other parameters as set in Table 5.3; default input values= tree.100 values using the default for temperate deciduous forest

Figure 5.4 indicates good performance of the DayCent model following calibration and code changes; modelled values for above ground biomass often fall within the range of the standard deviation of field data. The graphs in Figure 5.4 also indicate very poor performance for use of the default **tree.100** input values, which are intended to broadly represent mixed temperate deciduous forest. Performance was improved for the parameterised and calibrated input values, but it was necessary to apply the code changes to simulate changes in carbon metabolism and increased photosynthetic activity and above ground growth following coppicing in order to produce output representative of field data.

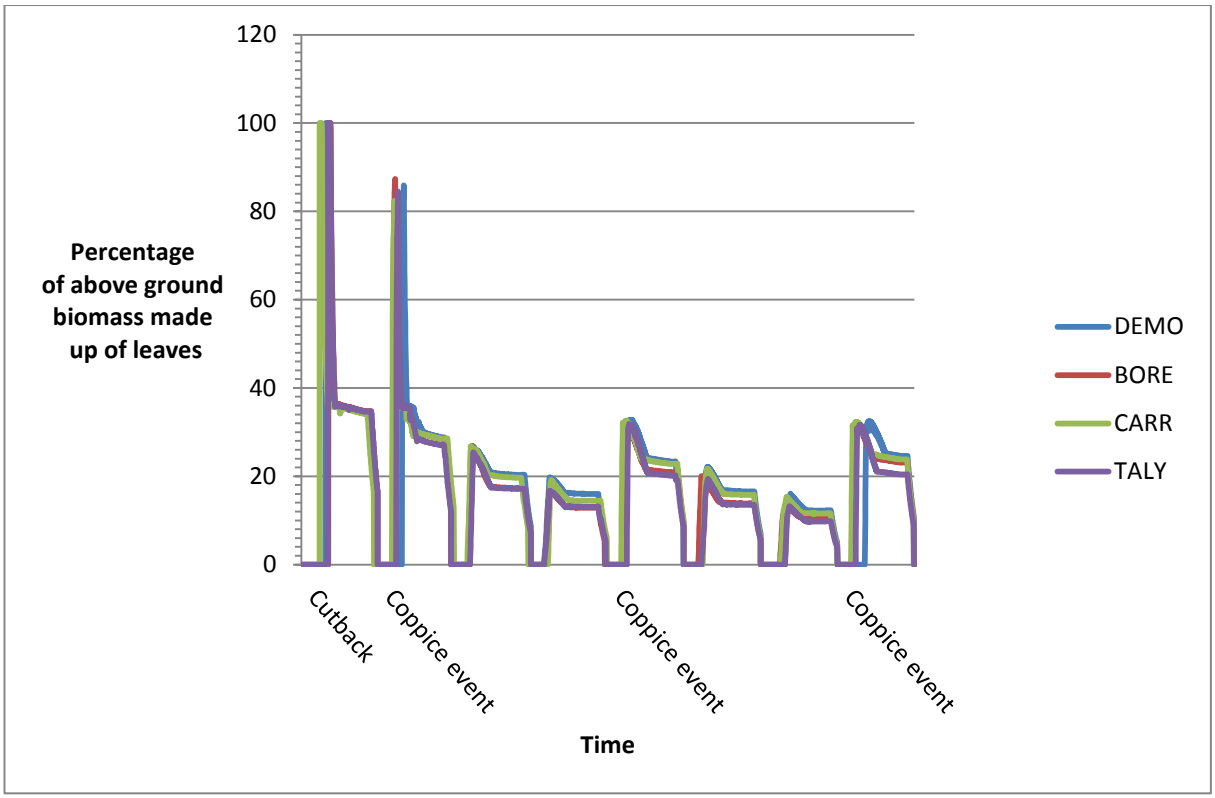

Figure 5.5 Leaf biomass as a proportion of total above ground biomass for the four calibration sites

Figure 5.5 indicates variation in the proportion of total biomass made up of leaves over the coppice cycle: modelled values compare well with measured values from Proe *et al.* (2002) of 40;18;12.

Dimitriou *et al.* (2009) recorded ET in the range of 36-59 cm a^{-1} which accounted for around 76 % of precipitation; proportional values for the four calibration sites as indicated in table 5.5 are significantly lower than this, but absolute values are mostly within range.

Table 5.5 Annual evapotranspiration at the four calibration sites, with reference to annual precipitation values

	Precipitation cm	ET cm	% ET
BORE / Average	**87.55**	**47.95**	**55.55**
1997	101.21	52.54	51.91
1998	76.32	49.91	65.39
1999	75.34	49.16	65.25
2000	99.84	47.32	47.40
2001	78.89	49.23	62.40
2002	78.77	38.12	48.39
2003	75.24	45.63	60.64
2004	101.11	48.21	47.68
2005	101.21	51.45	50.84
CARR / Average	**116.28**	**51.41**	**45.53**
1998	131.08	52.62	40.14
1999	101.18	53.40	52.78
2000	101.30	48.90	48.27
2001	101.32	49.13	48.49
2002	161.66	42.14	26.07
2003	131.08	64.55	49.24
2004	101.30	48.13	47.51
2005	101.29	52.44	51.77
DEMO / Average	**73.24**	**45.06**	**62.48**
1997	70.30	51.69	73.53
1998	75.34	49.21	65.31
1999	70.93	45.34	63.92
2000	78.51	46.15	58.79
2001	76.33	46.37	60.75
2002	81.49	31.00	38.04
2003	81.57	43.19	52.95
2004	54.38	41.68	76.65
2005	70.30	50.91	72.42
TALY / Average	**148.47**	**51.16**	**35.71**
1997	134.86	57.12	42.36
1998	159.20	50.90	31.97
1999	167.04	51.83	31.03
2000	188.60	51.24	27.17
2001	117.33	51.65	44.02
2002	189.36	49.31	26.04
2003	136.66	41.25	30.18
2004	108.32	50.31	46.45
2005	134.86	56.82	42.13

It is worth noting that potential ET is likely to correlate more strongly with factors controlling water demand, and that water availability may be affected more strongly by site drainage factors than by precipitation, hence ET may not be expected to make up a consistent proportion of

precipitation. Field data for poplar suggests lower yield from the first rotation, since roots are not yet fully established, followed by more consistent values of biomass both above and below ground in subsequent rotations (Deckmyn *et al.*, 2004). Modelled and measured values from studies on SRC willow also indicate slow establishment of roots, taking around 2 years to reach values over 1 t ha^{-1} increasing to around 5 t ha^{-1} by the third year of the rotation (Shibu *et al.*, 2012) and arriving at 35 t ha^{-1} 22 years from planting (Amichev *et al.*, 2011). Output from DayCent for the four calibration datasets shown in Figure 5.4 indicates faster initial root development, with 5 t ha^{-1} reached in the first year of the first rotation, and 35 t ha^{-1} achieved at some sites by 9 years from planting, although values appeared to level off at this point. During calibration, alternative partitioning parameters were tested, allocating smaller proportions to root biomass were tested, however due to the use of root biomass in calculation of nutrient and water supply, this approach resulted in under prediction of yield. This may indicate that DayCent fails to fully simulate the efficiency of water and nutrient uptake, or that the genotypes considered here have more prolific root systems than those assessed elsewhere. Ultimately, it is likely that good simulation of above ground growth rates was at the expense of accurate representation of below ground growth rates

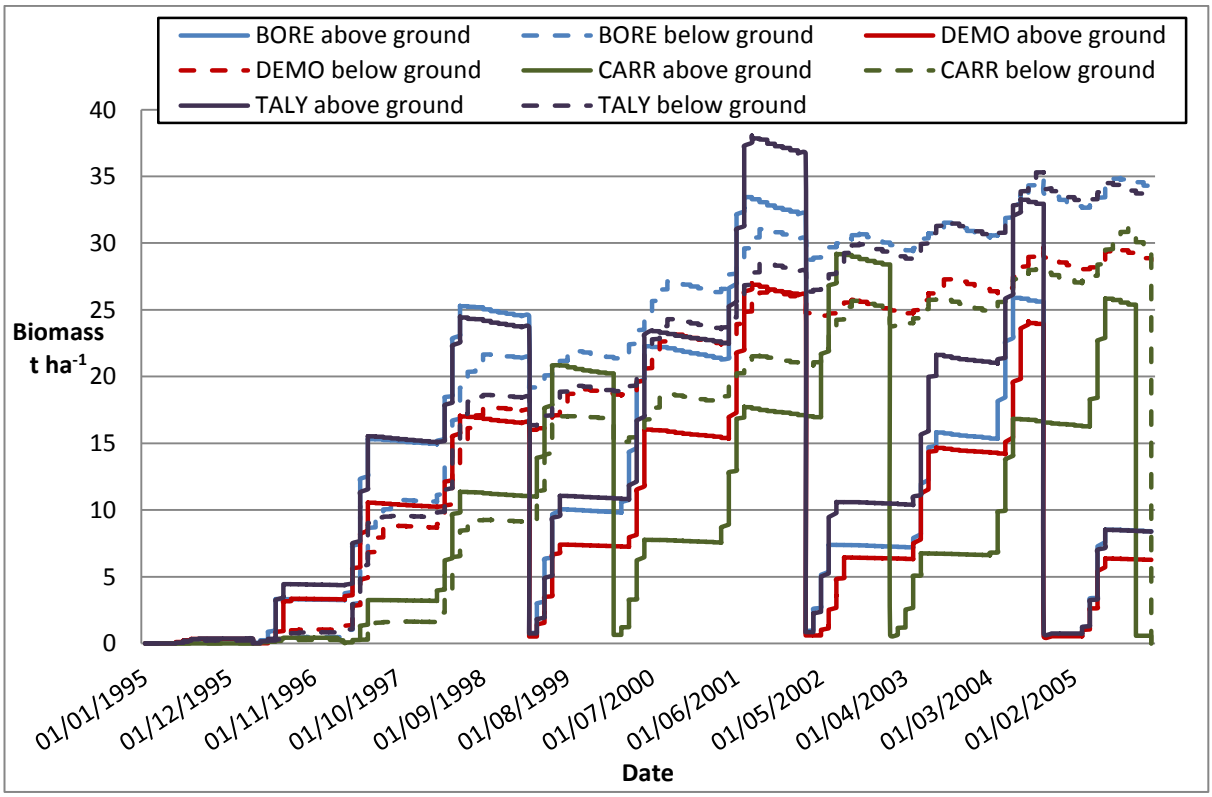

Figure 5.6 Above and below ground biomass for the four calibration datasets

5.4.3 Validation dataset

For the validation site, field data is based on harvested biomass, hence should account for impacts of pests and other damage, and it is not necessary to take into account potential error in allometric equations. Error may be introduced however if the harvested proportion of above ground biomass differs from the 95% applied in the model. Site properties for the validation site are listed in Table 5.6, and the model was run as for the calibration sites, but with tree parameters kept constant. Presence of a water table was simulated all year round in order to match measured values for WFPS. For the validation site, *Miscanthus* data were also available, along with N_2O measurements for both crops; since scenario analysis in Chapter 6 will also be performed for *Miscanthus*, and since output on N_2O emissions for both crops will be considered, it is useful to assess model performance using these data also.

Table 5.6 Site properties for the validation site

Soil horizon	**Depth to top (cm)**	**Depth to bottom (m)**	**Mean clay %**	**Mean silt %**	**Mean sand %**	**bd (CST)**	**pH**
1	0	20	25	29	46	1.38	6.75
2	20	45	22	32	46	1.4	6.75
3	45	70	44	32	24	1.26	6.75
4	70	150	42	38	20	1.26	6.75
Weather data	**Maximum temperature (°C)**		**Minimum temperature(°C)**		**Average annual precipitation (cm)**		
	31.3		-14.2		57.26		

5.4.4 Validation performance

Table 5.7 indicates model performance for yield simulation at the validation site; values of relative deviation for SRC willow are comparable to the 14.3 and -2.7 achieved for yield modelling with ForestGrowth by Tallis *et al.* (2013) suggesting that explicit simulation of stem numbers is not vital to reasonable prediction of yield.

Table 5.7 Relative deviation of yield predictions for the validation site

SRC willow	**Observed yield t ha^{-1}**	**Modelled yield t ha^{-1}**	**Relative deviation**
2004	18.9	18.1	-4.2
2007	30	27.4	-8.5

Figures 5.7 and 5.8 are included to indicate the impacts of applying lower values for SNFXMX(2). Figure 5.7 indicates that applying lower values for SNFXMX(2) caused simulated above ground biomass to be significantly underestimated from the first rotation. Whilst the pattern in response to interannual climate variation is the same for all simulated values of SNFXMX(2), the impact of root establishment to increase yields after the first rotation is not seen for simulations with reduced N fixation, presumably due to soil N depletion meaning that yields as high as those simulated during establishment can no longer be supported. As stated in Section 1.4.2.4, without fertiliser input N soil depletion may be observed in later years at former arable sites, however the effect simulated here is faster than would be expected, and causes yield to be underestimated by the first rotation. At lower values of N fixation, below ground biomass levels off more quickly, and does not reach the 35 t ha^{-1} peak identified by previous studies (Amichev *et al.*, 2011), whilst root growth during establishment is still faster than suggested elsewhere in the literature (Shibu *et al.*, 2012). Hence it appears that the 0.004 level of N fixation applied in the tree.100 file is necessary to simulate above ground and below ground biomass, particularly in later rotations.

Figure 5.8 indicates that altering N fixation has limited impact on soil nitrate and ammonium concentrations. Peak concentrations are higher at lower N fixation rates, however values are low for all conditions most of the time from the first rotation. Therefore, value of N fixation does not appear to affect simulation of N exhaustion. Given the very low level simulated for both ammonium and nitrate, it is useful to assess whether N retention may be poorly simulated by the model in general.

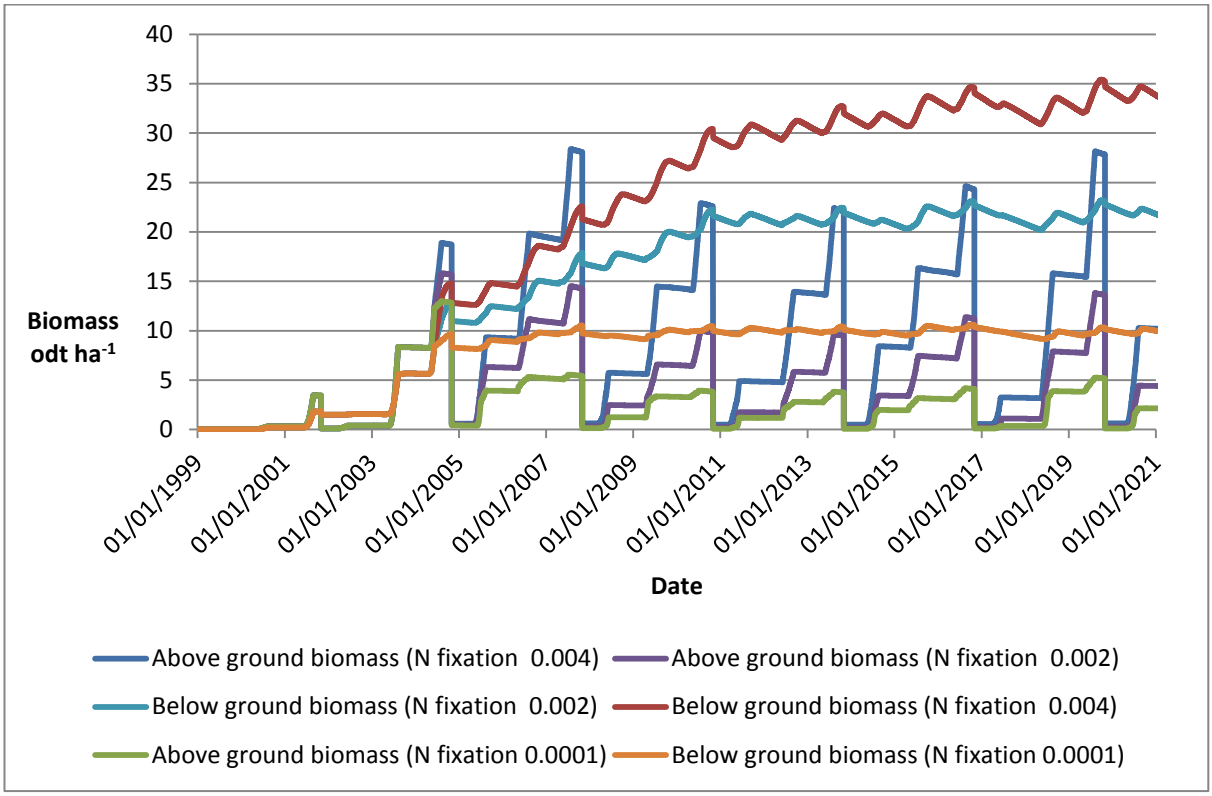

Figure 5.7 Modelled above and below ground biomass with a range of values for N fixation (SNFXMX(2)) for SRC simulated willow cultivation at the validation site.

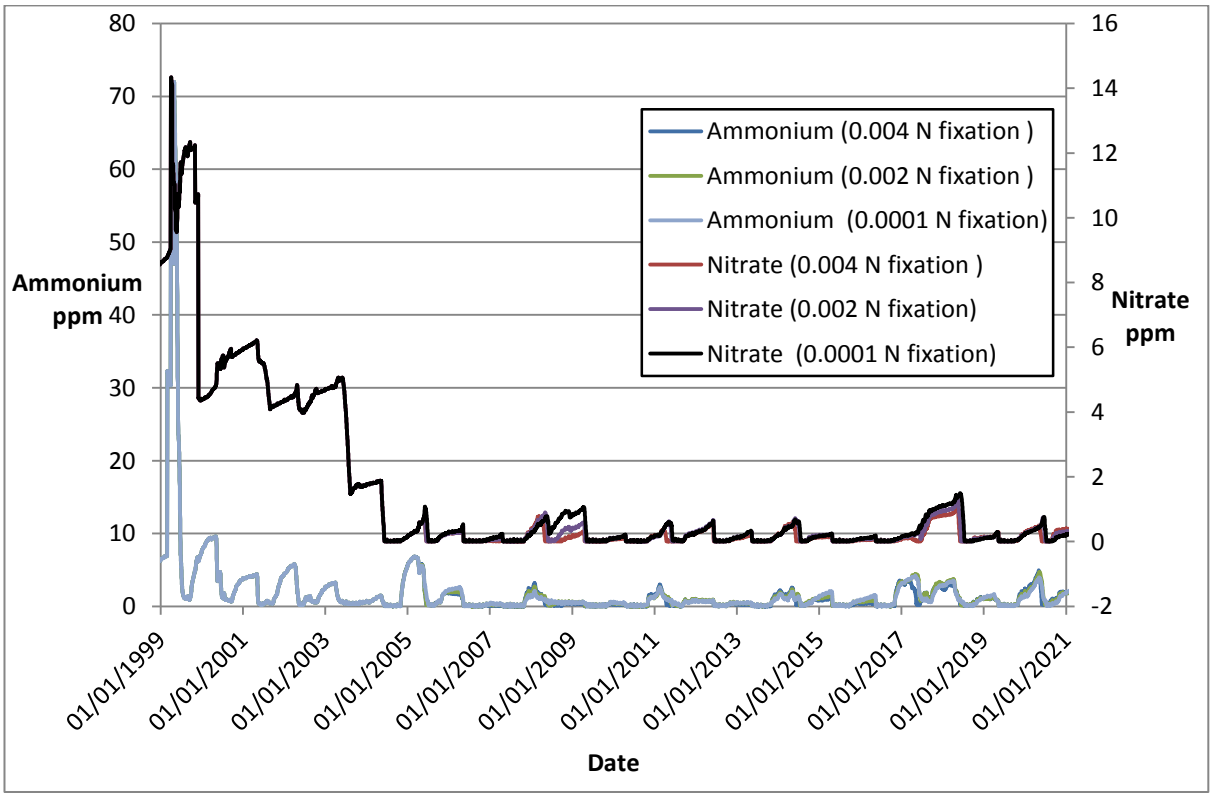

Figure 5.8 Modelled soil N with a range of values for N fixation (SNFXMX(2)) for simulated SRC willow cultivation at the validation site. For both ammonium and nitrate, little difference was simulated between conditions, meaning that the lines for 0.002 and 0.004 are often not visible behind the line for 0.001.

As was noted in Section 4.4.5, previous studies have identified poor simulation of soil nitrate, and ammonium with DayCent (Del Grosso *et al.*, 2008; Jarecki *et al.*, 2008). For the calibration studies, field data is not available to assess model performance; however Figure 5.9 and Figure 5.10 respectively indicate that both ammonium and nitrate fall to relatively low levels quite rapidly after fertiliser applications. Although a degree of retention is simulated under fertilised land use, both graphs indicate a baseline around zero under no fertiliser land use, with small peaks following crop inputs to soil. Figure 5.11 and Figure 5.12 indicate that for ammonium and nitrate respectively, measured values at the validation site were significantly higher than simulated by the model, in line with findings of previous studies. Poor representation of soil N availability may be a limitation in terms of simulating both crop growth and N_2O emissions. However, by applying a value of 0.004 for **SNFXMX(2),** observed levels of crop growth can be simulated in spite of under prediction of soil N. Under prediction of soil N availability may be a factor in the need to over-predict the rate of below ground biomass accumulation in order to simulate observed above ground biomass. Under prediction of soil N availability may reflect over prediction of leaching or gaseous losses (Del Grosso *et al.*, 2008; Jarecki *et al.*, 2008). As discussed in Section 4.4.5 there is not a convenient, universal solution to the identified issues with simulating soil nitrate and ammonium, hence it will be necessary to consider this as a possible limitation when drawing conclusions from model output.

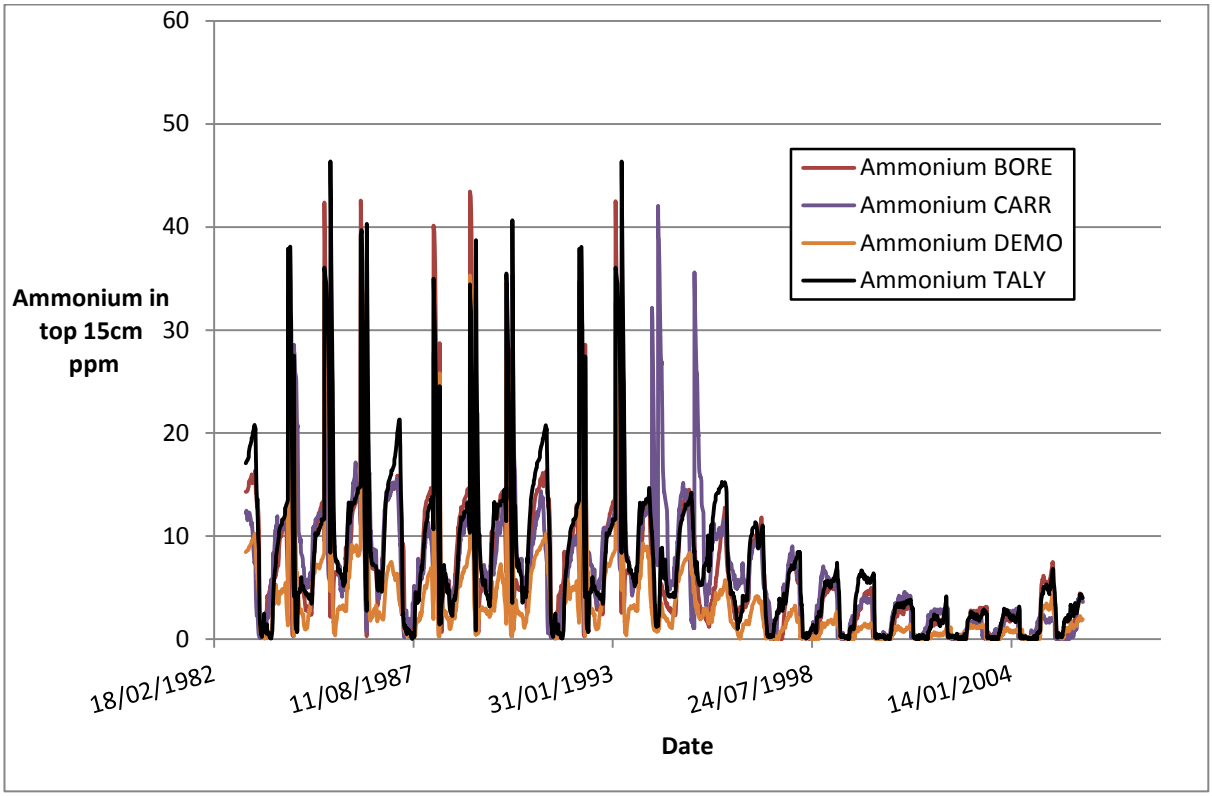

Figure 5.9 Simulated values of ammonium in the top 15cm of soil at all 4 calibration sites over a 20 year period

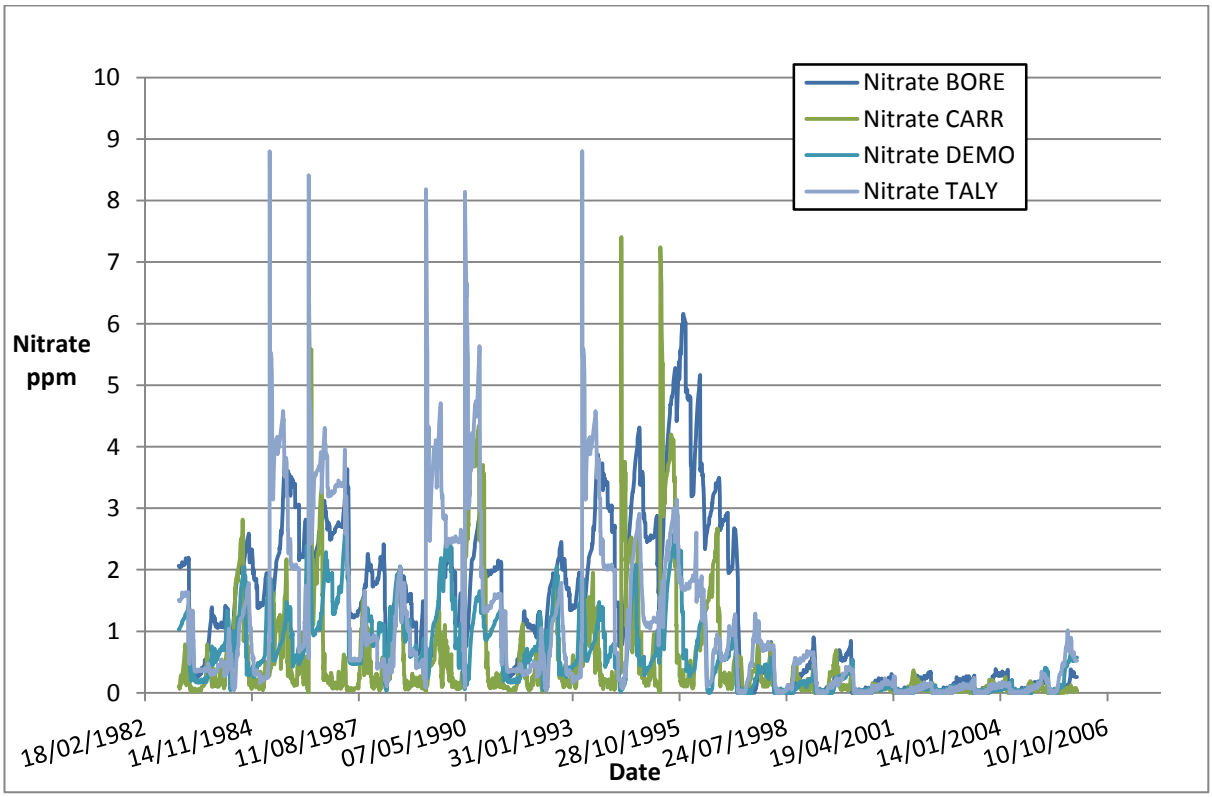

Figure 5.10 Simulated values of nitrate at all 4 calibration sites over a 20 year period

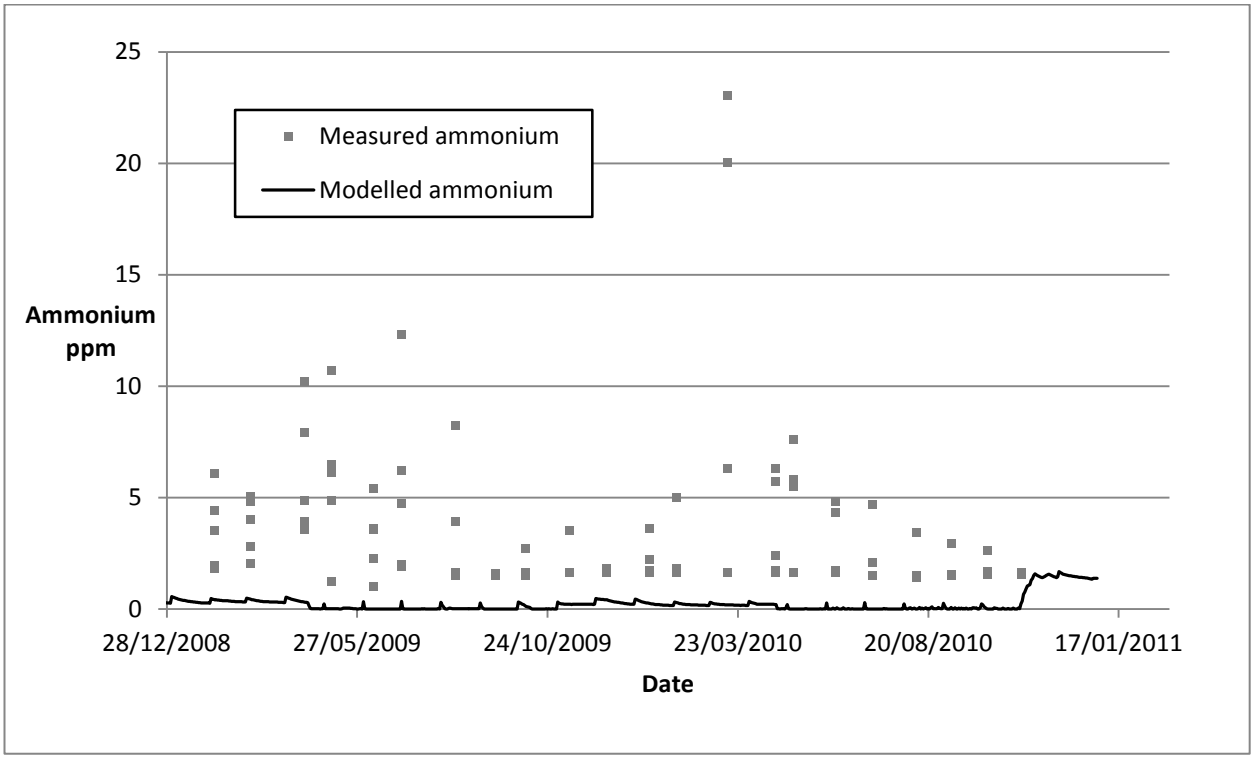

Figure 5.11 Comparison of modelled and measured soil ammonium for for SRC willow cultivation at the validation site. Measured values are indicated as dots, due to being point values, whereas simulated values are continuous, and are hence represented with a line.

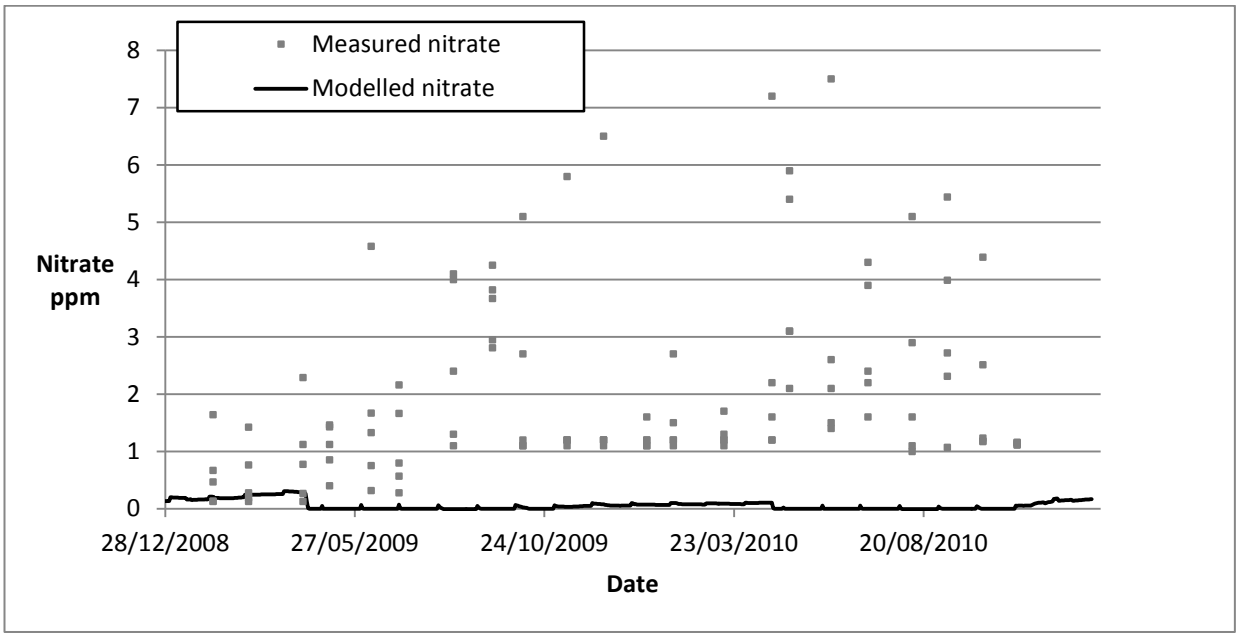

Figure 5.12 Comparison of modelled and measured soil nitrate for SRC willow cultivation at the validation site. Measured values are indicated as dots, due to being point values, whereas simulated values are continuous, and are hence represented with a line.

Error bars in Figure 5.13 representing spatial variation in measurements indicate that the SRC willow field showed significant variation in N_2O flux, in line with field scale variation identified by previous research (Green *et al.*, 2003; Strudley *et al.*, 2008). Modelled values were low, and

generally within the range of measurements for the date, which suggests that simulation of N_2O emissions may be acceptable in spite of issues with representation of soil N availability.

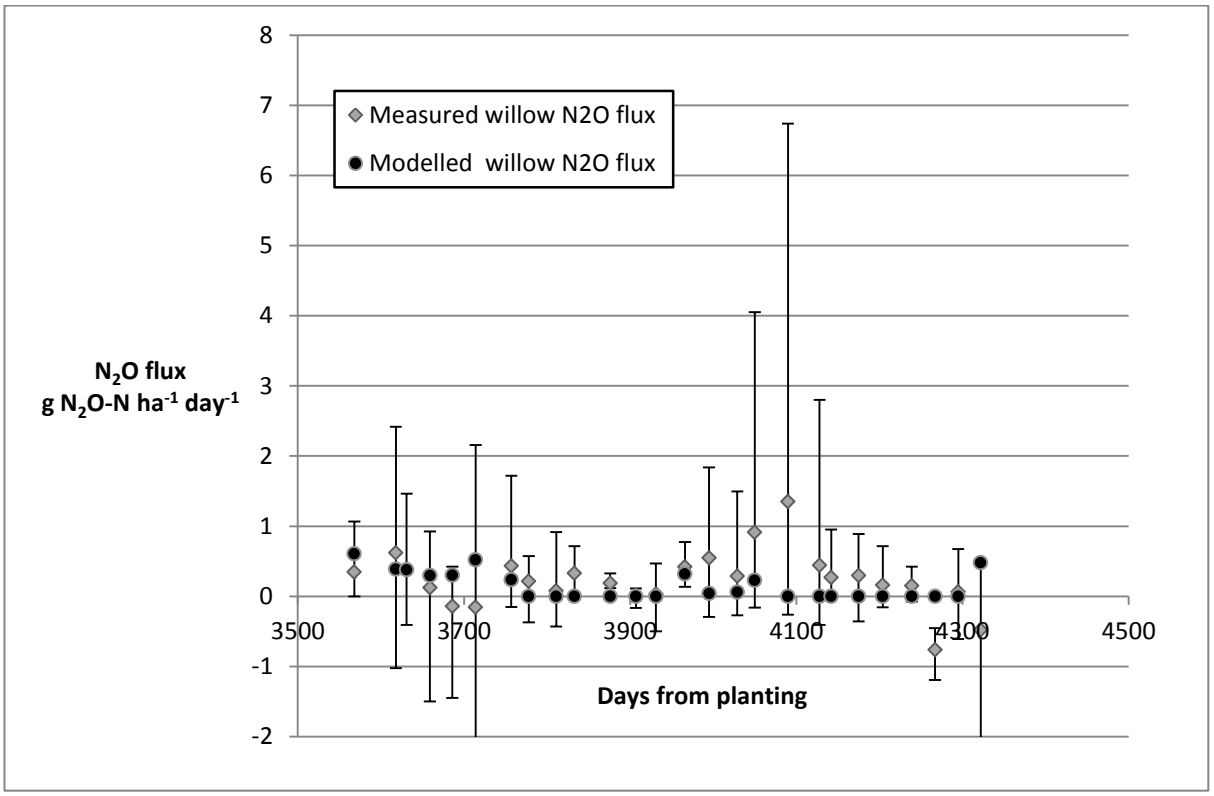

Figure 5.13 Comparison of modelled and measured soil N_2O flux for SRC willow cultivation at the validation site. Error bars on measured values indicate maximum and minimum of five measurements taken at different points over the field on the same day.

It is also useful to assess model performance for *Miscanthus* at the validation site, since field data for yield and N_2O emissions are also available. Field data for *Miscanthus* indicated lower yield for the first harvest; as for SRC willow, establishment yield for *Miscanthus* is generally lower, and the model does not appear able to simulate this. For this site, yields are lower for *Miscanthus* than SRC willow, meaning that the second harvest also shows high relative deviation in Table 5.8, although absolute deviation is only -0.84 t ha^{-1}.

Table 5.8 Relative deviation of yield predictions for the validation site

Miscanthus	Observed yield t/ha	Modelled yield t/ha	Relative deviation
2009	2.80	5.96	113.04
2010	4.14	3.30	-20.19

Figure 5.14 indicates that the *Miscanthus* field also showed significant spatiotemporal variation in N_2O flux, and again modelled values were low, and generally within the range of measurements for the date.

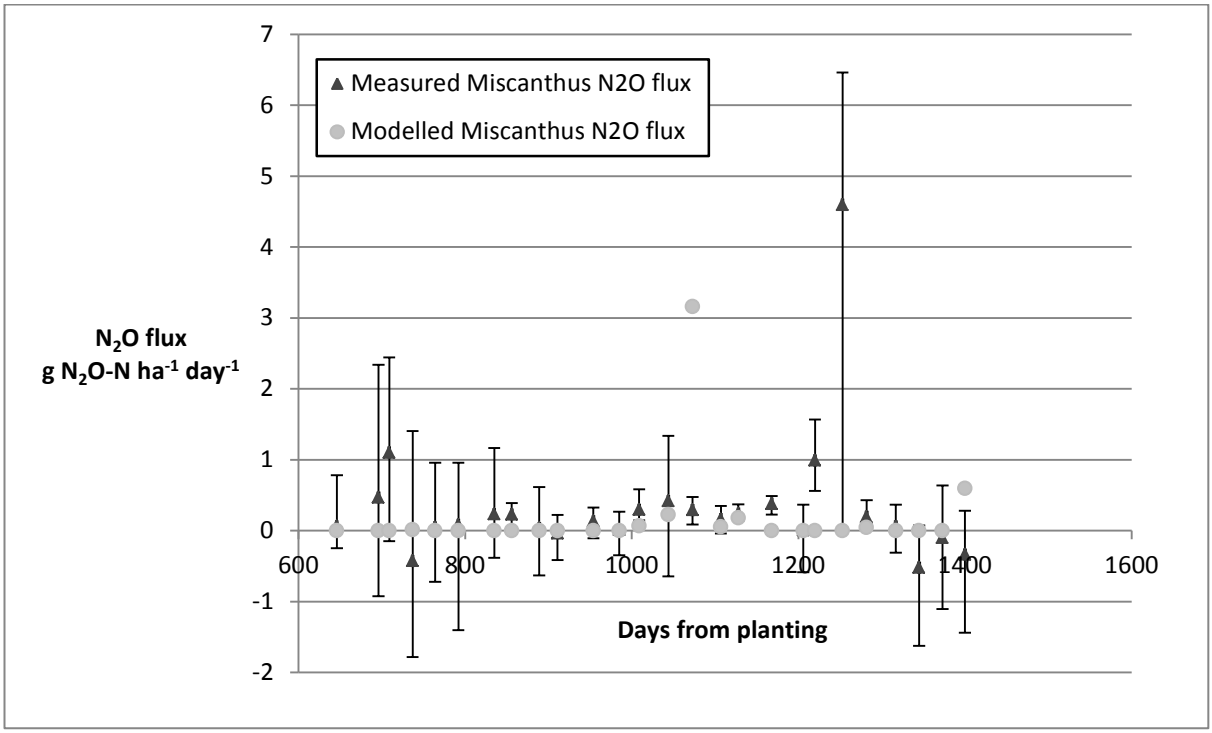

Figure 5.14 Comparison of modelled and measured soil N_2O flux for Miscanthus cultivation at the validation site. Error bars on measured values indicate maximum and minimum of five measurements taken at different points over the field on the same day.

5.5 Discussion

For the parameterisation of SRC willow growth rate, field data errors may be present in the calibration data, due to use of d100 values to estimate above ground biomass, and in the validation data due to possible variation in the proportion of above ground biomass harvested. In terms of input data, further potential sources of error include missing weather data, which was populated based on the same dates in previous years, and use of dates for first and last growth obtained from the literature, which may differ slightly from the dates at the specific sites, due to variation with climate and latitude.

Additionally, the use of average yield for all genotypes at each calibration site will have the limitation of preventing assessment of variation in genotype performance for the study sites to be assessed in Chapter 6. However, given the low level of variation in yield between genotypes for the sites assessed, calibrating the model to these separately may not have been useful; to calibrate to each genotype separately, it would have been better to choose sites with greater genotypic variation to identify which site properties are important.

For the calibration sites, modelled above ground biomass was generally within ± one standard deviation of measured data for year one of the rotation, indicating good simulation of regrowth following coppicing. Simulated above ground biomass was also generally within ± one standard deviation of measured data for year three of rotations, which points to potentially good performance for simulating yield, although confidence must be based on performance at validation. The adapted and parameterised model gives improved representation for the calibration sites, except the second year of the second rotation, when the parameterised version of the model which did not account for the impacts of coppice more closely matched field data at three of the four calibration sites (these appear to have experienced dieback, possibly due to frost, which is not simulated by the model). The adapted parameterised version of the model also gives best simulation of final yield for both rotations, and hence overall, is better.

Validation performance for simulating SRC willow yield was good, with less than 10% underestimation for both modelled rotations, hence confidence in model yield predictions in scenario analysis can be relatively high, although it is important to consider potential limitations if the model is applied to sites with climate and soil types outside of the range assessed here.

Below ground biomass was not as well simulated as above ground, although the model is theoretically capable of simulating the 130 cm rooting depth of SRC willow appropriately, using the **TLAYPG** value of 7 applied here. Poor simulation of below ground biomass for SRC willow may be attributed to failure of DayCent to fully simulate the efficiency of water and nutrient uptake. Although predicted below ground biomass is less important than above ground in terms of yield, requirement for water and nutrients to complete this growth may result in over prediction of crop water and nutrient demands.

In terms of the scenario analysis required by this study it is also important to note that the 250 cm rooting depth of *Miscanthus* (Christian 2006) can also be simulated by applying a value of 9 for the **crop.100** equivalent parameter. Using crop parameters from Davis *et al*. (2010), DayCent performance for simulation of *Miscanthus* yield was reasonable for the second harvest, but first harvest was significantly over-estimated.

Issues with simulation of soil N availability have also been identified. Potential associated deficiencies in simulation of N_2O emissions and N leaching must be considered, however parameterisation of symbiotic N fixation goes some way to resolving potential impacts on simulation of crop growth. Therefore, confidence in simulated N_2O emissions will be based on the assessment of validation performance in Chapter 4, and reasonable performance at the validation sites for SRC willow and *Miscanthus*, as shown in Figures 5.13 and 5.14 respectively. Simulated values for N leaching should be considered carefully in comparison to field data, and model verification performance in previous studies, since this study has not performed model verification for N leaching.

Since the **tree.100** file has 153 parameters, many of which cannot be measured directly, or vary with growing conditions in a way which cannot easily be measured, hence values used from other studies may not be reliable, likewise default values will only provide an approximation of the appropriate parameter value, and fitted values are simply the parameter value required to produce output matching field data. As a result, high confidence in model output should be limited to simulation of above ground biomass for sites relatively similar to those used in verification. In terms of timing and amount of water and nutrient uptake, confidence should be based on data used to parameterise the **tree.100** file, and data used to set first and last growth dates.

5.6 Summary

To predict yield, and to model how SRC willow differs from annuals in terms of amounts and timing of ET and nutrient uptake requires simulation of how growth processes vary seasonally, over the crop lifecycle, and in response to coppicing management. Alterations were made to the model code to enable the model to simulate variation in growth rate and C partitioning following coppice event. These changes theoretically give improved representation given the observed differences in tree growth following coppicing, but are reliant on use of appropriate values for the new parameters in the **tree.100** file. Since the model had not previously been applied for SRC willow, it was also necessary to adjust parameters in the **tree.100** file to better represent growth of SRC willow, using values from previous studies where available, and default or fitted values for the remaining parameters.

The updated model appeared better able to simulate the observed pattern of growth over the coppice cycle, and the updated parameters in the tree.100 file gave significantly improved yield prediction compared to defaults. The updated model parameters give improved representation of the relationship between simulated soil N and SRC willow growth, but this does not resolve simulation of soil N in terms of N cycling, leaching, gaseous emissions or soil response to crop uptake.

In terms of crop growth simulation, latitude and soil water availability are the most important site factors to be considered: the calibration datasets span a range of latitudes from 51 to 55 degrees North and available water capacity varies from 152 to 73 mm. Based on model performance over this range of sites, no limitations in representing yield under certain conditions were identified. Calibration focussed on fitting parameters in the **tree.100** and **trem.100** files, as well as altering presence or absence of water table to ensure model output for WFPS was in line with field observations on soil moisture status. For scenario analysis, such as application of the model to the "typical sites" identified in Chapter 2, there are no field data to match simulated WFPS to, so as was stated of N_2O emissions in Section 4.6, conclusions drawn about potential yield will only hold for sites where WFPS is in the range simulated by the model.

6. Scenario Development and Model output

Chapter 6 meets Objective 4; "For simulated cultivation of *Miscanthus* and SRC willow, assess spatial variation in: yield; N_2O emissions; soil C storage; evapotranspiration". The objective is met by performing scenario analysis for land use change to perennial energy crops at 12 sites typical of those identified as suitable for cultivation in Chapter 2, and comparing model output between these sites.

The first step was to select specific sites where common combinations of site properties occur, using the spatial database produced from the two-step cluster analysis in Section 2.10. Section 6.1 details the processing of this database to select representative "typical sites" at which to perform scenario analysis using the DayCent model. Chapter 6 does not consider the end use, or distance from end use- these were covered in Chapter 2, and will be discussed further in Chapter 7.

The DayCent model applied in this chapter was identified as suitable in Chapter 3 and developed to give improved representation in Chapters 4 and 5. Improvements made in Chapter 4 enable the model to simulate impacts of change in tillage regime on WFPS, where the previous version only simulated the effect on decomposition rates. This change should enable improved simulation of N_2O emissions. Improvements made to the DayCent model in Chapter 5 gave improved yield prediction for SRC managed SRC willow; in addition to enabling improved yield prediction in the scenario analysis, the improved simulation of crop growth should in turn enable improved representation of transfers of water and nutrients between plant and soil.

Section 6.1 describes the site selection process, and includes data on site locations, soil properties and precipitation. Section 6.2 then details how the improved model was applied at the identified sites, including preparation of input data for modelling, and how the model was run. The description includes details on how input files for the DayCent model were produced from the database and available historic local weather data, and points to information from the literature used to generate the cultivation schedule for *Miscanthus* and SRC willow. Once input data files have been produced, model running is relatively simple, so description of this stage is brief.

Section 6.3 explores model output, to address Objective 4; “For simulated cultivation of *Miscanthus* and SRC willow, assess spatial variation in: yield; N_2O emissions; soil C storage; evapotranspiration”. Analysis aims to identify some of the factors which may influence simulated spatial variation in the benefits of land use change for bioenergy. Section 6.4 will then draw these findings together, to answer the question; what is the variation in identified impacts of land use change for bioenergy at these sites? And consider the extent to which these findings may be extrapolated to sites with similar soil properties and precipitation regimes. Finally, Section 6.5 identifies limitations in the model and the approach taken which could be addressed in future research.

6.1 Site data for scenario analysis

Chapter 2 identified which of the locations identified as potentially suitable for *Miscanthus* cultivation by Lovett *et al.* (2009) were sufficiently close to appropriate energy end uses to be useful for energy crop cultivation. Given that both energy crop yield and the impacts of land use change are controlled by complex interaction of site factors, it is useful to perform modelling analysis for common combinations of site properties. A database of potential sites with latitude and longitude as well as soil properties, hydrological regime and precipitation was produced for the suitable locations, and cluster analysis used to identify common combinations of site properties, which were compiled in Tables 2.9 and 2.10.

These “typical sites” are intended to be representative in terms of the identified properties considered to be important controls of the impacts of land use change; topsoil and subsoil texture and packing density, hydrological regime and depth to gleyed horizon. As well as these site properties, the model requires latitude and local weather data, hence it was necessary to select specific locations from the database, in order to produce the required input files for the DayCent model. However, categories of precipitation which will be used to select sites are necessarily broad, to limit the number of modelled sites to fit with time constraints. Temperature and latitude are also key drivers of crop growth, which were not taken into account when identifying typical sites for practical reasons, but must be considered when analysing and extrapolating from findings.

The complete dataset of potential cultivation sites from Chapter 2 was filtered using the typical combinations of site properties identified in Section 2.10, listed in Table 2.9 and Table 2.10. This was done for each of the six typical combinations in turn, to produce six separate spreadsheets of all locations where this typical combination of properties is expressed. Given the importance of precipitation as a crop growth driver, each spreadsheet was then split into higher precipitation (greater than 75 cm per year) and lower precipitation (less than 75 cm per year) to give a total of 12 spreadsheets. The threshold was set at 75 cm because this was roughly the median precipitation of the sites in the database. One site was then selected at random from each spreadsheet, and the 12 chosen sites are mapped in Figure 6.1 and listed in Table 6.1.

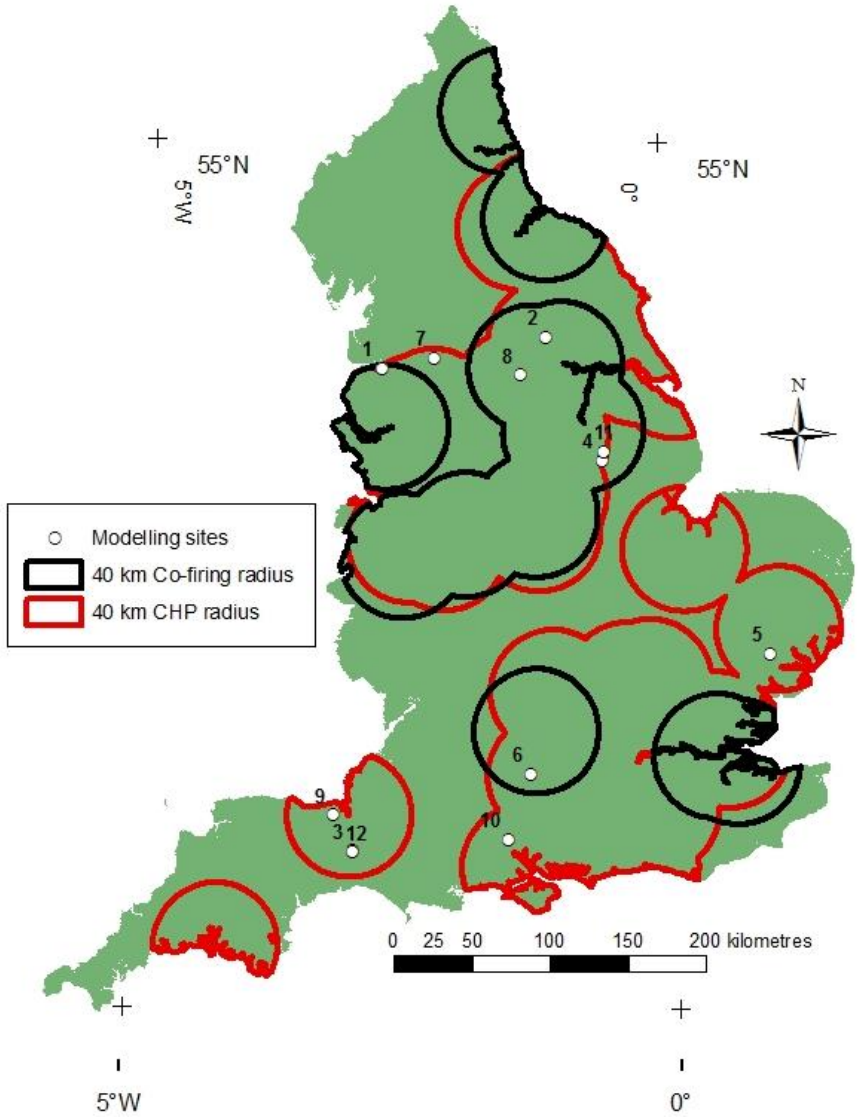

Figure 6.1 Locations of sites selected for scenario analysis, shown in relation to the 40km transport radii for feedstock end uses identified in Chapter 2

Table 6.1 Site data for model scenario locations

Site number	Annual total precipitation	pH	Topsoil texture	Topsoil packing density	Subsoil texture	Subsoil packing density	Depth to textural change	Depth to gleyed horizon	Water regime	Existing land use
1	1037	5-6	Medium	Low	Fine	High	20-40 cm	< 40 cm	Wet within 40 cm depth for over 11 months	Arable and horticulture
2	605									
3	1056	5-6	Fine	Medium	Fine	High	> 120 cm	< 40 cm	Wet within 80 cm for over 6 months, but not wet within 40 cm for over 11 months	
4	560									
5	543	6-7	Coarse	Medium	Medium	Medium	40-60 cm	> 120 cm	Not wet within 80 cm for over 3 months, nor wet within 40 cm for over 1 month	
6	837									
7	1445	5-6	Medium	Low	Fine	High	> 120 cm	< 40 cm	Wet within 40 cm depth for over 11 months	Grassland
8	687									
9	1172	6-7	Medium	Medium	Medium	Medium	> 120 cm	> 120 cm	Not wet within 80 cm for over 3 months, nor wet within 40 cm for over 1 month	
10	736									
11	570	5-6	Fine	Medium	Fine	High	> 120 cm	< 40 cm	Wet within 80 cm for over 6 months, but not wet within 40 cm for over 11 months	
12	1056									

Where textural compositions are;

Medium= (18% < clay < 35% and >= 15% sand, or 18% <clay and 15% < sand < 65%)
Fine = (35% < clay < 60%)
Coarse= (18% < clay and > 65% sand

6.2 Producing input files and running the model

As described in Section 3.7, the model runs by reading in values from formatted text files, some of which contain defaults, or pertain to specific event types, which should not be altered, except as part of parameterisation work, such as that performed in Chapter 5. In addition to these, in order to run for a specific scenario, the DayCent model requires data on site specific properties. For each scenario analysis, changes to two of the default input files were required, and three new input files had to be produced; these are detailed in Table 6.2.

Table 6.2 DayCent input files with input variables to be altered for scenario analyses; where the name of the input file is specific to the relevant scenario, the file ending only is given here. For the bottom two cases, the model requires the given file name and ending.

Input file	File name	Key input variables
Daily weather data file	*.wth*	Precipitation, maximum temperature, minimum temperature
Site file	*.100*	Monthly weather data: this section can be populated automatically, using the ancillary tools provided with the model to extract averages from the weather data file. Site data: Latitude and Longitude, soil textural composition, bulk density and pH.
Schedule file	*.sch*	Dates of all events to be simulated: Previous land use (start and end dates, management activity dates). Energy crop planting, coppicing or harvesting management dates, as well as first and last growth days for each year of SRC willow, and senescence dates for each year of *Miscanthus*
Default site properties file	*site.in*	Edited to simulate presence or absence of water table for months 1-12.
Soil properties file	*soil.in*	Properties of texture, field capacity, wilting point, bulk density, hydraulic conductivity and pH for each layer, varying with depth to represent the soil profile

Weather data were accumulated from the British Atmospheric Data Centre (Met Office) using data from the nearest Met Office station with the required daily values of maximum and minimum temperature and total precipitation. Data were accumulated for the period 1980 to 2000, using multiple Met Office sites where necessary to fill gaps in the data. Ideally, weather input data for DayCent would include solar radiation flux, relative humidity, and wind speed, to enable improved calculation of potential ET, however the model can be run using only precipitation, minimum and maximum temperature. Due to difficulty in obtaining the additional weather parameters at the required daily scale, the decision was taken to run the model using only precipitation, minimum and maximum temperature.

Since the soil data originally compiled in Chapter 2 were supplied in the form of a range, site files were produced for each of the 12 sites (labelled 1 to 12) from section 6.1.1 according to the maximum and minimum of the textural range (used to create an error bar in output graphs, accounting for uncertainty in soil input data). Bulk density was based on the expected value for the given soil texture according to Saxton *et al.* (1986), adjusted where necessary to account for high or low packing density values for that site.

Soil input files, given in Appendix 4.1, were produced from these site files using an ancillary program which was distributed with DayCent (The program is called file.100 and is included on the attached data stick). The JRC soil data includes separate values of texture and packing density for topsoil and subsoil, and a value for the depth to textural change. Therefore the tool was run twice to produce a soil input file for topsoil, then subsoil, and the two were combined to create a soil profile with two sections, accounting for change in properties with depth. All 24 soil profiles (maximum and minimum for each of the 12 sites) are included in the appendix Section 4.1.

Values for hydrological regime were used to decide whether a water table should be simulated; where wet soil was indicated, a water table was simulated for the appropriate portion of the year in the default site properties input file. For months where presence of water table is simulated, water is allowed to flow up into the soil profile from the deep storage layer. Values were converted as follows;

Wet within 40 cm depth for over 11 months; Water table simulated for 12 months of the year

Wet within 80 cm for over 6 months, but not wet within 40 cm for over 11 months; Water table simulated for 6 months of the year

Not wet within 80 cm for over 3 months, nor wet within 40 cm for over 1 month; Water table simulated for 0 months of the year

Schedule files were produced to simulate previous land use, land use change to the relevant energy crop, and multiple cycles of that energy crop. The full schedule files are included on the attached cd. The schedule file must include a spin up period to account for the impact of previous land use on site properties such as soil C and N. Around 2000 years is recommended, in the form

of 1800 years of native vegetation and 200 years of current cropping management (Adler, 2007). Therefore the schedule files begin at year 0014, with land forested until 1813, followed by 200 years of either grazing or arable use, depending on the current land use at the site. As previously stated, this is not likely to be a realistic representation of the land use history of the site, but is based on the recommended approach to setting soil C pools prior to a model run. Grassland was simulated using timings of activities taken from a distributed schedule file, no inputs were simulated, since improved grassland was ruled out at the constraints mapping stage, and a no-till management was assumed, although grasslands may be ploughed every few years and still defined as permanent pasture. Grassland sites simulated will include calcerous, acid and neutral, however since these types cannot be distinguished in the 1km resolution land cover data, there will be no distinction in the input data, and it is assumed that the pH values based on JRC soil layer data will account for the differences. The impacts of this variation in pH on SOM turnover are accounted for in DayCent pH using an arctangent function to calculate a decomposition rate modifier. Grassland sites selected based on cluster analysis were either acid, with pH 5-6, or neutral, with pH 6-7 as these conditions were most commonly occurring for grassland sites identified by spatial analysis in Chapter 2. Arable land management was simulated as a wheat and oilseed rape crop rotation, with scheduling of events based on information from the UK Agriculture website calendars for wheat (UK Agriculture, 2010b) and oilseed rape (UK Agriculture, 2010a) respectively. The simulation of either arable or grassland management before the energy crop is intended to set a baseline starting point for the scenario analysis.

The 20 years of weather data were looped for the entire spin up period. In order for the first energy crop lifecycle to be directly comparable to the previous time period, the weather data file was restarted from the year 1980 both at the start of the energy crop lifecycle in 2014, and exactly one lifecycle prior to the simulated land use change. Dates shown in the analysis are used simply to show the passage of time in a virtual experiment; weather data used are not intended to be representative of the time period stated.

The schedule file for tillage management was written according to Finch *et al.* (2009), who state that site preparation for planting of energy crops is likely to use the same equipment and be of similar intensity to traditional arable management, with ploughing operations performed the autumn prior to planting, and the field left bare over winter to aid breakdown. Since freeze thaw is not simulated a second tillage operation was scheduled prior to planting.

Scheduling data for SRC willow were produced as in Section 5.4.1; according to planting dates from Forestry Commission site data, and dates for first and last growth from Martin and Stephens (2006). For the *Miscanthus* schedule file, it is not necessary to stipulate first and last days of growth, however a value for SENM must be specified, and this is used to initiate simulation of stem senescence. Detailed study of green stem area by Finch *et al.* (2004) identified senescence from the start of August, so a value of (Julian day) 213 was used. Timing of harvests and scheduling of management was simulated according to guidance from DEFRA (2007) with no harvest in the first year due to low production during establishment, and annual harvesting on March first thereafter. Images of harvesting and planting equipment are included in the visual glossary; additional settling was simulated in an attempt to account for the compacting impact of this heavy machinery, in the absence of more appropriate specific equations.

At the end of the energy crop lifecycle, removal was simulated based on recommendations by Finch *et al.* (2009). For *Miscanthus*, a single herbicide application is usually sufficient, although it usually takes two years for complete removal, hence herbicide application was scheduled after the final harvest, in Spring 2034 and ploughing in of the residues; ploughing was performed again before the next rotation in 2035 to incorporate *Miscanthus* regrowth and weeds which are likely to spring up during the fallow period.

For SRC willow, removal options for a mature plantation include complete removal of stumps and roots, mulching in of stumps and roots down to 90cm using a modified peat cutter, both of which require specialised machinery and may damage soil structure and lead to erosion, or stump removal with planting of a cover or fodder crop (Finch *et al.*, 2009; Mitchell *et al.*, 1999). In order to avoid damage to soil structure, and minimise the economic and soil losses of a fallow year, cover cropping is likely to be preferred, hence the approach simulated clear cutting after the final harvest in 2040, shortly followed by growth of a fodder crop in 2041, which was partially harvested, and the remainder ploughed in at the end of 2041.

The model was run for multiple lifecycles of the new energy crop to assess model simulation of long term trends in soil C, and to enable consideration of the level at which dynamic equilibrium is reached, and what factors might affect this.

The standard process of running the model was described in greater detail in Section 3.7, and will not be repeated here. In brief: to run the model for the scenario sites, it was necessary to make sure that command prompt was pointing to the folder containing the model and ancillary files as detailed in Table 6.2. For each run, it was then necessary to set the default site properties file to simulate a water table for a number of months appropriate to the hydrological regime, and to populate the soil input file with the correct soil profile values.

For several of the sites, the model produced an error message during the first year of the run, indicating an NO_3 calculation error. This error message was generated by well drained sites due to rapid leaching causing the model to calculate negative NO_3. Hence for site 3 no output was generated, and only one set of output was generated for sites 9 and 10 (meaning that there is no output range for these sites).

6.3 Output analysis

The DayCent model produces multiple output files, although some of these are optional, for the purpose of this exercise, the full complement were generated in case they were required for later analysis. Assessment of sustainability of perennial energy crop cultivation in Section 1.4 identified potentially significant impacts on soil carbon storage (Section 1.4.1), N_2O emissions (Section 1.4.2), leaching of nitrates and associated indirect N_2O emissions (Section 1.4.3) and hydrology (Section 1.4.4).

Table 6.3 Variables of interest and their containing model output files

Variable	Output file	Variable name
Yield	dc_sip.csv	*Miscanthus*=aglivc+ stdedc Willow= fbrchc + rlwodc + wood1c + wood2c
Direct N_2O emissions	nflux.out	nit_N2O-N + dnit_N2O-N
Indirect N_2O emissions	Extracted from .bin using the list.100 executable file	(strmac(4) + strmac(8))0.025 ((IPCC indirect EF Groffman *et al.*, 2000)
Soil carbon	dc_sip.csv	strucc(1)+ metabc(1)+ strucc(2)+ metabc(2)+ som1c(1)+ som1c(2)+ som2c(1)+ som2c(2)+ som3c
Evapotranspiration and interception	waterbal.out	Intrcpt + evap + transp

Therefore output on soil C, N_2O emissions, leaching and evapotranspiration must be analysed to assess and compare these impacts. Model output for yield must also be considered due to impacts on the area of land use change required per unit of energy generation. The output files containing variables of interest are listed in Table 6.3. The output from the scenario modelling will be analysed to identify patterns, and consider what conclusions can be drawn from the findings in terms of spatial variation in benefits of bioenergy cultivation. This analysis aims to address Objective 4, to "assess spatial variation in: yield; N_2O emissions; soil C storage; evapotranspiration", and to consider how this would affect the benefits of bioenergy.

Section 6.3 assesses simulated values of yield, N_2O emissions, SOC storage and ET for all of the identified sites. It was first necessary to compare predicted values of yield, ET, N_2O and soil C to published data to check for systematic model errors. Further analysis considers site variation in yields and the identified environmental impacts, as well as looking for informative trends in model output.

Given the expectation that interaction between input variables will be a significant control on the outputs of interest, it is not appropriate to perform multiple regression analysis to look for a predictive relationship between input and output. Instead, correlation analysis will be used to consider controlling factors, through Pearson correlation coefficient. The discussion focusses on site factors which may be expected to cause positive or negative outcomes if the simulated land use change were to take place, and the extent to which findings may be extrapolated to other sites with the same soil properties and hydrological regime. This assessment may be limited by the relatively small number of data points.

Section 6.4 then looks at interactions between model outputs to identify where land use change would have the best outcomes in terms of emissions per unit energy generation.

6.3.1 Yield

Figure 6.2 shows *Miscanthus* yield over the seven complete energy crop lifecycles. Predicted values at all sites were unrealistically high for the first harvest of each cycle, resulting in an averaged value of nearly 20 odt ha^{-1} for year one in Figure 6.2. As described in Section 6.2, the

first year of *Miscanthus* growth is only around 2 odt ha^{-1}, and is not usually harvested, meaning that the first harvest accounts for two years of growth. The model is unable to simulate slower growth and different biomass partitioning during establishment when simulating perennial non-tree crops, and therefore overestimates growth during this period. Future work to develop the model to apply different growth parameters at different stages in the lifecycle, similar to the simulation of tree growth, as discussed for SRC willow in Chapter 5, could correct this issue. Simulation of excessive growth during establishment may result in oversimulation of N uptake, although since field studies have observed uptake of most available N during this period (Dufossé *et al.*, 2012), this is not a significant concern. Overestimation of establishment yield for *Miscanthus* will not, in itself, be discussed further, although it is important to consider knock on effects on simulation of water use during this period.

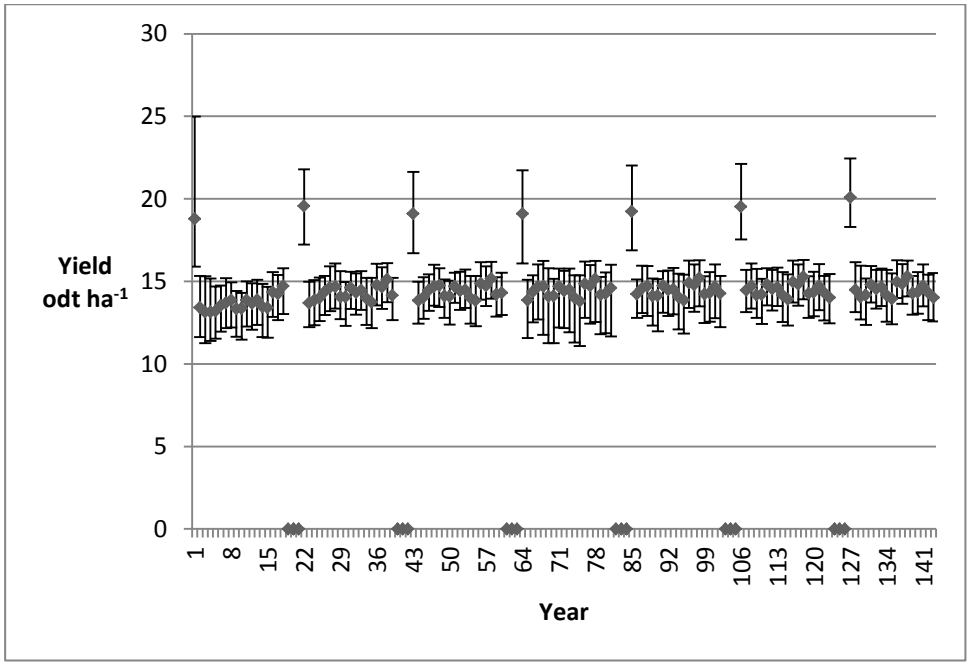

Figure 6.2 Annual Miscanthus yields over seven Miscanthus lifecycles, as simulated by DayCent, beginning with the first harvested yield, averaged across all of the modelled sites. Error bars indicate maximum and minimum values for that year. Years with zero yields indicate years between Miscanthus cycles.

Miscanthus field studies (e.g. Christian *et al.*, 2008b) have observed increase in yield up to 14 harvests, followed by falling yields. Modelled annual yields showed variation between years, which would be expected with inter-annual weather variation, and a general trend of slight increase over the first growing cycle (18 harvests), as can be seen from Figure 6.2. It has been suggested that the decline in *Miscanthus* productivity in later years occurs due to increasing space taken up by unproductive rhizome (Christian *et al.*, 2008a; Don *et al.*, 2012). DayCent could not represent this explicitly, since crop architecture is not simulated, however development to apply

different growth parameters at different stages in the lifecycle would enable the model to represent this trend. Figure 6.2 indicates that simulated yields were not reduced over seven *Miscanthus* lifecycles, indicating either that soils did not become N deficient, or that the model does not simulate any impact on yield from soil N depletion.

Figure 6.2 shows averaged yields ranging from 11.6 - 15.3 odt ha^{-1} following the first harvest. The raw yield data for all sites in the first cycle ranged from 11.26 - 15.80 odt ha^{-1}. These values seem reasonable compared to field data, for example Christian *et al.* (2008a) recorded yields from 10.53 - 16.94 odt ha^{-1} dry matter for unfertilised *Miscanthus* over 14 years on silty clay loam. However, from Table 6.4 it can be seen that DayCent predictions are often outside the range predicted by Lovett *et al.* (2009) for that specific location, although there is no consistent pattern of over or under estimation. Predicted yield values mapped in the Lovett *et al.* study (2009) were based on an empirical relationship formulated by Richter *et al.* (2008) according to relationships between yield, crop age, weather variables and soil available water capacity. Richter *et al.* (2008) reported model root mean square error (RMSE) of 1.38, and r^2 0.51 odt ha^{-1} , and their plot of modelled against measured yields indicated up to +/- 6 odt ha^{-1} error for individual sites. Therefore although simulated yields produced by DayCent were up to -2.18 or +1.56 outside of the range published in Lovett *et al.* (2009) they fall within that error margin, and may still be considered reasonable predictions.

Calibration of DayCent for modelling *Miscanthus* was not performed as part of this study; crop.100 values were provided by Sarah Davis, as calculated in the Davis *et al*. (2010) study. Davis *et al*. (2010) parameterised the model using data from European and US field trials, and the model showed good performance in calibration (Davis *et al*. 2010) and validation (Davis *et al.*, 2012) both against US field data.

Figure 6.3 indicates that for the first complete SRC willow lifecycle, DayCent simulated harvests which, averaged across all modelled sites, ranged from 14.7 - 29.5 odt ha^{-1}. Simulated values were lower for the first harvest, ranging from 4.79 - 33.12 odt ha^{-1}, producing an average of around 15 odt ha^{-1} across all modelled sites, which reflects higher allocation of new growth below ground and less root mass for uptake of water and nutrients. Defra state that first harvest will range from 21-36 odt ha^{-1} which could suggest establishment yields are underestimated at some sites (Hilton, 2002). However in the field dataset used in model calibration establishment year yields were as

low as 2.16 odt ha^{-1}. The average simulated SRC willow yield over all sites for the first cycle, excluding establishment yield, was 26.8, which falls within the range of genotype averages from 21.15 - 32.1 modelled elsewhere by Aylott *et al.* (2008).

Table 6.4 Average annual yield as simulated by DayCent, compared to predicted yields at that site taken from the Lovett et al. study (2009). "Difference" denotes how far outside of the range given by Lovett et al. (2009) the values simulated by DayCent fall. Note that sites 9 and 10 are based only on the minimum of the texture range, due to model errors for the maximum.

Site	**Predicted average annual *Miscanthus* yield odt ha^{-1} a^{-1}**		
	(Lovett *et al.*, 2009)	**DayCent**	**Difference**
1	13-14.9	13.8-13.9	-0.08
2	15 or greater	14.0-14.2	-1.85
4	9-12.9	12.0-12.2	1.16
5	15 or greater	13.4-13.6	2.59
6	9-12.9	13.5-13.7	-2.38
7	15 or greater	14.1	3.19
8	15 or greater	14.5-14.6	-1.43
9	15 or greater	14.7	-1.34
10	9-12.9	14.1	3.15
11	13-14.9	12.5-12.7	-1.34

Chapter 5 calibrated and validated DayCent for simulation of SRC willow yield over the first two coppice cycles, however field data were not available to verify model performance over subsequent cycles. The expected trend of increasing yield until the trees are 14 years old (4 or 5 harvests) identified by Pacaldo *et al.* (2012) was observed in calibration model runs, and is also simulated for these scenario analysis sites, as can be seen in Figure 6.4. Since the field dataset only covers the first two rotations, average yields from the model output for the full crop lifecycle may be expected to be higher than those observed in the field. Analysis of longer term model performance in Section 5.4 compared to literature values suggested that above ground growth rates are well simulated, at the expense of accurate representation of below ground growth rates. Poor simulation of below ground growth rates is likely to affect simulation of N, C, and water, as will be discussed in Sections 6.3.2, 6.3.3 and 6.3.4 respectively.

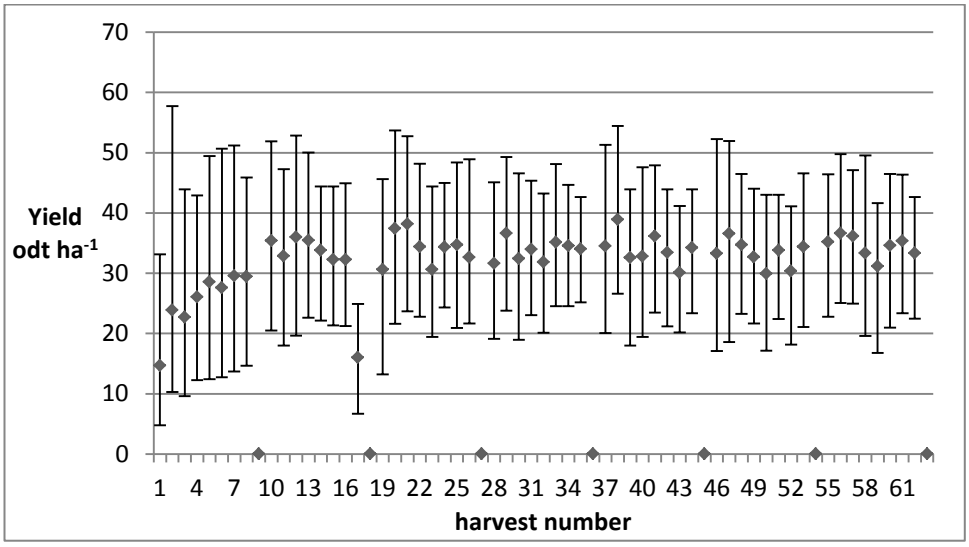

Figure 6.3 SRC willow yields over seven SRC willow cycles, with harvest simulated every three years. Yield was simulated by DayCent for each harvest, and is plotted here averaged across all of the modelled sites, beginning with the first harvested yield. Error bars indicate maximum and minimum values for that year. Years with zero yields indicate years between willow cycles.

Looking at longer term SRC willow yields in Figure 6.3, predicted values are much higher for subsequent rotations, and these do not include an establishment period (i.e. low yielding first harvest). This is likely caused by a modelling error; establishment growth partitioning is not applied in subsequent rotations, because the age of the tree is not reset. This limitation means that the model cannot currently be used to predict yields during subsequent rotations. This is due to the model not re-reading the input file and resetting the values when the same tree is grown in two consecutive periods; minor modification of the code should enable the age of the tree to be reset following replanting. This simulation issue may affect longer term simulation of soil C cycling, as will be discussed in Section 6.3.3.

Table 6.5 Comparison of DayCent simulated values of SRC willow and Miscanthus yield per year for all modelled sites, with descriptive statistics. SRC willow yields tabulated here are calculated as harvest/3 since a three year rotation was simulated.

Site	Predicted average *Miscanthus* yield odt ha^{-1} a^{-1}	Predicted average SRC willow yield odt ha^{-1} a^{-1}
1+	13.92	8.63
1-	13.82	8.38
2+	14.23	9.18
2-	14.08	8.70
4+	12.24	4.51
4-	11.98	5.17
5+	13.44	4.48
5-	13.63	4.30
6+	13.55	5.70
6-	13.70	5.36
7+	14.13	14.25
7-	14.14	14.29
8+	14.50	14.59
8-	14.64	15.73
9-	14.66	9.55
10-	14.10	8.98
11+	12.55	9.23
11-	12.68	9.91
Mean	13.67	8.94
Maximum	14.66	15.73
Minimum	11.98	4.30
Range	2.68	11.43
Standard deviation	0.78	3.62

Although per harvest SRC willow yields are higher than those predicted for *Miscanthus* (as can be seen from comparison of Figures 6.2 and 6.3), since harvesting interval is longer for SRC willow, yields per year are generally lower, as can be seen from Table 6.5. Variations in energy density, harvesting energy expenditure, processing and transport should also be considered when comparing the relative benefits of SRC willow or *Miscanthus*.

Table 6.5. indicates much greater variation in simulated yield for SRC willow than *Miscanthus*; maximum annualised yield values for SRC willow are higher than for *Miscanthus*, whilst minimum annualised yield values for SRC willow are much lower than for *Miscanthus*. This is in line with modelling by Hastings (2014) for the UK, which simulated higher yield for *Miscanthus* in most regions, but higher yields for SRC willow at lower temperatures. Sites where Lovett *et al.* (2009)

indicated yields below the economic threshold for *Miscanthus* were ruled out in Section 2.5, which explains why very low yields for *Miscanthus* were not simulated for any sites in this study; modelling could be performed for sites with low *Miscanthus* yield to assess whether economically feasible yields could be achieved for SRC willow.

Simulated SRC willow yields were lower on land formerly in arable usage (sites 1-6), where they did not reach 10 odt ha^{-1} a^{-1}. Bullard *et al.* (2002) note that the suggested economic threshold of 10-12 odt ha^{-1} a^{-1} may not be achieved without amendments, hence it may be worthwhile to run the model to assess whether viable yields would be simulated with the addition of fertiliser or irrigation amendments at these sites.

Although low simulated SRC willow yields at former arable sites appear to suggest this land use change may not be profitable or productive, good yields have been observed in field trials on former arable land, for example the Centre for Ecology and Hydrology field site in Lincolnshire used for model validation in Sections 5.4.3 and 5.4.4 produced a yield of 10 odt ha^{-1} a^{-1} for the second harvest; similar to the maximum simulated here for the former arable sites. Tendency for lower SRC willow yields on former arable sites, by around 1 odt ha^{-1} a^{-1} compared to former grassland or setaside sites was also noted by Aylott *et al.* (2008). To identify why the model simulates much higher yields for former grassland, it is first necessary to explore how other model outputs are affected by previous land use, therefore this will be discussed in Section 6.5.

Modelled SRC willow yields averaged by site range from 12.90 to 47.19 odt ha^{-1} per harvest; well within the 2.16 to 51.15 odt ha^{-1} per harvest recorded in the forestry commission field trials for the genotypes used for model parameterisation. However, for some harvests, yields as high as 58 odt ha^{-1} were simulated for sites 7 and 8, exceeding measured values from the study dataset for the UK, and maximum expected yields quoted by Defra of around 36 odt ha^{-1} per harvest (12 odt ha^{-1} a^{-1}) (Hilton, 2002), although they are within estimates for the UK in (Hastings *et al.*, 2014).

Converting yields simulated by DayCent into energy generation potential gives a range of 61.1 - 74.7 GJ ha^{-1} a^{-1} for *Miscanthus*, and 25.0 – 91.5 GJ ha^{-1} a^{-1} for SRC willow; assuming energy densities of 17 GJ odt^{-1} for *Miscanthus* (Department for Environment Food and Rural Affairs, 2007) and 19.4 GJ odt^{-1} for SRC willow (Volk and Luzadis, 2008) and a conversion efficiency of 30% as

co-firing with coal (Berndes *et al.*, 2010). For a more complete assessment, variation in energy inputs for cultivation, processing and transport should also be considered when comparing energy yield per area between SRC willow and *Miscanthus*.

Other factors which may affect farm yields, for example pests and diseases and altitude (Aylott *et al.*, 2008) are not modelled by DayCent. Additionally, significant variation in yields may be observed at field and landscape scales due to non-homogeneity of soil properties, and interaction with topographic factors controlling water flows (Richter *et al.* 2008). Aylott *et al.* (2008) note that in practice, field trial yields are unlikely to be replicated at commercial scale due, where management approaches may be less stringent and scientific. This may not mean that projected values based on field trials cannot be achieved, since improvements in crop varieties may balance out the discrepancy.

Table 6.6 Statistically significant correlations between yield and input variables

	***Miscanthus* Yield**		**SRC Yield**	
	Correlation Coefficient	**Significance (2-tailed)**	**Correlation Coefficient**	**Significance (2-tailed)**
Topsoil clay %	-.577	.012	-.084	.740
Subsoil available water capacity	.118	.642	.490	.039
Months with water table	.397	.103	.554	.017
Annual precipitation	.651	.003	.391	.109
Average temperature	.597	.009	.176	.485
Average maximum temperature	.656	.003	.260	.297
Average minimum temperature	-.443	.066	-.528	.024

Table 6.6 shows statistically significant correlations between yield and various data inputs. Although Richter *et al.* (2008) suggest that *Miscanthus* yield varies with available water capacity (AWC) not precipitation, as previously suggested by Heaton *et al.* (2004); Table 6.6 indicates a positive relationship between precipitation and yield for *Miscanthus*, whilst the relationship with AWC was not statistically significant. *Miscanthus* yield showed statistically significant positive correlations with average temperature and average maximum temperature. A statistically significant negative correlation was simulated between *Miscanthus* yield and topsoil clay percentage, this is presumably due to better infiltration into soils with lower clay content, leading to increased water availability.

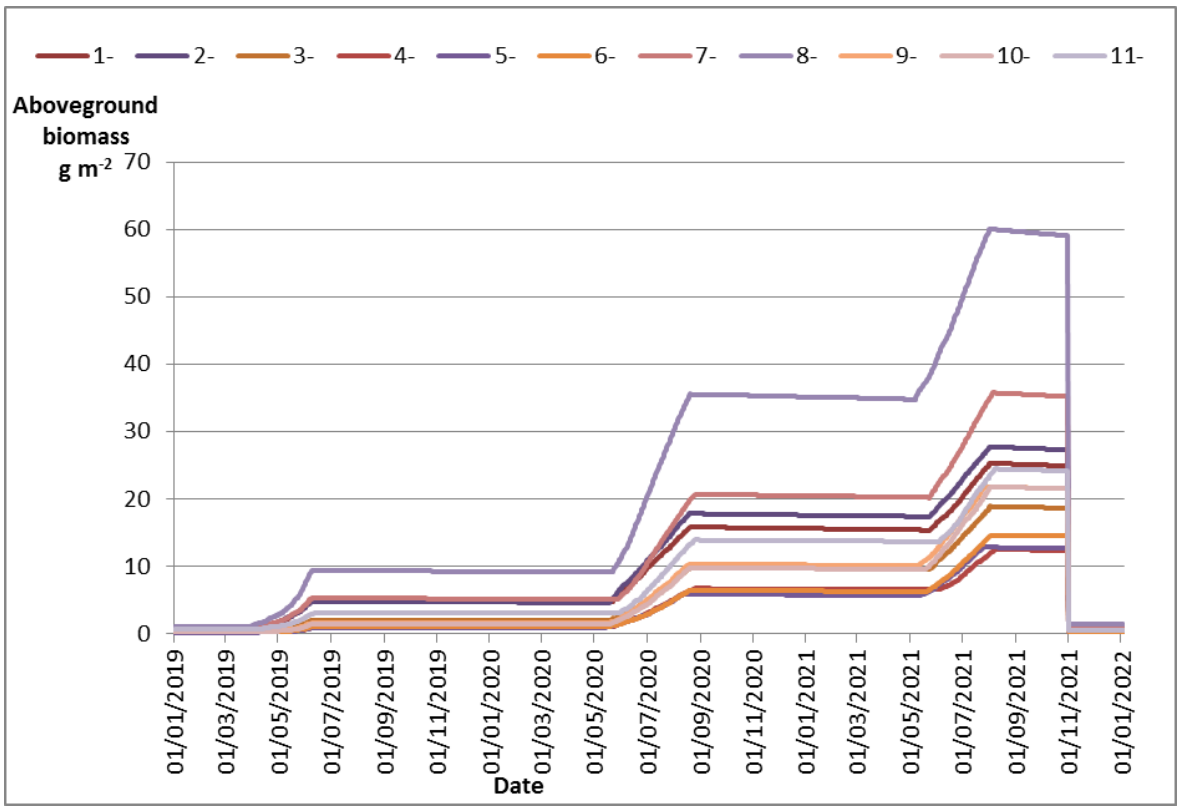

Figure 6.4 Graph of above ground carbon for one three year SRC willow rotation at half of the model sites (-VE) for the purpose of illustrating variation in start and end times of growth.

Willow showed positive correlation with both subsoil available water capacity and duration of water table, as would be expected from a crop with significant water demand, although the correlation with precipitation was not statistically significant. Willow yield shows a negative correlation with minimum temperature, which may indicate that the parameter to limit length of growing season ('FURGDYS' as mentioned in Table 5.3 of Chapter 5) should be more flexible. Examining time series above ground carbon for different sites in Figure 6.4, it can be seen that some sites (i.e. those with lower latitude and higher winter temperatures) begin growth earlier in the year, hence when simulated growth is curtailed at the end of a set number of days, this artificially limits yield.

Table 6.6 also shows a negative correlation between *Miscanthus* yield and minimum temperatures (although this trend is not statistically significant) suggesting that simulation of *Miscanthus* growth may suffer a similar issue. DayCent was calibrated for *Miscanthus* by Davis *et al.* (2010) using data from a trial in Illinois (published in Heaton *et al.*, 2008) where temperature

range is greater than the UK and average temperatures over winter months are often between -1 and -5°C, thus parameters may not describe growth as well for UK temperature regimes.

Both energy crops appear to produce higher yields at sites with greater water availability, although they differ in terms of the specific model inputs which are correlated with higher yields. Statistically significant correlations with temperature variables for yield of both *Miscanthus* and SRC willow mean that similar yield may not be simulated for other sites with the same soil properties and similar total precipitation.

6.3.2 N_2O emissions

Table 6.7 Average direct N_2O emissions over one crop lifecycle. Figures are also shown for averages excluding the planting and removal period, for purposes of comparison to the literature.

	Average direct N_2O emissions over one crop lifecycle kg N_2O-N $ha^{-1}a^{-1}$			
Site label	***Miscanthus* (full lifecycle; averaged over 21 years)**	***Miscanthus* (without planting and removal; averaged over 19 years)**	**Willow (full lifecycle; averaged over 27 years)**	**Willow (without planting and removal; averaged over 24 years)**
1+	1.49	0.96	2.26	0.92
1-	1.82	0.99	2.38	1.20
2+	1.50	0.92	2.04	0.87
2-	2.05	1.13	2.05	1.08
4+	0.51	0.25	0.59	0.34
4-	0.42	0.22	0.76	0.37
5+	0.46	0.30	0.43	0.27
5-	0.34	0.19	0.30	0.19
6+	0.67	0.42	0.56	0.41
6-	0.31	0.17	0.29	0.20
7+	2.72	1.94	3.03	2.19
7-	2.79	1.91	2.81	2.12
8+	2.01	0.94	1.95	1.27
8-	2.29	1.58	2.42	1.84
9-	1.29	0.94	1.36	1.05
10-	1.03	0.75	1.06	0.94
11+	0.70	0.41	0.73	0.62
11-	0.69	0.45	0.92	0.69
Maximum	2.79	1.94	3.03	2.19
Minimum	0.31	0.17	0.29	0.19
Range	2.47	1.77	2.74	2.00
Standard deviation	0.81	0.55	0.90	0.61

Table 6.7 shows that average annual emissions for the established energy crop (i.e. excluding the period following planting and removal) are 0.17 - 1.94 kg N_2O-N ha^{-1} a^{-1} for *Miscanthus* and 0.19 - 2.19 kg N_2O-N ha^{-1} a^{-1} for SRC willow. Values are higher where establishment and removal periods were included in the averaged time period, however available field data were mostly collected from established crops, and there is a shortage of data on the impacts of removal, hence values based on the full period are less useful for comparison. Figures for *Miscanthus* compare reasonably to values published in the literature, for example Behnke *et al.* (2012) measured 0.73

kg N_2O-N ha^{-1} a^{-1} for unfertilised *Miscanthus*, Roth *et al.* (2013) measured 0.37 kg N_2O-N ha^{-1} a^{-1} for established *Miscanthus* and 0.61 kg N_2O-N ha^{-1} a^{-1} for recently planted *Miscanthus*, and Drewer *et al.* (2012) measured 0.32 kg N_2O-N ha^{-1} a^{-1} from established *Miscanthus*, whilst Dufossé *et al.* (2012) modelled 0.4 kg N_2O-N ha^{-1} a^{-1} for unfertilised *Miscanthus*. Figures for SRC willow also compare reasonably to values published in the literature, for example Balasus *et al.* (2012) measured 0.7 kg N_2O-N ha^{-1} a^{-1} for newly planted SRC willow and Drewer *et al.* (2012) measured 0.017kg N_2O-N ha^{-1} a^{-1} from established SRC willow. The lower end of modelled values are in range of these literature values for unfertilised energy crop cultivation, ranging up to 2 or 3 times those values. The range of values seen with both modelling and field studies reflects the influence of variables other than crop type and fertilisation level on N_2O emission rate, making it difficult to draw direct comparisons. Given nonlinearity of equations to calculate N_2O emissions, combined with spatiotemporal variation in controlling parameters, model performance at simulation may be expected to be poor compared to other outputs. However, confidence in model output for N_2O emissions should be based on validation performance in Chapter 4; i.e. relative deviation from measurements may range from -66 % up to + 660 %, with greater proportional deviation at low levels of emissions.

Reliability of model output for N_2O emissions is dependent on accurate simulation of soil N, porosity and WFPS, which cannot be verified for this type of scenario analysis, however output can be assumed to be reasonable for cultivation on soils as simulated. Uncertainty surrounding input data, in particular the amount of soil settling following crop establishment and land use change will thus contribute to uncertainty in model output. Poor simulation of growth rates during *Miscanthus* establishment, as mentioned in Section 6.3.1, may affect simulation of N availability for nitrification and denitrification, contributing to N_2O emissions error. Similarly, poor simulation of below ground growth rates for SRC willow, as mentioned in Section 6.3.1, may also affect simulation of N availability for transformation reactions, thus creating additional error. Alternatively, the high levels of simulated symbiotic N fixation required to match field data may cause overestimation of N availability, resulting in overestimation of N_2O emissions.

Overall, simulated emissions from SRC willow and *Miscanthus* are low, with average complete lifecycle emissions of 0.31 to 2.79 kg N_2O-N ha^{-1} a^{-1} for *Miscanthus* and 0.29 to 3.03 kg N_2O-N ha^{-1} a^{-1} for SRC willow, compared to 1.40 to 14.74 kg N_2O-N ha^{-1} a^{-1} for arable crops. Range in simulated N_2O emissions is greater for SRC willow at 2.74 kg N_2O-N ha^{-1} a^{-1} compared to 2.47 kg N_2O-N ha^{-1} a^{-1} for *Miscanthus*. Figures 6.5 and 6.6 indicate that land use change to *Miscanthus* and Willow only

reduces direct N_2O emissions for arable sites (1-6); DayCent predicted slight increase in direct emissions for conversion of most of the grassland sites (7-12) to either energy crop. Emissions simulated for both energy crops were higher on former grassland, but the simulated increase mainly reflects lower emissions of the existing land use; grassland emissions were simulated at 0.67 to 3.10 kg N_2O-N ha^{-1} a^{-1}, which may be attributed to lower N inputs. Thus according to model output, the impact of land use change in terms of direct N_2O emissions is generally beneficial for conversion of arable land and detrimental for conversion of grassland. For comparison, using the IPCC tier 1 default emission factor of 0.125 (IPCC, 2006), emissions from arable land as simulated here are 17.5 kg N_2O-N ha^{-1} a^{-1}, whereas emissions from energy crops would be 0 kg N_2O-N ha^{-1} a^{-1} since annual fertiliser applications were not simulated, meaning a reduction following land use change of 17.5 kg N_2O-N ha^{-1} a^{-1}. It is more difficult to give an IPCC value for the grassland, since the defaults require given stocking density and animal type which are not modelled explicitly in DayCent.

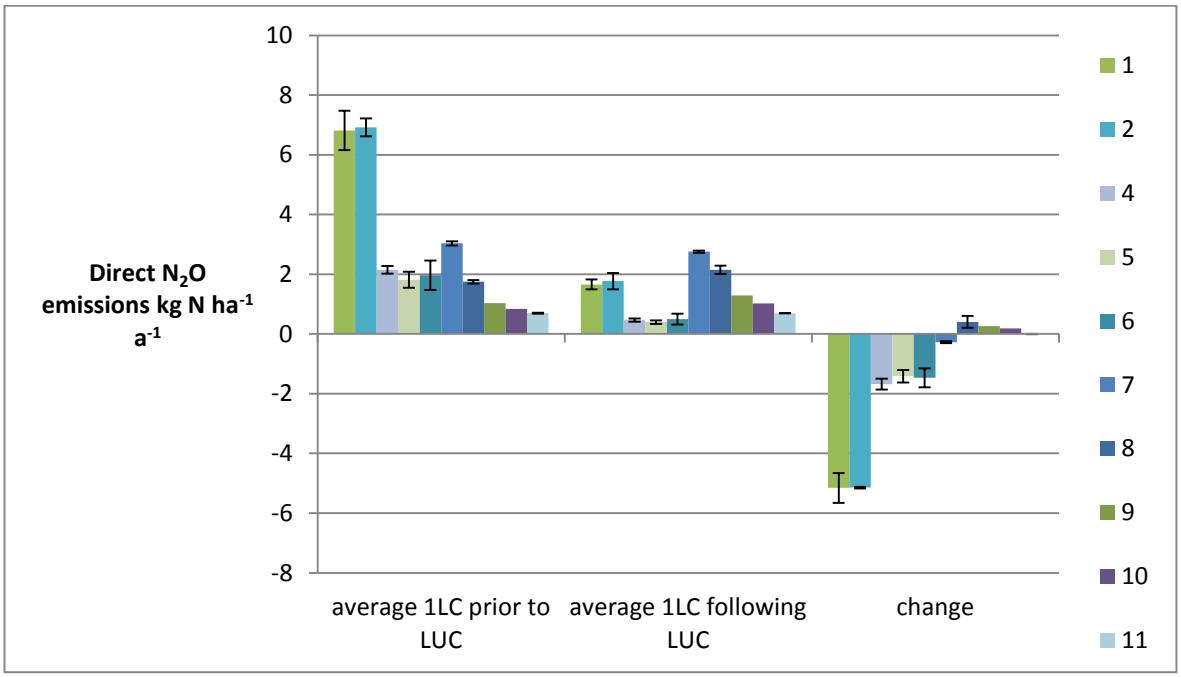

Figure 6.5 Impact of land use change for Miscanthus on N_2O emissions. Values at each site were averaged over a complete energy crop lifecycle (average 1LC following LUC) of 21 years, and compared to 21 years of the previous land use, simulated with the same weather data (average 1LC prior to LUC). Change in N_2O is calculated as after - before (negative values indicate a decrease)

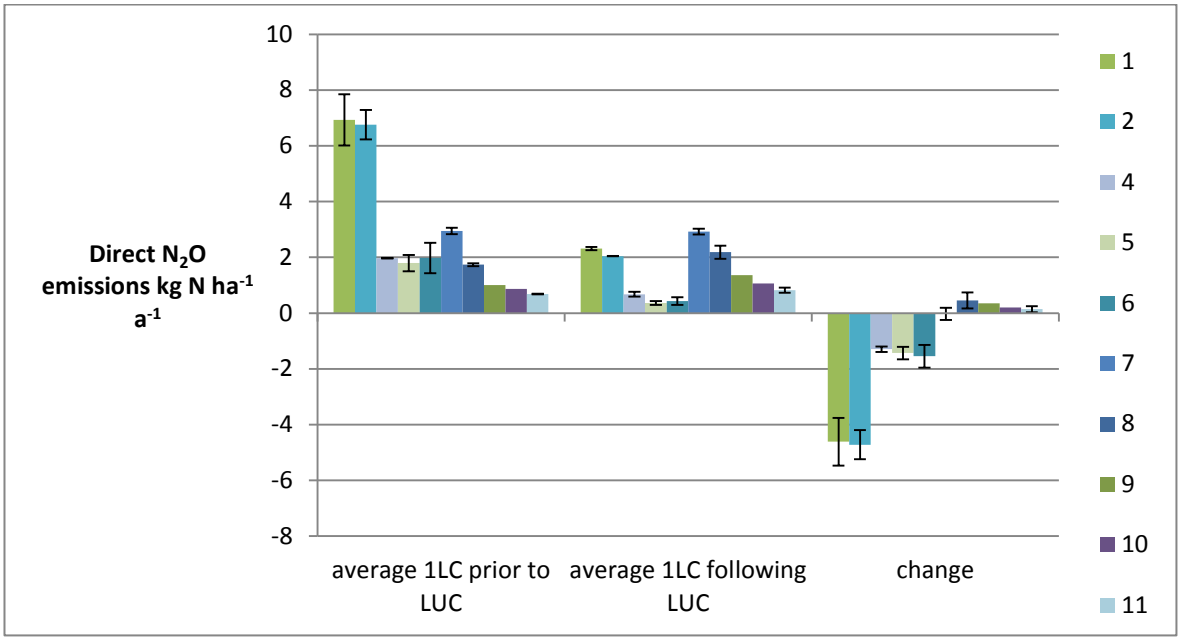

Figure 6.6 Impact of land use change for SRC willow on N_2O emissions. Values at each site were averaged over a complete energy crop lifecycle (average 1LC following LUC) of 27 years, and compared to 27 years of the previous land use, simulated with the same weather data (average 1LC prior to LUC). Change in N_2O is calculated as after - before (negative values indicate a decrease)

Over the lifecycle of the energy crop, N_2O emissions were generally relatively low, with significant peaks associated with the removal process, and the establishment period in the case of *Miscanthus*. For *Miscanthus*, as shown in Figure 6.7 removal peaks were simulated in 2034 and emissions at the start of the second energy crop cycle in 2035 were generally higher than at the start of the first cycle in 2014. For Willow, as shown in Figure 6.8, N_2O emissions peaks were simulated in 2040 and 2041, with emissions at the start of the second energy crop cycle in 2042 again higher than at the start of the first cycle in 2014. Due to a lack of data, it is not possible to verify these simulations with field observations, although Lavoie *et al.* (2013) provide some evidence for increase in N_2O following forest clearcut which they postulate reflects an increase in N availability. Although these emissions pulses are significant, lifecycle averages are more relevant for comparison, since N_2O is long lived.

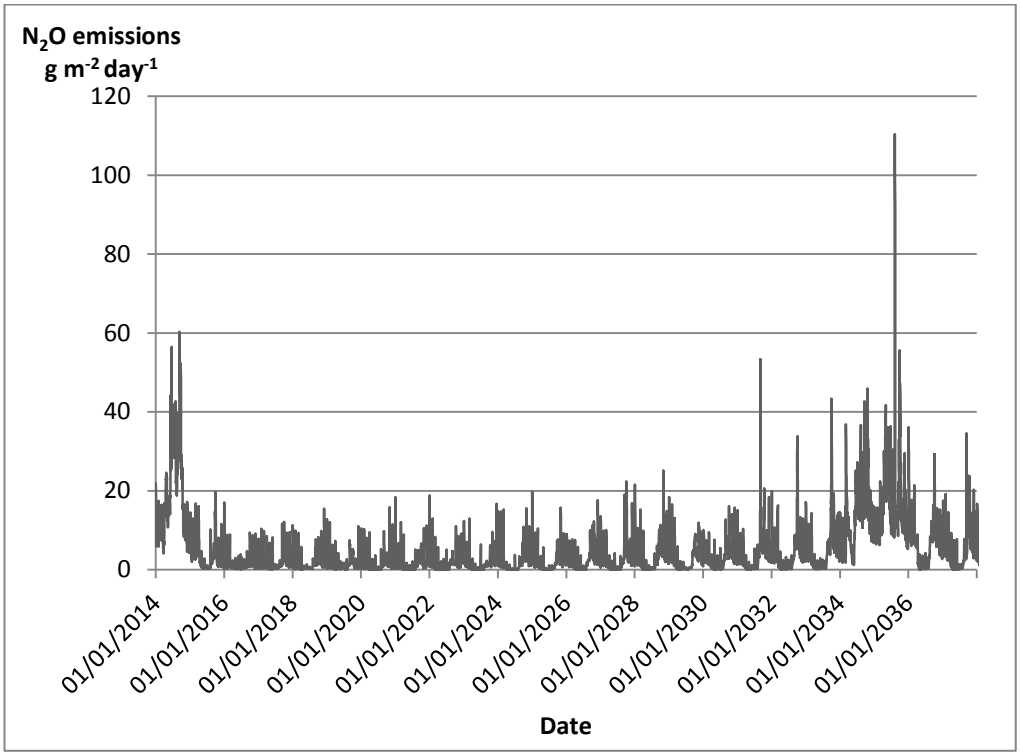

Figure 6.7 Time series N_2O emissions for a full lifecycle of Miscanthus, averaged across all sites

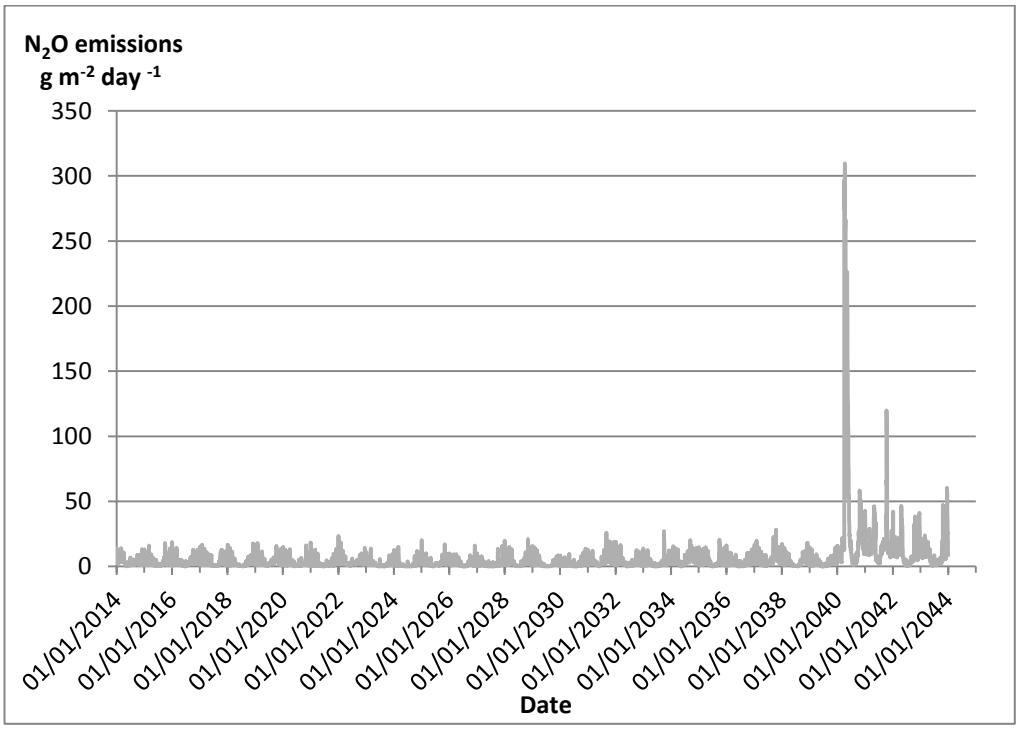

Figure 6.8 Time series N_2O emissions for a full lifecycle of SRC willow, averaged across all sites

Table 6.8 indicates statistically significant correlations between direct N_2O emissions and input variables. The correlation with latitude may be a result of covariance with other factors such as temperature. Given that the processes responsible for N_2O emissions from soil take place under

different conditions of soil moisture status, it is harder to draw conclusions about controlling factors or to interpret correlations with input variables. Positive correlations with water table and precipitation and negative correlations with topsoil sand content may indicate dominance of denitrification, or may reflect covariance with yield; simulated N_2O emissions for both energy crops correlate with yield, and yield is proportional to N fixation, and hence will increase N availability. Positive correlation with latitude and negative correlation with minimum temperatures may reflect covariance of these inputs with precipitation, and negative correlation with bulk density may well reflect the statistically significant correlation of -0.773 between bulk density and available water capacity. Statistically significant correlations with latitude for N_2O emissions under both *Miscanthus* and SRC willow, and with minimum temperature under *Miscanthus* mean that similar N_2O emissions may not be simulated for other sites with the same soil properties and similar total precipitation.

Table 6.8 Statistically significant correlations between direct N_2O emissions and input variables

	N_2O emissions for a full lifecycle of *Miscanthus*		**N_2O emissions for a full lifecycle of SRC willow**	
	Correlation Coefficient	**Significance (2-tailed)**	**Correlation Coefficient**	**Significance (2-tailed)**
Latitude	.722	.001	.735	.001
pH	-.568	.014	-.636	.005
Topsoil sand %	-.494	.037	-.527	.025
Topsoil bulk density	-.480	.044	-.492	.038
Topsoil available water capacity	.447	.063	.516	.028
Subsoil available water capacity	.569	.014	.643	.004
Months with water table	.809	<0.001	.842	<0.001
Annual precipitation	.695	.001	.733	.001
Average minimum temperature	-.543	.020	-.397	.103
***Miscanthus* yield**	.717	.001	.639	.004
SRC willow yield	.789	<0.001	.707	.001

Table 6.9 Average indirect N_2O emissions over one crop lifecycle.

	Average leached N over one crop lifecycle kg N $ha^{-1}a^{-1}$		Average indirect N_2O emissions over one crop lifecycle kg N_2O -N $ha^{-1}a^{-1}$	
	Miscanthus	**SRC willow**	***Miscanthus***	**SRC willow**
1+	449.14	241.49	11.23	6.04
1-	437.57	247.17	10.94	6.18
2+	526.19	271.65	13.15	6.79
2-	496.03	269.89	12.40	6.75
4+	551.94	181.41	13.80	4.54
4-	532.90	198.59	13.32	4.96
5+	667.69	171.38	16.69	4.28
5-	668.71	163.71	16.72	4.09
6+	680.13	205.92	17.00	5.15
6-	684.36	196.59	17.11	4.91
7+	456.83	648.37	11.42	16.21
7-	465.49	647.68	11.64	16.19
8+	596.02	720.14	14.90	18.00
8-	638.45	703.63	15.96	17.59
9-	599.54	531.09	14.99	13.28
10-	642.96	537.59	16.07	13.44
11+	552.51	615.21	13.81	15.38
11-	536.67	624.73	13.42	15.62

EF 5 for estimating N_2O emissions from leaching based on (Nevison, 2002)

Table 6.10 Literature values of indirect N_2O emissions

Source	**Context**	**Leaching kg N ha^{-1} a^{-1}**	**Emissions kg N_2O-N ha^{-1} a^{-1}**
(Mortensen, 1998)	SRC willow establishment year	136	3.4
	SRC willow, year 3	3	0.075
(Christian and Riche, 1998)	*Miscanthus* establishment year	154	3.85
	Miscanthus, year 2	8	0.2
	Miscanthus, year 3	3	0.075

Data in Table 6.10 suggest high leaching during establishment for both perennial energy crops, followed by very low leaching in later years, which may reflect N store exhaustion, or more efficient uptake of N. Goodlass *et al.* (2007) recorded leaching following removal of SRC poplar at similar levels to during the establishment phase, perhaps due to soil disturbance and organic matter breakdown. Modelled indirect N_2O emissions and leaching values in Table 6.9 are higher than measured values for established *Miscanthus* and SRC willow indicated in Table 6.10, although modelled SRC willow values for some sites were in the region of those measured for establishing SRC willow by Mortensen *et al.* (1998). Previous work by Del Grosso *et al.* (2005)

indicated good performance by DayCent in simulating leaching rates for a range of arable sites. Prior to land use change, simulated values were much higher for grassland sites than arable sites, as can be seen in Figures 6.10 and 6.11; this is in line with field data, where high leaching from grazed grassland is attributed to inputs from ruminant livestock (Ryden *et al.*, 1984).

Del Grosso *et al.* (2005) note that DayCent simulates leaching of N from N fixation; as such the high values of leaching simulated are likely due to high values of simulated symbiotic N fixation required to match yield. This suggestion is supported by time series data (Figure A4.1 in the Appendix) which indicate greater leaching during energy crop growth than establishment and removal periods. Significantly lower values by year three for *Miscanthus* and SRC willow in the studies referenced in Table 6.10 may suggest that levels of N fixation associated with *Miscanthus* and SRC willow cultivation in the field do not result in significant leaching. Therefore, high simulated values of leaching, which do not match well with measured data may indicate that the rate of symbiotic N fixation is set too high, and that N uptake efficiency is set too low. Excess soil N resulting from this model error may also be responsible for the increase in direct N_2O emissions simulated for grassland sites. Fixation rate is proportional to growth, thus the strong positive correlation of indirect N_2O emissions with energy crop yield with a coefficient of 0.981, significant at the 0.001 level displayed in Figure 6.9 would support the assertion that this model artefact is responsible for the simulated high levels of leaching. This also explains the observation in Section 5.4 that altering N fixation had limited impact on soil nitrate and ammonium concentrations, since fixed N appears to be leached as opposed to stored in soil. Figure 6.9 also shows that there is no discernible correlation for *Miscanthus* yield; analysis showed a weak negative correlation which was not statistically significant, hence high simulated levels of N leaching for *Miscanthus* may require further explanation.

In either case, model output poses an interesting question, as to what extent N fixation does take place in association with the roots of SRC willow and *Miscanthus* in the context of field scale cultivation, and points to a need for additional field data on N leaching, to make more confident predictions on what the water course pollution and GHG emissions impacts of energy crop cultivation might be.

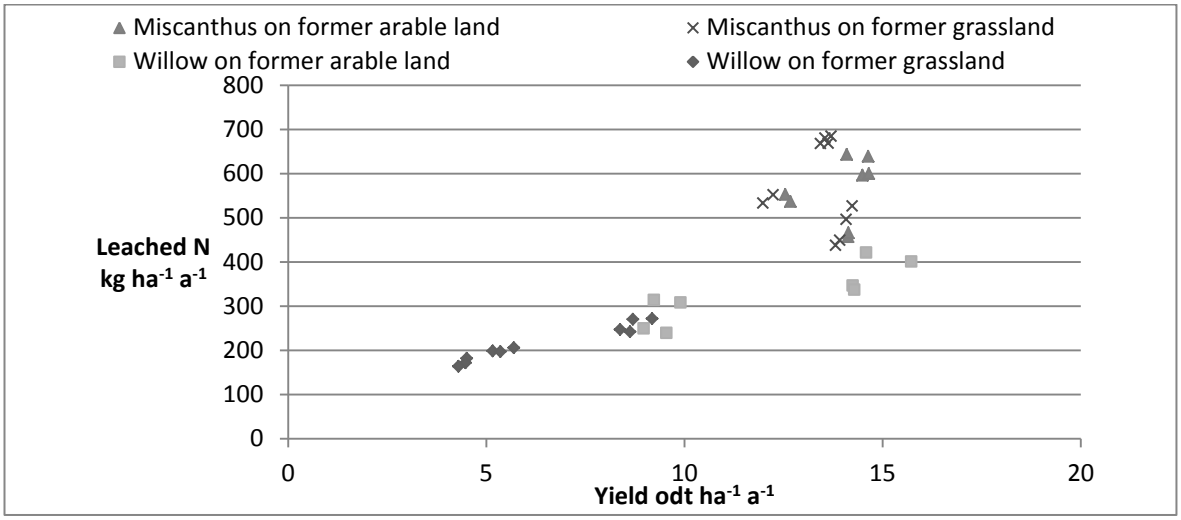

Figure 6.9 Graph to show simulated relationship between yield and N leaching

The model simulates an increase in indirect N_2O emissions for land use change to *Miscanthus* or SRC willow, as can be seen in Figure 6.11 and 6.12. Comparison of figures 6.10 and 6.11 with figures 6.5 and 6.6 indicates that, following land use change, simulated indirect N_2O emissions are somewhat higher than simulated direct emissions, although as indicated above this may reflect model error, and is not representative of field observations.

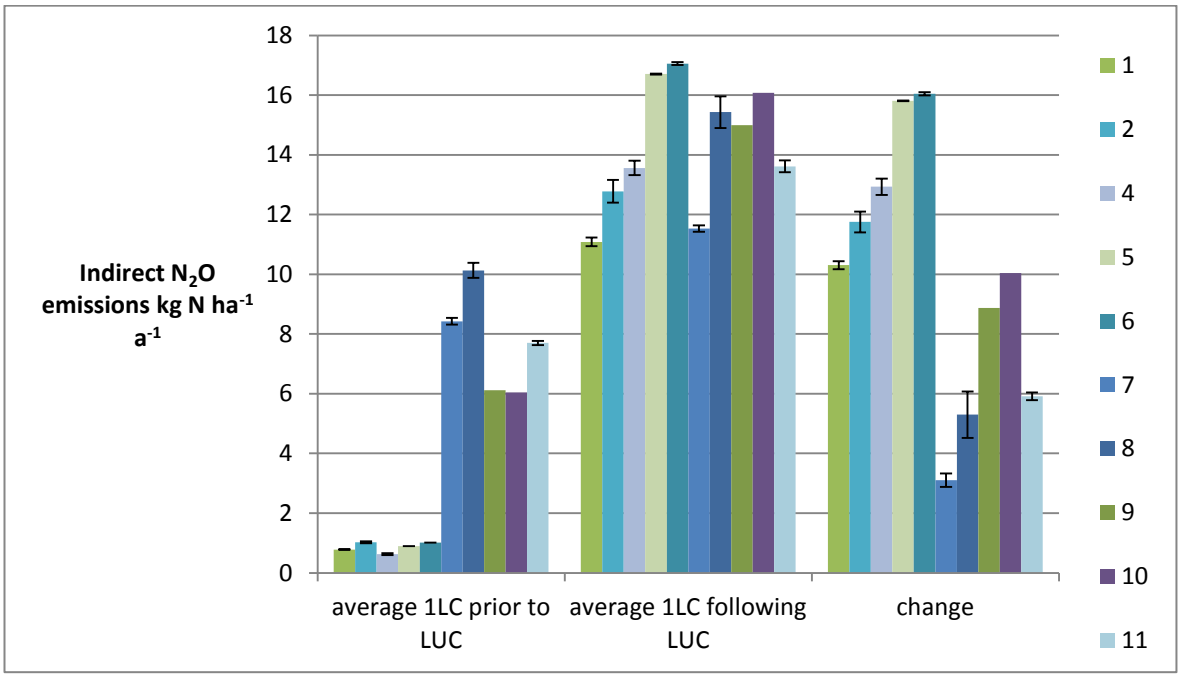

Figure 6.10 Impact of land use change for Miscanthus on indirect N_2O emissions. Values at each site were averaged over a complete energy crop lifecycle (average 1LC following LUC) of 21 years, and compared to 21 years of the previous land use, simulated with the same weather data (average 1LC prior to LUC). Change in N_2O is calculated as after - before (negative values indicate a decrease)

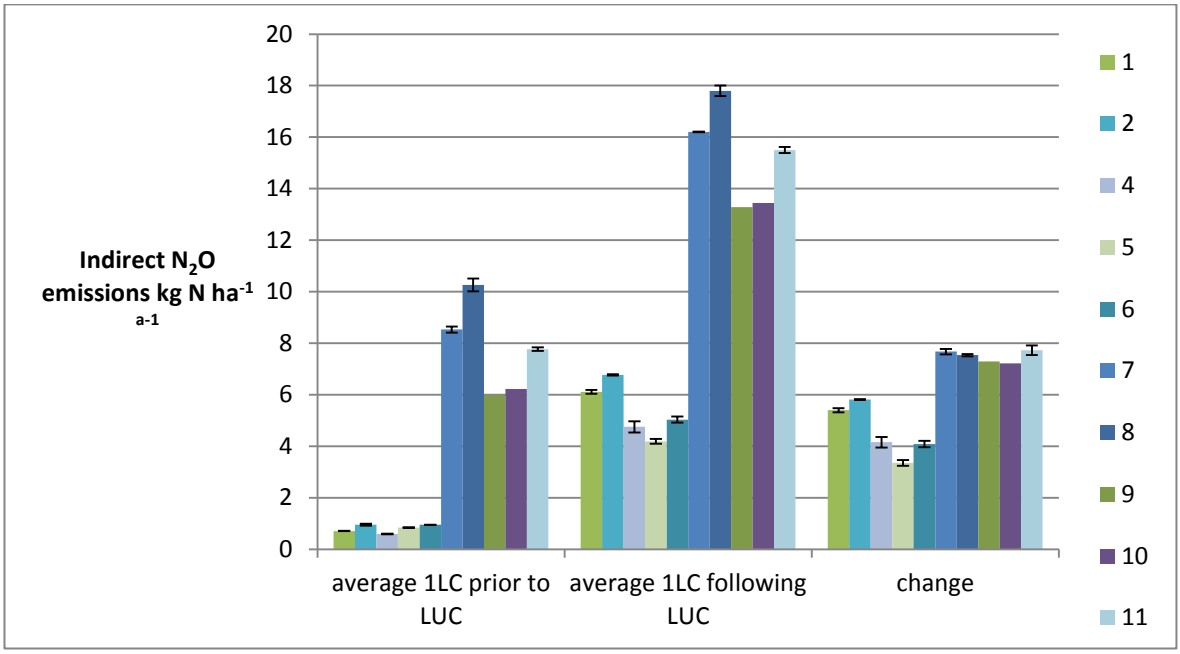

Figure 6.11 Impact of land use change for SRC willow on indirect N_2O emissions. Values at each site were averaged over a complete energy crop lifecycle (average 1LC following LUC) of 27 years, and compared to 27 years of the previous land use, simulated with the same weather data (average 1LC prior to LUC). Change in N_2O is calculated as after - before (negative values indicate a decrease)

6.3.3 Soil carbon

Given the uncertainty associated with amount and duration of Soil C storage associated with bioenergy crop cultivation, it may be excluded from inventories (Cannell, 1999; Keoleian and Volk, 2005; Matthews, 2001b). However, since DayCent has been shown to perform well at simulating SOC , modelling incorporating site factors and current land use should produce informative predicted values for individual sites.

Table 6.11 Modelled soil C increase over one crop lifecycle (excluding planting and the ploughing in of roots and residues associated with energy crop removal, for purposes of comparison to the literature)

	Increase in Soil C t ha^{-1} a^{-1} over the full energy crop lifecycle	
	***Miscanthus* (averaged over 19 years)**	**Willow (averaged over 24 years)**
1+	1.41	0.41
1-	1.53	0.41
2+	1.55	0.46
2-	1.60	0.43
4+	1.65	0.27
4-	1.63	0.33
5+	1.89	0.36
5-	1.77	0.31
6+	1.92	0.41
6-	1.84	0.37
7+	0.86	0.62
7-	0.92	0.60
8+	0.92	0.50
8-	1.06	0.50
9-	1.33	0.64
10-	1.52	0.63
11+	1.08	0.51
11-	1.05	0.54
Maximum	1.92	0.64
Minimum	0.86	0.27
Range	1.06	0.37
Mean	1.42	0.46
Standard Deviation	0.34	0.11

In general, the literature suggests that *Miscanthus* and SRC willow cultivation would result in increased soil C for former arable land and recent setaside, but may reduce soil C when cultivated on undisturbed land or longer term grassland and setaside (Fargione *et al.*, 2008; Rowe *et al.*, 2009; Smith, 2004). Table 6.11 shows that the model simulated an increase in SOC for all modelled sites; simulated soil C accumulation was 0.86 to 1.92 t C ha^{-1} a^{-1} for *Miscanthus* and 0.27 to 0.64 t C ha^{-1} a^{-1} for SRC willow. Accumulation was calculated prior to ploughing in of residues and roots at the end of the lifecycle, since time series data indicate that this tends to cause a short term C peak, and since available field data do not include this portion of the lifecycle.

The database value of SOC accumulation under *Miscanthus* is 0.62 t C ha^{-1} a^{-1} (Brandão *et al.*, 2011), which is lower than model output in Table 6.11. Model output shown in Figure 6.12 supports literature observations (e.g. by Smith, 2004) that SOC accumulation following land use

change is often greatest during establishment, and the average accumulation rate of 1.43 t C ha^{-1} a^{-1} over the first four years for grassland sites is comparable to the relative increase recorded by Kahle *et al.* (2001) under *Miscanthus* (compared to a grassland control) of 1.7 t C ha^{-1} a^{-1} over the first four years. Based on this comparison, it appears the DayCent model simulates the rate of initial accumulation under *Miscanthus* well, but may overestimate long term accumulation.

For cultivation of *Miscanthus*, a greater increase in soil C is simulated for land use change from arable than from grassland, as could be expected given the initially higher SOC value for grassland. Some field studies have recorded no increase in soil C, for *Miscanthus* compared to grassland despite high inputs during establishment; this may be attributed to a rhizosphere priming effect causing increased soil C decomposition, triggered by readily available C from root exudates (Zatta *et al.*, 2013; Zimmermann *et al.*, 2012). The DayCent model is not able to simulate this type of effect, and thus may overestimate SOC accumulation for affected sites.

The database values for SOC accumulation under SRC willow is 0.09 to 0.18 t C ha^{-1} a^{-1} (Brandão *et al.*, 2011), which is below model output in Table 6.11. Elsewhere Clair *et al.* (2008) modelled values which indicate accumulation of 0.115 t C ha^{-1} a^{-1} for conversion from annual tilled arable, but no accumulation for conversion from grassland whilst Matthews (2001b) states that conversion from grassland to SRC may result in SOC loss due to soil disruption for planting. Based on these figures, the model may slightly overestimate SOC accumulation for SRC cultivation on former arable land, and simulates accumulation on former grassland which is disputed elsewhere.

Previous work by Del Grosso *et al.* (2002) found DayCent performed well for simulation of soil C; although simulations deviated from measured values for specific cropping systems, variation according to land use was correctly simulated. Based on comparison of model output to values published in the literature, DayCent correctly simulates greater accumulation with *Miscanthus* compared to SRC willow, however simulation of greater SOC for energy crop systems than grassland may not be representative of field response. Furthermore, although DayCent correctly simulated higher soil C for the grassland than the arable site, total soil C values (for the top 20cm) are slightly low; with averages of 20.8 t C ha^{-1} for arable land and 35.4 t C ha^{-1} for grassland at the end of the spin up period, compared to reference values in the range 30 to 220 t C ha^{-1}. Given that constraints mapping ruled out organic soils and high quality farmland, modelled sites could be

expected to be towards the lower end of the SOC range; output from cluster analysis in Tables 2.7 and 2.8. indicates that site SOC values ranged from very low to medium, hence sites SOC may be underestimated at the end of the spin up period at sites 1, 2, 7, 8 and 11 where medium SOC is indicated by JRC data. A study by Foereid (2012) also used DayCent to predict soil C values for UK sites, and found a strong tendency to under predict SOC, particularly for grassland sites. These issues, combined with possible underestimation of SOC at the end of the spin up period may point to a need to improve model calibration of C cycling.

This research did not attempt to improve soil C cycling; although the model was successfully calibrated for SRC willow above ground biomass in Chapter 5, no calibration was performed for C cycling associated with SRC willow cultivation, since data on change in soil C was not available for the sites. Although analysis in Chapter 5 notes that simulated below ground biomass accumulation was initially too rapid, final values were reasonable; hence the overall SOC accumulation may not be affected. However, death rates for both above and below ground biomass were fitted based on model defaults and best fit to field data for above ground biomass, hence associated inputs to SOC may be misrepresented.

DayCent was calibrated by Davis *et al.* (2010) for above ground *Miscanthus* biomass, although the approach taken to set ratio of above to below ground biomass is not detailed, and there is no separate validation of soil C. Davis *et al.* (2010) simulated SOC accumulation of 4 t $ha^{-1}a^{-1}$over 10 years for the calibration site, and in a subsequent study simulated an average rate of 5.23 t $ha^{-1}a^{-1}$ over 10 years for a large area in the central US (Davis *et al.*, 2012). Although calibration for *Miscanthus* was not performed as part of this study, simulated SOC accumulation was closer to literature values than that simulated by Davis *et al.* (2010), suggesting that the model performs well for simulation of SOC accumulation under *Miscanthus* for English climate conditions.

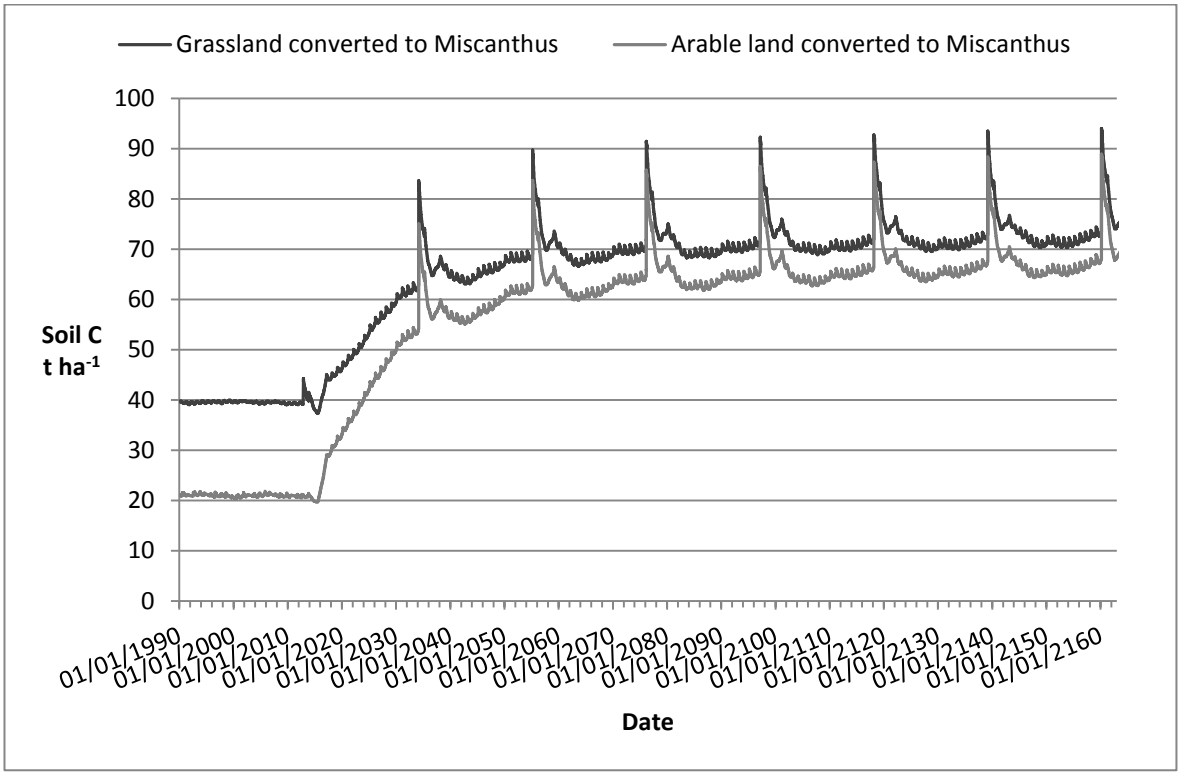

Figure 6.12 Soil carbon over seven complete lifecycles of Miscanthus

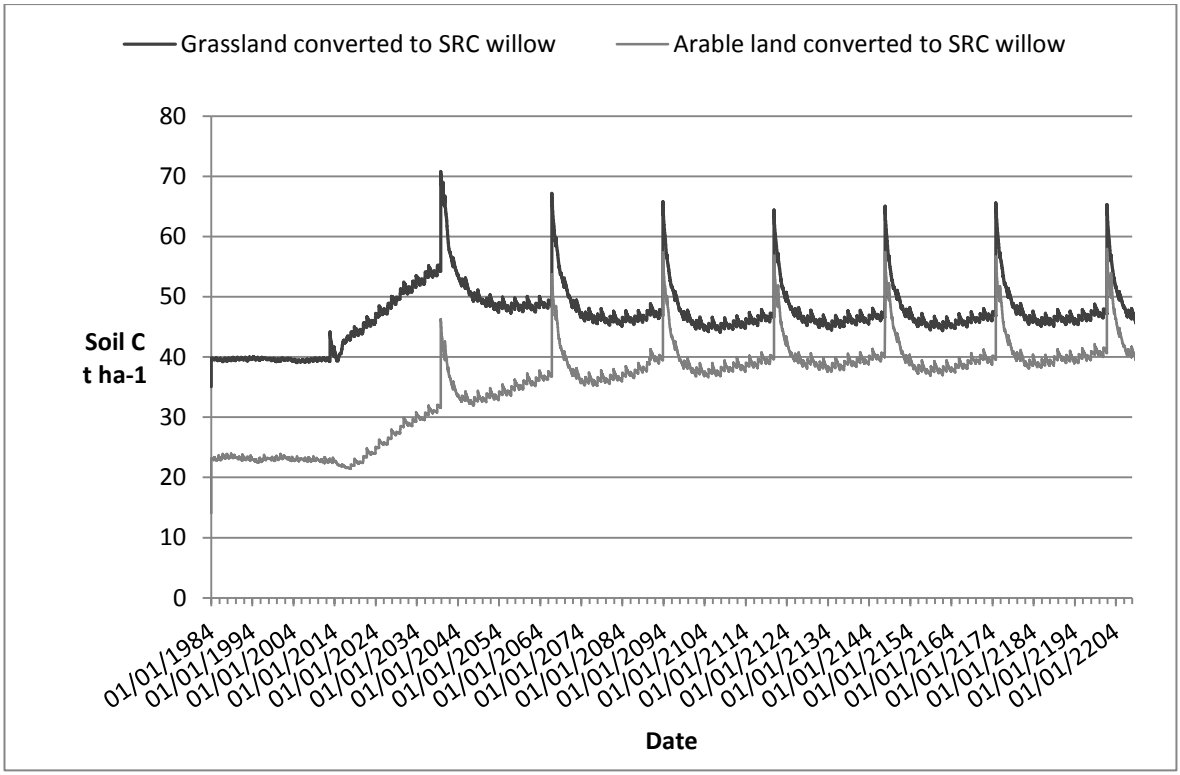

Figure 6.13 Soil carbon over seven complete lifecycles of SRC willow

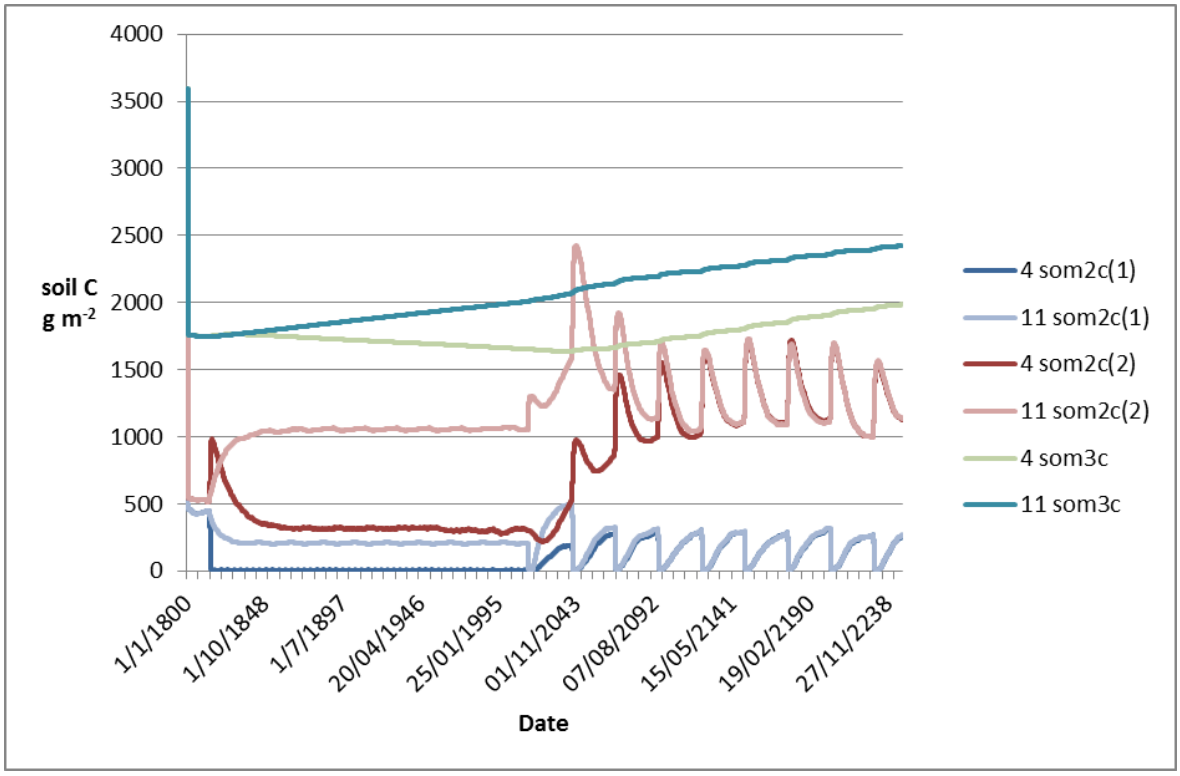

Figure 6.14 Simulated slow SOC pools for SRC willow cultivation at sites 4- (previously arable) and 11- (previously grassland). Forest was originally simulated at both sites to set soil C pools; the graph covers the modelled period from removal of forest, through over 200 years of energy crop cultivation commencing in 2014. som2c(1)=Carbon in surface slow soil organic matter; som2c(2)= Carbon in soil slow soil organic matter; som3c=Carbon in passive soil organic matter.

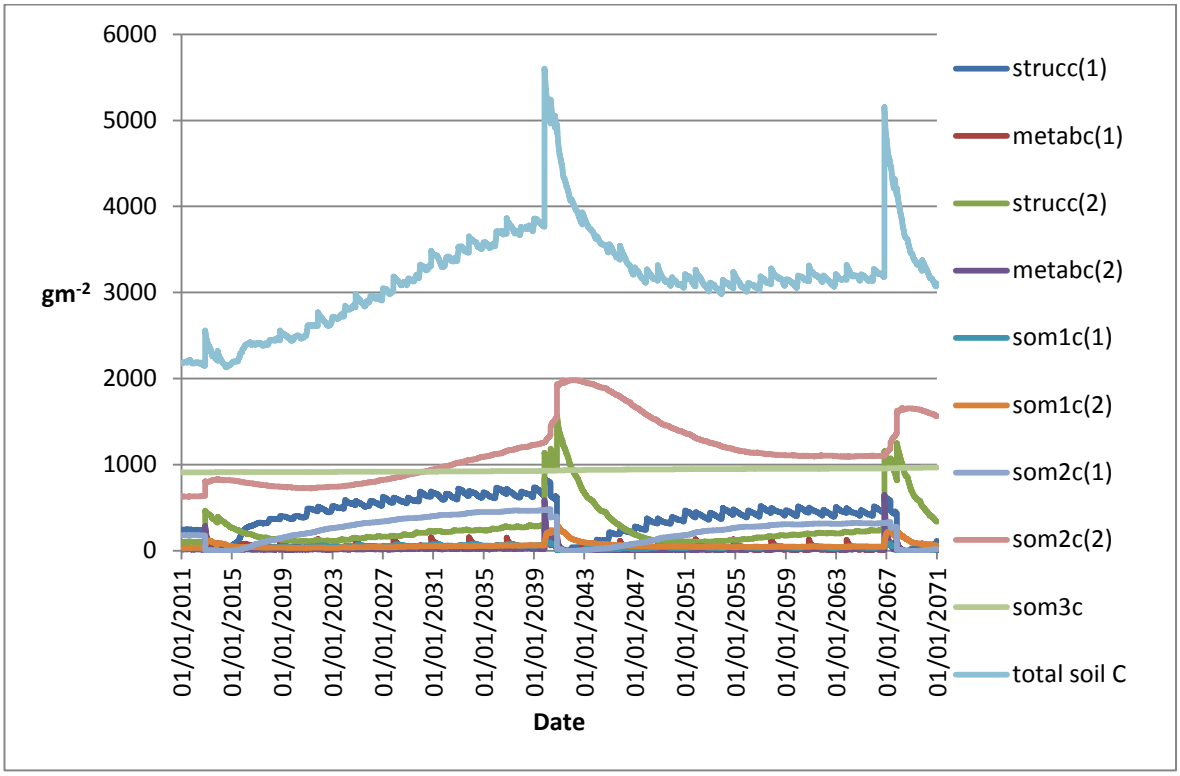

Figure 6.15 Simulated SOC pools for SRC willow cultivation at a former grassland site. strucc(1)=Carbon in structural component of surface litter; metabc(1)= Carbon in metabolic component of surface litter; strucc(2)= Carbon in structural component of soil litter; metabc(2) = Carbon in metabolic component of soil litter; som1c(1) = Carbon in surface active soil organic matter; som1c(2)= Carbon in soil active soil organic matter; som2c(1)=Carbon in surface slow soil organic matter; som2c(2)= Carbon in soil slow soil organic matter; som3c=Carbon in passive soil organic matter.

It was noted in Section 6.3.1 that yield is significantly overestimated where DayCent was run for more than one SRC willow lifecycle, and that this may affect soil C simulation for the relevant time period. Although simulated values of both above and below ground biomass were higher, model output shown in Figure 6.14 indicates lower SOC for these subsequent SRC willow lifecycles at former grassland sites. For conversion of arable land to SRC willow, Figure 6.14 shows slower increase for second rotation, in a similar trend to that seen for conversion of arable land to *Miscanthus* in Figure 6.13.

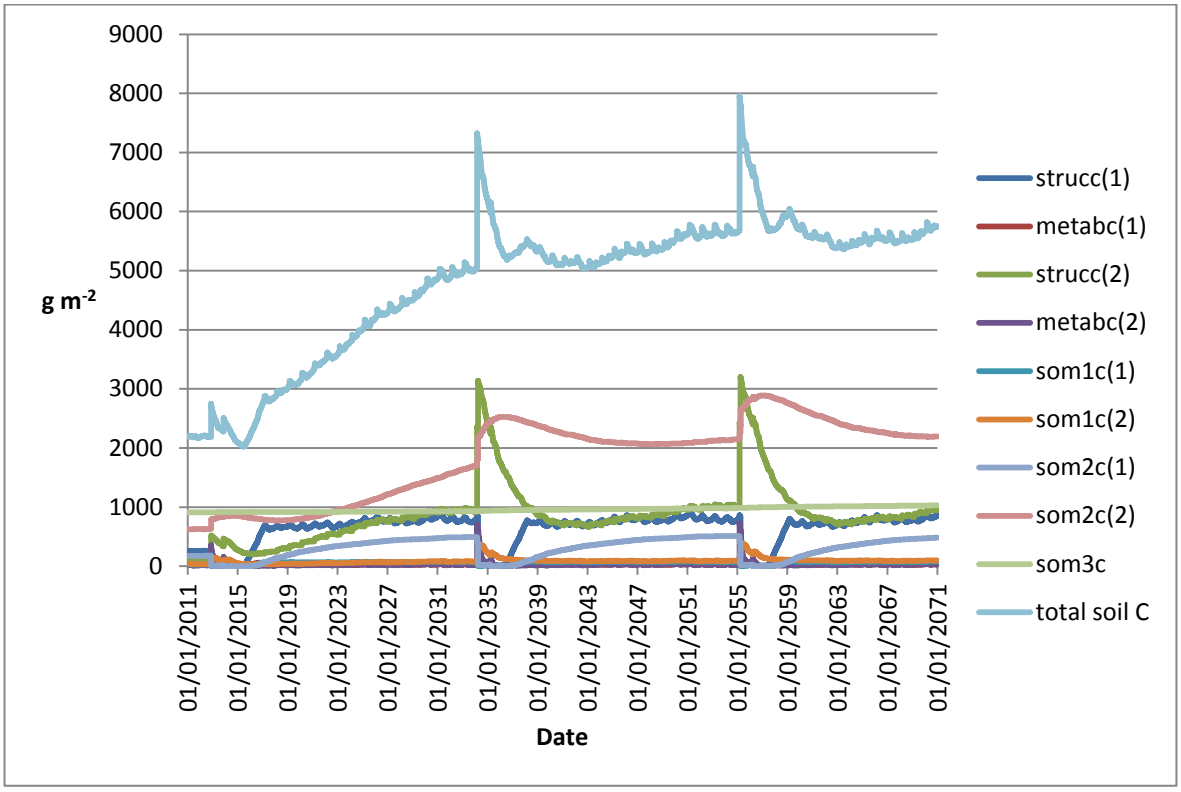

Figure 6.16 Simulated SOC pools for Miscanthus cultivation at a former grassland site. strucc(1)=Carbon in structural component of surface litter; metabc(1)= Carbon in metabolic component of surface litter; strucc(2)= Carbon in structural component of soil litter; metabc(2) = Carbon in metabolic component of soil litter; som1c(1) = Carbon in surface active soil organic matter; som1c(2)= Carbon in soil active soil organic matter; som2c(1)=Carbon in surface slow soil organic matter; som2c(2)= Carbon in soil slow soil organic matter; som3c=Carbon in passive soil organic matter.

Data collected from SRC poplar indicate that soil loss and erosion may occur for several years following establishment, but from 12-18 years, SOC accumulation (relative to arable control) was recorded (Hansen, 1993). Model output shown in Figure 6.13 indicates a one year dip in SOC on conversion of arable land to SRC willow, whereas in the case of grassland, rapid accumulation followed land use change, which may be attributed to input of plant organic C from the previous land use.

To understand patterns in total SOC, it is useful to break model output down into constituent pools; Foereid *et al.* (2012) note that differences between sites tends to reflect historical conditions, and associated recalcitrant C in slowly decomposing pools. In general, this was also true of model output: sites with initially higher soil C reached a higher dynamic equilibrium level of C. As stated in Section 6.2, a spin up period of 1800 years forestry was simulated for all sites, to set SOC pools; Figure 6.14 starts from the removal of this forest, and shows long term trends in

slow SOC pools at example arable (4) and grassland (11) sites, followed by changes with conversion to SRC willow cultivation. Following conversion from forest; passive soil organic matter (som3c), surface slow soil organic matter (som2c(1)) and soil slow soil organic matter (som2c(2)) all decrease much more rapidly at the arable site than the grassland site. The passive organic C pool som3c did not stabilise over 200 years of cropping or grassland; steady reduction was simulated for arable and steady increase for grassland, which may indicate a problem with C cycling simulation, since it could be expected that equilibrium would be reached during this time. For both sites, this pool increased following conversion to SRC willow in 2014, at a rate slightly steeper than that observed under grassland. The slow surface organic C pool som2c(1)) exhibits a slow increase during each 27 year SRC willow cultivation lifecycle, which is much greater for the former grassland site in the first lifecycle. Drops in surface slow C are accompanied by peaks in the soil slow organic C pool som2c(2) following conversion of grassland to SRC willow, and at the end of each complete SRC willow lifecycle, as directed by scheduled cultivation events. The increase in these pools following ploughing in of grassland crop C appears to be responsible for the higher total SOC during the first SRC willow lifecycle. From comparison of Figures 6.15 and 6.16, it can be seen that the greatest differences between SOC simulation for SRC willow compared to *Miscanthus* is the continuing high levels of som2c(1) and strucc(1) during the second *Miscanthus* lifecycle, presumably due to significant inputs from senescence. It is apparent that virtually no breakdown or loss of surface carbon pools is simulated in the absence of tillage, and this may contribute to unrealistically high predicted SOC values, given Zimmermann *et al.* (2013) recorded that 79.7% of SOC inputs from *Miscanthus* were in the form of labile particulate organic matter, and hence it would be more representative to allocate the majority of inputs to active pools, or to simulate faster breakdown of surface pools.

Failure to simulate the anticipated 12 year deficit in SOC on conversion to SRC willow may indicate that in general, decomposition of slow organic matter pools is too slow, or that too great a proportion of OM inputs are allocated to the slow and surface pools for grassland also. Further model calibration focussed on C cycling following conversion to SRC willow and *Miscanthus* would enable more informative predictions on SOC storage to be made.

Previous modelling work by Matthews and Grogan (2001a) simulated soil C accumulation as directly proportional to inputs, although simulation of C pools was less complex than in DayCent. Table 6.12 indicates that for cultivation of SRC willow, there is a statistically significant correlation between yield and SOC increase (as can be seen in Figure 6.17), with a correlation coefficient of

0 .738. This results in generally greater increase in soil C for land use change from grassland than from arable, contrary to what would be expected from previous studies (e.g. Clair *et al.*, 2008; Matthews, 2001b). Conversely, for cultivation of *Miscanthus*, a statistically significant negative relationship with yield was simulated, which may indicate greater control on soil C of factors controlling decomposition rate, or may suggest that lower yields result from greater loss of biomass to surface litter prior to harvest. Table 6.12 also indicates positive correlation between precipitation and SOC increase for SRC willow, which likely reflects covariance of precipitation and yield, and a negative correlation with pH. For *Miscanthus*, Table 6.12 indicates negative correlations between SOC accumulation and subsoil AWC, presence of water table and annual precipitation. In terms of SOC, it appears to be advantageous to cultivate *Miscanthus* at drier sites with high pH and SRC willow at wetter sites with low pH.

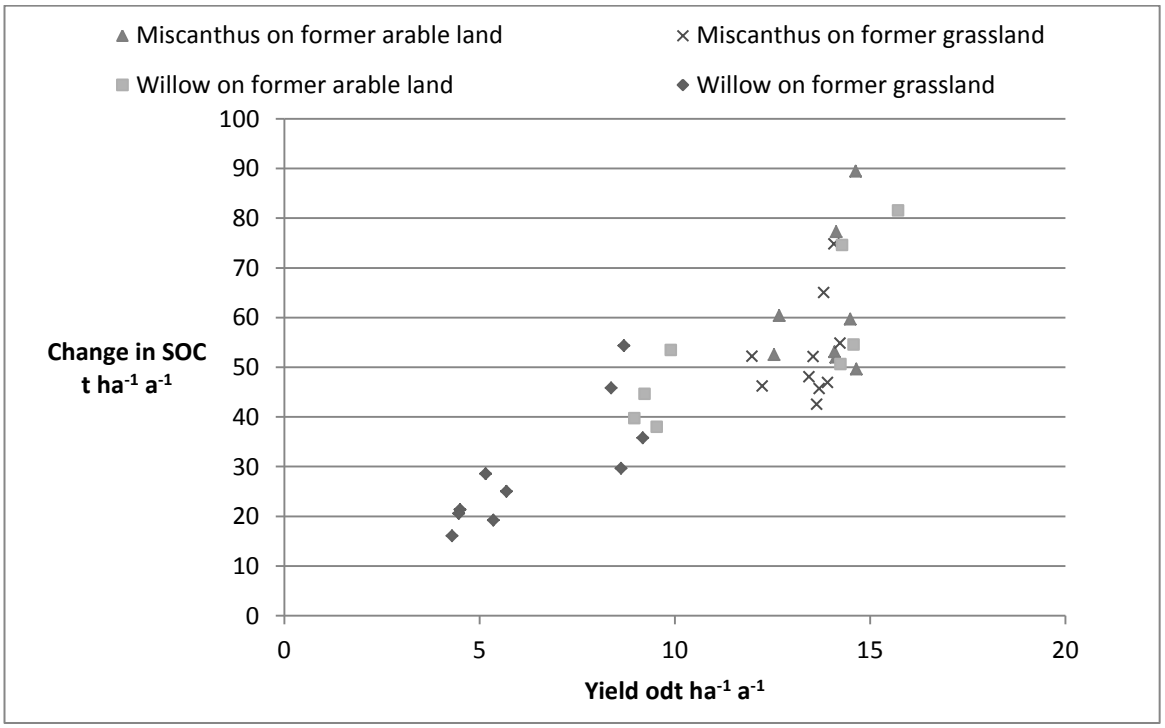

Figure 6.17 Modelled soil C increase over one crop lifecycle (excluding the ploughing in of roots and residues associated with energy crop removal) plotted against yield

Table 6.12 Statistically significant correlations between change in SOC and input variables

	SOC change under *Miscanthus*		SOC change under SRC willow	
	Correlation Coefficient	**Significance (2-tailed)**	**Correlation Coefficient**	**Significance (2-tailed)**
pH	.568	.014	-.091	.720
Subsoil available water capacity	-.569	.014	.184	.464
Months with water table	-.596	.009	.191	.449
Annual precipitation	-.388	.112	.480	.044
***Miscanthus* Yield**	-.513	.030		
SRC willow Yield			.829	<0.001

Although change in SOC shows no statistically significant correlations with temperature inputs or latitude, the strong correlations with yield may limit the potential to extrapolate findings to other sites with similar soil properties and precipitation.

6.3.4 Evapotranspiration

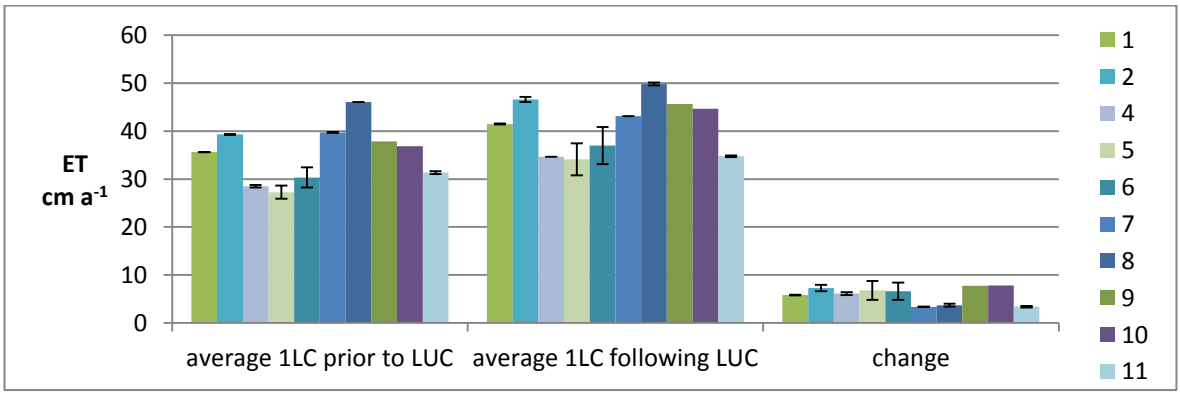

Figure 6.18 Impact of land use change for Miscanthus on evapotranspiration (ET). Values at each site were averaged over a complete energy crop lifecycle excluding establishment year (average 1LC following LUC) of 20 years, and compared to 20 years of the previous land use, simulated with the same weather data (average 1LC prior to LUC). Change is calculated as after - before (positive values indicate an increase).

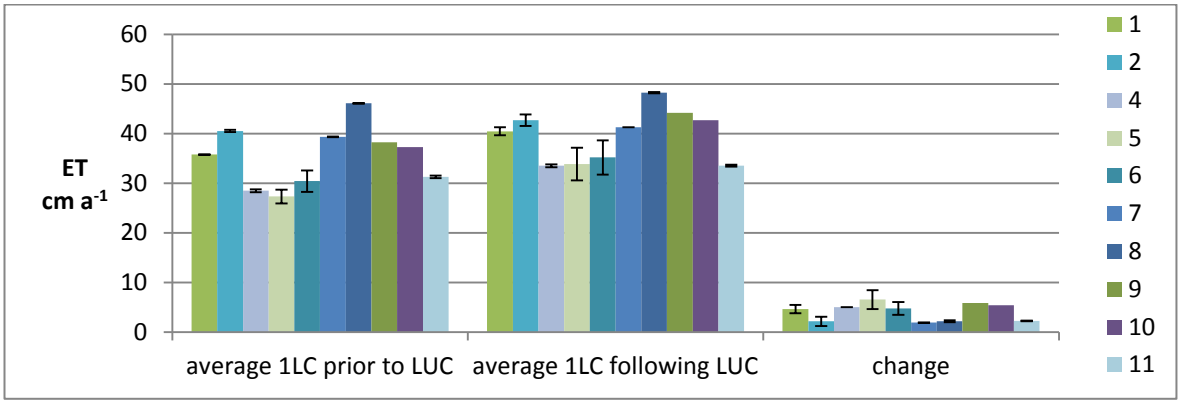

Figure 6.19 Impact of land use change for SRC willow on evapotranspiration (ET). Values at each site were averaged over a complete energy crop lifecycle (average 1LC following LUC) of 27 years, and compared to 27 years of the previous land use, simulated with the same weather data (average 1LC prior to LUC). Change is calculated as after - before (positive values indicate an increase).

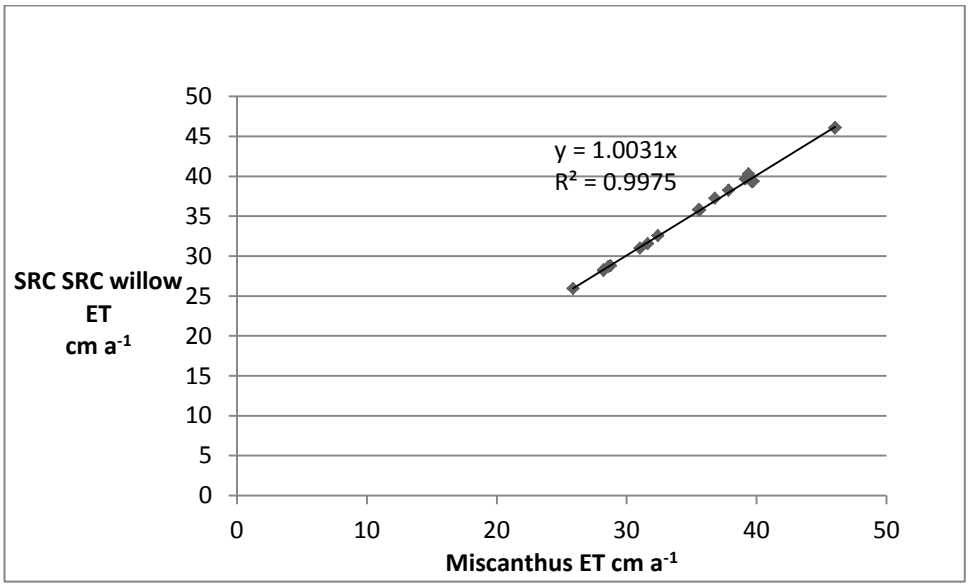

Figure 6.20 Comparison of average annual evapotranspiration (ET) for Miscanthus (excluding establishment year) and SRC willow: statistically significant positive correlation, coefficient 0.979

DayCent simulated increased evapotranspiration (ET) for all land use change to perennial energy crops, as can be seen from Figures 6.18 and 6.19. The increase is generally greater for transition from arable land than for transition from grassland, and comparable for SRC willow and *Miscanthus*.

Figure 6.20 shows a comparison of simulated ET for *Miscanthus* and SRC willow; the relationship between X and Y indicates that ET for *Miscanthus* was generally higher, although simulated values of ET were higher for SRC willow at some sites.

Elsewhere Jørgensen and Schelde (2001) fitted the COUP model to field data for fertilised SRC, and found higher ET for clones which produced higher yield, with values of 70.7 cm a^{-1} for 8.3 odt ha^{-1} $a^{-1}$and 87.8 cm a^{-1} for 9.1 odt ha^{-1} a^{-1}. Simulated annual evapotranspiration for SRC willow using the DayCent model was lower than this, ranging from 30.6 to 48.3 cm a^{-1}. These figures from DayCent were similar to field values tabulated in Dimitriou *et al.* (2009) which ranged from 35 to 59 cm a^{-1}. Although minimum values simulated by DayCent were slightly lower than literature values, this may be attributed to site factors causing lower yields; simulated values can be accepted as reasonable, but the possibility that ET is underestimated should also be considered.

Values of annual evapotranspiration simulated for *Miscanthus* using the DayCent model were in the range of 30.8 to 50.1 cm a^{-1}; these are in general slightly higher than values tabulated in Richter *et al.* (2008) which ranged from 25.9 to 45.6 cm a^{-1} but only covered the growing season, whilst Zeri *et al.* (2013) measured values from 58 to 75cm for a full year at a US site, with interannual variation due to amount and timing of precipitation relative to crop growth cycle. Again, minimum values simulated by DayCent were slightly lower than the literature values, although again this may reflect site and climate factors, for example higher temperatures for the US field site cited here, so the simulated values can be considered reasonable for site conditions.

Given that the DayCent model does not represent variation in water use efficiency, particularly between C3 and C4 photosynthesis, it could be expected that *Miscanthus* transpiration may be somewhat overestimated by the model. Elsewhere, models such as PALMS incorporate algorithms developed specifically to represent photosynthesis for C4 crops (e.g. Woo, 2013), in order to account for variation in water use efficiency, and potential benefits of C4 energy crops. Two parameters in the fix.100 input could be fitted to *Miscanthus* to give improved representation of water availability impacts on growth:

pprpts(3) the lowest ratio of available water to PET at which there is no restriction on production

pprpts(1) the minimum ratio of available water to PET which would completely limit production

Compared to the other outputs considered, short term trends in water availability have greater importance, therefore time series graphs were also produced to look at interannual variation, and how this was affected by land use. Graphs for *Miscanthus* (Figure 6.21) clearly indicated very low ET in year 1, hence this was excluded from site averages to ensure they were representative of the bulk of the crop lifecycle. It was noted in Section 6.3.1 that *Miscanthus* yield was overestimated for the first harvest, which could result in overestimation of ET; Figure 6.21 indicates that values of ET in year 2 are in line with simulation for later years, and thus they were included in site averages, although the possibility that field values of ET may be lower than simulated for this year should be considered when thinking about potential impacts on flood risk during crop establishment. Additionally, the possibility of influx of sediment to rivers during fallow years, or with soil disturbance on removal should be considered when thinking about possible impacts on flood risks. Interannual variation in ET at a site appeared to be similar for *Miscanthus* and previous land use, whereas ET for SRC willow did not correlate with either preceding land use, as can be seen from Figures 6.21 and 6.22 respectively.

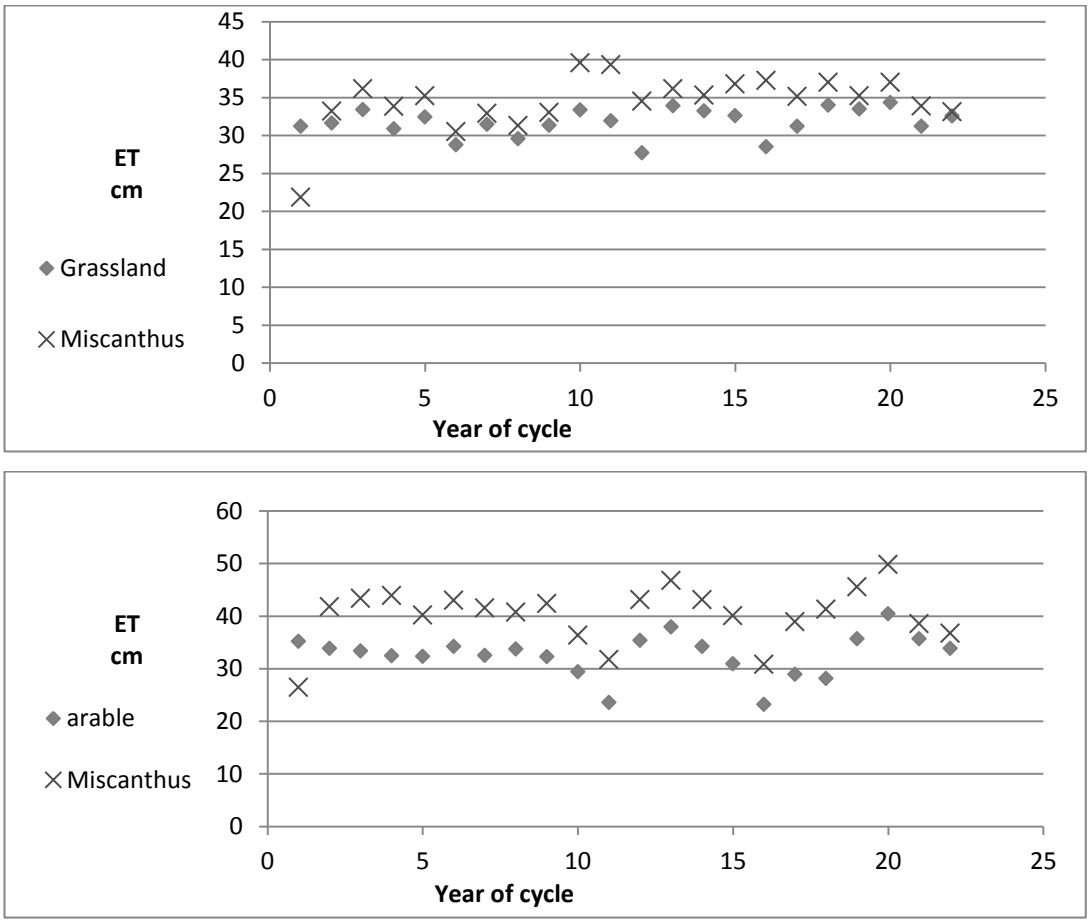

Figure 6.21 Time series data for evapotranspiration (ET) with transition to Miscanthus for an example arable site and an example grassland site.

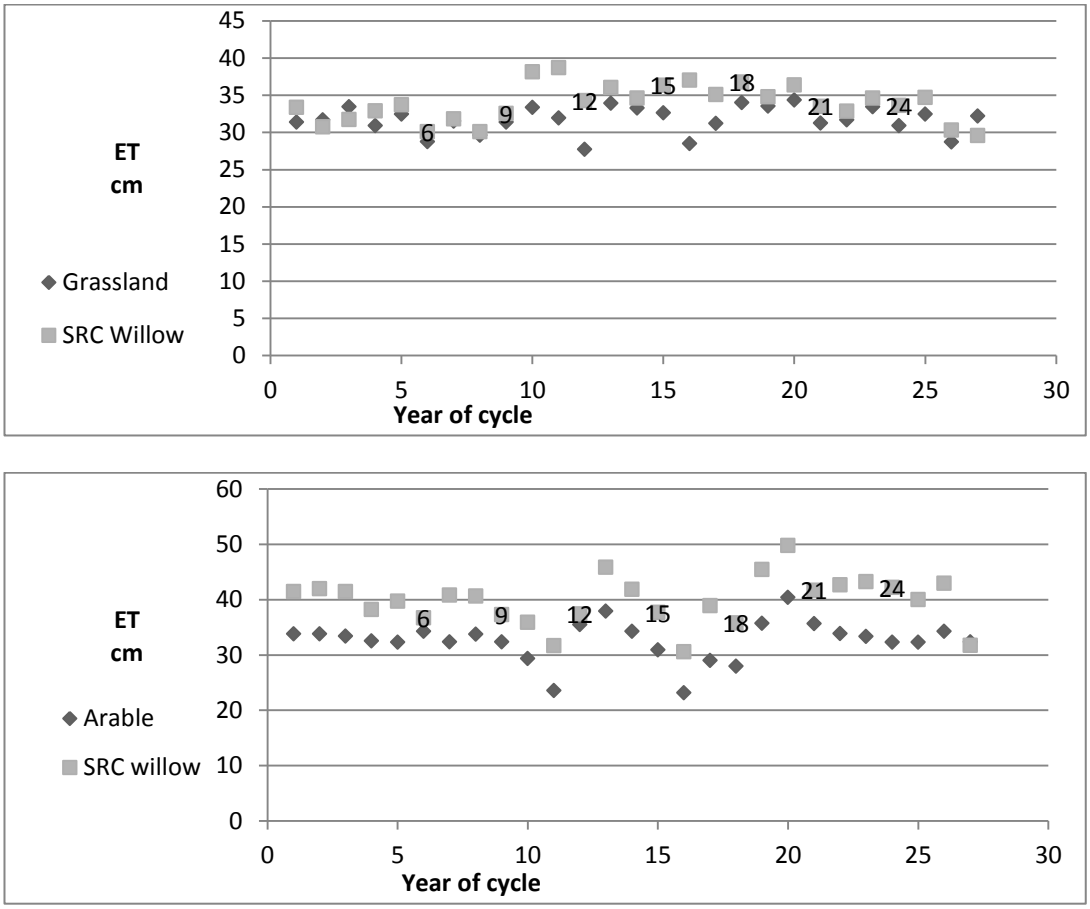

Figure 6.22 Time series data for evapotranspiration (ET) with transition to SRC willow for an example arable site and an example grassland site. Numbered years indicate the year after a coppice event, when crop growth parameters may cause a lower rate of ET.

In addition to climate and other factors causing interannual variation in ET, Borek *et al.* (2010) note that SRC managed systems have lowest ET in the year following coppicing, with annual increase over a three year cycle. The first year after coppicing is labelled in Figure 6.22; although the described pattern of ET is not always observed, there may be interaction between crop factors causing lower ET for labelled years, and climate factors causing additional interannual variation in ET.

For both *Miscanthus* and SRC willow the increased evapotranspiration may be during summer months, when water shortages are more likely; seasonality of water availability must be taken into account when considering the practical implications of changes in evapotranspiration. Therefore, monthly breakdown graphs for each site before and after land use change were also produced; Figures 6.23 and 6.24 show the simulated change in regime for an example arable and grassland site, with transition to *Miscanthus* and SRC willow. These indicate that DayCent simulated increase in ET from months 4 through to 9 or 10 at former arable sites (although the

difference was often negligible in months 6 and 7), and increase in ET from months 3 through to 8 at former grassland sites (although the difference was often negligible in months 5 and 6). In general, increased ET at times of high precipitation may have a positive impact on the catchment by reducing flood risk, whilst increases at times of low precipitation may have negative impacts on ecology and water availability for human usage. For site 4, precipitation is relatively high during the energy crop growing season, whereas for site 9 the precipitation profile is almost the reverse of the evapotranspiration profile; these site differences will affect the impacts of increases in ET. Although in the context of this thesis land use change is modelled at plot scale, findings must be contextualised in terms of local energy crop demand, and the likelihood that feedstock will be grown in a relatively concentrated area, meaning that a small increase in ET over a large area of a catchment may represent a significant volume of water: this will be discussed in Section 6.4.

Simulated timing of ET is dependent on simulated timings of growth, which has not been explicitly validated for SRC willow on a sub-annual scale, hence further work could improve confidence in this output. Additionally, poor simulation of below ground growth during establishment may result in overprediction of water uptake during this time period, and this may also benefit from further work.

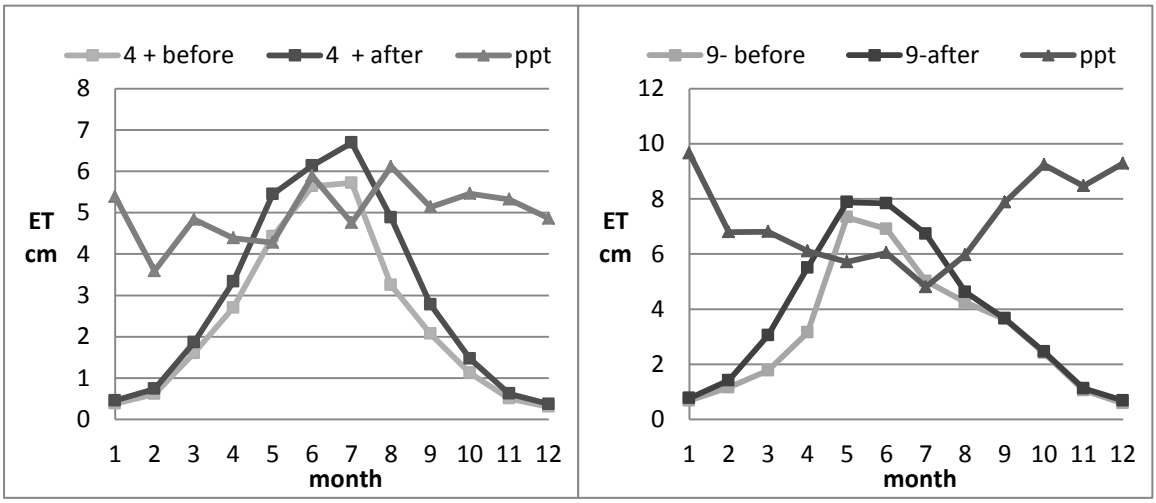

Figure 6.23 Monthly average precipitation and monthly average evapotranspiration (ET) with transition from an example arable site (4+) and an example grassland site (9-) to Miscanthus

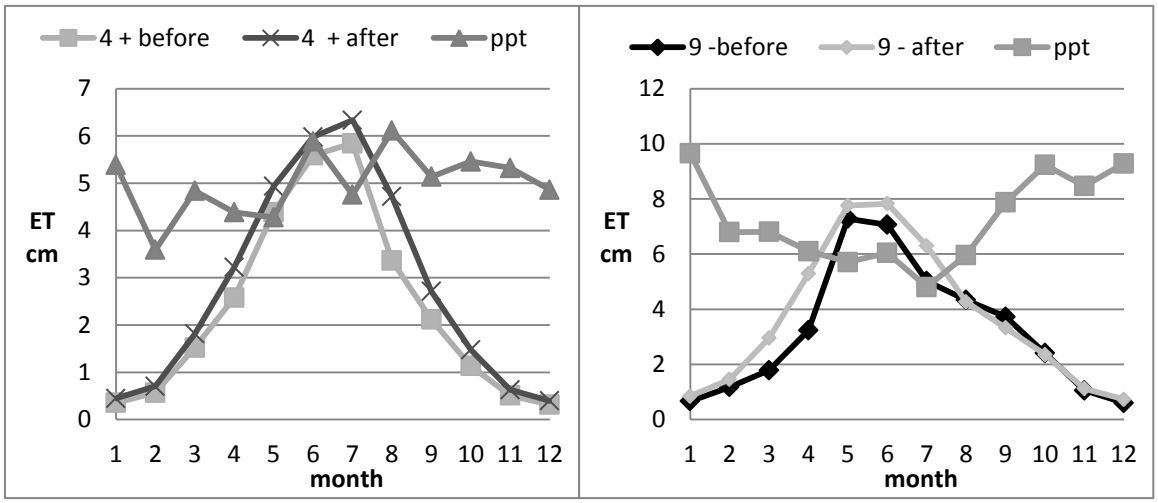

Figure 6.24 Monthly average precipitation and monthly average evapotranspiration (ET) with transition from an example arable site (4+) and an example grassland site (9-) to SRC willow

Change in ET ranged from 1.73 to 8.78 cm a^{-1}, which suggests that reduction in water availability is not necessarily a concern, whereas in some cases, even if water resources are currently plentiful, energy crop cultivation on the scale required for useful generation could cause water shortages to be an issue.

Table 6.13 Statistically significant correlations between ET output and input variables

	ET under *Miscanthus*		**ET under SRC willow**	
	Correlation Coefficient	**Significance (2-tailed)**	**Correlation Coefficient**	**Significance (2-tailed)**
Topsoil clay %	-0.491	0.039	-0.545	0.019
Subsoil sand %	0.396	0.104	0.471	0.049
Months with water table	0.559	0.016	0.485	0.041
Annual precipitation	0.522	0.026	0.516	0.028
Average temperature	0.499	0.035	0.542	0.020
Average maximum temperature	0.566	0.014	0.601	0.008
Average minimum temperature	-0.486	0.041	-0.367	0.134
Yield	0.893	<0.001	0.647	0.004

Table 6.13 indicates a strong relationship between ET and yield for both energy crops, also shown in Figure 6.26. Given the <0.001 significance level for correlation between *Miscanthus* yield and ET, it is possible that the other correlations for ET may largely reflect controls on Yield; Table 6.6 indicated that *Miscanthus* yield also showed strong positive relationships with annual precipitation, average temperature and average maximum temperature, and strong negative

correlation with topsoil clay. The correlation coefficient between SRC willow yield and ET is less strong, and there are fewer shared correlations with inputs. Positive correlations of ET for both energy crops with months with water table and annual precipitation and a negative correlation with topsoil clay content (high clay impedes infiltration) indicate a simulated link to water availability in the soil profile. Positive correlations with temperature variables result from the use of temperature to calculate potential ET (PET). The negative correlation between ET for *Miscanthus* and average minimum temperature is difficult to explain given the use of average minimum temperature to calculate PET. Given the positive correlations with yield, SRC willow and *Miscanthus* should not be located to minimise ET, but to ensure that negative impacts of high ET are minimised, i.e. planting should be favoured in catchments prone to flood risk and minimised in areas with water resource limitations. Given the strong correlations with temperature inputs and yield, there are limits to the potential to extrapolate findings on predicted ET to other sites with similar soil properties.

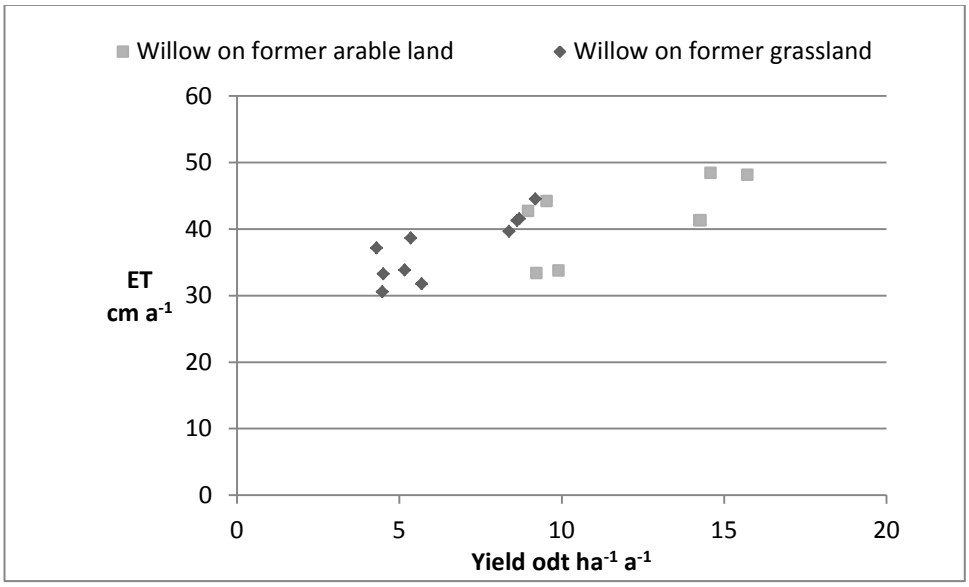

Figure 6.26 Relationship between average annual ET and yield for SRC willow: statistically significant with a coefficient of 0.647; and between average annual ET and yield for Miscanthus: statistically significant with a coefficient of 0. 893

It could be expected that increased water use would coincide with improvement in water quality, as has been observed by Dimitriou *et al.* (2009), due to a reduction in uptake; the model simulated the reverse pattern, due to high levels of simulated N fixation, but it is likely this would not be borne out in the field.

6.4 Spatial variation in benefits of land use change for bioenergy

Yield per hectare is significant in dictating area of land use change required, however as well as land, water must be considered as a finite resource, and it is also useful to consider variation in other land-use change impacts for a given energy generation. Output displayed in Sections 6.3.1 through to 6.3.4 can be synthesised to consider the degree of spatial variation in identified impacts of land use change for bioenergy. Therefore Figures 6.27 through to 6.29 indicate variation between sites in impacts per GJ of electricity generation if feedstock were used for co-firing with coal. Although total energy generation would be much greater if feedstock were used for CHP, coal is a useful metric for comparison of emissions, given that it is replaced directly in co-firing. This section will also discuss issues with extrapolating findings to sites with similar soil properties and precipitation, but different latitude and temperature regime.

Figure 6.27 indicates over 100m^3 per GJ variation in ET associated with feedstock cultivation, and suggests that SRC willow generally has greater ET per GJ, but the reverse is true at sites 7 and 8, which were the highest yielding sites for SRC willow. This may indicate co-benefits of land-use efficiency and water-use efficiency under the conditions modelled for sites 7 and 8. There remains a possibility that ET may be underestimated for SRC willow, as discussed in Section 6.3.4. Given the observation by Jørgensen and Schelde (2001) that per hectare ET is increased for high yielding varieties (although this may not translate to higher ET per odt) this is a particular concern for high yielding sites, where significant areas of cultivation within the same catchment could risk depleting water resources.

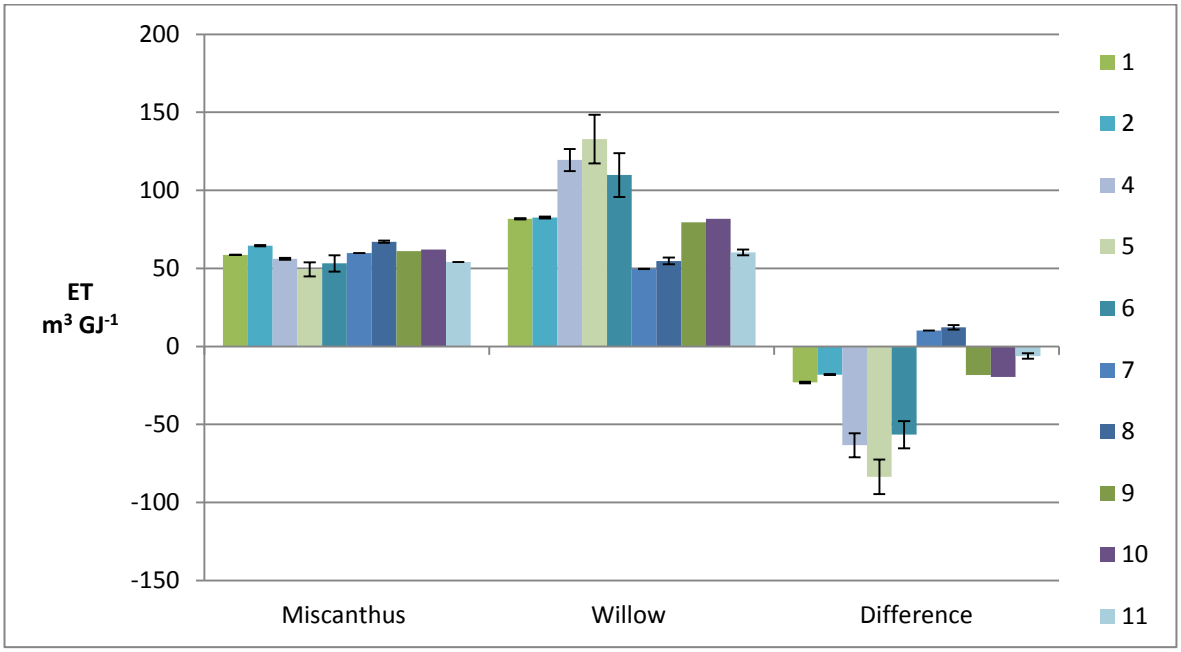

Figure 6.27 Variation between sites in evapotranspiration per GJ of electricity yield, if feedstock were used for co-firing with coal. Evapotranspiration is generally expressed as a depth over the hectare, but is here expressed as volume of water, to account for variation in size of land area required to generate 1 GJ energy. Difference indicates how much more evapotranspiration is associated with Miscanthus cultivation than the same energy generation from willow feedstock cultivated at the same site.

There will be further site specific issues for ET, in terms of whether increased water usage may have beneficial or adverse impacts. Scaling up, for example to meet the demand of 3.7 PJ for 10 % co-firing at West Burton, the nearest co-firing plant to sites 4 and 11, water taken up by ET for feedstock cultivation could range from 53 m^3 GJ^{-1} for cultivation of *Miscanthus* at site 11, which would equate to 1.96 10^8 m^3, up to 126 m^3 GJ^{-1} for cultivation of SRC willow at site 4, which would equate to 4.6610^8 m^3. It is noteworthy that simulated SRC willow yields for site 4 may not be economically feasible even before impacts of ET on local hydrology and water resources are considered.

Figure 6.28 indicates direct N_2O emissions in kg CO_2 equivalents per GJ of electricity yield from the cultivation of both bioenergy feedstocks, variation between sites and crop types is over 13 kg CO_2 equivalents per GJ, which is significant compared to the highest value of around 15 kg CO_2 equivalents per GJ. Emissions are generally greater for the cultivation of SRC willow, except for at the two sites with highest SRC willow yields, again suggesting that benefits may be co-located by maximising yield, and minimising the area of land to supply the same energy.

These N_2O emissions are significantly lower than from the combustion of the coal replaced by these bioenergy feedstocks, which is in the region of 92 kg CO_2 equivalent per GJ (de Mira and Kroeze, 2006): potential total emissions savings will be considered in Chapter 7. Figure 6.29 shows variation in change in N_2O emissions per GJ: reduction in emissions is seen for both crops when grown at the former arable sites (1 to 6) however, displacement of current arable agriculture is likely to counterbalance this, although without knowing if and where such land use change may take place, this cannot be factored in to calculations. Reduction in emissions per GJ are greater for SRC willow feedstock, however, since total emissions per unit energy were generally higher, it is likely that this reflects greater land use, and would thus result in greater displacement of agriculture, and associated emissions. Therefore, whether this appears to be beneficial may be dependent on the inventory approach used, but it should not be regarded as a benefit in decision making.

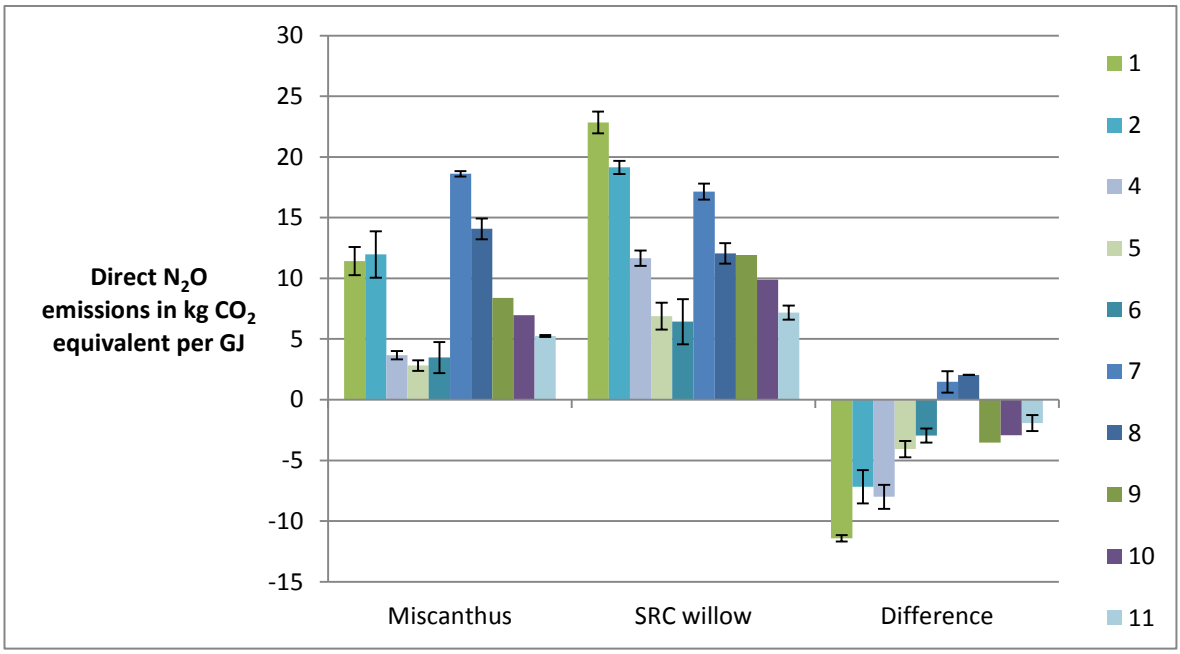

Figure 6.28 Variation between sites in direct N_2O emissions in kg CO_2 equivalents per GJ of electricity yield, if feedstock were used for co-firing with coal. Difference indicates how much more direct N_2O emissions are associated with Miscanthus cultivation than the same energy generation from willow feedstock cultivated at the same site.

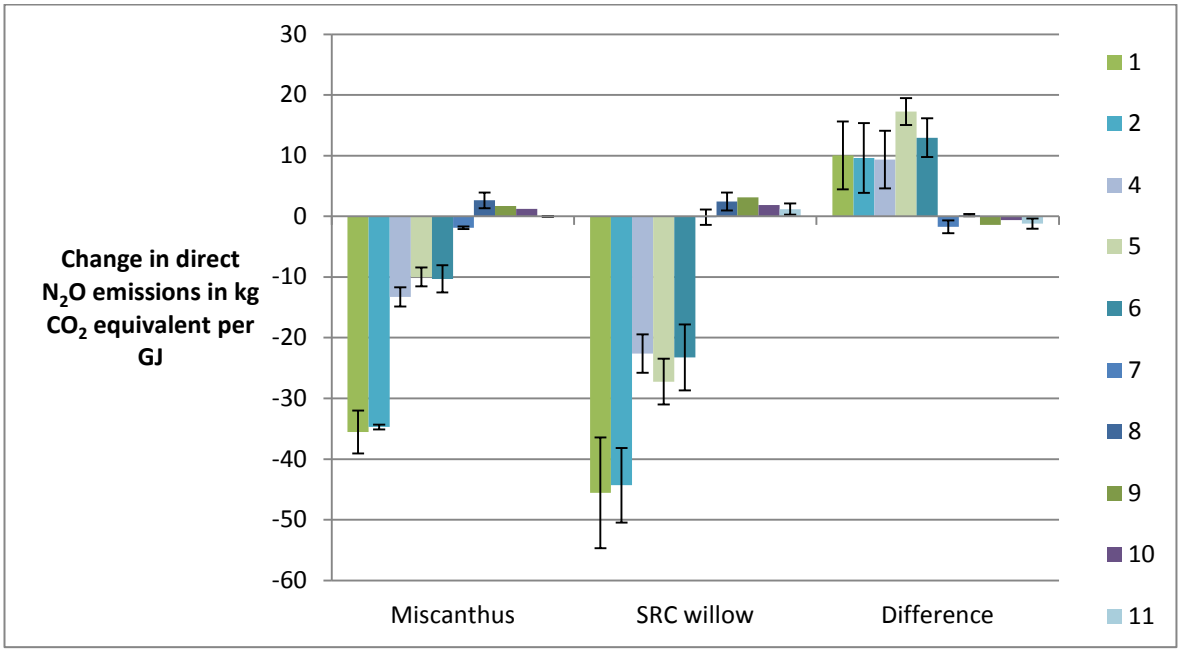

Figure 6.29 Variation between sites in change in direct N_2O emissions in kg CO_2 equivalents per GJ of electricity yield, if feedstock were used for co-firing with coal. Difference indicates how much more direct N_2O emissions are associated with Miscanthus cultivation than the same energy generation from willow feedstock cultivated at the same site.

Figure 6.30 indicates that both energy crops result in SOC sequestration, indicating further benefits in comparison to the 92 kg CO_2 equivalent per GJ associated with coal combustion. For many sites, SOC sequestration attributed to 2 GJ of generation from *Miscanthus* would counterbalance the emissions associated with 1 GJ of coal generation. Whilst encouraging, given that SOC storage is temporary, this should be regarded as an ancillary short term benefit, and it may not be appropriate to include these values in inventories. Again, there is significant variation in SOC storage between sites, and storage is greater for *Miscanthus* than SRC willow for all sites.

In general, modelled benefits are greatest for cultivation of SRC willow at sites 7 and 8, or *Miscanthus* at sites 5 and 6; in terms of maximising energy yield and minimising area of land use change, which tends to also minimise ET and N_2O emissions per unit energy. SOC storage per unit energy was also lowest for cultivation of SRC willow at sites 7 and 8, however this was due to high yields meaning low area of land conversion per unit energy; SOC storage per area of land use change compared favourably to other sites. The process of extrapolating findings from the modelled sites to the database of locations with similar soil properties and precipitation regimes is complicated by identified strong correlations between model output and inputs such as latitude and temperature regime which were not accounted for by the site selection process. Additionally, simulation of previous land use and management is highly generalised, and in particular the wide

range in conditions at former grassland sites may not be well represented. Nonetheless, model output is in theory more informative about impacts at these sites than application of default factors and database values.

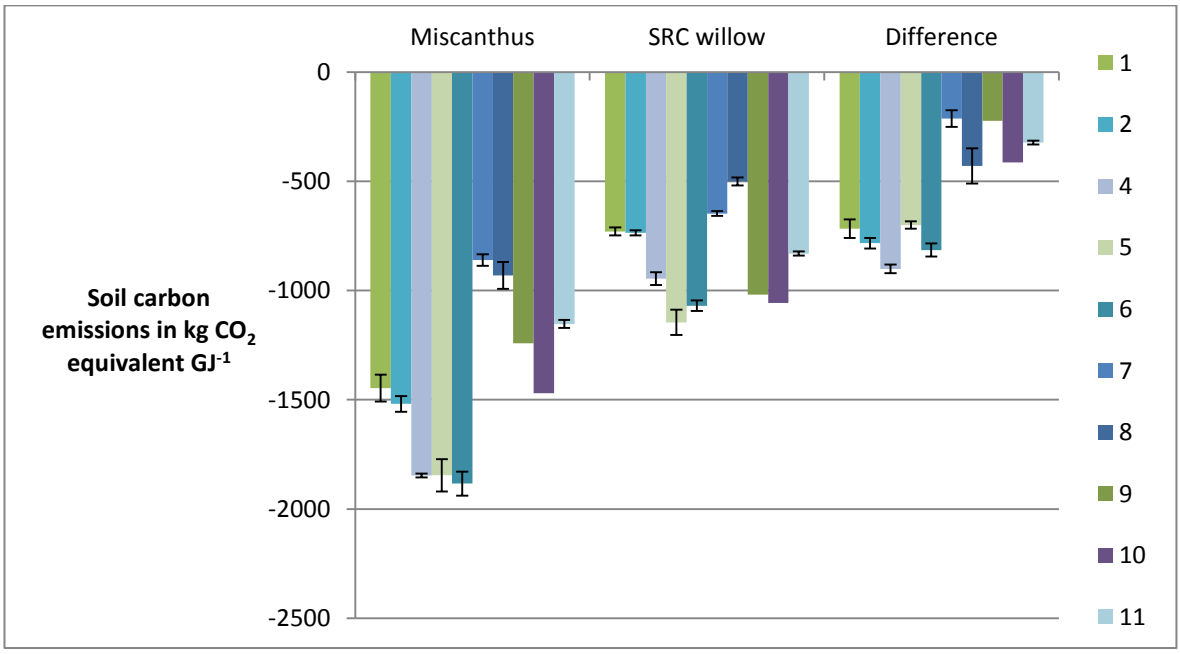

Figure 6.30 Variation between sites in soil carbon emissions in kg CO_2 equivalents per GJ of electricity yield, if feedstock were used for co-firing with coal. Difference indicates how much more soil carbon emissions are associated with Miscanthus cultivation than the same energy generation from willow feedstock cultivated at the same site.

6.5 Discussion of model limitations

Sources of error in model output can be separated into; input data errors and model structural error associated with parameters and algorithms. The model was run using soil input data for the maximum and minimum of the supplied range, in an effort to account for some of the impacts of input error. AWC values were calculated by a tool distributed with the model by applying pedotransfer functions to user defined values for soil textural properties; this approach has been identified as a common source of input error for modelling (Richter, Riche *et al.* 2008), and may have significant impact on model output due to relationships with yield, N_2O emissions and SOC storage as discussed in Sections 6.3.1, 6.3.2 and 6.3.3 respectively.

Weather data may also include errors, owing to use of data from nearby met office sites, as opposed to data collected from the specific location of the modelled site, and the use of a looped

20 year record to represent historic conditions, and future conditions, as opposed to using a complete historic record and projected future weather based on climate change scenarios. The use of looped weather data from a nearby site to represent historic conditions was justified by the intention that model output be indicative of the impacts of land use change at sites similar to the modelled site, as opposed to specific to that site. It would however be useful to consider the impacts of future changes in climate and atmospheric CO_2 on model simulations; predictions of reduced lowland precipitation in future UK climates (e.g. Hulme *et al.*, 2002) may reduce potential energy crop yields, given the correlation with water availability variables for both SRC willow and *Miscanthus*. However reduced stomatal conductance under increased CO_2 levels may be expected to counterbalance this, by reducing demand for water; this will have less impact on C4 crops such as *Miscanthus* (Cure, 1986). C:N ratio may also be expected to increase under elevated CO_2 , reducing crop demand for N, potentially increasing yield for sites where N availability is currently a limiting factor. Schedule files were also intended to represent averaged management and event dates, and do not factor in land management decisions or variation in senescence dates associated with variation in growing season at different latitudes.

In the context of scenario analysis, it is not possible to account for internal model error, although likely contribution to output error can be discussed based on findings from previous studies and identified limitations of the model. Previous work by Del Grosso *et al.* (2010) identified that at an annual, national scale for the US the DayCent 95% confidence interval for simulating N_2O emissions was +50% and -35%, 85% of which was attributed to model structural error, with the remainder reflecting input data. Analysis in Section 4.4.5 identified relative deviation of model output from measurements from - 66 % up to + 660 %; again this was at an annual scale, however resolution of soil input data was finer than available for this scenario analysis.

Soil water is an important control on crop growth representation; hence limitations in model simulation of crop available water can also be considered an important source of uncertainty in model output. As well as being affected by parameter uncertainty in terms of calculation of AWC, and values assigned for rooting depth and presence of water table, crop available water will also be affected by structural uncertainty in the simulation of soil drainage. Inability of DayCent to simulate small-scale variations in drainage and soil texture affects simulation of WFPS, contributing to model error in terms of N_2O emissions simulation, as discussed in Section 4.4.2 and 4.4.3.

Poor simulation of response of WFPS to land management was discussed in Chapter 4; whilst model development resulted in a noticeable improvement in simulation of immediate change in WFPS, longer term changes are more complex. Blanco-Canqui (2010) suggests that bulk density is generally reduced under perennial grasses, whilst Schmer *et al.* (2011) identified site specific variation in the response of soil bulk density to perennials. Since DayCent cannot account for changes to soil structure over time under no tillage, which improve drainage as opposed to increasing soil water availability as discussed in Section 4.2.2, schedule files produced for this study simulated settling following tillage to prepare the site for the energy crop (which caused a variable increase in bulk density) and no subsequent changes. Figure 6.31 indicates the change in bulk density due to tillage and settling up to the start of cultivation of the energy crop; due to calculation of tillage and settling factors based on soil texture, and constraints set on application of these factors, bulk density may be increased or decreased depending on schedule file, initial bulk density value, and soil texture. In general, updated bulk density was lower for former arable sites. Given the impact of the constraints on application of tillage and settling factors, bulk density during the simulation of energy crop growth may be regarded as a model artefact. In practice, the impact of tillage regime on bulk density would be dependent on moisture content at time of tillage as well as the variables included in the calculation (tillage type and soil texture). Furthermore, bulk density following settling will be site specific, and affected by climate and biotic factors, leading to an unpredictable equilibrium value. Further work to calibrate bulk density, could give improved simulation of nitrogen cycling and organic matter decomposition rates before and after land use change.

Since simulation of tillage and settling under arable management results in reduced bulk density for site 4, where lowest SRC willow yields were simulated, it does not appear that the tendency to simulate lower bulk density at grassland sites is directly responsible for the higher yields, however, it remains important to assess the impact this may have on model output.

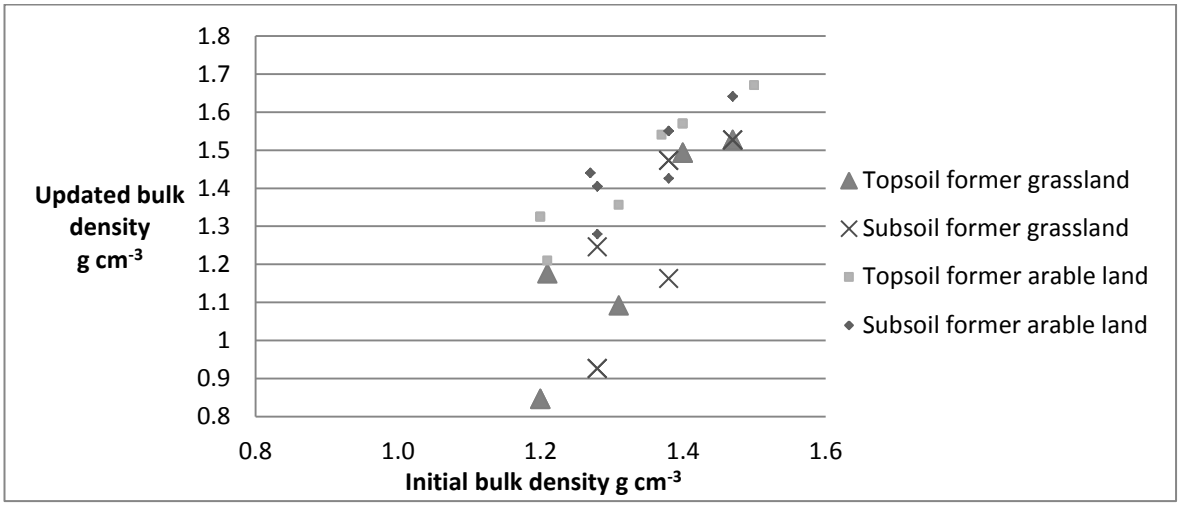

Figure 6.31 Graph to display relationship between initial bulk density and bulk density following spin up and land use change; i.e. during first energy crop lifecycle

Additional model runs were performed for a chosen site to consider:

i) whether reduction in bulk density should have been simulated under energy crops, to account for aggregate formation over time (run b)

ii) whether bulk density increases simulated for some arable sites had a significant impact on output (run c)

Simulations were run for SRC willow, to compare sites 1 and 7, due to similarities in initial site and soil properties, and differences in both calculated bulk density values after simulation of settling, and predicted yields. For site 7, topsoil bulk density was 0.08 lower and subsoil bulk density was 0.48 lower, whilst yield was over 5 odt ha^{-1} a^{-1} greater for the former grassland site. Run b simulated a reduction in bulk density to account for increased aggregate formation one year into land use change to SRC willow. Run c simulated a reduction in settling under the arable land management, which resulted in lower bulk density under previous land use.

It can be seen from Table 6.14 that reducing bulk density during SRC willow growth reduced N_2O emissions and increased SRC willow yield slightly, whereas reducing bulk density under the previous land use reduced N_2O emissions more, and increased yield more, even though bulk density during SRC willow cultivation was not reduced by as much. From comparison with site 7, it does not appear that bulk density is the main control on either output. Figure 6.32 compares soil C for the same set of model runs, and indicates that soil C is higher for 7 than 1 (for both maximum (+) and minimum (-) of the soil textural range) and that reducing settling under the arable land management reduces this difference.

Table 6.14 Comparison of bulk density, lifecycle N_2O emissions and average yield for SRC willow at sites 1 and 7. For site 1, three different versions of the schedule file were tested; the original (1) as described in Section 6.2, 1b, in which bulk density was reduced in year 2 of willow growth and 1c, in which settling was reduced under arable usage. Each schedule file was applied for maximum (+) and minimum (-) of the soil textural range, as described in Section 6.2.

run	+ or -	initial bulk density topsoil	topsoil bulk density during SRC willow growth	initial bulk density subsoil	subsoil bulk density during SRC willow growth	lifecycle N_2O emissions	average yield
1	+	1.40	1.57	1.38	1.55	2.26	8.63
	-	1.20	1.32	1.28	1.40	2.38	8.38
1b	+	1.40	1.30	1.38	1.28	2.18	8.70
	-	1.20	0.98	1.28	1.06	2.10	8.86
1c	+	1.40	1.34	1.38	1.32	2.04	9.13
	-	1.20	0.98	1.28	1.06	1.92	9.31
7	+	1.40	1.49	1.38	1.47	3.03	14.25
	-	1.20	0.85	1.28	0.93	2.81	14.29

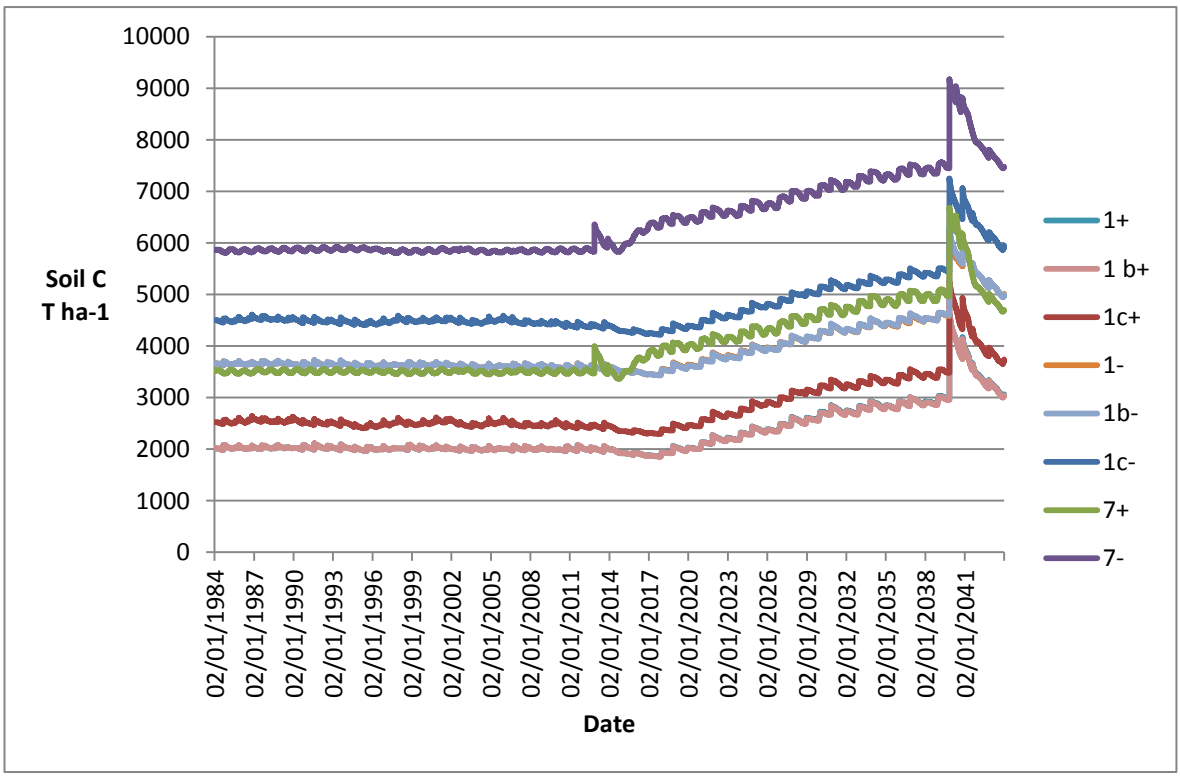

Figure 6.32 Comparison of soil C under SRC willow at sites 1 and 7. For site 1, three different versions of the schedule file were tested; the original (1) as described in Section 6.2, 1b, in which bulk density was reduced in year 2 of willow growth and 1c, in which settling was reduced under arable usage.

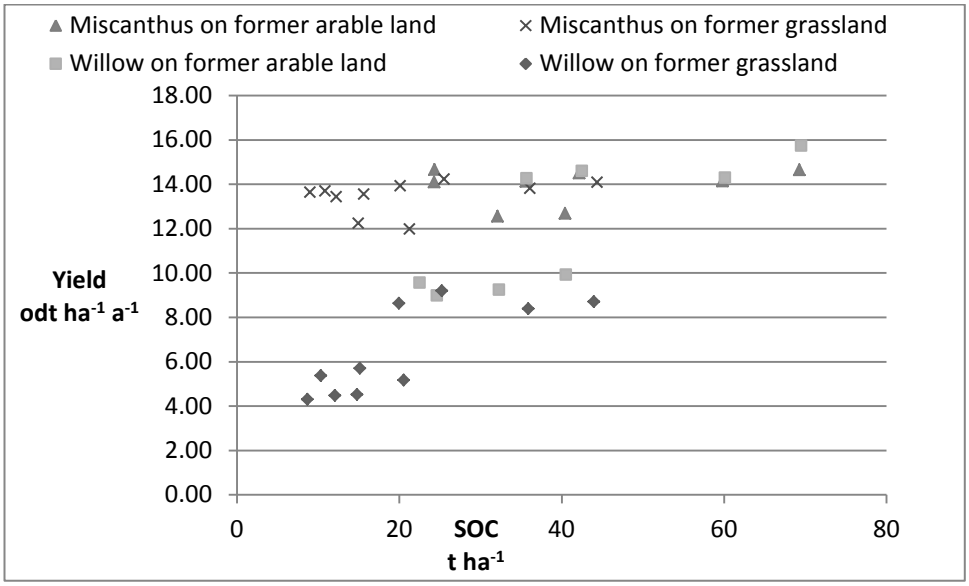

Figure 6.33 Graph to indicate relationship between soil C at land use change and yield. The relationship is stronger for willow, with a correlation coefficient of 0.827 and a significance of <0.001 , compared to a correlation coefficient of 0.513 and a significance of 0.030 for Miscanthus.

Table 6.15 Comparison of field data with simulated soil C for the four sites used in parameterisation of the SRC willow crop model. Failure to simulate field values of C during parameterisation may reduce confidence in model output, however since the same spin up approach was applied to set soil C levels for these parameterisation sites was applied to scenario analysis (as described in Section 6.2), soil C may be underestimated at the scenario analysis sites 1-11 as well, and crop parameters may be set appropriately to simulate yield for underestimated soil C.

Site	TALY	CARR	DEMO	BORE
Field data SOC T/ha	125.57	No data	88.58	57.31
Model output T/ha	30.72	30.72	31.65	39.18
Relative deviation %	-75.54	N/A	-64.27	-31.64

Adler *et al.* (2007) suggest that soil C may be important in determining yield. Given that C and N are coupled in soil organic matter, the strong relationship between soil C and yield observed for SRC willow, as indicated in Figure 6.33, may also reflect a dependence on soil N availability. This relationship may also contribute to the overestimation of SRC willow yields in the second SRC lifecycle (harvest 10 onwards in Figure 6.3). The model was parameterised for SRC willow without calibration of soil C, and Table 6.15 indicates that SOC was underestimated by up to 75%. It is possible that this underprediction of initial soil C at the parameterisation sites may have led to the need for a high value of symbiotic N fixation to match yield. Model verification based on yield data only is commonly applied, e.g. Chamberlain *et al.* (2011) took a very similar approach to use the DayCent model to predict yield, N_2O emissions and changes in system C associated with

switchgrass cultivation, as stated in Section 5.4.2. Similarly regression model approaches in Richter *et al.* (2008) do not account for any impact of SOC on yield.

Although soil C was underestimated for parameterisation sites in Chapter 5 and may also be underestimated in the scenario analysis in this chapter, previous studies applying the same approach to SOC setting have stated that levels were reasonable (Adler, 2007), and within 11% of measured values (Del Grosso S, 2002). Underprediction of soil C at the former arable (1-6) scenario analysis sites may result in underprediction of SRC willow yield, and may have contributed to simulation of yields below economic limits at some of these sites, in spite of high simulated levels of N fixation. As stated in Section 5.5 "high confidence in model output should be limited to simulation of above ground biomass for sites relatively similar to those used in verification"; simulated soil C for the sites with SRC yield below economic values was much lower than that simulated in the calibration studies (8.7 to 20.6 t ha^{-1} compared to 30.7 to 39.2 t ha^{-1} respectively) which may limit confidence in output. Simulation of yields in excess of those observed in the field at former grassland sites was not limited to sites where soil C was outside the range simulated for the calibration sites, since for the sandy end of the soil texture range at site 7, an SRC yield of 14.25 odt ha^{-1} a^{-1} was simulated for starting soil C of 35.6 t ha^{-1}, in a similar range to the calibration sites. In general work to parameterise the SRC willow model for a wider range of site conditions could improve confidence in the yield values simulated in Section 6.3.1.

The rate of N fixation calculated for SRC willow in Chapter 5 may not be considered that high, since Davis *et al.* (2010) identified higher N fixation for *Miscanthus* in a study which did calibrate for soil C. High simulated N fixation for *Miscanthus* may explain the weak relationship between *Miscanthus* yield and soil C in Figure 6.33. It is important to also consider that symbiotic N fixation rates will vary according to soil availability, given the metabolic expense involved, and that potential rates may vary according to geneotype and preparation, and that higher values may be possible in the future with selective breeding (Keymer and Kent, 2013).

In addition to the need to improve calibration of soil C as identified in Section 6.3.3, further work may be necessary to re-set the value of symbiotic N fixation for SRC willow, to account for higher than simulated C, and associated N at the parameterisation sites used in Section 5.4. Improved parameterisation of rates of symbiotic N fixation and improved simulation of soil C during the spin up period would in turn improve the simulation of changes in soil C and N under energy crops; as

mentioned in Section 5.4 low levels simulated for both ammonium and nitrate suggest that N retention may be poorly simulated by the model in general. Some field studies have observed that depletion is a greater risk for former arable sites (Ian Shield Rothamsted personal communication 2013), whereas elsewhere it has been observed that mineralisation resulting from disturbance of grassland in preparation for planting of SRC created an excess of available soil N (Jug, 1999).

Given the likely impact of simulated N fixation on simulated N leaching as postulated in Section 6.3.2, this further work may also be expected to yield improved simulation of N leaching. However, work by Davis *et al.* (2010) to calculate the maximum rate of N fixation for *Miscanthus* included calibration for soil C, and thus may not be altered by this work. Since simulated N leaching for *Miscanthus* was also much greater than field values, it may therefore be expected that there are additional issues with simulation of N leaching which must be addressed.

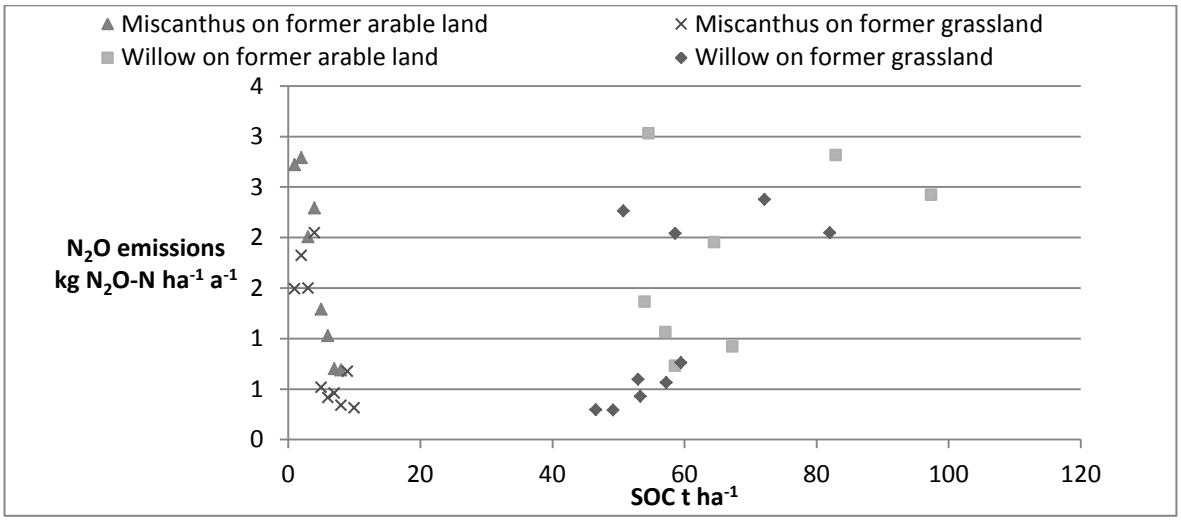

Figure 6.34 Graph to indicate relationship between soil C at land use change and N_2O emissions. The relationship is strong for both crops; willow has a correlation coefficient of 0.789 and a significance of <0.001 , and Miscanthus has a correlation coefficient of 0.853 and a significance of <0.001 .

Figure 6.34 indicates that there is also a strong relationship between soil C at the start of the simulated energy crop cultivation period and simulated direct N_2O emissions. As such, soil C is an additional factor to consider when predicting impacts of land use change for energy crops, and improved model simulation of C should also give more reliable simulation of N_2O emissions.

6.6 Chapter summary

Input data were compiled for 12 sites representative of the typical soil property and land use combinations identified in Chapter 2. Input files for the DayCent model were produced from these data, to be run for the maximum and minimum of soil data value ranges at each site. Analysis was run successfully for most sites, although the model terminated with error messages at sites 3 and 12.

Additional model errors identified during initial assessment of results were; overestimation of yield during *Miscanthus* establishment, and overestimation of SRC willow yields in subsequent lifecycles if removal and replanting is simulated. A more significant issue is simulation of N leaching at levels much higher than those observed by field studies; output for this variable cannot be considered reliable, hence a complete GHG balance cannot be calculated.

The model simulated the greatest benefits from energy crop cultivation where yields were highest, since this minimised associated ET and direct N_2O emissions per unit energy generation. Although SOC storage per unit energy was greater for lower yields, since a greater land area is subject to accumulation, this benefit is temporary, and may not counterbalance the negative impacts of associated indirect land use change for the displaced agriculture. Similarly, reduction in direct N_2O emissions from soil per GJ was greater where lower yields required a greater area of land use change, however, again, this benefit would likely not be upheld once indirect land use change impacts were taken into account.

Extrapolation to other sites with similar soil properties and precipitation was complicated by additional influence from latitude and temperature variables, but this approach should still represent an improvement over the application of a constant EF.

Calibration in Chapter 5 which overlooked SOC resulted in limitations in model performance for SRC willow yield at some sites, and may also limit confidence in other outputs; further work on developing this aspect of the model is recommended.

References

Abdalla, M., Jones, M., Yeluripati, J., Smith, P., Burke, J., Williams, M., 2010. Testing DayCent and DNDC model simulations of N_2O fluxes and assessing the impacts of climate change on the gas flux and biomass production from a humid pasture. Atmospheric Environment 44, 2961-2970.

Abdalla, M., Kumar, S., Jones, M., Burke, J., Williams, M., 2011. Testing DNDC model for simulating soil respiration and assessing the effects of climate change on the CO2 gas flux from Irish agriculture. Global and Planetary Change 78, 106-115.

Adler, P.R., Stephen J. Del Grosso, and William J. Parton, 2007. Life-cycle assessment of net greenhouse-gas flux for bioenergy cropping systems. Ecological Applications 17, 675-691.

Aggarwal, P., Kalra, N., Chander, S., Pathak, H., 2006. InfoCrop: A dynamic simulation model for the assessment of crop yields, losses due to pests, and environmental impact of agro-ecosystems in tropical environments. I. Model description. Agricultural Systems 89, 1-25.

Ahuja, L.R., Fiedler, F., Dunn, G.H., Benjamin, J.G., Garrison, A., 1998. Changes in soil water retention curves due to tillage and natural reconsolidation. Soil Science Society of America Journal 62, 1228-1233.

Akgul, O., Shah, N., Papageorgiou, L.G., 2012. Economic optimisation of a UK advanced biofuel supply chain. Biomass and Bioenergy 41, 57-72.

Alexander, P., Moran, D., Rounsevell, M.D.A., Hillier, J., Smith, P., 2014a. Cost and potential of carbon abatement from the UK perennial energy crop market. GCB Bioenergy 6, 156-168.

Alexander, P., Moran, D., Smith, P., Hastings, A., Wang, S., Sünnenberg, G., Lovett, A., Tallis, M.J., Casella, E., Taylor, G., Finch, J., Cisowska, I., 2014b. Estimating UK perennial

energy crop supply using farm-scale models with spatially disaggregated data. GCB Bioenergy 6, 142-155.

Alexander, R.B., 2002. Estimating the sources and transport of nutrients in the Waikato River Basin, New Zealand. Water Resources Research 38, 12, 14-23.

Alletto, L., Coquet, Y., 2009. Temporal and spatial variability of soil bulk density and near-saturated hydraulic conductivity under two contrasted tillage management systems. Geoderma 152, 85-94.

Almaraz, J.J., Zhou, X., Mabood, F., Madramootoo, C., Rochette, P., Ma, B.-L., Smith, D.L., 2009. Greenhouse gas fluxes associated with soybean production under two tillage systems in southwestern Quebec. Soil and Tillage Research 104, 134-139.

Amichev, B.Y., Hangs, R.D., Van Rees, K.C.J., 2011. A novel approach to simulate growth of multi-stem willow in bioenergy production systems with a simple process-based model (3PG). Biomass and Bioenergy 35, 473-488.

Amthor, J.S., Chen, J.M., Clein, J.S., Frolking, S.E., Goulden, M.L., Grant, R.F., Kimball, J.S., King, A.W., McGuire, A.D., Nikolov, N.T., Potter, C.S., Wang, S., Wofsy, S.C., 2001. Boreal forest CO_2 exchange and evapotranspiration predicted by nine ecosystem process models: Intermodel comparisons and relationships to field measurements. Journal of Geophysical Research 106, 623-648.

An, G.-H., Miyakawa, S., Kawahara, A., Osaki, M., Ezawa, T., 2008. Community structure of arbuscular mycorrhizal fungi associated with pioneer grass species *Miscanthus* sinensis in acid sulfate soils: Habitat segregation along pH gradients. Soil Science and Plant Nutrition 54, 517-528.

Atkinson, C.J., 2009. Establishing perennial grass energy crops in the UK: A review of current propagation options for *Miscanthus*. Biomass and Bioenergy 33, 5, 752–759.

Aylott, M., McDermott, F., 2012. Domestic Energy Crops; Potential and Constraints Review. Project Number: 12-021. A report for DECC. URN: 12D/081, In: Consultants, N.T.B. (Ed.).

Aylott, M.J., Casella, E., Tubby, I., Street, N.R., Smith, P., Taylor, G., 2008. Yield and spatial supply of bioenergy poplar and willow short-rotation coppice in the UK. New Phytologist 178, 358-370.

Azooz, R.H., Arshad, M.A., 1996. Soil infiltration and hydraulic conductivity under long-term no-tillage and conventional tillage systems. Can J Soil Sci 76, 143-152.

Babus'Haq, R.F., Probert, S.D., 1996. Combined Heat-and-Power Implementation in the UK: Past, Present and Prospective Developments. Applied Energy 53, 41-76.

Baggs, E.M.S., M.; Pihlatie, M.; Regar, A.; Cook, H.; Cadisch,G., 2003. Nitrous oxide emissions following application of residues and fertiliser under zero and conventional tillage. Plant and Soil 254, 361-370.

Balasus, A., Bischoff, W.-A., Schwarz, A., Scholz, V., Kern, J., 2012. Nitrogen fluxes during the initial stage of willows and poplars in short-rotation coppices. Journal of Plant Nutrition and Soil Science 175, 729-738.

Ball, B.C., Scott, A., Parker, J.P., 1999. Field N_2O, CO_2 and CH_4 fluxes in relation to tillage, compaction and soil quality in Scotland. Soil & Tillage Research 53, 29-39.

Balland, V., Pollacco, J.A.P., Arp, P.A., 2008. Modeling soil hydraulic properties for a wide range of soil conditions. Ecological Modelling 219, 300-316.

Baresel, C., & Destouni, G. , 2005. Novel quantification of coupled natural and cross-sectoral water and nutrient/pollutant flows for environmental management. Environ Sci Technol 39, 6182-6190.

Baresel, C., Destouni, G., 2006. Estimating subsurface nitrogen accumulation–depletion in catchments by input–output flow analysis. Physics and Chemistry of the Earth, Parts A/B/C 31, 1030-1037.

Basset-Mens, C., Anibar, L., Durand, P., van der Werf, H.M., 2006. Spatialised fate factors for nitrate in catchments: modelling approach and implication for LCA results. The Science of The Total Environment 367, 367-382.

Bateman, E.J., Baggs, E.M., 2005. Contributions of nitrification and denitrification to N_2O emissions from soils at different water-filled pore space. Biology and Fertility of Soils 41, 379-388.

Bauen, A.W., Dunnett, A.J., Richter, G.M., Dailey, A.G., Aylott, M., Casella, E., Taylor, G., 2010. Modelling supply and demand of bioenergy from short rotation coppice and *Miscanthus* in the UK. Bioresource Technology 101, 8132-8143.

Beale, C.V., Long, S.P., 1997. Seasonal dynamics of nutrient accumulation and partitioning in the perennial C4-grasses *Miscanthus* X Giganteus and Spartina Cynosuroides. Biomass and Bioenergy 12, 419-428.

Beaujouan, V.r., Durand, P., Ruiz, L., Aurousseau, P., Cotteret, G., 2002. A hydrological model dedicated to topography-based simulation of nitrogen transfer and transformation: rationale and application to the geomorphology- denitrification relationship. Hydrological Processes 16, 493-507.

Beheydt, D., Boeckx, P., Sleutel, S., Li, C., Vancleemput, O., 2007. Validation of DNDC for 22 long-term N_2O field emission measurements. Atmospheric Environment 41, 6196-6211.

Behnke, G.D., David, M.B., Voigt, T.B., 2012. Greenhouse Gas Emissions, Nitrate Leaching, and Biomass Yields from Production of *Miscanthus* × giganteus in Illinois, USA. BioEnergy Research 5, 801-813.

Bell, M.J., Jones, E., Smith, J., Smith, P., Yeluripati, J., Augustin, J., Juszczak, R., Olejnik, J., Sommer, M., 2011. Simulation of soil nitrogen, nitrous oxide emissions and mitigation scenarios at 3 European cropland sites using the ECOSSE model. Nutrient Cycling in Agroecosystems 92, 161-181.

Berndes, G., 2002. Bioenergy and water—the implications of large-scale bioenergy production for water use and supply. Global Environmental Change 12, 253-271.

Berndes, G., Hansson, J., Egeskog, A., Johnsson, F., 2010. Strategies for 2nd generation biofuels in EU – Co-firing to stimulate feedstock supply development and

process integration to improve energy efficiency and economic competitiveness. Biomass and Bioenergy 34, 227-236.

Berntsen, J., Petersen, B.M., Olesen, J.E., 2006. Simulating trends in crop yield and soil carbon in a long-term experiment—effects of rising CO2, N deposition and improved cultivation. Plant and Soil 287, 235-245.

The UK Department for Business, Enterprise and Regulatory Reform (BERR), 2008. UK Renewable Energy Strategy-consultation. Available at: http://webarchive.nationalarchives.gov.uk/+/http://www.berr.gov.uk/files/file46799.pdf [accessed 1⁄42014].

Bessou, C., Mary, B., Léonard, J., Roussel, M., Gréhan, E., Gabrielle, B., 2010. Modelling soil compaction impacts on nitrous oxide emissions in arable fields. European Journal of Soil Science 61, 348-363.

Blanco-Canqui, H., 2010. Energy Crops and Their Implications on Soil and Environment. Agron J 102, 403-419.

Bøhm, B., Kristjansson, H., Ottosson, U., Rämä, M., Sipilä, K., 2008. District heating distribution in areas with low heat demand density, In: Zinko, H. (Ed.), IEA R&D Programme on “District Heating and Cooling, including the integration of CHP”. IEA.

Bollmark, L., Sennerby-Forsse, L., and Ericsson, T. , 1999. Seasonal dynamics and effects of nitrogen and carbohydrate reserves in cutting-derived Salix viminalis plants. Can. J. For. Res 29, 85-94.

Borek R, F.A., Kozyra J, 2010. Water implications of selected energy crops cultivated on a field scale. Journal of Food Agriculture & Environment 8, 1345-1351.

Bouwman, A.F., 1996. Direct emission of nitrous oxide from agricultural soils. Nutrient Cycling in Agroecosystems 46, 53-70.

Boyd, J., Christerson, L., & Dinkelbach, L., 2000. Energy from willow. SAC.

Boyer, E.W., Alexander, R.B., Parton, W.J., Li, C., Butterbach-Bahl, K., Donner, S.D., Wayne Skaggs, R., J., D.G.S., 2006. Modeling denitrification in terrestrial and aquatic ecosystems at regional scales. Ecological Applications 16, 2123-2142.

Bradford, J.M., Huang, C.-h., 1994. Interrill soil erosion as affected by tillage and residue cover. Soil & Tillage Research 31, 353-361.

Brandão, M., Milà i Canals, L., Clift, R., 2011. Soil organic carbon changes in the cultivation of energy crops: Implications for GHG balances and soil quality for use in LCA. Biomass and Bioenergy 35, 2323-2336.

Brechbill, S.C., Tyner, W.E., Ileleji, K.E., 2011. The Economics of Biomass Collection and Transportation and Its Supply to Indiana Cellulosic and Electric Utility Facilities. BioEnergy Research 4, 141-152.

Brereton, N.J., Pitre, F.E., Shield, I., Hanley, S.J., Ray, M.J., Murphy, R.J., Karp, A., 2013. Insights into nitrogen allocation and recycling from nitrogen elemental analysis and 15N isotope labelling in 14 genotypes of willow. Tree Physiol. tpt081, 00, 1-11

Brisson, N., Gary, C., Justes, E., Roche, R., Mary, B., Ripoche, D., Zimmer, D., Sierra, J., Bertuzzi, P., Burger, P., Bussière, F., Cabidoche, Y.M., Cellier, P., Debaeke, P., Gaudillère, J.P., Hénault, C., Maraux, F., Seguin, B., Sinoquet, H., 2003. An overview of the crop model STICS. Europ. J. Agronomy 18, 309-332.

Brisson, N., Mary, B., Ripoche, D., Jeuffroy, M.H., Ruget, F., Nicoullaud, B., Gate, P., Devienne-Barret, F., Antonioletti, R., Durr, C., Richard, G., Beaudoin, N., Recous, S., Tayot, X., Plenet, D., Cellier, P., Machet, J., Meynard, J.M., Delécolle, R., 1998. STICS: a generic model for the simulation of crops and their water and nitrogen balances. 1. Theory and parameterization applied to wheat and corn. Agronomie 18, 311-346.

Bronick, C.J., Lal, R., 2005. Soil structure and management: a review. Geoderma 124, 3-22.

Brown, L., Syed, B., Jarvis, S.C., Sneath, R.W., Phillips, V.R., Goulding, K.W.T., Li, C., 2002. Development and application of a mechanistic model to estimate emission of nitrous oxide from UK agriculture. Atmospheric Environment 36, 917-928.

Bullard, M.J., Mustill, S.J., McMillan, S.D., Nixon, P.M.I., Carver, P., Britt, C.P., 2002. Yield improvements through modification of planting density and harvest frequency in short rotation coppice Salix spp.—1. Yield response in two morphologically diverse varieties. Biomass and Bioenergy 22, 15–25.

Cadoux, S., Riche, A.B., Yates, N.E., Machet, J.-M., 2012. Nutrient requirements of *Miscanthus* x giganteus: Conclusions from a review of published studies. Biomass and Bioenergy 38, 14-22.

Cannell MGR, M.R., Hargreaves KJ, Brown TA, Cruickshank MM, Bradley RI, Spencer T, Hope D, Billett MF, Adger WN, Subak S., 1999. National inventories of terrestrial carbon sources and sinks: the UK experience. Climatic Change 42, 3 505-530.

Capowiez, Y., Cadoux, S., Bouchant, P., Ruy, S., Roger-Estrade, J., Richard, G., Boizard, H., 2009. The effect of tillage type and cropping system on earthworm communities, macroporosity and water infiltration. Soil and Tillage Research 105, 209-216.

CBD, 2008. The potential impacts of biofuels on biodiversity. Matters arising from SBSTA recommendation XII/7. UNEP/CBD/COP/9/26 Convention on Biological Diversity, 16 pp.

Center for Ecology and Hydrology, 2011. Land Cover Map (1km dominant target class, GB) 2007 Version 1.0, Available at: https://gateway.ceh.ac.uk/download?fileIdentifier=337f9dea-726e-40c7-9f9b-e269911c9db6 [accessed 1/8/2011].© NERC (CEH) 2011. © Crown Copyright 2007. Ordnance Survey Licence number 100017572. © Crown Copyright 2011. Licence number 100,427. © third-party licensors.

Ceulemans, R., A. J. S. McDonald, and J. S. Pereira, 1996. A comparison among eucalypt, poplar and willow characteristics with particular reference to a coppice, growth-modelling approach. Biomass and Bioenergy 11, 215-231.

Chamberlain, J.F., Miller, S.A., Frederick, J.R., 2011. Using DAYCENT to quantify on-farm GHG emissions and N dynamics of land use conversion to N-managed switchgrass in the Southern U.S.. Agriculture, Ecosystems and Environment 141, 332-341.

Chatskikh, D., Olesen, J.E., 2007. Soil tillage enhanced CO2 and N_2O emissions from loamy sand soil under spring barley. Soil and Tillage Research 97, 5-18.

Chatskikh, D., Olesen, J.E., Berntsen, J., Regina, K., Yamulki, S., 2005. Simulation of Effects of Soils, Climate and Management on N_2O Emission from Grasslands. Biogeochemistry 76, 395-419.

Chatskikh, D., Olesen, J.E., Hansen, E.M., Elsgaard, L., Petersen, B.M., 2008. Effects of reduced tillage on net greenhouse gas fluxes from loamy sand soil under winter crops in Denmark. Agriculture, Ecosystems & Environment 128, 117-126.

Chen, D., Li, Y., Grace, P., Mosier, A.R., 2008. N_2O emissions from agricultural lands: a synthesis of simulation approaches. Plant and Soil 309, 169-189.

Chen, S.-J., Hwang, C.-L., 1992. Fuzzy Multiple Attribute Decision Making: Methods and Applications. Springer, Berlin.

Chen, Y., S. Tessier, and J. Gallichand, 1998a. Estimates of tillage effects on saturated hydraulic conductivity. Canadian Agricultural Engineering 40, 169-178.

Chen, Y., Tessier, S., Rouffignat, J., 1998b. Soil bulk density estimation for tillage systems and soil textures. Transactions of the American society of engineers. 41, 1601-1610.

Cherubini, F., 2010. GHG balances of bioenergy systems – Overview of key steps in the production chain and methodological concerns. Renewable Energy 35, 1565-1573.

Cherubini, F., Bird, N.D., Cowie, A., Jungmeier, G., Schlamadinger, B., Woess-Gallasch, S., 2009. Energy- and greenhouse gas-based LCA of biofuel and bioenergy systems: Key issues, ranges and recommendations. Resources, Conservation and Recycling 53, 434-447.

Chicco, G., Mancarella, P., 2009. Distributed multi-generation: A comprehensive view. Renewable and Sustainable Energy Reviews 13, 535-551.

Chirinda, N., Kracher, D., Lægdsmand, M., Porter, J.R., Olesen, J.E., Petersen, B.M., Doltra, J., Kiese, R., Butterbach-Bahl, K., 2010. Simulating soil N_2O emissions and

heterotrophic CO2 respiration in arable systems using FASSET and MoBiLE-DNDC. Plant and Soil 343, 139-160.

Christensen, L., Riley, W.J., Ortiz-Monasterio, I., 2006. Nitrogen Cycling in an Irrigated Wheat System in Sonora, Mexico: Measurements and Modeling. Nutrient Cycling in Agroecosystems 75, 175-186.

Christian, D., Poulton, P., Riche, A., Yates, N., Todd, A., 2006. The recovery over several seasons of 15N-labelled fertilizer applied to *Miscanthus*×giganteus ranging from 1 to 3 years old. Biomass and Bioenergy 30, 125-133.

Christian, D., Riche, A., Yates, N., 2008a. Growth, yield and mineral content of *Miscanthus*×giganteus grown as a biofuel for 14 successive harvests. Industrial Crops and Products 28, 320-327.

Christian DG, P.P., Riche AB, Yates NE. , 1997. The recovery of 15N-labelled fertilizer applied to *Miscanthus* giganteus. Biomass and BioEnergy 12, 21-24.

Christian, D.G., Riche, A.B., 1998. Nitrate leaching losses under *Miscanthus* grass planted on a silty clay loam soil. Soil Use and Management 14, 131-135.

Christian, D.G., Riche, A.B., Yates, N.E., 2008b. Growth, yield and mineral content of *Miscanthus*×giganteus grown as a biofuel for 14 successive harvests. Industrial Crops and Products 28, 320-327.

Chum, H., A. Faaij, J. Moreira, G. Berndes, P. Dhamija, H. Dong, B. Gabrielle, A. Goss Eng, W. Lucht, M. Mapako, O. Masera Cerutti, T. McIntyre, T. Minowa, K. Pingoud, 2011. Bioenergy. In IPCC Special Report on Renewable Energy Sources and Climate Change Mitigation [O. Edenhofer, R. Pichs-Madruga, Y. Sokona, K. Seyboth, P. Matschoss, S. Kadner, T. Zwickel, P. Eickemeier, G. Hansen, S. Schlömer, C. von Stechow (eds)]. Cambridge University Press, Cambridge, United Kingdom and New York, NY, USA.

Clair, S., Hillier, J., Smith, P., 2008. Estimating the pre-harvest greenhouse gas costs of energy crop production. Biomass and Bioenergy 32, 442-452.

Clifton-Brown, J.C., Breuer, J., Jones, M.B., 2007. Carbon mitigation by the energy crop, *Miscanthus*. Global Change Biology 13, 2296-2307.

Clifton-Brown, J.C., Lewandowski, I., Andersson, B., Basch, G., Christian, D.G., Kjeldsen, J.B., Jorgensen, U., Mortensen, J.V., Riche, A.B., Schwarz, K.U., Tayebi, K., Teixeira, F., 2001. Performance of 15 *Miscanthus* genotypes at five sites in Europe. Agron J 93, 1013-1019.

Crow, P., Houston, T.J., 2004. The influence of soil and coppice cycle on the rooting habit of short rotation poplar and willow coppice. Biomass and Bioenergy 26, 497-505.

Culman, S.W., DuPont, S.T., Glover, J.D., Buckley, D.H., Fick, G.W., Ferris, H., Crews, T.E., 2010. Long-term impacts of high-input annual cropping and unfertilized perennial grass production on soil properties and belowground food webs in Kansas, USA. Agr Ecosyst Environ 137, 13-24.

Cure, J.D., Acock. B., 1986. Crop responses to carbon dioxide doubling: A literature survey. Agricultural and Forest Meteorology 38, 127-145.

Curley, E.M., O'Flynn, M.G., McDonnell, K.P., 2009. Nitrate leaching losses from *Miscanthus* x giganteus impact on groundwater quality. J. Agronomy 8, 107-112.

Danalatos, N., Archontoulis, S., Mitsios, I., 2007. Potential growth and biomass productivity of *Miscanthus*×giganteus as affected by plant density and N-fertilization in central Greece. Biomass and Bioenergy 31, 145-152.

Dao, T.H., 1998. Tillage and crop residue effects on carbon dioxide evolution and carbon storage in a Paleustoll. Soil Sci. Soc. Am. J. 62, 250-256.

David, M.B., J., S., Grosso, D., Hu, X., Marshall, E.P., McIsaac, G.F., Parton, W.J., Tonitto, C., Youssef, M.A., 2009. Modeling denitrification in a tile-drained, corn and soybean agroecosystem of Illinois, USA. Biogeochemistry 93, 7-30.

Davidson, E.A., Potter, C.S., Schlesinger, P., Klooster, S.A., 1998. Model estimates of regional nitric oxide emissions from Soils of the Southeastern United States. Ecological Applications 8, 748-759.

Davis, S.C., Parton, W.J., Dohleman, F.G., Smith, C.M., Grosso, S.D., Kent, A.D., DeLucia, E.H., 2010. Comparative Biogeochemical Cycles of Bioenergy Crops Reveal

Nitrogen-Fixation and Low Greenhouse Gas Emissions in a *Miscanthus* × giganteus Agro-Ecosystem. Ecosystems 13, 144-156.

Davis, S.C., Parton, W.J., Grosso, S.J.D., Keough, C., Marx, E., Adler, P.R., DeLucia, E.H., 2012. Impact of second-generation biofuel agriculture on greenhouse-gas emissions in the corn-growing regions of the US. Frontiers in Ecology and the Environment 10, 69-74.

de Fraiture, C., Giordano, M., Liao, Y., 2008. Biofuels and implications for agricultural water use: blue impacts of green energy. Water Policy 10, 1, 67-81.

de Fraiture, C., Berndes, G., 2008. Biofuels: Environmental Consequences and Interactions with Changing Land Use; Biofuels and Water, In: Howarth, R.W., Bringezu, S. (Eds.), Scientific Committee on Problems of the Environment (SCOPE) International Biofuels Project Rapid Assessment, Gummersbach Germany.Cornell University, Ithaca NY, USA, pp. 139-142.

de Fraiture, C.d., Berndes, G., 2009. Biofuels and water. Pages 139-153 in R.W. Howarth and S. Bringezu (eds.) Biofuels: Environmental Consequences and Interactions with Changing Land Use. Proceedings of the Scientific Committee on Problems of the Environment (SCOPE) International Biofuels Project Rapid Assessment, 22-25 September 2008, Gummersbach Germany. Cornell University, Ithaca NY, USA. (http://cip.cornell.edu/biofuels/).

de Mira, R.R., Kroeze, C., 2006. Greenhouse gas emissions from willow-based electricity: a scenario analysis for Portugal and The Netherlands. Energy Policy 34, 1367-1377.

de Vries, S.C., van de Ven, G.W.J., van Ittersum, M.K., Giller, K.E., 2010. Resource use efficiency and environmental performance of nine major biofuel crops, processed by first-generation conversion techniques. Biomass and Bioenergy 34, 588-601.

De Vries, W., Kros, J., Kuikman, P.J., Velthof, G.L., Voogd, J.C.H., Wieggers, H.J.J., Butterbach-Bahl, K., Denier Van Der Gon, H.A.C., Van Amstel, A.R., 2005. Use of

measurements and models to improve the national IPCC based assessments of soil emissions of nitrous oxide. Environmental Sciences 2, 217-233.

Deckmyn, G., Laureysens, I., Garcia, J., Muys, B., Ceulemans, R., 2004. Poplar growth and yield in short rotation coppice: model simulations using the process model SECRETS. Biomass and Bioenergy 26, 221-227.

Defra, 2007. Department for Environment, Food and Rural Affairs (DEFRA) UK Biomass Strategy, Available at: http://www.biomassenergycentre.org.uk/pls/portal/docs/PAGE/RESOURCES/REF_LIB_RES/PUBLICATIONS/UKBIOMASSSTRATEGY.PDF. [accessed 17/10/2011], p. 49.

Del Grosso, S., Mosier, A., Parton, W., Ojima, D., 2005. DAYCENT model analysis of past and contemporary soil NO and net greenhouse gas flux for major crops in the USA. Soil and Tillage Research 83, 9-24.

Del Grosso S.J., Parton W.J., Mosier A.R., Peterson G., Schimel D., 2002. Simulated effects of dryland cropping intensification on soil organic matter and greenhouse gas exchanges using the DAYCENT ecosystem model. . Environmental Pollution 116, 75-83.

Del Grosso, S.J., Halvorson, A.D., Parton, W.J., 2008. Testing DAYCENT Model Simulations of Corn Yields and Nitrous Oxide Emissions in Irrigated Tillage Systems in Colorado. Journal of Environment Quality 37, 4, 1383-1389.

Del Grosso, S.J., Ogle, S.M., Parton, W.J., Breidt, F.J., 2010. Estimating uncertainty in N_2O emissions from US cropland soils. Global Biogeochemical Cycles 24, 1 pp 12.

Del Grosso, S.J., Parton, W.J., Mosier, A.R., Ojimal, D.S., Kulmala, A.E., Phongpan, S., 2000. General model for N_2O and N_2 gas emissions from soils due to dentrification. Global Biogeochemical Cycles 14, 1045-1060.

Del Grosso, S.J., Wirth, T., Ogle, S. M., & Parton, W. J. , 2008. Estimating Agricultural Nitrous Oxide Emissions. Transactions American Geophysical Union 89, 529-529.

Delgado, J.A., Del Grosso, S.J., Ogle, S.M., 2010. 15N isotopic crop residue cycling studies and modeling suggest that IPCC methodologies to assess residue contributions to N_2O-N emissions should be reevaluated. Nutrient Cycling in Agroecosystems 86, 383-390.

Delgrosso, S., Mosier, A., Parton, W., Ojima, D., 2005. DAYCENT model analysis of past and contemporary soil NO and net greenhouse gas flux for major crops in the USA. Soil and Tillage Research 83, 9-24.

Delon, C., SerÇA, D., Boissard, C., Dupont, R., Dutot, A., Laville, P., De Rosnay, P., Delmas, R., 2007. Soil NO emissions modelling using artificial neural network. Tellus B 59, 502-513.

Department for Environment Food and Rural Affairs, 2007. *Miscanthus* Growers' Handbook.

Department for Environment Food and Rural Affairs, 2011. TRP - Technical Report : UK Agricultural GHG Inventory 2011 projections summary v3 http://randd.defra.gov.uk/Default.aspx?Menu=Menu&Module=More&Location=None&Completed=0&ProjectID=15542

Department for Environment Food and Rural Affairs, 2012. Agriculture in the UK, Available at: http://www.defra.gov.uk/statistics/foodfarm/cross-cutting/auk/ [accessed 1/10/2013].

Department for Transport, 2011. Biofuel statistics: Year 3 (2010 to 2011), Biofuels statistics https://www.gov.uk/government/publications/biofuels-statistics-quarterly-year-to-april-2011. [accessed 22 March 2014].

Department of Energy & Climate Change, D.f.E., Food & Rural Affairs, Department for Transport, 2012. UK Bioenergy Strategy. Department of Energy & Climate Change, London.

Department of Energy and Climate Change, 2010. UK energy consumption statistics, Available at: http://www.decc.gov.uk/en/content/cms/statistics/publications/ecuk/ecuk.aspx [accessed 23/3/2011].

Department of Energy and Climate Change, 2011. Renewable Heat Incentive, Available at: http://www.decc.gov.uk/assets/decc/What%20we%20do/UK%20energy%20supply/Energy%20mix/Renewable%20energy/policy/renewableheat/1387-renewable-heat-incentive.pdf [accessed 1/4/2011].

Department of Energy and Climate Change, 2011 UK Energy Sector Indicators. URN 11D/193. http://www.decc.gov.uk/assets/decc/11/stats/publications/indicators/3327-uk-energy-sector-indicators-2011.pdf [accessed 1/4/2011].

Department of Energy and Climate Change, 2012. Digest of UK Energy Statistics (DUKES), Chapter 7, Available at: http://www.decc.gov.uk/en/content/cms/statistics/energy_stats/source/chp/chp.aspx [accessed 20/09/12].

Department of Energy and Climate Change, 2013a. Digest of UK Energy Statistics (DUKES), Chapter 6, Available at :https://www.gov.uk/government/publications/digest-of-united-kingdom-energy-statistics-dukes-2013-printed-version-excluding-cover-pages [accessed 20/09/13].

Department of Energy and Climate Change, 2013b. https://www.gov.uk/government/news/new-biomass-sustainability-criteria-to-provide-certainty-for-investors-to-2027 [accessed 1/2/2014]

Derpsch, R., Friedrich, T., Kassam, A., & Hongwen, L. , 2010. Current status of adoption of no-till farming in the world and some of its main benefits. Int J Agric & Biol Eng 3, 1 - 25.

Dimitriou, G., Busch, S., Jacobs, P., Schmidt-Walter, N., 2009. A review of the impacts of Short Rotation Coppice cultivation on water issues Landbauforschung vTI. Agriculture and Forestry Research 59, 197-206.

DNDC User Guide, 2009. User's Guide for the DNDC Model. Version 9.3. Institute for the Study of Earth, Oceans and Space. University of New Hampshire.

Dockerty, T., Appleton, K., Lovett, A., 2012. Public opinion on energy crops in the landscape: considerations for the expansion of renewable energy from biomass. Journal of Environmental Planning and Management 55, 1134-1158.

Doltra, J., Lægdsmand, M., Olesen, J.E., 2010. Cereal yield and quality as affected by nitrogen availability in organic and conventional arable crop rotations: A combined modeling and experimental approach. European Journal of Agronomy. 34, 2, 83–95

Don, A., Osborne, B., Hastings, A., Skiba, U., Carter, M.S., Drewer, J., Flessa, H., Freibauer, A., Hyvönen, N., Jones, M.B., Lanigan, G.J., Mander, Ü., Monti, A., Djomo, S.N., Valentine, J., Walter, K., Zegada-Lizarazu, W., Zenone, T., 2012. Land-use change to bioenergy production in Europe: implications for the greenhouse gas balance and soil carbon. GCB Bioenergy 4, 372-391.

Dondini, M., Van Groenigen, K.-J., Del Galdo, I., Jones, M.B., 2009. Carbon sequestration under *Miscanthus*: a study of 13C distribution in soil aggregates. GCB Bioenergy 1, 321-330.

Doty, S.L., Brian Oakley, Gang Xin, Jun Won Kang, Glenda Singleton, Zareen Khan, Azra Vajzovic, and James T. Staley, 2009. Diazotrophic endophytes of native black cottonwood and willow. Symbiosis 47, 23-33.

Drewer, J., Finch, J.W., Lloyd, C.R., Baggs, E.M., Skiba, U., 2012. How do soil emissions of N_2O, CH_4 and CO_2 from perennial bioenergy crops differ from arable annual crops? GCB Bioenergy 4, 408-419.

Drigo, R., Masera, O.R., Trossero, M.A., 2002. Woodfuel integrated supply/demand overview mapping—WISDOM: a geographical representation of woodfuel priority areas. Unasylva 211, 36-40.

Drury, C.F., Yang, X.M., Reynolds, W.D., Tan, C.S., 2004. Influence of crop rotation and aggregate size on carbon dioxide production and denitrification. Soil and Tillage Research 79, 87-100.

DS4DS, 2013. Project. available at: http://www.ds4ds.org [accessed 10/1/2014].

Dufossé, K., Gabrielle, B., Drouet, J.-L., Bessou, C., 2012. Using Agroecosystem Modeling to Improve the Estimates of N_2O Emissions in the Life-Cycle Assessment of Biofuels. Waste and Biomass Valorization 4, 593-606.

Eckert B., Kirchhof G, Halbritter A, Stoffels M, Hartmann A., 2001. Azospirillum doebereinerae sp nov., a nitrogen fixing bacterium associated with the C-4-grass *Miscanthus*. Int J Syst Evol Microbiol 51, 17-26.

Edwards R., Neuwahl F, Mahieu V, 2008. Biofuels in the European context: Facts and uncertainties. , In: European Commission, J.R.C. (Ed.), Brussels.

Ekholm, P., 2005. Phosphorus loss from different farming systems estimated from soil surface phosphorus balance. Agriculture, Ecosystems & Environment 110, 266-278.

Elmi, A., Madramootoo, C., Hamel, C., & Liu, A., 2003. Denitrification and nitrous oxide to nitrous oxide plus dinitrogen ratios in the soil profile under three tillage systems. Biology and Fertility of Soils 38, 340-348.

Elowson, S., 1999. Willow as a vegetation filter for cleaning of polluted drainage water from agricultural land. Biomass Bioenergy 16, 281-290.

Environment Agency, 2013. Environment Agency Geostore http://www.geostore.com/environment-agency/WebStore?xml=environment-agency/xml/ogcDataDownload.xml [accessed 8/12/2013].

Environment Agency, 2013b. Catchment abstraction management strategies (CAMS) http://www.environment-agency.gov.uk/business/topics/water/119927.aspx 7/12/2013.

European Commission - Joint Research Centre, Institute for Environment and Sustainability, 2013. European Soil Database v2 Raster Library, © European Communities, 1995-2013. Last updated: 6/9/2013 http://eusoils.jrc.ec.europa.eu/projects/ProjectsData.html.

European Commission, 2008a. Document SEC 85 V2; accompanying the package of implementation measures for the EU's objectives on climate change and renewable energy for 2020.

European Commission, 2008b. Proposal for a Directive of the European Parliament and of the Council on the promotion of the use of energy from renewable sources.

Falster, H. Gamborg, C., Gundersen, P., Hansen, L., Heding, N., Houmann Jakobsen, H., Kofman, P., Nikolaisen, L., Thomsen, I. M. 2002. CHP and Power Plants, In: Serup, H. (Ed.), Wood for Energy Production. Technology - Environment - Economy. Danish centre for biomass.

Fargione, J., Hill, J., Tilman, D., Polasky, S., Hawthorne, P., 2008. Land Clearing and the Biofuel Carbon Debt. Science 319, 1235-1238.

Farina, R., Seddaiu, G., Orsini, R., Steglich, E., Roggero, P.P., Francaviglia, R., 2011. Soil carbon dynamics and crop productivity as influenced by climate change in a rainfed cereal system under contrasting tillage using EPIC. Soil and Tillage Research 112, 36-46.

Farmer's Weekly Interactive, 2011. Contracts aim to entice more *Miscanthus* growers. Available at: http://www.fwi.co.uk/Articles/26/08/2011/128649/Contracts-aim-to-entice-more-*Miscanthus*-growers.htm [accessed 26/10/12].

Farmer's Weekly Interactive, 2012. Renewables gathers pace at Cereals. Available at: http://www.fwi.co.uk/Articles/16/05/2012/132935/Renewables-gathers-pace-at-Cereals.htm [accessed 26/10/12].

Farrell AE, P.R., Turner BT, Jones AD, O'Hare M, Kammen DM., 2006. Ethanol can contribute to energy and environmental goals. Science 311, 506-508.

Finch, J.W., Hall, R.L., Rosier, P.T.W., Clark, D.B., Stratford, C., Davies, H.N., Marsh, T.J., Roberts, J.M., Riche, A., Christian, D., 2004. The hydrological impacts of energy crop production in the UK. Final report. CEH Project Number: C01937, 151pp.

Finch, J.W., Karp, A., McCabe, D.P.M., Nixon, S., Riche, A.B., Whitmore, A.P., 2009. *Miscanthus*, short-rotation coppice and the historic environment. Available at: http://nora.nerc.ac.uk/7566/1/EngHerit_Report_final.pdf [accessed 6/7/13].

Finney, K.N., Sharifi, V.N., Swithenbank, J., 2012. The negative impacts of the global economic downturn on funding decentralised energy in the UK. Energy Policy 51, 290-300.

Firbank, L.G., 2008. Assessing the Ecological Impacts of Bioenergy Projects. BioEnergy Research 1, 12-19.

Foereid, B., Bellamy, P.H., Holden, A., Kirk, G.J.D., 2012. On the initialization of soil carbon models and its effects on model predictions for England and Wales. European Journal of Soil Science 63, 32-41.

Foereid, B., de Neergaard, A., Høgh-Jensen, H., 2004a. Turnover of organic matter in a *Miscanthus* field: effect of time in *Miscanthus* cultivation and inorganic nitrogen supply. Soil Biology and Biochemistry 36, 1075-1085.

Foereid, B., Deneergaard, A., Hoghjensen, H., 2004b. Turnover of organic matter in a *Miscanthus* field: effect of time in *Miscanthus* cultivation and inorganic nitrogen supply. Soil Biology and Biochemistry 36, 1075-1085.

Forestry Commission, 2013. UK biomass power stations. Version 1.4 March 2013 ed.

Fornara, D.A.a.T., D., 2009. Ecological mechanisms associated with the positive diversity–productivity relationship in an N-limited grassland. Ecology Letters 90, 408-418.

Thornton, F., Bock, B., Bandaranayake, W., Tyler, D., Pettry, D., Green, T., Makik, R., Bingham, L., Houston, A., Shires, M., Dewey, J., 1998. Soil and Water Quality Aspects of Herbaceous and Woody Energy Crop Productions: Lessons from Research-Scale Comparisons with Agricultural Crops. Paper presented at BioEnergy '98: Expanding Bioenergy Partnerships, Madison, Wisconsin, October 4-8, .

Franzluebbers, A.J., Hons, F.M., Zuberer, D.A., 1995. Tillage and crop effects on seasonal dynamics of soil CO 2 evolution, water content, temperature, and bulk density. Applied Soil Ecology 2, 95-109.

Franzluebbers, A.J., Langdale, G.W., Schomberg, H.H., 1999. Soil Carbon, Nitrogen, and Aggregation in Response to Type and Frequency of Tillage. Soil Sci. Soc. Am. J. 63, 349-355.

Frolking, S.E., Mosier, A.R., Ojima, D.S., Li, C., Parton, W.J., Potter, C.S., Priesack, E., Stenger, R., Haberbosch, C., Dörsch, P., Flessa, H., Smith, K.A., 1998. Comparison of N_2O

emissions from soils at three temperate agricultural sites: simulations of year-round measurements by four models. Nutrient Cycling in Agroecosystems 52, 77-105.

Gabrielle, B., Laville, P., Hénault, C., Nicoullaud, B., Germon, J.C., 2006. Simulation of Nitrous Oxide Emissions from Wheat-cropped Soils using CERES. Nutrient Cycling in Agroecosystems 74, 133-146.

Galloway, J.N., Schlesinger, W. H., Levy, H., Michaels, A., & Schnoor, J. L. , 1995. Nitrogen fixation: Anthropogenic enhancement-environmental response. Global Biogeochemical Cycles 9, 235-252.

Gascuel-Odoux, C., Aurousseau, P., Durand, P., Ruiz, L., Molenat, J., 2010. The role of climate on inter-annual variation in stream nitrate fluxes and concentrations. Science of The Total Environment 408, 5657-5666.

Gasol, C.M., Gabarrell, X., Rigola, M., González-García, S., Rieradevall, J., 2011. Environmental assessment: (LCA) and spatial modelling (GIS) of energy crop implementation on local scale. Biomass and Bioenergy 35, 2975-2985.

Gassman, P.W., Reyes, M.R., Green, C.H., Arnold, J.G., 2007. The Soil and Water Assessment Tool: Historical Development, Applications, and Future Research Directions. Transactions of the ASABE: American Society of Agricultural and Biological Engineers 50, 1211-1250.

Gawel, E., Ludwig, G., 2011. The iLUC dilemma: How to deal with indirect land use changes when governing energy crops? Land Use Policy 28, 846-856.

Gerbens-Leenes, P.W., Hoekstra, A.Y., van der Meer, T., 2009. The water footprint of energy from biomass: A quantitative assessment and consequences of an increasing share of bio-energy in energy supply. Ecological Economics 68, 1052-1060.

Giltrap, D.L., Li, C., Saggar, S., 2010. DNDC: A process-based model of greenhouse gas fluxes from agricultural soils. Agriculture, Ecosystems & Environment 136, 292-300.

Goodlass G, G.M., Hilton B, McDonough S, 2007. Nitrate leaching from short-rotation coppice. Soil Use Manage 23, 178-184.

Goodrich, D.C., Scott, R., Qi, J., Goff, B., Unkrich, C.L., Moran, M.S., Williams, D., Schaeffer, S., Snyder, K., MacNish, R., Maddock, T., Pool, D., Chehbouni, A., Cooper, D.I., Eichinger, W.E., Shuttleworth, W.J., Kerr, Y., Marsett, R., Ni, W., 2000. Seasonal estimates of riparian evapotranspiration using remote and in situ measurements. Agricultural and Forest Meteorology 105, 281-309.

Gopalakrishnan, G., Cristina Negri, M., Salas, W., 2012. Modeling biogeochemical impacts of bioenergy buffers with perennial grasses for a row-crop field in Illinois. GCB Bioenergy 4, 739-750.

Grant, R., 1995. Dynamics of energy water, carbon and nitrogen in agricultural ecosystems: simulation and experimental validation. Ecological Modelling 81, 169-181.

Grant, R.F., Pattey, E., 2003. Modelling variability in N_2O emissions from fertilized agricultural fields. Soil Biology and Biochemistry 35, 225-243.

Grant, R.F., Pattey, E., Goddard, T.W., Kryzanowski, L.M., Puurveen, H., 2006. Modeling the Effects of Fertilizer Application Rate on Nitrous Oxide Emissions. Soil Science Society of America Journal 70, 1, 235-248.

Green, T.R., Ahuja, L.R., Benjamin, J.G., 2003. Advances and challenges in predicting agricultural management effects on soil hydraulic properties. Geoderma 116, 3-27.

Groffman, P.M., Brumme, R., Butterbach-Bahl, K., Dobbie, K.E., Mosier, A.R., Ojima, D., Papen, H., Parton, W.J., Smith, K.A., Wagner-Ridd, C., 2000a. Evaluating annual nitrous oxide fluxes at the ecosystem scale. Global Biogeochemical Cycles 14, 1061-1070.

Groffman, P.M., Gold, A.J., Addy, K., 2000b. Nitrous oxide production in riparian zones and its importance to national emission inventories. Chemosphere - Global Change Science 2, 291-299.

Gross, R., 2003. Progress in renewable energy. Environment International 29, 105-122.

Guitouni, A., Martel, J.M., 1998. Tentative guidelines to help choosing an appropriate MCDA method. European Journal of Operational Research 109, 501-521.

Gupta, S.C., Larson, W.E., 1979. Estimating Soil Water Retention Characteristics From Particle Size Distribution, Organic Matter Percent, and Bulk Density. Water Resources Research 15, 1633-1655.

Gupta, S.C., Lowery, B., Moncrief, J.F., Larson,W.E., 1991. Modeling tillage effects on soil physical properties. Soil Tillage Research 20, 293-318.

H. G. Adegbidi, T.A. Volk, E. H. White, L. P. Abrahamson, R. D. Briggs, Bickelhaupt, D.H., 2001. Biomass and nutrient removal by willow clones in experimental bioenergy plantations in New York State. Biomass and Bioenergy 20, 399-411.

H.J. Hellebrand, V.S., J. Kern, 2008. Nitrogen conversion and nitrous oxide hot spots in energy crop cultivation. RES. AGR. ENG. 54, 58-67.

Hamelin, L., Jørgensen, U., Petersen, B.M., Olesen, J.E., Wenzel, H., 2012. Modelling the carbon and nitrogen balances of direct land use changes from energy crops in Denmark: a consequential life cycle inventory. GCB Bioenergy 4, 889-907.

Hamelinck, C.N., Suurs, R.A.A., Faaij, A.P.C., 2005. International bioenergy transport costs and energy balance. Biomass and Bioenergy 29, 114-134.

Hanegraaf, M.C., Biewinga, E.E., Van der Bijl, G., 1998. Assessing the ecological and economic sustainability of energy crops. Biomass and Bioenergy 15, 345-355.

Hansen, E.A., 1993. Soil carbon sequestration beneath hybrid poplar plantations in the north central United States. Biomass and Bioenergy 5, 431-436.

Hastings, A., Clifton-Brown, J., Wattenbach, M., Mitchell, C.P., Smith, P., 2009. The development of MISCANFOR, a new*Miscanthus*crop growth model: towards more robust yield predictions under different climatic and soil conditions. GCB Bioenergy 1, 154-170.

Hastings, A., Tallis, M.J., Casella, E., Matthews, R.W., Henshall, P.A., Milner, S., Smith, P., Taylor, G., 2014. The technical potential of Great Britain to produce ligno-cellulosic biomass for bioenergy in current and future climates. GCB Bioenergy 6, 108-122.

Hawkes, A., Leach, M., 2008. On policy instruments for support of micro combined heat and power. Energy Policy 36, 2973-2982.

Heaton, E., 2004. A quantitative review comparing the yields of two candidate C4 perennial biomass crops in relation to nitrogen, temperature and water. Biomass and Bioenergy 27, 21-30.

Heaton, E.A., Dohleman, F.G., Long, S.P., 2008. Meeting US biofuel goals with less land: the potential of *Miscanthus*. Global Change Biology 14, 2000-2014.

Heaton, E.A., Dohleman, F.G., Long, S.P., 2009. Seasonal nitrogen dynamics of*Miscanthus*×giganteusandPanicum virgatum. GCB Bioenergy 1, 297-307.

Heaton, E.A., Dohleman, F.G., Miguez, A.F., Juvik, J.A., Lozovaya, V., Widholm, J., Zabotina, O.A., McIsaac, G.F., David, M.B., Voigt, T.B., Boersma, N.N., Long, S.P., 2010. *Miscanthus*: A Promising Biomass Crop, In: Turkan, I. (Ed.), Advances in Botanical Research. Elsevier, pp. 76-137

Heide, C., Böttcher, J., Deurer, M., Duijnisveld, W.H.M., Weymann, D., Well, R., 2009. Spatial and temporal variability of N_2O in the surface groundwater: a detailed analysis from a sandy aquifer in northern Germany. Nutrient Cycling in Agroecosystems 87, 33-47.

Heinen, M., 2006. Simplified denitrification models: Overview and properties. Geoderma 133, 444-463.

Hellebrand, H., Kern, J., Model, A., and Berg, W. 2006. Nitrous Oxide Fluxes from Loamy Sand Soil in Northeast Germany - Seasonal Variations and Influence of Nitrogen Fertilization, Precipitation, and Crop Types. Workshop on Agricultural Air Quality, Washington 682-692

Hellebrand, H., Scholz, V., Kern, J., 2008. Fertiliser induced nitrous oxide emissions during energy crop cultivation on loamy sand soils. Atmospheric Environment 42, 8403-8411.

Hellebrand, H.J., Scholz, V., Kern, J., & Kavdir, Y. , 2005. N_2O release during cultivation of energy crops. Agrartechnische Forschung 11, 114-124.

Hellebrand, H.J., Strähle, M., Scholz, V., Kern, J., 2010. Soil carbon, soil nitrate, and soil emissions of nitrous oxide during cultivation of energy crops. Nutrient Cycling in Agroecosystems 87, 175-186.

Hendriks, R.F.A., Wolleswinkel, R.J., van den Akker Alterra, J.J.H., 2008. Predicting greenhouse gas emission from peat soils depending on water management with the SWAP–ANIMO model, In: Farrell, C., Feehan, J. (Eds.), 13th International Peat Congress After Wise Use - The Future of Peatlands International Peat Society, Tullamore, Ireland, Jyväskylä, Finland, pp. 583-586.

Hillier, J., Whittaker, C., Dailey, G., Aylott, M., Casella, E., Richter, G.M., Riche, A., Murphy, R., Taylor, G., Smith, P., 2009. Greenhouse gas emissions from four bioenergy crops in England and Wales: Integrating spatial estimates of yield and soil carbon balance in life cycle analyses. GCB Bioenergy 1, 267-281.

Hilton, B., 2002. Growing short rotation coppice, best practice guidelines. DEFRA Publication.

Hofmann-Schielle, C., A. Jug, F. Makeschin, and K. E. Rehfuess., 1999. Short-rotation plantations of balsam poplars, aspen and willows on former arable land in the Federal Republic of Germany. I. Site–growth relationships. Forest Ecology and Management 121, 41-55.

Hoogeveen, J., Faurès, J.-M., van de Giessen, N., 2009. Increased biofuel production in the coming decade: to what extent will it affect global freshwater resources? Irrigation and Drainage 58, S148-S160.

Hosseini, S.A., Shah, N., 2011. Multi-scale process and supply chain modelling: from lignocellulosic feedstock to process and products. Interface Focus 1, 255-262.

Howarth, R.W.B., S., Martinelli, l.A., Santoro, R., Messem, D. and Sala, O.E., 2009. Introduction: Biofuels and the Environment in the 21st Century, In: Howarth, R.W.a.B., S. (Ed.), Biofuels: Environmental Consequences and Interactions with Changing Land Use. Proceedings of the Scientific Committee on Problems of the Environment (SCOPE) International Biofuels Project Rapid Assessment. Cornell University, Ithaca NY, USA, Gummersbach Germany, pp. 14-36.

Hulme, M., Jenkins, G., Lu, X., Turnpenny, J., Mitchell, T., Jones, R., Lowe, J., Murphy, J., Hassell, D., Boorman, P.e.a., 2002. Climate change scenarios for the United Kingdom: the UKCIP02 scientific report., Norwich, UK: Tyndall Centre for Climate Change Research.

Hutchings, N., Olesen, J., Petersen, B., Berntsen, J., 2007. Modelling spatial heterogeneity in grazed grassland and its effects on nitrogen cycling and greenhouse gas emissions. Agriculture, Ecosystems & Environment 121, 153-163.

Hutchins, M.G., Deflandre-Vlandas, A., Posen, P.E., Davies, H.N., Neal, C., 2010. How Do River Nitrate Concentrations Respond to Changes in Land-use? A Modelling Case Study of Headwaters in the River Derwent Catchment, North Yorkshire, UK. Environmental Modeling & Assessment 15, 93-109.

Huth, N.I., Thorburn, P.J., Radford, B.J., Thornton, C.M., 2010. Impacts of fertilisers and legumes on N_2O and CO_2 emissions from soils in subtropical agricultural systems: A simulation study. Agriculture, Ecosystems & Environment 136, 351-357.

Hwang, C.L., Youn, K., 1981. Multiple Attribute Decision Making - Methods and Application: A State of the Art Survey. Springer, New York.

International Energy Agency, 2008. World energy outlook

International Energy Agency, 2009. Bioenergy - a sustainable and reliable energy source. A review of status and prospects, Available at: http://www.ieabioenergy.com/LibItem.aspx?id=6479 [accessed 1/3/2011].

IPCC, 2000. Robert T. Watson, Ian R. Noble, Bert Bolin, N. H. Ravindranath, David J. Verardo and David J. Dokken (Eds.) Cambridge University Press, UK. pp. 375 Available from Cambridge University Press, The Edinburgh Building Shaftesbury Road, Cambridge CB2 2RU ENGLAND Summary for Policymakers IPCC, Geneva, Switzerland. pp. 20. Available from IPCC Secretariat in Arabic, Chinese, English, French, Spanish and Russian.

IPCC, 2003. Good Practice Guidance for Land Use, Land-Use Change and Forestry, pp. 89-112.

IPCC, 2006a. IPCC Guidelines for National Greenhouse Gas Inventories, In: Rodel D. Lasco, S.O., John Raison, Louis Verchot, Reiner Wassmann, K.Y., Sumana Bhattacharya, John S. Brenner, Julius Partson Daka, Sergio P. González, Thelma Krug, Y.L., Daniel L. Martino, Brian G. McConkey, Pete Smith, Stanley C. Tyler, and Washington Zhakata (Eds.).

IPCC, 2006b. IPCC Guidelines For National Greenhouse Gas Inventories, In: Eggleston H.S., B.L., Miwa K., Ngara T. and Tanabe K. (Ed.), Prepared by the National Greenhouse Gas Inventories Programme. Published: IGES.

IPCC, 2007. Intergovernmental Panel on Climate Change (IPCC) AR4 Climate Change: Synthesis Report, 2007, Available at: http://www.ipcc.ch/publications_and_data/ar4/syr/en/main.html [accessed 1/4/2011]. In: Allali, A., Bojariu, R., Diaz,S., Elgizouli, I., Griggs, D., Hawkins, D., Hohmeyer,O., Jallow, B. P., Kajfez-Bogataj, L., Leary, N., Lee, H., Wratt, D. (Ed.), pp. 23-73.

IPCC [Core Writing Team, P., R.K and Reisinger, A. (eds.)], 2007. Climate Change 2007: Synthesis Report. Contribution of Working Groups I, II and III to the Fourth Assessment Report of the Intergovernmental Panel on Climate Change, p. 104 pp.

Koppejan, J., Sokhansanj, S., Melin, S., Madrali, S., 2012. FINAL REPORT; Status overview of torrefaction technologies, IEA Bioenergy Task 32

Jablonski, S., Pantaleo, A., Bauen, A., Pearson, P., Panoutsou, C., Slade, R., 2008. The potential demand for bioenergy in residential heating applications (bio-heat) in the UK based on a market segment analysis. Biomass and Bioenergy 32, 635-653.

Jarecki, M.K., Parkin, T.B., Chan, A.S.K., Hatfield, J.L., Jones, R., 2008. Comparison of DAYCENT-Simulated and Measured Nitrous Oxide Emissions from a Corn Field. Journal of Environment Quality 37, 5, 1685-1690.

Jarvis, N.J., 2007. A review of non-equilibrium water flow and solute transport in soil macropores: principles, controlling factors and consequences for water quality. European Journal of Soil Science 58, 523-546.

Jenkinson, D.S., D.D. Harkness, E.D. Vance, D.E. Adams, A.F. Harrison., 1992. Calculating net primary production and annual input of organic matter to soil from the amount and radiocarbon content of soil organic matter. Soil Biol. Biochem 24, 4, 295-308.

Jensen, K., Clark, C., Ellis, P., English, B., Menard, J., Walsh, M., Delatorreugarte, D., 2007. Farmer willingness to grow switchgrass for energy production. Biomass and Bioenergy 31, 773-781.

Jørgensen, R.N., Jørgensen, B. J., Nielsen, N. E., Maag, M., & Lind, A. M. , 1997. N_2O emission from energy crop fields of *Miscanthus* "Giganteus" and winter rye. Atmospheric Environment 31, 2899-2904.

Jørgensen, U., Schelde, K., 2001. Energy crop water and nutrient use efficiency, IEA Bioenergy Task 17, Short Rotation Crops. The International Energy Agency.

Jug, A., Hofmann-Schielle, C., Makeschin, F., Rehfuess, K.E., 1999. Short-rotation plantations of balsam poplars, aspen and willows on former arable land in the Federal Republic of Germany. II. Nutritional status and bioelement export by harvested shoot axes. Forest Ecology and Management 121, 67-83.

Jug, A., Hofmann-Schielle, C., Makeschin, F., Rehfuess, K.E., 1999. Short-rotation plantations of balsam poplars, aspen and willows on former arable land in the Federal Republic of Germany. III. Soil ecological effects. For. Ecol. Manage. 121, 85-99.

Henderson, JV. 1988. Locational Pattern of Heavy Industries - Decentralization Is More Efficient. Journal of Policy Model 10, 569-580.

K. L. Weier, J.W.D., J. F. Power, and D. T. Walters, 1993. Denitrification and the Dinitrogen/Nitrous Oxide Ratio as Affected by Soil Water, Available Carbon, and Nitrate. Soil Sci. Soc. Am. J. 57, 66-72.

Kaharabata, S.K., Drury, C.F., Priesack, E., Desjardins, R.L., McKenney, D.J., Tan, C.S., Reynolds, D., 2003. Comparing measured and Expert-N predicted NO emissions from 2 conventional till and no till corn treatments. Nutrient Cycling in Agroecosystems 66, 107-118.

Kahle, P., Beuch, S., Boelcke, B., Leinweber, P., Schulten, H.R., 2001. Cropping of *Miscanthus* in Central Europe: biomass production and influence on nutrients and soil organic matter. European Journal of Agronomy 15, 171-184.

Karp, A., Shield, I., 2008. Bioenergy from plants and the sustainable yield challenge. New Phytol 179, 15-32.

Kaufman, L., Rousseeuw, P.J., 2009. Finding Groups in Data: An Introduction to Cluster Analysis. 344. John Wiley & Sons.

Kavdir, Y., Hellebrand, H., Kern, J., 2008. Seasonal variations of nitrous oxide emission in relation to nitrogen fertilization and energy crop types in sandy soil. Soil and Tillage Research 98, 175-186.

Keoleian, G., Volk, T., 2005. Renewable Energy from Willow Biomass Crops: Life Cycle Energy, Environmental and Economic Performance. Critical Reviews in Plant Sciences 24, 385-406.

Keymer, D.P., Kent, A.D., 2013. Contribution of nitrogen fixation to first year *Miscanthus* × giganteus. GCB Bioenergy, in press.

Kim, S., Dale, B.E., Ong, R.G., 2012. An alternative approach to indirect land use change: Allocating greenhouse gas effects among different uses of land. Biomass and Bioenergy 46, 447-452.

Kishore, V., 2004. Biomass energy technologies for rural infrastructure and village power—opportunities and challenges in the context of global climate change concerns. Energy Policy 32, 801-810.

Knoth, J., 2012. Analysis of the Potential for Diazotrophic Endophytes to Increase Efficiency of Bioenergy Crop Production: Growth promotion effects of the endophytes isolated from Populus trichocarpa and Salix sitchensis. University of Washington.

Kopp, R.F., L. P. Abrahamson, E. H. White, T. A. Volk, C. A. Nowak, and R. C. Fillhart., 2001. Willow biomass production during ten successive annual harvests. Biomass and Bioenergy 20, 1-7.

Kramer, S.B., 2006. Reduced nitrate leaching and enhanced denitrifier activity and efficiency in organically fertilized soils. Proceedings of the National Academy of Sciences 103, 4522-4527.

Lal, R., 2004. Soil Carbon Sequestration Impacts on Global Climate Change and Food Security. Science 304, 1623-1627.

Landsberg, J.J., Waring, R.H., 1997. A generalised model of forest productivity using simplified concepts of radiation-use efficiency, carbon balance and partitioning Forest Ecology and Management 95, 209-228.

Lane, S.N., Reaney, S.M., Heathwaite, A.L., 2009. Representation of landscape hydrological connectivity using a topographically driven surface flow index. Water Resources Research 45, 10.

Laville, P., Hénault, C., Gabrielle, B., Serça, D., 2005. Measurement and Modelling of NO Fluxes on Maize and Wheat Crops During their Growing Seasons: Effect of Crop Management. Nutrient Cycling in Agroecosystems 72, 159-171.

Lavoie, M., Kellman, L., Risk, D., 2013. The effects of clear-cutting on soil CO2, CH4, and N_2O flux, storage and concentration in two Atlantic temperate forests in Nova Scotia, Canada. Forest Ecology and Management 304, 355-369.

Leij, F.J., Ghezzehei, T.A., Or, D., 2002a. Analytical models for soil pore-size distribution after tillage. Soil Science Society of America Journal 66, 1104-1114.

Leij, F.J., Ghezzehei, T.A., Or, D., 2002b. Modeling the dynamics of the soil pore-size distribution. Soil & Tillage Research 64, 61-78.

Lemke, R.L., Izaurralde, R. C., Nyborg, M. and Solberg, E. D., 1999. Tillage and N source influence soil-emitted nitrous oxide in the Alberta Parkland region. Can. J. Soil Sci. 79, 15-24.

Lesur, C., Bazot, M., Bio-Beri, F., Mary, B., Jeuffroy, M.-H., Loyce, C., 2013. Assessing nitrate leaching during the three-first years of *Miscanthus* × giganteus from on-farm measurements and modeling. GCB Bioenergy, 6, 4, 439–449.

Lewandowski, I., Schmidt, U., 2006. Nitrogen, energy and land use efficiencies of *Miscanthus*, reed canary grass and triticale as determined by the boundary line approach. Agriculture, Ecosystems & Environment 112, 335-346.

Lewis, D., McGechan, M.B., 2002. SW—Soil and Water A Review of Field Scale Phosphorus Dynamics Models. Biosystems Engineering 82, 359-380.

Li, C., Aber, J., Stange, F., Butterbach-Bahal, K., Papen, H., 2000. A process-oriented model of N_2O and NO emissions from forest soils. 1. Model development. Journal of Geophysical Research 105, 4369-4384.

Li, C., Frolking, S., Butterbach-Bahl, K., 2005a. Carbon Sequestration in Arable Soils is Likely to Increase Nitrous Oxide Emissions, Offsetting Reductions in Climate Radiative Forcing. Climatic Change 72, 321-338.

Li, C., Frolking, S., Frolking, T.A., 1992. A model of nitrous oxide evolution from soil driven by rainfall events: 1. Model Structure and sensetivity. Journal of Geophysical research 97, 9759-9776.

Li, C., Frolking, S. and Harriss, R.C. 1994. Modeling carbon biogeochemistry in agricultural soils. Global Biogeochemical Cycles 8, 237-254.

Li, Y., Chen, D., 2010. Modelling N_2O emissions from agroecosystems: the WNMM experience. 19th World Congress of Soil Science, Soil Solutions for a Changing World

Li, Y., Chen, D., Zhang, Y., Edis, R., Ding, H., 2005b. Comparison of three modeling approaches for simulating denitrification and nitrous oxide emissions from loam-textured arable soils. Global Biogeochemical Cycles 19, 3, pp 15.

Li, Y., Tullberg, J., Freebairn, D., McLaughlin, N., Li, H., 2008. Effects of tillage and traffic on crop production in dryland farming systems: I. Evaluation of PERFECT soil-crop simulation model. Soil and Tillage Research 100, 15-24.

Li, Y., White, R., Chen, D., Zhang, J., Li, B., Zhang, Y., Huang, Y., Edis, R., 2007. A spatially referenced water and nitrogen management model (WNMM) for (irrigated) intensive cropping systems in the North China Plain. Ecological Modelling 203, 395-423.

Lindegaard, K., 2013. Why we need an Energy Crops Scheme 3. Position paper. Crops for Energy Ltd. pp 14.

Lindroth, A., and A. Båth. , 1999. Assessment of regional willow coppice yield in Sweden on basis of water availability. Forest Ecology and Management 121, 57-65.

Lindroth, A., Verwijst, T., and Halldin, S. 1994. Water-use efficiency of willow: variation with season, humidity and biomass allocation. Journal of Hydrology 156, 1-19.

Linn, D.M., and Doran, J.W. 1984. Effect of water-filled pore space on carbon dioxide and nitrous oxide production in tilled and nontilled soils. Soil Science Society of America Journal 48, 1267-1272.

Logsdon, S.D., 1995. Flow mechanisms through continuous and buried macropores. Soil Science 160, 237-242.

Lokupitiya, E., Paustian, K., 2006. Agricultural Soil Greenhouse Gas Emissions. Journal of Environment Quality 35, 1413.

Lovett, A., Sünnenberg, G., Dockerty, T., 2014. The availability of land for perennial energy crops in Great Britain. GCB Bioenergy 6, 99-107.

Lovett, A.A., Sünnenberg, G.M., Richter, G.M., Dailey, A.G., Riche, A.B., Karp, A., 2009. Land Use Implications of Increased Biomass Production Identified by GIS-Based Suitability and Yield Mapping for *Miscanthus* in England. BioEnergy Research 2, 17-28.

Low Carbon Transport Steering Group, 2010. Scope 3 Third party Road Freight CO_2 emissions pilot model. Rev 21-07-10 In: http://www.google.co.uk/url?q=https://www.gov.uk/government/uploads/system/uploads/attachment_data/file/218576/lct-steering-group-carbon-em.xls&sa=U&ei=Ag4iU-6CCY7whQeb-4D4Aw&ved=0CCsQFjAD&usg=AFQjCNEgLOFJnxfpWiVTwXY4uPYTo4Utwg

Borzêcka-Walker, M., and Borek, R. 2008. Evaluation of carbon sequestration in energetic crops (*Miscanthus* and coppice willow). Int. Agrophysics 22, 185-190.

Martens, A., 1998. The energetic feasibility of CHP compared to the separate production of heat and power. Appl Therm Eng 18, 935-946.

Martin, P.J., Stephens, W., 2006. Willow growth in response to nutrients and moisture on a clay landfill cap soil. I. Growth and biomass production. Bioresource Technology 97, 437-448.

Matthews, R.B., Grogan, P., Bullard, M. J., Christian, D. G., Knight, J. D., Lainsbury, M. A., & Parker, S. R. , 2001a. Potential C-sequestration rates under short-rotation coppiced willow and *Miscanthus* biomass crops: a modelling study. In Biomass and Energy Crops II, University of York, York, UK, 18-21 December 2001. (No. 65, pp. 303-312). Association of Applied Biologists.

Matthews, R.W., 2001b. Modeling of energy and carbon budgets of wood fuel coppice systems. Biomass and Bioenergy 21, 1-19.

McCown, R.L., Hammer, G.L., Hargreaves, J.N.G., Holzworth, D.P., Freebairn, D.M., 1996. APSIM: a Novel Software System for Model Development, Model Testing and Simulation in Agricultural Systems Research. Agricultural Systems 50, 255-271.

McKay, H.e., 2011. Short Rotation Forestry: review of growth and environmental impacts. . Forest Research Monograph, 2, Forest Research, Surrey, 212pp.

McKendry, P., 2002a. Energy production from biomass (part 1): overview of biomass. Bioresource Technology 83, 37-46.

McKendry, P., 2002b. Review paper. Energy production from biomass (part 2): conversion technologies. Bioresource Technology 83, 47-54.

Melillo, J.M., Reilly, J.M., Kicklighter, D.W., Gurgel, A.C., Cronin, T.W., Paltsev, S., Felzer, B.S., Wang, X., Sokolov, A.P., Schlosser, C.A., 2009. Indirect emissions from biofuels: how important? Science 326, 1397-1399.

Meisinger J.J., Delgado J.A., 2002. Principles for managing nitrogen leaching. Journal of Soil Water Conservation 57:485–498.

Met Office, Met Office Land Surface Stations Data (1900-2000), http://badc.nerc.ac.uk/browse/badc/ukmo-surface/data/united_kingdom.

Metay, A., Oliver, R., Scopel, E., Douzet, J.-M., Aloisio Alves Moreira, J., Maraux, F., Feigl, B.J., Feller, C., 2007. N_2O and CH_4 emissions from soils under conventional and no-till management practices in Goiânia (Cerrados, Brazil). Geoderma 141, 78-88.

Metivier, K.A., Pattey, E., Grant, R.F., 2009. Using the ecosys mathematical model to simulate temporal variability of nitrous oxide emissions from a fertilized agricultural soil. Soil Biology and Biochemistry 41, 2370-2386.

Mishra, U., Torn, M.S., Fingerman, K., 2013. *Miscanthus* biomass productivity within US croplands and its potential impact on soil organic carbon. GCB Bioenergy 5, 391-399.

Mitchell, C., Bauknecht, D., Connor, P.M., 2006. Effectiveness through risk reduction: a comparison of the renewable obligation in England and Wales and the feed-in system in Germany. Energy Policy 34, 297-305.

Mitchell, C.P., Stevens, E.A., Waters, M.P., 1999. Short-rotation forestry - operations, productivity and costs based on experience gained in the UK. Forest Ecology and Management 121, 123-136.

Mitchell, D., 2008. A Note on Rising Food Prices, The World Bank Development Prospects Group, 21. pp 20.

Miyake, S., Renouf, M., Peterson, A., McAlpine, C., Smith, C., 2012. Land-use and environmental pressures resulting from current and future bioenergy crop expansion: A review. Journal of Rural Studies 28, 650-658.

Mola-Yudego, B., Aronsson, P., 2008. Yield models for commercial willow biomass plantations in Sweden. Biomass and Bioenergy 32, 829-837.

Moldrup, P., Olesen, T., Komatsu, T., Schjønning, P., & Rolston, D. E. , 2001. Tortuosity, diffusivity, and permeability in the soil liquid and gaseous phases. Soil Science Society of America Journal 65, 613-623.

Moldrup, P.O., T.; Yoshikawa, S.; Komatsu, T.; Rolston, D. E.; , 2004. Three-Porosity Model for Predicting the Gas Diffusion Coefficient in Undisturbed Soil. Soil Sci. Soc. Am. J. 68, 750-759.

Möller, B., Lund, H., 2010. Conversion of individual natural gas to district heating: Geographical studies of supply costs and consequences for the Danish energy system. Applied Energy 87, 1846-1857.

Mollersten, K., 2003. Potential market niches for biomass energy with CO_2 capture and storage?Opportunities for energy supply with negative CO_2 emissions. Biomass and Bioenergy 25, 273-285.

Monzon, J.P., V.O. Sadras, and F.H. Andrade., 2006. Fallow soil evaporation and water storage as affected by stubble in sub-humid (Argentina) and semi-arid (Australia) environments. Field Crops Research 98, 83-90.

Moret, D., Arrue, J.L., 2007. Dynamics of soil hydraulic properties during fallow as affected by tillage. Soil & Tillage Research 96, 103-113.

Morgan, M.E., Kingston, J. D., & Marino, B. D., 1994. Carbon isotopic evidence for the emergence of C4 plants in the Neogene from Pakistan and Kenya. Nature 367, 162-165.

Mortensen, H.C., Overgaard, B., 1992. Chp Development in Denmark - Role and Results. Energy Policy 20, 1198-1206.

Mortensen, J., Nielsen, K. H., and Jorgensen, U., 1998. Nitrate leaching during establishment of willow (Salix viminalis) on two soil types and at two fertilization levels. Biomass and Bioenergy 15, 457-466.

Mortimer N.D., E.M.A., Horne R.E., 2004. Energy and greenhouse gas emissions for bioethanol production from wheat grain and sugar beet, pp. P9-11.

Mosier, A., Kroeze, C., Nevison, C., Oenema, O., Seitzinger, S., & Van Cleemput, O., 1998. Closing the global N_2O budget: nitrous oxide emissions through the agricultural nitrogen cycle. Nutrient cycling in Agroecosystems 52, 225-248.

Moukoumi, J., Farrell, R.E., Rees, K.J.C., Hynes, R.K., Bélanger, N., 2012. Intercropping Caragana arborescens with Salix miyabeana to Satisfy Nitrogen Demand and Maximize Growth. BioEnergy Research 5, 719-732.

Mulder, K., Hagens, N., Fisher, B., 2010. Burning Water: A Comparative Analysis of the Energy Return on Water Invested. AMBIO 39, 30-39.

Müller, C., Sherlock, R.R., Williams, P.H., 1997. Mechanistic model for nitrous oxide emission via nitrification and denitrification. Biol Fertil Soils 24, 231-238.

Natural England, 2006. Energy Crops Scheme 1: http://www.naturalengland.org.uk/Images/ECS1_tcm6-26820.pdf [accessed 6/4/2014].

Natural England, 2009a. Environmental Appraisal of Applications Under The Energy Crops (ECS) Scheme For *Miscanthus*, Short Rotation Coppice (SRC) and Short Rotation Energy Crops (SREC): Guidance Notes For Natural England and Forest Commission Appraisers, Available from Natural England: ecsqueries@naturalengland.org.uk., 26. pp.

Natural England, 2009b. Rural Development Programme for England. Energy Crops Scheme. Establishment Grants Handbook. 3rd Edition.

Natural England, 2013. Environmental Appraisal of Applications Under The Energy Crops (ECS) Scheme For *Miscanthus*, Short Rotation Coppice (SRC) and Short Rotation Energy Crops (SREC):Guidance Notes For Natural England and Forest Commission Appraisers, Available from Natural England: ecsqueries@naturalengland.org.uk.

Nelson, C.O.S.a.R., 1993. Cropping Systems Simulation Model: User's Manual, In: Campbell, G.S., Donatelli, M., Yan, Y., Ferrer, F., Evert, F.V., McCool, D., Martin, S., Mulla, D., Bechini, L., Deabaeke, P. (Eds.). Biological Systems Engineering Department, Washington State University.

Nevison, C., 2000. Review of the IPCC methodology for estimating nitrous oxide emissions associated with agricultural leaching and runoff. Chemosphere-Global Change Science 2, 493-500.

Nevison, C., 2002. Indirect N_2O emissions from agriculture, Background Papers: IPCC Expert Meetings on Good Practice Guidance and Uncertainty Management in National Greenhouse Gas Inventories. IPCC. Kanagawa, Japan, Intergovernmental Panel on Climate Change, pp. 381-397.

Nixon P, B.M., 2001. Planting and growing *Miscanthus*, best practice guidelines. DEFRA Publications.

Nonhebel, S., 2005. Renewable energy and food supply: will there be enough land? Renewable and Sustainable Energy Reviews 9, 191-201.

Novoa, R.S.A., Tejeda, H.R., 2006. Evaluation of the N_2O emissions from N in plant residues as affected by environmental and management factors. Nutrient Cycling in Agroecosystems 75, 29-46.

Ofgem, 2013a. Non-Domestic Renewable Heat Incentive (RHI). Available at: https://www.ofgem.gov.uk/publications-and-updates/non-domestic-renewable-heat-incentive-guidance-published [accessed 26/2/14]

Ofgem, 2013b. Renewables Obligation - total obligation levels for 2012-13. Available at: https://www.ofgem.gov.uk/publications-and-updates/renewables-obligation-total-obligation-levels-2012-13 [accessed 26/2/14]

Ofgem, 2013c. Renewables Obligation: Guidance for Generators. Available at: https://www.ofgem.gov.uk/publications-and-updates/renewables-obligation-guidance-generators-may-2013 [accessed 26/2/14]

Ogle, S.M., Breidt, F.J., Easter, M., Williams, S., Paustian, K., 2007. An empirically based approach for estimating uncertainty associated with modelling carbon sequestration in soils. Ecological Modelling 205, 453-463.

Ogle, S.M., Swan, A., Paustian, K., 2012. No-till management impacts on crop productivity, carbon input and soil carbon sequestration. Agriculture, Ecosystems & Environment 149, 37-49.

Onstad, C.A., Wolfe, M. L., Larson, C. L., & Slack, D. C., 1984. Tilled soil subsidence during repeated wetting [Forman, egan, clay loams, Barnes loam, sverdrup sandy loam]. . Transactions of the ASAE[American Society of Agricultural Engineers](USA).

Or, D., Leij, F. J., Snyder, V., & Ghezzehei, T. A., 2000. Stochastic model for post tillage soil pore space evolution. Water Resources Research 36, 1641-1652.

Pacaldo, R.S., Volk, T.A., Briggs, R.D., 2012. Greenhouse Gas Potentials of Shrub Willow Biomass Crops Based on Below- and Aboveground Biomass Inventory Along a 19-Year Chronosequence. BioEnergy Research 6, 252-262.

Paice, J., 2011. International Food Expo, London, UK.

Paine, L.K., Peterson, T.L., Undersander, D.J., Rineer, K., Bartelt, G.A., emple, S., Sample, D.W., Klemm, R.M., 1996. Some Ecological and Socio-Economic Considerations for Biomass Energy Crop Production. Biomass and Bioenergy 10, 231-242.

Pala, M., C.O. Stöckle, and H.C. Harris., 1996. Simulation of durum wheat (triticum durum) growth under differential water and nitrogen regimes in a mediterranean type of environment using CropSyst. Agricultural Systems 51, 147-163.

Parkin, T.B., Tiedje, J.M., 1984. Application of a soil core method to investigate the effect of oxygen concentration on denitrification. Soil Biology and Biochemistry 16, 331-334.

Parton, W., Hartman, M., Ojima, D., Schimel, D., 1998. DAYCENT and its land surface submodel: description and testing. Global and Planetary Change 19, 35-48.

Parton, W.J., A. R. Mosier, D. S. Ojima, D. W. Valentine, D. S. Schimel, K. Weier, and Airi E. Kulmala., 1996. Generalized model for N2 and N_2O production from nitrification and denitrification. Global Biogeochemical Cycles 10, 401-412.

Parton, W.J., D. S. Schimel, C. V. Cole, and D. S. Ojima, 1987. Analysis of factors controlling soil organic matter levels in Great Plains grasslands. Soil Sci. Soc. Am. J. 51, 1173-1179.

Parton, W.J., Hanson, P.J., Swanston, C., Torn, M., Trumbore, S.E., Riley, W., Kelly, R., 2010. ForCent model development and testing using the Enriched Background Isotope Study experiment. Journal of Geophysical Research 115 pp 15.

Parton, W.J., Hartman, M., Ojima, D., & Schimel, D., 1998. DAYCENT and its land surface submodel: description and testing Original Research Article. Global and Planetary Change 19, 35-48.

Parton, W.J., Ojima, D.S., Cole, C.V., Schimel, D.S., 1994. A general model for soil organic matter dynamics: sensitivity to litter chemistry, texture and management. Quantitative Modelling of Soil Forming Processes. Soil Science Society of America, Madison, 147-167.

Patzek, T.W., 2004. Thermodynamics of the Corn-Ethanol Biofuel Cycle. Critical Reviews in Plant Sciences 23, 519-567.

Paustian, K., Six, J., Elliott, E. T., & Hunt, H. W., 2000. Management options for reducing CO2 emissions from agricultural soils. Biogeochemistry 48, 147-163.

Perlack, R.D., Wright, L. L., Turhollow, A. F., Graham, R. L., Stokes, B. J., & Erbach, D. C. , 2005. Biomass as feedstock for a bioenergy and bioproducts industry: the technical feasibility of a billion-ton annual supply. Oak Ridge National Lab TN.

Perrin, C., Michel, C., Andreâassian, V., 2001. Does a large number of parameters enhance model performance? Comparative assessment of common catchment model structures on 429 catchments. Journal of Hydrology 242, 275 - 301.

Perry, M., Rosillocalle, F., 2008. Recent trends and future opportunities in UK bioenergy: Maximising biomass penetration in a centralised energy system. Biomass and Bioenergy 32, 688-701.

Perry, M.a.R.-C., F. , 2006. Co-firing report—United Kingdom. , IEA Task 40, p. 75.

Petersen, S., Schjonning, P., Thomsen, I., Christensen, B., 2008. Nitrous oxide evolution from structurally intact soil as influenced by tillage and soil water content. Soil Biology and Biochemistry 40, 967-977.

Philippot, S., 1996. Simulation models of short-rotation forestry production and coppice biology. . Biomass and Bioenergy 11, 85-93.

Pirmoradian, N., Sepaskhah, A.R., Hajabbasi, M.A., 2005. Application of Fractal Theory to quantify Soil Aggregate Stability as influenced by Tillage Treatments. Biosystems Engineering 90, 227-234.

Piterou, A., Shackley, S., Upham, P., 2008. Project ARBRE: Lessons for bio-energy developers and policy-makers. Energy Policy 36, 2044-2050.

Porporato, A., Odorico, P.D., Laio, F., Rodriguez-Iturbe, I., 2003. Hydrologic controls on soil carbon and nitrogen cycles. I. Modeling scheme. Advances in Water Resources 26, 45-58.

Post, J., Hattermann, F.F., Krysanova, V., Suckow, F., 2008. Parameter and input data uncertainty estimation for the assessment of long-term soil organic carbon dynamics. Environmental Modelling & Software 23, 125-138.

Potter, C.S., Matson, P.A., Vitousek, P.M., Davidson, E.A., 1996. Process modeling of controls on nitrogen trace gas emissions from soils worldwide. Journal Of Geophysical Research 101, 1361-1377.

Powlson, D.S., Riche, A.B., Shield, I., 2005. Biofuels and other approaches for decreasing fossil fuel emissions from agriculture. Annals of Applied Biology 146, 193-201.

Price, L., 2004. Identifying the yield potential of *Miscanthus* x giganteus: an assessment of the spatial and temporal variability of M. x giganteus biomass productivity across England and Wales. Biomass and Bioenergy 26, 3-13.

Price, L., Bullard, M., Lyons, H., Anthony, S., Nixon, P., 2004. Identifying the yield potential of *Miscanthus* x giganteus: an assessment of the spatial and temporal variability of M. x giganteus biomass productivity across England and Wales. Biomass and Bioenergy 26, 3-13.

Priesack, E., 2012. Expert-N research group: http://www.helmholtz-muenchen.de/en/iboe/expertn/, In: Ecology, M.g.o.t.I.o.S. (Ed.).

Proe MF, G.J., Craig J 2002. Effects of spacing, species and coppicing on leaf area, light interception and photosynthesis in short rotation forestry. Biomass and BioEnergy 23, 315-326.

Raphael Slade, Robert Saunders, Robert Gross, Bauen, A., 2011. Energy from biomass: the size of the global resource. Imperial College Centre for Energy Policy and Technology and UK Energy Research Centre, London.

Rawls, W.J., Pachepsky, Y.A., Ritchie, J.C., Sobecki, T.M., Bloodworth, H., 2003. Effect of soil organic carbon on soil water retention. Geoderma 116, 61-76.

Reay, D.S., Edwards, A.C., Smith, K.A., 2009. Importance of indirect nitrous oxide emissions at the field, farm and catchment scale. Agriculture, Ecosystems & Environment 133, 163-169.

Regina, K., Alakukku, L., 2010. Greenhouse gas fluxes in varying soils types under conventional and no-tillage practices. Soil and Tillage Research 109, 144-152.

Renaud, L.V., Roelsma, J., Groenendijk, P., 2006. ANIMO 4.0. User's guide of the ANIMO 4.0 nutrient leaching model, p. 191.

Richards, G.P., 2001. The FullCAM Carbon Accounting Model: Development, Calibration and Implementation, IEA Bioenergy Task 38: Workshop in Canberra/Australia, March 2001. Carbon Accounting and Emissions Trading Related to Bioenergy, Wood Products and Carbon Sequestration, p. 56.

Richter, G.M., Riche, A.B., Dailey, A.G., Gezan, S.A., Powlson, D.S., 2008. Is UK biofuel supply from *Miscanthus* water-limited? Soil Use and Management 24, 235-245.

Riley, W.J., Matson, P.A., 2000. NLoss: A Mechanistic model of denitrified N_2O and N_2 evolution from soil. Soil Science 165, 237-250.

Robbins, M.P., Evans, G., Valentine, J., Donnison, I.S., Allison, G.G., 2012. New opportunities for the exploitation of energy crops by thermochemical conversion in Northern Europe and the UK. Prog Energ Combust 38, 138-155.

Roberts, S., 2008. Infrastructure challenges for the built environment. Energy Policy 36, 4563-4567.

Rochette, P., 2008. No-till only increases N_2O emissions in poorly-aerated soils. Soil and Tillage Research 101, 97-100.

Rochette, P., Angers, D.A., Chantigny, M.H., Bertrand, N., 2008. Nitrous Oxide Emissions Respond Differently to No-Till in a Loam and a Heavy Clay Soil. Soil Science Society of America Journal 72, 1363–1369.

Rochette, P., Eriksen-Hamel, N.S., 2008. Chamber Measurements of Soil Nitrous Oxide Flux: Are Absolute Values Reliable? Soil Science Society of America Journal 72, 331–342.

Roelandt, C., van Wesemael, B., Rounsevell, M., 2005. Estimating annual N_2O emissions from agricultural soils in temperate climates. Global Change Biology 11, 1701-1711.

Rooney, D.C., Killham, K., Bending, G.D., Baggs, E., Weih, M., Hodge, A., 2009. Mycorrhizas and biomass crops: opportunities for future sustainable development. Trends Plant Sci 14, 542-549.

Roth, B., Jones, M., Burke, J., Williams, M., 2013. The Effects of Land-Use Change from Grassland to *Miscanthus* x Giganteus on Soil N_2O Emissions. Land 2, 437-451.

Rowe, R., Street, N., Taylor, G., 2009. Identifying potential environmental impacts of large-scale deployment of dedicated bioenergy crops in the UK. Renewable and Sustainable Energy Reviews 13, 271-290.

Rüdig, W., 1986. Energy conservation and electricity utilities A comparative analysis of organizational obstacles to CHP/DH. . Energy policy 14, 104-116.

Ryan, M., Müller, C., Di, H.J., Cameron, K.C., 2004. The use of artificial neural networks (ANNs) to simulate N_2O emissions from a temperate grassland ecosystem. Ecological Modelling 175, 189-194.

Ryden, J.C., Ball, P.R., Garwood, E.A., 1984. Nitrate leaching from grassland. Nature 311, 50-53.

Saxton, K.E., W_J Rawls, J. S. Romberger, and R. I. Papendick., 1986. Estimating generalized soil-water characteristics from texture. Soil Science Society of America Journal 50, 1031-1036.

Schmer, M.R., Liebig, M.A., Vogel, K.P., Mitchell, R.B., 2011. Field-scale soil property changes under switchgrass managed for bioenergy. GCB Bioenergy 3, 439-448.

Schmidt, J., Leduc, S., Dotzauer, E., Kindermann, G., Schmid, E., 2010. Potential of biomass-fired combined heat and power plants considering the spatial distribution of biomass supply and heat demand. International Journal of Energy Research 34, 970-985.

Schoumans, O.F., Silgram, M., Groenendijk, P., Bouraoui, F., Andersen, H.E., Kronvang, B., Behrendt, H., Arheimer, B., Johnsson, H., Panagopoulos, Y., Mimikou, M., Lo Porto, A., Reisser, H., Le Gall, G., Barr, A., Anthony, S.G., 2009a. Description of nine nutrient loss models: capabilities and suitability based on their characteristics. Journal of Environmental Monitoring 11, 506-514.

Schoumans, O.F., Silgram, M., Walvoort, D.J.J., Groenendijk, P., Bouraoui, F., Andersen, H.E., Lo Porto, A., Reisser, H., Le Gall, G., Anthony, S., Arheimer, B., Johnsson, H., Panagopoulos, Y., Mimikou, M., Zweynert, U., Behrendt, H., Barr, A., 2009b. Evaluation of the difference of eight model applications to assess diffuse annual nutrient losses from agricultural land. Journal of Environmental Monitoring 11, 540.

Schoumans, O.F., Silgram, M.E., Andersen, H.E., Anthony, S., Arheimer, B., Barr, A., Behrendt, H., Bouraoui, F., Ejhed, H., Groenendijk, P., Jeuken, M., Johnsson, H., B. Kronvang, Le Gall, G., Murdock, A., Lo Porto, A., Price, L., Schoumans, O., Silgram, M., Smit, R., Varanou, E., Zweynert, U.A., 2003. Review and literature evaluation of nutrient quantification tools. EUROHARP report 1, NIVA report SNO 4739-2003, 120 pp.

Schwen, A., Bodner, G., Scholl, P., Buchan, G. D., & Loiskandl, W. , 2011. Temporal dynamics of soil hydraulic properties and the water-conducting porosity under different tillage Soil and Tillage Research 113, 89-98.

Searchinger, T., Heimlich, R., Houghton, R.A., Dong, F., Elobeid, A., Fabiosa, J., Tokgoz, S., Hayes, D., Yu, T.H., 2008. Use of U.S. Croplands for Biofuels Increases Greenhouse Gases Through Emissions from Land-Use Change. Science 319, 1238-1240.

Sherrington, C., Moran, D., 2010. Modelling farmer uptake of perennial energy crops in the UK. Energy Policy 38, 3567-3578.

Shibu, M.E., Matthews, R.B., Bakam, I., Moffat, A.J., Baggaley, N.J., 2012. Estimating greenhouse gas abatement potential of biomass crops in Scotland under various management options. Biomass and Bioenergy 47, 211-227.

Silgram, M., Anthony, S.G., Collins, A.L., Strőmqvist, J., Bouraoui, F., Schoumans, O., Lo Porto, A., Groenendijk, P., Arheimer, B., Mimikou, M., Johnsson, H., 2009. Evaluation of diffuse pollution model applications in EUROHARP catchments with limited data. Journal of Environmental Monitoring 11, 3, 554-571.

Sims, R.E.H., Hastings, A., Schlamadinger, B., Taylor, G., Smith, P., 2006. Energy crops: current status and future prospects. Global Change Biology 12, 2054-2076.

Sims, R.E.H., Venturi, P., 2003. All-year-round harvesting of short rotation coppice eucalyptus compared with the delivered costs of biomass from more conventional short season, harvesting systems. Biomass and Bioenergy 26, 27-37.

Six, J., Bossuyt, H., Degryze, S., Denef, K., 2004a. A history of research on the link between (micro)aggregates, soil biota, and soil organic matter dynamics. Soil and Tillage Research 79, 7-31.

Six, J., Elliott, E.T., Paustian, K., 2000. Soil macroaggregate turnover and microaggregate formation: a mechanism for C sequestration under no-tillage agriculture. Soil Biology & Biochemistry 32, 2099-2103.

Six, J., Ogle, S.M., Jay breidt, F., Conant, R.T., Mosier, A.R., Paustian, K., 2004b. The potential to mitigate global warming with no-tillage management is only realized when practised in the long term. Global Change Biology 10, 155-160.

Skiba, U.v.D., S.; Ball, B.C., 2002. The influence of tillage on NO and N_2O fluxes under spring and winter barley. Soil Use and Management 18, 340-345.

Smart, L.B., Volk, T. A., Lin, J., Kopp, R. F., Phillips, I. S., Cameron, K. D., White, E. H., Abrahamson, L. P. , 2005. Genetic improvement of shrub willow (Salix spp.) crops for bioenergy and environmental applications in the United States. UNASYLVA-FAO 56, 51-55.

Smeets, E.M.W., Bouwman, L.F., Stehfest, E., van Vuuren, D.P., Posthuma, A., 2009. Contribution of N_2O to the greenhouse gas balance of first-generation biofuels. Global Change Biology 15, 1-23.

Smith, J., Gottschalk, P., Bellarby, J., Chapman, S., Lilly, A., Towers, W., Bell, J., Coleman, K., Nayak, D., Richards, M., Hillier, J., Flynn, H., Wattenbach, M., Aitkenhead, M., Yeluripati, J., Farmer, J., Milne, R., Thomson, A., Evans, C., Whitmore, A., Falloon, P., Smith, P., 2010a. Estimating changes in Scottish soil carbon stocks using ECOSSE. I. Model description and uncertainties. Climate Research 45, 179-192.

Smith, P., 2004. Carbon sequestration in croplands: the potential in Europe and the global context. European Journal of Agronomy 20, 229-236.

Smith, P., D. Martino, Z. Cai, D. Gwary, H. Janzen, P. Kumar, B. McCarl, S. Ogle, F. O'Mara, C. Rice, B. Scholes, O. Sirotenko, 2007. Agriculture. In Climate Change 2007: Mitigation. Contribution of Working Group III to the Fourth Assessment Report of the Intergovernmental Panel on Climate Change, In: [B. Metz, O.R.D., P.R. Bosch, R. Dave, L.A. Meyer (eds)]

Smith, P., Gregory, P.J., van Vuuren, D., Obersteiner, M., Havlik, P., Rounsevell, M., Woods, J., Stehfest, E., Bellarby, J., 2010b. Competition for land. Philos Trans R Soc Lond B Biol Sci 365, 2941-2957.

Smith, P., Martino, D., Cai, Z., Gwary, D., Janzen, H., Kumar, P., McCarl, B., Ogle, S., O'Mara, F., Rice, C., Scholes, B., Sirotenko, O., Howden, M., McAllister, T., Pan, G., Romanenkov, V., Schneider, U., Towprayoon, S., Wattenbach, M., Smith, J., 2008. Greenhouse gas mitigation in agriculture. Philosophical Transactions of the Royal Society B: Biological Sciences 363, 789-813.

Smith, P., Smith, J.U., Powlson, D.S., McGill, W.B., Arah, J.R.M., Cherto, O.G., Coleman, K., Franko, U., Frolking, S., Jenkinson, D.S., Jensen , L.S., Kelly, R.H., Klein-Gunnewiek, H., Komarov, A.S., Li, C., Molina J, J.A.E., Mueller, T., Parton , W.J., Thornley, J.H.M., Whitmore, A.P., 1997. A comparison of the performance of nine soil organic matter models using datasets from seven long-term experiments. Geoderma 81, 153-225.

Smith, W.N.G., B. B.; Desjardins,R. L.; Rochette, P.; Drury,C. F.; and LiC.; , 2008. Evaluation of two process-based models to estimate soil N_2O emissions in Eastern Canada. Can J Soil Sci 88, 2, 251-260.

Soane, B.D., Ball, B.C., Arvidsson, J., Basch, G., Moreno, F., Roger-Estrade, J., 2012. No-till in northern, western and south-western Europe: A review of problems and opportunities for crop production and the environment. Soil and Tillage Research 118, 66-87.

Socolow, R.H., 1999. Nitrogen management and the future of food: lessons from the management of energy and carbon. Proceedings of the National Academy of Sciences 96, 6001-6008.

Spackman, P., 2011. Burning ambitions for biomass. Farmer's Weekly Interactive, 2011, Available at: http://www.fwi.co.uk/Articles/07/04/2011/126268/Burning-ambitions-for-biomass.htm [accessed 26/10/12], Farmers Weekly. Reed Business information ltd, p. 2.

Speirs, J., Gross, R., Deshmukh, S., Heptonstall, P., Munuera, L., Leach, M., Torriti, J., 2010. Building a roadmap for heat 2050 scenarios and heat delivery in the UK, Combined Heat and Power Association Reports, p. 44.

Stehfest, E., Bouwman, L., 2006. N_2O and NO emission from agricultural fields and soils under natural vegetation: summarizing available measurement data and modeling of global annual emissions. Nutrient Cycling in Agroecosystems 74, 207-228.

Stenger, R., Priesack, E., Barkle, G., Sperr, C., 1999. Expert-N. A tool for simulating nitrogen and carbon dynamics in the soil-plant-atmosphere system, In: Tomer, M., Robinson, M., Gielen, G. (Eds.), NZ Land Treatment Collective. Proceedings Technical Session 20: Modelling of Land Treatment Systems. New Plymouth, pp. 19-28.

Stöckle, C., Roger Nelson, M., 2003. CropSyst, a cropping systems simulation model. European Journal of Agronomy 18, 289-307.

Stöckle, C., Campbell, G.S., Donatelli, M., Yan, Y., Ferrer, F., Evert, F.V., McCool, D., Martin, S., Mulla, D., Bechini, L., Deabaeke, P., Nelson, P.R., 2004. Cropping Systems Simulation Model: User's Manual, Washington State University.

Stöckle, C., Higgins, S., Kemanian, A., Nelson, R., Huggins, D., Marcos, J., Collins, H., 2012. Carbon storage and nitrous oxide emissions of cropping systems in eastern Washington: A simulation study. Journal of Soil and Water Conservation 67, 365-377.

Stockmann, U., Adams, M.A., Crawford, J.W., Field, D.J., Henakaarchchi, N., Jenkins, M., Minasny, B., McBratney, A.B., Courcelles, V.d.R.d., Singh, K., Wheeler, I., Abbott, L., Angers, D.A., Baldock, J., Bird, M., Brookes, P.C., Chenu, C., Jastrow, J.D., Lal, R., Lehmann, J., O'Donnell, A.G., Parton, W.J., Whitehead, D., Zimmermann, M., 2013. The knowns, known unknowns and unknowns of sequestration of soil organic carbon. Agriculture, Ecosystems & Environment 164, 80-99.

Strudley, M., Green, T., Ascoughii, J., 2008. Tillage effects on soil hydraulic properties in space and time: State of the science. Soil and Tillage Research 99, 4-48.

Styles, D., Jones, M., 2007a. Current and future financial competitiveness of electricity and heat from energy crops: A case study from Ireland. Energy Policy 35, 4355-4367.

Styles, D., Jones, M., 2007b. Energy crops in Ireland: Quantifying the potential life-cycle greenhouse gas reductions of energy-crop electricity. Biomass and Bioenergy 31, 759-772.

Tallis, M.J., Casella, E., Henshall, P.A., Aylott, M.J., Randle, T.J., Morison, J.I.L., Taylor, G., 2013. Development and evaluation of ForestGrowth-SRC a process-based model for short rotation coppice yield and spatial supply reveals poplar uses water more efficiently than willow. GCB Bioenergy 5, 53-66.

Taylor, S.C., Firth, S.K., Wang, C., Allinson, D., Quddus, M., Smith, P., 2014. Spatial mapping of building energy demand in Great Britain. GCB Bioenergy 6, 123-135.

Thomas, A.R.C., Bond, A.J., Hiscock, K.M., 2013a. A GIS based assessment of bioenergy potential in England within existing energy systems. Biomass and Bioenergy. 55, 107-121

Thomas, A.R.C., Bond, A.J., Hiscock, K.M., 2013b. A multi-criteria based review of models that predict environmental impacts of land use-change for perennial energy crops on water, carbon and nitrogen cycling. GCB Bioenergy 5, 227-242.

Thorburn, P.J., Biggs, J.S., Collins, K., Probert, M.E., 2010. Using the APSIM model to estimate nitrous oxide emissions from diverse Australian sugarcane production systems. Agriculture, Ecosystems & Environment 136, 343-350.

Thornley, P., 2006. Increasing biomass based power generation in the UK. Energy Policy 34, 2087-2099.

Tilman, D., Hill, J., Lehman, C., 2006. Carbon-Negative Biofuels from Low-Input High-Diversity Grassland Biomass. Science 314, 1598-1600.

Toenshoff, C., Joergensen, R.G., Stuelpnagel, R., Wachendorf, C., 2013. Dynamics of soil organic carbon fractions one year after the re-conversion of poplar and willow plantations to arable use and perennial grassland. Agriculture, Ecosystems & Environment 174, 21-27.

Toenshoff, C., Stuelpnagel, R., Joergensen, R.G., Wachendorf, C., 2012. Carbon in plant biomass and soils of poplar and willow plantations—implications for SOC distribution in different soil fractions after re-conversion to arable land. Plant and Soil 367, 407-417.

Toma, Y.O., Fernández, F.G., Sato, S., Izumi, M., Hatano, R., Yamada, T., Nishiwaki, A.Y.A., Bollero, G., Stewart, J.R., 2010. Carbon budget and methane and nitrous oxide emissions over the growing season in a *Miscanthus* sinensis grassland in Tomakomai, Hokkaido, Japan. GCB Bioenergy 3, 116-134.

Tonini, D., Hamelin, L., Wenzel, H., Astrup, T., 2012. Bioenergy production from perennial energy crops: a consequential LCA of 12 bioenergy scenarios including land use changes. Environ Sci Technol 46, 13521-13530.

Uchida, Y., Clough, T., Kelliher, F., Sherlock, R., 2008. Effects of aggregate size, soil compaction, and bovine urine on N_2O emissions from a pasture soil. Soil Biology and Biochemistry 40, 924-931.

UK Agriculture, 2010a. Oilseed rape production cycle. Available at: http://www.ukagriculture.com/production_cycles/oilseed_rape_production_cycle.cfm. [accessed 2/7/2014],

UK Agriculture, 2010b. Wheat production cycle. Available at: http://www.ukagriculture.com/production_cycles/wheat_production_cycle.cfm [accessed 2/7/2014]

UK Agriculture, 2010c.Grassland in the UK- an introduction. Available at: http://www.ukagriculture.com/crops/grassland_uk.cfm[accessed 29/8/2014]

United Nations Environment Programme, 2007. Buildings and Climate Change: Status,Challenges and Opportunities, Available at: http://www.unep.fr/scp/publications/details.asp?id=DTI/0916/PA [accessed 2/4/2011], United Nations Environment Programme.

Upham, P., Speakman, D., 2007. Stakeholder opinion on constrained 2030 bioenergy scenarios for North West England. Energy Policy 35, 5549-5561.

Vallios, I., Tsoutsos, T., Papadakis, G., 2009. Design of biomass district heating systems. Biomass and Bioenergy 33, 659-678.

Van Breemen, N., Boyer, E.W., Goodale, C.L., Jaworski, N.A., Paustian, K., Seitzinger, S.P., Lajtha, K., Mayer, B., Vandam, D., Howarth, R.W., Nadelhoffer1, K.J., Eve, M., Billen, G., 2002. Where did all the nitrogen go? Fate of nitrogen inputs to large watersheds in the northeastern U.S.A. Biogeochemistry 57/58, 267-293.

van Kessel, C., Clough, T., van Groenigen, J.W., 2009. Dissolved Organic Nitrogen: An Overlooked Pathway of Nitrogen Loss from Agricultural Systems? Journal of Environment Quality 38, 393.

Vanloocke, A., Bernacchi, C.J., Twine, T.E., 2010. The impacts of *Miscanthus* × giganteus production on the Midwest US hydrologic cycle. GCB Bioenergy, 180-191.

Venturi, P., Gigler, J. K., & Huisman, W., 1999 Economical and technical comparison between herbaceous *Miscanthus* x giganteus and woody energy crops Salix viminalis. Renewable Energy 16, 1023-1026.

Verchot, L.V., Davidson, E.A., Henrique Cattanio, J., Ackerman, l.L., Erickson, H.E., Keller, M., 1999. Land use change and biogeochemical controls of nitrogen oxide emissions from soils in eastern Amazonia. Global Biogeochemical Cycles 13, 31-46.

Verchot, L.V., Hutabarat, L., Hairiah, K., van Noordwijk, M., 2006. Nitrogen availability and soil N_2O emissions following conversion of forests to coffee in southern Sumatra. Global Biogeochemical Cycles 13, 31–46.

Verlinden, M.S., Broeckx, L.S., Zona, D., Berhongaray, G., De Groote, T., Camino Serrano, M., Janssens, I.A., Ceulemans, R., 2013. Net ecosystem production and carbon balance of an SRC poplar plantation during its first rotation. Biomass and Bioenergy 56, 412-422.

Vogeler, I., Giltrap, D., Cichota, R., 2013. Comparison of APSIM and DNDC simulations of nitrogen transformations and N_2O emissions. The Science of The Total Environment 465, 147-155.

Volk, T.A., Luzadis, V.A., 2008. Willow biomass production for bioenergy, biofuels, and bioproducts in New York, Renewable Energy from Forest Resources in the United States p. 238.

Wagener, T., Gupta, H.V., 2005. Model identification for hydrological forecasting under uncertainty. Stochastic Environmental Research and Risk Assessment 19, 378-387.

Waller, I., Lundgren, G., Bailey, N., Bradley, D., Labastida, R.R., 2011. Building Robust Regional and International Supply Chains, World Biofuels Markets, Rotterdam.

Wang, S., Hastings, A., Smith, P., 2012. An optimization model for energy crop supply. GCB Bioenergy 4, 88-95.

Wang, S., Hastings, A., Wang, S., Sunnenberg, G., Tallis, M.J., Casella, E., Taylor, S., Alexander, P., Cisowska, I., Lovett, A., Taylor, G., Firth, S., Moran, D., Morison, J., Smith, P., 2014. The potential for bioenergy crops to contribute to meeting GB heat and electricity demands. GCB Bioenergy 6, 136-141.

Webster, C.P., T.S.Scott., 2004. Rothamsted project number 074454.

Webster, C.P.S., T and Goulding, K. W. T., 2003. Can tillage practice affect the contribution of nitrous oxide to the total greenhouse gas production from arable agriculture. Controlling N Flows and Losses. Abstracts for the 12th Nitrogen Workshop, Exeter Theme 3a.

Weigelt, A., Weisser, W.W., Buchmann, N. and Scherer-Lorenzen, M., 2009. Biodiversity for multifunctional grasslands: equal productivity in high-diversity low-input and low-diversity high-input systems. Biogeosciences 6, 1695-1706.

Wetterlund, E., Leduc, S., Dotzauer, E., Kindermann, G., 2012. Optimal use of forest residues in Europe under different policies—second generation biofuels versus combined heat and power. Biomass Conversion and Biorefinery 3, 3-16.

Whitehead, P., Wilson, E., Butterfield, D., 1998. A semi-distributed integrated nitrogen model for multiple source assessment in catchments (INCA): Part I — model structure and process equations. Science of The Total Environment 210/211, 547-558.

Wilhelm, W.W.J., J.M.F. Hatfield, J.L. Voorhees, W.B. and Linden D.R., 2004. Crop and Soil Productivity Response to Corn Residue Removal: A Literature Review. Agronomy Journal 96, 1-17.

Williams, J.R., 1990. The Erosion-Productivity Impact Calculator (EPIC) Model: A Case History. Philosophical Transactions of the Royal Society B: Biological Sciences 329, 421-428.

Williams, J.R., Izaurralde, R. C., & Steglich, E. M., 2008. Agricultural Policy/Environmental eXtender Model: Theoretical documentation version 0604. BREC Report, 17.

Williams, J.R., Jones, C.A., Dyke, P.T., 1984. A modeling approach to determining the relationship between erosion and soil productivity. Trans. ASAE 27, 129- 142.

Wolf, J., Broeke, M., Rotter, R., 2005. Simulation of nitrogen leaching in sandy soils in The Netherlands with the ANIMO model and the integrated modelling system STONE. Agriculture, Ecosystems & Environment 105, 523-540.

Woo, D.K., 2013. Soil carbon and nitrogen cycle modeling for bioenergy crops, Civil Engineering. University of Illinois at Urbana-Champaign, Urbana, Illinois.

Wood, G., Dow, S., 2011. What lessons have been learned in reforming the Renewables Obligation? An analysis of internal and external failures in UK renewable energy policy. Energy Policy 39, 2228-2244.

Yang, X., Drury, C., Reynolds, W., Tan, C., 2008. Impacts of long-term and recently imposed tillage practices on the vertical distribution of soil organic carbon. Soil and Tillage Research 100, 120-124.

Zatta, A., Clifton-Brown, J., Robson, P., Hastings, A., Monti, A., 2013. Land use change from C3 grassland to C4 *Miscanthus*: effects on soil carbon content and estimated mitigation benefit after six years. GCB Bioenergy, 6, 4, 360-370.

Zeri, M., Hussain, M.Z., Anderson-Teixeira, K.J., DeLucia, E., Bernacchi, C.J., 2013. Water use efficiency of perennial and annual bioenergy crops in central Illinois. Journal of Geophysical Research: Biogeosciences 118, 581-589.

Zimmermann, J., Dauber, J., Jones, M.B., 2012. Soil carbon sequestration during the establishment phase of *Miscanthus* × Giganteus: a regional-scale study on commercial farms using 13C natural abundance. GCB Bioenergy 4, 453-461.

Zimmermann, J., Dondini, M., Jones, M.B., 2013. Assessing the impacts of the establishment of *Miscanthus* on soil organic carbon on two contrasting land-use types in Ireland. European Journal of Soil Science 64, 747-756.

Visual glossary

Moldbord plough

(Farm Weekly, 23 Feb, 2009)

(National Resources Conservation Service, 2010)

Rotovator

(Chetak Agro Industries)

Rototiller

The primary difference between the rotovator and the rototiller is user control over rate of rotation; the rotovator has a gearbox enabling change in rate of movement over soil- combined with constant rate of tine rotation this enables user control over degree of “engagement” of soil

(Aliimg.com global trade site)

Ridger

(National Resources Conservation Service, 2010)

Rotary Harrow

(National Resources Conservation Service, 2010)

A 'lay-flat planter'

For planting of SRC willow: images from defra best practice guide (Hilton, 2002)

Direct chip harvesting of SRC willow: images from defra best practice guide (Hilton, 2002)

Miscanthus harvesting images from defra best practice guide Nixon (2001)

Farm Weekly, 23 Feb, 2009. Available at: http://www.farmweekly.com.au/news/agriculture/cropping/general-news/mouldboard-ploughing-could-be-a-saviour-for-sandplain-farmers/1441500.aspx [acessed 28/4/2014].

Aliimg.com global trade site Available at: http://i00.i.aliimg.com/photo/247117397/Rotary_tiller.jpg [acessed 28/4/2014]

National Resources Conservation Service, 2010. Tillage Equipment Pocket Identification Guide, Available at: http://www.nrcs.usda.gov/Internet/FSE_DOCUMENTS/nrcs142p2_007135.pdf [acessed 28/4/2014]

Chetak Agro Industries, Available at: http://uttar-pradesh.all.biz/agricultural-rotavator-g200475#show0 [acessed 28/4/2014]

Hilton, B., 2002. Growing short rotation coppice, best practice guidelines. DEFRA Publication.

Nixon P, B.M., 2001. Planting and growing *Miscanthus*, best practice guidelines. DEFRA Publications.

Appendix 1: Mapping

Table A1.1 Calculations of potential supply and demand for co-firing using Miscanthus from a 40 km supply radius

Coal Plant	10% demand (odt)	Group	Feedstock (odt) in 40 km	excess 10 % (odt)	excess 20 % (odt)
Cottam	730893.18	1			
Drax	1435815.53	1			
Eggborough	727183.06	1			
Ferrybridge C	725328.00	1			
West Burton	716794.73	1	3566133	-769881	-5105896
Ironbridge	359881.41	2			
Ratcliffe	742023.53	2			
Rugeley	362107.48	2	3385085	1921072	457060
Kingsnorth	732377.22	3			
Tilbury B Generation Aggregates	378432.00	3	1434945	324136	-786673
Didcot A Generation Aggregates	749443.76	N	1044671	295227	-454217
Fiddlers Ferry	727554.07	N	988798.5	261244	-466310
Lynemouth	155824.94	N	1051191	895366	739541.1
Wilton	37101.18	N	1275017	1237915	1200814
Whole area	8580760.09		13091313	4934960	2397415
			useful feedstock	**10% (odt)**	**20% (odt)**
useful feedstock = total - excess				8156353	10693898

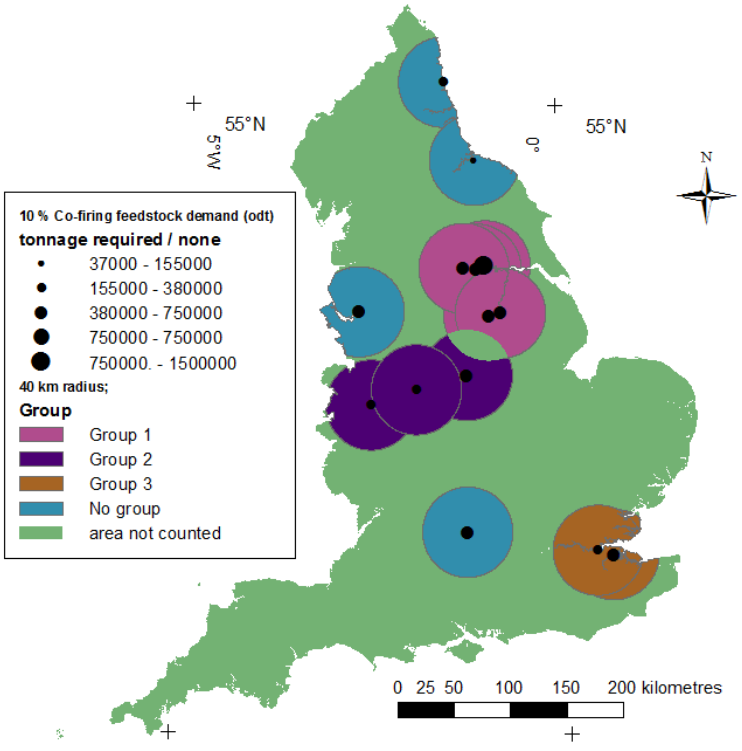

Figure A1.1 Map to show groupings of 40 km demand zones for co-firing.

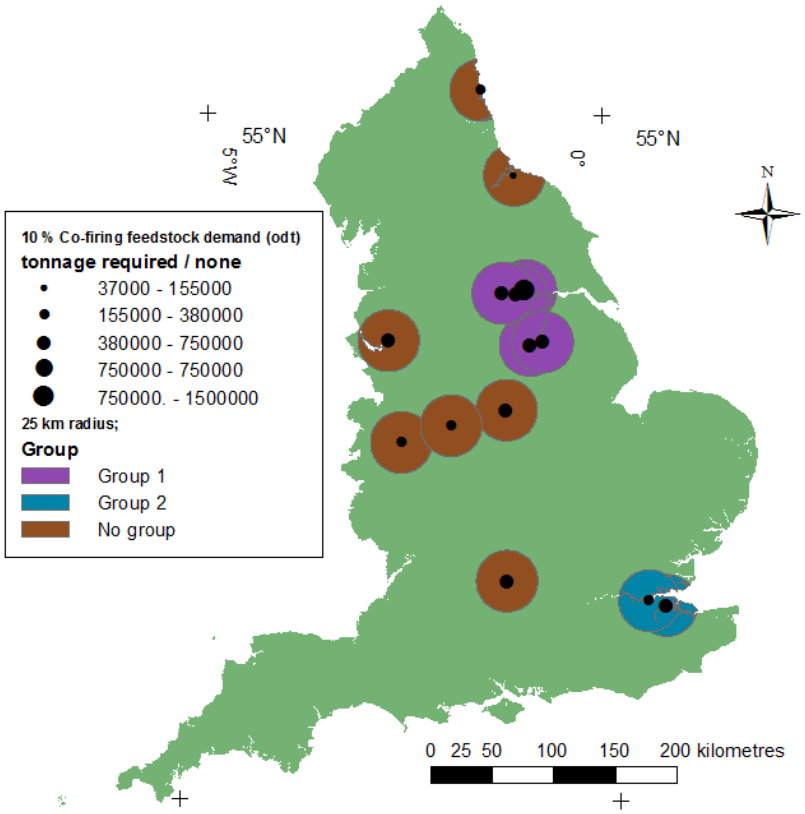

Figure A1.2 Map to show groupings of 25 km demand zones for co-firing.

Table A1.2 Calculations of potential supply and demand for co-firing using Miscanthus from a 25 km supply radius

Coal Plant	10% demand (odt)	Group	Feedstock (odt) in 25 km	excess 10 % (odt)	excess 20 % (odt)
Cottam	730893	1			
Drax	1435816	1			
Eggborough	727183	1			
Ferrybridge C	725328	1			
West Burton	716795	1	4336014	-2186726	-6522740
Kingsnorth	732377	2			
Tilbury B Generation Aggregates	378432	2	1110809	-608389	-1719198
Ironbridge	359881	N	446593.5	86712	-273169
Didcot A Generation Aggregates	749444	N	388647	-360797	-1110241
Fiddlers Ferry	727554	N	488085	-239469	-967023
Lynemouth	155825	N	535287	379462	223637
Ratcliffe	742024	N	811881	69857	-672166
Rugely	362107	N	672252	310145	-51963
Wilton	37101	N	527713.5	490612	453511
Whole area	8580760		9317283	1336788	677148
			useful feedstock	**10% (odt)**	**20% (odt)**
useful feedstock = total - excess				7980495	8640135

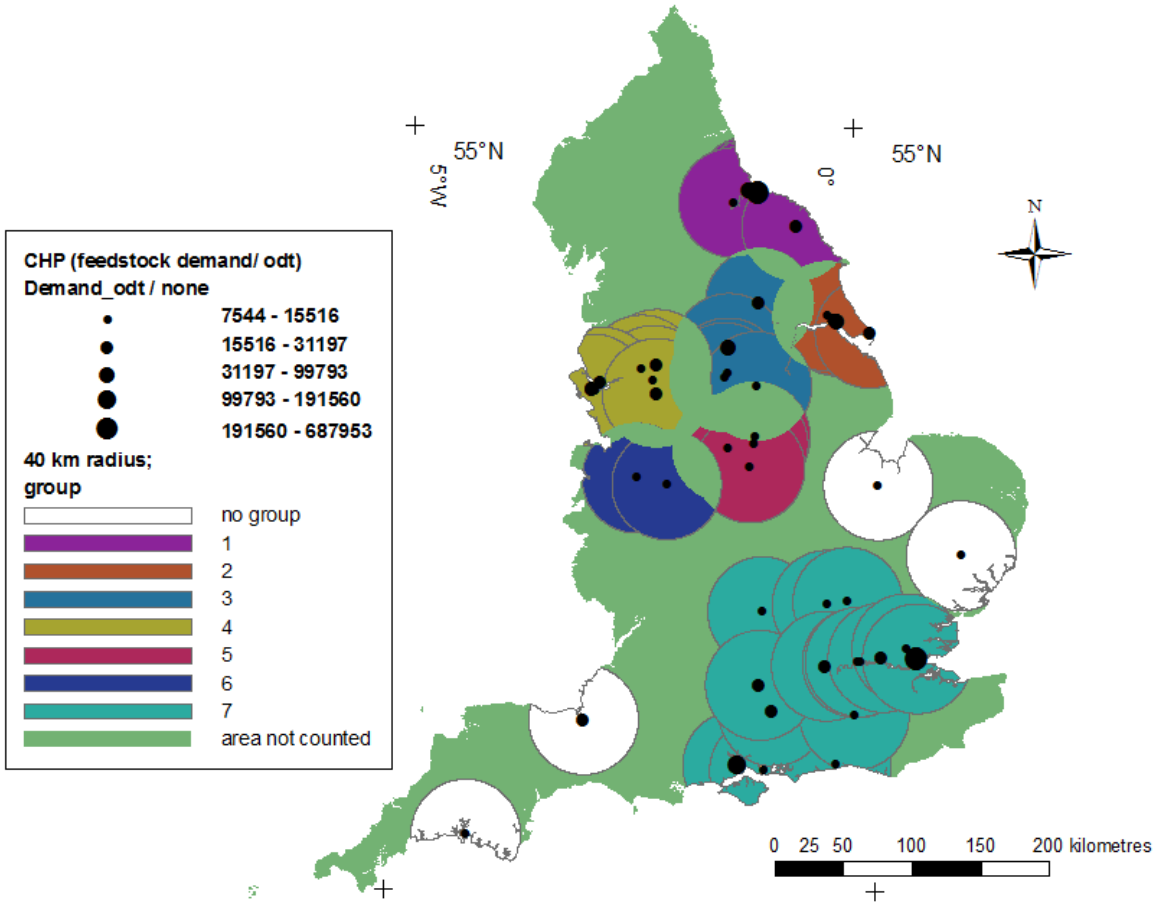

Figure A1.3 Map to show groupings of 40 km demand zones for industrial and large scale Combined Heat and Power

Table A1.3 Calculations of potential supply and demand for CHP using Miscanthus from a 40 km supply radius

Site name	Demand (odt)	Feedstock 40 km (odt)	Group	Group demand (odt)	Exclusive feedstock (odt)	Excess feedstock (odt)
SembCorp Utilities (UK) Limited	473114	1207476	1	598387	1940693	1342305
Petroplus Refining Teesside Ltd and Phillips-Imperial Petroleum Ltd	99793	1377530				
Elementis Chromium LLP	8256	1689995				
TG Power Limited	17223	623270				
BP Chemicals Ltd	79929	1352775	2	138999	1291731	1152732
Aarhus United UK Ltd	23319	1324442				
Croda Chemicals Europe Ltd	14477	1504619				
Gassco AS	21274	882389				
Harworth Power Ltd	23089	1823495	3	120886	1967348	1846461
Redfearn Glass Ltd and Rexam Glass Barnsley Ltd and Rockware Glass Ltd	68755	930141				
Sheffield Teaching Hospitals NHS Trust	11515	893103				
Sheffield Teaching Hospitals NHS Trust	9451	794400				
Campbell Grocery Products Limited	8076	1792433				
The University of Manchester	16212	803823	4	149107	1050492	901385
Basell Polyolefins UK Ltd	13493	915525				
Manchester Airport plc	9196	839672				
Vauxhall Motors Ltd	20635	708402				
Eastham Refinery Ltd	19796	686673				
Ford Motor Company Ltd and Jaguar Cars Ltd	16582	846000				
Innospec Ltd	10529	737993				
Vauxhall Motors Ltd	20635	708402				
AstraZeneca UK Ltd	22029	889466				
Nottingham University Hospitals NHS Trust	10924	2160576	5	44122	2234486	2190364
University Of Nottingham	8481	2195975				
Rolls-Royce plc	10276	1697514				
AstraZeneca plc	14441	2591816				
Ministry of Defence	9336	1103070	6	21820	571434	549614
SI Group UK Ltd	12485	1312976				
Ministry of Defence	7732	1651575	7	1063172	6683670	5620498
IBC Vehicles Ltd	9810	2118485				
GlaxoSmithKline plc	11231	1819329				

ExxonMobil Chemical Limited	191561	730908				
Fleet Support Ltd	10460	492785				
SmithKline Beecham plc and Glaxosmithkline Plc	12308	632253				
Star Energy UK Onshore Ltd	16389	1233599				
Gatwick Airport Ltd	8431	1013304				
AWE plc	31198	1134353				
Heathrow Airport Ltd and British Airways plc	19111	22391921				
Guys & St Thomas' Hospital NHS Trust	9977	1396452				
Guys & St Thomas' Hospital NHS Trust	7544	1332315				
Ford Motor Company Ltd	31110	1273154				
Ford Motor Company Ltd	8356	1299812				
BP Oil UK Ltd	687954	1238657				
Not grouped						
Garden Isle Frozen Foods Ltd	7642	701126				693483
Muntons plc	15516	2314878				2299362
Innovia Films Ltd	18524	762515				743991
Devonport Royal Dockyard Ltd	14197	45920				31722

	Total useful feedstock (odt)
Useful feedstock = sum of demands which can be met	2009251

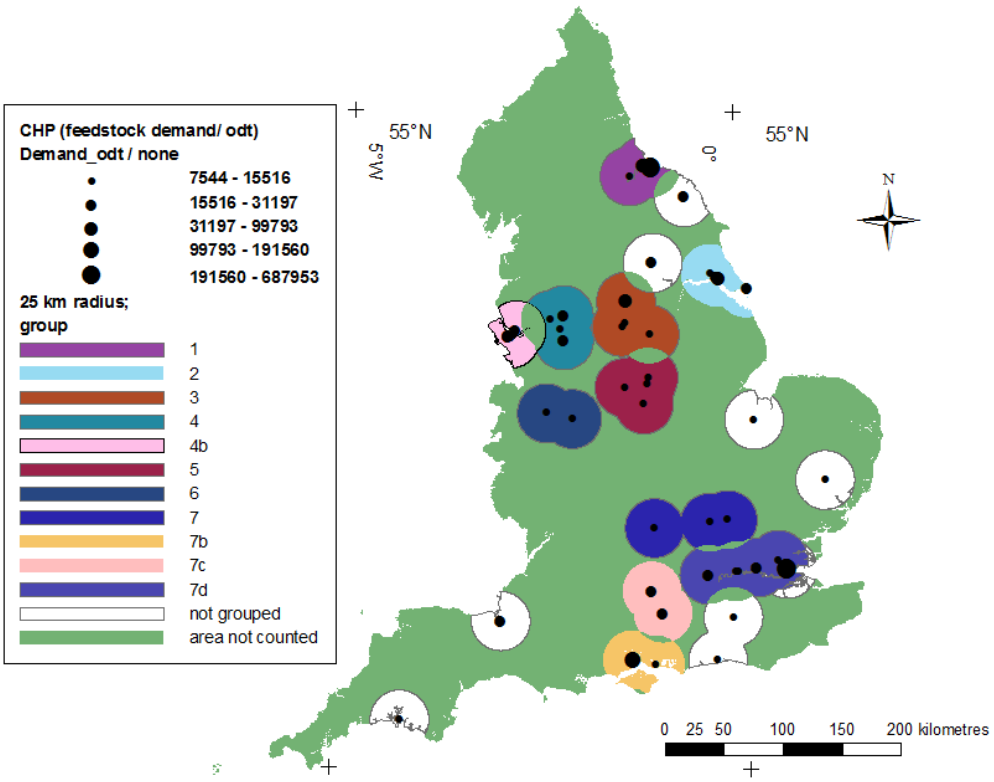

Figure A1.4 Map to show groupings of 25 km demand zones for industrial and large scale Combined Heat and Power

Table A1.4 Calculations of potential supply and demand for CHP using Miscanthus from a 25 km supply radius

Site name	Demand (odt)	Feedstock 25 km (odt)	Group	Group demand (odt)	Exclusive feedstock (odt)	Excess feedstock (odt)
SembCorp Utilities (UK) Limited	473114	473592	1	581164	1054806	473642
Petroplus Refining Teesside Ltd and Phillips-Imperial Petroleum Ltd	99793	645128				
Elementis Chromium	8256	1002741				
BP Chemicals Ltd	79929	579038	2	138999	832050	693051
Aarhus United UK Ltd	23319	590051				
Croda Chemicals Europe Ltd	14477	658658				
Gassco AS	21274	274749				
Redfearn Glass Ltd and Rexam Glass Barnsley Ltd and Rockware Glass Ltd	68755	472421	3	97797	921716	823918
Sheffield Teaching Hospitals NHS Trust	11515	328704				
Sheffield Teaching Hospitals NHS Trust	9451	283934				

Site name	Demand (odt)	Feedstock 25 km (odt)	Group	Group demand (odt)	Exclusive feedstock (odt)	Excess feedstock (odt)
Campbell Grocery Products Limited	8076	627525				
The University of Manchester	16212	370449	4	60929	504371	443441
Basell Polyolefins UK Ltd	13493	522000				
Manchester Airport plc	9196	471920				
AstraZeneca UK Ltd	22029	426587				
Nottingham University Hospitals NHS Trust	10924	785487	5	44122	1547643	1503521
University Of Nottingham	8481	773076				
Rolls-Royce plc	10276	666968				
AstraZeneca plc	14441	924740				
Ministry of Defence	9336	538197	6	21820	745221	723401
SI Group UK Ltd	12485	469661				
Ministry of Defence	7732	772667	7	28773	1930910	1902137
IBC Vehicles Ltd	9810	999431				
GlaxoSmithKline plc	11231	897471				
Eastham Refinery Ltd	19796	235040	4b	88177	204606	116429
Ford Motor Company Ltd and Jaguar Cars Ltd	16582	340839				
Innospec Ltd	10529	269019				
Vauxhall Motors Ltd	20635	249909				
Vauxhall Motors Ltd	20635	249909				
ExxonMobil Chemical Limited	191561	251105	7b	202021	298922	96901
Fleet Support Ltd	10460	194156				
Star Energy UK Onshore Ltd	16389	587037	7c	47587	674697	627110
AWE plc	31198	496784				
Heathrow Airport Ltd and British Airways plc	19111	305411	7d	76098	777728	701630
Guys & St Thomas' Hospital NHS Trust	9977	251297				
Guys & St Thomas' Hospital NHS Trust	7544	292010				
Ford Motor Company Ltd	31110	529872				
Ford Motor Company Ltd	8356	699933				
Not grouped						
TG Power Limited	17223	250559			244008	226785
Harworth Power Ltd	23089	899037			838725	815636
SmithKline Beecham plc and Glaxosmithkline Plc	12308	237581			116775	104467
Gatwick Airport Ltd	8431	541748			349711	341281

Site name	Demand (odt)	Feedstock 25 km (odt)	Group	Group demand (odt)	Exclusive feedstock (odt)	Excess feedstock (odt)
Garden Isle Frozen Foods Ltd	7642	139619			139618	131976
Muntons plc	15516	1220090			1220089	1204573
Innovia Films Ltd	18524	367718			367717	349194
Devonport Royal Dockyard Ltd	14197	4094	Not viable			
BP Oil UK Ltd	687954	587733	Not viable			
					Total useful feedstock (odt)	
Useful feedstock = sum of demands which can be met					1490221	

Appendix 2: Model development for tillage

2.1 Code development for simulation of changes in bulk density

2.1.1 Filename bd_till.c

```
#include <stdio.h>
#include <stdlib.h>
#include "n2o_model.h"
#include "soilwater.h"
#include "swconst.h"
#include <math.h>


extern LAYERPAR_SPT layers;
float hydr_cond(float satcond, float theta, float thetas, float soiltavg,
          float volmin);
void bd_till(float *bdc, float *bulkden, float *rsetbd, float *thetas_bd, float *A)
{
          int ilyr;

for (ilyr=0; ilyr < layers->numlyrs; ilyr++) {

          if((layers->rsetbd[ilyr] > layers->bulkd[ilyr] - 0.2) && (*bdc < 0.0)) {
                    layers->rsetbd[ilyr] = layers->rsetbd[ilyr] + *bdc;

          }else if((layers->rsetbd[ilyr] < layers->bulkd[ilyr] + 0.1) && (*bdc > 0.0)) {
                    layers->rsetbd[ilyr] = layers->rsetbd[ilyr] + *bdc;

          }else {
                    layers->rsetbd[ilyr] = layers->rsetbd[ilyr];}
          printf("layers->rsetbd[%1d] = %8.6f\n", ilyr, layers->rsetbd[ilyr]);

    layers->thetas_bd[ilyr] = 95*(1-layers->rsetbd[ilyr]/(float)PARTDENS);
}

return;
}
```

2.1.2 Filename org_bdc.c

```
#include <stdio.h>
#include <stdlib.h>
#include "n2o_model.h"
#include "soilwater.h"
#include <math.h>

extern LAYERPAR_SPT layers;
void org_bdc(float *obdc)
{
/*          calculate organic matter for tillage calculation*/
 *obdc = (layers->orgfrac[0]*layers->width[0] +
             layers->orgfrac[1]*layers->width[1] +
             layers->orgfrac[2]*layers->width[2]) /
            (layers->width[0] + layers->width[1] + layers->width[2]);

}
```

2.1.3 Changes to enable call to bd_till and org_bdc from simsom.f (in simsom.f)

```
c ... Fortran to C prototype
    INTERFACE

SUBROUTINE org_bdc(obdc)
       !MS$ATTRIBUTES ALIAS:'_org_bdc' :: org_bdc
            REAL    obdc
     END SUBROUTINE org_bdc

SUBROUTINE bd_till(bdc, bulkden, clyr, nlayer, bulkd)
       !MS$ATTRIBUTES ALIAS:'_bd_till' :: bd_till
       REAL    bdc
            REAL    bulkden
            INTEGER clyr
            INTEGER nlayer
            REAL    bulkd
     END SUBROUTINE bd_till

  END INTERFACE
……..

  if (docult .and. (cultday .eq. curday) .or.
   &     (cultcnt .gt. 0. .and. cultcnt .lt. 31)) then
       do 34 ii = 1, 4
        cltfac(ii) = clteff(ii)
```

```
34      continue
        do 47 ii = 1, 5
         cultbd(ii) = cultc(ii)

47      continue

            if (cultday .eq. curday) then
         cultcnt = 0
                    endif
c..... bdc is bd multiplier to calculate the effect of cult on bd.
c ..... calculate newbd using       = bd (asread in) * bdc

c ..... chen 1999 equationto calc bdc: bdc = cultc(1) + cultc(2) * clayfrac + cultc(3) *
c.......siltfrac + cultc(4) * sandfrac + cultc(5) * orgfrac

c ..... cultc is the effect of cultivation on bulk density;read from
c ..... the cult.100 file.

c ..... if we are within 1 month of cult, apply bd multiplier
       if (cultcnt .eq. 0) then

            do 49 ii = 1, 5
         cultbd(ii) = cultc(ii)

49      continue

       call org_bdc(obdc)
            bdc= cultbd(1) + cultbd(2) * clay + cultbd(3) *
   &   silt + cultbd(4) * sand
   &   + cultbd(5)          * obdc

            print *, "bdc", bdc


           call bd_till(bdc, bulkden, clyr, nlayer, bulkd)
c48     continue
                   endif
       cultcnt = cultcnt + 1

          else
       do 35 ii = 1, 4
        cltfac(ii) = 1.0
35      continue
       cultcnt = 0
             endif
```

2.1.4 Application of newly calculated rsetbd

Initlyrs.c: layers->rsetbd[ilyr] = layers->bulkd[ilyr];

This sets the initial value of rsetbd

Wfps.c: porespace = 1.0f - layers->rsetbd[ilyr] / (float)PARTDENS;

This applies the updated value of bd to porespace calculations

2.1.5 Added to cultin.f

```
read(16, *) cultc(1), name
call ckdata('schedl','cultc',name)
read(16, *) cultc(2), name
call ckdata('schedl','cultc',name)
read(16, *) cultc(3), name
call ckdata('schedl','cultc',name)
read(16, *) cultc(4), name
call ckdata('schedl','cultc',name)
read(16, *) cultc(5), name
call ckdata('schedl','cultc',name)
```

2.1.6 Added parameter listings

Parameters which have been added must be listed in .inc (for fortran) or .h (for c) ancillary files to ensure that the model recognises them

```
soilwater.h:    float  rsetbd[MAXLYR];
soilwater.h:    void bd_till(float *bdc);
soilwater.h:    void obdc(float *obdc);
Param.inc:      &    cgresp(3),fgresp(6), obdc,
Param.inc:      &       cgresp,fgresp, obdc,
Dovars.inc:     c ... cultcnt     number of days that cultivation effect on decomposition
Dovars.inc:     &            omadday, plntday, seneday, tremday, cultcnt,
Dovars.inc:     integer  cultcnt, fertcnt, erodcnt, grazcnt, irricnt, plntcnt,
Parcp.inc:      &    cfrtcn(2),cfrtcw(2),clteff(4),cultc(5),cthc(2),cmxturn,
Parcp.inc:      &     cfrtcn,cfrtcw,clteff,cultc,cthc,cmxturn,crprtf,cultra,
```

2.2 Types of tillage

Site 5 states “moldbord plough” (See p# visual glossary)
Site 4 states “conventional till” (assume moldbord plough)
Sites 3 and 6 state “moldbord plough”

```
K     Moldbord_Plough
0.0                'CULTRA(1)'
0.05               'CULTRA(2)'
0.95               'CULTRA(3)'
0.05               'CULTRA(4)'
0.95               'CULTRA(5)'
0.95               'CULTRA(6)'
1.0                'CULTRA(7)'
1.0                'CLTEFF(1)'
3.0               'CLTEFF(2)'
3.0               'CLTEFF(3)'
```

```
1.15                'CLTEFF(4)'
-0.363              'CULTC(1)'
0.000               'CULTC(2)'
0.000               'CULTC(3)'
0.389               'CULTC(4)'
0.000               'CULTC(5)'
```

Site 2 states “rotovator”: this is similar to the rototiller in terms of morphology and functionality (see p# visual glossary)

Values were taken from Chen for CULTC(1-4) and the other parameters are from the existing DayCent input files

```
ROT     rotavator_rototiller_cultivator
0.0                 'CULTRA(1)'
0.4                 'CULTRA(2)'
0.6                 'CULTRA(3)'
0.1                 'CULTRA(4)'
0.6                 'CULTRA(5)'
0.25                'CULTRA(6)'
0.7                 'CULTRA(7)'
1.700               'CLTEFF(1)'
1.700               'CLTEFF(2)'
2.000               'CLTEFF(3)'
2.000               'CLTEFF(4)'
-0.23000            'CULTC(1)'
0.0000              'CULTC(2)'
0.0000              'CULTC(3)'
0.0000               'CULTC(4)'
0.0000               'CULTC(5)'
```

Site 2 states “rotary harrowing to 8–10 cm”: this is similar to ridger (see p# visual glossary)

Values were taken from Chen for CULTC(1-4) and the other parameters are from the existing DayCent input files

```
D     Field_and_Row_Cultivators_ridger
0.0                 'CULTRA(1)'
0.4                 'CULTRA(2)'
0.6                 'CULTRA(3)'
0.1                 'CULTRA(4)'
0.6                 'CULTRA(5)'
0.25                'CULTRA(6)'
0.7                 'CULTRA(7)'
1.0                 'CLTEFF(1)'
1.0                 'CLTEFF(2)'
1.0                 'CLTEFF(3)'
```

```
1.0                 'CLTEFF(4)'
-0.292              'CULTC(1)'
-0.4135             'CULTC(2)'
0.000                  'CULTC(3)'
0.0000                 'CULTC(4)'
0.0485                 'CULTC(5)'
```

2.3 Calibrating Cult.100 decomposition factor

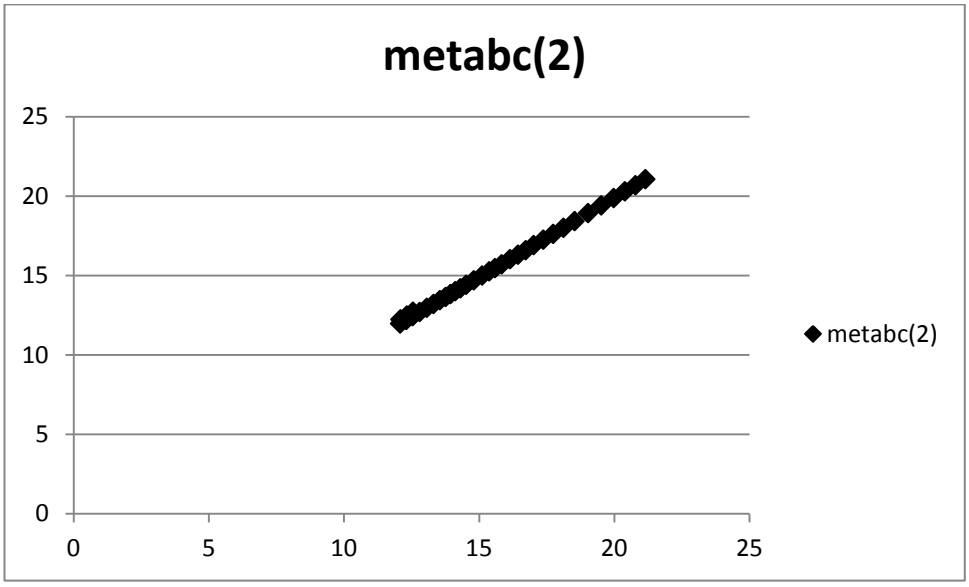

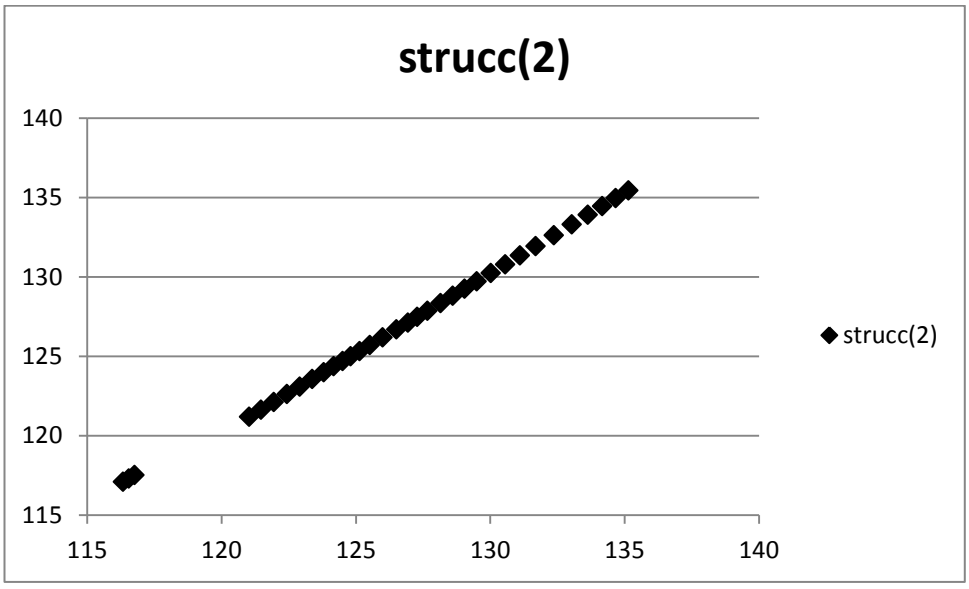

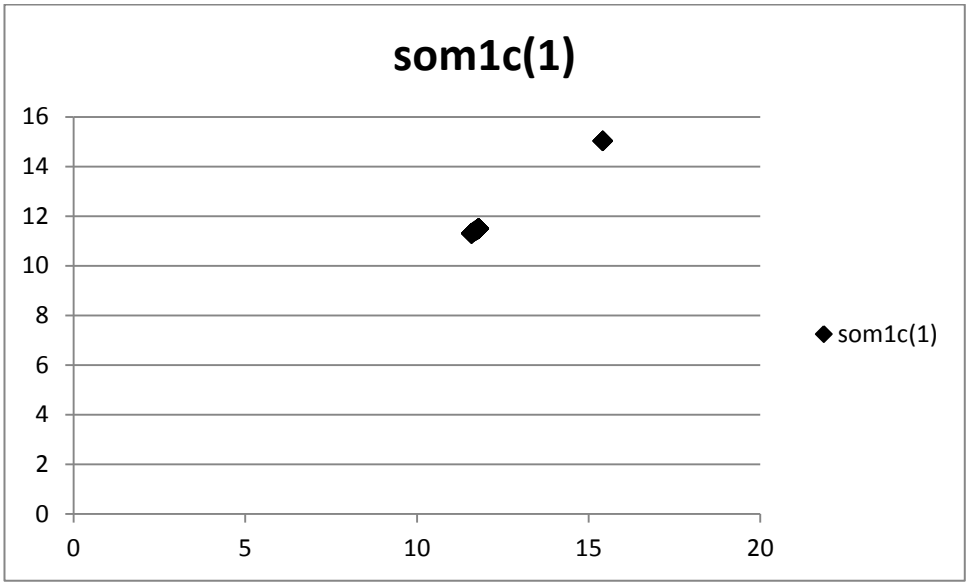
som1c(1)
16
14
12
10
8
6
4
2
0
0
5
10
15
20
som1c(1)

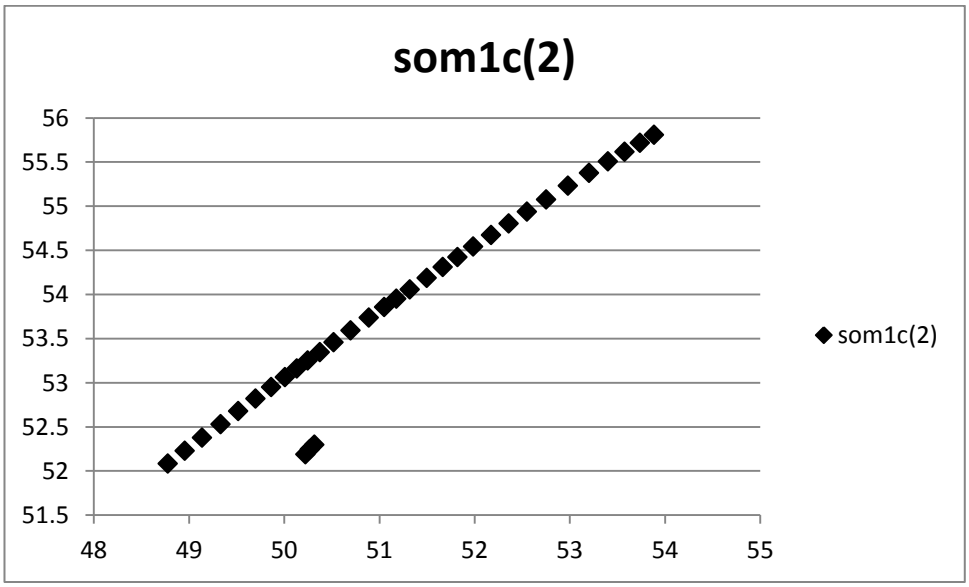
som1c(2)
56
55.5
55
54.5
54
53.5
53
52.5
52
51.5
48
49
50
51
52
53
54
55
som1c(2)

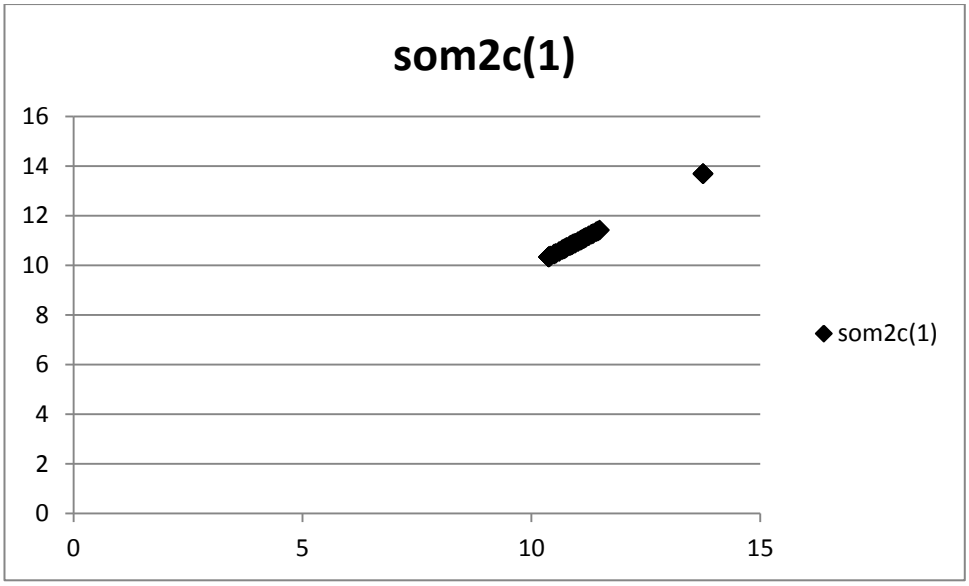
som2c(1)
16
14
12
10
8
6
4
2
0
0
5
10
15
som2c(1)

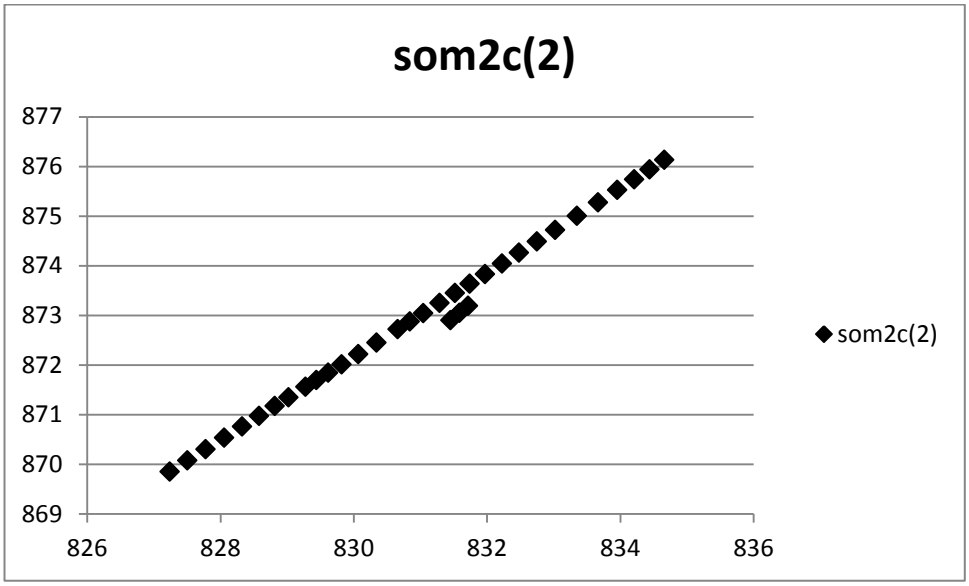

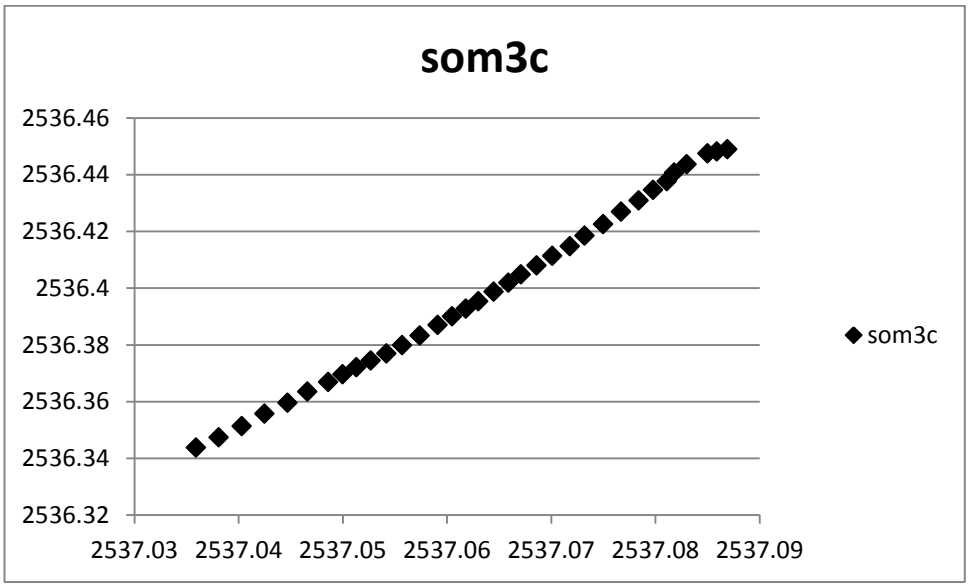

Figure A.2.1Graphs produced for cult.100 type ROT, listed in Appendix Section 2.2, produced at tillage calibration site 2, to indicate relationship between soil C pool as simulated with the DayCent model as distributed (X axis) and the adapted DayCent model (Y axis) over 30 days following simulated tillage. Where all values are in Daily carbon in soil organic matter pools g m^{-2} and:
metabc(2) = metabolic C in soil litter
strucc(2) = soil litter structural C
som1c(1) = C in surface active pool soil organic matter
som1c(2) = C in soil active soil pool organic matter
som2c(1) = C in surface slow pool soil organic matter
som2c(2) = C in soil slow pool soil organic matter
som3c = C in passive pool soil organic matter

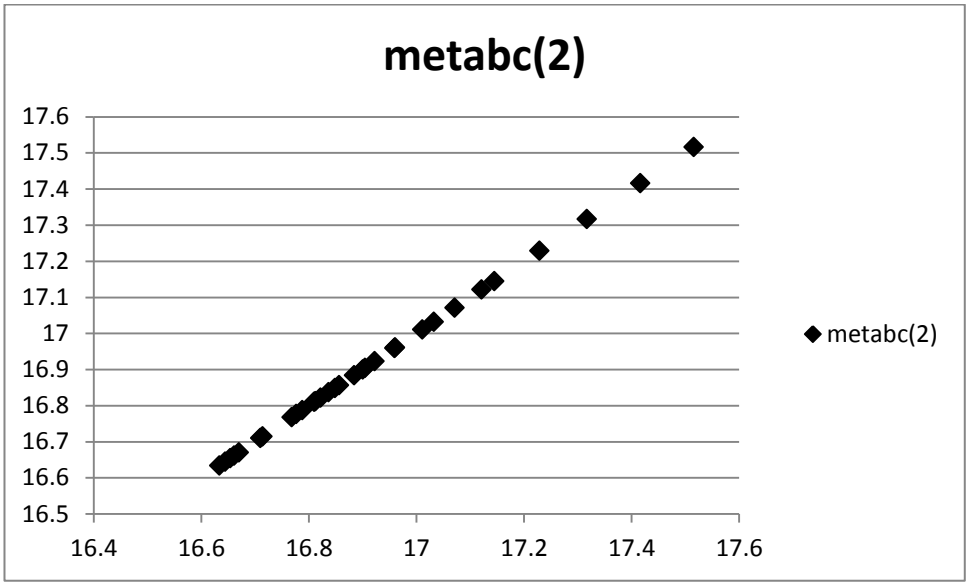
metabc(2)
17.6
17.5
17.4
17.3
17.2
17.1
17
16.9
16.8
16.7
16.6
16.5
16.4
16.6
16.8
17
17.2
17.4
17.6
metabc(2)

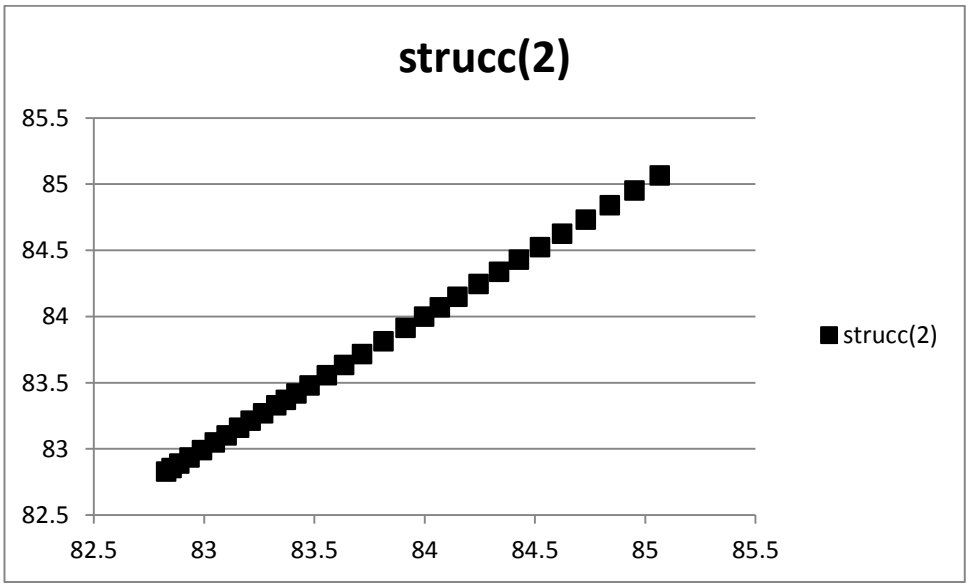
strucc(2)
85.5
85
84.5
84
83.5
83
82.5
82.5
83
83.5
84
84.5
85
85.5
strucc(2)

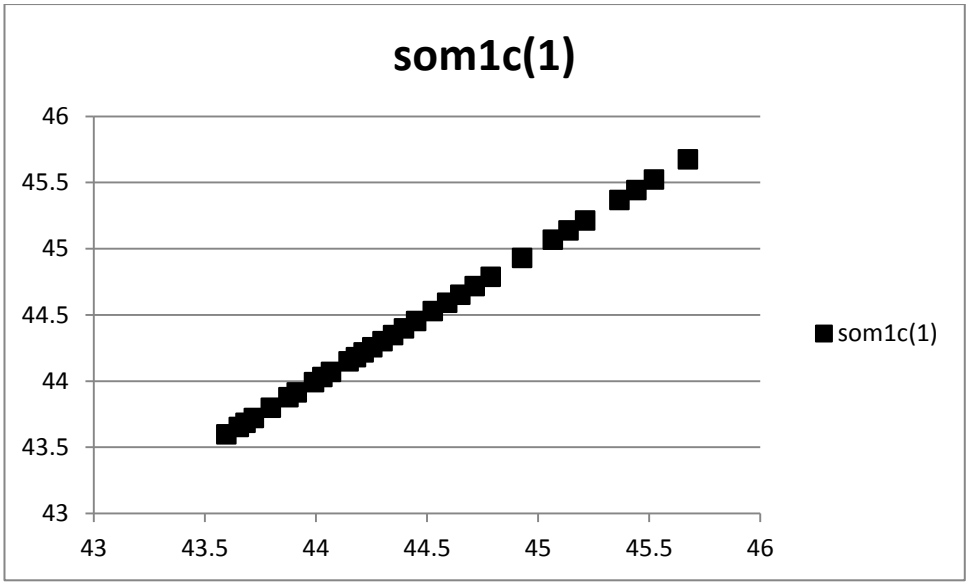
som1c(1)
46
45.5
45
44.5
44
43.5
43
43
43.5
44
44.5
45
45.5
46
som1c(1)

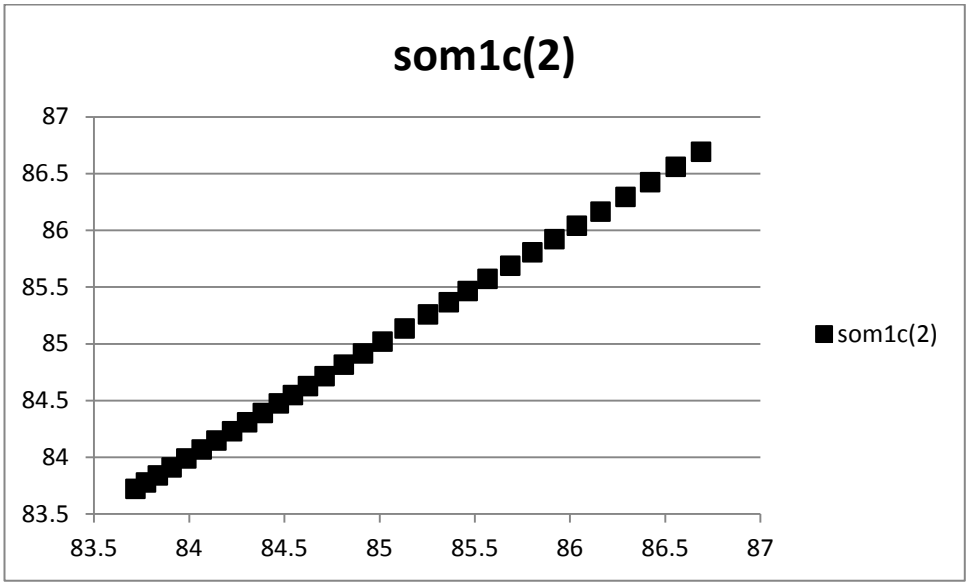
som1c(2)
87
86.5
86
85.5
85
84.5
84
83.5
83.5
84
84.5
85
85.5
86
86.5
87
som1c(2)

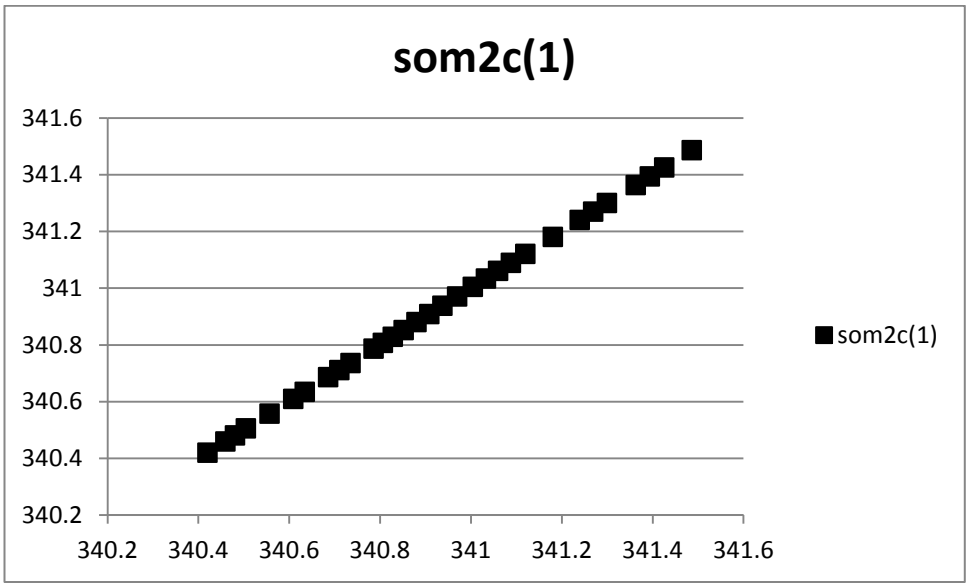
som2c(1)
341.6
341.4
341.2
341
340.8
340.6
340.4
340.2
340.2
340.4
340.6
340.8
341
341.2
341.4
341.6
som2c(1)

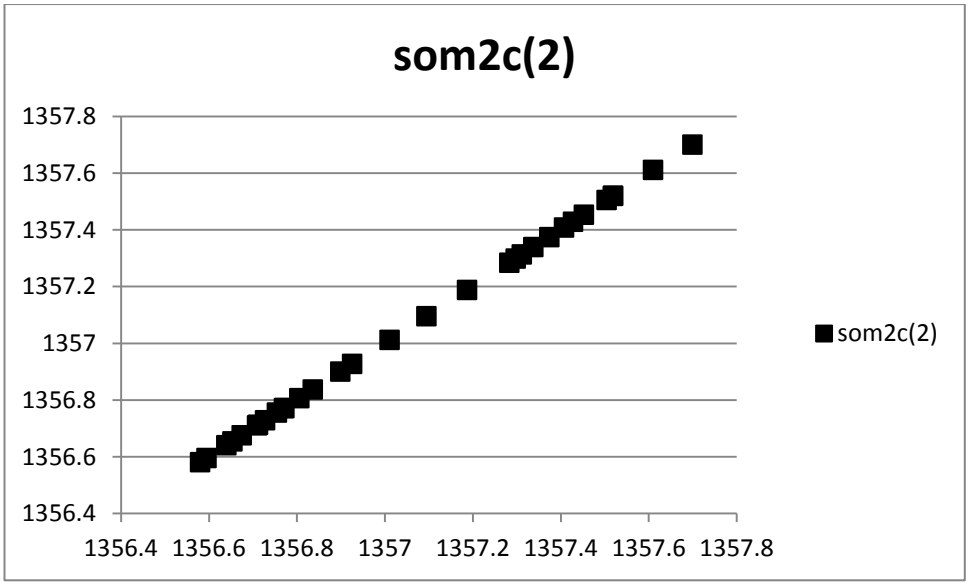
som2c(2)
1357.8
1357.6
1357.4
1357.2
1357
1356.8
1356.6
1356.4
1356.4
1356.6
1356.8
1357
1357.2
1357.4
1357.6
1357.8
som2c(2)

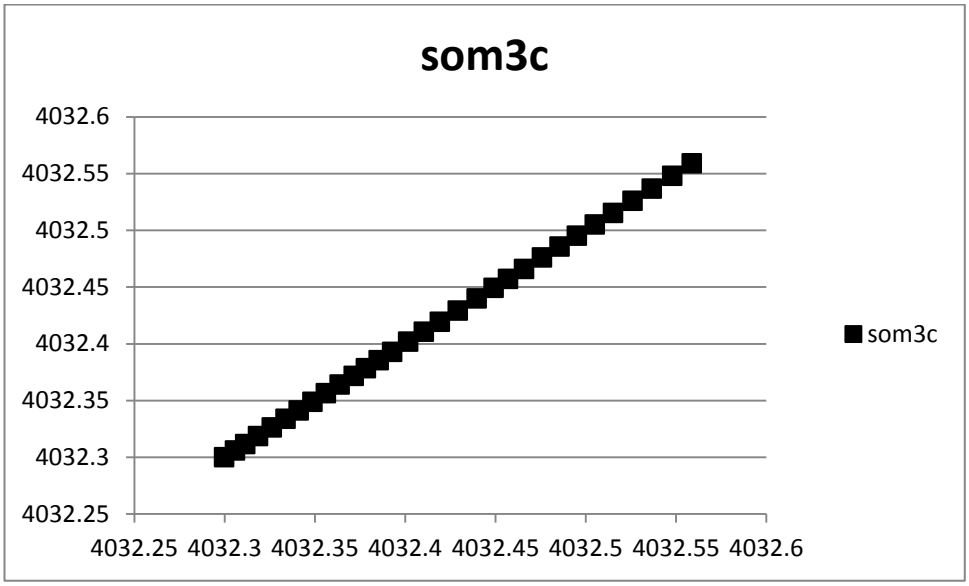

Figure A.2.2Graphs produced for cult.100 type K, listed in Appendix Section 2.2, produced at tillage calibration site 3, to indicate relationship between soil C pool as simulated with the DayCent model as distributed (X axis)and the adapted DayCent model (Y axis) over 30 days following simulated tillage. Where all values are in Daily carbon in soil organic matter pools g m^{-2} and:
metabc(2) = metabolic C in soil litter
strucc(2) = soil litter structural C
som1c(1) = C in surface active pool soil organic matter
som1c(2) = C in soil active soil pool organic matter
som2c(1) = C in surface slow pool soil organic matter
som2c(2) = C in soil slow pool soil organic matter
som3c = C in passive pool soil organic matter

2.4 Figures from publications used to calibrate tillage

Figure A2.1: Figure 1 from Rochette et al. (2008a) Time series WFPS and N_2O emissions for the heavy clay soil

This figure could not be included for copyright reasons, but can be found in:

Rochette, P., Angers, D.A., Chantigny, M.H., Bertrand, N., 2008. Nitrous Oxide Emissions Respond Differently to No-Till in a Loam and a Heavy Clay Soil. Soil Science Society of America Journal 72, 1363–1369.

This figure shows the pattern of WFPS in m^3m^{-3} for the clay soil measured by Rochette et al. (2008a) which was between 0.6 m^3m^{-3} and 0.8 m^3m^{-3} for much of the measured period, dropping to around half this value in summer. Minimum measured WFPS was around 0.2 m^3m^{-3}. Significantly, the figure indicates 0.1 – 0.2 m^3m^{-3} lower saturation for the conventional till site from September to May, and this difference between sites may be important for N_2O emissions. The figure also shows measured data for N_2O emissions over the same period, indicating generally similar emissions for T and NT sites, with higher emissions from the NT site in the period following tillage in September. Measured emissions were low for much of the study period with very large peaks for the NT condition, particularly in September and October, in the region of 10 to 15 mg m^{-3} h^{-1}. These peaks were much smaller in 2002. There are no data for December through to April in any of these years for N_2O or WFPS.

Figure A2.2: Figure 3 from Rochette et al. (2008a). Time series WFPS and N_2O emissions for the loam soil

This figure could not be included for copyright reasons, but can be found in:

Rochette, P., Angers, D.A., Chantigny, M.H., Bertrand, N., 2008. Nitrous Oxide Emissions Respond Differently to No-Till in a Loam and a Heavy Clay Soil. Soil Science Society of America Journal 72, 1363–1369.

This figure shows the pattern of WFPS for the loamy soil measured by Rochette et al. (2008) which was between 0.4 m^3m^{-3} and 0.6 m^3m^{-3} for much of the measured period, with minimum values below 0.1 m^3m^{-3}, and 0.1 – 0.3 m^3m^{-3} lower saturation for the conventional till site from September 2001 to May 2002, and May to June, as well as much of August through September in 2003. The figure also shows measured data for N_2O emissions over the same period, indicating generally similar emissions for T and NT sites, with higher emissions from the conventional till site in the period following tillage. Measured emissions over the whole study period were much lower than values recorded for either management on the clay soil, generally below 0.1 mg m^{-3} h^{-1}, with peaks at the tilled site following tillage, reaching around 0.2 mg m^{-3} h^{-1}. Measured N_2O emissions

were slightly elevated at both T and NT sites between April and July, but never exceeded 0.4 mg m^{-3} h^{-1}. There are no data for December through to April in any of these years for N_2O or WFPS.

Figure A2.3: Figure 2 from Lemke et al. (1999). Time series N_2O emissions

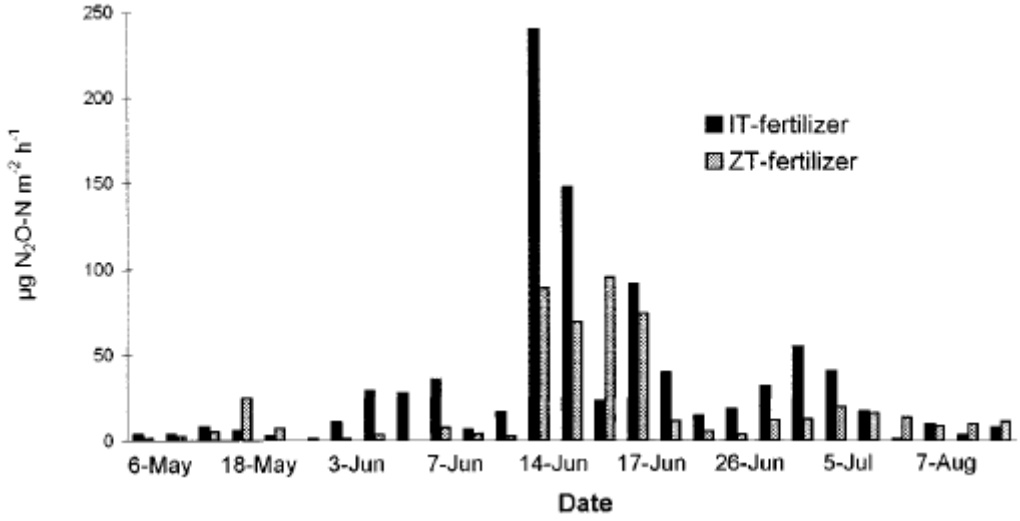

Figure A2.4: Figure 3 from Chatskikh et al. (2007). Time series soil water content and N_2O emissions

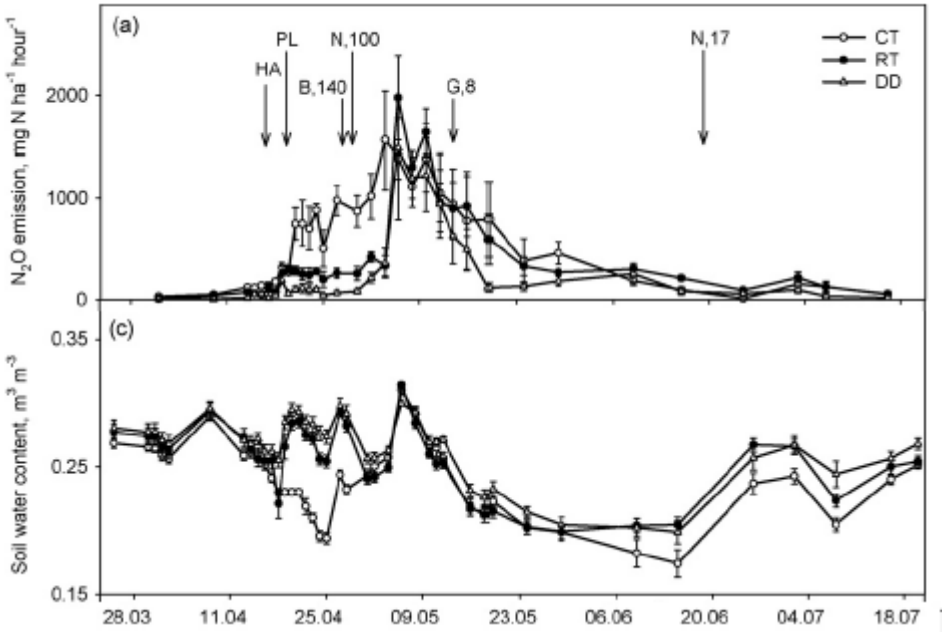

Figure A2.5: Figure 3 from Baggs et al. (2003). Time series WFPS and N_2O emissions –the model run in chapter 4 represents the fertilised bean (residue) condition. Arrow indicates timing of fertiliser application.

This figure could not be included for copyright reasons, but can be found in:

Baggs, E.M.S., M.; Pihlatie, M.; Regar, A.; Cook, H.; Cadisch,G., 2003. Nitrous oxide emissions following application of residues and fertiliser under zero and conventional tillage. Plant and Soil 254, 361-370.

Field data in Baggs et al. (2003) show the N_2O emissions peak in response to fertiliser which was significantly higher for the NT condition; around 300 compared to 60g N_2O-N $ha^{-1}d^{-1}$. For both tillage conditions, emissions peaked 2 or 3 days after fertiliser input, halved by around 5 days after the peak, and returned to a baseline of 10-20 g N_2O-N $ha^{-1}d^{-1}$ around 10 days after the peak. WFPS data for the site were not included in the publication.

Appendix 3: Model development for coppicing of trees (SRC willow)

3.1 Code development for coppicing of trees

3.1.1 Added to tremin.f

```
c ... Number of lines to read for each tree removal type

     parameter (TREMLNS = 21)

      call ckdata('schedl','copp',name)

          print *, "copp", copp
```

3.1.2 Ammendment of killrt.f

```
c ... Death of COARSE ROOTS

     if (crootc .gt. 0.001) then
       crd = crootc * fd(2)

c ... Amendment to transfer  C and nutrients into forest growth pool instead of dead root OM pool
if c ... COPP event scheduled

              if (copp .lt. 0) then
             do 23 iel = 1, nelem
           dethe = crd * (croote(iel)/crootc)

        call flow(croote(iel),forstg(iel),time,dethe)
23      continue

       call csched(crd,crtcis(LABELD),crootc,
     &           crtcis(UNLABL),carbostg(FORSYS,UNLABL),
     &           crtcis(LABELD),carbostg(FORSYS,LABELD),
     &           1.0,accum)
          Endif
c ... Where:
c ... croote(iel)          Coarse root nutrients (N, P and S are flowed separately)
c ... forstg(iel)          Forest store of nutrients (N, P and S)
c ... crtcis                        Coarse root carbon
c ... carbostg             Carbon storage
c ... FORSYS               denotes that this is a forest system (as opposed to crop or grassland)
c ... LABELD and UNLABL          refer to whether or not C is labelled
c ... End amendment
```

```
            do 20 iel = 1, nelem
          dethe = crd * (croote(iel)/crootc)


          call flow(croote(iel),wood3e(iel),time,dethe)
20        continue

         call csched(crd,crtcis(LABELD),crootc,
     &              crtcis(UNLABL),wd3cis(UNLABL),
     &              crtcis(LABELD),wd3cis(LABELD),
     &              1.0,accum)
        endif
```

3.1.3 Added to treein.f

```
c ... Number of lines to read for each tree type
      parameter (TREELNS = 153)


       read(11, *) prdc, name
       call ckdata('treein','prdc',name)
```

3.1.4 Added to potfor.f

```
if (copp .ge. 2) then
            prdx(2)= prdx(2)
            else
            prdx(2)= prdc
```

3.1.5 Added to treegrow.f

```
if (copp .ge. 2) then
            if (trage .le. swold) then
c ..... Use juvenile forest C allocation fractions
       iptr = 1

      else
c ..... Use mature forest C allocation fractions
       iptr = 2

            endif
            else
c ..... Use coppice C allocation fractions
       iptr = 3
```

```
      Endif

c ..... Increment the counter that is tracking the number of days to
c ..... apply COPP growth parameters

                              copp= copp +1
```

3.1.6 Added to default.f

```
            prdc = 0.0
```

3.1.7 Added parameter listings

Parameters which have been added must be listed in .inc (for fortran) or .h (for c) ancillary files to ensure that the model recognises them

Param.inc: & trage, prdc

3.2 Willow input values in tree.100

```
WILL     Willow_[Callibrate]
1.00000          'DECID'
0.6            'PRDX(2)'
0.80            'PRDC'
20.00000          'PPDF(1)'
40.00000          'PPDF(2)'
1.70000           'PPDF(3)'
3.70000           'PPDF(4)'
22.99000          'CERFOR(1,1,1)'
396.00000         'CERFOR(1,1,2)'
40.00000          'CERFOR(1,1,3)'
64.98723         'CERFOR(1,2,1)'
500.00000         'CERFOR(1,2,2)'
83.00000          'CERFOR(1,2,3)'
100.98589        'CERFOR(1,3,1)'
500.00000         'CERFOR(1,3,2)'
70.00000          'CERFOR(1,3,3)'
120.98589           'CERFOR(1,4,1)'
479.00000         'CERFOR(1,4,2)'
131.00000         'CERFOR(1,4,3)'
112.9807          'CERFOR(1,5,1)'
833.00000         'CERFOR(1,5,2)'
100.00000         'CERFOR(1,5,3)'
40.01242          'CERFOR(2,1,1)'
396.00000         'CERFOR(2,1,2)'
40.00000          'CERFOR(2,1,3)'
```

```
70.01277          'CERFOR(2,2,1)'
500.00000         'CERFOR(2,2,2)'
83.00000          'CERFOR(2,2,3)'
200.00000         'CERFOR(2,3,1)'
500.00000         'CERFOR(2,3,2)'
70.00000          'CERFOR(2,3,3)'
220.01411          'CERFOR(2,4,1)'
479.00000         'CERFOR(2,4,2)'
113.02000         'CERFOR(2,4,3)'
200.0193          'CERFOR(2,5,1)'
833.00000         'CERFOR(2,5,2)'
100.00000         'CERFOR(2,5,3)'
38               'CERFOR(3,1,1)'
396.00000         'CERFOR(3,1,2)'
40.00000          'CERFOR(3,1,3)'
50               'CERFOR(3,2,1)'
500.00000         'CERFOR(3,2,2)'
83.00000          'CERFOR(3,2,3)'
98.00000          'CERFOR(3,3,1)'
500.00000         'CERFOR(3,3,2)'
70.00000          'CERFOR(3,3,3)'
98                'CERFOR(3,4,1)'
479.00000         'CERFOR(3,4,2)'
131.00000         'CERFOR(3,4,3)'
113                'CERFOR(3,5,1)'
833.00000         'CERFOR(3,5,2)'
100.00000         'CERFOR(3,5,3)'
1.50000           'DECW1'
0.50000           'DECW2'
0.60000           'DECW3'
0.37             'FCFRAC(1,1)'
0.15              'FCFRAC(2,1)'
0.12              'FCFRAC(3,1)'
0.21              'FCFRAC(4,1)'
0.15              'FCFRAC(5,1)'
0.339991           'FCFRAC(1,2)'
0.038439          'FCFRAC(2,2)'
0.347103          'FCFRAC(3,2)'
0.248706          'FCFRAC(4,2)'
0.025762          'FCFRAC(5,2)'
0.20             'FCFRAC(1,3)'
0.01              'FCFRAC(2,3)'
0.44              'FCFRAC(3,3)'
0.34              'FCFRAC(4,3)'
0.01              'FCFRAC(5,3)'
0.15000             'TFRTCN(1)'
0.0100            'TFRTCN(2)'
0.1500            'TFRTCW(1)'
0.0100           'TFRTCW(2)'
0.00000           'LEAFDR(1)'
0.00000           'LEAFDR(2)'
0.00000           'LEAFDR(3)'
0.00000           'LEAFDR(4)'
0.00000           'LEAFDR(5)'
0.00000           'LEAFDR(6)'
0.03000           'LEAFDR(7)'
0.03000           'LEAFDR(8)'
0.03000           'LEAFDR(9)'
0.03000           'LEAFDR(10)'
```

```
0.00000           'LEAFDR(11)'
0.00000           'LEAFDR(12)'
0.0130           'BTOLAI'
441.00           'KLAI'
-0.47000          'LAITOP'
8.00000           'MAXLAI'
1.00000           'MAXLDR'
0.750000           'FORRTF(1)'
0.75000           'FORRTF(2)'
0.75000           'FORRTF(3)'
1500.00           'SAPK'
1000.00           'SWOLD'
0.20300           'WDLIG(1)'
0.16000           'WDLIG(2)'
0.25000           'WDLIG(3)'
0.25000           'WDLIG(4)'
0.25000           'WDLIG(5)'
0.25000           'WDLIG(6)'
1.000          'WOODDR(1)'
0.0400           'WOODDR(2)'
0.0400           'WOODDR(3)'
0.01000           'WOODDR(4)'
0.00200           'WOODDR(5)'
0.12000           'WOODDR(6)'
0.14000           'WRDSRFC'
0.05000           'WMRTFRAC'
0.004         'SNFXMX(2)'
-26.000           'DEL13C'
1.25000           'CO2IPR'
0.75000           'CO2ITR'
1.25000           'CO2ICE(1,1,1)'
1.00000           'CO2ICE(1,1,2)'
1.00000           'CO2ICE(1,1,3)'
1.25000           'CO2ICE(1,2,1)'
1.00000           'CO2ICE(1,2,2)'
1.00000           'CO2ICE(1,2,3)'
1.00000           'CO2IRS'
1.00000           'BASFC2'
1.00000           'BASFCT'
0.80000           'SITPOT'
13.5000           'MAXNP'
0.01525           'FKMRSPMX(1)'
0.30000           'FKMRSPMX(2)'
0.01525           'FKMRSPMX(3)'
0.01525           'FKMRSPMX(4)'
0.01525           'FKMRSPMX(5)'
0.16000           'FKMRSPMX(6)'
0.00000           'FMRSPLAI(1)'
0.00000           'FMRSPLAI(2)'
0.75000           'FMRSPLAI(3)'
1.00000           'FMRSPLAI(4)'
2.00000           'FMRSPLAI(5)'
2.00000           'FMRSPLAI(6)'
0.23000           'FGRESP(1)'
0.23000           'FGRESP(2)'
0.23000           'FGRESP(3)'
0.23000           'FGRESP(4)'
0.23000           'FGRESP(5)'
```

```
0.23000           'FGRESP(6)'
0.50000           'NO3PREF(2)'
7                 'TLAYPG'
0                 'TRAGE'
0.25000           'TMIX'
5.00000           'TMPLFF'
8.0000           'TMPLFS'
100.0             'FURGDYS'
1.0               'FLSGRES'
0.12              'TMXTURN'
1.0               'NPP2CS(2)'
```

3.3 Coppice input values in trem.100

```
COPP   coppice
0.00000           'EVNTYP'
1.00000           'REMF(1)'
1.00000          'REMF(2)'
0.95000           'REMF(3)'
1.00000           'REMF(4)'
0.95000            'REMF(5)'
0.00000           'FD(1)'
0.20000           'FD(2)'
1.00000           'RETF(1,1)'
1.00000           'RETF(1,2)'
0.00000           'RETF(1,3)'
0.00000           'RETF(1,4)'
0.00000           'RETF(2,1)'
0.00000           'RETF(2,2)'
0.00000           'RETF(2,3)'
0.00000           'RETF(2,4)'
0.00000           'RETF(3,1)'
0.00000           'RETF(3,2)'
0.00000           'RETF(3,3)'
0.00000           'RETF(3,4)'
-150                 'COPP'
```

Appendix 4: Scenario analysis

4.1 Soil input files

Column 1 - Minimum depth of soil layer (cm)
Column 2 - Maximum depth of soil layer (cm)
Column 3 - Bulk density of soil layer (g cm^{-3})
Column 4 - Field capacity of soil layer, volumetric
Column 5 - Wilting point of soil layer, volumetric
Column 6 - Evaporation coefficient for soil layer (currently not being used)
Column 7 - Percentage of roots in soil layer, these values must sum to 1.0
Column 8 - Fraction of sand in soil layer, 0.0 - 1.0
Column 9 - Fraction of clay in soil layer, 0.0 - 1.0
Column 10 - Organic matter in soil layer, fraction 0.0 - 1.0
Column 11 - Minimum volumetric soil water content below wilting point for soil layer, soil water content will not be allowed to drop below this value
Column 12 - Saturated hydraulic conductivity of soil layer (cm s^{-1})
Column 13 - pH of soil layer

1+ 2+

```
0.0   2.0  1.40  0.23365  0.10340  0.80  0.01  0.65  0.18  0.01
0.08  0.00060  5.50
  2.0   5.0  1.40  0.23365  0.10340  0.20  0.04  0.65  0.18  0.01
0.06  0.00060  5.50
  5.0  10.0  1.40  0.23365  0.10340  0.00  0.25  0.65  0.18  0.01
0.04  0.00060  5.50
 10.0  20.0  1.40  0.23365  0.10340  0.00  0.30  0.65  0.18  0.01
0.01  0.00060  5.50
 20.0  30.0  1.40  0.23365  0.10340  0.00  0.10  0.65  0.18  0.01
0.00  0.00060  5.50
30.0  45.0  1.38  0.35334  0.16525  0.00  0.05  0.33  0.35  0.01
0.00  0.00018  5.50
 45.0  60.0  1.38  0.35334  0.16525  0.00  0.04  0.33  0.35  0.01
0.00  0.00018  5.50
 60.0  75.0  1.38  0.35334  0.16525  0.00  0.03  0.33  0.35  0.01
0.00  0.00018  5.50
 75.0  90.0  1.38  0.35334  0.16525  0.00  0.02  0.33  0.35  0.01
0.00  0.00018  5.50
 90.0 105.0  1.38  0.35334  0.16525  0.00  0.01  0.33  0.35  0.01
0.00  0.00018  5.50
105.0 120.0  1.38  0.35334  0.16525  0.00  0.00  0.33  0.35  0.01
0.00  0.00018  5.50
120.0 150.0  1.38  0.35334  0.16525  0.00  0.00  0.33  0.35  0.01
0.00  0.00018  5.50
150.0 180.0  1.38  0.35334  0.16525  0.00  0.00  0.33  0.35  0.01
0.00  0.00018  5.50
180.0 210.0  1.38  0.35334  0.16525  0.00  0.00  0.33  0.35  0.01
0.00  0.00018  5.50
```

1+ 2+ Bulk density under energy crop

layers->rsetbd[0] = 1.569405
layers->rsetbd[1] = 1.569405
layers->rsetbd[2] = 1.569405
layers->rsetbd[3] = 1.569405
layers->rsetbd[4] = 1.569405
layers->rsetbd[5] = 1.549405
layers->rsetbd[6] = 1.549405
layers->rsetbd[7] = 1.549405
layers->rsetbd[8] = 1.549405
layers->rsetbd[9] = 1.549405
layers->rsetbd[10] = 1.549405
layers->rsetbd[11] = 1.549405
layers->rsetbd[12] = 1.549405
layers->rsetbd[13] = 1.549405

1- 2-

```
  0.0   2.0  1.20  0.38649  0.16504  0.80  0.01  0.15  0.35  0.01
0.13  0.00026  5.50
  2.0   5.0  1.20  0.38649  0.16504  0.20  0.04  0.15  0.35  0.01
0.10  0.00026  5.50
  5.0  10.0  1.20  0.38649  0.16504  0.00  0.25  0.15  0.35  0.01
0.07  0.00026  5.50
 10.0  20.0  1.20  0.38649  0.16504  0.00  0.30  0.15  0.35  0.01
0.02  0.00026  5.50
 20.0  30.0  1.20  0.38649  0.16504  0.00  0.10  0.15  0.35  0.01
0.00  0.00026  5.50
 30.0  45.0  1.28  0.51250  0.29618  0.00  0.05  0.20  0.60  0.01
0.00  0.00013  5.50
 45.0  60.0  1.28  0.51250  0.29618  0.00  0.04  0.20  0.60  0.01
0.00  0.00013  5.50
 60.0  75.0  1.28  0.51250  0.29618  0.00  0.03  0.20  0.60  0.01
0.00  0.00013  5.50
 75.0  90.0  1.28  0.51250  0.29618  0.00  0.02  0.20  0.60  0.01
0.00  0.00013  5.50
 90.0 105.0  1.28  0.51250  0.29618  0.00  0.01  0.20  0.60  0.01
0.00  0.00013  5.50
105.0 120.0  1.28  0.51250  0.29618  0.00  0.00  0.20  0.60  0.01
0.00  0.00013  5.50
120.0 150.0  1.28  0.51250  0.29618  0.00  0.00  0.20  0.60  0.01
0.00  0.00013  5.50
150.0 180.0  1.28  0.51250  0.29618  0.00  0.00  0.20  0.60  0.01
0.00  0.00013  5.50
180.0 210.0  1.28  0.51250  0.29618  0.00  0.00  0.20  0.60  0.01
0.00  0.00013  5.50
```

1- 2- Bulk density under energy crop

layers->rsetbd[0] = 1.324396
layers->rsetbd[1] = 1.324396
layers->rsetbd[2] = 1.324396
layers->rsetbd[3] = 1.324396
layers->rsetbd[4] = 1.324396
layers->rsetbd[5] = 1.404397
layers->rsetbd[6] = 1.404397
layers->rsetbd[7] = 1.404397
layers->rsetbd[8] = 1.404397
layers->rsetbd[9] = 1.404397
layers->rsetbd[10] = 1.404397
layers->rsetbd[11] = 1.404397
layers->rsetbd[12] = 1.404397
layers->rsetbd[13] = 1.404397

4+

```
0.0   2.0  1.31  0.35334  0.16525  0.80  0.01  0.33  0.35  0.01
0.13  0.00018  5.50
  2.0   5.0  1.31  0.35334  0.16525  0.20  0.04  0.33  0.35  0.01
0.10  0.00018  5.50
  5.0  10.0  1.31  0.35334  0.16525  0.00  0.25  0.33  0.35  0.01
0.07  0.00018  5.50
 10.0  20.0  1.31  0.35334  0.16525  0.00  0.30  0.33  0.35  0.01
0.02  0.00018  5.50
 20.0  30.0  1.31  0.35334  0.16525  0.00  0.10  0.33  0.35  0.01
0.00  0.00018  5.50
 30.0  45.0  1.31  0.35334  0.16525  0.00  0.05  0.33  0.35  0.01
0.00  0.00018  5.50
 45.0  60.0  1.31  0.35334  0.16525  0.00  0.04  0.33  0.35  0.01
0.00  0.00018  5.50
 60.0  75.0  1.31  0.35334  0.16525  0.00  0.03  0.33  0.35  0.01
0.00  0.00018  5.50
 75.0  90.0  1.31  0.35334  0.16525  0.00  0.02  0.33  0.35  0.01
0.00  0.00018  5.50
 90.0 105.0  1.31  0.35334  0.16525  0.00  0.01  0.33  0.35  0.01
0.00  0.00018  5.50
105.0 120.0  1.38  0.35334  0.16525  0.00  0.00  0.33  0.35  0.01
0.00  0.00018  5.50
120.0 150.0  1.38  0.35334  0.16525  0.00  0.00  0.33  0.35  0.01
0.00  0.00018  5.50
150.0 180.0  1.38  0.35334  0.16525  0.00  0.00  0.33  0.35  0.01
0.00  0.00018  5.50
180.0 210.0  1.38  0.35334  0.16525  0.00  0.00  0.33  0.35  0.01
0.00  0.00018  5.50
```

4+ Bulk density under energy crop

layers->rsetbd[0] = 1.355653
layers->rsetbd[1] = 1.355653
layers->rsetbd[2] = 1.355653
layers->rsetbd[3] = 1.355653
layers->rsetbd[4] = 1.355653
layers->rsetbd[5] = 1.355653
layers->rsetbd[6] = 1.355653
layers->rsetbd[7] = 1.355653
layers->rsetbd[8] = 1.355653
layers->rsetbd[9] = 1.355653
layers->rsetbd[10] = 1.425653
layers->rsetbd[11] = 1.425653
layers->rsetbd[12] = 1.425653
layers->rsetbd[13] = 1.425653

4-

```
0.0   2.0  1.21  0.51250  0.29618  0.80  0.01  0.20  0.60  0.01
0.24  0.00013  5.50
  2.0   5.0  1.21  0.51250  0.29618  0.20  0.04  0.20  0.60  0.01
0.18  0.00013  5.50
  5.0  10.0  1.21  0.51250  0.29618  0.00  0.25  0.20  0.60  0.01
0.12  0.00013  5.50
 10.0  20.0  1.21  0.51250  0.29618  0.00  0.30  0.20  0.60  0.01
0.03  0.00013  5.50
 20.0  30.0  1.21  0.51250  0.29618  0.00  0.10  0.20  0.60  0.01
0.00  0.00013  5.50
 30.0  45.0  1.21  0.51250  0.29618  0.00  0.05  0.20  0.60  0.01
0.00  0.00013  5.50
 45.0  60.0  1.21  0.51250  0.29618  0.00  0.04  0.20  0.60  0.01
0.00  0.00013  5.50
 60.0  75.0  1.21  0.51250  0.29618  0.00  0.03  0.20  0.60  0.01
0.00  0.00013  5.50
 75.0  90.0  1.21  0.51250  0.29618  0.00  0.02  0.20  0.60  0.01
0.00  0.00013  5.50
 90.0 105.0  1.21  0.51250  0.29618  0.00  0.01  0.20  0.60  0.01
0.00  0.00013  5.50
105.0 120.0  1.21  0.51250  0.29618  0.00  0.00  0.20  0.60  0.01
0.00  0.00013  5.50
120.0 150.0  1.28  0.51250  0.29618  0.00  0.00  0.20  0.60  0.01
0.00  0.00013  5.50
150.0 180.0  1.28  0.51250  0.29618  0.00  0.00  0.20  0.60  0.01
0.00  0.00013  5.50
180.0 210.0  1.28  0.51250  0.29618  0.00  0.00  0.20  0.60  0.01
0.00  0.00013  5.50
```

4- Bulk density under energy crop

layers->rsetbd[0] = 1.208802
layers->rsetbd[1] = 1.208802
layers->rsetbd[2] = 1.208802
layers->rsetbd[3] = 1.208802
layers->rsetbd[4] = 1.208802
layers->rsetbd[5] = 1.208802
layers->rsetbd[6] = 1.208802
layers->rsetbd[7] = 1.208802
layers->rsetbd[8] = 1.208802
layers->rsetbd[9] = 1.208802
layers->rsetbd[10] = 1.208802
layers->rsetbd[11] = 1.278802
layers->rsetbd[12] = 1.278802
layers->rsetbd[13] = 1.278802

5+ 6+

```
0.0   2.0  1.37  0.25474  0.16569  0.80  0.01  0.65  0.35  0.01
0.13  0.00011  6.50
  2.0   5.0  1.37  0.25474  0.16569  0.20  0.04  0.65  0.35  0.01
0.10  0.00011  6.50
  5.0  10.0  1.37  0.25474  0.16569  0.00  0.25  0.65  0.35  0.01
0.07  0.00011  6.50
 10.0  20.0  1.37  0.25474  0.16569  0.00  0.30  0.65  0.35  0.01
0.02  0.00011  6.50
 20.0  30.0  1.37  0.25474  0.16569  0.00  0.10  0.65  0.35  0.01
0.00  0.00011  6.50
 30.0  45.0  1.37  0.25474  0.16569  0.00  0.05  0.65  0.35  0.01
0.00  0.00011  6.50
 45.0  60.0  1.37  0.25474  0.16569  0.00  0.04  0.65  0.35  0.01
0.00  0.00011  6.50
 60.0  75.0  1.27  0.25474  0.16504  0.00  0.03  0.15  0.35  0.01
0.00  0.00026  6.50
 75.0  90.0  1.27  0.25474  0.16504  0.00  0.02  0.15  0.35  0.01
0.00  0.00026  6.50
 90.0 105.0  1.27  0.25474  0.16504  0.00  0.01  0.15  0.35  0.01
0.00  0.00026  6.50
105.0 120.0  1.27  0.25474  0.16504  0.00  0.00  0.15  0.35  0.01
0.00  0.00026  6.50
120.0 150.0  1.27  0.25474  0.16504  0.00  0.00  0.15  0.35  0.01
0.00  0.00026  6.50
150.0 180.0  1.27  0.25474  0.16504  0.00  0.00  0.15  0.35  0.01
0.00  0.00026  6.50
180.0 210.0  1.27  0.25474  0.16504  0.00  0.00  0.15  0.35  0.01
0.00  0.00026  6.50
```

5+ 6+ Bulk density under energy crop

layers->rsetbd [0] = 1.539405
layers->rsetbd[1] = 1.539405
layers->rsetbd[2] = 1.539405
layers->rsetbd[3] = 1.539405
layers->rsetbd[4] = 1.539405
layers->rsetbd[5] = 1.539405
layers->rsetbd[6] = 1.539405
layers->rsetbd[7] = 1.439405
layers->rsetbd[8] = 1.439405
layers->rsetbd[9] = 1.439405
layers->rsetbd[10] = 1.439405
layers->rsetbd[11] = 1.439405
layers->rsetbd[12] = 1.439405
layers->rsetbd[13] = 1.439405

5- 6-

```
0.0   2.0  1.50  0.21260  0.10540  0.80  0.01  0.82  0.18  0.01
0.08  0.00057  6.50
  2.0   5.0  1.50  0.21260  0.10540  0.20  0.04  0.82  0.18  0.01
0.06  0.00057  6.50
  5.0  10.0  1.50  0.21260  0.10540  0.00  0.25  0.82  0.18  0.01
0.04  0.00057  6.50
 10.0  20.0  1.50  0.21260  0.10540  0.00  0.30  0.82  0.18  0.01
0.01  0.00057  6.50
 20.0  30.0  1.50  0.21260  0.10540  0.00  0.10  0.82  0.18  0.01
0.00  0.00057  6.50
 30.0  45.0  1.50  0.21260  0.10540  0.00  0.05  0.82  0.18  0.01
0.00  0.00057  6.50
 45.0  60.0  1.50  0.21260  0.10540  0.00  0.04  0.82  0.18  0.01
0.00  0.00057  6.50
 60.0  75.0  1.47  0.23365  0.10340  0.00  0.03  0.65  0.18  0.01
0.00  0.00060  6.50
 75.0  90.0  1.47  0.23365  0.10340  0.00  0.02  0.65  0.18  0.01
0.00  0.00060  6.50
 90.0 105.0  1.47  0.23365  0.10340  0.00  0.01  0.65  0.18  0.01
0.00  0.00060  6.50
105.0 120.0  1.47  0.23365  0.10340  0.00  0.00  0.65  0.18  0.01
0.00  0.00060  6.50
120.0 150.0  1.47  0.23365  0.10340  0.00  0.00  0.65  0.18  0.01
0.00  0.00060  6.50
150.0 180.0  1.47  0.23365  0.10340  0.00  0.00  0.65  0.18  0.01
0.00  0.00060  6.50
180.0 210.0  1.47  0.23365  0.10340  0.00  0.00  0.65  0.18  0.01
0.00  0.00060  6.50
```

5- 6- Bulk density under energy crop

layers->rsetbd[0] = 1.670512
layers->rsetbd[1] = 1.670512
layers->rsetbd[2] = 1.670512
layers->rsetbd[3] = 1.670512
layers->rsetbd[4] = 1.670512
layers->rsetbd[5] = 1.670512
layers->rsetbd[6] = 1.670512
layers->rsetbd[7] = 1.640512
layers->rsetbd[8] = 1.640512
layers->rsetbd[9] = 1.640512
layers->rsetbd[10] = 1.640512
layers->rsetbd[11] = 1.640512
layers->rsetbd[12] = 1.640512
layers->rsetbd[13] = 1.640512

7+ 8+

```
0.0   2.0  1.40  0.23365  0.10340  0.80  0.01  0.65  0.18  0.01
0.08  0.00060  5.50
  2.0   5.0  1.40  0.23365  0.10340  0.20  0.04  0.65  0.18  0.01
0.06  0.00060  5.50
  5.0  10.0  1.40  0.23365  0.10340  0.00  0.25  0.65  0.18  0.01
0.04  0.00060  5.50
 10.0  20.0  1.40  0.23365  0.10340  0.00  0.30  0.65  0.18  0.01
0.01  0.00060  5.50
 20.0  30.0  1.40  0.23365  0.10340  0.00  0.10  0.65  0.18  0.01
0.00  0.00060  5.50
 30.0  45.0  1.40  0.23365  0.10340  0.00  0.05  0.65  0.18  0.01
0.00  0.00060  5.50
 45.0  60.0  1.40  0.23365  0.10340  0.00  0.04  0.65  0.18  0.01
0.00  0.00060  5.50
 60.0  75.0  1.40  0.23365  0.10340  0.00  0.03  0.65  0.18  0.01
0.00  0.00060  5.50
 75.0  90.0  1.40  0.23365  0.10340  0.00  0.02  0.65  0.18  0.01
0.00  0.00060  5.50
 90.0 105.0  1.40  0.23365  0.10340  0.00  0.01  0.65  0.18  0.01
0.00  0.00060  5.50
105.0 120.0  1.40  0.23365  0.10340  0.00  0.00  0.65  0.18  0.01
0.00  0.00060  5.50
120.0 150.0  1.38  0.35334  0.16525  0.00  0.00  0.33  0.35  0.01
0.00  0.00018  5.50
150.0 180.0  1.38  0.35334  0.16525  0.00  0.00  0.33  0.35  0.01
0.00  0.00018  5.50
180.0 210.0  1.38  0.35334  0.16525  0.00  0.00  0.33  0.35  0.01
0.00  0.00018  5.50
```

7+ 8+ Bulk density under energy crop

layers->rsetbd[0] = 1.492550
layers->rsetbd[1] = 1.492550
layers->rsetbd[2] = 1.492550
layers->rsetbd[3] = 1.492550
layers->rsetbd[4] = 1.492550
layers->rsetbd[5] = 1.492550
layers->rsetbd[6] = 1.492550
layers->rsetbd[7] = 1.492550
layers->rsetbd[8] = 1.492550
layers->rsetbd[9] = 1.492550
layers->rsetbd[10] = 1.492550
layers->rsetbd[11] = 1.472550
layers->rsetbd[12] = 1.472550
layers->rsetbd[13] = 1.472550

7- 8-

```
  0.0   2.0  1.20  0.38649  0.16504  0.80  0.01  0.15  0.35  0.01
0.13  0.00026  5.50
  2.0   5.0  1.20  0.38649  0.16504  0.20  0.04  0.15  0.35  0.01
0.10  0.00026  5.50
  5.0  10.0  1.20  0.38649  0.16504  0.00  0.25  0.15  0.35  0.01
0.07  0.00026  5.50
 10.0  20.0  1.20  0.38649  0.16504  0.00  0.30  0.15  0.35  0.01
0.02  0.00026  5.50
 20.0  30.0  1.20  0.38649  0.16504  0.00  0.10  0.15  0.35  0.01
0.00  0.00026  5.50
 30.0  45.0  1.20  0.38649  0.16504  0.00  0.05  0.15  0.35  0.01
0.00  0.00026  5.50
 45.0  60.0  1.20  0.38649  0.16504  0.00  0.04  0.15  0.35  0.01
0.00  0.00026  5.50
 60.0  75.0  1.20  0.38649  0.16504  0.00  0.03  0.15  0.35  0.01
0.00  0.00026  5.50
 75.0  90.0  1.20  0.38649  0.16504  0.00  0.02  0.15  0.35  0.01
0.00  0.00026  5.50
 90.0 105.0  1.20  0.38649  0.16504  0.00  0.01  0.15  0.35  0.01
0.00  0.00026  5.50
105.0 120.0  1.20  0.38649  0.16504  0.00  0.00  0.15  0.35  0.01
0.00  0.00026  5.50
120.0 150.0  1.28  0.51250  0.29618  0.00  0.00  0.20  0.60  0.01
0.00  0.00013  5.50
150.0 180.0  1.28  0.51250  0.29618  0.00  0.00  0.20  0.60  0.01
0.00  0.00013  5.50
180.0 210.0  1.28  0.51250  0.29618  0.00  0.00  0.20  0.60  0.01
0.00  0.00013  5.50
```

7- 8- Bulk density under energy crop

```
layers->rsetbd[0] = 0.845400
layers->rsetbd[1] = 0.845400
layers->rsetbd[2] = 0.845400
layers->rsetbd[3] = 0.845400
layers->rsetbd[4] = 0.845400
layers->rsetbd[5] = 0.845400
layers->rsetbd[6] = 0.845400
layers->rsetbd[7] = 0.845400
layers->rsetbd[8] = 0.845400
layers->rsetbd[9] = 0.845400
layers->rsetbd[10] = 0.845400
layers->rsetbd[11] = 0.925400
layers->rsetbd[12] = 0.925400
layers->rsetbd[13] = 0.925400
```

9- 10-

```
0.0   2.0  1.47  0.23365  0.10340  0.80  0.01  0.65  0.18  0.01
0.08  0.00060  6.50
  2.0   5.0  1.47  0.23365  0.10340  0.20  0.04  0.65  0.18  0.01
0.06  0.00060  6.50
  5.0  10.0  1.47  0.23365  0.10340  0.00  0.25  0.65  0.18  0.01
0.04  0.00060  6.50
 10.0  20.0  1.47  0.23365  0.10340  0.00  0.30  0.65  0.18  0.01
0.01  0.00060  6.50
 20.0  30.0  1.47  0.23365  0.10340  0.00  0.10  0.65  0.18  0.01
0.00  0.00060  6.50
 30.0  45.0  1.47  0.23365  0.10340  0.00  0.05  0.65  0.18  0.01
0.00  0.00060  6.50
 45.0  60.0  1.47  0.23365  0.10340  0.00  0.04  0.65  0.18  0.01
0.00  0.00060  6.50
 60.0  75.0  1.47  0.23365  0.10340  0.00  0.03  0.65  0.18  0.01
0.00  0.00060  6.50
 75.0  90.0  1.47  0.23365  0.10340  0.00  0.02  0.65  0.18  0.01
0.00  0.00060  6.50
 90.0 105.0  1.47  0.23365  0.10340  0.00  0.01  0.65  0.18  0.01
0.00  0.00060  6.50
105.0 120.0  1.47  0.23365  0.10340  0.00  0.00  0.65  0.18  0.01
0.00  0.00060  6.50
120.0 150.0  1.47  0.23365  0.10340  0.00  0.00  0.65  0.18  0.01
0.00  0.00060  6.50
150.0 180.0  1.47  0.23365  0.10340  0.00  0.00  0.65  0.18  0.01
0.00  0.00060  6.50
180.0 210.0  1.47  0.23365  0.10340  0.00  0.00  0.65  0.18  0.01
0.00  0.00060  6.50
```

9- 10- Bulk density under energy crop

ayers->rsetbd[0] = 1.526600
layers->rsetbd[1] = 1.526600
layers->rsetbd[2] = 1.526600
layers->rsetbd[3] = 1.526600
layers->rsetbd[4] = 1.526600
layers->rsetbd[5] = 1.526600
layers->rsetbd[6] = 1.526600
layers->rsetbd[7] = 1.526600
layers->rsetbd[8] = 1.526600
layers->rsetbd[9] = 1.526600
layers->rsetbd[10] = 1.526600
layers->rsetbd[11] = 1.526600
layers->rsetbd[12] = 1.526600
layers->rsetbd[13] = 1.526600

11+

```
0.0   2.0  1.31  0.35334  0.16525  0.80  0.01  0.33  0.35  0.01
0.13  0.00018  5.50
  2.0   5.0  1.31  0.35334  0.16525  0.20  0.04  0.33  0.35  0.01
0.10  0.00018  5.50
  5.0  10.0  1.31  0.35334  0.16525  0.00  0.25  0.33  0.35  0.01
0.07  0.00018  5.50
 10.0  20.0  1.31  0.35334  0.16525  0.00  0.30  0.33  0.35  0.01
0.02  0.00018  5.50
 20.0  30.0  1.31  0.35334  0.16525  0.00  0.10  0.33  0.35  0.01
0.00  0.00018  5.50
 30.0  45.0  1.31  0.35334  0.16525  0.00  0.05  0.33  0.35  0.01
0.00  0.00018  5.50
 45.0  60.0  1.31  0.35334  0.16525  0.00  0.04  0.33  0.35  0.01
0.00  0.00018  5.50
 60.0  75.0  1.31  0.35334  0.16525  0.00  0.03  0.33  0.35  0.01
0.00  0.00018  5.50
 75.0  90.0  1.31  0.35334  0.16525  0.00  0.02  0.33  0.35  0.01
0.00  0.00018  5.50
 90.0 105.0  1.31  0.35334  0.16525  0.00  0.01  0.33  0.35  0.01
0.00  0.00018  5.50
105.0 120.0  1.38  0.35334  0.16525  0.00  0.00  0.33  0.35  0.01
0.00  0.00018  5.50
120.0 150.0  1.38  0.35334  0.16525  0.00  0.00  0.33  0.35  0.01
0.00  0.00018  5.50
150.0 180.0  1.38  0.35334  0.16525  0.00  0.00  0.33  0.35  0.01
0.00  0.00018  5.50
180.0 210.0  1.38  0.35334  0.16525  0.00  0.00  0.33  0.35  0.01
0.00  0.00018  5.50
```

11+ Bulk density under energy crop

layers->rsetbd[0] = 1.091540
layers->rsetbd[1] = 1.091540
layers->rsetbd[2] = 1.091540
layers->rsetbd[3] = 1.091540
layers->rsetbd[4] = 1.091540
layers->rsetbd[5] = 1.091540
layers->rsetbd[6] = 1.091540
layers->rsetbd[7] = 1.091540
layers->rsetbd[8] = 1.091540
layers->rsetbd[9] = 1.091540
layers->rsetbd[10] = 1.161540
layers->rsetbd[11] = 1.161540
layers->rsetbd[12] = 1.161540
layers->rsetbd[13] = 1.161540

11-

```
0.0   2.0  1.21  0.51250  0.29618  0.80  0.01  0.20  0.60  0.01
0.24  0.00013  5.50
  2.0   5.0  1.21  0.51250  0.29618  0.20  0.04  0.20  0.60  0.01
0.18  0.00013  5.50
  5.0  10.0  1.21  0.51250  0.29618  0.00  0.25  0.20  0.60  0.01
0.12  0.00013  5.50
 10.0  20.0  1.21  0.51250  0.29618  0.00  0.30  0.20  0.60  0.01
0.03  0.00013  5.50
 20.0  30.0  1.21  0.51250  0.29618  0.00  0.10  0.20  0.60  0.01
0.00  0.00013  5.50
 30.0  45.0  1.21  0.51250  0.29618  0.00  0.05  0.20  0.60  0.01
0.00  0.00013  5.50
 45.0  60.0  1.21  0.51250  0.29618  0.00  0.04  0.20  0.60  0.01
0.00  0.00013  5.50
 60.0  75.0  1.21  0.51250  0.29618  0.00  0.03  0.20  0.60  0.01
0.00  0.00013  5.50
 75.0  90.0  1.21  0.51250  0.29618  0.00  0.02  0.20  0.60  0.01
0.00  0.00013  5.50
 90.0 105.0  1.21  0.51250  0.29618  0.00  0.01  0.20  0.60  0.01
0.00  0.00013  5.50
105.0 120.0  1.21  0.51250  0.29618  0.00  0.00  0.20  0.60  0.01
0.00  0.00013  5.50
120.0 150.0  1.28  0.51250  0.29618  0.00  0.00  0.20  0.60  0.01
0.00  0.00013  5.50
150.0 180.0  1.28  0.51250  0.29618  0.00  0.00  0.20  0.60  0.01
0.00  0.00013  5.50
180.0 210.0  1.28  0.51250  0.29618  0.00  0.00  0.20  0.60  0.01
0.00  0.00013  5.50
```

11- Bulk density under energy crop

layers->rsetbd[0] = 1.175600
layers->rsetbd[1] = 1.175600
layers->rsetbd[2] = 1.175600
layers->rsetbd[3] = 1.175600
layers->rsetbd[4] = 1.175600
layers->rsetbd[5] = 1.175600
layers->rsetbd[6] = 1.175600
layers->rsetbd[7] = 1.175600
layers->rsetbd[8] = 1.175600
layers->rsetbd[9] = 1.175600
layers->rsetbd[10] = 1.175600
layers->rsetbd[11] = 1.245600
layers->rsetbd[12] = 1.245600
layers->rsetbd[13] = 1.245600

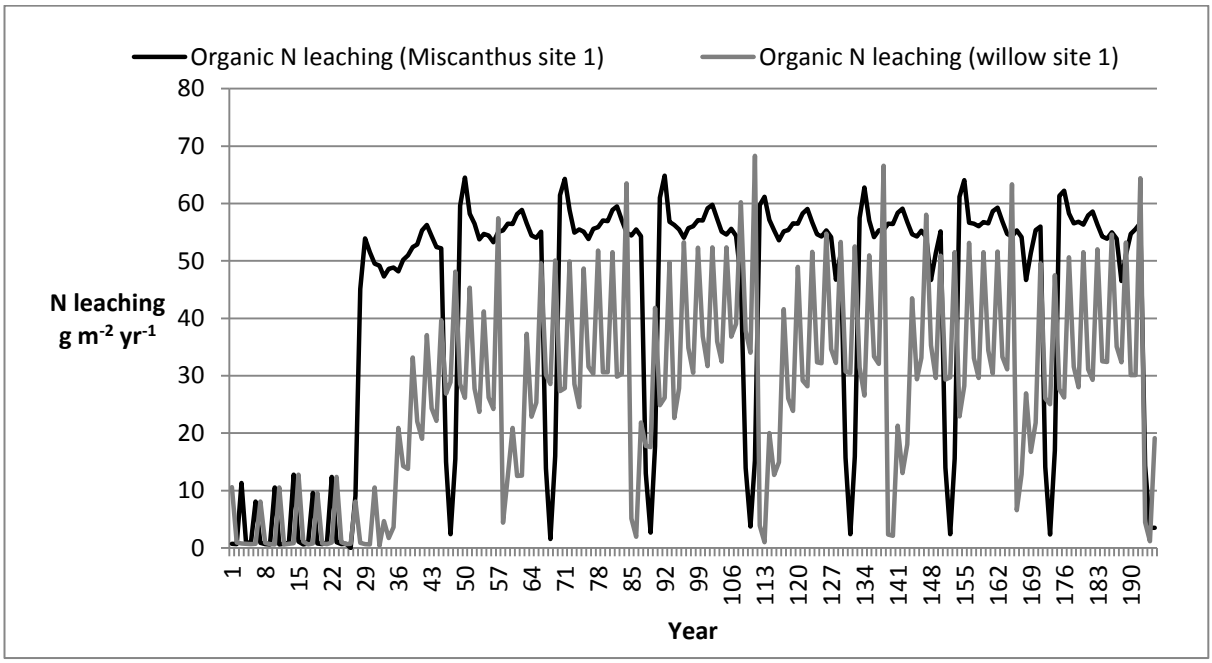

Figure A4.1Time series (by year) organic N leaching over the full simulated period at site1 for willow and Miscanthus